Communications and Control Engineering

Thomas Meurer

Control of Higher–Dimensional PDEs

Flatness and Backstepping Designs

Springer

Communications and Control Engineering

Thomas Meurer

Control of Higher-Dimensional PDEs

Flatness and Backstepping Designs

Springer

Author
PD Dr.-Ing. Thomas Meurer
Vienna University of Technology
Austria

ISSN 0178-5354
ISBN 978-3-642-30014-1 e-ISBN 978-3-642-30015-8
DOI 10.1007/978-3-642-30015-8
Springer Heidelberg New York Dordrecht London

British Library Cataloguing in Publication Data
A catalogue record for this book is available from the British Library

Library of Congress Control Number: 2012937231

Mathematics Subject Classification (2010): 60J27, 60J25, 60J35, 60J40, 60J60, 60K15, 62F15, 60G40, 32U20, 93C30, 34A38, 49J40, 49J55, 49L20, 49L25, 35J99, 47B34, 45H05

Printed on acid-free paper

Springer is part of Springer Science+Business Media (www.springer.com)

Für Barbara

Preface

The analysis of distributed–parameter systems governed by partial differential equations (PDEs) has in recent years gained increasing attention and importance. This is on the one hand motivated by the need to continuously advance the technological state–of–the–art, which requires the detailed resolution of the temporal and the spatial dynamics of the involved devices. On the other hand, new application areas emerge, which essentially rely on the exploitation of the spatial–temporal system evolution. Examples include smart, flapping, and flexible structures in aerospace applications, fusion reactors and electrochemical devices for energy generation and storage, quantum systems and quantum computing, or interconnected systems in mobile actuator and sensor networks and traffic congestion. The dynamic operation of these multi–physics systems inherently requires sophisticated control and observer strategies that explicitly address the spatial–temporal system dynamics. For this, infinite–dimensional system and control theory has been developed and continuously refined to provide a unifying mathematical framework to address the arising analysis and design tasks.

Based on the steady progress in nonlinear control and its success in applications novel and promising lines of development have been identified by their generalization to distributed–parameter systems. This, for instance, comprises differential flatness for inversion–based trajectory planning and feedforward control and Lyapunov–based techniques for (robust) feedback stabilization and observer design such as backstepping, dissipativity, or passivity concepts. Moreover, tracking controllers can be deduced from the suitable composition of these approaches. While many significant contributions have already been achieved for the control design of mainly linear systems the analysis and control of distributed–parameter systems involving nonlinearities and higher–dimensional spatial domains poses challenges for both methodic and applied research.

This research monograph aims at addressing some of these challenges by presenting recent developments for the control of systems governed by PDEs. Herein, the main focus is on systems with higher–dimensional spatial domain by suitably developing systematic model–based design approaches to realize trajectory planning and feedforward control, feedback stabilization and observer design, and

trajectory tracking. Techniques including flatness and backstepping build the core of the treatise and provide the starting point of the presented methodic extensions and generalizations. Moreover, semi–numerical approaches are deduced by integrating suitable methods of approximation into the design systematics to enlarge the domain of applicability. The theoretic analysis is combined with both simulation examples and state–of–the–art experimental results, which enables to bridge the gap between mathematical theory and control engineering practice in the rapidly evolving PDE control area.

The presentation is split into five parts starting with an introduction and survey of PDE control in Part I. Mathematical modeling of heat transfer problems, multi–agent networks, and flexible structures is considered in Part II. The derived model equations serve as the basis for flatness–based trajectory planning and feedforward control in Part III for PDE systems with both in–domain and boundary control. Part IV addresses feedback stabilization and observer design by generalizing backstepping techniques and considering their combination with trajectory planning and feedforward control towards the realization of tracking controllers for PDE systems. Simulation and experimental results are provided in the individual chapters to support the methodic developments and to illustrate their application. Selected mathematical tools and results from complex analysis, entire function theory, and functional analysis are summarized in Part V. Thus, the book is adequate as an advanced research monograph for graduate students in applied mathematics and control theory or as a reference to recent developments for researchers and control engineers interested in the analysis and the control of systems governed by PDEs.

This book would not have been possible without help, support, and suggestions of colleagues and family. In particular I am indebted to Andreas Kugi for his support and suggestions, many fruitful discussions, and his academic and personal advice. I want to acknowledge my students and co–workers in Vienna, especially the members of my work group Johannes Schröck, Lukas Jadachowski, Tilman Utz, and Marc Oliver Wagner. Moreover, I am particularly grateful to Miroslav Krstic for his suggestions and advice. During the work on PDEs I have enjoyed the interaction with Ansgar Jüngel, Pierre Rouchon, Birgit Schörkhuber, Kurt Schlacher, Andrey Smyshlyaev, Rafael Vazquez, Michael Zeitz. I am also thankful to my Viennese colleagues at the CDS group for collectively creating an open and friendly environment. In addition, the financial support of the German Research Council (DFG) is gratefully acknowledged. Last but not least I would like to thank my parents for their continuous support and Barbara for her encouragement and patience in the course of creating this book.

Vienna, January 2012 Thomas Meurer

Contents

List of Symbols and Abbreviations

The following list only contains symbols that are used consecutively throughout the text neglecting only locally introduced symbols.

Coordinates and Units

$\imath$	Imaginary unit $\imath^2 = -1$
$\mathtt{n}_j$	Node in communication graph with integer or multi–index j
t	Time coordinate
z^i	Spatial coordinate
z	Coordinate r–tuple $z = (z^1, z^2, \ldots, z^r)$
$z_{(i\|)}$	Coordinate $(r-1)$–tuple $z_{(i\|)} = (z^1, z^2, \ldots, z^{i-1}, z^{i+1}, \ldots, z^r)$
$z_{(i\|L_i, j\|L_j)}$	Coordinate r–tuple z with $z^i = L_i$ and $z^j = L_j$
$z_{(i\|L_i)}$	Coordinate r–tuple z with $z^i = L_i$
$z_{(i\|\zeta)}$	Coordinate r–tuple z with $z^i = \zeta$
s	Laplace variable

Variables

$\xi^{*,k}(z,t)$	k–th component of desired basic output vector with $(z,t) \in \Omega \times \mathbb{R}^+_{t_0}$
$\hat{\xi}(z,s)$	Laplace transform of $\xi(z,t)$
$\boldsymbol{\xi}(z,t)$	Basic output (vector) with $(z,t) \in \Omega \times \mathbb{R}^+_{t_0}$
$\boldsymbol{\xi}^*(z,t)$	Desired basic output (vector) with $(z,t) \in \Omega \times \mathbb{R}^+_{t_0}$
$\hat{\boldsymbol{\xi}}(z,s)$	Laplace transform of $\boldsymbol{\xi}(z,t)$
$\xi^k(z,t)$	k–th component of basic output vector with $(z,t) \in \Omega \times \mathbb{R}^+_{t_0}$
$\xi(z,t)$	Basic output (scalar) with $(z,t) \in \Omega \times \mathbb{R}^+_{t_0}$
$\xi^*(z,t)$	Desired basic output (scalar) with $(z,t) \in \Omega \times \mathbb{R}^+_{t_0}$
$\tilde{w}(z,t)$	State of target system for state–observer design with $(z,t) \in \Omega \times \mathbb{R}^+_{t_0}$
$w(z,t)$	State of target system for state–feedback design with $(z,t) \in \Omega \times \mathbb{R}^+_{t_0}$
$u^k(\mathtt{n}_j,t)$	k–th component of input vector with $(\mathtt{n}_j,t) \in \mathbb{N} \times \mathbb{R}^+_{t_0}$
$u^k(z,t)$	k–th component of input vector with $(z,t) \in \Omega \times \mathbb{R}^+_{t_0}$
$u_{\partial\Omega}$	Scalar boundary input (where distinguished from in–domain control u_Ω)

$u^{*,k}(\mathtt{n}_j,t)$	k–th component of feedforward control with $(\mathtt{n}_j,t)\in\mathtt{N}\times\mathbb{R}^+_{t_0}$
$u^*(\mathtt{n}_j,t)$	Feedforward control (scalar) with $(\mathtt{n}_j,t)\in\mathtt{N}\times\mathbb{R}^+_{t_0}$
$u^{*,k}(z,t)$	k–th component of feedforward control with $(z,t)\in\Omega\times\mathbb{R}^+_{t_0}$
$u^*(z,t)$	Feedforward control (scalar) with $(z,t)\in\Omega\times\mathbb{R}^+_{t_0}$
u_Ω	Scalar in–domain input (where distinguished from boundary control $u_{\partial\Omega}$)
$\hat{u}(z,s)$	Laplace transform of $u(z,t)$
$u(\mathtt{n}_j,t)$	Input (scalar) with $(\mathtt{n}_j,t)\in\mathtt{N}\times\mathbb{R}^+_{t_0}$
$u(z,t)$	Input (scalar) with $(z,t)\in\Omega\times\mathbb{R}^+_{t_0}$
$\boldsymbol{u}(\mathtt{n}_j,t)$	Input (vector) with $(\mathtt{n}_j,t)\in\mathtt{N}\times\mathbb{R}^+_{t_0}$
$\boldsymbol{u}(z,t)$	Input (vector) with $(z,t)\in\Omega\times\mathbb{R}^+_{t_0}$
$\boldsymbol{u}_{\partial\Omega}$	Boundary input vector (where distinguished from in–domain control $\boldsymbol{u}_\Omega$)
$\boldsymbol{u}^*(\mathtt{n}_j,t)$	Feedforward control (vector) with $(\mathtt{n}_j,t)\in\mathtt{N}\times\mathbb{R}^+_{t_0}$
$\boldsymbol{u}^*(z,t)$	Feedforward control (vector) with $(z,t)\in\Omega\times\mathbb{R}^+_{t_0}$
$\boldsymbol{u}_\Omega$	In–domain input vector (where distinguished from boundary control $\boldsymbol{u}_{\partial\Omega}$)
$\hat{\boldsymbol{u}}(z,s)$	Laplace transform of $\boldsymbol{u}(z,t)$
$\hat{x}(z,t)$	Observer state with $(z,t)\in\Omega\times\mathbb{R}^+_{t_0}$
$\tilde{x}(z,t)$	Observer error state with $(z,t)\in\Omega\times\mathbb{R}^+_{t_0}$
$\boldsymbol{x}(\mathtt{n}_j,t)$	State (vector) with $(\mathtt{n}_j,t)\in\mathtt{N}\times\mathbb{R}^+_{t_0}$
$x^k(z,t)$	k–th component of state vector with $(z,t)\in\Omega\times\mathbb{R}^+_{t_0}$
$x^*(\mathtt{n}_j,t)$	Desired state (scalar) with $(\mathtt{n}_j,t)\in\mathtt{N}\times\mathbb{R}^+_{t_0}$
$x^*(z,t)$	Desired state (scalar) with $(z,t)\in\Omega\times\mathbb{R}^+_{t_0}$
$\hat{x}(z,s)$	Laplace transform of $x(z,t)$
$x^k(\mathtt{n}_j,t)$	k–th component of state vector with $(\mathtt{n}_j,t)\in\mathtt{N}\times\mathbb{R}^+_{t_0}$
$x(\mathtt{n}_j,t)$	State (scalar) with $(\mathtt{n}_j,t)\in\mathtt{N}\times\mathbb{R}^+_{t_0}$
$x(z,t)$	State (scalar) with $(z,t)\in\Omega\times\mathbb{R}^+_{t_0}$
$\boldsymbol{x}(z,t)$	State (vector) with $(z,t)\in\Omega\times\mathbb{R}^+_{t_0}$
$\boldsymbol{x}^*(\mathtt{n}_j,t)$	Desired state (vector) with $(\mathtt{n}_j,t)\in\mathtt{N}\times\mathbb{R}^+_{t_0}$
$\boldsymbol{x}^*(z,t)$	Desired state (vector) with $(z,t)\in\Omega\times\mathbb{R}^+_{t_0}$
$\hat{\boldsymbol{x}}(z,s)$	Laplace transform of $\boldsymbol{x}(z,t)$
$y^k(\mathtt{n}_j,t)$	k–th component of output vector with $(\mathtt{n}_j,t)\in\mathtt{N}\times\mathbb{R}^+_{t_0}$
$y^k(z,t)$	k–th component of output vector with $(z,t)\in\Omega\times\mathbb{R}^+_{t_0}$
$y^{k,*}(\mathtt{n}_j,t)$	k–th component of desired output vector with $(\mathtt{n}_j,t)\in\mathtt{N}\times\mathbb{R}^+_{t_0}$
$y^*(\mathtt{n}_j,t)$	Desired output (scalar) with $(\mathtt{n}_j,t)\in\mathtt{N}\times\mathbb{R}^+_{t_0}$
$y^{k,*}(z,t)$	k–th component of desired output vector with $(z,t)\in\Omega\times\mathbb{R}^+_{t_0}$
$y^*(z,t)$	Desired output (scalar) with $(z,t)\in\Omega\times\mathbb{R}^+_{t_0}$
$\hat{y}(z,s)$	Laplace transform of $y(z,t)$
$y(\mathtt{n}_j,t)$	Output (scalar) with $(\mathtt{n}_j,t)\in\mathtt{N}\times\mathbb{R}^+_{t_0}$
$y(z,t)$	Output (scalar) with $(z,t)\in\Omega\times\mathbb{R}^+_{t_0}$
$\boldsymbol{y}(\mathtt{n}_j,t)$	Output (vector) with $(\mathtt{n}_j,t)\in\mathtt{N}\times\mathbb{R}^+_{t_0}$

$\boldsymbol{y}(z,t)$	Output (vector) with $(z,t) \in \Omega \times \mathbb{R}^+_{t_0}$
$\boldsymbol{y}^*(\mathtt{n}_j,t)$	Desired output (vector) with $(\mathtt{n}_j,t) \in \mathtt{N} \times \mathbb{R}^+_{t_0}$
$\boldsymbol{y}^*(z,t)$	Desired output (vector) with $(z,t) \in \Omega \times \mathbb{R}^+_{t_0}$
$\hat{\boldsymbol{y}}(z,s)$	Laplace transform of $\boldsymbol{y}(z,t)$

Dimensions

m	Dimension of $\boldsymbol{u}$
n	Dimension of $\boldsymbol{x}$
p	Dimension of $\boldsymbol{y}$

Bases, Vectors, Matrices, and Operators

$\mathfrak{A}^*$	Adjoint of $\mathfrak{A}$
$r^a,\ r^g$	Algebraic and geometric multiplicity of eigenvalue λ
θ_k	Constant $\theta_k = 1 + r^a_k - r^g_k$
Δ	Laplace operator $\Delta = \nabla \cdot \nabla$
$\mathcal{D}(\mathfrak{A})$	Domain of $\mathfrak{A}$
ψ	Basis function or eigenfunction of $\mathfrak{A}^*$
$\boldsymbol{\psi}$	Base vector or eigenvector of $\mathfrak{A}^*$
ϕ	Basis function or eigenfunction of $\mathfrak{A}$
$\boldsymbol{\phi}$	Base vector or eigenvector of $\mathfrak{A}$
λ	Eigenvalue of $\mathfrak{A}$
∇	Nabla operator
$\mathfrak{A}$	System operator
$\mathfrak{B}$	Input operator
$\mathfrak{C}$	Output operator
$\mathfrak{K}$	Boundary input operator
$\mathfrak{I}$	Identity operator or identity matrix
$\mathfrak{o}$	Zero operator or zero matrix

Function Spaces and Classes

$\mathcal{L}(X,Y)$	Space of bounded linear operators from X to Y
$\mathcal{L}(X)$	Space of bounded linear operators from X to X
$C^n(\Omega)$	Class of n–times continuously differentiable functions from Ω to $\mathbb{C}$ or $\mathbb{R}$
$G_{D,\alpha}(\Lambda)$	Gevrey class of order α on domain Λ
$G_{D,\alpha,\beta}(\Lambda)$	Gevrey class of order α in the first argument and β in the second argument on domain Λ
$H^p(\Omega)$	Sobolev space of order p
ℓ^∞	Space of bounded sequences $(f_k)_{k\in\mathbb{N}^r}$ with $\sup_{k\in\mathbb{N}} \lvert f_k\rvert < \infty$
$L^\infty(\Omega)$	Class of Lebesgue measurable bounded functions from Ω to $\mathbb{C}$
ℓ^p	Space of sequences $(f_k)_{k\in\mathbb{N}^r}$ with $\sum_{k\in\mathbb{N}} \lvert f_k\rvert^p < \infty$
$L^p(\Omega)$	Class of Lebesgue measurable functions with $\int_\Omega \lvert f(t)\rvert^p \mathrm{d}t < \infty$
$L^p(\Omega;X)$	Class of Lebesgue measurable X–valued functions with $\int_\Omega \lvert f(t)\rvert^p \mathrm{d}t < \infty$

$\ell_k^2(0,\tau)$	Space of square summable sequences $(f_k(t))_{k\in\mathbb{N}^r}$ on the interval $t \in [0,\tau]$, i.e., $\forall t \in [0,\tau] : \sum_{k\in\mathbb{N}^r} \lvert f_k(t)\rvert^2 < \infty$
X_{-1}	see Lemma B.4
X_1	see Lemma B.3

Entire and Special Functions

γ	Convergence exponent (see Section B.2.2)
$\mathcal{N}(\eta)$	Counting function (see Section B.2.2)
g^f	Genus of entire function (see Section B.2.2)
ϱ	Order of entire function (see Section B.2.2)
τ	Type of entire function (see Section B.2.2)
σ	Heaviside function
$\sigma(t-t_0)$	Heaviside function with $\sigma(t-t_0) = 0$ for $t < t_0$ and $\sigma(t-t_0) = 1$ else
δ_{ij}, $\delta_{i,j}$	Kronecker delta function with $\delta_{ij} = \delta_{i,j} = 1$ if $i = j$ and zero else
$\varrho^\epsilon(z)$	Indicator function satisfying $\varrho^\epsilon(z < 0) = 0$, $\varrho^\epsilon(z > \epsilon) = 1$, and $\varrho^\epsilon(z) \in C^4([0,\epsilon])$ for $\epsilon > 0$. If $\epsilon = 0$, then $\varrho^0(z) = \sigma(z)$.
$\mathcal{G}$	Weierstrass primary factor (see Section B.2.2)
$\mathit{\Pi}$	Weierstrass canonical product (see Section B.2.2)
g^s	Genus of sequence (see Section B.2.2)

Integral Kernels

$k(z^i,\zeta,t)$	Kernel of backstepping transformation in state–feedback control design
$g(z^i,\zeta,t)$	Kernel of inverse backstepping transformation in state–feedback control design
$l(z^i,\zeta,t)$	Kernel of backstepping transformation in state–observer design
$m(z^i,\zeta,t)$	Kernel of inverse backstepping transformation in state–observer design

Sets

$\mathbb{C}$	Set of complex numbers
ker	Kernel
$\mathbb{N}$	Set of natural numbers $\{0,1,2,\ldots\}$
$\mathbb{N}_1$	Set of natural numbers excluding 0
$\mathtt{N}$	Set of nodes (vertex set)
ran	Range
$\mathbb{R}$	Set of real numbers
$\mathbb{R}_{t_0}^+$	Set of real numbers $t \in \{t \in \mathbb{R} : t > t_0\}$
I_r	Index set $I_r = (1,2,\ldots,r)$
I_r^i	Index set $I_r^i = I_r \setminus \{i\} = (1,2,\ldots,i-1,i+1,\ldots,r)$
I_m	Index set $I_m = (1,2,\ldots,m)$
I_m^i	Index set $I_m^i = I_m \setminus \{i\} = (1,2,\ldots,i-1,i+1,\ldots,m)$
I_p	Index set $I_p = (1,2,\ldots,p)$
I_p^i	Index set $I_p^i = I_p \setminus \{i\} = (1,2,\ldots,i-1,i+1,\ldots,p)$
$\mathbb{Z}$	Set of integers $\{\ldots,-2,-1,0,1,2,\ldots\}$
$\mathbb{Z}_1$	Set of integers excluding 0

Algebra

$\#$	Number of elements in a set
$\bigtimes$	Cartesian product $\bigtimes_{j\in\{1,\ldots,r\}}[0,L_j]=[0,L_1]\times\ldots\times[0,L_r]$
$\wedge$	Logical conjunction
$\vee$	Logical disjunction

Abbreviations

2DOF	Two–degrees–of–freedom
BVP	Boundary–value problem
DCRS	Diffusion–convection–reaction system
DPS	Distributed–parameter system
DRS	Diffusion–reaction system
IEOK	Integral equation with operator kernel
IVP	Initial–value problem
MFC	Macro–fiber composite
MIMO	Multiple inputs multiple outputs
ODE	Ordinary differential equation
PDE	Partial differential equation
PdE	Partial difference equation
SISO	Single input single output

Chapter 1
Introduction

Although exhibiting a long history and tradition, partial differential equations (PDEs) are just nowadays starting to evolve as the fundamental mathematical description of many technical processes. It can be thereby observed that the success story of PDEs entering new areas of applied research is related to the vast progress in information technology and (computational) mathematics, which provide access to an almost unlimited computational power and newly developed efficient algorithms. With this, the attention is focused on previously unthought problems such as high resolution climate simulation using increasingly finer spatial grids covering the earth's surface or the study of multi–phase compressible reactive flows in complex geometrical domains.

In general, the distributed–parameter description becomes an essential ingredient of the modeling and analysis process if the spatial or property–related distribution of the process variables can no longer be neglected. Some characteristic examples are summarized below:

- chemical or biochemical reactors [65] such as three-way catalysts for exhaust after–treatment in automotive applications, (reactive) distillation and adsorption processes [140], or activated sludge processes for wastewater treatment [75];
- thermal systems [6] or the reheating and cooling of metal slabs during the steel processing to achieve desired metallurgical changes [146];
- electrochemical systems such as fuel cells [141] and Li–ion or Li–polymer battery devices for energy production and storage [26, 58];
- smart materials and vibratory systems [88, 10, 109];
- flexible structures arising in aerospace and mechanical applications including novel adaptive or flapping wing structures [139], micro–mechanic bending cantilevers in atomic force microscopes [15], or deformable mirrors in adaptive optics [114];
- fluid dynamical systems [1, 14], mixing processes and coupled fluid–structure interactions;
- wave propagation in optical fibers [130] and traffic congestion [152, 61];
- energy production in fusion reactors [142, 3].

T. Meurer: Control of Higher-Dimensional PDEs, CCE, pp. 3–20.
springerlink.com

However, the dynamic operation of these distributed–parameter systems (DPSs) essentially relies on the incorporation of suitable control strategies to influence the system dynamics and to enlarge the operating range. For this, it can be observed that in addition to the stabilization problem, the consideration of the trajectory tracking control problem, i.e. the design of a control such that the controlled variables of the distributed–parameter system follow prescribed desired reference trajectories, has gained increasing attraction. This is in particular due to the rising demands on product quality and efficiency, which require to turn away from the pure stabilization of an operating point towards the realization of specific start–up, transition, or tracking tasks. Selective academic and industrial applications, which illustrate and confirm the increasing interest in the study of tracking control problems for distributed–parameter systems can be found, e.g., in [108, 33, 100] and the references therein.

Nevertheless, although being of increasing practical interest, traditional control design approaches seem to provide only indirect and often unsatisfactory solutions to the tracking control problem. This is mainly due to the methodical focus on the feedback stabilization of a given distributed–parameter system without the consideration of the assignment and the realization of a suitable desired spatial–temporal dynamics.

1.1 Feedback Stabilization of PDE Systems

Model–based feedback control for distributed–parameter systems[1] can in general be classified in terms of early and late lumping. In the early lumping approach, the governing PDEs are reduced to a finite–dimensional description by making use of suitable approximation and model reduction techniques prior to the feedback control design. This includes the application of finite difference or finite element techniques [88, 109], modal or spectral approaches [56, 8, 88, 51, 54], balanced truncation and proper orthogonal decomposition [4, 11, 131], or Galerkin's method [111, 1] and its variants such as (approximate) inertial manifold techniques [49, 28, 27, 64]. Thereby, well–developed feedback control design methods can be applied originating from linear and nonlinear finite–dimensional control theory. However, depending on the order of approximation, the early lumping approach may lead to high–dimensional and complex feedback control structures, which do not fully exploit the physical structure of the system. In addition, the neglected dynamics may lead to a degradation of the control performance or even the destabilization of the closed–loop system due to the well–known control and observer spillover [7]. Furthermore, for nonlinear distributed–parameter systems the validity of the finite–dimensional approximation and hence the determined controller is usually restricted to a certain subset of the state space. As a result, situations may arise, where the

[1] In this section, only a brief overview of the major analysis as well as design approaches and techniques will be given, which are available for control problems governed by distributed–parameter systems. This can naturally include only a selection of methods and literature without any claim of being comprehensive.

domain of model validity is violated due to the control action. This leads to a loss of robustness and eventually to an unstable behavior of the closed–loop system (see, e.g., [66] for a fluid dynamical example).

On the other hand, in the late lumping approach the distributed nature is explicitly integrated into the system analysis and the control design. This in particular enables a rigorous extension of finite–dimensional systems and control theory to systems governed by partial differential equations, see, e.g., [123, 36, 81, 145] for modern and comprehensive treatises. For linear systems, the operator–theoretic representation of the distributed–parameter system using semigroup theory allows a mathematically profound generalization of well–known control design approaches for finite–dimensional systems. Examples include frequency domain techniques [24, 40, 18, 101, 76, 100], eigenvalue and structural assignment exploiting certain (Riesz) spectral properties of the system operator [73, 34, 113, 154], and LQR state–feedback control [36, 10], which, however, requires the rather involving solution of operator Riccati equations. In any case, special emphasis is required for the analysis of the asymptotic or the exponential stability of the closed–loop distributed–parameter systems. For this, typically linear and nonlinear semigroup and contraction theory as well as spectral analysis are applied [37, 143, 110, 105, 36, 25, 81].

Moreover, while Lyapunov's theory is a well–developed tool for finite–dimensional linear and nonlinear systems certain structural restrictions arise for its extension to the distributed–parameter case, which are mainly related to the existence and the construction of an appropriate Lyapunov functional and the loss of compactness of infinite–dimensional function spaces [38, 60, 104, 133, 39, 81]. Nevertheless significant generalizations to linear and nonlinear distributed–parameter systems are available including the celebrated LaSalle's invariance principle [60, 133, 78, 80]. Based on these mathematical tools various stabilization tasks have been addressed for both linear and nonlinear parabolic, hyperbolic, and biharmonic PDEs, see, e.g., [21, 71, 30, 81, 9, 32, 150, 12] and the many references therein. In addition, promising results are obtained utilizing dissipativity concepts and distributed–parameter port–Hamiltonian systems [125, 124, 83, 43, 87, 126, 41].

However, for systems governed by linear time varying PDEs, linear PDEs with nonlinear boundary conditions (BCs), and nonlinear PDEs the development of systematic feedback control design approaches ensuring at least local asymptotic stability is still a widely open question with only few available results (see, e.g., [53, 112, 31]). Besides the application of Lyapunov–based techniques for the verification that a particular choice of feedback control implies asymptotic or possibly exponential stability, the so–called backstepping approach provides a systematics for the design of exponentially stabilizing state–feedback controllers. Backstepping in its extension to PDE systems is thereby based on the determination of the kernel of an invertible Volterra integral equation to achieve a one–to–one correspondence between the possibly unstable plant dynamics and a suitably selected exponentially stable target system. This, however, requires the solution of a higher–dimensional PDE governing the evolution of the kernel. Once the kernel is determined, the respective state–feedback controller realizing the desired transformation is immediately obtained [19, 20, 79, 134, 136, 68, 67, 69, 137, 29, 138]. The backstepping

technique inherently relies on the knowledge of the spatial–temporal state evolution such that the control has to be complemented by a suitable state–observer. For this, backstepping can be similarly applied [135, 68], which results in dynamic output feedback controllers. In addition to linear systems with constant or spatially varying parameters, results on the incorporation of a single time varying reaction parameter [136], time and spatially varying parameters [94], as well as the extension to distributed–parameter systems with nonlinearities in terms of Volterra series [148, 149] are available.

Nevertheless, it has to be pointed out that with the exception of optimal control [22, 77, 111, 45, 52, 63, 144], whose methods are in general computationally expensive in the case of distributed–parameter systems, and certain extensions of the geometric theory of output regulation [23] with its restriction to linear systems, periodic desired trajectories, and the necessity to solve operator Lyapunov equations, the control of distributed–parameter systems is in general limited to the stabilization problem. On the other hand, enhanced operation demands and evolving novel applications require to consider the trajectory planning problem. Selected examples thereby include:

- the start–up, the shutdown, and the transition between operating points for chemical and thermal processes such as tubular and fixed–bed reactors in chemical engineering [108, 33];
- the realization of desired microstructural transitions during, e.g., annealing, quenching, and tempering in metallurgical applications [146];
- flexible smart structures such as piezoelectric stack actuators [55, 57, 2, 103, 96] and beam and plate systems [100, 128] with possible applications in injection valves, micro– and nano–positioning devices, and atomic force microscopy;
- adaptive optics in telescopes, adaptive wings, or so-called smart skins, where it is desired to suitably affect the shape of a structure to achieve, e.g., the modulation of optical wave fronts, the reduction of drag, or the improvement of aeroelastic characteristics [114, 155, 70];
- quantum control systems, e.g., to realize tunnel transitions between energy levels [117];
- the formation control of interconnected networks of mobile agents [91, 50, 92].

1.2 Trajectory Planning and Tracking Control for PDE Systems

The problem of trajectory planning, i.e. the design of an open–loop control to realize prescribed desired spatial–temporal output paths, is of fundamental interest in control theory and its applications. For the solution of the trajectory planning and tracking control problem for finite–dimensional linear and nonlinear systems, differential flatness as introduced by Fliess and co–workers [46] is nowadays a well established tool [115, 85, 102, 86, 119, 132]. Differential flatness basically implies that the system states and the control inputs can be parametrized in terms of a flat or so–called basic output and its time–derivatives up to a certain problem dependent

order. By prescribing appropriate trajectories for the flat output the respective state and input trajectories can be directly evaluated without integration of any differential equation. Within the context of differential algebra and differential geometry, this implies that a differentially flat system is endogenously equivalent to a system without dynamics described by a collection of independent variables, namely the flat output, having the same number of components as the number of system inputs [46, 48].

Observing that the underlying idea of equivalence and flatness, i.e. the existence of a one–to–one correspondence between trajectories of systems, can be also adapted to systems governed by PDEs [72, 116, 120, 89, 153], recent work on the flatness concept has mainly dealt with its extension to trajectory planning for boundary controlled linear and certain nonlinear distributed–parameter systems in a single spatial coordinate. Thereby, for parabolic and biharmonic PDEs the application of operational calculus or formal power series yields the parametrization of the system states and the system inputs by the flat or basic output, respectively, in terms of fractional differentiation operators or infinite power series representations. The series coefficients depend on time–derivatives of the basic output, which has to be chosen from a certain Gevrey class to ensure uniform convergence of the series. Selective examples concern trajectory planning for the linear heat equation [72] and for the linear diffusion equation with spatially dependent coefficients [72, 82] in several state variables [47, 89]. In addition, certain semi– and quasi–linear diffusion–convection–reaction systems modeling tubular reactors are considered, e.g., in [82, 98, 89, 99, 147], while a moving boundary problem (Stefan problem) is studied in [42, 121]. Besides parabolic PDEs, results on the trajectory planning for hyperbolic systems exhibiting wave dynamics are available [106, 120, 153, 151].

Nevertheless, in contrast to possible applications, e.g., for the selective reheating or cooling in material processing and forming, thermal management for energy production and storage units or problems of flow control, so far only very few results are available for the solution of the trajectory planning problem for PDEs defined on higher–dimensional domains. In [13], trajectory planning is considered for the boundary controlled linear heat equation with rectangular domain by using truncated Fourier series expansion, which, however, results in the loss of the essential effects arising from the infinite–dimensional system character. Trajectory planning for the temperature evolution inside a cylinder is considered in [120] by exploiting the rotational symmetry of the domain, which reduces the problem to two decoupled 1–dimensional systems. The motion of a fluid represented by linearized wave equations under the shallow water approximation inside a moving tank being subject to controlled translations and rotations is analyzed in [107]. The trajectory planning problem is thereby in principle solved by superimposing the solution of two decoupled 1–dimensional problems. Computations with entire functions are suggested in [118] for the 2– and 3–dimensional wave equation with a finite–dimensional control acting simultaneously on all of the domain's boundary. The resulting flatness–based parametrizations are thereby shown to diverge in general. For boundary controlled diffusion–convection–reaction systems with spatially and time varying parameters defined on a parallelepiped domain a solution to the trajectory planning problem is

provided in [95] by considering a formal integration of the PDE. With this, rather general results are obtained, which, however, rely on the particular shape of the spatial domain and the assumption of an infinite–dimensional boundary control. While the latter assumption is rather common, in particular for the controllability and observability analysis of diffusion–convection–reaction systems with higher–dimensional domain (see, e.g., [44, 122, 5, 74]), it represents a significant practical restriction. In order to address this, a design systematics is presented in [90] for boundary controlled linear diffusion–reaction systems with parallelepiped spatial domain, which is simultaneously applicable to both infinite– and finite–dimensional control configurations. Here, the Riesz spectral properties of the system operator are exploited to determine a flatness–based parametrization of the system variables in terms of differential operators of infinite order.

Besides the determination of open–loop input trajectories, flatness–based trajectory planning can be complemented by suitable feedback control techniques for distributed–parameter systems within the so–called two–degrees–of–freedom (2DOF) control concept. While the underlying idea of an independent design of the reference dynamics and the feedback stabilization traces back to [62] in the case of linear finite–dimensional control problems, recent extensions consider the application of the 2DOF concept to nonlinear finite–dimensional systems [59] and systems governed by PDEs [97]. The underlying schematic set–up is shown in Figure 1.1. Given the distributed–parameter system Σ_∞ with output $\boldsymbol{y}(t)$, the control structure comprises trajectory planning Σ^* and feedforward control Σ_{ff} to impose the desired output trajectory $\boldsymbol{y}^*(t)$ by means of $\boldsymbol{u}^*(t)$ and error feedback control Σ^e_{fb} to provide the state–feedback $\boldsymbol{u}_e(t)$ in terms of the estimated error state $\hat{\boldsymbol{x}}_e(t)$ obtained from an error system observer Σ^e_{ob} processing the tracking error $\boldsymbol{y}_e(t) = \boldsymbol{y}(t) - \boldsymbol{y}^*(t)$. In particular, in the nominal case of an exact plant model Σ_∞, no exogenous disturbances, and perfectly known initial conditions, the feedforward control in combination with trajectory planning ensures that the output $\boldsymbol{y}(t)$ exactly tracks a prescribed desired trajectory $\boldsymbol{y}^*(t)$. In order to account for model uncertainties and disturbances and to make this approach applicable to unstable systems, a feedback controller is designed to stabilize the tracking error dynamics, i.e. the evolution of the deviation between the actual state and its desired value. The latter is herein known from the flatness–based state and input parametrization. Moreover, it is in general necessary to integrate a distributed–parameter state–observer to estimate the unmeasured state evolution from the available measurements. Applications of the 2DOF concept for distributed–parameter systems comprise linear and semi–linear diffusion–convection–reaction systems [97, 93, 94], where flatness–based trajectory planning was combined with PI output error feedback control and backstepping–based state–feedback control, respectively, or flexible structures such as piezoelectric stack actuators and elastic beams with flatness–based techniques being integrated together with PID control [100, 84], modal finite–dimensional state–feedback control [156] and passivity–based dynamic output error feedback control [96, 129, 127]. In addition, complex periodically operated adsorption processes are addressed in [16, 17] within the early–lumping approach. Thereby, the experimental results presented in [16, 100, 127]

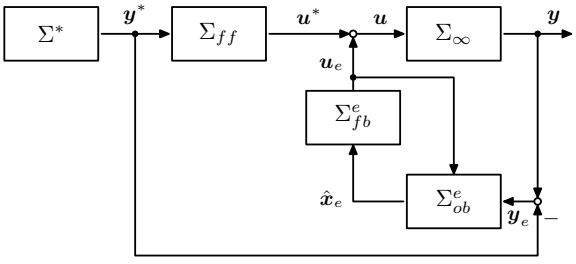

Fig. 1.1 Block diagram of the 2DOF control concept for the DPS Σ_∞ with trajectory planning Σ^*, feedforward control Σ_{ff}, error feedback control Σ^e_{fb}, error system observer Σ^e_{ob} for tracking control $\boldsymbol{y} \to \boldsymbol{y}^*$.

directly illustrate the robustness and the high tracking performance, which can be achieved by means of a suitable combination of these design methods within the 2DOF concept.

These introductory remarks constitute the starting point for this contribution, where systematic model–based trajectory planning, feedback stabilization, and tracking control methods are developed for distributed–parameter systems with a particular focus on higher–dimensional spatial domains.

1.3 Objectives of this Book

Although many significant contributions both on the methodic and the applied level are available for the control design for distributed–parameter systems many questions still remain unanswered. This in particular includes the analysis of distributed–parameter systems with higher–dimensional spatial domain, where from a control perspective various challenges arise, which can be currently only approached in an unsatisfactory way:

- Rather sophisticated approaches exist for trajectory planning given linear and certain classes of nonlinear boundary controlled distributed–parameter systems with 1–dimensional spatial domain. Nevertheless, their extension and systematization to complex higher–dimensional domains, in–domain control, and time varying or even nonlinear PDE systems is unsolved but of great interest in view of the many applications.
- Different techniques such as spectral, semigroup, and Lyapunov theory are available to verify that a particular type of output or state–feedback control stabilizes a given distributed–parameter systems. However, there is still a great lack in design methodologies, which systematically enable the feedback stabilization and are generically applicable to PDE control problems.
- The combination of trajectory planning and feedback stabilization is well established for finite–dimensional and distributed–parameter systems with

1–dimensional domain. However, their suitable integration within the 2DOF control design concept might lead to promising generalizations towards the solution of the tracking control problem for distributed–parameter systems with higher–dimensional spatial domain involving varying parameters and nonlinearities.
- In many applications complex geometrical domains have to be considered and nonlinearities arise due to, e.g., chemical reactions, fluid flow, or large displacements, which in general prevent the application of analytical approaches to the solution of trajectory planning, feedback stabilization, and tracking control problems. Hence, suitable semi–numeric techniques are required by combining analytical design methods with well–developed numerical tools.
- In general, numerical simulation is used to validate control and observer design concepts for distributed–parameter systems. Nevertheless, the thorough evaluation of their applicability, real–time capability, and performance essentially requires implementation and the proof–of–concept based on sophisticated experimental facilities.

In order to address these challenges, in this monograph recent developments are presented with the desire to extend the state–of–the–art both at the methodic as well as the applied level. For this, the analysis focuses on the trajectory planning and tracking control problem with the latter inherently covering the feedback stabilization task. In view of the individual components of the presented 2DOF control design concept and their realization, this comprises the following objectives:

- The generalization of flatness–based trajectory planning to distributed–parameter systems with higher–dimensional domain and both boundary as well as in–domain control.
- The development of backstepping–based design methodologies for the systematic feedback stabilization and the state–observer design for distributed–parameter systems with higher–dimensional parallelepiped domain covering both single input single output (SISO) and multiple inputs multiple outputs (MIMO) configurations.
- The combination of flatness–based trajectory planning and backstepping–based feedback control to realize exponentially stable tracking control for distributed–parameter systems with higher–dimensional domain.
- The development of efficient semi–numerical design techniques by combining the developed analytical design techniques with methods of numerical approximation to enable the consideration of complex multi–domain PDE control problems.
- The proof–of–concept by the application of the developed techniques in simulation and state–of–the–art experiments to verify the control and tracking performance.

It is herein desired to address these objectives based on theoretical and numerical results. Therefore, different application examples are studied within the various chapters both in simulation and experiment and extensions are provided whenever possible to generalize the underlying ideas.

1.4 Outline and Structure

The structure of this contribution can be directly deduced from the objectives stated above. Following this introductory Part I, the monograph is organized into Parts II–V. Part II considers the modeling of selective application examples that are governed by distributed–parameter systems. This comprises the established areas of non–convective and convective heat transfer in Chapter 2 as well as an emerging area dealing with the mathematical representation of interconnected network structures including cooperative sensor and actuator networks in Chapter 3. Moreover, flexible mechanical structures are considered in Chapter 4 with a particular focus on smart adaptive systems with spatially distributed piezoelectric actuators. It is thereby shown that the application areas can be embedded into the class of parabolic (or biharmonic) PDEs with the control being either located on the boundary or in the interior of the PDE domain. For this, fundamental modeling and analysis issues are presented, which are in addition required for the proper formulation of the respective stabilization and tracking control design tasks.

In order to address these, Part III considers the generalization and systematization of flatness–based techniques for trajectory planning and feedforward control for distributed–parameter systems with complex higher–dimensional spatial domain as well as spatially and time varying system parameters. Thereby, a spectral approach is presented in Chapter 6, which exploits the spectral properties of the system operator. Following a brief survey on the abstract formulation of PDE control problems in appropriate function spaces, Riesz spectral operators are introduced, which share the favorable properties that their eigenvalues are purely discrete and their eigenvectors and adjoint eigenvectors form a Riesz basis. It is thereby important to observe that many physically relevant problems can be embedded into the class of Riesz spectral operators as is outlined, e.g., in [35, 36]. By suitably re–formulating the resolvent of a generic Riesz spectral operator with eigenvalues of differing algebraic and geometric multiplicity, it is shown that a basic output can be systematically introduced under the assumption of approximate controllability to formally parametrize any system variable. Thereby, differential operators of infinite–order arise, which, however, can be interpreted as entire functions in the operational domain. This correspondence can be utilized for the convergence analysis of the formal parametrizations, where generic results are determined by making use of the theory of entire functions and Weierstrass canonical products. Here, additional conditions arise, which have to be taken into account for the admissible trajectory assignment for the parametrizing basic output. To address this, a generic set–up is proposed to realize finite time transitions between stationary and non–stationary profiles. The application of this design method is furthermore illustrated in numerical simulations for the heat and wave equation on a 1–dimensional domain as well as for boundary controlled diffusion–convection–reaction equations on both general Riemannian manifolds and 3–dimensional parallelepiped domains. These results are complemented by the analysis of a flexible piezoactuated plate, where the weak formulation of the equations of motion is utilized for the flatness–based design. With this, on the one hand an efficient semi–numerical design approach can be deduced

making use of weighted–residuals. On the other hand, experimental results are presented for high–speed rest–to–rest motion along predefined spatial–temporal deflection paths of the piezoactuated structure, which illustrate and confirm the tracking performance. In order to incorporate also time varying system parameters, a design approach based on the formal integration of the governing PDE is presented in Chapter 7. Given the example of a linear diffusion–convection–reaction system with the input being restricted to one boundary hypersurface of the parallelepiped domain, the uniform convergence of the state and input parametrizations is verified generically depending on the Gevrey order of the basic output trajectory. Moreover, the assignment of admissible desired trajectories is generalized by explicitly taking into account the time–variance of the governing PDE. The applicability and tracking performance is evaluated by simulation results for a 3–dimensional spatial domain.

The analysis of the trajectory tracking problem is complemented in Part IV by the development of feedback stabilization techniques for distributed–parameter systems with boundary actuation and their combination with trajectory planning and feedforward control within the 2DOF control concept. This covers boundary controlled diffusion–convection–reaction systems with spatially and time varying parameters defined on both 1–dimensional and higher–dimensional domains. For this, the backstepping approach is suitably extended for the state–feedback and state–observer design. Herein, both SISO as well as MIMO systems are considered, where in particular the latter configuration poses challenging problems due to the broad variety of boundary input and boundary output configurations. In order to address these tasks, the general formulation of the backstepping approach for linear diffusion–convection–reaction systems with spatially and time varying parameters and 1–dimensional domain is presented first in Chapter 8. Here, successive approximation techniques are introduced to solve the arising PDE for the backstepping integral kernel. With these preliminaries, extensions to distributed–parameter systems defined on higher–dimensional domains and MIMO configuration are considered in Chapter 9. It is herein shown that the MIMO case requires to introduce multi–linear Volterra integral transformations. In addition to the state–feedback control and state–observer design a separation principle is verified for the backstepping approach, which yields that feedback and observer can be designed separately. Moreover, it is shown that the backstepping technique, which transforms the original and possibly unstable distributed–parameter system into a target distributed–parameter system with prescribed stability properties, can be directly combined with differential flatness to determine exponentially stabilizing tracking controllers. This is confirmed in simulation scenarios, where the exponentially stable tracking of prescribed spatial–temporal paths is validated for both 1–dimensional and 3–dimensional settings arising in chemical engineering applications as well as the synchronization of a large scale multi–agent network.

Finally, the Appendix in Part V provides a brief overview of the used notation and the required mathematical background covering selected results from complex analysis, entire function theory, and functional analysis.

References

1. Aamo, O., Krstic, M.: Flow Control by Feedback. Springer, London (2003)
2. Adriaens, H., Koning, W.D., Banning, R.: Modeling piezoelectric actuators. IEEE/ASME Trans. Mechatr. 5(4), 331–341 (2000)
3. Ambrosino, G., Albanese, R.: Magnetic control of plasma current, position, and shape in Tokamaks: a survey of modeling and control approaches. IEEE Contr. Sys. Magazine 25(5), 76–92 (2005)
4. Atwell, J., King, B.: Proper orthogonal decompostion for reduced basis feedback controllers for parabolic equations. Math. Comput. Model 33, 1–19 (2001)
5. Avdonin, S., Ivanov, S.: Families of Exponentials. Cambridge University Press, Cambridge (1995)
6. Baehr, H., Stephan, K.: Heat and Mass Transfer, 2nd edn. Springer, Berlin (2006)
7. Balas, M.: Active control of flexible dynamic systems. J. Optim. Theory and Appl. 25(3), 415–436 (1978)
8. Balas, M.: Modal control of certain flexible dynamic systems. SIAM J. Control Optim. 16(3), 450–462 (1978)
9. Balogh, A., Krstic, M.: Burgers' Equation with Nonlinear Boundary Feedback: H^1 Stability, Well–Posedness and Simulation. Math. Probl. Eng. 6, 189–200 (2000)
10. Banks, H., Smith, R., Wang, Y.: Smart Material Structures: Modeling, Estimation and Control. John Wiley & Sons, Chichester (1996)
11. Banks, H., del Rosario, R., Tran, H.: Proper Orthogonal Decomposition-Based Control of Transverse Beam Vibration: Experimental Implementation. IEEE Trans. Contr. Sys. Techn. 10(5) (2002)
12. Beauchard, K., Zuazua, E.: Large Time Asymptotics for Partially Dissipative Hyperbolic Systems. Arch. Ration Mech. An. 199, 177–227 (2011)
13. Belghith, N., Fliess, M., Ollivier, F., Sedoglavic, A.: Platitude différentielle de l'équation de la chaleur bidimensionnelle. Actes des Journées Doctorales d'Automatique (2003)
14. Bewley, T.: Flow control: New Challenges for a new Renaissance. Prog. Aerosp. Sci. 37, 21–58 (2000)
15. Bining, G., Quate, C., Gerber, C.: Atomic force microscope. Phys. Rev. Letter 56(9), 930–933 (1986)
16. Bitzer, M.: Control of Periodically Operated Adsorption Processes. Fortschr.–Ber. VDI Reihe 8 Nr. 1038. VDI Verlag, Düsseldorf (2004)
17. Bitzer, M.: Model-based Nonlinear Tracking Control of Pressure Swing Adsorption Plants. In: Meurer, T., et al. (eds.) Control and Observer Design for Nonlinear Finite and Infinite Dimensional Systems. LNCIS, vol. 322, pp. 403–418. Springer, Berlin (2005)
18. Bontsema, J., Curtain, R., Schumacher, J.: Robust Control of Flexible Structures: A Case Study. Automatica 24(2), 177–186 (1988)
19. Bošković, D., Krstic, M., Liu, W.: Boundary control of an unstable heat equation via measurement of domain-averaged temperature. IEEE Trans. Automat. Control 46(12), 2022–2028 (2001)
20. Bošković, D., Balogh, A., Krstic, M.: Backstepping in infinite dimension for a class of parabolic distributed parameter systems. Math. Control Signal 16, 44–75 (2003)
21. Buis, G., Eisen, M., Vogt, W.: Lyapunov stability for partial differential equations. Part 1 - Lyapunov stability theory and the stability of solutions to partial differential equations. Part 2 - Contraction groups and equivalent norms. Tech. Rep. NASA-CR-1100, NASA (1968)

22. Butkovskiy, A.: Distributed Control Systems. Elsevier, New York (1969)
23. Byrnes, C., Laukó, I., Gilliam, D., Shubov, V.: Output Regulation for Linear Distributed Parameter Systems. IEEE Trans. Automat. Control 40(12), 2236–2252 (2000)
24. Callier, F., Desoer, C.: An Algebra of Transfer Functions for Distributed Linear Time–Invariant Systems. IEEE Trans. Circuits Syst. 25(9), 651–662 (1978)
25. Cazenave, T., Haraux, A.: An Introduction to Semilinear Evolution Equations. Clarendon Press, Oxford (1998)
26. Chen, Y., Evans, J.: Thermal analysis of lithium-ion batteries. J. Electrochem. Soc. 143(9), 2708–2712 (1996)
27. Christofides, P.: Nonlinear and Robust Control of PDE Systems. Birkhäuser, Basel (2001)
28. Christofides, P., Daoutidis, P.: Finite–Dimensional Control of Parabolic PDE Systems Using Approximate Inertial Manifolds. J. Math. Anal Appl. 216, 398–420 (1997)
29. Cochran, J., Krstic, M.: Motion planning and trajectory tracking for three–dimensional Poiseuille flow. J. Fluid Mech. 626, 307–332 (2009)
30. Conrad, F., Pierre, M.: Stabilization of second order evolution equations by unbounded nonlinear feedback. Ann. Inst. H Poincaré Anal Non Linéaire 11(5), 485–515 (1994)
31. Coron, J.M.: Control and Nonlinearity. American Mathematical Society, Providence, Rhode Island (2007)
32. Coron, J.M., d'Andrea Novel, B., Bastin, G.: A Strict Lyapunov Function for Boundary Control of Hyperbolic Systems of Conservation Laws. IEEE Trans. Autom. Control 52(1), 2–11 (2007)
33. Corriou, J.P.: Process Control – Theory and Applications. Springer, London (2004)
34. Curtain, R.: Pole Assignment for Distributed Systems by Finite–Dimensional Control. Automatica 21(1), 57–67 (1985)
35. Curtain, R., Pritchard, A.: Infinite Dimensional Linear Systems Theory. LNCIS, vol. 8. Springer, Berlin (1978)
36. Curtain, R., Zwart, H.: An Introduction to Infinite–Dimensional Linear Systems Theory. Texts in Applied Mathematics, vol. 21. Springer, New York (1995)
37. Dafermos, C., Slemrod, M.: Asymptotic behavior of nonlinear contraction semigroups. J. Funct. Anal. 13, 97–106 (1973)
38. Datko, R.: An extension of a theorem of A. M. Lyapunov to semi–groups of operators. J. Math. Anal. Appl. 24(2), 290–295 (1968)
39. Datko, R.: Extending a theorem of A. M. Liapunov to Hilbert space. J. Math. Anal. Appl. 32(3), 610–616 (1970)
40. Desoer, C., Wang, Y.T.: On the Generalized Nyquist Stability Criterion. IEEE Trans. Automat. Control 25(2), 187–196 (1980)
41. Duindam, V., Macchelli, A., Stramigioli, S., Bruyninckx, H. (eds.): Modeling and Control of Complex Physical Systems: The Port–Hamiltonian Approach. Springer, Heidelberg (2009)
42. Dunbar, W., Petit, N., Rouchon, P., Martin, P.: Motion Planning for a nonlinear Stefan Problem. ESAIM Contr. Optim. Ca. 9, 275–296 (2003)
43. Eberard, D., Maschke, B.: An extension of port hamiltonian systems with boundary port variables to irreversible systems: the example of the heat conduction. In: Proc. 6th IFAC Symposium Nonlinear Control Systems (NOLCOS 2004), Stuttgart, Germany (2004)
44. Fattorini, H.: Boundary control of temperature distributions in a parallelepipedon. SIAM J. Control 13(1), 1–13 (1975)

45. Fattorini, H.: Infinite Dimensional Optimization and Control Theory. Encyclopedia of Mathematics and its Applications, vol. 68. Cambridge University Press, Cambridge (1999)
46. Fliess, M., Lévine, J., Martin, P., Rouchon, P.: Flatness and defect of non–linear systems: introductory theory and examples. Int. J. Control 61, 1327–1361 (1995)
47. Fliess, M., Mounier, H., Rouchon, P., Rudolph, J.: A distributed parameter approach to the control of a tubular reactor: a multi–variable case. In: Proc. 37th Conference on Decision and Control, Tampa, FL, USA, pp. 439–442 (1998)
48. Fliess, M., Lévine, J., Martin, P., Rouchon, P.: A Lie-Bäcklund Approach to Equivalence and Flatness of Nonlinear systems. IEEE Trans. Automatic Control 44(5), 922–937 (1999)
49. Foias, C., Sell, G., Titi, E.: Exponential tracking and approximation of inertial manifolds for dissipative nonlinear equations. J. Dyn. Differ. Equ. 1, 199–244 (1989)
50. Frihauf, P., Krstic, M.: Leader–Enabled Deployment Onto Planar Curves: A PDE-Based Approach. IEEE Trans. Automat. Control 56(8), 1791–1806 (2011)
51. Fuller, C., Elliott, S., Nelson, P.: Active Control of Vibration. Academic Press, London (1996)
52. Fursikov, A.: Optimal control of distributed systems. Theory and applications. American Mathematical Society, Providence (1999)
53. Fursikov, A.: Stabilization for the 3D Navier–Stokes system by feedback boundary control. Disc. Cont. Dyn. Sys. A 10(1-2), 289–314 (2004)
54. Gawronski, W.: Dynamics and Control of Structures. Springer, New York (1998)
55. Ge, P., Jouaneh, M.: Tracking Control of a Piezoceramic Actuator. IEEE Trans. Control Sys. Techn. 4(3), 209–215 (1996)
56. Georgakis, C., Aris, R., Amundson, N.: Studies in the control of tubular reactors – I, II, III. Chem. Eng. Sc. 32, 1359–1387 (1977)
57. Goldfarb, M., Celanovic, N.: Modeling piezoelectric stack actuators for control of micromanipulation. IEEE Contr. Sys. Magazine 17(3), 69–79 (1997)
58. Gu, W., Wang, C.: Thermal–Electrochemical Modeling of Battery Systems. J. Electrochem. Soc. 147(8), 2910–2922 (2000)
59. Hagenmeyer, V.: Robust nonlinear tracking control based on differential flatness. Fortschr.–Ber. VDI Reihe 8 Nr. 978. VDI Verlag, Düsseldorf (2003)
60. Hale, J.: Dynamical systems and stability. J. Math. Anal. Appl. 26(1), 39–59 (1969)
61. Helbing, D.: Traffic and related self–driven many-particle systems. Rev. Mod. Phys. 73(4), 1067–1141 (2001)
62. Horowitz, I.: Synthesis of Feedback Systems. Academic Press, New York (1963)
63. Ito, K., Kunisch, K.: Receding horizon optimal control for infinite dimensional systems. ESAIM Contr. Optim. Ca. 8, 741–760 (2002)
64. Ito, K., Kunisch, K.: Reduced order control based on approximate inertial manifolds. Linear Algebra and its Applications 415(2-3), 531–541 (2006)
65. Jakobsen, H.: Chemical Reactor Modeling – Multiphase Reactive Flows. Springer, Heidelberg (2008)
66. King, R., Seibold, M., Lehmann, O., Noack, B., Morzyński, M., Tadmor, G.: Nonlinear Flow Control Based on a Low Dimensional Model of Fluid Flow. In: Meurer, T., et al. (eds.) Control and Observer Design for Nonlinear Finite and Infinite Dimensional Systems. LNCIS, vol. 322, pp. 369–386. Springer, Berlin (2005)
67. Krstic, M., Smyshlyaev, A.: Boundary Control of PDEs: A Course on Backstepping Designs. SIAM, Philadelphia (2008)

68. Krstic, M., Guo, B., Balogh, A., Smyshlyaev, A.: Output–feedback stabilization of an unstable wave equation. Automatica 44(1), 63–74 (2008)
69. Krstic, M., Magnis, L., Vazquez, R.: Nonlinear Stabilization of Shock–Like Unstable Equilibria in the Viscous Burgers PDE. IEEE Trans. Automat. Control 53(7), 1678–1683 (2008)
70. Kudva, J.: Overview of the DARPA Smart Wing Project. J. Intel Mat. Syst. Str. 15(4), 261–267 (2004)
71. Lagnese, J.: Boundary stabilization of thin plates. Studies in applied mathematics. SIAM, Philadelphia (1989)
72. Laroche, B., Martin, P., Rouchon, P.: Motion planning for the heat equation. Int. J. Robust Nonlinear Control 10, 629–643 (2000)
73. Lasiecka, I., Triggiani, R.: Stabilization and structural assignment of Dirichlet boundary feedback parabolic equations. SIAM J. Control Optim. 21(5), 766–803 (1983)
74. Lebeau, G., Robbiano, L.: Contrôle exact de l'équation de la chaleur. Comm. PDE 20(1-2), 335–356 (1995)
75. Lee, T., Wang, F., Newell, R.: Advances in distributed parameter approach to the dynamics and control of activated sludge processes for wastewater treatment. Water Research 40(5), 853–869 (2006)
76. Lenz, K., Özbay, H., Tannenbaum, A., Turi, J., Morton, B.: Frequency Domain Analysis and Robust Control Design for an Ideal Flexible Beam. Automatica 27(6), 947–961 (1991)
77. Lions, J.: Optimal Control of Systems Governed by Partial Differential Equations. Springer, Heidelberg (1971)
78. Littman, W.: A generalization of a theorem of Datko and Pazy. In: Porter, W., Kak, S., Aravena, J. (eds.) Advances in Computing and Control. LNCIS, vol. 130, pp. 318–323. Springer, Heidelberg (1989)
79. Liu, W.: Boundary feedback stabilization of an unstable heat equation. SIAM J. Control Optim. 42(3), 1033–1043 (2003)
80. Liu, Z., Zheng, S.: Semigroups associated with dissipative systems. Chapman&Hall/CRC, Boca Raton, London (1999)
81. Luo, Z., Guo, B., Morgül, O.: Stability and Stabilization of Infinite Dimensional Systems with Applications. Springer, London (1999)
82. Lynch, A., Rudolph, J.: Flatness–based boundary control of a class of quasilinear parabolic distributed parameter systems. Int J. Control 75(15), 1219–1230 (2002)
83. Macchelli, A., Melchiorri, C.: Modeling and Control of the Timoshenko Beam. The Distributed Port Hamiltonian Approach. SIAM J. Control Optim. 43(3), 743–767 (2004)
84. Macchelli, A., Melchiorri, C.: A formal method for improving the transient behaviour of a non–linear flexible link. Math. Comp. Model Dyn. Sys. (MCMDS) 17(1), 3–18 (2011)
85. Martin, P., Murray, R., Rouchon, P.: Flat systems. In: 4th European Control Conference (ECC), Brussels, Belgium. Plenary Lectures and Mini–Courses, pp. 211–264 (1997)
86. Martin, P., Murray, R., Rouchon, P.: Flat Systems: Open Problems, Infinite Dimensional Extension, Symmetries and Catalog. In: Advances in the Control of Nonlinear Systems. LNCIS, vol. 264, pp. 33–57. Springer, Heidelberg (2000)
87. Maschke, B., van der Schaft, A.: From conservation laws to port Hamiltonian formulation of distributed parameter systems. In: 16th IFAC World Congress, Prague (CZ), pp. 483–488 (2005)
88. Meirovitch, L.: Dynamics and Control of Structures. Wiley, New York (1990)

89. Meurer, T.: Feedforward and Feedback Tracking Control of Diffusion–Convection–Reaction Systems using Summability Methods. Fortschr.–Ber. VDI Reihe 8 Nr. 1081. VDI Verlag, Düsseldorf (2005)
90. Meurer, T.: Flatness–based Trajectory Planning for Diffusion–Reaction Systems in a Parallelepipedon — A Spectral Approach. Automatica 47(5), 935–949 (2011)
91. Meurer, T., Krstic, M.: Nonlinear PDE–based motion planning for the formation control of mobile agents. In: Proc (CD–ROM) 8th IFAC Symposium Nonlinear Control Systems (NOLCOS 2010), Bologna (I), pp. 599–604 (2010)
92. Meurer, T., Krstic, M.: Finite–time multi–agent deployment: A nonlinear PDE motion planning approach. Automatica 47(11), 2534–2542 (2011)
93. Meurer, T., Kugi, A.: Tracking control for a diffusion–convection–reaction system: combining flatness and backstepping. In: Proc. 7th IFAC Symposium Nonlinear Control Systems (NOLCOS 2007), Pretoria (SA), pp. 583–588 (2007)
94. Meurer, T., Kugi, A.: Tracking control for boundary controlled parabolic PDEs with varying parameters: combining backstepping and flatness. Automatica 45(5), 1182–1194 (2009)
95. Meurer, T., Kugi, A.: Trajectory planning for boundary controlled parabolic PDEs with varying parameters on higher-dimensional spatial domains. IEEE T. Automat. Contr. 54(8), 1854–1868 (2009)
96. Meurer, T., Kugi, A.: Tracking control design for a wave equation with dynamic boundary conditions modeling a piezoelectric stack actuator. Int. J. Robust Nonlin. 21(5), 542–562 (2011)
97. Meurer, T., Zeitz, M.: Two-degree-of-freedom tracking control design for boundary controlled distributed parameter systems using formal power series. In: Proc (CD–ROM) IEEE Conference on Decision and Control (CDC), Bahamas, pp. 3307–3312 (2004)
98. Meurer, T., Zeitz, M.: Feedforward and feedback tracking control of nonlinear diffusion–convection–reaction systems using summability methods. Ind. Eng. Chem. Res. 44, 2532–2548 (2005)
99. Meurer, T., Zeitz, M.: Model inversion of boundary controlled parabolic partial differential equations using summability methods. Math. Comp. Model Dyn. Sys. (MCMDS) 14(3), 213–230 (2008)
100. Meurer, T., Thull, D., Kugi, A.: Flatness–based tracking control of a piezoactuated Euler–Bernoulli beam with non–collocated output feedback: theory and experiments. Int. J. Contr. 81(3), 475–493 (2008)
101. Morris, K., Vidyasagar, M.: A Comparison of Different Models for Beam Vibrations From the Standpoint of Control Design. J. Dyn. Meas. Contr. 112, 349–356 (1990)
102. van Nieuwstadt, M., Rathinam, M., Murray, R.: Differential Flatness and Absolute Equivalence of Nonlinear Control Systems. SIAM J. Control Optim. 36(4), 1225–1239 (1998)
103. Niezrecki, C., Brei, D., Balakrishnan, S., Moskalik, A.: Piezoelectric Actuation: State of the Art. The Shock and Vibration Digest. 33(4), 269–280 (2001)
104. Pazy, A.: On the applicability of Lyapunov's theorem in Hilbert spaces. SIAM J. Math. Anal. 3(2), 291–294 (1972)
105. Pazy, A.: Semigroups of Linear Operators and Applications to Partial Differential Equations. Springer, New York (1992)
106. Petit, N., Rouchon, P.: Flatness of Heavy Chain Systems. SIAM J. Control Optim. 40(2), 475–495 (2001)

107. Petit, N., Rouchon, P.: Dynamics and Solutions to some Control Problems for Water-tank Systems. IEEE Trans. Automatic Control 47(4), 594–609 (2002)
108. Petit, N., Rouchon, P., Boueilh, J.M., Guérin, F., Pinvidic, P.: Control of an industrial polymerization reactor using flatness. J. Proc. Contr. 12(5), 659–665 (2002)
109. Preumont, A.: Vibration Control of Active Structures, 2nd edn. Kluwer Academic, Dordrecht (2002)
110. Pritchard, A., Zabczyk, J.: Stability and Stabilizability of Infinite Dimensional Systems. SIAM Review 23(1), 25–52 (1981)
111. Ray, W.: Advanced Process Control. McGraw-Hill, New York (1981)
112. Raymond, J.: Feedback boundary stabilization of the three–dimensional incompressible Navier–Stokes equations. J Math. Pures. Appl. 87(6), 627–669 (2007)
113. Rebarber, R.: Spectral assignability for distributed parameter systems with unbounded scalar control. SIAM J. Control Optim. 27(1), 148–169 (1989)
114. Roddier, F. (ed.): Adaptive Optics in Astronomy. Cambridge University Press, Cambridge (1999)
115. Rothfuß, R., Rudolph, J., Zeitz, M.: Flatness–based control of a nonlinear chemical reactor model. Automatica 32, 1433–1439 (1996)
116. Rouchon, P.: Motion planning, equivalence, and infinite dimensional systems. Int. J. Appl. Math. Comp. Sc. 11, 165–188 (2001)
117. Rouchon, P.: Flatness based trajectory generation of quantum systems. In: Proc. 6th IFAC Symposium Nonlinear Control Systems (NOLCOS 2004), Stuttgart (D), pp. 183–188 (2004)
118. Rouchon, P.: Flatness–based control of oscillators. Z Angew. Math. Mech. 85(6), 411–421 (2005)
119. Rudolph, J.: Beiträge zur flachheitsbasierten Folgeregelung linearer und nichtlinearer Systeme endlicher und unendlicher Dimension. Berichte aus der Steuerungs– und Regelungstechnik. Shaker–Verlag, Aachen (2003)
120. Rudolph, J.: Flatness Based Control of Distributed Parameter Systems. Berichte aus der Steuerungs– und Regelungstechnik. Shaker–Verlag, Aachen (2003)
121. Rudolph, J., Winkler, J., Woittennek, F.: Flatness Based Approach to a Heat Conduction Problem in a Crystal Growth Process. In: Meurer, T., et al. (eds.) Control and Observer Design for Nonlinear Finite and Infinite Dimensional Systems. LNCIS, vol. 322, pp. 387–401. Springer, Berlin (2005)
122. Russell, D.: A Unified Boundary Controllability Theory for Hyperbolic and Parabolic Partial Differential Equations. Studies Appl. Math. 52, 189–211 (1973)
123. Salamon, D.: Infinite Dimensional Linear Systems With Unbounded Control and Observation: A Functional Analytic Approach. Trans. Am. Math. Soc. 300(2), 383–431 (1987)
124. van der Schaft, A., Maschke, B.: Hamiltonian representation of distributed parameter systems with boundary energy flow. J. Geom. Phys. 42, 166–194 (2002)
125. van der Schaft, A., Maschke, B., Ortega, R.: Network Modelling of Physical Systems: A Geometric Approach. In: Banos, A., Lamnabhi-Lagarrigue, F., Montoya, F. (eds.) Advances in the Control of Nonlinear Systems, vol. 264, pp. 253–276. Springer, London (2001)
126. Schlacher, K.: Mathematical modeling for nonlinear control: a Hamiltonian approach. Math. Comput. Simulat. 79(4), 829–849 (2008)
127. Schröck, J.: Mathematical Modeling and Tracking Control of Piezo–actuated Flexible Structures. PhD thesis, Automation and Control Institute, Vienna University of Technology (2011)

128. Schröck, J., Meurer, T., Kugi, A.: Motion planning for a flexible beam structure with macro–fiber composite actuators. In: Proc (CD–ROM) European Control Conference (ECC), Budapest (H), pp. 2193–2198 (2009)
129. Schröck, J., Meurer, T., Kugi, A.: Non–collocated Feedback Stabilization of a Non–Uniform Euler–Bernoulli Beam with In–Domain Actuation. In: Proc. IEEE Conference on Decision and Control (CDC), Orlando (FL), USA, pp. 2776–2781 (2011)
130. Shaw, J.: Mathematical Principles of Optical Fiber Communications. SIAM, Philadelphia (2004)
131. Singler, J., Batten, B.: A proper orthogonal decomposition approach to approximate balanced truncation of infinite dimensional linear systems. Int. J. Comput. Math. 86, 355–371 (2009)
132. Sira-Ramirez, H., Agrawal, S.: Differentially Flat Systems. Marcel Dekker Inc., New York (2004)
133. Slemrod, M.: The linear stabilization problem in Hilbert space. J. Funct. Anal. 11(3), 334–345 (1972)
134. Smyshlyaev, A., Krstic, M.: Closed–Form Boundary State Feedbacks for a Class of 1–D Partial Integro–Differential Equations. IEEE Trans. Automat. Control 49(12), 2185–2202 (2004)
135. Smyshlyaev, A., Krstic, M.: Backstepping observers for a class of parabolic PDEs. Systems & Control Letters 54, 613–625 (2005)
136. Smyshlyaev, A., Krstic, M.: On control design for PDEs with space–dependent diffusivity or time–dependent reactivity. Automatica 41, 1601–1608 (2005)
137. Smyshlyaev, A., Guo, B.Z., Krstic, M.: Arbitrary decay rate for Euler–Bernoulli beam by backstepping boundary feedback. IEEE Trans. Autom. Control 54(5), 1134–1141 (2009)
138. Smyshlyaev, A., Cerpa, E., Krstic, M.: Boundary stabilization of a 1–D wave equation with in–domain anti–damping. SIAM J. Control Optim. 48(6), 4014–4031 (2010)
139. Stanewsky, E.: Adaptive wing and flow control technology. Prog. Aerosp. Sci. 37, 583–667 (2001)
140. Sundmacher, K., Kienle, A. (eds.): Reactive Distillation – Status and Future Directions. Wiley–VCH, Weinheim (2002)
141. Sundmacher, K., Kienle, A., Pesch, H., Berndt, J., Huppmann, G. (eds.): Molten Carbonate Fuel Cells: Modeling, Analysis, Simulation, and Control. Wiley–VCH Verlag GmbH, Weinheim (2007)
142. Taylor, T.: Physics of advanced tokamaks. Plasma Physics and Controlled Fusion 39(12B), B47 (1997)
143. Triggiani, R.: On the Stabilizability Problem in Banach Spaces. J. Math. Anal. Appl. 52, 383–403 (1975)
144. Tröltzsch, F.: Optimale Steuerung partieller Differentialgleichungen. Vieweg, Wiesbaden (2005)
145. Tucsnak, M., Weiss, G.: Observation and Control for Operator Semigroups. Birkhäuser, Basel (2009)
146. Unger, A., Tröltzsch, F.: Fast Solution of Optimal Control Problems in the Selective Cooling of Steel. Z Angew. Math. Mech. 81(7), 447–456 (2001)
147. Utz, T., Meurer, T., Kugi, A.: Motion planning for parabolic distributed–parameter systems based on finite–difference semi–discretizations. Int. J. Contr. 83(6), 1093–1106 (2010)

148. Vazquez, R., Krstic, M.: Control of 1-D parabolic PDEs with Volterra nonlinearities – Part I: Design. Automatica 44, 2778–2790 (2008)
149. Vazquez, R., Krstic, M.: Control of 1-D parabolic PDEs with Volterra nonlinearities – Part II: Analysis. Automatica 44, 2791–2803 (2008)
150. Villegas, J., Zwart, H., Gorrec, Y.L., Maschke, B.: Exponential Stability of a Class of Boundary Control Systems. IEEE Trans. Automat. Control 54(1), 142–147 (2009)
151. Wagner, M., Meurer, T., Kugi, A.: Feedforward control design for the inviscid Burger equation using formal power series and summation methods. In: Proc (CD–ROM) 17th IFAC World Congress, Seoul (KR), pp. 8743–8748 (2008)
152. Whitham, G.: Linear and Nonlinear Waves. John Wiley & Sons, New York (1999)
153. Woittennek, F.: Beiträge zum Steuerungsentwurf für lineare, örtlich verteilte Systeme mit konzentrierten Stelleingriffen. Berichte aus der Steuerungs– und Regelungstechnik. Shaker–Verlag, Aachen (2007)
154. Xu, C., Sallet, G.: On Spectrum and Riesz Basis Assignment of Infinite–Dimensional Linear Systems by Bounded Linear Feedbacks. SIAM J. Control Optim. 34(2), 521–541 (1996)
155. Yousefi-Koma, A., Zimcik, D.: Applications of Smart Structures to Aircraft for Performance Enhancement. Canadian Aeronautics and Space Journal 49(4), 163–173 (2003)
156. Zimmert, N., Pertsch, A., Sawodny, O.: 2–DOF Control of a Fire–Rescue Turntable Ladder. IEEE Trans. Control Sys. Tech. 20(2), 438–452 (2012)

Chapter 2
Model Equations for Non–Convective and Convective Heat Transfer

In the following, the fundamental balance equations are derived for non–convective and convective heat transfer. For this, thermodynamic principles are applied by considering a suitable control volume, which is either fixed in space or moving within a fluid. With this, selected application examples and the related control problems are introduced and briefly discussed towards their analysis in subsequent chapters.

2.1 Non–Convective Heat Transfer

In the following, the equations governing the evolution of the temperature field $x(z,t)$ in a heat conducting body are determined by making use of the first law of thermodynamics for a closed system, i.e. a coherent region of volume Ω from the conductive body (cf. Figure 2.1). With the internal energy $E(t)$ this yields

$$\partial_t E(t) = \dot{Q}(t) + P(t), \tag{2.1}$$

where $\dot{Q}(t)$ denotes the heat flow and $P(t)$ the (electrical or mechanical) power crossing the surface $\partial\Omega$ of Ω [3]. Assuming a solid body, the change in the material density $\rho(z,t)$ due to temperature and pressure variations can be neglected such that $\rho(z,t) = \rho$. With $E(t) = \int_\Omega \rho e(z,t)\mathrm{d}\Omega$ and the caloric equation of state $\mathrm{d}e(z,t) = c(x(z,t))\mathrm{d}x(z,t)$ with the specific heat capacity $c(x(z,t))$, this yields

$$\partial_t E(t) = \rho \int_\Omega c(x(z,t))\partial_t x(z,t)\mathrm{d}\Omega = \dot{Q}(t) + P(t) \tag{2.2}$$

For the determination of $\dot{Q}(t)$ consider a surface element $\mathrm{d}\partial\Omega$ with outer normal vector $\mathfrak{n}$ as shown in Figure 2.1. With the sign convention that the flow is positive if it enters the volume, the heat flow rate follows as

$$\mathrm{d}\dot{Q}(z,t) = -\dot{\boldsymbol{q}}(z,t)\cdot\mathfrak{n}\,\mathrm{d}\partial\Omega \tag{2.3}$$

T. Meurer: Control of Higher-Dimensional PDEs, CCE, pp. 23–35.
springerlink.com

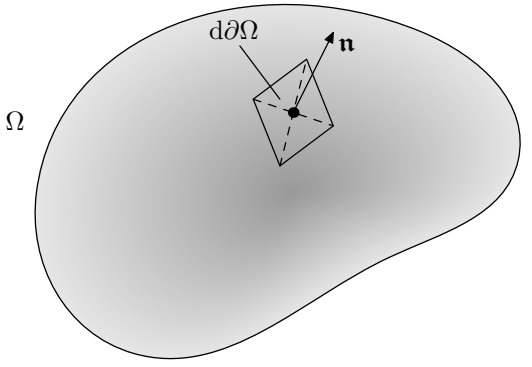

Fig. 2.1 Material volume Ω of the conducting body with surface element $\mathrm{d}\partial\Omega$ and outer normal vector $\mathfrak{n}$

with the vector field of the heat flux $\dot{\boldsymbol{q}}(z,t)$. The integration of the heat flow rate over the surface $\partial\Omega$ yields the total heat flow

$$\dot{Q}(t) = -\int_{\partial\Omega} \dot{\boldsymbol{q}}(z,t)\cdot\mathfrak{n}\,\mathrm{d}\partial\Omega = -\int_{\Omega} \nabla\cdot\dot{\boldsymbol{q}}(z,t)\mathrm{d}\Omega. \tag{2.4}$$

The latter equation thereby follows from the divergence theorem.

In order to determine $P(t)$ observe that $P(t)$ in general consists of two contributions, namely the power caused by a change of volume and the power $P_D(t)$ dissipated inside the volume Ω. While the first contribution equals zero for an incompressible body the dissipative part can be made up of, e.g., the ohmic resistance of a heat and electricity conduction material or the energy rich radiation absorbed by the body. To cover these dissipative and hence irreversible energy conversions a so–called power density $\dot{W}(x(z,t),u_\Omega(z,t),z,t)$ with $u_\Omega(z,t)$ denoting an external quantity is introduced such that

$$P(t) = P_D(t) = \int_{\Omega} \dot{W}(x(z,t),u_\Omega(z,t),z,t)\mathrm{d}\Omega. \tag{2.5}$$

Obviously, the dissipative energy conversions act like heat sources thus increasing the internal energy of the body. Note that a similar effect is obtained whenever (exothermic) chemical or nuclear reactions take place inside the body. However, it is in many situations possible to neglect the change in the chemical composition of the body and hence the material properties and to cover the reactive contributions by means of the power density.

As a result, substituting (2.4) and (2.5) into (2.2) yields

$$\int_{\Omega} \big(\rho c(x(z,t))\partial_t x(z,t) + \nabla\cdot\dot{\boldsymbol{q}}(z,t) - \dot{W}(x(z,t),u_\Omega(z,t),z,t)\big)\mathrm{d}\Omega = 0.$$

Since this expression has to hold for any material volume Ω equality can be only achieved if

$$\rho c(x(z,t))\partial_t x(z,t) = -\nabla \cdot \dot{\boldsymbol{q}}(z,t) + \dot{W}(x(z,t), u_\Omega(z,t), z, t).$$

By making use of Fourier's law, the heat flux can be determined as

$$\dot{\boldsymbol{q}}(z,t) = -\lambda(x(z,t))\nabla x(z,t) \tag{2.6}$$

with the in general temperature–dependent thermal conductivity $\lambda(x(z,t))$. Hence, the evolution of the temperature field $x(z,t)$ is obtained in terms of the PDE

$$\begin{aligned}\rho c(x(z,t))\partial_t x(z,t) = \nabla \cdot \big(\lambda(x(z,t))\nabla x(z,t)\big) \\ + \dot{W}(x(z,t), u_\Omega(z,t), z, t).\end{aligned} \tag{2.7}$$

In the special case of an anisotropic material such as certain crystals or laminated materials using Einstein's summation convention (cf. Appendix A.1) it follows that

$$\dot{q}^i(z,t) = -\lambda^{ij}(x(z,t))\partial_{z^j} x(z,t), \tag{2.8}$$

which yields the heat equation according to

$$\begin{aligned}\rho c(x(z,t))\partial_t x(z,t) = \partial_{z^i}\big(\lambda^{ij}(x(z,t))\partial_{z^j} x(z,t)\big) \\ + \dot{W}(x(z,t), u_\Omega(z,t), z, t).\end{aligned} \tag{2.9}$$

In order to completely establish the temperature field, the PDE has to be complemented by boundary conditions and an initial condition. For this, three types of boundary conditions on $(z,t) \in \partial\Omega \times \mathbb{R}^+$ are distinguished in general, see, e.g., [3]:

(i) The temperature is given as a function of time and surface position, i.e.

$$x(z,t) = u_{\partial\Omega}(z,t). \tag{2.10}$$

This is called a boundary condition of first type or a Dirichlet condition.

(ii) The heat flux normal to the surface is prescribed as a function of time and surface position with

$$\begin{aligned}\dot{\boldsymbol{q}}(z,t)\cdot\mathfrak{n} &= -\lambda(x(z,t))\nabla x(z,t)\cdot\mathfrak{n} \\ &= -\lambda(x(z,t))\partial_{\mathfrak{n}} x(z,t) = u_{\partial\Omega}(z,t).\end{aligned} \tag{2.11}$$

This boundary condition of second type is also called a Neumann condition.

(iii) If the body of temperature $x(z,t)$ is in contact with another medium of temperature $u_{\partial\Omega}(z,t)$, energy is exchanged along the boundary. Here, it is necessary to further distinguish between the firm or loose contact of conducting solid bodies or the contact with a fluid. In the first case, assuming a firm contact

between two bodies, it is obvious that both the temperatures as well as the normal heat flux at the interface must coincide, i.e.

$$\begin{aligned} x(z,t) &= u_{\partial\Omega}(z,t) \\ -\lambda(x(z,t))\partial_{\mathbf{n}} x(z,t) &= -\lambda(u_{\partial\Omega}(z,t))\partial_{\mathbf{n}} u_{\partial\Omega}(z,t). \end{aligned} \tag{2.12}$$

If the contact is loose, an additional resistance occurs, which results in a temperature jump along the interface. The resistance is thereby described in terms of the heat transfer coefficient α_{cs} such that

$$-\lambda(x(z,t))\partial_{\mathbf{n}} x(z,t) = \alpha_{cs}\big(x(z,t) - u_{\partial\Omega}(z,t)\big). \tag{2.13}$$

On the other hand, if the conducting body of temperature $x(z,t)$ is in contact with a fluid of temperature $u_{\partial\Omega}(z,t)$ a boundary layer develops along the interface. With α denoting the heat transfer coefficient, a balance of energy along the boundary yields

$$-\lambda(x(z,t))\partial_{\mathbf{n}} x(z,t) = \alpha\big(x(z,t) - u_{\partial\Omega}(z,t)\big). \tag{2.14}$$

In mathematical terms boundary conditions of the form (2.13) and (2.14) are called mixed or Robin boundary conditions. Note that if α is large (2.14) can be approximately reduced to the Dirichlet condition

$$x(z,t) = u_{\partial\Omega}(z,t).$$

Moreover, it should be pointed out that α could be a function of $x(z,t)$ and $u_{\partial\Omega}(z,t)$ rendering the boundary condition nonlinear. A typical example is thereby given by free convection along the boundary surface. Similarly, nonlinear boundary conditions are obtained in the case of radiative heat transfer, see, e.g., [3] for further details.

For further considerations as well as analytical and numerical solution methods for the equations governing non–convective heat conduction, the reader is referred to, e.g., [7, 5, 3] and the references therein.

2.2 Convective Heat Transfer in Single Phase Flow

With the exception of, e.g., heat conduction in solids, typically convective effects have to be taken into account for the modeling of heat transfer problems. In order to address this, subsequently, the equations governing convective heat transfer are briefly derived and illustrated in selective application examples and related control problems. Subsequently, let $\mathbb{M} \subset \mathbb{R}^3$ be a space (or a Riemannian manifold) filled with a fluid, which is itself in motion. For the derivation of the balance equations governing the state of the fluid Reynold's transport theorem is used following [2, 3]. In order to introduce this kinematical principle, consider the deformation of a closed

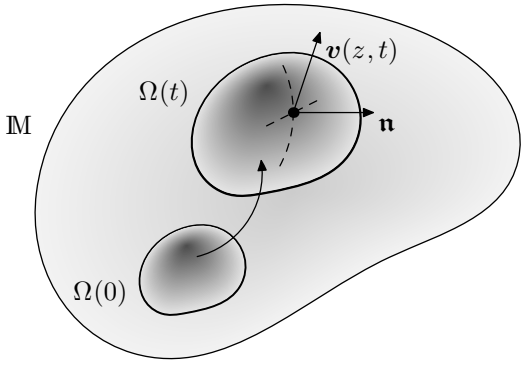

Fig. 2.2 Deformation of a closed volume $\Omega(0)$ moving with the flow into $\Omega(t)$ at time t. Here, $\mathbf{n}$ and $\boldsymbol{v}(z,t)$ denote the normal vector and the velocity at a point on the boundary of $\Omega(t)$.

material volume $\Omega(t)$ with surface $\partial\Omega(t)$ moving with the fluid, i.e. consisting of the same fluid particles during the motion. The unit normal to the surface is denoted by $\mathbf{n}$ and the surface velocity is given by $\boldsymbol{v}(z,t)$ (cf. Figure 2.2). Let $f(z,t)$ be any function of the spatial coordinates z and time t. Then Reynold's transport theorem states that the rate of change of the volume integral $F(t) = \int_{\Omega(t)} f(z,t)\mathrm{d}\Omega$ is the volume integral of the rate of change at a point plus the net flow of $f(z,t)$ over the volume's surface [2], i.e.

$$\mathrm{d}_t F(t) = \int_{\Omega(t)} \partial_t f(z,t)\mathrm{d}\Omega + \int_{\partial\Omega(t)} f(z,t)\boldsymbol{v}(z,t)\cdot\mathbf{n}\mathrm{d}\partial\Omega \tag{2.15a}$$

$$= \int_{\Omega(t)} \big(\partial_t f(z,t) + \nabla\cdot(\boldsymbol{v}(z,t)f(z,t))\big)\mathrm{d}\Omega, \tag{2.15b}$$

where the second equality follows from the divergence theorem. Herein, the integrand can be re–written as

$$\begin{aligned}
&\partial_t f(z,t) + \nabla\cdot(\boldsymbol{v}(z,t)f(z,t)) \\
&= \underbrace{\partial_t f(z,t) + \boldsymbol{v}(z,t)\cdot\nabla f(z,t)}_{=\mathrm{D}_t f(z,t)} + f(z,t)\nabla\cdot\boldsymbol{v}(z,t) \\
&= \mathrm{D}_t f(z,t) + f(z,t)\nabla\cdot\boldsymbol{v}(z,t)
\end{aligned}$$

in terms of the so–called material derivative D_t, i.e. the rate of change observed when moving with the particle, while ∂_t represents the rate of change at a fixed point.

By replacing the function $f(z,t)$ with the density $\rho(z,t)$ times an intensive quantity such as the specific internal energy, the specific enthalpy, or the specific entropy, Reynold's transport theorem yields the rate of change of the respective extensive quantity $F(t)$, e.g., the internal energy, enthalpy, or entropy. This fact is exploited

subsequently to determine the differential and the respective integral formulation of the energy balance for a single phase pure substance and to outline the necessary modifications towards the consideration of a reactive multi–component mixture.

From Reynold's transport theorem, the mass balance for a pure substance yields

$$\mathrm{d}_t m = \mathrm{d}_t \int_{\Omega(t)} \rho(z,t)\mathrm{d}\Omega = \int_{\Omega(t)} \big(\partial_t \rho(z,t) + \nabla\cdot(\boldsymbol{v}(z,t)\rho(z,t))\big)\mathrm{d}\Omega = 0$$

since the mass m is constant for any control volume $\Omega(t)$ (Lagrangian description). With this, the continuity equation follows as

$$\partial_t \rho(z,t) + \nabla\cdot(\boldsymbol{v}(z,t)\rho(z,t)) = 0. \tag{2.16}$$

By considering the first law of thermodynamics, i.e. (2.1) for the non–convective case, the change of the internal energy $E(t)$ is determined by

$$\mathrm{d}_t E(t) = \dot{Q}(t) + P(t).$$

With $E(t) = \int_{\Omega(t)} \rho(z,t)e(z,t)\mathrm{d}\Omega$ and the specific inner energy $e(z,t)$ the application of (2.15a) implies

$$\begin{aligned}\mathrm{d}_t E(t) &= \int_{\Omega(t)} \big(\partial_t(\rho(z,t)e(z,t)) + \nabla\cdot(\boldsymbol{v}(z,t)\rho(z,t)e(z,t))\big)\mathrm{d}\Omega \\ &= \dot{Q}(t) + P(t),\end{aligned}$$

which in view of (2.16) reduces to

$$\int_{\Omega(t)} \rho(z,t)\mathrm{D}_t e(z,t)\mathrm{d}\Omega = \dot{Q}(t) + P(t). \tag{2.17}$$

The heat $\dot{Q}(t)$ entering the control volume over its surface $\partial\Omega(t)$ is governed by (2.4) but with the domain of integration replaced by $\Omega(t)$, i.e.

$$\dot{Q}(t) = -\int_{\partial\Omega(t)} \dot{\boldsymbol{q}}(z,t)\cdot\mathfrak{n}\,\mathrm{d}\partial\Omega = -\int_{\Omega(t)} \nabla\cdot\dot{\boldsymbol{q}}(z,t)\mathrm{d}\Omega. \tag{2.18}$$

The total power $P_{tot}(t)$ generated from the surface forces, which is exchanged with the control volume, comprises the so–called drag $P_S(t)$, i.e. the part contributing only to the potential and kinetic energies, and the part $P(t)$ contributing to the internal energy. Their determination relies on continuum mechanical considerations describing the state of the fluid. Hence, following, e.g., [3], the total power is obtained[1] as

$$P_{tot}(t) = \int_{\partial\Omega(t)} v^i(z,t)\delta_{ij}(\boldsymbol{\sigma}(z,t)\cdot\mathfrak{n})^j\mathrm{d}\partial\Omega$$

[1] Note that the Einstein summation convention (cf. Appendix A.1) is used subsequently with δ_{ij} denoting the Kronecker delta function.

$$= \int_{\Omega(t)} \partial_{z^k} \left(v^i(z,t) \delta_{ij} \sigma^{kj}(z,t) \right) \mathrm{d}\Omega,$$

where $\boldsymbol{\sigma}(z,t)$ is the Cauchy stress tensor, $\boldsymbol{\sigma}(z,t) \cdot \mathfrak{n}$ is the Cauchy traction vector, and $(\boldsymbol{\sigma}(z,t) \cdot \mathfrak{n})^j = \sigma^{kj}(z,t) \delta_{kl} \mathfrak{n}^l$ [1, p. 505f]. Moreover, the drag can be determined by restricting the analysis to those forces only resulting in the dilatation of the control volume such that

$$P_S(t) = \int_{\Omega(t)} \partial_{z^k} \sigma^{kj}(z,t) \delta_{ji} v^i(z,t) \mathrm{d}\Omega.$$

By considering the difference $P_{tot}(t) - P_S(t)$ the fraction $P(t)$ is obtained, which contributes to the internal energy, i.e.

$$P(t) = \int_{\Omega(t)} \partial_{z^k} v^i(z,t) \delta_{ij} \sigma^{kj}(z,t) \mathrm{d}\Omega. \tag{2.19}$$

With this, (2.17) can be evaluated to obtain the differential form of the energy balance

$$\rho(z,t) \mathrm{D}_t e(z,t) = -\partial_{z^k} \dot{q}^k(z,t) + \partial_{z^k} v^i(z,t) \delta_{ij} \sigma^{kj}(z,t). \tag{2.20}$$

By taking into account the caloric equations of state different formulations of the energy equation can be obtained, where in particular the description in terms of the temperature field is subsequently considered in further detail.

Remark 2.1. To provide a complete description of the governing equations for a pure substance, it is in addition to the continuity equation (2.16) and the energy balance (2.20) necessary to introduce the Navier–Stokes equation

$$\rho(z,t) \mathrm{D}_t v^i(z,t) = \rho(z,t) k^i(z,t) + \partial_{z^j} \sigma^{ij}(z,t) \tag{2.21}$$

with the body forces $k^i(z,t)$, $i = 1,2,3$, such as gravity, to express the evolution of the velocity field [2, 1, 3]. Thereby, a constitutive equation relating stress and strain and hence stress and velocity is required to obtain a closed–form expression. However, for the sake of simplicity, these facts are neglected in the following by assuming a known velocity field $\boldsymbol{v}(z,t)$ in order to focus solely on the convective heat transfer.

It is well–known in thermodynamics that the specific enthalpy $h(z,t)$ and the specific inner energy $e(z,t)$ are related by $h(z,t) = e(z,t) + p(z,t)\nu(z,t)$ with the pressure $p(z,t)$ and the specific volume $\nu(z,t) = 1/\rho(z,t)$. This yields for the material derivative of $e(z,t)$ after some intermediate computations involving the continuity equation (2.16) that

$$\rho(z,t) \mathrm{D}_t e(z,t) = \rho(z,t) \mathrm{D}_t h(z,t) - \mathrm{D}_t p(z,t) - p(z,t) \nabla \cdot \boldsymbol{v}(z,t).$$

Hence, (2.17) can be re–formulated in terms of the specific enthalpy according to

$$\rho(z,t)\mathrm{D}_t h(z,t) = -\partial_{z^k}\dot{q}^k(z,t) + \partial_{z^k}v^i(z,t)\delta_{ij}\sigma^{kj}(z,t) + \mathrm{D}_t p(z,t) + p(z,t)\nabla\cdot\boldsymbol{v}(z,t).$$

Moreover, specific enthalpy $h(z,t)$ and temperature $x(z,t)$ are related by

$$\mathrm{d}h(z,t) = c_p(z,t)\mathrm{d}x(z,t) - \left[\vartheta(\partial_x\nu)_p - \nu(z,t)\right]\mathrm{d}p(z,t)$$

with the thermodynamic temperature ϑ and $(\partial_x\nu)_p$ referring to the derivative of the specific volume $\nu(z,t)$ with respect to the temperature $x(z,t)$ for constant pressure [15]. In the general case of anisotropic heat conduction making use of Fourier's law (2.8) results in

$$\begin{aligned}\rho(z,t)c_p(z,t)\mathrm{D}_t x(z,t) &= \partial_{z^k}\left(\lambda^{kj}(x(z,t))\partial_{z^j}x(z,t)\right)\\ &+ \partial_{z^k}v^i(z,t)\delta_{ij}\sigma^{kj}(z,t) + \frac{\vartheta(\partial_x\nu)_p}{\nu(z,t)}\mathrm{D}_t p(z,t) + p(z,t)\nabla\cdot\boldsymbol{v}(z,t).\end{aligned} \tag{2.22}$$

Note that similar to the previous section, the thermal energy balance can be complemented by dissipative contributions summarized in terms of the power density $\dot{W}(x(z,t),u_\Omega(z,t),z,t)$ with $u_\Omega(z,t)$ an external quantity. With this, (2.22) reads as

$$\begin{aligned}\rho(z,t)c_p(z,t)\mathrm{D}_t x(z,t) &= \partial_{z^k}\left(\lambda^{kj}(x(z,t))\partial_{z^j}x(z,t)\right)\\ &+ \partial_{z^k}v^i(z,t)\delta_{ij}\sigma^{kj}(z,t) + \frac{\vartheta(\partial_x\nu)_p}{\nu(z,t)}\mathrm{D}_t p(z,t) + p(z,t)\nabla\cdot\boldsymbol{v}(z,t)\\ &+ \dot{W}(x(z,t),u_\Omega(z,t),z,t).\end{aligned} \tag{2.23}$$

Based on this temperature form of the energy equation, certain simplifications of (2.23) can be introduced depending on the properties of the fluid:

(i) For incompressible fluids with $\nabla\cdot\boldsymbol{v}(z,t) = 0$ and hence $\mathrm{D}_t\rho(z,t) = 0$, the term $p(z,t)\nabla\cdot\boldsymbol{v}(z,t)$ is dropped.
(ii) If the flow is isobaric, then $\mathrm{D}_t p(z,t) = 0$.
(iii) Given an ideal gas with $p\nu = R\vartheta$, then $\vartheta(\partial_x\nu)_p/\nu = \vartheta(\partial_\vartheta\nu)_p/\nu = 1$ can be directly deduced [3].

In addition, boundary and initial conditions have to be specified to completely establish the evolution of the temperature field. For this, similar to the previous section, three types of boundary conditions are distinguished in general such that (2.10)–(2.14) can be transferred to the considered configuration.

Remark 2.2 (Extensions to multi–component reactive mixtures). In order to address chemical reactions in N–component mixtures several modifications have to be taken into account. In addition to the overall continuity equation (2.16), this includes $N-1$ component continuity equations, where reaction rates have to be considered and the individual flow velocities of each component in the mixture have to be introduced for the application of Reynold's transport theorem. The energy balance has to be modified in terms of the reaction heat generated from the specific enthalpies and the

diffusive fluxes. Moreover, it is necessary to balance entropy. For a detailed treatise, the reader is, e.g., referred to [14, 2, 3, 12] and the references therein.

2.3 Selected Applications and Control Problems

Based on the previously derived equations governing non–convective and convective heat transfer a broad variety of control problems arising in different physical domains can be identified from the standpoint of feedback stabilization. However, various applications require to analyze the trajectory planning or tracking control problem, respectively, or rely on an accurate real–time estimation of the evolving states from the available measurement data. In order to motivate the analysis and the examples considered in the subsequent sections selected applications are briefly outlined below. Simulation results, which cover directly related problems for diffusion–convection–reaction systems on 3–dimensional geometries are subsequently presented in Sections 6.5.3, 7.5, 9.8.1.

2.3.1 Thermal Battery Management

The problem of energy storage poses challenging control problems. This, e.g., comprises the thermal management of Li–Ion, Li–polymer, and related battery concepts. Thereby, the proper battery operation is essential to achieve optimal performance. Here, self–acceleration effects of exothermic side reactions have to be taken into account, which eventually lead to thermal runaway [9, 10, 11]. As a result, the high uniformity of the spatial–temporal temperature distribution inside a battery cell or the battery stack constitutes a thermal requirement for battery operation.

The thermal battery model can be considered either thermally and electrochemically coupled or decoupled depending on the treatment of the heat generation term. As pointed out, e.g., in [11] the heat generation rate depends not only on the cell temperature but also on the charging or discharging state. Thus a coupled model has to include the full coverage of the electrochemical processes within the cell. Decoupled models on the other hand employ empirical relations, which describe the heat generation rate in terms of temperature and experimentally determined discharge and/or charge curves.

Following [8], a Li–ion battery is divided into three portions namely the core consisting of individual cells connected in parallel, the case, and the contact layer between core and case, which is typically filled with liquid electrolyte. Moreover, the liquid electrolyte in general shows only limited mobility such that convective effects can be neglected[2] together with radiative effects inside the opaque battery

[2] The incorporation of convection requires to analyze the energy balance in the form (2.23) with the velocity field being either imposed from empirical or measurement data or by a detailed modeling of the interior flow conditions [11].

core. Hence, heat conduction is the major mode of energy transfer inside the battery such that the spatial–temporal temperature evolution in the battery can be derived from (2.7) according to

$$\rho c(z)\partial_t x(z,t) = \sum_{i=1}^{3} \partial_{z^i}\big(\lambda^i(z)\partial_{z^i} x(z,t)\big) + \dot{W}(x(z,t), u_\Omega(z,t), z, t). \quad (2.24a)$$

Herein, it is sufficient to consider only spatially varying heat capacity and thermal conductivity. As pointed out above, the determination of the power density $\dot{W}(x(z,t), u_\Omega(z,t), z, t)$ — also called heat generation rate in the context of thermal battery modeling — either relies on a suitable coupling with the electrochemistry or empirical relations. In order to simplify the analysis typically the ansatz suggested by [4] is used to express the heat generation rate, i.e.

$$\dot{W}(x(z,t), u_\Omega(z,t), z, t) = \frac{I}{V_{tot}}\big[R_{oc}(x(z,t)) - R(t) - x(z,t)\partial_x R_{oc}(x(z,t))\big], \quad (2.24b)$$

where I, V_{tot}, $R_{oc}(x(z,t))$, and $R(t)$ denote the total current of the battery, the total volume of the core region, the open circuit potential, and the working voltage, respectively [8]. If no electrochemical model is employed, then the potentials in (2.24b) have to be determined from measurement data. Note that typically R_{oc} and $\partial_x R_{oc}(x(z,t))$ are considered as constants (ignoring the abuse of notation) and $R(t)$ is determined from experimental data depending on the charge or discharge state of the battery by making use of the Shepherd equation [9]. The remaining parameters have to be evaluated depending on the geometric and material properties of the individual cells as well as their connection (for details, the reader is referred to, e.g., [8]). In general, it should be pointed out that the spatial variation of $c(z)$ and $\lambda^i(z)$, $i = 1, 2, 3$ is neglected. Finally boundary conditions have to be taken into account to model the energy exchange at the boundary. Here, the physical conditions imply Robin boundary conditions, i.e.

$$-\lambda(z)\partial_{\mathbf{n}} x(z,t) = \alpha(z)\big(x(z,t) - u_{\partial\Omega}(z,t)\big). \quad (2.24c)$$

In general, the heat transfer coefficient $\alpha(z)$ is a function of $x(z,t)$ and $u_{\partial\Omega}(z,t)$ for $z \in \partial\Omega$, which renders the problem nonlinear [8].

The PDE–formulation above on the one hand enables to perform numerical simulations to study the thermal dynamics of the battery under different charging and discharging conditions. On the other hand, it allows to address control and state estimation tasks to deduce the interior temperature profile by means of model–based observer techniques for monitoring purposes and to realize modern state feedback control strategies, e.g., to prevent thermal runaway. Moreover, trajectory planning and tracking control problems arise during the charging phase.

2.3.2 Building Climate Control

Increasing the energy efficiency of buildings is closely tied to the incorporation of suitable automation techniques. While a detailed analysis and modeling of a whole building is immensely complex due to its inherent multi–physics and multi–scale characteristics, the consideration of individual subsystems provides an initial demonstration and evaluation test bench. For this, sensor and actuator placement for optimal climate control inside a room are considered, e.g., in [6]. Here, convective heat transfer governed by (2.23) is analyzed together with the Navier–Stokes equations (2.21) to model the temperature and flow field evolution due to a controlled inflow of air through suitably placed vents along the room's boundary. The control task thereby concerns the determination of a feedback strategy to control the room temperature near a workplace and minimize energy.

Assuming for the sake of simplicity an incompressible fluid such that $\nabla \cdot \boldsymbol{v}(z,t) = 0$ with a known velocity field $\boldsymbol{v}(z,t)$, then the problem reduces to the analysis of (2.23). Following [6], in this case the analysis can be restricted to

$$\partial_t x(z,t) + \boldsymbol{v}(z,t) \cdot \nabla x(z,t) = \frac{\lambda}{\rho c_p} \Delta x(z,t), \qquad (z,t) \in \Omega \times \mathbb{R}^+, \tag{2.25a}$$

where $\Omega = (0, L_1) \times (0, L_2) \times (0, L_3)$. The respective boundary conditions can be, e.g., chosen of Robin type, i.e.

$$-\lambda \partial_{\mathbf{n}} x(z,t) = \begin{cases} \alpha\big(x(z,t) - x^o(z,t)\big), & z \in \partial\Omega_0 \\ \alpha\big(x(z,t) - u_{\partial\Omega}(z,t)\big), & z \in \partial\Omega_1 \end{cases} \tag{2.25b}$$

with $\partial\Omega = \partial\Omega_0 \cup \partial\Omega_1$, $x^o(z,t)$ denoting the temperature of the exterior, and $u_{\partial\Omega}(z,t)$ representing the control input. As outlined above, the control task concerns the design of $u_{\partial\Omega}(z,t)$ such that the weighted averaged temperature over a subdomain $\Omega_c \subset \Omega$ of the room

$$y(t) = \int_{\Omega_c} c(z) x(z,t) \mathrm{d}\Omega_c \tag{2.25c}$$

or more general $y(z,t) = x(z,t)|_{z \in \Omega_c}$ follows a prescribed path $y^*(t)$ or $y^*(z,t)$, respectively. On the other hand, the reconstruction of the temperature evolution from the available data obtained from suitably placed sensors inside or along the boundary of the domain Ω poses a challenging observation problem in view of the distributed–parameter system characteristics.

2.3.3 Medical Applications

Besides energy storage and building climate control, trajectory planning and tracking control problems for heat transfer or similarly diffusion problems can be identified, e.g., in the operation of decontamination rigs [16] or medical applications such as hyperthermia [13]. Here, it is desired to plan and to track the spatial–temporal evolution of desired global and regional temperature profiles by means of suitable control strategies. While the arising control problems are essentially distributed in space and time, the presented control designs typically rely on the early lumping approach by making use of approximation techniques to reduce the governing PDEs to a low–dimensional set of ordinary differential equations (ODEs). Hence, by incorporating directly the distributed–parameter system character of the process significant improvements can be expected.

References

1. Abraham, R., Marsden, J., Ratiu, T.: Manifolds, Tensor Analysis, and Applications, Applied Mathematical Sciences, 2nd edn., vol. 75. Springer, New York (1993)
2. Aris, R.: Vectors, Tensors, and the Basic Equations of Fluid Mechanics. Dover Publications Inc., New York (1989)
3. Baehr, H., Stephan, K.: Heat and Mass Transfer, 2nd edn. Springer, Berlin (2006)
4. Bernardi, D., Pawlikowski, E., Newman, J.: A General Energy Balance for Battery Systems. J. Electrochem. Soc. 132(1), 5–12 (1985)
5. Bird, R., Stewart, W., Lightfoot, E.: Transport Phenomena. John Wiley & Sons, Inc., New York (2002)
6. Borggaard, J., Burns, J., Surana, A., Zietsman, L.: Control, Estimation and Optimization of Energy Efficient Buildings. In: Proc. American Control Conference, St. Louis (MO), USA, pp. 837–841 (2009)
7. Carslaw, H., Jaeger, J.: Conduction of Heat in Solids, 2nd edn. Oxford University Press, Oxford (1959)
8. Chen, S., Wan, C., Wang, Y.: Thermal analysis of lithium–ion batteries. J. Power Sources 140, 111–124 (2005)
9. Chen, Y., Evans, J.: Three-Dimensional Thermal Modeling of Lithium-Polymer Batteries under Galvanostatic Discharge and Dynamic Power Profile. J. Electrochem. Soc. 141(11), 2947–2955 (1994)
10. Chen, Y., Evans, J.: Thermal analysis of lithium-ion batteries. J. Electrochem. Soc. 143(9), 2708–2712 (1996)
11. Gu, W., Wang, C.: Thermal–Electrochemical Modeling of Battery Systems. J. Electrochem. Soc. 147(8), 2910–2922 (2000)
12. Jakobsen, H.: Chemical Reactor Modeling – Multiphase Reactive Flows. Springer, Heidelberg (2008)
13. Mattingly, M., Roemer, R., Devasia, S.: Exact temperature tracking for hyperthermia: a model–based approach. IEEE Trans. Control Syst. Technol. 8(6), 979–992 (2000)

14. Merk, H.: The macroscopic equations for simultaneous heat and mass transfer in isotropic, continuous, and closed systems. App. Sci. Res. A 8, 73–99 (1959)
15. Stephan, P., Schaber, K., Stephan, K., Mayinger, F.: Thermodynamik Band 1: Einstoffsysteme, 18th edn. Springer, Heidelberg (2009)
16. Ulloa, R., Rouaud, O., Havet, M., Boillereaux, L.: Observer–based tracking control of superficial temperature. Journal of Food Engineering 76(1), 70–78 (2006)

Chapter 3
Model Equations for Multi–Agent Networks

In the past decades, extensive research has been conducted on the cooperative control of multi–agent systems with possible applications ranging from UAVs and sensor networks over transportation systems to micro–satellite clusters (see, e.g., [19] for a rather recent overview). Thereby, different analysis and design approaches have emerged depending on the available communication topology and the considered formation control task.

In the behavior–based approach a desired set of behaviors is assigned to the individual agents and the overall behavior of the system is achieved by defining the relative importance between the individual behaviors [3]. The virtual structure approach relies on the consideration of the entire formation as a single (rigid) entity and the desired state is assigned to the rigid structure [22]. Alternatively, constraint functions relating the positions and orientations of the individual agents can be defined [27]. The potential field approach is based on the introduction of structural interaction forces between neighboring agents to stabilize the system to the equilibrium manifold [20]. Moreover, optimization–based approaches are analyzed to minimize the individual and cumulative error [7, 19]. In general, an additional distinction arises between leaderless and leader–follower systems. In the latter either a real or a virtual agent is chosen as the leader, whose state follows a desired trajectory. The follower agents track the state of the leader while maintaining their overall formation. Thereby in general feedback interconnection strategies are analyzed, which either rely on global or local information corresponding to a centralized or decentralized control scheme to achieve the agent synchronization, e.g., the realize the deployment into prescribed formations. For a general treatise, the reader is also referred to the monographs [23, 5, 16].

Besides the discrete analysis of the interconnected individual agents continuous models based on partial differential equations (PDEs) have been used to model, analyze, and control many particle systems (see, e.g, the review in [11]), large vehicular platoons [4], and traffic flow [1, 11]. In view of the analysis of multi–agent systems, [8] introduce a semi–discrete continuous–time partial difference equation (PdE) framework over graphs, where the spatial discretization corresponds to the individual agent. It is thereby shown that the graph Laplacian control proposed in [21]

T. Meurer: Control of Higher-Dimensional PDEs, CCE, pp. 37–49.
springerlink.com

coincides with the linear heat equation. In order to incorporate certain parameter uncertainties for multi–agent systems modeled by PdEs adaptive control approaches are proposed [14]. A wave–like PDE model in the limit as the number of vehicles in a platoon moving in a straight line tends to infinity is proposed in [4]. With this, the stability margin of large vehicular platoons under bidirectional decentralized control was analyzed and improved by introducing a forward–backward asymmetry in the control gains. Linear diffusion–advection–reaction equations with dynamic boundary conditions were studied in [9, 10] for the leader–follower formation control into deployment profiles governed by the respective (unstable) equilibrium profiles. For this, PDE–backstepping [15] was applied to exponentially stabilize the equilibrium profiles. Results on flatness–based motion planning using nonlinear Burgers–type equations can be found in [17, 18].

3.1 Distributed–Parameter Modeling of Networks of Mobile Agents

The following treatise provides a brief introduction to the modeling of distributed agent networks by making use of distributed–parameter systems theory. For this, the main focus is on time–invariant communication topologies preserving interconnection between neighboring agents[1]. Thereby, leader–follower configurations are considered with the trajectories of the leader agents serving as the manipulated variables. The collective leader–follower agent dynamics is hence introduced in terms of time varying PDEs governing the individual agent states. This set–up enables a solution of consensus, synchronization as well as formation control and deployment problems along desired paths independent of the actual communication topology. It is shown that the discretization of the PDE model directly induces a decentralized communication and interconnection structure for the multi–agent system, which is required to achieve the desired spatial–temporal behavior.

3.1.1 Agent Models — Discrete and Continuous Formulations

In general, graph theory is used to model the communication network between the agents. Hence, let $\mathtt{G} = \mathtt{G}(\mathtt{N}, \mathtt{E})$ be an undirected graph defined by a non–empty set $\mathtt{N}$ of nodes (also called vertex set) and a set $\mathtt{E} \subset \mathtt{N} \times \mathtt{N}$ of edges. Herein, each node represents an agent. Two nodes $\mathtt{n}_i$ and $\mathtt{n}_j$ are neighbors abbreviated by $\mathtt{n}_i \sim \mathtt{n}_j$ if $(\mathtt{n}_i, \mathtt{n}_j) \in \mathtt{E}$, which means that $\mathtt{n}_i$ and $\mathtt{n}_j$ share information about their state. Two nodes $\mathtt{n}_i$ and $\mathtt{n}_j$ are connected by a path if there exists a sequence $\{\mathtt{n}_{i_0}, \mathtt{n}_{i_1}, \ldots, \mathtt{n}_{i_n}\}$

[1] Alternative descriptions relying on switched topologies, where neighboring agents are defined, e.g., as those within a circle of specified radius around an agent trace back to [26] and are analyzed in a control context, e.g., in [12].

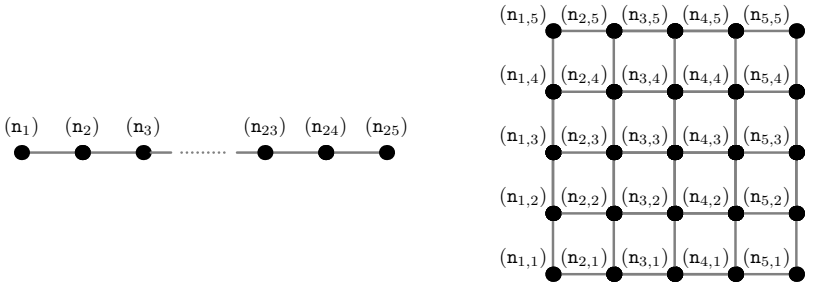

(a) Chain–like graph. (b) Mesh–like graph.

Fig. 3.1 Examples of graphs with the agents represented by the dots • and the communication paths (undirected) shown in light gray

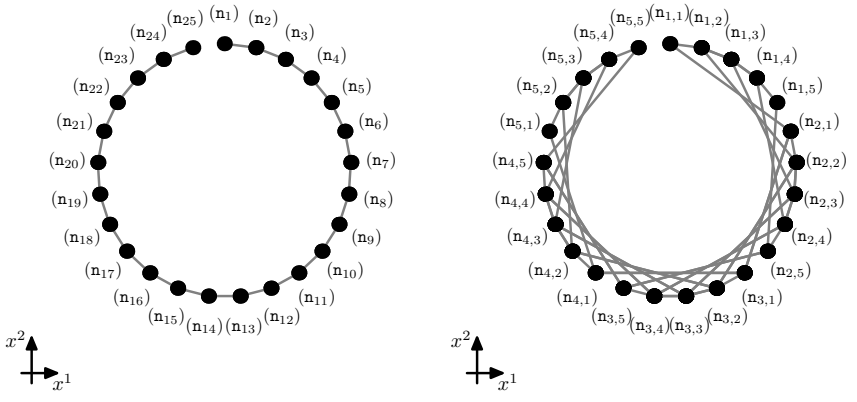

(a) Chain–like communication graph. (b) Mesh–like communication graph.

Fig. 3.2 Examples of mobile agent formations with the agents represented by the dots • and the communication connections according to Figure 3.1 shown in light gray

for some finite n such that $\mathtt{n}_i = \mathtt{n}_{i_0}$, $\mathtt{n}_j = \mathtt{n}_{i_n}$, and $\mathtt{n}_{i_k} \sim \mathtt{n}_{i_{k+1}}$ for each $k \in \{0, 1, \ldots, n\}$. The graph $\mathtt{G}$ is called connected when each pair of nodes is connected by a path and is called complete if $\mathtt{E} = \mathtt{N} \times \mathtt{N}$. In order to introduce the leader–follower concept it is necessary to consider a non–empty connected subgraph $\mathtt{S}$ of $\mathtt{G}$. The boundary of $\mathtt{S}$ is defined according to $\partial\mathtt{S} := \{\mathtt{n} \in \mathtt{G} \setminus \mathtt{S} : \exists\, \mathtt{m} \in \mathtt{S} \text{ s.t. } \mathtt{m} \sim \mathtt{n}\}$. Let $\mathtt{S}_f$ and $\mathtt{S}_l$ be two subgraphs of $\mathtt{G}$ and assume that $\mathtt{S}_l = \partial\mathtt{S}_f$ together with $\mathtt{S}_f \cup \mathtt{S}_l = \mathtt{G}$. Here, the subscripts f and l refer to follower and leader agents.

3.1.1.1 Discrete Formulation

Based on these preliminary notions, PdEs and graph Laplacian control are used to motivate the continuous reformulation in terms of PDEs. Under the assumption of a

time–invariant communication topology, let $\boldsymbol{x}(\mathtt{n},t) \in (L^2([0,\tau];L^2(\mathtt{S}_f)))^n$ denote the state of agent $\mathtt{n}$ at time $t > 0$ [13]. Taking into account the simple integrator dynamics

$$\partial_t \boldsymbol{x}(\mathtt{n},t) = \boldsymbol{v}(\mathtt{n},t) \tag{3.1}$$

the choice $\boldsymbol{v}(\mathtt{n},t) = \Delta\boldsymbol{x}(\mathtt{n},t)$ is the (graph) Laplacian control, where $\Delta\boldsymbol{x}(\mathtt{n},t) := \sum_{\mathtt{m}\in\mathtt{N},\,\mathtt{m}\sim\mathtt{n}}(\boldsymbol{x}(\mathtt{m},t) - \boldsymbol{x}(\mathtt{n},t))$. By denoting the trajectories of the leader agents by $\boldsymbol{u}(\mathtt{n},t)$ the collective motion of the agents follows as

$$\partial_t \boldsymbol{x}(\mathtt{n},t) = \Delta\boldsymbol{x}(\mathtt{n},t) = \sum_{\mathtt{m}\in\mathtt{N},\,\mathtt{m}\sim\mathtt{n}} (\boldsymbol{x}(\mathtt{m},t) - \boldsymbol{x}(\mathtt{n},t)), \qquad \mathtt{n}\in\mathtt{S}_f \tag{3.2a}$$

$$\boldsymbol{x}(\mathtt{n},t) = \boldsymbol{u}(\mathtt{n},t), \qquad \mathtt{n}\in\mathtt{S}_l \tag{3.2b}$$

with the initial condition $\boldsymbol{x}(\mathtt{n},0) = \boldsymbol{x}_0(\mathtt{n}) \in (L^2(\mathtt{S}_f))^n$. Obviously, (3.2) is a continuous time PdE with non–homogeneousDirichlet boundary conditions governed by the leader agents. This formulation enables to analyze certain rendezvous and containment problems (see, e.g. [8, 13] and the references therein).

It is obvious that different control strategies can be applied to analyze the integrator dynamics (3.1). In particular, feedback of diffusion–reaction type, i.e. $\boldsymbol{v}(\mathtt{n},t) = \Delta\boldsymbol{x}(\mathtt{n},t) + c(\mathtt{n},t)\boldsymbol{x}(\mathtt{n},t)$, yields

$$\begin{aligned} \partial_t \boldsymbol{x}(\mathtt{n},t) &= \Delta\boldsymbol{x}(\mathtt{n},t) + c(\mathtt{n},t)\boldsymbol{x}(\mathtt{n},t), && \mathtt{n}\in\mathtt{S}_f \\ \boldsymbol{x}(\mathtt{n},t) &= \boldsymbol{u}(\mathtt{n},t), && \mathtt{n}\in\mathtt{S}_l. \end{aligned}$$

Moreover, nonlinear dynamics can be assigned by a suitable selection of $\boldsymbol{v}(\mathtt{n},t)$ [18]. Nevertheless, each of these feedback control strategies and thus the resulting communication topology requires a careful analysis to be able to deduce the dynamical properties related to consensus, synchronization, rendezvous, containment, or deployment formations. For this, the remaining degrees–of–freedom in terms of the leader agents can be suitably exploited to impose a prescribed collective dynamics of the agent network.

Assuming that $\mathtt{G}$ is given by the simple chained graph shown in Figure 3.1(a), the evaluation of (3.2) yields

$$\begin{aligned} \partial_t \boldsymbol{x}(\mathtt{n}_i,t) &= \boldsymbol{x}(\mathtt{n}_{i+1},t) - 2\boldsymbol{x}(\mathtt{n}_i,t) + \boldsymbol{x}(\mathtt{n}_{i-1},t), && \forall \mathtt{n}_i \in \mathtt{S}_f \\ \partial_t \boldsymbol{x}(\mathtt{n}_1,t) &= \boldsymbol{x}(\mathtt{n}_2,t) - \boldsymbol{x}(\mathtt{n}_1,t), && \text{if } \mathtt{n}_1 \in \mathtt{S}_f \\ \partial_t \boldsymbol{x}(\mathtt{n}_{25},t) &= \boldsymbol{x}(\mathtt{n}_{24},t) - \boldsymbol{x}(\mathtt{n}_{25},t), && \text{if } \mathtt{n}_{25} \in \mathtt{S}_f \\ \boldsymbol{x}(\mathtt{n}_j,t) &= \boldsymbol{u}(\mathtt{n}_j,t), && \forall \mathtt{n}_j \in \mathtt{S}_l. \end{aligned}$$

These expressions directly illustrate the formal relationship with the linear heat equation on the line since the right–hand side of the differential equations can be interpreted as a finite difference discretization of the respective PDE with Neumann boundary conditions and in–domain or Dirichlet boundary control depending on the

subgraph $\mathtt{S}_l$. A similar picture is obtained for the meshed graph of Figure 3.1(b), where (3.2) implies

$$
\begin{aligned}
\partial_t \boldsymbol{x}(\mathtt{n}_{i,j},t) &= \boldsymbol{x}(\mathtt{n}_{i+1,j},t) - 2\boldsymbol{x}(\mathtt{n}_{i,j},t) + \boldsymbol{x}(\mathtt{n}_{i-1,j},t) \\
&\quad + \boldsymbol{x}(\mathtt{n}_{i,j+1},t) - 2\boldsymbol{x}(\mathtt{n}_{i,j},t) + \boldsymbol{x}(\mathtt{n}_{i,j-1},t), \qquad \forall \mathtt{n}_{i,j} \in \mathtt{S}_f \\
\partial_t \boldsymbol{x}(\mathtt{n}_{1,j},t) &= \boldsymbol{x}(\mathtt{n}_{1,j-1},t) + \boldsymbol{x}(\mathtt{n}_{1,j+1},t) - 3\boldsymbol{x}(\mathtt{n}_{1,j},t) \\
&\quad + \boldsymbol{x}(\mathtt{n}_{2,j},t), \qquad \text{if } \mathtt{n}_{1,j} \in \mathtt{S}_f \\
\partial_t \boldsymbol{x}(\mathtt{n}_{5,j},t) &= \boldsymbol{x}(\mathtt{n}_{5,j-1},t) + \boldsymbol{x}(\mathtt{n}_{5,j+1},t) - 3\boldsymbol{x}(\mathtt{n}_{1,j},t) \\
&\quad + \boldsymbol{x}(\mathtt{n}_{4,j},t), \qquad \text{if } \mathtt{n}_{5,j} \in \mathtt{S}_f \\
\partial_t \boldsymbol{x}(\mathtt{n}_{i,1},t) &= \boldsymbol{x}(\mathtt{n}_{i-1,1},t) + \boldsymbol{x}(\mathtt{n}_{i+1,1},t) - 3\boldsymbol{x}(\mathtt{n}_{i,1},t) \\
&\quad + \boldsymbol{x}(\mathtt{n}_{i,2},t), \qquad \text{if } \mathtt{n}_{i,1} \in \mathtt{S}_f \\
\partial_t \boldsymbol{x}(\mathtt{n}_{i,5},t) &= \boldsymbol{x}(\mathtt{n}_{i-1,5},t) + \boldsymbol{x}(\mathtt{n}_{i+1,5},t) - 3\boldsymbol{x}(\mathtt{n}_{i,5},t) \\
&\quad + \boldsymbol{x}(\mathtt{n}_{i,4},t), \qquad \text{if } \mathtt{n}_{i,5} \in \mathtt{S}_f \\
\partial_t \boldsymbol{x}(\mathtt{n}_{1,1},t) &= \boldsymbol{x}(\mathtt{n}_{1,2},t) - 2\boldsymbol{x}(\mathtt{n}_{1,1},t) + \boldsymbol{x}(\mathtt{n}_{2,1},t), \qquad \text{if } \mathtt{n}_{1,1} \in \mathtt{S}_f \\
\partial_t \boldsymbol{x}(\mathtt{n}_{1,5},t) &= \boldsymbol{x}(\mathtt{n}_{1,4},t) - 2\boldsymbol{x}(\mathtt{n}_{1,5},t) + \boldsymbol{x}(\mathtt{n}_{2,5},t), \qquad \text{if } \mathtt{n}_{1,5} \in \mathtt{S}_f \\
\partial_t \boldsymbol{x}(\mathtt{n}_{5,1},t) &= \boldsymbol{x}(\mathtt{n}_{5,2},t) - 2\boldsymbol{x}(\mathtt{n}_{5,1},t) + \boldsymbol{x}(\mathtt{n}_{4,1},t), \qquad \text{if } \mathtt{n}_{5,1} \in \mathtt{S}_f \\
\partial_t \boldsymbol{x}(\mathtt{n}_{5,5},t) &= \boldsymbol{x}(\mathtt{n}_{5,4},t) - 2\boldsymbol{x}(\mathtt{n}_{5,5},t) + \boldsymbol{x}(\mathtt{n}_{4,5},t), \qquad \text{if } \mathtt{n}_{5,5} \in \mathtt{S}_f \\
\boldsymbol{x}(\mathtt{n}_{i,j},t) &= \boldsymbol{u}(\mathtt{n}_{i,j},t), \qquad \forall \mathtt{n}_{i,j} \in \mathtt{S}_l.
\end{aligned}
$$

Here, the formal correspondence to the finite difference discretization of the linear heat equation with quadratic domain and Neumann boundary conditions as well as in–domain or Dirichlet boundary control in terms of the leader agents according to the subgraph $\mathtt{S}_l$ becomes apparent. Corresponding circular formation examples are shown Figure 3.2 for the motion of mobile agents in the (x^1, x^2)–plane with the communication topologies according to Figure 3.1. Each agent only processes the information exchanged with all of its nearest neighbors in the communication graph.

Moreover, if the number of agents increases, then the previous analysis illustrates that the PdE–description approaches the continuous PDE–formulation. This observation is exploited subsequently, where it is shown that the PDE–setting can be suitably applied for the analysis of multi–agent networks with the communication topology between the individual agents, i.e. the graph $\mathtt{G}$ as well as the subgraphs $\mathtt{S}_f$ and $\mathtt{S}_l$, being imposed by the spatial discretization of the differential operators.

3.1.1.2 Continuous Formulation

Motivated by the results of the previous paragraph consider first the graph in Figure 3.3, which is a generalization of the meshed graph shown in 3.1(b) to the node set $\mathtt{N} = \{\mathtt{n}_{i,j}\}_{i=1,\ldots,N_1,\, j=1,\ldots,N_2}$ with N_1 and N_2 two arbitrary integers. Herein, follower agents, i.e., the subgraph $\mathtt{S}_f$, are marked by black dots while leader agents, i.e., the subgraph $\mathtt{S}_l$, are shown with light gray dots. Moreover, assume that the dynamics of the agents follows (3.1). However, differing from classical graph Laplacian control let

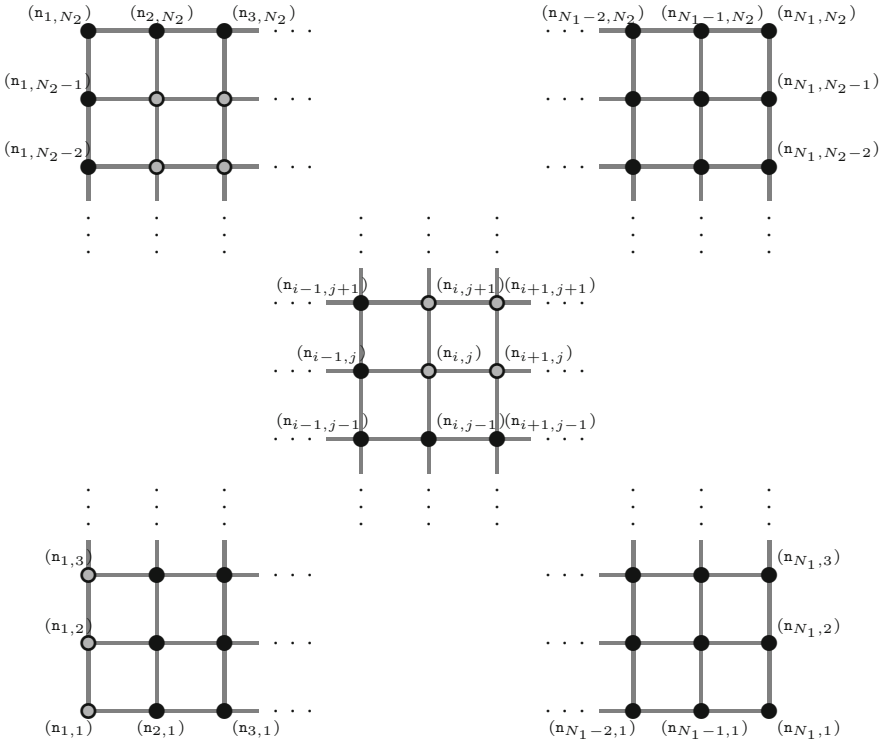

Fig. 3.3 Planar discrete communication configuration with agents $(\mathtt{n}_{i,j})$, $i = 1, \dots, N_1$, $j = 1, \dots, N_2$ represented by the dots. Here, the pairing (i, j) refers to the agent index in the communication graph. Follower agents are represented in black while leader agents are in addition marked with a light gray dot.

$$\boldsymbol{v}(\mathtt{n}_{i,j},t) = \begin{cases} \displaystyle\sum_{\substack{\mathtt{m}_j \in \{(i,j)\}_{i=1,\dots,N_1}, \\ \mathtt{m}_j \sim \mathtt{n}_{i,j}}} \frac{a_{\mathtt{m}_j}}{(\mathrm{d}z^1)^2}\big(\boldsymbol{x}(\mathtt{m}_j,t) - \boldsymbol{x}(\mathtt{n}_{i,j},t)\big) \\ \quad + \displaystyle\sum_{\substack{\mathtt{m}_i \in \{(i,j)\}_{j=1,\dots,N_2}, \\ \mathtt{m}_i \sim \mathtt{n}_{i,j}}} \frac{a_{\mathtt{m}_i}}{(\mathrm{d}z^2)^2}\big(\boldsymbol{x}(\mathtt{m}_i,t) - \boldsymbol{x}(\mathtt{n}_{i,j},t)\big) \\ \quad + c(\mathtt{n}_{i,j},t)\boldsymbol{x}(\mathtt{n}_{i,j},t), & \text{if } \mathtt{n}_{i,j} \in \mathtt{S}_f \\ \boldsymbol{u}(\mathtt{n}_{i,j},t), & \text{if } \mathtt{n}_{i,j} \in \mathtt{S}_l. \end{cases} \tag{3.3}$$

Here, $a_{\mathtt{m}_i}$, $a_{\mathtt{m}_j}$, and $c(\mathtt{n}_{i,j}, t)$ represent variable diffusion and reaction parameters while $\mathrm{d}z^1$ and $\mathrm{d}z^2$ so far denote constants. In view of the graph structure, the evaluation of (3.1) with (3.3) results in

$$\begin{aligned}
&\partial_t \boldsymbol{x}(\mathtt{n}_{i,j},t) = \\
&\quad \frac{a_{\mathtt{m}_j}}{(\mathrm{d}z^1)^2}\big(\boldsymbol{x}(\mathtt{n}_{i+1,j},t) - 2\boldsymbol{x}(\mathtt{n}_{i,j},t) + \boldsymbol{x}(\mathtt{n}_{i-1,j},t)\big) \\
&\quad + \frac{a_{\mathtt{m}_i}}{(\mathrm{d}z^2)^2}\big(\boldsymbol{x}(\mathtt{n}_{i,j+1},t) - 2\boldsymbol{x}(\mathtt{n}_{i,j},t) + \boldsymbol{x}(\mathtt{n}_{i,j-1},t)\big) \\
&\quad + c(\mathtt{n}_{i,j},t)\boldsymbol{x}(\mathtt{n}_{i,j},t), \qquad \forall \mathtt{n}_{i,j} \in \mathtt{S}_f \quad (3.4a)\\
&\boldsymbol{x}(\mathtt{n}_{i,j},t) = \boldsymbol{u}(\mathtt{n}_{i,j},t), \qquad \forall \mathtt{n}_{i,j} \in \mathtt{S}_l. \quad (3.4b)
\end{aligned}$$

By interpreting $\mathrm{d}z^1$ and $\mathrm{d}z^2$ as discretization step–sizes according to $\mathrm{d}z^1 = 1/(N_1 - 1)$ and $\mathrm{d}z^2 = 1/(N_2 - 1)$ the graph $\mathtt{G}$ represents the discretization of a unit square. For the planar graph of Figure 3.3 this imposes that

$$\mathtt{n}_{i,j} \equiv ((i-1)\mathrm{d}z^1, (j-1)\mathrm{d}z^2). \tag{3.5}$$

With this, consider the limit as the number of agents N_1, N_2 approach infinity (and thus $\mathrm{d}z^1,\ \mathrm{d}z^2 \to 0$) such that the discrete agent setting approaches an agent continuum distributed in the plane $\Omega = (0,1)\times(0,1)$ with each $\mathtt{n}_{i,j}$ being uniquely correlated with a point $(z_i^1, z_j^2) \in \Omega$. In view of (3.4) and the arising difference quotients this implies that the state of the agent continuum $\boldsymbol{x}(z,t) = [x^1(z,t),\ldots,x^n(z,t)]^T$ with $z = (z^1, z^2)$ can be re–formulated by means of the PDEs

$$\begin{aligned}
\partial_t x^k(z,t) = a_1(z^1)\partial^2_{z^1} x^k(z,t) + a_2(z^2)\partial^2_{z^2} x^k(z,t) \\
+ c(z,t)x^k(z,t) + u^k(z,t), \qquad k = 1,\ldots,n, \quad (3.6)
\end{aligned}$$

where the input can be, e.g., represented by

$$u^k(z,t) = \sum_{l=1}^{m} \mathfrak{b}^{k,l}(z)u^{l,k}(t). \tag{3.7}$$

in terms of the spatial characteristics $\mathfrak{b}^{k,l}(z)$ imposing the actuation by the leader agents. Obviously, (3.6) is a diffusion–reaction equation with orthotropic thermal conductivity. However, differing from the results of the previous chapter, the independent coordinates z^1 and z^2 correspond to the location in the communication graph while $x^k(z,t)$ describes the agent's state.

3.1.1.3 Distributed–Parameter Agents Models

By generalizing this preliminary analysis, subsequently the evolution of the agent network is described in terms of the diffusion–convection–reaction system

$$\begin{aligned}
\partial_t x^k(z,t) = \sum_{i=1}^{r}\big[a_i(z^i)\partial^2_{z^i} x^k(z,t) + b_i(z^i)\partial_{z^i} x^k(z,t)\big] \\
+ c(z,t)x^k(z,t) + u^k_\Omega(z,t), \qquad k = 1,\ldots,n \quad (3.8a)
\end{aligned}$$

for $(z,t) \in \Omega \times \mathbb{R}^+_{t_0}$, $\Omega = (0,1)^r$, with spatially and time varying parameters and in–domain control $u^k_\Omega(z,t)$, e.g., by imposing the velocity of particular leader agents. Note that besides the decoupled communication configuration in (3.8a) also a coupling between the individual states $x^k(z,t)$, $k = 1,\ldots,n$, can be imposed by introducing diffusion, convection, as well as reaction matrices.

In addition, conditions along the boundary $\partial\Omega$ of the domain Ω have to be assigned. For this, certain subsets along the boundary can be chosen as either leader or follower agents towards the realization of desired formations. This results in

(i) Dirichlet conditions

$$x^k(z,t) = u^k_{\partial\Omega}(z,t), \qquad (z,t) \in \partial\Omega_0 \times \mathbb{R}^+_{t_0}, \tag{3.8b}$$

(ii) Neumann conditions

$$\epsilon^0 \partial_{\mathbf{n}} x^k(z,t) = u^k_{\partial\Omega}(z,t), \qquad (z,t) \in \partial\Omega_1 \times \mathbb{R}^+_{t_0}, \tag{3.8c}$$

(iii) and mixed conditions

$$\epsilon^0 \partial_{\mathbf{n}} x^k(z,t) + p^0 x^k(z,t) = u^k_{\partial\Omega}(z,t), \qquad (z,t) \in \partial\Omega_2 \times \mathbb{R}^+_{t_0} \tag{3.8d}$$

in such a way that $\partial\Omega_1 \cup \partial\Omega_2 \cup \partial\Omega_3 = \partial\Omega$. Herein, it should be pointed out that the input not necessarily has to act on all of the respective boundary but that $u^k_{\partial\Omega}(z,t)$ might be of compact support such that $u^k_{\partial\Omega}(z,t) = 0$ for $z \in \partial\Omega'_i \subseteq \partial\Omega_i$ for $i = 1,2,3$.

Finally, the initial configuration has to be taken into account in terms of the initial state

$$x^k(z,t_0) = x^k_0(z), \qquad z \in \overline{\Omega}. \tag{3.8e}$$

As is shown below and illustrated in the subsequent parts by means of simulation results, the PDE–setting presented above enables a rather generic analysis of the collective dynamics of the agent network, which is in particular independent of the actual communication topology. Starting with (3.8), the latter follows directly by reverting the presented procedure, i.e. from the transfer of the continuous to the discrete description by means of suitable (finite difference) discretizations.

3.1.2 Communication Topology by Discretization

As pointed out above, the realization of this generic continuous formulation in a discrete setting follows directly from the consistent discretization of the governing equations, which imposes the communication topology. Hence, given (3.8), consistent finite difference representations of the arising spatial derivatives can be, e.g.,

found in [25]. Consistency thereby implies that the discretization approaches the continuous formulation in the limit as the discretization stepsize approaches zero.

Hence, let $j = (j_1, \ldots, j_r)$ and $N = (N_1, \ldots, N_r)$ denote multi–indexes (see also Appendix A.2), let $\mathtt{N} = \{\mathtt{n}_j\}_{j_i=1,\ldots,N_i,\, i=1,\ldots,r}$ represent the node set, and let $\mathtt{n}_{(j_i|j_i')}$ express the node $\mathtt{n}_{j_1,\ldots,j_{i-1},j_i',j_{i+1},\ldots,j_r}$. Similar to (3.5), it hence follows that

$$\mathtt{n}_j \equiv ((j_1 - 1)\mathrm{d}z^1, (j_2 - 1)\mathrm{d}z^2, \ldots, (j_r - 1)\mathrm{d}z^r). \tag{3.9}$$

Three–point central differences imply that the spatial derivatives at a node $\mathtt{n}_j$ can be represented according to

$$\partial_{z^i} x^k(\mathtt{n}_j, t) = \frac{x^k(\mathtt{n}_{(j_i|j_i+1)}, t) - x^k(\mathtt{n}_{(j_i|j_i-1)}, t)}{2\mathrm{d}z^i} + \tag{3.10a}$$

$$\partial_{z^i}^2 x^k(\mathtt{n}_j, t) = \frac{x^k(\mathtt{n}_{(j_i|j_i+1)}, t) - 2x^k(\mathtt{n}_j, t) + x^k(\mathtt{n}_{(j_i|j_i-1)}, t)}{(\mathrm{d}z^i)^2} \tag{3.10b}$$

with $\mathrm{d}z^i = 1/(N_i - 1)$ and the approximation error of order $O((\mathrm{d}z^i)^2)$. Similarly higher–order (five–point central difference) approximations can be introduced, i.e.,

$$\begin{aligned}
\partial_{z^i} x^k(\mathtt{n}_j, t) = {} & \frac{1}{12\mathrm{d}z^i}\big[-x^k(\mathtt{n}_{(j_i|j_i+2)}, t) + 8x^k(\mathtt{n}_{(j_i|j_i+1)}, t) \\
& - 8x^k(\mathtt{n}_{(j_i|j_i-1)}, t) + x^k(\mathtt{n}_{(j_i|j_i-2)}, t)\big] + O((\mathrm{d}z^i)^4) \\
\partial_{z^i}^2 x^k(\mathtt{n}_j, t) = {} & \frac{1}{12(\mathrm{d}z^i)^2}\big[-x^k(\mathtt{n}_{(j_i|j_i+2)}, t) + 16x^k(\mathtt{n}_{(j_i|j_i+1)}, t) \\
& - 30x^k(\mathtt{n}_j, t) + 16x^k(\mathtt{n}_{(j_i|j_i-1)}, t) - x^k(\mathtt{n}_{(j_i|j_i-2)}, t)\big] + O((\mathrm{d}z^i)^4).
\end{aligned}$$

While the latter two equations provide an approximation of the continuous description of the order $O((\mathrm{d}z^i)^4)$ for each $i = 1, \ldots, r$, their realization obviously relies on a communication topology differing from the one depicted in Figure 3.3. In particular, both the position information of all nearest neighbors as well as a subset of their nearest neighbors is required. Nevertheless, these observations illustrate the generality of the presented distributed–parameter formulation of the agent dynamics, where the additional degree–of–freedom in terms of the discretization scheme can be appropriately exploited for the implementation of the determined results.

By making use of (3.10), the finite difference discretization of (3.8a) yields

$$\begin{aligned}
\partial_t x^k(\mathtt{n}_j, t) = {} & \sum_{i=1}^{r} \frac{1}{(\mathrm{d}z^i)^2}\left[\left(a_i^{j_i} + \frac{\mathrm{d}z^i b_i^{j_i}}{2}\right) x^k(\mathtt{n}_{(j_i|j_i+1)}, t)\right. \\
& \left. + \left(a_i^{j_i} - \frac{\mathrm{d}z^i b_i^{j_i}}{2}\right) x^k(\mathtt{n}_{(j_i|j_i-1)}, t)\right] + \left(c(\mathtt{n}_j, t) - 2\sum_{i=1}^{r} \frac{a_i^{j_i}}{(\mathrm{d}z^i)^2}\right) x^k(\mathtt{n}_j, t) \\
& + u_\Omega^k(\mathtt{n}_j, t), \qquad k = 1, \ldots, n
\end{aligned} \tag{3.11}$$

with $a_i^{j_i} = a_i((j_i - 1)\mathrm{d}z^i)$ and $b_i^{j_i} = b_i((j_i - 1)\mathrm{d}z^i)$. In case of Dirichlet boundary conditions (3.8b), the system of ODEs (3.11) holds for all $j_i = 2, \ldots, N_i - 1$,

$i = 1, \ldots, r$, with $x^k(\mathtt{n}_j, t) = u^k_{\partial\Omega}(\mathtt{n}_j, t)$ for $j_i = 1$ or $j_i = N_i$, $i = 1, \ldots, r$. For Neumann or mixed boundary conditions according to (3.8c) and (3.8d) additional differential equations arise along the boundary of the domain.

The resulting system of linear and inhomogeneous ODEs represents the communication structure and interconnection protocol of the agent network. The inputs $u^k_\Omega(\mathtt{n}_j, t)$ for the interior nodes and $u^k_{\partial\Omega}(\mathtt{n}_j, t)$ for the boundary nodes $j_i = 1$ or $j_i = N_i$, $i = 1, \ldots, r$, correspond to the trajectories of the leader agents. Their suitable design is required to enable the agent network to realize particular tasks as is outlined below.

3.2 Selected Applications and Control Problems

From the many different interaction protocols for multi–agent systems to realize, for instance, consensus, formations, coverage, flocking, swarming, or distributed estimation subsequently the application of distributed–parameter systems and control theory is presented for a continuum of agents to achieve consensus and deployment into desired formation profiles. These examples thereby provide an initial confirmation that the establishment of a link between graph theory, functional analysis, and modern control techniques for distributed–parameter systems provides promising opportunities for the study of communication networks such as sensor and actuator networks or so–called smart grids within a common framework. Besides, the already available results (see, e.g., [24]) illustrate that this approach might enable to conjecture certain system theoretic properties of the multi–agent network.

3.2.1 Consensus and Stabilization

Consensus refers to the agreement of the multi–agent system to a global state value. In view of interconnected structure, consensus problems arise, e.g., in the synchronization of mobile agent networks [23, 5], complex networks including power networks [2] or the load balancing for distributed memory multiprocessors [6]. In order to motivate the respective control task assume that the state of a multi–agent system is governed by (3.8) in the continuous limit and (3.11) in the discrete setting. Here, $\boldsymbol{x}(z, t)$ could describe the spatial location of a continuum of mobile agents or the number of tasks to be done by a distributed multiprocessor network. The available degrees–of–freedom, i.e., $u^k_\Omega(z, t)$, $z \in \Omega$, and $\boldsymbol{u}^k_{\partial\Omega}(z, t)$, $z \in \partial\Omega$, can be hence utilized to achieve a desired dynamical behavior. For consensus, this implies that the inputs are determined to ensure exponential convergence

$$\|\boldsymbol{x}(z, t) - \boldsymbol{x}_s(z)\|_X \leq Me^{-\alpha t}, \qquad M,\ \alpha > 0$$

or at least asymptotic convergence

$$\|\boldsymbol{x}(z,t) - \boldsymbol{x}_s(z)\|_X \to 0$$

of the state $\boldsymbol{x}(z,t)$ to an equilibrium state $\boldsymbol{x}_s(z)$ starting at an arbitrary initial state $\boldsymbol{x}(z,t_0) = \boldsymbol{x}_0(z)$. Design methods to achieve the feedback stabilization for distributed–parameter systems of the form (3.8) are analyzed in Chapters 8 and 9. Thereby, it is shown that state observer techniques can be integrated to obtain an estimate of the spatial–temporal state evolution from a set of measurements.

3.2.2 Leader–Enabled Formation Deployment

The formation control problem refers to making the agents move to a desired geometric shape. In the following, the realization of finite time transitions between desired formation profiles along prescribed spatial–temporal paths is introduced for a network of mobile agents moving in the plane in a leader–follower configuration. For this, the motion of a network of mobile agents in the (x^1, x^2)–plane is considered with the x^k–dynamics being imposed according to (3.8), i.e.

$$\begin{aligned}\partial_t x^k(z,t) = &\sum_{i=1}^{r}\left[a_i(z^i)\partial^2_{z^i}x^k(z,t) + b_i(z^i)\partial_{z^i}x^k(z,t)\right]\\ &+ c(z,t)x^k(z,t)\end{aligned} \tag{3.12}$$

for $k = 1, 2$ and $(z,t) \in \Omega \times \mathbb{R}^+_{t_0}$. Here, it is assumed that the leader agents are only located at the boundary $\partial\Omega$ of the communication domain $\Omega = (0,1)^r$. The respective boundary conditions are given by (3.8b)–(3.8d) with the input $u^k_{\partial\Omega}(z,t)$, $z \in \partial\Omega$ being of compact support. The deployment formations $(x^1_s(z), x^2_s(z))$ thereby correspond to equilibrium profiles of (3.12) governing the agents motion, i.e.

$$\sum_{i=1}^{r}\left[a_i(z^i)\partial^2_{z^i}x^k_s(z) + b_i(z^i)\partial_{z^i}x^k_s(z)\right] + c(z,t)x_s(z) = 0,\ z \in \Omega \tag{3.13a}$$

with

$$x^k_s(z) = u^k_{\partial\Omega,s}(z), \qquad z \in \partial\Omega_0 \tag{3.13b}$$

$$\epsilon^0\partial_{\mathbf{n}}x^k_s(z) = u^k_{\partial\Omega,s}(z), \qquad z \in \partial\Omega_1 \tag{3.13c}$$

$$\epsilon^0\partial_{\mathbf{n}}x^k_s(z) + p^0x^k_s(z) = u^k_{\partial\Omega,s}(z), \qquad z \in \partial\Omega_2 \tag{3.13d}$$

such that $\partial\Omega = \partial\Omega_1 \cup \partial\Omega_2 \cup \partial\Omega_3$. Solutions to (3.13) require that the parameter $c(z,t)$ is non–analytical, i.e., there exists a $t_s \geq t_0$ such that $c(z,t) = c_s(z)$ for all $t \geq t_s$ with $\partial^l_t c(z,t) = 0$ for $t = t_s$ and all $l \in \mathbb{N}$.

The leader–enabled formation deployment hence relies on the suitable determination of the spatial–temporal leader trajectories $(u^1_{\partial\Omega}(z,t), u^2_{\partial\Omega}(z,t))$, $z \in \partial\Omega$ to achieve finite time transitions between different equilibrium profiles

$$(x^1_{0,s}(z), x^2_{0,s}(z)) \xrightarrow[t\in[t_0,t_0+T]]{(u^1_{\partial\Omega}(z,t),u^2_{\partial\Omega}(z,t))} (x^1_{T,s}(z), x^2_{T,s}(z))$$

along prescribed transition paths $(x^{1,*}(z,t), x^{2,*}(z,t))$. For the solution of this tracking control problem motion planning techniques to achieve the desired transition in open–loop and feedback control strategies to exponentially stabilize the tracking error dynamics are presented in Parts III and IV. This involves the analysis of possible collisions as well as the spatial localization of the individual agents by means of state observers. The realization of the tracking control for a discrete set of mobile agents moreover requires to impose a particular communication and interconnection topology as outlined in Section 3.1.2 in terms of a finite difference discretization of the agent continuum.

References

1. Alvarez, L., Horowitz, R., Li, P.: Traffic flow control in automated highway systems. Control Eng. Practice 7, 1071–1078 (1999)
2. Arenas, A., Diaz-Guilera, A., Kurths, J., Moreno, Y., Zhou, C.: Synchronization in complex networks. Physics Reports 469(3), 93–153 (2008)
3. Balch, T., Arkin, R.: Behavior–Based Formation Control for Multirobot Teams. IEEE Trans. Robotics Automat. 14(6), 926–939 (1998)
4. Barooah, P., Mehta, P., Hespanha, J.: Mistuning–Based Control Design to Improve Closed–Loop Stability Margin of Vehicular Platoons. IEEE Trans. Automat. Control 54(9), 2100–2113 (2009)
5. Bullo, F., Cortés, J., Martínez, S.: Distributed Control of Robotic Networks. Applied Mathematics Series. Princeton University Press (2009)
6. Cybenko, G.: Dynamic Load Balancing for Distributed Memory Multiprocessors. J. Parallel Distr. Com. 7, 279–301 (1989)
7. Dunbar, W., Murray, R.: Distributed Receding Horizon Control for Multi–Vehicle Formation Stabilization. Automatica 42(4), 549–558 (2006)
8. Ferrari-Trecate, G., Buffa, A., Gati, M.: Analysis and Coordination in Multi–Agent Systems Through Partial Difference Equations. IEEE Trans. Automat. Control 51(6), 1058–1063 (2006)
9. Frihauf, P., Krstic, M.: Rapidly convergent leader-enabled multi-agent deployment into planar curves. In: Proc. American Control Conference, St. Louis (MO), USA, pp. 1994–1999 (2009)
10. Frihauf, P., Krstic, M.: Leader–Enabled Deployment Onto Planar Curves: A PDE-Based Approach. IEEE Trans. Automat. Control 56(8), 1791–1806 (2011)
11. Helbing, D.: Traffic and related self–driven many-particle systems. Rev. Mod. Phys. 73(4), 1067–1141 (2001)

12. Jadbabaie, A., Lin, J., Morse, A.: Coordination of groups of mobile autonomous agents using nearest neighbor rules. IEEE Trans. Autom. Control 48(6), 988–1001 (2003)
13. Ji, M., Ferrari-Trecate, G., Egerstedt, M., Buffa, A.: Containment Control in Mobile Networks. IEEE Trans. Autom. Control 53(8), 1972–1975 (2008)
14. Kim, J., Kim, K.D., Natarajan, V., Kelly, S., Bentsman, J.: PdE–based model reference adaptive control of uncertain heterogeneous multiagent networks. Nonlinear Analysis: Hybrid Systems 2, 1152–1167 (2008)
15. Krstic, M., Smyshlyaev, A.: Boundary Control of PDEs: A Course on Backstepping Designs. SIAM, Philadelphia (2008)
16. Mesbahi, M., Egerstedt, M.: Graph Theoretic Methods in Multiagent Networks. Princeton Univeristy Press, Princeton (2010)
17. Meurer, T., Krstic, M.: Nonlinear PDE–based motion planning for the formation control of mobile agents. In: Proc (CD–ROM) 8th IFAC Symposium Nonlinear Control Systems (NOLCOS 2010), Bologna (I), pp. 599–604 (2010)
18. Meurer, T., Krstic, M.: Finite–time multi–agent deployment: A nonlinear PDE motion planning approach. Automatica 47(11), 2534–2542 (2011)
19. Murray, R.: Recent Research in Cooperative Control of Multivehicle Systems. J. Dyn. Meas. Contr. 129, 571–583 (2007)
20. Olfati-Saber, R.: Flocking for Multi–Agent Dynamic Systems: Algortihms and Theory. IEEE Trans. Automat. Control 51(3), 401–420 (2006)
21. Olfati-Saber, R., Murray, R.: Consensus Problems in Networks of Agents With Switching Topology and Time-Delays. IEEE Trans. Automat. Control 49(9), 1520–1533 (2004)
22. Ren, W., Beard, R.: Formation feedback control for multiple spacecraft via virtual structures. IEE Proceedings 151(3), 357–368 (2004)
23. Ren, W., Beard, R.: Distributed Consensus in Multi–vehicle Cooperative Control. Springer, London (2008)
24. Sarlette, A., Sepulchre, R.: A PDE viewpoint on basic properties of coordination algorithms with symmetries. In: Proc. IEEE Conference on Decision and Control (CDC), pp. 5139–5144 (2009)
25. Schwarz, H.: Numerische Mathematik. Teubner-Verlag, Stuttgart (1997)
26. Vicsek, T., Czirók, A., Ben-Jacob, E., Cohen, I., Shochet, O.: Novel Type of Phase Transition in a System of Self-Driven Particles. Phys. Rev. Lett. 75(6), 1226–1229 (1995)
27. Zhang, W., Hu, J.: Optimal multi–agent coordination under tree formation constraints. IEEE Trans. Automat. Control 53(3), 692–705 (2008)

Chapter 4
Model Equations for Flexible Structures with Piezoelectric Actuation

Smart material systems, where active distributed actuators and sensors are bonded or embedded in an elastic structure, occur in a large variety of applications with the purpose of vibration suppression, static or dynamic shape control, or fault detection [2, 11, 18]. Moreover, due to the vast progress in actuator development new application areas emerge such as adaptive optics in telescopes, adaptive wings, or so–called smart skins [24]. Here, it is desired to realize a transiently varying shape of a structure to achieve, e.g., the modulation of optical wave fronts, the reduction of drag, or the improvement of aeroelastic characteristics. Thereby, piezoelectric elements typically serve as actuators by exploiting the indirect piezoelectric effect, which allows to convert electrical voltage into mechanical strain. Due to their spatial extension, the modeling of these systems leads to a distributed–parameter description in terms of partial differential equations.

This is subsequently illustrated for the benchmark example of a flexible thin plate with Lipschitz domain and spatially distributed macro–fiber composite (MFC) actuators. In order to keep this section self–contained, at first some preliminary continuum mechanical results are summarized towards the introduction of Hamilton's principle (see, e.g., [7, 12]), which enables a systematic energy–based derivation of the equations of motion.

Notation. Throughout this section, Einstein's summation convention is used according to Appendix A.1.

4.1 Continuum Mechanical Preliminaries

In the following, the basic notions and concepts of continuum mechanics in the Euclidean space $\mathbb{R}^3$ are introduced, which are essential for the energy–based modeling of smart flexible structures with a particular focus on piezoactuated structures. For a comprehensive (differential geometric) treatment of continuum mechanics, the interested reader is referred to, e.g., [6, 3, 17].

T. Meurer: Control of Higher-Dimensional PDEs, CCE, pp. 51–75.
springerlink.com

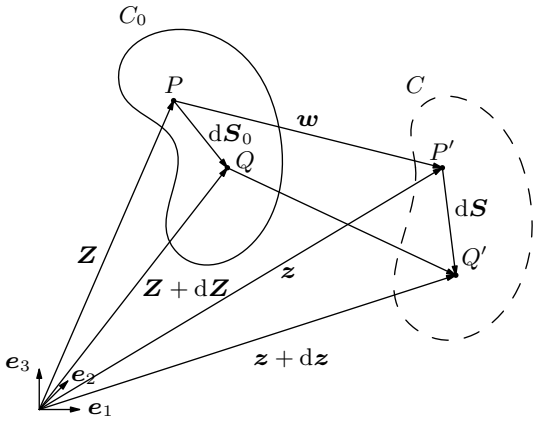

Fig. 4.1 Elastic deformation of a body in Euclidean space $\mathbb{R}^3$

By considering the first law of thermodynamics, i.e. the energy equation, the so–called strain energy density w_s can be introduced according to

$$w_s = \int_0^{\epsilon_{ij}} \sigma^{ij} \mathrm{d}\epsilon_{ij}. \tag{4.1}$$

Here, σ^{ij} and ϵ_{ij} denote the components of the stress and Green's strain tensor, respectively [12]. With this, the strain energy W_s follows immediately from the integration of (4.1) over the volume occupied by the considered deformable body, i.e.

$$W_s = \int_V w_s \mathrm{d}V. \tag{4.2}$$

In order to determine W_s both the strain components ϵ_{ij} and the stress components σ^{ij} have to be determined. For the strain components, kinematic relations between the undeformed and the deformed configuration of a body are utilized while for the stress components the constitutive equations are introduced relating σ^{ij} and ϵ_{kl} depending on the material properties of the body under consideration.

For the description of the motion of a deformable body, a fixed reference frame in $\mathbb{R}^3$ is introduced as illustrated in Figure 4.1. Here, C_0 represents the unstressed state of the body at time $t = t_0$, i.e. the configuration to which the body will return after the removal of the forces causing the elastic deformation, while C represents the deformed state of the body at an arbitrary time $t > t_0$. The motion of a material particle, which was located in the unstressed state at $\boldsymbol{Z} = Z^i \boldsymbol{e}_i$, to the position $\boldsymbol{z} = z^i \boldsymbol{e}_i$ in the deformed body can be expressed by the (invertible) transformation $z^i = z^i(\boldsymbol{Z}, t)$ or $Z^i = Z^i(\boldsymbol{z}, t)$, respectively, with $\boldsymbol{z}(\boldsymbol{Z}, t_0) = \boldsymbol{Z}$. Moreover, the distance between the two (arbitrary) neighboring material points P and Q in the undeformed and the deformed state follows as $\|\mathrm{d}\boldsymbol{S}_0\|^2 = \mathrm{d}Z^i \delta_{ij} \mathrm{d}Z^j$ or $\|\mathrm{d}\boldsymbol{S}\|^2 = \mathrm{d}z^i \delta_{ij} \mathrm{d}z^j$, respectively. With this, the change of distance between P and Q due to the deformation of the body can be determined according to

$$\begin{aligned}\|\mathrm{d}\boldsymbol{S}\|^2 - \|\mathrm{d}\boldsymbol{S}_0\|^2 &= \mathrm{d}z^i\delta_{ij}\mathrm{d}z^j - \mathrm{d}Z^i\delta_{ij}\mathrm{d}Z^j \\ &= \partial_{Z^k} z^i \delta_{ij} \partial_{Z^m} z^j \mathrm{d}Z^k \mathrm{d}Z^m - \mathrm{d}Z^i\delta_{ij}\mathrm{d}Z^j \\ &= \left(\partial_{Z^i} z^k \delta_{km} \partial_{Z^j} z^m - \delta_{ij}\right) \mathrm{d}Z^i \mathrm{d}Z^j,\end{aligned}$$

where equality in the second line follows from the total differential. Herein, $\boldsymbol{F} = \partial_{\boldsymbol{Z}}\boldsymbol{z}$ or $F_l^k = \partial_{Z^l} z^k$ denotes the deformation gradient, which accordingly fulfills $\det \boldsymbol{F} \neq 0$. These computations directly imply the components ϵ_{ij} of the Green strain tensor $\boldsymbol{\epsilon}(\boldsymbol{Z}, t) = (\boldsymbol{F}^T\boldsymbol{F} - \boldsymbol{\delta})/2$ in the form

$$\epsilon_{ij} = \frac{1}{2}\left(\partial_{Z^i} z^k \delta_{km} \partial_{Z^j} z^m - \delta_{ij}\right).$$

Together with the displacement vector $\boldsymbol{w}(\boldsymbol{Z}, t) = \boldsymbol{z}(\boldsymbol{Z}, t) - \boldsymbol{Z}$ the strain can be expressed as

$$\epsilon_{ij} = \frac{1}{2}\left(\partial_{Z^j} w^i + \partial_{Z^i} w^j + \partial_{Z^i} w^k \delta_{km} \partial_{Z^j} w^m\right). \tag{4.3}$$

Herein, the displacement gradient $\boldsymbol{H} = \partial_{\boldsymbol{Z}}\boldsymbol{w}$ with $H_l^k = \partial_{Z^l} w^k$ can be introduced. For small displacements with $|H_l^k| \ll 1$ a geometric linearization can be applied such that (4.3) reduces to

$$e_{ij} = \frac{1}{2}\left(\partial_{Z^j} w^i + \partial_{Z^i} w^j\right). \tag{4.4}$$

As pointed out above, the evaluation of (4.1) and (4.2) requires to introduce a constitutive equation, which relates the components σ^{ij} of the stress tensor[1] $\boldsymbol{\sigma}$ with the components ϵ_{ij} or e_{ij} of the strain tensor $\boldsymbol{\epsilon}$ and hence with the displacement vector $\boldsymbol{w}$. In the linear elastic case under the assumption of small displacements, the generalized Hooke's law yields

$$\sigma^{ij} = c^{ijkl} e_{kl}, \tag{4.5}$$

where the 4–th rank elasticity tensor $\boldsymbol{c}$ with components c^{ijkl} represents the elastic material properties of the deformable body. The material is said to be homogeneous if the 81 components c^{ijkl} are independent of the location within the body. However, observe that due to the symmetry of σ^{ij} and e_{kl} it follows that

$$c^{ijkl} = c^{jikl}, \quad c^{ijkl} = c^{ijlk},$$

which reduces the number of material parameters to 36. In general, the components c^{ijkl} depend on the orientation of the coordinate system. In this case, the material is called anisotropic. However, if three mutually orthogonal planes of elastic symmetry exist the material is called orthotropic. Thereby, the notion elastic symmetry refers

[1] The corresponding stress tensor to the Green strain tensor $\boldsymbol{\epsilon}$ is the so–called Piola–Kirchhoff stress tensor $\boldsymbol{\sigma}$.

to the invariance of the elastic moduli c^{ijkl} at a material point for every pair of coordinate systems that are mirror images to each other in a plane, which is called a plane of elastic symmetry [12]. Given an orthotropic material, the constitutive equation (4.5) can be expressed as

$$\sigma^{ii} = c^{iijj} e_{jj}, \quad \sigma^{ij} = 2c^{ijij} e_{ij} \ (i \neq j). \tag{4.6}$$

Finally, a material is called isotropic if an infinite number of planes of elastic symmetry exist, i.e. the components c^{ijkl} are independent of the orientation of the coordinate system. In this case, the stress–strain relationship is given by

$$\sigma^{ij} = \Big(\mu\big(\delta^{ik}\delta^{jl} + \delta^{il}\delta^{jk}\big) + \lambda\delta^{ij}\delta^{kl}\Big) e_{kl}, \tag{4.7}$$

where μ and λ represent the so–called Lamé constants. These are related to the shear modulus G, the Young modulus E, and the Poisson ratio ν according to

$$\mu = G = \frac{E}{2(1+\nu)}, \quad \lambda = \frac{\nu E}{(1+\nu)(1-2\nu)}.$$

Depending on the considered application, the thermal or the electrical properties of the material can be suitably incorporated into the constitutive equations. In order to illustrate this, subsequently the constitutive equations for a piezoelectric material are introduced following the treatise in [10]. Thereby, nonlinear effects such as hysteresis or creep are neglected. In particular, it follows that

$$\sigma^{ij} = c^{ijkl} e_{kl} - a_k^{ij} D^k \tag{4.8}$$

$$E_i = -a_i^{kl} e_{kl} + \beta_{ik} D^k. \tag{4.9}$$

Similar to (4.5), σ^{ij} and e_{ij} denote the mechanical stress and strain while D^k and E_i represent the electric flux density and electric field strength, a_k^{ij} refers to the tensor of piezoelectric material parameters, and β_{ik} are the components of the dielectricity tensor. The components thereby satisfy the symmetry conditions $a_k^{ij} = a_k^{ji}$ and $\beta_{ik} = \beta_{ki}$. Obviously, according to (4.9) mechanical strain imposes a change in the electric field, which is called the direct piezoelectric effect. On the other hand, with (4.8) a change in the electric flux density results in a mechanical deformation. This is commonly referred to as the indirect piezoelectric effect.

Remark 4.1. An alternative formulation of the constitutive equations for piezoelectric material is given by

$$e_{ij} = s_{ijkl}\sigma^{kl} + d_{ij}^k E_k \tag{4.10}$$

$$D^i = d_{kl}^i \sigma^{kl} + p^{ik} E_k. \tag{4.11}$$

in terms of the tensor of elastic compliances s_{ijkl} with $s_{ijkl} = s_{jikl} = s_{ijlk} = s_{klij}$, the tensor d_{ij}^k with $d_{ij}^k = d_{ji}^k$ describing the piezoelectric effect, and the dielectric permittivity tensor p^{kl} satisfying $p^{kl} = p^{lk}$. Considering as an example the

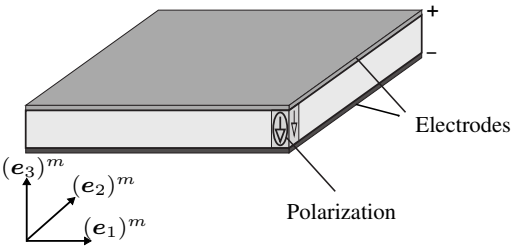

Fig. 4.2 Schematics of a piezoelectric patch actuator in the material coordinate system $(\boldsymbol{e}_i)^m$

commonly used piezoelectric material PZT–5A, with its orthorhombic crystal structure, the tensor $\boldsymbol{d}$ in Voigt–Kelvin notation is expressed as

$$\boldsymbol{d} = \begin{bmatrix} 0 & 0 & d_{11}^3 \\ 0 & 0 & d_{22}^3 \\ 0 & 0 & d_{33}^3 \\ 0 & d_{23}^2 & 0 \\ d_{13}^1 & 0 & 0 \\ 0 & 0 & 0 \end{bmatrix}.$$

Consider Figure 4.2, where $(\boldsymbol{e}_k)^m$, $k = 1, 2, 3$, denotes the unit vectors in the material–fixed coordinate system. In view of the presented configuration with material polarization in $(\boldsymbol{e}_3)^m$–direction and correspondingly electrodes on top and bottom, it is reasonable to assume that $E_1 = E_2 = 0$ and $E_3 \neq 0$. In other words, the main electric field component is directed in the $(\boldsymbol{e}_3)^m$–direction. Moreover, it is reasonable to neglect the stress and strain components perpendicular to the plane spanned by $(\boldsymbol{e}^1)^m$ and $(\boldsymbol{e}^2)^m$. Hence, (4.10) implies that the strength of the piezoelectric effect depends only on d_{11}^3 and d_{22}^3. For transversely isotropic piezoelectric material this is also referred to as the d_{31}–effect [21].

In view of the previous analysis, the overall potential energy of a piezoelectric elastically deformable body consists of the mechanical strain energy (4.2), i.e.

$$W_s = \frac{1}{2}\int_V \sigma^{ij}\epsilon_{ij}\mathrm{d}V. \tag{4.12}$$

and the electro–static field energy

$$W_e = \frac{1}{2}\int_V E_i D^i \mathrm{d}V.$$

For the linear elastic case with (4.8) and (4.9), this reduces to

$$W_p = W_s + W_e = \frac{1}{2}\int_V \left(\sigma^{ij}e_{ij} + E_i D^i\right)\mathrm{d}V$$

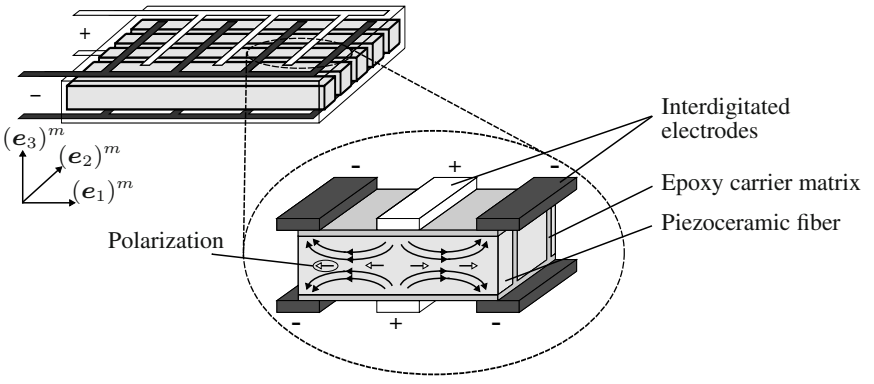

Fig. 4.3 Schematic structure of the MFC patch actuator in the material coordinate system $(\boldsymbol{e}_i)^m$

$$= \frac{1}{2}\int_V \left(c^{ijkl} e_{kl} e_{ij} - 2a_k^{ij} D^k e_{ij} + \beta_{ik} D^k D^i \right) \mathrm{d}V. \quad (4.13)$$

In the case of a coupled structure with a flexible carrier layer and local piezoelectric actuators or sensors, the volume integral in (4.13) has to be suitably decomposed into the different layers and their geometric and material properties. In particular the evaluation of the terms originating from the electric field evolving inside the actuator requires to address the individual actuator set–up in terms of location and orientation. For this, subsequently MFC actuators are considered, which enable to overcome the limitations of the classically used monolithic piezoceramic actuators such as brittleness of the material, poor conformability, and overall low strain energy density. Their schematics is depicted in Figure 4.3. The actuator is build up as a fiber composite actuator, where piezoceramic fibers are embedded into an epoxy carrier matrix. Interdigitated electrode patterns on the faces of the carrier produce in–plane electric fields, which permit the realization of large, directional, in–plane actuation strains. With this configuration of piezoceramic fibers, electrodes, and polarization the so–called d_{33}–effect is exploited, which is significantly larger than the d_{31}–effect utilized in classic piezoelectric actuators [20, 21].

Throughout the subsequent analysis of MFC actuated flexible structures, it is convenient to introduce a local actuator–fixed coordinate system as is shown in Figure 4.3 and to consider the transformation of the local results into a global body–fixed coordinate system. Besides the incorporation of the dynamic effects of arbitrarily placed actuators this in addition enables a concise determination of the respective components a_k^{ij} and β_{ik} of the material and dielectricity tensor, which are typically provided by the manufacturer in terms of the local coordinates. In order to address this, consider two coordinate systems with origins o_r and o_m and basis vectors $(\boldsymbol{e}_k)^r$ and $(\boldsymbol{e}_k)^m$ referring to a global reference system (r–system) and a local material system (m–system), respectively. Hence, the position vector to an arbitrary point can be expressed in the i–system, $i \in \{r, m\}$, with the coordinates $(Z^k)_i$ as $\boldsymbol{Z}_i = (Z^k)_i (\boldsymbol{e}_k)^i$

in the undeformed configuration and as $\boldsymbol{z}_i = (z^k)_i(\boldsymbol{e}_k)^i$ in the deformed configuration. Let $\boldsymbol{S}_r^m$ and $\boldsymbol{s}_r^m(t)$ denote the position vectors to the origin of the m–system expressed in the r–system, i.e. $\boldsymbol{S}_r^m$ and $\boldsymbol{s}_r^m(t)$ describe the translation from the origin o_r to the origin o_m in the undeformed and deformed configuration. Moreover, let $\boldsymbol{R}_r^m \in SO(3)$ denote the rotation tensor with components $(R_l^k)_r^m = (\boldsymbol{e}_k)^m \cdot (\boldsymbol{e}_l)_r^m$, where $\cdot$ is the dot product and $(\boldsymbol{e}_l)_r^m$ denotes $(\boldsymbol{e}_l)^m$ expressed in coordinates of the r–system. This in particular implies that $\boldsymbol{R}_r^m(\boldsymbol{R}_r^m)^T = (\boldsymbol{R}_r^m)^T\boldsymbol{R}_r^m = \boldsymbol{\delta}$ and $\det \boldsymbol{R}_r^m = 1$ [19]. The indexes herein refer to the rotation from the m–system to the r–system. The inverse rotation from the r–system to the m–system hence follows as $\boldsymbol{R}_m^r = (\boldsymbol{R}_r^m)^{-1} = (\boldsymbol{R}_r^m)^T$. Note that the parametrization of the rotation is not unique. In particular, direction cosines, Euler angles, or roll–pitch–yaw angles can be used depending on the application (cf., e.g., [19]). If not stated otherwise, the subsequent analysis refers to roll–pitch–yaw angles. Observe that the rotation tensor in general depends on time such that $\boldsymbol{R}_r^m = \boldsymbol{R}_r^m(t)$.

With these preparations, the transformations of the position vectors from the m–system to the r–system are obtained as $\boldsymbol{Z}_r = \boldsymbol{S}_r^m + \boldsymbol{R}_r^m(t_0)\boldsymbol{Z}_m$ in the undeformed and $\boldsymbol{z}_r(\boldsymbol{Z}_m, t) = \boldsymbol{s}_r^m(t) + \boldsymbol{R}_r^m(t)\boldsymbol{z}_m(\boldsymbol{Z}_m, t)$ in the deformed configuration. In addition, this implies the introduction of the local displacement vector $\boldsymbol{w}_m(\boldsymbol{Z}_m, t) = \boldsymbol{z}_m(\boldsymbol{Z}_m, t) - \boldsymbol{Z}_m$ and the global displacement vector $\boldsymbol{w}_r(\boldsymbol{Z}_m, t) = \boldsymbol{z}_r(\boldsymbol{Z}_m, t) - \boldsymbol{Z}_r$ or equivalently $\boldsymbol{w}_r(\boldsymbol{Z}_m, t) = (\boldsymbol{R}_r^m(t) - \boldsymbol{R}_r^m(t_0))\boldsymbol{Z}_m + \boldsymbol{R}_r^m(t)\boldsymbol{w}_m(\boldsymbol{Z}_m, t) + \boldsymbol{s}_r^m(t) - \boldsymbol{S}_r^m$ by making use of the relations between the coordinate systems introduced above.

Moreover, the transformation rules for the Green strain tensor and the second Piola–Kirchhoff stress tensor can be deduced as

$$\begin{aligned}\boldsymbol{\epsilon}_r(\boldsymbol{Z}_m, t) &= \boldsymbol{R}_r^m(t_0)\boldsymbol{\epsilon}_m(\boldsymbol{Z}_m, t)\boldsymbol{R}_m^r(t_0)\\ (\epsilon_{kl})_r &= (R_k^p)_r^m(t_0)(\epsilon_{pq})_m(R_l^q)_m^r(t_0) = (R_k^p)_r^m(t_0)(R_l^q)_r^m(t_0)(\epsilon_{pq})_m\end{aligned}$$

and

$$(\sigma^{ij})_r = (R_p^i)_r^m(t_0)(\sigma^{pq})_m(R_q^j)_m^r(t_0) = (R_p^i)_r^m(t_0)(R_q^j)_r^m(t_0)(\sigma^{pq})_m.$$

In addition, the components of the electric flux density and electric field strength transform according to $(D^k)_r = (R_p^k)_r^m(D^p)_m$ and $(E_i)_r = (R_i^p)_r^m(E_p)_m$. With this, the transformation of the components of the stress tensor and the electric field strength satisfying the constitutive equations (4.8) and (4.9), respectively, can be directly determined by means of the transformed components of the tensors c^{ijkl}, a_k^{ij}, and β_{ik} given by the relationships

$$(c^{ijkl})_r = (R_p^i)_r^m(t_0)(R_q^j)_r^m(t_0)(R_s^k)_r^m(t_0)(R_t^l)_r^m(t_0)(c^{pqst})_m \tag{4.14}$$

$$(a_k^{ij})_r = (R_k^s)_r^m(t_0)(R_p^i)_r^m(t_0)(R_q^j)_r^m(t_0)(a_s^{pq})_m \tag{4.15}$$

$$(\beta_{ik})_r = (R_i^p)_r^m(t_0)(R_k^q)_r^m(t_0)(\beta_{pq})_m. \tag{4.16}$$

Hence, for the evaluation of the potential energy (4.13) it is sufficient to consider the components of the strain tensor and the electric flux density solely in the global

r-system with the respective tensor components $(c^{ijkl})_r$, $(a_k^{ij})_r$, and $(\beta_{ik})_r$ obtained from the introduced transformations (4.14)–(4.16).

In order to complement the energetic considerations, the kinetic energy W_k of the deformable body follows as

$$W_k = \int_V \rho \partial_t(\boldsymbol{w}_r)^T \partial_t \boldsymbol{w}_r \mathrm{d}V, \tag{4.17}$$

where ρ denotes the density of the body. Note that W_k is associated with the macroscopically observable velocity of the continuum, while the (microscopic) motions of the molecules of the continuum is a part of the strain energy. With these preliminaries, Hamilton's principle for a piezoelectric continuum can be stated in terms of the first variation of the functional

$$\mathcal{I} = \int_{t_1}^{t_2} \big(W_k - W_p\big)\mathrm{d}t.$$

Hamilton's principle implies that from the set of all admissible spatial–temporal paths for a material particle $\boldsymbol{w}_r$, the true path renders $\mathcal{I}$ stationary [12, 23]. For conservative systems, this can be equivalently expressed as

$$\delta\mathcal{I} = \delta \int_{t_1}^{t_2} \big(W_k - W_p\big)\mathrm{d}t = 0, \quad \delta\boldsymbol{w}_r(t_1) = \delta\boldsymbol{w}_r(t_2) = 0,$$

where δ denotes the variational operator. In order to include non–conservative forces that cannot be derived from a potential energy function such as damping this approach can be generalized to the so–called extended Hamilton's principle. Here, the equations of motion are obtained from

$$\begin{aligned} &\delta\mathcal{I}^{ex} = \delta \int_{t_1}^{t_2} \big(W_k - W_p\big)\mathrm{d}t + \int_{t_1}^{t_2} \delta W_{nc}\mathrm{d}t = 0, \\ &\delta\boldsymbol{w}_r(t_1) = \delta\boldsymbol{w}_r(t_2) = 0, \end{aligned} \tag{4.18}$$

where δW_{nc} represents the variational form of the virtual work of the non–conservative contributions. In the following, the application of the extended Hamilton's principle is illustrated for a piezoactuated thin flexible plate.

4.2 Flexible Plate with Distributed MFC Actuators

Based on the previous analysis the equations of motion are derived for an adaptive structure consisting of a thin plate with spatially distributed MFC patch actuators[2] as schematically shown in Figure 4.4. Thereby, it is assumed that the $l \in M$ individual MFC patches are located pairwise symmetrically on the top and bottom of the plate

[2] Note that subsequently the superscript p refers to piezoelectric actuators.

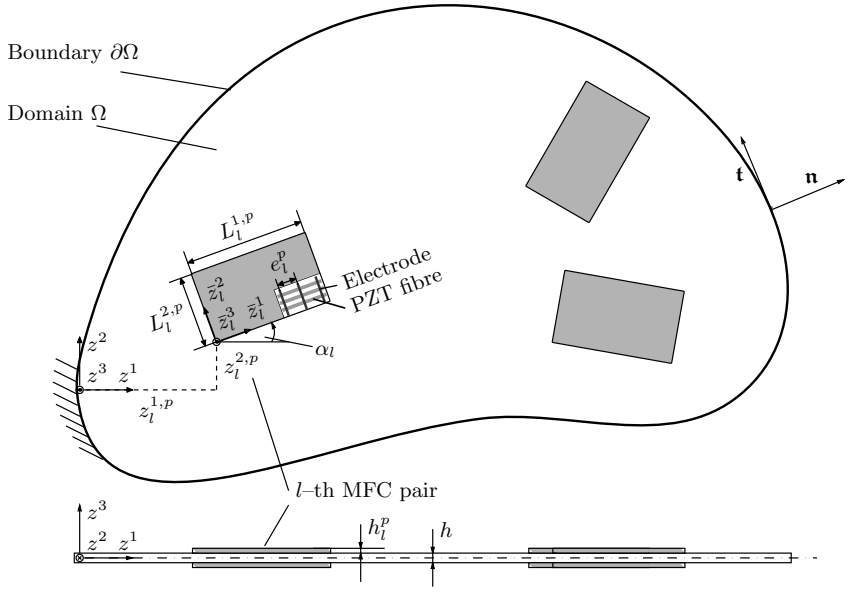

Fig. 4.4 Schematics of the considered plate with MFC actuators distributed over the plate domain Ω and boundary $\partial\Omega$. The vectors $\mathbf{t}$ and $\mathbf{n}$ denote the tangent and normal vector at a point on $\partial\Omega$.

with anti–symmetric voltage supply to each MFC actuator pair. Furthermore, for modeling purposes the MFC actuator pairs are equipped with a local actuator–fixed coordinate system in terms of the coordinate tuple $(\bar{z}_l^1, \bar{z}_l^2, \bar{z}_l^3)$, which describes the rotation of the l–th patch pair by an angle α_l with respect to the global plate–fixed coordinate system represented by the coordinate tuple (z^1, z^2, z^3). Note that subsequently all overlined quantities refer to a description in terms of the actuator–fixed coordinate system.

Assumption 4.1. For modeling, the following assumptions are imposed:

(i) The Kirchhoff–Love assumptions hold for both the carrier plate and the MFC actuators [12], i.e.

(a) Deflections are small compared to the plate thickness such that $\epsilon_{ij} = e_{ij}$
(b) There is no force resultant on the cross–sectional area of a plate element. The midsurface of the plate is a neutral plane, i.e. it does not undergo deformations during bending.
(c) The transverse normal stress σ^{33} is small compared to the remaining stress components and is neglected.
(d) Plane sections initially normal to the midsurface remain plane and normal to the midsurface during bending. Hence, it follows that e_{13} and e_{23} are negligible. Together with the assumption of an orthotropic material this yields $\sigma^{13} = \sigma^{23} = 0$.

(ii) The carrier plate material is homogeneous and orthotropic with respect to the (z^1, z^2, z^3) coordinate system and the constitutive equations are given by (4.6).
(iii) Linear[3] piezoelectric material is considered satisfying the constitutive equations (4.8) and (4.9) with respect to the $(\bar{z}^1, \bar{z}^2, \bar{z}^3)$ coordinate system. The MFC actuator material is assumed homogeneous and orthotropic.
(iv) The MFC actuators neither touch the plate boundary nor do they overlap or contact directly.
(v) The supply voltage U_l^p to each MFC pair is applied anti–symmetrically, i.e. $U_l^p = U_l^{p,t} = -U_l^{p,b}$, where t and b refer to the top and bottom patch, respectively.

Assumption 4.1 (i), i.e., the plane stress assumption, in particular implies that

$$(w^1)_r = w^1 - z^3 \partial_{z^1} w^3, \quad (w^2)_r = w^2 - z^3 \partial_{z^2} w^3, \quad (w^3)_r = w^3, \tag{4.19}$$

where $w^i = w^i(z^1, z^2, t)$ denote the components of the displacement vector of the material point at $(z^1, z^2, 0)$ when the plate is in equilibrium.

Remark 4.2. In order to ensure consistency with the examples considered in Sections 2 and 3, with a slight abuse of notation subsequently z^k is used to refer to the coordinate in the undeformed state initially denoted as Z^k.

The substitution of (4.19) into (4.4) hence yields the respective components of the strain tensor, i.e.

$$\begin{aligned} e_{11} &= \partial_{z^1} w^1 - z^3 \partial_{z^1}^2 w^3, \quad e_{22} = \partial_{z^2} w^2 - z^3 \partial_{z^2}^2 w^3, \\ e_{12} &= e_{21} = \frac{1}{2}\Big(\partial_{z^2} w^1 + \partial_{z^1} w^2 - 2 z^3 \partial_{z^1 z^2}^2 w^3\Big). \end{aligned} \tag{4.20}$$

4.2.1 Preparations

In order to determine the individual energy contributions of the carrier plate and the MFC patch actuator pairs, the respective constitutive equations have to be evaluated in view of Assumption 4.1.

4.2.1.1 Constitutive Equations for the Carrier Plate

From Assumptions 4.1(i)(c), (i)(d), and (ii) it follows that

$$\sigma^{ij} e_{ij} = Y^{1111} e_{11}^2 + 2 Y^{1122} e_{11} e_{22} + Y^{2222} e_{22}^2 + 2\big(Y^{1212} + Y^{2121}\big) e_{12}^2 \tag{4.21}$$

with the material constants

[3] While piezoceramic material essentially shows hysteresis and creep behavior this assumption can be fulfilled by incorporating a suitable hysteresis and creep compensation as is introduced and analyzed, e.g., in [14, 15] for MFC actuators.

$$Y^{ijkl} = \frac{1}{2}\left(c^{ijkl} + c^{klij}\right). \tag{4.22}$$

4.2.1.2 Constitutive Equations for the MFC Patch Actuators

For the mathematical representation of the actuator contributions to the potential energy, according to Assumption 4.1 (iii) the constitutive equations (4.8), (4.9) are considered for linear orthotropic piezoelectric material. Thereby, special emphasis is required for the analysis of the different actuator orientations given in the local actuator–fixed coordinate systems in terms of $(\bar{z}_l^1, \bar{z}_l^2, \bar{z}_l^3)$ with respect to the global plate–fixed coordinate system. As already outlined in Section 4.1, the components $(c^{ijkl,p})_l$, $(a_k^{ij})_l$, and $(\beta_{ik})_l$ of the elasticity, the piezoelectric material, and the dielectricity tensors have to be transformed into the global coordinate system with components (z^1, z^2, z^2) according to (4.14)–(4.16). This is subsequently outlined for the l–th MFC pair for arbitrary $l \in M$ from the actuator index set M with $\#M = m$.

From Figure 4.4 it follows that the rotation tensor $(\boldsymbol{R})_r^l$ between the local and global coordinate system can be represented as

$$(\boldsymbol{R})_r^l = \begin{bmatrix} \cos(\alpha_l) & -\sin(\alpha_l) & 0 \\ \sin(\alpha_l) & \cos(\alpha_l) & 0 \\ 0 & 0 & 1 \end{bmatrix}.$$

The electrode orientation along the $\bar{z}_l^2$–direction implies that the electric field only evolves along the $\bar{z}_l^1$–direction (cf. Figures 4.3 and 4.4) such that the only non–zero components of the flux density and field strength $(D^k)_l$ and $(E_i)_l$ are given by $(D^1)_l$ and $(E_1)_l$. Thus, let $(R_p^q)_r^l$ denote the elements of $(\boldsymbol{R})_r^l$, then (4.14) together with Assumptions 4.1(i) and (iii) yields for the components of the elasticity tensor $c^{ijkl,p} = (c^{ijkl,p})_r = (R_o^i)_r^l (R_q^j)_r^l (R_s^k)_r^l (R_t^l)_r^l (c^{oqst,p})_m$ while (4.15) and (4.16) evaluate to $a_k^{ij} = (a_k^{ij})_r = (R_k^1)_r^l (R_p^i)_r^l (R_q^j)_r^l (a_1^{mn})_l$ and $\beta_{ik} = (\beta_{ik})_r = (R_i^1)_r^l (R_k^1)_r^l (\beta_{11})_l$. As a result, taking into account Assumption 4.1 (i)(c) the constitutive equations (4.8) and (4.9) for the l–th actuator evaluate to

$$\begin{bmatrix} \sigma^{11} \\ \sigma^{22} \\ \sigma^{12} \\ \sigma^{21} \end{bmatrix} = \begin{bmatrix} c^{1111,p} & c^{1122,p} & c^{1112,p} & c^{1121,p} \\ c^{2211,p} & c^{2222,p} & c^{2212,p} & c^{2221,p} \\ c^{1211,p} & c^{1222,p} & c^{1212,p} & c^{1221,p} \\ c^{2111,p} & c^{2122,p} & c^{2112,p} & c^{2121,p} \end{bmatrix} \begin{bmatrix} e_{11} \\ e_{22} \\ e_{12} \\ e_{21} \end{bmatrix} - \begin{bmatrix} a_1^{11} & a_2^{11} \\ a_1^{22} & a_2^{22} \\ a_1^{12} & a_2^{12} \\ a_1^{21} & a_2^{21} \end{bmatrix} \begin{bmatrix} D^1 \\ D^2 \end{bmatrix}$$

$$\begin{bmatrix} E_1 \\ E_2 \end{bmatrix} = -\begin{bmatrix} a_1^{11} & a_1^{22} & a_1^{12} & a_1^{21} \\ a_2^{11} & a_2^{22} & a_2^{12} & a_2^{21} \end{bmatrix} \begin{bmatrix} e_{11} \\ e_{22} \\ e_{12} \\ e_{21} \end{bmatrix} + \begin{bmatrix} \beta_{11} & \beta_{12} \\ \beta_{21} & \beta_{22} \end{bmatrix} \begin{bmatrix} D^1 \\ D^2 \end{bmatrix}$$

Herein, the components of the electric flux density are given by $D^k = (D^k)_r = (R_1^k)_r^l (D^1)_l$ such that $D^1 = \cos(\alpha_l)(D^1)_l$ and $D^2 = \sin(\alpha_l)(D^1)_l$. Note that in

general certain symmetries of the tensor components for the orthotropic actuator material are preserved under the transformations (4.14)–(4.16). These are, however, not explicitly taken into account throughout the following analysis since their incorporation does neither simplify the notation nor the necessary computations. Thus, it follows that

$$\begin{aligned}\sigma^{ij}e_{ij} + E_i D^i &= Y^{1111,p}e_{11}^2 + 2\big(Y^{1212,p} + Y^{2121,p}\big)e_{12}^2 + Y^{2222,p}e_{22}^2 \\ &\quad + 2Y^{1122,p}e_{11}e_{22} + 4Y^{1112,p}e_{11}e_{12} + 4Y^{2212,p}e_{22}e_{12} \\ &\quad - 2\big(a_1^{11}D^1 + a_1^{11}D^2\big)e_{11} - 2\big(a_1^{22}D^1 + a_2^{22}D^2\big)e_{22} \\ &\quad - 2\big(\big[a_1^{12} + a_1^{21}\big]D^1 + \big[a_2^{12} + a_2^{21}\big]D^2\big)e_{12} \\ &\quad + \beta_{11}D^1D^1 + (\beta_{12} + \beta_{21})D^1D^2 + \beta_{22}D^2D^2,\end{aligned} \tag{4.23}$$

where

$$Y^{ijkl,p} = \frac{1}{4}\left(c^{ijkl,p} + c^{ijlk,p} + c^{klji,p} + c^{lkji,p}\right). \tag{4.24}$$

Based on these preparations, subsequently the potential and the kinetic energies of the carrier plate and the MFC actuators are determined individually. These serve as the basis for the application of the extended Hamilton's principle, which enables a systematic derivation of the equations of motion of the considered thin plate with distributed MFC actuators.

Notation. In the following, the additional subscript l in both the piezoelectric material parameters given in the global plate–fixed coordinate system and the applied voltages refers to the general configuration with each MFC actuator $l \in M$ possessing individual properties.

4.2.2 Potential Energy, Kinetic Energy, and Virtual Work of Non–Conservative Forces

The overall potential and kinetic energy of the flexible plate with MFC actuators consists of the energetic contributions of the individual components, i.e. the carrier plate and the m actuators. For their determination only the major results are provided while the intermediate computations for the evaluation of the volume integrals (4.2) or (4.13), respectively, as well as (4.17) are omitted. In order to suitably integrate the contribution of the MFC patch actuators the spatial actuator characteristic $\Lambda_l^\epsilon(z^1, z^2)$ is introduced as

$$\begin{aligned}\Lambda_l^\epsilon = \big[\varrho^\epsilon\big(\bar{z}_l^1(z^1, z^2)\big) - \varrho^\epsilon\big(\bar{z}_l^1(z^1, z^2) - L_l^{1,p}\big)\big] \times \\ \big[\varrho^\epsilon\big(\bar{z}_l^2(z^1, z^2)\big) - \varrho^\epsilon\big(\bar{z}_l^2(z^1, z^2) - L_l^{2,p}\big)\big]\end{aligned} \tag{4.25}$$

with the indicator function $\varrho^\epsilon(\cdot)$ satisfying the conditions $\varrho^\epsilon(z<0)=0$, $\varrho^\epsilon(z>\epsilon)=1$, and $\varrho^\epsilon(z)\in C^4([0,\epsilon])$ if $\epsilon>0$. If $\epsilon=0$ the indicator function is replaced by the Heaviside function, i.e. $\varrho^0(x)=\sigma(x)$. In addition,

$$\begin{aligned}\bar{z}_l^1(z^1,z^2)&=\cos(\alpha_l)\big(z^1-z_l^{1,p}\big)+\sin(\alpha_l)\big(z^2-z_l^{2,p}\big)\\ \bar{z}_l^2(z^1,z^2)&=-\sin(\alpha_l)\big(z^1-z_l^{1,p}\big)+\cos(\alpha_l)\big(z^2-z_l^{2,p}\big),\end{aligned}$$

where α_l denotes the angle of rotation of the actuator–fixed $(\bar{z}^1,\bar{z}^2,\bar{z}^3)$ coordinate system with respect to the global plate–fixed (z^1,z^2,z^3) coordinate system (cf. Figure 4.4). The appearing volume integrals are reduced to integrals over the plate domain Ω by considering that

$$\int_V f\mathrm{d}V=\begin{cases}\int_\Omega\int_{-\frac{h}{2}}^{\frac{h}{2}} f\mathrm{d}z^3\mathrm{d}\Omega, & \text{for the carrier plate}\\ \int_\Omega\left[\int_{-(\frac{h}{2}+h_l^p)}^{-\frac{h}{2}} f\mathrm{d}z^3+\int_{\frac{h}{2}}^{\frac{h}{2}+h_l^p} f\mathrm{d}z^3\right]\mathrm{d}\Omega, & \text{for the } l\text{–th actuator pairing.}\end{cases}$$

Moreover note that

- the evaluation of the potential and kinetic energies yields a decoupling of the w^1 and w^2 motion from the w^3 motion. Due to the anti–symmetric voltage supply according to Assumption 4.1(v) it can be shown that only the bending deflection w^3 is excited by the MFC actuators such that all terms involving w^1 and w^2 are directly dropped throughout the derivation of the energy contributions;
- gravitational forces are neglected but can be directly incorporated into the potential energy contributions of the carrier plate and the MFC actuators;
- independent coordinates are dropped whenever the relation is clear from the context to shorten notation.

Kinetic Energy of the Carrier Plate

The kinetic energy of the plate is obtained by evaluating (4.17) with (4.19), i.e.

$$W_k^c(t)=\frac{1}{2}\Big(\varsigma_k^{c,1}\big(\partial_t w^3,\partial_t w^3\big)+\varsigma_k^{c,2}\big(\partial_t w^3,\partial_t w^3\big)\Big) \tag{4.26}$$

with

$$\begin{aligned}\varsigma_k^{c,1}(w,\hat{w})&=\int_\Omega \rho^c h w\hat{w}\mathrm{d}\Omega\\ \varsigma_k^{c,2}(w,\hat{w})&=\int_\Omega \rho^c I^c\nabla w\cdot\nabla\hat{w}\mathrm{d}\Omega,\end{aligned} \tag{4.27}$$

where ρ^c is the density of the carrier material, h is the plate height, $I^c=h^3/12$, and ∇ is the Nabla operator. Note that the term $\varsigma_k^{c,2}(\cdot,\cdot)$ vanishes when neglecting the contributions of $(w^1)_r$ and $(w^2)_r$ defined in (4.19).

Kinetic Energy of the MFC Patch Actuators

The kinetic energy contribution of the MFC patch actuator pairs is obtained from (4.17) such that

$$W_k^p(t) = \frac{1}{2}\Big(\varsigma_k^{p,1}\big(\partial_t w^3, \partial_t w^3\big) + \varsigma_k^{p,2}\big(\partial_t w^3, \partial_t w^3\big)\Big) \tag{4.28}$$

with

$$\begin{aligned}\varsigma_k^{p,1}(w,\hat{w}) &= 2\int_\Omega \sum_{l\in M} \rho_l^p \Lambda_l^\varepsilon h_l^p w\hat{w}\,\mathrm{d}\Omega\\ \varsigma_k^{p,2}(w,\hat{w}) &= 2\int_\Omega \sum_{l\in M} \rho_l^p \Lambda_l^\varepsilon I_l^p \nabla w\cdot\nabla\hat{w}\,\mathrm{d}\Omega.\end{aligned} \tag{4.29}$$

Here, ρ_l^p is the homogenized density of the actuator material, h_l^p is the height of a single actuator, and $I_l^p = ([h/2 + h_l^p]^3 - [h/2]^3)/3$. The multiplication by 2 in (4.29) is due to the consideration of an actuator pair with actuators mounted symmetrically on the top and bottom surface of the plate. Similar to above, the term $\varsigma_k^{p,2}(\cdot,\cdot)$ vanishes if the contributions $(w^1)_r$ and $(w^2)_r$ are neglected in (4.19).

Potential Energy of the Carrier Plate

The potential energy of the carrier plate is solely determined by the strain energy (4.12) together with (4.19)–(4.21), which can be represented as

$$W_p^c(t) = \frac{1}{2}\varsigma_p^c(w^3, w^3) \tag{4.30}$$

with

$$\begin{aligned}\varsigma_p^c(w,\hat{w}) = \int_\Omega I^c\Big(&q^1\partial_{z^1}^2 w\partial_{z^1}^2\hat{w} + q^2\partial_{z^2}^2 w\partial_{z^2}^2\hat{w}\\ &+ q^3\Delta w\Delta\hat{w} + q^4\partial_{z^1}\partial_{z^2} w\partial_{z^1}\partial_{z^2}\hat{w}\Big)\mathrm{d}\Omega.\end{aligned} \tag{4.31}$$

Here, $\Delta = \nabla\cdot\nabla = \partial_{z^1}^2 + \partial_{z^2}^2$ is the Laplacian and the constants q^i follow as

$$q^1 = Y^{1111} - Y^{1122},\ q^2 = Y^{2222} - Y^{1122},\ q^3 = Y^{1122},\ q^4 = 4\big(Y^{1212} + Y^{2121}\big).$$

Potential Energy of the MFC Patch Actuators

The potential energy contribution (4.13) of the MFC patch actuator pairs consists of two terms due to the strain energy and the electric field, i.e.

$$W_p^p(t) = \frac{1}{2}\varsigma_p^{p,b}\big(w^3, w^3\big) + \varsigma_p^{p,e}\big(w^3\big) \tag{4.32}$$

with

$$\begin{aligned}\varsigma_p^{p,b}(w,\hat{w}) = 2\int_\Omega \sum_{l\in M} \Lambda_l^\epsilon I_l^p \Big(& q_l^{1,p}\partial_{z^1}^2 w \partial_{z^1}^2 \hat{w} + q_l^{2,p}\partial_{z^2}^2 w \partial_{z^2}^2 \hat{w} \\ & + q_l^{3,p}\Delta w \Delta\hat{w} + q_l^{4,p}\partial_{z^1}\partial_{z^2} w \partial_{z^1}\partial_{z^2}\hat{w} \\ & + q_l^{5,p}\big(\partial_{z^1}^2 w + \partial_{z^1}\partial_{z^2} w\big)\big(\partial_{z^1}^2\hat{w} + \partial_{z^1}\partial_{z^2}\hat{w}\big) \\ & + q_l^{6,p}\big(\partial_{z^2}^2 w + \partial_{z^1}\partial_{z^2} w\big)\big(\partial_{z^2}^2\hat{w} + \partial_{z^1}\partial_{z^2}\hat{w}\big)\Big)\mathrm{d}\Omega.\end{aligned} \tag{4.33}$$

The constants $q_l^{i,p}$ are thereby given by

$$\begin{aligned} & q_l^{1,p} = Y_l^{1111,p} - 2Y_l^{1112,p} - Y_l^{1122,p},\ q_l^{2,p} = Y_l^{2222,p} - 2Y_l^{2212,p} - Y_l^{1122,p} \\ & q_l^{3,p} = Y_l^{1122,p},\ q_l^{4,p} = 2\big(Y_l^{1212,p} + Y_l^{2121,p} - Y_l^{1112,p} - Y_l^{2212}\big), \\ & q_l^{5,p} = 2Y_l^{1112,p},\ q_l^{6,p} = 2Y_l^{2212,p}. \end{aligned}$$

The second term in (4.32) yields the contribution of the electro–mechanical coupling given by

$$\begin{aligned}\varsigma_p^{p,e}(w) = \int_\Omega \sum_{l\in M} \Lambda_l^\epsilon h_l^p (h + h_l^p)\times \\ \Big(\big[a_{1,l}^{11}\partial_{z^1}^2 w + a_{1,l}^{22}\partial_{z^2}^2 w + \big(a_{1,l}^{12} + a_{1,l}^{21}\big)\partial_{z^1}\partial_{z^2} w\big]\tilde{D}_l^1 \\ + \big[a_{2,l}^{11}\partial_{z^1}^2 w + a_{2,l}^{22}\partial_{z^2}^2 w + \big(a_{2,l}^{12} + a_{2,l}^{21}\big)\partial_{z^1}\partial_{z^2} w\big]\tilde{D}_l^2\Big)\mathrm{d}\Omega.\end{aligned} \tag{4.34}$$

Here, Assumption 4.1(v) on the anti–symmetric voltage supply implies $\tilde{D}_l^k = D_l^{k,t} - D_l^{k,b}$, where t and b refer to the top and bottom MFC patch actuator of the respective actuator pair.

Supply Voltages and Electric Flux Density

The relationship between the electric flux density D^1 and the applied voltage U_1^p can be determined by considering the constructive set–up of an individual MFC actuator (cf. Figures 4.3 and 4.4). For this, assume that the self–generated electric field due to the direct piezoelectric effect, i.e. $a_i^{kl}e_{kl}$, $i,k,l = 1,2$, is insignificant compared to the applied electric field E_i, $i = 1,2$. Then integration in the $\bar{z}^1$–direction between two neighboring electrodes located at $\bar{z}_e^1$ and $\bar{z}_e^1 + e^p$ with e^p denoting the electrode spacing provides

$$U^p = U_1^p = \int_{\bar{z}_l^1}^{\bar{z}_l^1 + e^p} (E_1)_l \,\mathrm{d}\bar{z}_l^1 = e^p(\beta_{11})_l (D^1)_l.$$

Hence, in the local actuator–fixed coordinate system this yields

$$(D^1)_l = \frac{U^p}{e_l^p(\beta_{11})_l},$$

which implies in the global coordinate system that

$$\begin{aligned} D^1 &= (D^1)_r = (R_1^1)_r^l (D^1)_l = \frac{\cos(\alpha_l) U^p}{e_l^p(\beta_{11})_l} \\ D^2 &= (D^2)_r = (R_1^2)_r^l (D^2)_l = \frac{\sin(\alpha_l) U^p}{e_l^p(\beta_{11})_l}. \end{aligned}$$

By recalling that $\tilde{D}_l^k = D_l^{k,t} - D_l^{k,b}$ it follows for the l–th MFC actuator pair together with Assumption 4.1(v) that

$$\begin{aligned} \tilde{D}_l^1 &= \frac{\cos(\alpha_l)}{e_l^p(\beta_{11,l})_l}\big(U_l^{p,t} - U_l^{p,b}\big) = \frac{2\cos(\alpha_l)}{e_l^p(\beta_{11,l})_l} U_l^p \\ \tilde{D}_l^2 &= \frac{\sin(\alpha_l)}{e_l^p(\beta_{11,l})_l}\big(U_l^{p,t} - U_l^{p,b}\big) = \frac{2\sin(\alpha_l)}{e_l^p(\beta_{11,l})_l} U_l^p. \end{aligned} \tag{4.35}$$

Virtual Work of Non–Conservative Forces

Mechanical structures in general exhibit energy dissipation due to damping. As outlined above, for its incorporation the variational form of the respective virtual work is considered, which for viscous (external) damping can be expressed as

$$\delta W_{nc}(t) = \varsigma_{cn}^c\big(\partial_t w^3, \delta w^3\big) + \varsigma_{cn}^p\big(\partial_t w^3, \delta w^3\big) \tag{4.36}$$

with the contributions of the carrier plate and the MFC patch actuator pairs

$$\varsigma_{cn}^c(w, \hat{w}) = \int_\Omega \nu^c w \hat{w} \mathrm{d}\Omega \tag{4.37}$$

$$\varsigma_{cn}^p(w, \hat{w}) = 2 \int_\Omega \sum_{l \in M} \nu_l^p \Lambda_l^\epsilon w \hat{w} \mathrm{d}\Omega, \tag{4.38}$$

where ν^c and ν_l^p, $l \in M$, represent the respective viscous damping coefficients.

4.2.3 Strong Form of the Equations of Motion

The equations of motion of the piezoactuated flexible plate are subsequently derived by considering the extended Hamilton's principle (4.18). By recalling that the variational operator δ can be interchanged with both differential and integral operators,

the variational forms $\delta W_k(t)$ and $\delta W_p(t)$ of the overall kinetic and potential energy $W_k(t) = W_k^c(t) + W_k^p(t)$ and $W_p(t) = W_p^c(t) + W_p^p(t)$, respectively, can be directly determined as

$$\begin{aligned}\delta W_k(t) &= \varsigma_k^{c,1}\big(\partial_t w^3, \partial_t\big(\delta w^3\big)\big) + \varsigma_k^{c,2}\big(\partial_t w^3, \partial_t\big(\delta w^3\big)\big)\\ &\quad + \varsigma_k^{p,1}\big(\partial_t w^3, \partial_t\big(\delta w^3\big)\big) + \varsigma_k^{p,2}\big(\partial_t w^3, \partial_t\big(\delta w^3\big)\big)\\ \delta W_p(t) &= \varsigma_p^{c}\big(w^3, \delta w^3\big) + \varsigma_p^{p,b}\big(w^3, \delta w^3\big) + \varsigma_p^{p,e}\big(\delta w^3\big).\end{aligned}$$

Together with the divergence theorem, i.e.

$$\int_\Omega \nabla\cdot(u\boldsymbol{v})\mathrm{d}\Omega = \int_\Omega (\boldsymbol{v}\cdot\nabla u + u\nabla\cdot\boldsymbol{v})\mathrm{d}\Omega = \int_{\partial\Omega} u\boldsymbol{v}\cdot\mathrm{d}\boldsymbol{s} \tag{4.39}$$

with $\mathrm{d}\boldsymbol{s} = \mathfrak{n}\mathrm{d}s$, where $\mathfrak{n} = [\mathfrak{n}^1, \mathfrak{n}^2]^T$ denotes the normal pointing outward on the boundary $\partial\Omega$, the equality (see, e.g., [4, p. 12])

$$\begin{aligned}&\int_{\partial\Omega}(m_1\partial_{z^1}u + m_2\partial_{z^2}u)\mathrm{d}s\\ &\qquad = \int_{\partial\Omega}\big([\mathfrak{n}^1 m_1 + \mathfrak{n}^2 m_2]\partial_{\mathfrak{n}}u + u\partial_{\mathfrak{t}}[\mathfrak{n}^2 m_1 - \mathfrak{n}^1 m_2]\big)\mathrm{d}s\end{aligned} \tag{4.40}$$

with the tangent vector $\mathfrak{t} = [-\mathfrak{n}^2, \mathfrak{n}^1]^T$ orthogonal to $\mathfrak{n}$ such that $\partial_{\mathfrak{t}} = \mathfrak{t}\cdot\nabla$, and the fundamental lemma of variational calculus the equations of motion follow after some tedious but basically straightforward computations. In particular, the PDE

$$\begin{aligned}&\rho\partial_t^2 w^3 - \rho I\Delta\partial_t^2 w^3 + \nu\partial_t w^3 + \partial_{z^1}^2\big(\mu^1\partial_{z^1}^2 w^3\big) + \partial_{z^2}^2\big(\mu^2\partial_{z^2}^2 w^3\big)\\ &+\Delta(\mu^3\Delta w^3) + \partial_{z^1}\partial_{z^2}\big(\mu^4\partial_{z^1}\partial_{z^2}w^3\big) + \partial_{z^1}^2\big(\mu^5\big(\partial_{z^1}^2 w^3 + \partial_{z^1}\partial_{z^2}w^3\big)\big)\\ &+\partial_{z^1}\partial_{z^2}\big(\mu^5\big(\partial_{z^1}^2 w^3 + \partial_{z^1}\partial_{z^2}w^3\big)\big) + \partial_{z^1}\partial_{z^2}\big(\mu^6\big(\partial_{z^1}\partial_{z^2}w^3 + \partial_{z^2}^2 w^3\big)\big)\\ &+\partial_{z^2}^2\big(\mu^6\big(\partial_{z^1}\partial_{z^2}w^3 + \partial_{z^2}^2 w^3\big)\big) = \sum_{l\in M} I_l^p U_l^p\end{aligned} \tag{4.41a}$$

is obtained governing the evolution of $w^3(z^1, z^2, t)$ for $(z^1, z^2, t) \in \Omega\times(0,T)$. Herein, the following abbreviations are used summarizing the various material parameters

$$\begin{aligned}\rho &= \rho^c h + 2\sum_{l\in M}\Lambda_l^\epsilon\rho_l^p h_l^p\\ \rho I &= \rho^c I^c + 2\sum_{l\in M}\Lambda_l^\epsilon\rho_l^p I_l^p\\ \nu &= \nu^c + 2\sum_{l\in M}\Lambda_l^\epsilon\nu_l^p\\ \mu^j &= \begin{cases} q^j I^c + 2\sum_{l\in M} q_l^{j,p} I_l^p \Lambda_l^\epsilon, & j = 1,\dots,4\\ 2\sum_{l\in M} q_l^{j,p} I_l^p \Lambda_l^\epsilon, & j = 5,6\end{cases}\end{aligned}$$

$$\Gamma_l^p = \Gamma_l^1 \cos(\alpha_l) + \Gamma_l^2 \sin(\alpha_l)$$

with

$$\Gamma_l^j = \Gamma_l^0 \left[a_{j,l}^{11} \partial_{z^1}^2 \Lambda_l^\epsilon + a_{j,l}^{22} \partial_{z^2}^2 \Lambda_l^\epsilon + \left(a_{j,l}^{12} + a_{j,l}^{21} \right) \partial_{z^1} \partial_{z^2} \Lambda_l^\epsilon \right]$$

and

$$\Gamma_l^0 = -\frac{2 h_l^p (h + h_l^p)}{e_l^p (\beta_{11,l})_l}.$$

The respective boundary conditions follow depending on the boundary configuration by taking into account Assumption 4.1(iv) and the assumption that $\partial\Omega = \partial\Omega_c \cup \partial\Omega_f \cup \partial\Omega_h$:

(i) clamped conditions for $(z^1, z^2) \in \partial\Omega_c$

$$w^3 = \partial_{\mathfrak{n}} w^3 = 0 \tag{4.41b}$$

(ii) free conditions for $(z^1, z^2) \in \partial\Omega_f$

$$\mathfrak{n}^1 \mathfrak{n}^1 \kappa^{11} + \mathfrak{n}^1 \mathfrak{n}^2 \left(\kappa^{12} + \kappa^{21} \right) + \mathfrak{n}^2 \mathfrak{n}^2 \kappa^{22} = 0 \tag{4.41c}$$

$$\begin{aligned} &\partial_{\mathfrak{t}} \left(\mathfrak{n}^2 \mathfrak{n}^2 \kappa^{12} + \mathfrak{n}^1 \mathfrak{n}^2 \left(\kappa^{11} - \kappa^{22} \right) - \mathfrak{n}^1 \mathfrak{n}^1 \kappa^{21} \right) - \mathfrak{n}^1 \left(\partial_{z^1} \kappa^{11} + \partial_{z^2} \kappa^{12} \right) \\ &- \mathfrak{n}^2 \left(\partial_{z^1} \kappa^{21} + \partial_{z^2} \kappa^{22} \right) - \rho I \partial_{\mathfrak{n}} \partial_t^2 w^3 = 0 \end{aligned} \tag{4.41d}$$

(iii) hinged conditions for $(z^1, z^2) \in \partial\Omega_h$

$$w^3 = 0 \tag{4.41e}$$

$$\mathfrak{n}^1 \mathfrak{n}^1 \kappa^{11} + \mathfrak{n}^1 \mathfrak{n}^2 \left(\kappa^{12} + \kappa^{21} \right) + \mathfrak{n}^2 \mathfrak{n}^2 \kappa^{22} = 0. \tag{4.41f}$$

Thereby, κ^{ij} abbreviates

$$\begin{aligned} \kappa^{11} &= \mu^1 \partial_{z^1}^2 w^3 + \mu^3 \Delta w^3 + \mu^5 \left(\partial_{z^1}^2 w^3 + \partial_{z^1} \partial_{z^2} w^3 \right) \\ \kappa^{12} &= \mu^4 \partial_{z^1} \partial_{z^2} w^3 + \mu^5 \left(\partial_{z^1}^2 w^3 + \partial_{z^1} \partial_{z^2} w^3 \right) \\ \kappa^{21} &= \mu^6 \left(\partial_{z^1} \partial_{z^2} w^3 + \partial_{z^2}^2 w^3 \right) \\ \kappa^{22} &= \mu^2 \partial_{z^2}^2 w^3 + \mu^3 \Delta w^3 + \mu^6 \left(\partial_{z^1} \partial_{z^2} w^3 + \partial_{z^2}^2 w^3 \right). \end{aligned}$$

For the unique determination of the motion, initial conditions for displacement and velocity have to be imposed, i.e.

$$w^3 = w_0^3, \quad \partial_t w^3 = w_1^3, \qquad (z^1, z^2) \in \overline{\Omega},\ t = 0. \tag{4.41g}$$

An additional simplification arises from the remark below.

Remark 4.3. In most situations, the kinetic energy contributions of $\varsigma_k^{c,2}\left(\partial_t w^3, \partial_t w^3\right)$ and $\varsigma_k^{p,2}\left(\partial_t w^3, \partial_t w^3\right)$ are insignificant compared to those of $\varsigma_k^{c,1}\left(\partial_t w^3, \partial_t w^3\right)$ and

$\varsigma_k^{p,1}\big(\partial_t w^3, \partial_t w^3\big)$, respectively. Hence, subsequently $\rho I(z^1, z^2) = 0$ is considered to simplify the analysis.

Throughout the following chapters, the two cases $\epsilon = 0$ and $\epsilon > 0$ of spatial patch characteristics Λ_j^ϵ are analyzed. However, note that due to the appearance of derivatives of Λ_j^ϵ with respect to z^1 and z^2 on the right–hand side of the governing PDE (4.41a), special emphasis is required for the case $\epsilon = 0$, where Λ_j^ϵ is no longer continuously differentiable. In order to analyze also this case, the weak or variational form has be considered by introducing a class of suitable test functions. Moreover, the weak form provides a useful basis for the numerical analysis of the equations of motion by means of a weighted residual approach.

4.2.4 Weak or Variational form of the Equations of Motion

For $\epsilon = 0$, the indicator function $\varrho^\epsilon(\cdot)$ is by assumption equivalent to the Heaviside function such that $\varrho^0(\cdot) = \sigma(\cdot)$. In this case, the strong form (4.41a)–(4.41g) is not well–defined and the analysis of the system dynamics requires to introduce the respective weak or variational form. For this, subsequently only the case of $\partial\Omega_c \neq \emptyset$ is considered but more general situations can be analyzed similarly. Hence, set $z = (z^1, z^2)$ and introduce the Hilbert space

$$H^2_{\partial\Omega_c}(\Omega) = \{w \in H^2(\Omega) : \, w|_{z\in\partial\Omega_c} = \partial_{\mathfrak{n}} w|_{z\in\partial\Omega_c} = 0\}. \tag{4.42}$$

Subsequently, let $\mathcal{V} = H^2_{\partial\Omega_c}(\Omega)$ and let $\mathcal{H} = L^2(\Omega)$ equipped with the inner product

$$\langle w, \hat{w}\rangle_{\mathcal{H}} = \int_\Omega \rho w \overline{\hat{w}} \, \mathrm{d}\Omega, \tag{4.43}$$

where $\rho = \rho(z)$ denotes the spatially varying density per unit area, which is strictly positive and real. Multiplication of the PDE (4.41a) with a test function $\Upsilon(z) \in \mathcal{V}$ and sequentially applying the divergence theorem (4.39) taking into account (4.40) and the boundary conditions (4.41b)–(4.41f) results in

$$\begin{aligned}
&\big\langle \partial_t^2 w^3(t), \Upsilon\big\rangle_{\mathcal{H}} + \big\langle \tilde{\nu}\partial_t w^3(t), \Upsilon\big\rangle_{\mathcal{H}} + \varsigma_p^c\big(w^3(t), \Upsilon\big) + \varsigma_p^{p,b}\big(w^3(t), \Upsilon\big) = \\
&- \sum_{l\in M} U_l^p(t) \Gamma_l^0 \times \\
&\Bigg(\Big\langle \Lambda_l^\epsilon, \frac{1}{\rho}\big[a_{1,l}^{11}\partial_{z^1}^2\Upsilon + a_{1,l}^{22}\partial_{z^2}^2\Upsilon + \big(a_{1,l}^{12} + a_{1,l}^{21}\big)\partial_{z^1}\partial_{z^2}\Upsilon\big]\cos\alpha_l \Big\rangle_{\mathcal{H}} + \\
&\Big\langle \Lambda_l^\epsilon, \frac{1}{\rho}\big[a_{2,l}^{11}\partial_{z^1}^2\Upsilon + a_{2,l}^{22}\partial_{z^2}^2\Upsilon + \big(a_{2,l}^{12} + a_{2,l}^{21}\big)\partial_{z^1}\partial_{z^2}\Upsilon\big]\sin\alpha_l \Big\rangle_{\mathcal{H}} \Bigg)
\end{aligned} \tag{4.44}$$

with $\tilde{\nu} = \nu/\rho$. Consider now the linear functionals

$$\begin{aligned}\varsigma^1(w,\hat{w}) &= \varsigma_p^c\big(w,\hat{w}\big) + \varsigma_p^{p,b}\big(w,\hat{w}\big)\\ &= \int_\Omega \Big(\mu^1\partial_{z^1}^2 w\overline{\partial_{z^1}^2\hat{w}} + \mu^2\partial_{z^2}^2 w\overline{\partial_{z^2}^2\hat{w}} + \mu^3\Delta w\overline{\Delta\hat{w}}\\ &\quad + \mu^4\partial_{z^1}\partial_{z^2}w\overline{\partial_{z^1}\partial_{z^2}\hat{w}}\\ &\quad + \mu^5\big(\partial_{z^1}^2 w + \partial_{z^1}\partial_{z^2}w\big)\overline{\big(\partial_{z^1}^2\hat{w} + \partial_{z^1}\partial_{z^2}\hat{w}\big)}\\ &\quad + \mu^6\big(\partial_{z^2}^2 w + \partial_{z^1}\partial_{z^2}w\big)\overline{\big(\partial_{z^2}^2\hat{w} + \partial_{z^1}\partial_{z^2}\hat{w}\big)}\Big)\mathrm{d}\Omega \qquad (4.45)\\ \varsigma^2(w,\hat{w}) &= \big\langle\tilde{\nu}w,\hat{w}\big\rangle_{\mathcal{H}} \qquad (4.46)\end{aligned}$$

for $w,\ \hat{w} \in \mathcal{V}$ such that $\varsigma^1 : \mathcal{V}\times\mathcal{V} \to \mathbb{C}$ and $\varsigma^2 : \mathcal{H}\times\mathcal{H} \to \mathbb{C}$. It can be easily shown that ς^j, $j = 1, 2$, represent sesquilinear forms according to Definition B.10. Furthermore, the following properties can be verified.

Lemma 4.1. *The sesquilinear forms* $\varsigma^1 : \mathcal{V}\times\mathcal{V} \to \mathbb{C}$ *and* $\varsigma^2 : \mathcal{H}\times\mathcal{H} \to \mathbb{C}$ *defined by* (4.45) *and* (4.46) *satisfy*

(i) $\forall w, \hat{w} \in \mathcal{V} :\ \varsigma^j(w,\hat{w}) = \overline{\varsigma^j(\hat{w},w)}$
(ii) $\exists c_1 \geq 0$ *s.t.* $\forall w, \hat{w} \in \mathcal{V} :\ |\varsigma^1(w,\hat{w})| \leq c_1\|w\|_{\mathcal{V}}\|\hat{w}\|_{\mathcal{V}}$
(iii) $\exists k_1 > 0$ *s.t.* $\forall w \in \mathcal{V} :\ \Re\{\varsigma^1(w,w)\} = \varsigma^1(w,w) \geq k_1\|w\|_{\mathcal{V}}^2$
(iv) $\exists c_2 \geq 0$ *s.t.* $\forall w, \hat{w} \in \mathcal{H} :\ |\varsigma^2(w,\hat{w})| \leq c_2\|w\|_{\mathcal{H}}\|\hat{w}\|_{\mathcal{H}}$
(v) $\exists k_2 > 0$ *s.t.* $\forall w \in \mathcal{H} :\ \Re\{\varsigma^2(w,w)\} = \varsigma^2(w,w) \geq k_2\|w\|_{\mathcal{H}}^2$

i.e. both ς^1 *and* ς^2 *are symmetric, continuous, and coercive, which implies that* ς^1 *is* $\mathcal{V}$*–elliptic and* ς^2 *is* $\mathcal{H}$*–elliptic.*

Proof. The symmetry property (i) is obviously satisfied, which implies that $\varsigma^j(w,\hat{w})$, $j = 1, 2$ are real. For the proof of property (ii) let $c_1' = \max_j(\sup_{z\in\Omega}|\mu^j(z)|)$ and take into account the Hölder inequality. Then the sequence of inequalities is obtained

$$\begin{aligned}&|\varsigma^1(w,\hat{w})|\\ &\leq c_1'\Big\{\int_\Omega\big|\partial_{z^1}^2 w\overline{\partial_{z^1}^2\hat{w}}\big|\mathrm{d}\Omega + \int_\Omega\big|\partial_{z^2}^2 w\overline{\partial_{z^2}^2\hat{w}}\big|\mathrm{d}\Omega + \int_\Omega\big|\Delta w\overline{\Delta\hat{w}}\big|\mathrm{d}\Omega\\ &\quad + \int_\Omega\big|\partial_{z^1}\partial_{z^2}w\overline{\partial_{z^1}\partial_{z^2}\hat{w}}\big|\mathrm{d}\Omega\\ &\quad + \int_\Omega\big|\big(\partial_{z^1}^2 w + \partial_{z^1}\partial_{z^2}w\big)\overline{\big(\partial_{z^1}^2\hat{w} + \partial_{z^1}\partial_{z^2}\hat{w}\big)}\big|\mathrm{d}\Omega\\ &\quad + \int_\Omega\big|\big(\partial_{z^2}^2 w + \partial_{z^1}\partial_{z^2}w\big)\overline{\big(\partial_{z^2}^2\hat{w} + \partial_{z^1}\partial_{z^2}\hat{w}\big)}\big|\mathrm{d}\Omega\Big\}\\ &\leq c_1'\Big\{2\big\|\partial_{z^1}^2 w\big\|_{L^2}\big\|\partial_{z^1}^2\hat{w}\big\|_{L^2} + 2\big\|\partial_{z^2}^2 w\big\|_{L^2}\big\|\partial_{z^2}^2\hat{w}\big\|_{L^2}\\ &\quad + \big\|\partial_{z^1}\partial_{z^2}w\big\|_{L^2}\big\|\partial_{z^1}\partial_{z^2}\hat{w}\big\|_{L^2} + \big\|\partial_{z^1}^2 w + \partial_{z^1}\partial_{z^2}w\big\|_{L^2}\big\|\partial_{z^1}^2\hat{w} + \partial_{z^1}\partial_{z^2}\hat{w}\big\|_{L^2}\\ &\quad + \big\|\partial_{z^2}^2 w + \partial_{z^1}\partial_{z^2}w\big\|_{L^2}\big\|\partial_{z^2}^2\hat{w} + \partial_{z^1}\partial_{z^2}\hat{w}\big\|_{L^2}\Big\}\end{aligned}$$

$$\leq 7c_1'\|w\|_{\mathcal{V}}\|\hat{w}\|_{\mathcal{V}} = c_1\|w\|_{\mathcal{V}}\|\hat{w}\|_{\mathcal{V}}$$

for all $w,\ \hat{w} \in \mathcal{V}$. To verify (iii) observe that for any $w \in \mathcal{V}$ and $\mu^j \geq 0$

$$\begin{aligned}
\varsigma^1(w,w) &= \int_\Omega \Big\{\mu^1\big|\partial_{z^1}^2 w\big|^2 + \mu^2\big|\partial_{z^2}^2 w\big|^2 + \mu^3\big|\Delta w\big|^2 + \mu^4\big|\partial_{z^1}\partial_{z^2} w\big|^2 \\
&\quad + \mu^5\big|\big(\partial_{z^1}^2 w + \partial_{z^1}\partial_{z^2} w\big)\big|^2 + \mu^6\big|\big(\partial_{z^2}^2 w + \partial_{z^1}\partial_{z^2} w\big)\big|^2\Big\}\mathrm{d}\Omega \\
&\geq \int_\Omega \left\{\mu^1\big|\partial_{z^1}^2 w\big|^2 + \mu^2\big|\partial_{z^2}^2 w\big|^2 + 2\frac{\mu^4}{2}\big|\partial_{z^1}\partial_{z^2} w\big|^2\right\}\mathrm{d}\Omega \\
&\geq k_1 \int_\Omega \left\{\big|\partial_{z^1}^2 w\big|^2 + \big|\partial_{z^2}^2 w\big|^2 + 2\big|\partial_{z^1}\partial_{z^2} w\big|^2\right\}\mathrm{d}\Omega \\
&= k_1\|w\|_{\mathcal{V}}^2
\end{aligned}$$

for $k_1 = \min\{\inf_{z\in\Omega}\mu^1(z)), \inf_{z\in\Omega}\mu^2(z)), \inf_{z\in\Omega}\mu^4(z))/2\}$. Taking into account property (i) implies (iii).

Proceeding similarly yields the existence of a constant $c_2 > 0$ such that

$$|\varsigma^2(w,\hat{w})| \leq \int_\Omega \rho\tilde{\nu} w\overline{\hat{w}}\mathrm{d}\Omega \leq c_2\|w\|_{\mathcal{H}}\|\hat{w}\|_{\mathcal{H}},$$

for all $w,\ \hat{w} \in \mathcal{H}$, which proves (iv). Moreover, property (v) holds since $\varsigma^2(w,\hat{w})$ is symmetric and since $\tilde{\nu}$ is bounded and strictly non–negative. □

With these properties, the Lax–Milgram theorem implies the existence of bounded, invertible linear operators $\mathfrak{A}^1 \in \mathcal{L}(\mathcal{V},\mathcal{V}')$ and $\mathfrak{A}^2 \in \mathcal{L}(\mathcal{H},\mathcal{H}')$ such that $\varsigma^1(w,\hat{w}) = \langle\mathfrak{A}^1 w,\hat{w}\rangle_{\mathcal{V}',\mathcal{V}}$ and $\varsigma^2(w,\hat{w}) = \langle\mathfrak{A}^2 w,\hat{w}\rangle_{\mathcal{H}',\mathcal{H}}$, where $\mathcal{V}'$ and $\mathcal{H}'$ are the dual spaces to $\mathcal{V}$ and $\mathcal{H}$, respectively, and $\langle\cdot,\cdot\rangle_{\mathcal{V}',\mathcal{V}}$ as well as $\langle\cdot,\cdot\rangle_{\mathcal{H}',\mathcal{H}}$ denote so–called duality pairings [22, 2, 1]. For their interpretation note that any element $w \in \mathcal{H}$ can be considered as a linear functional on $\mathcal{V} \subset \mathcal{H}$ by the mapping $v \mapsto \langle w,v\rangle_{\mathcal{H}} \in \mathbb{R}$ for all $v \in \mathcal{V}$ and thus as an element of the dual space $\mathcal{V}'$. Furthermore, $\mathcal{H}$ can be identified with $\mathcal{H}'$ by the Riesz representation theorem B.7. With this, the sequence of continuous and dense embeddings $\mathcal{V} \hookrightarrow \mathcal{H} \cong \mathcal{H}' \hookrightarrow \mathcal{V}'$ is obtained, which forms a so–called Gelfand triple with $\mathcal{H}$ serving as the pivot space. It is a consequence of the Riesz representation theorem that linear functionals $f \in \mathcal{V}'$ acting on $\mathcal{V}$ can be continuously extended to the larger space $\mathcal{H}$ if and only if f is of the form $f(x) = \langle y,x\rangle_{\mathcal{H}}$ for fixed $y \in \mathcal{H}$ and all $x \in \mathcal{V}$. By considering the duality pairing $\langle f,v\rangle_{\mathcal{V}',\mathcal{V}}$, which is the extension of the inner product $\langle\cdot,\cdot\rangle_{\mathcal{H}}$ from $\mathcal{V}\times\mathcal{H}$ to $\mathcal{V}'\times\mathcal{H}$, linear functions $f \in \mathcal{V}'$ admit the representation $f(v) = \langle f,v\rangle_{\mathcal{V}',\mathcal{V}}$. As a result, the weak or variational form (4.44) can be equivalently either written as

$$\begin{aligned}
&\big\langle\partial_t^2 w^3(t),\Upsilon\big\rangle_{\mathcal{V}',\mathcal{V}} + \big(\mathfrak{A}^1 w^3(t)\big)(\Upsilon) + \big(\mathfrak{A}^2\partial_t w^3(t)\big)(\Upsilon) = f(\Upsilon,t) \\
&w^3(0) = w_0^3,\ \partial_t w^3(0) = w_1^3
\end{aligned} \tag{4.47a}$$

with

$$
\begin{aligned}
f(\Upsilon,t) = &- \sum_{l\in M} U_l^p(t)\Gamma_l^0 \times \\
&\Bigg(\left\langle \Lambda_l^\epsilon, \frac{1}{\rho}\left[a_{1,l}^{11}\partial_{z^1}^2\Upsilon + a_{1,l}^{22}\partial_{z^2}^2\Upsilon + \left(a_{1,l}^{12}+a_{1,l}^{21}\right)\partial_{z^1}\partial_{z^2}\Upsilon\right]\cos\alpha_l \right\rangle_{\mathcal{H}} \\
&+ \left\langle \Lambda_l^\epsilon, \frac{1}{\rho}\left[a_{2,l}^{11}\partial_{z^1}^2\Upsilon + a_{2,l}^{22}\partial_{z^2}^2\Upsilon + \left(a_{2,l}^{12}+a_{2,l}^{21}\right)\partial_{z^1}\partial_{z^2}\Upsilon\right]\sin\alpha_l \right\rangle_{\mathcal{H}} \Bigg).
\end{aligned}
\tag{4.47b}
$$

or interpreted as an abstract differential equation

$$
\begin{aligned}
&\partial_t^2 w^3(t) + \mathfrak{A}^1 w^3(t) + \mathfrak{A}^2 \partial_t w^3(t) = f(t) \\
&w^3(0) = w_0^3,\ \partial_t w^3(0) = w_1^3
\end{aligned}
\tag{4.48}
$$

in the dual space $\mathcal{V}'$. With these considerations existence and uniqueness of solutions can be established following [2, Theorem 4.1] by making use of Lemma 4.1 and the Lax–Milgram theorem, as is summarized below.

Theorem 4.1. *Let $w_0^3 \in \mathcal{V}$, $w_1^3 \in \mathcal{H}$, and $f \in L^2((0,\tau),\mathcal{H}')$. Then there exists a unique solution of* (4.47) *or* (4.48)*, respectively, with $w^3 \in L^2((0,\tau),\mathcal{V})$, $\partial_t w^3 \in L^2((0,\tau),\mathcal{H})$, and $\partial_t^2 w^3 \in L^2((0,\tau),\mathcal{V}')$. The map $(w_0^3, w_1^3, f) \to (w^3, \partial_t w^3)$ is continuous from $\mathcal{V}\times\mathcal{H}\times L^2((0,\tau),\mathcal{H}')$ to $L^2((0,\tau),\mathcal{V})\times L^2((0,\tau),\mathcal{H})$.*

Similar results are, e.g., obtained in [22]. Note that this result obviously holds for both $\epsilon = 0$ and $\epsilon > 0$ in the indicator function $\varrho^\epsilon(\cdot)$ describing the spatial actuator characteristics, which enables a treatment of the governing equations in a common framework.

4.3 Selected Applications and Control Problems

The example of a thin plate with distributed MFC actuators can be considered as a prototypical smart structure involving actuators embedded into a flexible carrier layer. The level of smartness thereby relies on the appropriate coordination of actuation and sensing by means of control and optimization. Since this benchmark example exhibits the main features of smart flexible structures generalizations can be derived both in view of the development of control design systematics and novel applications. While a comprehensive discussion is outside the scope of this contribution, subsequently selected control problems are briefly highlighted together with prospective application areas.

4.3.1 Motion Planning and Transient Elastic Shaping of Structures

The realization of prescribed transient changes in the deflection profile of flexible structures facilitates new and innovative applications comprising

- adaptive optics, where deformable mirrors are used, e.g., in earth bound telescopes to compensate atmospheric distortions;
- flow control, where transient deformations are used to influence the evolving boundary layers and the resulting flow field;
- flapping wing structures mimicking the flight motion of insects or birds;
- morphing structures involving large deformations of the structural configuration to achieve shape changes.

Herein, it is on the one hand desired to develop systematic strategies for the determination of input signals to the actuators to realize the desired elastic motion of the in general 2– or 3–dimensional flexible structure. This feedforward control problem moreover includes motion planning approaches to derive spatial–temporal trajectories for deflection or strain in certain regions of interest Ω_y^i of the spatial domain Ω. In view of the considered thin plate with distributed MFC actuators, this implies that

$$y^i(t) = \int_{\Omega_y^i} c^i(z) w^3(z,t) \mathrm{d}\Omega_y^i, \qquad i = 1, \ldots, p \tag{4.49}$$

or more generally $y^i(z,t) = w^3(z,t)|_{z \in \Omega_y^i}$, $i = 1, \ldots, p$, has to follow a desired spatial–temporal path $y^{i,*}(t)$ or $y^{i,*}(z,t)$, respectively. Note that the problem formulation includes rest–to–rest motion as is commonly used in multi–body or robot dynamics. This is thoroughly addressed in Section 6.6, where experimental results are presented for a flexible plate structure with spatially distributed piezoelectric patch actuators.

On the other hand, the realization of the desired motion in general relies on the incorporation of suitable feedback control strategies to compensate model errors or exogenous disturbances acting on the structure.

4.3.2 Vibration Suppression and Elastic Motion Tracking

Vibration suppression can be essentially interpreted as the robust stabilization of an equilibrium by suitably processing measurement data. However, in view of the realization of prescribed spatial–temporal deflection profiles $w^*(z,t)$ this is equivalent to either the exponential

$$\|w(z,t) - w^*(z,t)\|_X \leq M e^{-\alpha t}, \qquad M,\, \alpha > 0$$

or asymptotic

$$\|w(z,t) - w^*(z,t)\|_X \to 0 \quad \text{as} \quad t \to \infty$$

convergence to the desired state. In order to achieve tracking of the desired elastic motion in general feedforward control and methods of feedback stabilization

are combined according to the 2DOF control concept schematically depicted in Figure 1.1. Examples of the application and the resulting tracking performance achieved by making use of the 2DOF control concept for elastomechanical structures can be, e.g., found in [9, 8, 16, 13, 5, 25] and the references therein.

References

1. Alt, H.: Lineare Funktionalanalysis, 4th edn. Springer, New York (2000)
2. Banks, H., Smith, R., Wang, Y.: Smart Material Structures: Modeling, Estimation and Control. John Wiley & Sons, Chichester (1996)
3. Haupt, P.: Continuum Mechanics and Theory of Materials, 2nd edn. Springer, Heidelberg (2002)
4. Lagnese, J., Lions, J.L.: Modelling analysis and control of thin plates. Collection recherches en mathématiques appliquées. Masson, Paris (1989)
5. Macchelli, A., Melchiorri, C.: A formal method for improving the transient behaviour of a non–linear flexible link. Math. Comp. Model Dyn. Sys (MCMDS) 17(1), 3–18 (2011)
6. Marsden, J., Hughes, T.: Mathematical Foundations of Elasticity. Dover Publications Inc., Mineola (1994)
7. Meirovitch, L.: Principles and Techniques of Vibrations. Prentice Hall, New Jersey (1997)
8. Meurer, T., Kugi, A.: Tracking control design for a wave equation with dynamic boundary conditions modeling a piezoelectric stack actuator. Int. J. Robust Nonlin. 21(5), 542–562 (2011)
9. Meurer, T., Thull, D., Kugi, A.: Flatness–based tracking control of a piezoactuated Euler–Bernoulli beam with non–collocated output feedback: theory and experiments. Int. J. Contr. 81(3), 475–493 (2008)
10. Nowacki, W.: Dynamic Problems of Thermoelasticity. Noordhoff Int. Publ., PWN–Polish Scientific Publ., Warszawa (1975)
11. Preumont, A.: Vibration Control of Active Structures, 2nd edn. Kluwer Academic, Dordrecht (2002)
12. Reddy, J.: Energy and Variational Methods in Applied Mechanics. Wiley–Interscience, New York (1984)
13. Schröck, J.: Mathematical Modeling and Tracking Control of Piezo–actuated Flexible Structures. PhD thesis, Automation and Control Institute, Vienna University of Technology (2011)
14. Schröck, J., Meurer, T., Kugi, A.: Control of a flexible beam actuated by macro-fiber composite patches – Part I: Modelling and feedforward trajectory control. Smart Mater. Struct. 20(1), article 015015, 7 pages (2011)
15. Schröck, J., Meurer, T., Kugi, A.: Control of a flexible beam actuated by macro-fiber composite patches – Part II: Hysteresis and creep compensation, experimental results. Smart Mater. Struct. 20(1), article 015016, 11 pages (2011)
16. Schröck, J., Meurer, T., Kugi, A.: Non–collocated Feedback Stabilization of a Non–Uniform Euler–Bernoulli Beam with In–Domain Actuation. In: Proc. IEEE Conference on Decision and Control (CDC), Orlando (FL), USA, pp. 2776–2781 (2011)
17. Slaughter, W.: The Linearized Theory of Elasticity. Birkhäuser, Basel (2002)
18. Smith, R.: Smart Material Systems: Model Development. SIAM, Philadelphia (2005)

19. Spong, M., Vidyasagar, M.: Robot Dynamics and Control. John Wiley & Sons, New York (1989)
20. Wilkie, W., Bryant, R., High, J., Fox, R., Hellbaum, R., Jalink, A., Little, B., Mirick, P.: Low–Cost Piezocomposite Actuator for Structural Control Applicationd. In: Smart Structures and Materials 2000: Industrial and Commercial Applications of Smart Structures Technologies, SPIE, Newport Beach (CA), USA, vol. 3991, pp. 323–334 (2000)
21. Williams, R., Park, G., Inman, D., Wilkie, W.: An overview of composite actuators with piezoceramic fibers. In: Proc. 20th Modal Analysis Conference, Los Angeles (CA), USA (2002)
22. Wloka, J.: Partial Differential Equations. Cambridge University Press, Cambridge (1987)
23. Yourgrau, W., Mandelstam, S.: Variational Principles in Dynamics and Quantum Theory, 3rd edn. Dover Publications Inc., Mineola (2007)
24. Yousefi-Koma, A., Zimcik, D.: Applications of Smart Structures to Aircraft for Performance Enhancement. Canadian Aeronautics and Space Journal 49(4), 163–173 (2003)
25. Zimmert, N., Pertsch, A., Sawodny, O.: 2–DOF Control of a Fire–Rescue Turntable Ladder. IEEE Trans. Control Sys. Tech. 20(2), 438–452 (2012)

Chapter 5
Mathematical Problem Formulation

The results obtained for the modeling examples of Chapters 2–4 can be embedded in a general mathematical setting involving parabolic diffusion–convection–reaction systems (Chapters 2 and 3) or so–called biharmonic Petrowski systems (Chapter 4) defined on bounded higher–dimensional domains. This enables a rigorous formulation of the subsequently analyzed control problems.

5.1 General System Setting

Let Ω be an open bounded subset of $\mathbb{R}^r$ and set $\mathcal{Q}_T = \Omega \times (t_0, t_0 + \tau)$ for some fixed $\tau > 0$ as well as $\partial\mathcal{Q}_T := \partial\Omega \times (t_0, t_0+\tau)$ with $\partial\Omega$ the boundary of Ω. Multi–index notation is used with the multi–index $k = \{k^1, \ldots, k^r\}$, $|k| = k^1 + \cdots + k^r$ such that $D^k = D_{z^1}^{k^1} \cdots D_{z^r}^{k^r}$ with $D_{z^i}^1 = \partial_{z^i}$ and $D_{z^i}^0 = 1$. Hence, let

$$\begin{aligned} \mathfrak{L}(z,t)\boldsymbol{x}(z,t) &:= \left[\sum_{j=1}^{n} \mathfrak{L}_{i,j}(z,t)x^j(z,t)\right]_{i=1}^{n} \\ \mathfrak{L}_{i,j}(z,t) &= \sum_{1\le|k|\le 2K} a_{i,j}^k(z)D^k + a_{i,j}^0(z,t) \end{aligned} \tag{5.1}$$

$$\begin{aligned} \mathfrak{K}(z,t)\boldsymbol{x}(z,t) &:= \left[\sum_{j=1}^{n} \mathfrak{K}_{i,j}(z,t)x^j(z,t)\right]_{i=1}^{n'} \\ \mathfrak{K}_{i,j}(z,t) &= \sum_{1\le|k|<2K} p_{i,j}^k(z)D^k + p_{i,j}^0(z,t) \end{aligned} \tag{5.2}$$

$$\begin{aligned} \mathfrak{G}(z)\boldsymbol{x}(z,t) &:= \left[\sum_{j=1}^{n} \mathfrak{G}_{i,j}(z)x^j(z,t)\right]_{i=1}^{p} \\ \mathfrak{G}_{i,j}(z)x^j(z,t) &= \int_\Omega \sum_{|k|<2K} r_{i,j}^k(z,\zeta)D^k x^j(\zeta,t)\mathrm{d}\Omega \end{aligned} \tag{5.3}$$

T. Meurer: Control of Higher-Dimensional PDEs, CCE, pp. 77–80.
springerlink.com

denote operators acting on the state vector $\boldsymbol{x}(z,t) = [x^1(z,t), \ldots, x^n(z,t)]^T$ with $K \in \{1,2\}$. Since $\mathfrak{L}(z,t)$ is a differential operator of order $2K$ defined on the domain Ω, in general $n' = 2nr$ boundary conditions are required, which are subsequently described by $\mathfrak{K}(z,t)$ in terms of the coefficients $p^k_{i,j}(z)$ and $p^0_{i,j}(z,t)$. The coefficients $r^k_{i,j}(z,\zeta)$ are introduced to represent spatial sensor characteristics so that $\mathfrak{G}(z,t)$ denotes the output operator.

Notation. If $\mathfrak{L}(z,t)$, $\mathfrak{K}(z,t)$, and $\mathfrak{G}(z,t)$ are independent of t then $\mathfrak{L}(z)$, $\mathfrak{K}(z)$, and $\mathfrak{G}(z)$ is used, respectively. If in addition the dependency is clear from the context, then $\mathfrak{L}$, $\mathfrak{K}$, and $\mathfrak{G}$ are used to refer to (5.1)–(5.3), respectively. Without loss of generality in these cases $t_0 = 0$.

With these preparations, the distributed–parameter systems considered in Chapters 2– 4 can be embedded into the following class of initial–boundary–value problems

$$\partial_t \boldsymbol{x}(z,t) = \mathfrak{L}(z,t)\boldsymbol{x}(z,t) + \mathfrak{F}(z)\boldsymbol{u}_\Omega(z,t), \qquad (z,t) \in \mathcal{Q}_T \tag{5.4a}$$

$$\mathfrak{K}(z,t)\boldsymbol{x}(z,t) = \boldsymbol{u}_{\partial\Omega}(z,t), \qquad (z,t) \in \partial\mathcal{Q}_T \tag{5.4b}$$

$$\boldsymbol{y}(z,t) = \mathfrak{G}(z)\boldsymbol{x}(z,t), \qquad t \in \overline{\mathbb{R}^+_{t_0}} \tag{5.4c}$$

$$\boldsymbol{x}(z,t_0) = \boldsymbol{x}_0(z), \qquad z \in \overline{\Omega}. \tag{5.4d}$$

Here, $\mathfrak{F}(z)$ is an input operator describing the spatial actuator characteristics and location. The vectors $\boldsymbol{u}_\Omega(z,t) = [u^1_\Omega(z,t) \ldots, u^{m_\Omega}_\Omega(z,t)]^T$ and $\boldsymbol{u}_{\partial\Omega}(z,t) = [u^1_{\partial\Omega}(z,t), \ldots, u^{m_{\partial\Omega}}_{\partial\Omega}(z,t)]^T$ with $m = m_\Omega + m_{\partial\Omega}$ represent the distributed in–domain and boundary input, respectively, where so far no distinction is made between infinite– and finite–dimensional control inputs. Note that besides inhomogeneous boundary conditions a suitable choice of the components $\boldsymbol{u}_{\partial\Omega}(z,t)$ enables to introduce locally or globally homogeneous Robin boundary conditions. The notions 'local' and 'global' thereby refer to the fact that each of the components of $\boldsymbol{u}_{\partial\Omega}(z,t)$ might be zero only on a subset of $\partial\Omega$ (local) or zero for all $(z,t) \in \partial\mathcal{Q}_T$ (global). Similarly, Dirichlet and Neumann boundary conditions can be included for each of the components by means of the operator $\mathfrak{K}(z,t)$. The system output is given by $\boldsymbol{y}(z,t) = [y^1(z,t), \ldots, y^p(z,t)]^T$ and relates $\boldsymbol{x}(z,t)$ and its derivatives $D^k\boldsymbol{x}(z,t)$ up to order $|k| = 2K-1$ according to $\mathfrak{G}(z,t)$, which provides spatially averaged or pointwise information depending on the coefficients $r^k_{i,j}(z,\zeta)$.

In the following, additional assumptions are imposed to restrict the analysis to parabolic PDEs (in the sense of Petrowski) with bounded and suitably differentiable coefficients.

Assumption 5.1. Consider (5.1) and (5.4), then it is assumed that

(i) the PDE (5.4a) is uniformly parabolic in the sense of Petrowski, i.e. there exists a constant $\theta > 0$ such that all roots ς_l of

$$\det\left[\sum_{|k|=2K} a^k_{i,j}(z)(\imath\xi)^k - \delta_{ij}\varsigma\right]_{i,j=1,\ldots,n} = 0$$

with $\xi \in \mathbb{R}^r$, $|\xi| = 1$ satisfy $\max_l \sup_{|\xi|=1} \Re\{\varsigma_l\} \leq -\theta$ for all $z \in \Omega$;
(ii) the coefficients $a_{i,j}^k(z)$ of (5.1) are continuous bounded functions on $\mathcal{Q}_T$.

Together with additional restrictions on the domains of $\boldsymbol{u}_\Omega(z,t)$ and $\boldsymbol{u}_{\partial\Omega}(z,t)$ these assumptions imply existence, uniqueness, and regularity of in general only weak solutions to (5.4). For further details, the reader is referred, e.g., to [2, 4, 3, 1].

5.2 Trajectory Planning and Tracking Control

The considered trajectory planning and tracking control problem for (5.4) concerns the design of input trajectories $(\boldsymbol{u}_\Omega(z,t), \boldsymbol{u}_{\partial\Omega}(z,t))$ to realize transitions from an initial (stationary) profile $\boldsymbol{x}_0(z)$ to a desired final profile

$$\boldsymbol{x}(z, t_0 + T) = \boldsymbol{x}_T(z), \qquad z \in \overline{\Omega} \tag{5.5}$$

along a prescribed spatial–temporal transition path $\boldsymbol{x}^*(z,t)$ within the finite time–interval $t \in [t_0, t_0 + T]$, i.e.

$$\boldsymbol{x}_0(z) = \boldsymbol{x}(z,t_0) \xrightarrow[t\in[t_0,t_0+T]]{(\boldsymbol{u}_{\partial\Omega}(z,t),\, \boldsymbol{u}_\Omega(z,t))} \boldsymbol{x}(z, t_0+T) = \boldsymbol{x}_T(z). \tag{5.6}$$

Here, $T > 0$ denotes the specified transition time. This configuration in particular includes the finite time transition problem between stationary profiles, where the final profile is required to satisfy $\boldsymbol{x}(z,t) = \boldsymbol{x}_T(z)$ for $t \geq t_0 + T$ with $\boldsymbol{x}_T(z)$ representing a steady state solution of (5.4). From a practical point of view, this corresponds to important control tasks such as the start–up and the shutdown of reactors, or the transition between operating points, which typically arise in thermal, chemical, and biochemical engineering as well as related areas.

For the solution of the control problem, flatness–based methods for trajectory planning are presented in Part III. Here, at first a spectral design approach is introduced in Chapter 6 for the case of time–invariant PDE–systems defined on a rather general spatial domain Ω. Secondly, a formal integration approach is proposed in Chapter 7 for time varying scalar diffusion–convection–reaction systems, i.e. $n = 1$ in (5.4), with parallelepiped domain. The state–feedback stabilization and state–observer design is addressed in Part IV by exploiting and extending the backstepping technique to boundary controlled distributed–parameter systems with spatially and time varying parameters. Besides the analysis of PDEs defined on the line in Section 8 this covers higher–dimensional parallelepiped domains and configurations comprising multiple inputs and outputs in Section 9. In addition, it is thereby shown that a suitable reformulation of the backstepping approach enables an integrated tracking control design to achieve the exponentially stable tracking of desired trajectories for unstable distributed–parameter systems.

References

1. Evans, L.: Partial Differential Equations, Graduate Studies in Mathematics, vol. 19. American Mathematical Society, Rhode Island (2002)
2. Friedman, A.: Partial differential equations of parabolic type. Prentice–Hall, Englewood Cliffs (NJ) (1964)
3. Ladyženskaja, O., Solonnikov, V., Ural'ceva, N.: Linear and Quasi–linear Equations of Parabolic Type. Translations of Mathematical Monographs, 5th edn., vol. 23. American Mathematical Society, Rhode Island (1998)
4. Lions, J., Magenes, E.: Non–Homogeneous Boundary Value Problems and Applications, vol. 3. Springer, Berlin (1973)

Chapter 6
Spectral Approach for Time–Invariant Systems with General Spatial Domain

The spectral analysis of a finite– or infinite–dimensional linear operator is a well–established and profound mathematical tool for stability analysis and feedback control design. The dynamic system properties are thereby determined based on the eigenvalue distribution and the respective set of eigenvectors. For infinite–dimensional systems governed by PDEs certain restrictions apply, which are in particular related to the possible existence of continuous spectra. Fortunately, a wide class of physically important systems including, e.g., diffusion–convection–reaction, wave, Euler–Bernoulli, and Timoshenko beam equations, yields so–called Riesz spectral operators, which exhibit a purely discrete eigenvalue distribution and whose eigenvectors and adjoint eigenvectors, respectively, span a basis for the underlying function space. These properties can be advantageously exploited for the controllability and observability analysis similar to the finite–dimensional case [14]. Furthermore, Riesz spectral operators satisfy the spectrum determined growth assumption such that the stability properties of the system can be directly determined based on the eigenvalue distribution [14, 37]. This property can be in particular utilized for the stabilizability and stability analysis as well as for the design of stabilizing state–feedback controllers, see, e.g., [65, 33, 13, 48, 49, 37] and the references therein.

In the following, a spectral approach is proposed for the solution of the trajectory planning problem for time–invariant distributed–parameter systems governed by Riesz spectral operators defined on a general spatial domain. For this, it is at first required to re–formulate the governing PDE(s) and boundary conditions in an abstract operator theoretic framework in suitable Hilbert spaces. Herein, special emphasis is required for the case of unbounded input operators arising, e.g., in the case of boundary control or pointwise in–domain control. As outlined in Section 6.1, this leads to the introduction of admissible control operators and hence well–posed systems by interpreting the range of the operators in a larger sense. Thereby, two approaches based on either suitable operator extensions or homogenization of boundary conditions are presented to cover boundary control problems. In order to be able to consider a large class of systems in a common framework, Riesz spectral operators are introduced in a rather general setting by taking into account operators whose generalized eigenfunctions and generalized adjoint eigenfunctions form

T. Meurer: Control of Higher-Dimensional PDEs, CCE, pp. 83–188.
springerlink.com

a orthonormal Riesz basis. This in particular includes the case when the geometric multiplicity of an eigenvalue is strictly less than its algebraic multiplicity.

Given a well–posed abstract system with Riesz spectral system operator, the trajectory planning problem is considered in Section 6.2. Here it is shown that a general systematic solution can be obtained by a suitable re–interpretation of the resolvent operator and the introduction of a flat or basic output, which allows to parametrize system states and control inputs. Hence, by prescribing an appropriate desired trajectory for the basic output the evaluation of the input parametrization directly yields the feedforward control, which realizes the corresponding spatial–temporal state profile imposed by the state parametrization. This, however, requires to ensure the uniform convergence of the state and input parametrizations by means of differential operators of infinite order applied to the basic output. As is shown in Section 6.3, the convergence problem has to be addressed twofold. On the one hand, convergence can be reduced to a problem of trajectory assignment for the basic output, which in general has to be restricted to a certain Gevrey class. On the other hand, additional restrictions apply, which are related to the controllability property. The latter essentially depends on the geometry of the spatial domain and the number, the dimension, and the location of the control inputs. The determination of spatial–temporal paths for the basic output ensuring convergence is considered in Section 6.4. Herein, finite time transitions between stationary operating profiles as well as non–stationary states are embedded into a systematic framework including their numerical evaluation.

The spectral trajectory planning approach is analyzed and validated by means of simulations in Section 6.5 for a selection of application examples. This comprises the heat and wave equation with in–domain control and 1–dimensional spatial domain in Section 6.5.1. The results obtained for the wave equation confirm that the presented approach is also applicable to hyperbolic systems with a finite speed of wave propagation. Here, it is shown that the parametrizations in terms of differential operators of infinite order converge to shift operators, which reflect the wave speed. Moreover, the trajectory planning problem is solved for systems with higher–dimensional spatial domains. For this, a linear diffusion–reaction equation on an Riemannian manifold and a linear diffusion–convection–reaction system on a parallelepiped domain are analyzed in Sections 6.5.2 and 6.5.3, respectively. Thereby, it is assumed that the control input is restricted to a subset of the domain's boundary. In addition, two control configurations are analyzed, namely infinite–dimensional and finite–dimensional boundary control. While the first is mainly of theoretical interest it allows to determine rather general results. For finite–dimensional boundary control in terms of a finite number of patch actuators, it is shown that the state and input parametrizations in general diverge for the realization of finite time transitions between stationary profiles. However, it is exemplarily shown that the incorporation of divergent parametrizations involving suitable summability methods into the presented spectral design methodology significantly enhances its domain of applicability.

Finally an experimental validation of the design systematics is provided in Section 6.6 for a flexible plate structure with spatially distributed piezoelectric patch

actuators. Herein, the weak formulation of the equations of motion is utilized for the theoretical analysis and the determination of an efficient semi–numerical implementation of the spectral design technique. Thereby, the weighted–residual approach is considered for the determination of a finite–dimensional approximation of the distributed–parameter system, which enables the numerical computation of the eigenvalue and eigenvector distribution. With this, the formal parametrizations can be reduced to differential operators of finite order and enable an approximate evaluation of the state and input parametrizations. The presented experimental results confirm the applicability of this approach and illustrate the tracking performance for high–speed rest–to–rest bending and torsional motions of the plate structure.

Notation. Throughout this chapter the explicit dependency of variables on the tuple z of spatial coordinates is consecutively dropped in accordance with the common control and operator theoretic literature. However, in certain situations the spatial argument is added to clarify and emphasize the specific character of the particular variable.

6.1 Abstract Formulation and Spectral Analysis

In order to provide a rigorous and general analysis, subsequently an abstract operational system formulation is introduced for the trajectory planning problem. For this, consider the abstract control problem governed by

$$\partial_t \boldsymbol{x}(t) = \mathfrak{L}\boldsymbol{x}(t) + \mathfrak{F}\boldsymbol{u}_\Omega(t), \qquad \boldsymbol{x}(0) = \boldsymbol{x}_0 \subset \mathcal{D}(\mathfrak{L}) \tag{6.1a}$$

$$\mathfrak{K}\boldsymbol{x}(t) = \boldsymbol{u}_{\partial\Omega}(t) \tag{6.1b}$$

$$\boldsymbol{y}(t) = \mathfrak{G}\boldsymbol{x}(t). \tag{6.1c}$$

Here, $\mathfrak{L} : \mathcal{D}(\mathfrak{L}) \subseteq Z \to X$ denotes a linear time–invariant strongly elliptic differential operator with domain $\mathcal{D}(\mathfrak{L})$ (cf. (5.1)). The space Z is called the solution space while X represents the state space. It is in particular assumed that $Z \subset X$ with continuous embedding (cf. Appendix B.3). The distributed input $\boldsymbol{u}_\Omega(t) = \boldsymbol{u}_\Omega(\cdot, t)$ is assumed to be defined on the Hilbert space U and is assigned in terms of the operator $\mathfrak{F} : \mathcal{D}(\mathfrak{F}) \subseteq U \to X$ with domain $\mathcal{D}(\mathfrak{F})$. The boundary conditions are imposed in terms of the boundary operator $\mathfrak{K} : \mathcal{D}(\mathfrak{K}) \subseteq Z \to V$ (cf. (5.2)), e.g., in terms of the boundary trace operator, with the input $\boldsymbol{u}_{\partial\Omega}(t) = \boldsymbol{u}_{\partial\Omega}(\cdot, t)$ from the Hilbert space V. Moreover, the compatibility condition $\mathfrak{K}(\cdot)\boldsymbol{x}(\cdot, 0) = \boldsymbol{u}_{\partial\Omega}(\cdot, 0)$ is assumed to hold. The output $\boldsymbol{y}(t)$ is defined on the Hilbert space Y in terms of the operator $\mathfrak{G} : X \to Y$.

Due to the in general inhomogeneous boundary conditions the abstract analysis of the evolution equation (6.1) requires special emphasis. In particular, it is desired to transfer the governing equations into the abstract form

$$\partial_t \boldsymbol{x}(t) = \mathfrak{A}\boldsymbol{x}(t) + \mathfrak{B}\boldsymbol{u}(t), \qquad t > 0 \tag{6.2a}$$

$$\boldsymbol{x}(0) = \boldsymbol{x}_0 \in \mathcal{D}(\mathfrak{A}) \tag{6.2b}$$

$$\boldsymbol{y}(t) = \mathfrak{C}\boldsymbol{x}(t), \qquad t \geq 0 \tag{6.2c}$$

with the possibly unbounded input and output operators $\mathfrak{B}$ and $\mathfrak{C}$ but purely homogeneous boundary conditions included into the proper definition of the domain $\mathcal{D}(\mathfrak{A})$ of the system operator $\mathfrak{A}$ who is the generator of a semigroup. Thereby, the well–posedness of (6.2) requires that $\mathfrak{B}$ and $\mathfrak{C}$ represent so–called admissible control and observation operators (see, e.g., [64] or [66]), which are briefly introduced in the following section.

6.1.1 Admissible Control and Observation Operators

The admissibility of the control operator $\mathfrak{B}$ follows from the continuity of mild solutions $\boldsymbol{x}(t) \in X$ of (6.2). For this, let $\boldsymbol{x}_0 \in X$, $\boldsymbol{u}(t) \in L^2_{\text{loc}}([0,\infty);U)$, $\mathfrak{B} \in \mathcal{L}(U, X_{-1})$ with X_{-1} as introduced in Lemma B.4, and assume that $\mathfrak{A}$ is the infinitesimal generator of a C_0–semigroup $\mathfrak{T}(t)$. Motivated by the classical variation of constants formula, consider the operator $\mathcal{B}_\tau \in \mathcal{L}(L^2([0,\infty);U), X_{-1})$ defined by

$$\mathcal{B}_\tau \boldsymbol{u} = \int_0^\tau \mathfrak{T}(\tau - s)\mathfrak{B}\boldsymbol{u}(s)\mathrm{d}s. \tag{6.3}$$

Note that $\mathcal{B}_\tau$ is also called the controllability map [14, Section 4], which is used for the definition of exact and approximate controllability, where either $\mathrm{ran}\mathcal{B}_\tau = X$ (exact controllability) or $\overline{\mathrm{ran}\mathcal{B}_\tau} = X$ (approximate controllability).

Definition 6.1 (Admissible control operator). The operator $\mathfrak{B} \in \mathcal{L}(U, X_{-1})$ is called an admissible control operator for $\mathfrak{T}(t)$ if $\mathrm{ran}\mathcal{B}_\tau \subset X$ for some $\tau > 0$ [66].

It should be pointed out that if $\mathfrak{B}$ is admissible then the integration in (6.3) is evaluated in X_{-1} but the integral is in X, which by definition is a dense subspace of X_{-1}. The input operator is called bounded if it can be restricted to $\mathfrak{B} \in \mathcal{L}(U, X)$ and unbounded otherwise. Moreover, it can be shown that if $\mathfrak{B}$ is admissible and $\mathrm{ran}\mathcal{B}_\tau \subset X$ for some $\tau > 0$ then $\mathcal{B}_t \in \mathcal{L}(L^2([0,\infty);U), X)$ for every $t > 0$. As a result, given an admissible control operator $\mathfrak{B} \in \mathcal{L}(U, X_{-1})$ for $\mathfrak{T}(t)$, then for every $\boldsymbol{x}_0 \in X$ and $\boldsymbol{u}(t) \in L^2_{\text{loc}}([0,\infty);U)$ the initial–value problem (6.2) has a unique solution in X_{-1} given by

$$\boldsymbol{x}(t) = \mathfrak{T}(t)\boldsymbol{x}_0 + \mathcal{B}_t\boldsymbol{u},$$

which satisfies $\boldsymbol{x}(t) \in C([0,\infty);X) \cap H^1_{\text{loc}}((0,\infty);X_{-1})$. Hence, the existence of a mild solution is guaranteed. By assuming that $\boldsymbol{u}(t) \in H^1_{\text{loc}}((0,\tau);U)$ or $\boldsymbol{u}(t) \in H^2_{\text{loc}}((0,\tau);U)$ for some $\tau \in (0,\infty)$ different regularity properties of the solution to (6.2) can be determined (cf. [66, Section 4.3]).

For the introduction of the dual concept of an admissible observation operator consider (6.2) with $\mathfrak{B} = \mathfrak{o}$, where $\mathfrak{o}$ denotes the zero operator. Let $\mathfrak{C} \in \mathcal{L}(X_1, Y)$ with X_1 given by Lemma B.3, $\boldsymbol{x}_0 \in X_1$, and assume $\mathfrak{A}$ is the infinitesimal generator of a C_0–semigroup $\mathfrak{T}(t)$. Then the resulting initial–value problem has a unique (mild) solution $\boldsymbol{x}(t) = \mathfrak{T}(t)\boldsymbol{x}_0$ [14]. Hence, in view of (6.2c), the (truncated) observation map

$$\big(\mathcal{C}_\tau \boldsymbol{x}_0\big) = \begin{cases} \mathfrak{C}\mathfrak{T}(t)\boldsymbol{x}_0, & t \in [0, \tau] \\ \mathbf{0}, & t > \tau \end{cases}$$

can be introduced such that $\mathcal{C}_\tau \in \mathcal{L}(X_1, L^2([0, \infty); Y))$. Note that the observation map can be used to define both the exact observability of the autonomous system (6.2) with $\mathfrak{B} = \mathfrak{o}$ if $\mathcal{C}_\tau$ is injective with bounded inverse as well as the approximate observability if $\ker \mathcal{C}_\tau = \{\mathbf{0}\}$ [14, Definition 4.1.12].

Definition 6.2 (Admissible observation operator). The operator $\mathfrak{C} \in \mathcal{L}(X_1, Y)$ is called an admissible observation operator for $\mathfrak{T}(t)$ if for some $\tau > 0$ the observability map $\mathcal{C}_\tau$ has a continuous extension to X [66].

This definition implies that the operator $\mathfrak{C} \in \mathcal{L}(X_1, Y)$ is an admissible observation operator for $\mathfrak{T}(t)$ if and only if for some $\tau > 0$ there exists a constant K_τ such that

$$\int_0^\tau \big\| \mathfrak{C}\mathfrak{T}(t)\boldsymbol{x}_0 \big\|_Y^2 \mathrm{d}t \leq K_\tau^2 \|\boldsymbol{x}_0\|_X^2 \qquad \forall \boldsymbol{x}_0 \in \mathcal{D}(\mathfrak{A}).$$

Moreover, an admissible observation operator $\mathfrak{C} \in \mathcal{L}(X_1, Y)$ is called bounded if it can be extended such that $\mathfrak{C} \in \mathcal{L}(X, Y)$ and unbounded otherwise.

For a detailed discussion and the summary of further properties of admissible control and observation operators the interested reader is referred to [64, 66].

6.1.2 Abstract Boundary Control Systems

With these preparations, it is now possible to transfer the inhomogeneous boundary control problem (6.1) into the abstract operator form (6.2), which serves as the fundamental basis for the subsequent sections. For this, basically two approaches are available, which either rely on suitable operator extensions [26, 48, 49, 64, 66] or are based on the homogenization of the boundary conditions and the consideration of the resulting system on an extended state space [18, 14].

6.1.2.1 Operator Extension Approach

At first let $\mathfrak{F} = \mathfrak{o}$ in (6.1) with $\mathfrak{o}$ the zero operator such that the only forcing of the system arises from the inhomogeneous boundary condition. The following treatise is

based on [66], which provides a concise generalization of the results of [26, 48, 49] on admissible input elements and their relationship to boundary control problems. Proceeding as in [66, Section 10], a boundary control system on V, Z, and X is a pair of operators $(\mathfrak{L}, \mathfrak{K})$, where $\mathfrak{L} \in \mathcal{L}(Z, X)$ and $\mathfrak{K} \in \mathcal{L}(Z, V)$ if there exists a $\beta \in \mathbb{C}$ such that the following properties hold:

(i) $\mathfrak{K}$ is onto,
(ii) $\ker\mathfrak{K}$ is dense in X,
(iii) $\beta\mathfrak{I} - \mathfrak{L}$ restricted to $\ker\mathfrak{K}$ is onto, and
(iv) $\ker(\beta\mathfrak{I} - \mathfrak{L}) \cap \ker\mathfrak{K} = \{\mathbf{0}\}$.

Under these assumptions, it is at first required to introduce the Hilbert space $X_1 = \ker\mathfrak{K}$ and the operator $\mathfrak{A} = \mathfrak{L}|_{X_1}$, i.e. the restriction of $\mathfrak{L}$ to X_1, to recast (6.1) into the familiar form (6.2). In view of (ii) it follows that X_1 is a closed subspace of Z and $\mathfrak{A} \in \mathcal{L}(X_1, X)$. Moreover, property (iii) implies that $\operatorname{ran}(\beta\mathfrak{I} - \mathfrak{L})|_{X_1} = \operatorname{ran}(\beta\mathfrak{I} - \mathfrak{A}) = X$ such that $\beta\mathfrak{I} - \mathfrak{A}$ is surjective. Since property (iv) yields $\ker(\beta\mathfrak{I} - \mathfrak{A}) = \{\mathbf{0}\}$ and thus the injectivity of $\beta\mathfrak{I} - \mathfrak{A}$ the bijectivity of $\beta\mathfrak{I} - \mathfrak{A}$ is guaranteed. Hence, for $\beta \in \rho(\mathfrak{A})$ it follows that $(\beta\mathfrak{I} - \mathfrak{A})^{-1} \in \mathcal{L}(X)$. On the other hand, the definition of X_1 and $\mathfrak{A}$ implies that $(\beta\mathfrak{I} - \mathfrak{A})^{-1} \in \mathcal{L}(X, X_1)$, which illustrates that for any $\beta \in \rho(\mathfrak{A})$ the norm on X_1 is equivalent to the norm $\|\boldsymbol{x}\|_1 = \|(\beta\mathfrak{I} - \mathfrak{A})\boldsymbol{x}\|$. As pointed out in Lemma B.3 the norms generated for different β are equivalent in the graph norm and hence independent of the particular choice of β. Let X_{-1} denote the completion of X with respect to the norm $\|\boldsymbol{x}\|_{-1} = \|(\beta\mathfrak{I} - \mathfrak{A})^{-1}\boldsymbol{x}\|$. Then by Lemma B.4 the operator $\mathfrak{A}$ has an extension, also identified with $\mathfrak{A}$, such that $\mathfrak{A} \in \mathcal{L}(X, X_{-1})$. With these preliminaries, the existence of a unique operator $\mathfrak{B}$ in the sense of (6.2) can be guaranteed.

Lemma 6.1. *Let $(\mathfrak{L}, \mathfrak{K})$ be a boundary control system on V, Z, and X in the sense defined above. Let $\mathfrak{A} = \mathfrak{L}|_{X_1} \in \mathcal{L}(X_1, X)$ and X_{-1} be the completion of X_1 under the norm $\|\boldsymbol{x}\|_{-1} = \|(\beta\mathfrak{I} - \mathfrak{A})^{-1}\boldsymbol{x}\|_X$ for $\beta \in \rho(\mathfrak{A})$. Then there exists a unique operator $\mathfrak{B} \in \mathcal{L}(V, X_{-1})$ such that*

$$\mathfrak{L} = \mathfrak{A} + \mathfrak{B}\mathfrak{K}, \tag{6.4}$$

where $\mathfrak{A}$ is regarded as the extended operator from X to X_{-1}. For every $\beta \in \rho(\mathfrak{A})$ it follows that $(\beta\mathfrak{I} - \mathfrak{A})^{-1}\mathfrak{B} \in \mathcal{L}(V, Z)$ and

$$\mathfrak{K}(\beta\mathfrak{I} - \mathfrak{A})^{-1}\mathfrak{B} = \mathfrak{I}, \tag{6.5}$$

so that $\mathfrak{B}$ is bounded from below.

For a proof of this result consult [66, Section 10.1]. Hence, the evaluation of (6.1) with (6.4) directly yields $\partial_t \boldsymbol{x}(t) = (\mathfrak{A} + \mathfrak{B}\mathfrak{K})\boldsymbol{x}(t) = \mathfrak{A}\boldsymbol{x}(t) + \mathfrak{B}\boldsymbol{u}_{\partial\Omega}(t)$. In principle $\mathfrak{B}$ follows from (6.4) since $\mathfrak{K} \in \mathcal{L}(Z, V)$ implies the existence of at least a bounded right inverse of $\mathfrak{K}$. However, for an explicit computation of $\mathfrak{B}$ it is convenient to follow one of the two approaches presented below (see [66, Remarks 10.1.5, 10.1.6]):

(i) Compute the solution $\boldsymbol{x} = (\beta\mathfrak{I} - \mathfrak{L})^{-1}\mathfrak{B}\boldsymbol{u}_{\partial\Omega}$ for $\beta \in \rho(\mathfrak{L})$ to the elliptic boundary–value problem

$$\mathfrak{L}\boldsymbol{x} = \beta\boldsymbol{x}, \quad \mathfrak{K}\boldsymbol{x} = \boldsymbol{u}_{\partial\Omega}.$$

With this, $\mathfrak{B}$ can be directly identified.

(ii) From (6.4), it follows that

$$\langle \mathfrak{L}\boldsymbol{x}, \boldsymbol{\psi}\rangle_X = \langle (\mathfrak{A} + \mathfrak{B}\mathfrak{K})\boldsymbol{x}, \boldsymbol{\psi}\rangle_X = \langle \boldsymbol{x}, \mathfrak{A}^*\boldsymbol{\psi}\rangle_X + \langle \mathfrak{K}\boldsymbol{x}, \mathfrak{B}^*\boldsymbol{\psi}\rangle_X$$

for any $\boldsymbol{x} \in Z$ and $\boldsymbol{\psi} \in \mathcal{D}(\mathfrak{A}^*)$. Hence, in many applications the adjoint $\mathfrak{B}^*$ can be determined from

$$\langle \mathfrak{K}\boldsymbol{x}, \mathfrak{B}^*\boldsymbol{\psi}\rangle_X = \langle \mathfrak{L}\boldsymbol{x}, \boldsymbol{\psi}\rangle_X - \langle \boldsymbol{x}, \mathfrak{A}^*\boldsymbol{\psi}\rangle_X \tag{6.6}$$

using, e.g., integration by parts or the divergence theorem, respectively[1].

If $\mathfrak{F} \neq \mathfrak{o}$, then the control operator follows directly as the composite operator

$$\mathfrak{B} \mapsto [\mathfrak{F}, \mathfrak{B}] \tag{6.7a}$$

with the operator $\mathfrak{B}$ on the right–hand side defined as above and the composite input

$$\boldsymbol{u}(t) \mapsto \left[\boldsymbol{u}_\Omega^T(t), \boldsymbol{u}_{\partial\Omega}^T(t)\right]^T. \tag{6.7b}$$

Hence, assuming that $\mathfrak{B}$ as defined in (6.7a) is an admissible control operator in the sense of Definition 6.1, a mild solution to (6.1) can be determined provided that $\boldsymbol{u}(t) \in L^2_{\mathrm{loc}}([0,\infty); U)$ with $\boldsymbol{u}(t)$ from (6.7b) with higher regularity obtained if $\boldsymbol{u}(t) \in H^1_{\mathrm{loc}}([0,\tau); U)$ or $\boldsymbol{u}(t) \in H^2_{\mathrm{loc}}([0,\tau); U)$ for some $\tau \in (0,\infty)$. This naturally leads to the definition of a well–posed boundary control system according to [66] (see, e.g., [24] for related results given that $\mathfrak{A}$ is a so–called Riesz spectral operator, which is considered in Section 6.1.3).

Definition 6.3. The boundary control system $(\mathfrak{L}, \mathfrak{K})$ is called well–posed if $\mathfrak{A}$ as introduced in Lemma 6.1 is the generator of a C_0–semigroup $\mathfrak{T}(t)$ on X and $\mathfrak{B}$ defined in (6.7a) is an admissible control operator for $\mathfrak{T}(t)$.

6.1.2.2 Homogenization Approach

As an alternative, [18] introduces a homogenization approach[2] by considering a suitable change of the dependent coordinates. For this, consider the change of variables

[1] It should be pointed out that this approach is well–established for the solution of DPSs with inhomogeneous BCs using the so–called modal transformation (see, e.g., [20]) though embedded in a less rigorous theoretical framework.

[2] The underlying idea is extensively discussed, e.g., in structural mechanics [38], however in general in a less rigorous framework.

$$\boldsymbol{x}(t) \mapsto \boldsymbol{x}(t) + \mathfrak{K}'\boldsymbol{u}_{\partial\Omega}(t),$$

where $\mathfrak{K}' \in \mathcal{L}(V, X)$ is a bounded operator satisfying

$$\mathfrak{K}\mathfrak{K}'\boldsymbol{u}_{\partial\Omega}(t) = \boldsymbol{u}_{\partial\Omega}(t).$$

With this, (6.1) reduces to

$$\begin{aligned}
\partial_t \boldsymbol{x}(t) &= \mathfrak{L}\boldsymbol{x}(t) + \mathfrak{F}\boldsymbol{u}_{\Omega}(t) + \mathfrak{L}\mathfrak{K}'\boldsymbol{u}_{\partial\Omega}(t) - \mathfrak{K}'\partial_t\boldsymbol{u}_{\partial\Omega}(t) \\
\mathfrak{K}\boldsymbol{x}(t) &= \mathbf{0} \\
\boldsymbol{x}(0) &= \boldsymbol{x}_0 - \mathfrak{K}'\boldsymbol{u}_{\partial\Omega}(0)
\end{aligned}$$

with homogeneous boundary conditions. As a result, (6.1) can be re–formulated in an abstract operational framework in an extended state space $X \mapsto X \oplus V$ according to (6.2) with

$$\boldsymbol{x}(t) \mapsto \left[\boldsymbol{x}^T(t), \boldsymbol{u}_{\partial\Omega}^T(t)\right]^T \tag{6.8a}$$

$$\boldsymbol{u}(t) \mapsto \left[\boldsymbol{u}_{\Omega}^T(t), \partial_t\boldsymbol{u}_{\partial\Omega}^T(t)\right]^T \tag{6.8b}$$

$$\mathfrak{A} = \begin{bmatrix} \mathfrak{L} & \mathfrak{L}\mathfrak{K}' \\ \mathfrak{o} & \mathfrak{o} \end{bmatrix} \tag{6.8c}$$

$$\mathfrak{B} = \begin{bmatrix} \mathfrak{F} & -\mathfrak{K}' \\ \mathfrak{o} & \mathfrak{I} \end{bmatrix} \tag{6.8d}$$

$$\mathfrak{C} = \left[\mathfrak{G}, \mathfrak{o}\right]^T. \tag{6.8e}$$

In addition, it follows that $\mathcal{D}(\mathfrak{A}) = \mathcal{D}(\mathfrak{L}) \oplus V$, $\mathfrak{B} : \mathcal{D}(\mathfrak{B}) = \mathcal{D}(\mathfrak{F}) \oplus V \to X$, and $\mathfrak{C} : X \oplus V \to Y$. As indicated by the mappings (6.8a) and (6.8b), note that no notational distinction is made between the dependent coordinates in the original and the extended set–up. Similar to the previous paragraph it is again assumed that the input and output operators $\mathfrak{B}$ and $\mathfrak{C}$ defined in (6.8d) and (6.8e) are admissible control and observation operators in the sense of Definitions 6.1 and 6.2.

Based on the general abstract operational system formulation (6.2) with the operators determined by means of either operational extension or homogenization, subsequently, the class of so–called Riesz spectral operators is introduced, which allows for a rather intuitive system representation by exploiting the spectral properties of the operator $\mathfrak{A}$. Thereby, it has to be pointed out that many physically relevant problems such as linear diffusion–convection–reaction systems, wave–type equations, Euler–Bernoulli and Timoshenko beam equations, as well as Kirchhoff and Mindlin plate equations can in general be re–formulated in terms of Riesz spectral operators, which makes this a rather important and attractive class both from a theoretical and application point of view.

6.1.3 Bases of Hilbert Spaces, Riesz Bases, and Spectral Operators

In order to motivate the notion of a Riesz basis and to determine the properties of the important class of (Riesz) spectral operators, at first some preliminary results on normed linear spaces and spectral analysis are summarized subsequently. For this, let B be a Banach space with norm $\|\cdot\|_B$ and let X denote a Hilbert space with inner product $\langle\cdot,\cdot\rangle_X$ and induced norm $\|\boldsymbol{x}\|_X = \sqrt{\langle \boldsymbol{x}, \boldsymbol{x}\rangle_X}$.

A sequence $(\boldsymbol{e}_k)_{k\in\mathbb{N}}$ of vectors in a Banach space B is called a (Schauder) basis of B if every vector $\boldsymbol{x} \in B$ can be expanded uniquely in a series

$$\boldsymbol{x} = \sum_{k\in\mathbb{N}} x_k \boldsymbol{e}_k, \tag{6.9}$$

which converges in the strong (norm) topology of B, i.e. $\|\boldsymbol{x} - \sum_{k=1}^{n} x_k \boldsymbol{e}_k\|_B \to 0$ as $n \to \infty$ [69]. Given a basis $(\boldsymbol{e}_k)_{k\in\mathbb{N}}$ of a Hilbert space X, the following theorem holds, which traces back to S. Banach and whose proof can be found, e.g., in [21].

Theorem 6.1. *The sequence $(\boldsymbol{f}_k)_{k\in\mathbb{N}}$ biorthogonal to a basis $(\boldsymbol{e}_k)_{k\in\mathbb{N}}$ of a Hilbert space X is also a basis of X.*

Consequently, any $\boldsymbol{x} \in X$ can be uniquely expanded into the series

$$\boldsymbol{x} = \sum_{k\in\mathbb{N}} \big\langle \boldsymbol{x}, \boldsymbol{f}_k \big\rangle_X \boldsymbol{e}_k, \tag{6.10}$$

which is convergent in the norm $\|\cdot\|_X$.

Let $\mathfrak{A}$ be a linear bounded and invertible operator on X and let $(\boldsymbol{e}_k)_{k\in\mathbb{N}}$ be an arbitrary orthonormal basis of X. Hence, for any $\boldsymbol{x} \in X$ it follows from (6.9) or (6.10), respectively, that

$$\mathfrak{A}^{-1}\boldsymbol{x} = \sum_{k\in\mathbb{N}} \big\langle \mathfrak{A}^{-1}\boldsymbol{x}, \boldsymbol{e}_k \big\rangle_X \boldsymbol{e}_k = \sum_{k\in\mathbb{N}} \big\langle \boldsymbol{x}, (\mathfrak{A}^{-1})^* \boldsymbol{e}_k \big\rangle_X \boldsymbol{e}_k$$

and hence with $\boldsymbol{\kappa}_k = (\mathfrak{A}^{-1})^* \boldsymbol{e}_k$ and $\boldsymbol{f}_k = \mathfrak{A}\boldsymbol{e}_k$

$$\boldsymbol{x} = \sum_{k\in\mathbb{N}} \big\langle \boldsymbol{x}, \boldsymbol{\kappa}_k \big\rangle_X \boldsymbol{f}_k. \tag{6.11}$$

Moreover, since $\langle \boldsymbol{f}_j, \boldsymbol{\kappa}_k\rangle_X = \langle \mathfrak{A}\boldsymbol{e}_j, (\mathfrak{A}^{-1})^*\boldsymbol{e}_k\rangle_X = \langle \boldsymbol{e}_j, \boldsymbol{e}_k\rangle_X = \delta_{j,k}$ the expansion (6.11) is unique and equivalent to (6.9). Thus every linear bounded invertible operator transforms any orthonormal basis of X into another, but not necessarily orthonormal, basis of X. Following [6, 21] a basis $(\boldsymbol{f}_k)_{k\in\mathbb{N}}$ of X, which is obtained from an orthonormal basis $(\boldsymbol{e}_k)_{k\in\mathbb{N}}$ of X by means of such a transformation is called a basis equivalent to an orthonormal basis or a Riesz basis. In addition, since $\mathfrak{A}$ transforms the orthonormal basis $(\boldsymbol{e}_k)_{k\in\mathbb{N}}$ into the basis $(\boldsymbol{f}_k)_{k\in\mathbb{N}}$, as shown above, the operator $(\mathfrak{A}^{-1})^*$ transforms $(\boldsymbol{e}_k)_{k\in\mathbb{N}}$ into the basis $(\boldsymbol{\kappa}_k)_{k\in\mathbb{N}}$, which is biorthogonal

to $(\boldsymbol{f}_k)_{k\in\mathbb{N}}$. Hence, a basis which is biorthogonal to a Riesz basis is itself equivalent to an orthonormal basis [21].

Remark 6.1. If not stated otherwise throughout this chapter the natural numbers $\mathbb{N}$ are considered as the index set. However, all results hold similarly if another countable index set is used, e.g., $\mathbb{Z}$. The choice thereby depends on the particular system under consideration. In addition note that Riesz bases can be similarly defined for non–separable spaces by allowing an arbitrary index set (cf. [44, Lemma 5.17.17]).

With this, the following theorem can be introduced, which provides a procedure to deduce that a given sequence indeed represents a Riesz basis.

Theorem 6.2. *The following assertions are equivalent:*

(i) The sequence $(\boldsymbol{e}_k)_{k\in\mathbb{N}}$ forms a basis of the Hilbert space X equivalent to an orthonormal basis, i.e. $(\boldsymbol{e}_k)_{k\in\mathbb{N}}$ is a Riesz basis.

(ii) The sequence $(\boldsymbol{e}_k)_{k\in\mathbb{N}}$ becomes an orthonormal basis of the space X by an appropriate replacement of the inner product $\langle\cdot,\cdot\rangle_X$ by some topologically equivalent new inner product $\langle\cdot,\cdot\rangle_1$, i.e. there exist positive constants $c_1,\ c_2$ such that for all $\boldsymbol{x}\in X$ the induced norms satisfy $c_1\langle\boldsymbol{x},\boldsymbol{x}\rangle_X \le \langle\boldsymbol{x},\boldsymbol{x}\rangle_1 \le c_2\langle\boldsymbol{x},\boldsymbol{x}\rangle_X$.

(iii) The sequence $(\boldsymbol{e}_k)_{k\in\mathbb{N}}$ is complete in X and there exists positive constants $m,\ M$ such that for any positive integer k' and arbitrary $\alpha_k,\ k=1,\dots,k'$, one has $m\sum_{k=1}^{k'}|\alpha_k|^2 \le \|\sum_{k=1}^{k'}\alpha_k\boldsymbol{e}_k\| \le M\sum_{k=1}^{k'}|\alpha_k|^2$.

(iv) The sequence $(\boldsymbol{e}_k)_{k\in\mathbb{N}}$ is complete in X, there exists a complete biorthogonal sequence $(\boldsymbol{f}_k)_{k\in\mathbb{N}}$, and for any $\boldsymbol{x}\in X$ one has $\sum_{k\in\mathbb{N}}|\langle\boldsymbol{x},\boldsymbol{e}_k\rangle_X|^2<\infty$ and $\sum_{k\in\mathbb{N}}|\langle\boldsymbol{x},\boldsymbol{f}_k\rangle_X|^2<\infty$.

(v) The sequence $(\boldsymbol{e}_k)_{k\in\mathbb{N}}$ is complete in X and the Gramian matrix given by $[\langle\boldsymbol{e}_k,\boldsymbol{e}_j\rangle_X]_{k,j\in\mathbb{N}}$ generates a bounded invertible operator on ℓ^2.

The equivalences (i)–(iv) are also known as the Bari Theorem for which a proof can be found, e.g. in [7], [21, Theorem. VI.2.1], or [69, Theorem. 9], respectively. The latter reference in particular points out the equivalence with (v). For further properties of Riesz bases and generalizations such as Bari bases the interested reader is referred to [21]. As a main assertion of the Bari Theorem it follows that any $\boldsymbol{x}\in X$ can be represented as a linear combination of the individual $\boldsymbol{e}_k,\ k\in\mathbb{N}$, even if these are not mutually orthogonal but form a Riesz basis [14, 24, 66].

Corollary 6.1. *Let $(\boldsymbol{e}_k)_{k\in\mathbb{N}}$ be a Riesz basis. Then*

(i) there exists a sequence $(\boldsymbol{f}_k)_{k\in\mathbb{N}}$ biorthogonal to $(\boldsymbol{e}_k)_{k\in\mathbb{N}}$, which forms a Riesz basis for X;

(ii) every $\boldsymbol{x}\in X$ can be uniquely expressed as

$$\boldsymbol{x}=\sum_{k\in\mathbb{N}}\big\langle\boldsymbol{x},\boldsymbol{f}_k\big\rangle_X\boldsymbol{e}_k$$

and there exist constants $m,\ M>0$ such that

$$m\sum_{k\in\mathbb{N}}\big|\big\langle\boldsymbol{x},\boldsymbol{f}_k\big\rangle_X\big|^2 \le \|\boldsymbol{x}\|_X^2 \le M\sum_{k\in\mathbb{N}}\big|\big\langle\boldsymbol{x},\boldsymbol{f}_k\big\rangle_X\big|^2.$$

The properties of Riesz bases briefly summarized above can be directly exploited to define and characterize so–called (Riesz) spectral operators on Hilbert spaces. Note that subsequently not the most general case of a spectral operator is introduced but that the notation and the presented results are adjusted to the class of systems under consideration by following mainly [28, 24, 61] and the references therein. For a general spectral theory of non–selfadjoint linear operators, the interested reader is in particular referred to [16].

Definition 6.4 (Scalar operator). Let $(\boldsymbol{e}_k)_{k\in\mathbb{N}}$ be a Riesz basis in a Hilbert space X, let $(\boldsymbol{f}_k)_{k\in\mathbb{N}}$ be the Riesz basis biorthogonal to $(\boldsymbol{e}_k)_{k\in\mathbb{N}}$, and let $(\lambda_k)_{k\in\mathbb{N}}$ be a sequence in $\mathbb{C}$. The linear operator

$$\mathfrak{A}\boldsymbol{x} = \sum_{k\in\mathbb{N}} \lambda_k \langle \boldsymbol{x}, \boldsymbol{f}_k\rangle_X \boldsymbol{e}_k$$

in X with domain

$$\mathcal{D}(\mathfrak{A}) = \left\{ \boldsymbol{x} \in X : \sum_{k\in\mathbb{N}} |\lambda_k|^2 |\langle \boldsymbol{x}, \boldsymbol{f}_k\rangle_X|^2 < \infty \right\}$$

is called a scalar operator.

Definition 6.5 (Spectral operator). An operator $\mathfrak{A}$ in X is called a spectral operator if it can be represented in the form

$$\mathfrak{A} = \mathfrak{S} + \mathfrak{N} \tag{6.12}$$

with $\mathfrak{S}$ a scalar operator and $\mathfrak{N}$ a bounded finite rank nilpotent operator commuting with $\mathfrak{S}$.

By imposing a restriction on the sequence $(\lambda_k)_{k\in\mathbb{N}}$ the following Lemma can be verified [66].

Lemma 6.2. *Let $(\boldsymbol{e}_k)_{k\in\mathbb{N}}$ and $(\boldsymbol{f}_k)_{k\in\mathbb{N}}$ be orthonormal Riesz bases and let $(\lambda_k)_{k\in\mathbb{N}}$ be a sequence in $\mathbb{C}$. Then the following statements are equivalent:*

(i) The sequence $(\lambda_k)_{k\in\mathbb{N}}$ is bounded.
(ii) The series $\mathfrak{A}\boldsymbol{x} = \sum_{k\in\mathbb{N}} \lambda_k \langle \boldsymbol{x}, \boldsymbol{f}_k\rangle_X \boldsymbol{e}_k$ is convergent for every $\boldsymbol{x} \in X$ and the thus defined operator $\mathfrak{A}$ is bounded on X.

If the above statements are true, then $\sup_{k\in\mathbb{N}} |\lambda_k| \leq \|\mathfrak{A}\| \leq \sqrt{M/m}\sup_{k\in\mathbb{N}} |\lambda_k|$, where m, M as introduced in Theorem 6.2(iii).

Given a bounded operator $\mathfrak{A} \in \mathcal{L}(X)$, the last statement implies that $\lambda_k \in \sigma_p(\mathfrak{A})$, where $\sigma_p(\mathfrak{A})$ denotes the point spectrum of the operator $\mathfrak{A}$ [66, Proposition 2.2.10]. By restricting the analysis to operators with a pure point spectrum, the relationship between the spectral properties of the operator and the properties of a the Riesz basis of the Hilbert space X can be further exploited by analyzing the Riesz basis properties of the root vectors or generalized eigenvectors, respectively, of a linear operator $\mathfrak{A}$, i.e. the sequence of its eigenvectors and associated vectors.

For this recall, that the spectrum $\sigma(\mathfrak{A})$ of the closed linear operator $\mathfrak{A}$ contains all eigenvalues, i.e. all $\lambda \in \mathbb{C}$ for which the equation

$$\big(\mathfrak{A} - \lambda\mathfrak{I}\big)\boldsymbol{\phi} = \mathbf{0}$$

has at least one nonzero solution $\boldsymbol{\phi} \in X$. In this case $\boldsymbol{\phi}$ is called an eigenvector. The vector $\boldsymbol{\phi}_k \in X$ is called a generalized eigenvector of the operator $\mathfrak{A}$ corresponding to the eigenvalue λ_k if

$$\big(\mathfrak{A} - \lambda_k\mathfrak{I}\big)^{n_k}\boldsymbol{\phi}_k = \mathbf{0}$$

for some $n_k \in \mathbb{N}$. Here, n_k is denoted as the order or the index of λ_k, cf. [14, Definition A.4.5] or [2, Section 9.9]. The dimension of the set of all generalized eigenvectors corresponding to λ_k, i.e. $\dim\ker\big(\mathfrak{A} - \lambda_k\mathfrak{I}\big)^{n_k}$, is called the algebraic multiplicity r_k^a of the eigenvalue λ_k. The dimension of the space consisting of all eigenvectors of $\mathfrak{A}$ corresponding to λ_k is called the geometric or proper multiplicity r_k^g of the eigenvalue λ_k. Since the set of all eigenvectors to λ_k is by definition part of the set of all generalized eigenvectors to λ_k it follows that $r_k^g \leq r_k^a$. If $r_k^g < r_k^a$ then the chain of associated vectors has to be introduced according to

$$\big(\mathfrak{A} - \lambda_k\mathfrak{I}\big)\boldsymbol{\phi}_{k_j} = \boldsymbol{\phi}_{k_{j-1}}, \quad j = r_k^g + 1, \ldots, r_k^a.$$

with $\boldsymbol{\phi}_{k_{r_k^g}}$ denoting the eigenvector to the eigenvalue λ_k. In order to provide a concise formulation, the following notational convention is imposed.

Notation. The sets $((\boldsymbol{\phi}_{k_j})_{j=1,\ldots,r_k^a})_{k\in\mathbb{N}}$ and $((\boldsymbol{\psi}_{k_j})_{j=1,\ldots,r_k^a})_{k\in\mathbb{N}}$ of generalized eigenvectors of the operator $\mathfrak{A}$ and its adjoint $\mathfrak{A}^*$, respectively, are composed according to the following rules: For each $k \in \mathbb{N}$,

(i) the first $j = 1, \ldots, r_k^g$ elements correspond to the eigenvectors to λ_k,
(ii) the final $j = r_k^g + 1, \ldots, r_k^a$ elements are the associated vectors to λ_k.

With these preliminaries and conventions the main result on the representation of the considered class of (Riesz) spectral operators can be formulated as follows (see also [24, Theorems. 2.9, 2.12] and [61, Theorem. 4]).

Theorem 6.3. *Let $\mathfrak{A}$ be a closed linear operator with isolated (point) spectrum $\sigma_p(\mathfrak{A}) = (\lambda_k)_{k\in\mathbb{N}}$ and $\overline{\sigma_p(\mathfrak{A})}$ being totally disconnected*[3] *and $r_k^a < \infty$ for all $k \in \mathbb{N}$. Suppose that the set of generalized eigenvectors $((\boldsymbol{\phi}_{k_j})_{j=1,\ldots,r_k^a})_{k\in\mathbb{N}}$ forms a Riesz basis for X. Then*

(i) the set of generalized eigenvectors $((\boldsymbol{\psi}_{k_j})_{j=1,\ldots,r_k^a})_{k\in\mathbb{N}}$ of the adjoint operator $\mathfrak{A}^*$ forms a Riesz basis for X, which is biorthogonal to $((\boldsymbol{\phi}_{k_j})_{j=1,\ldots,r_k^a})_{k\in\mathbb{N}}$;
(ii) $\mathfrak{A} = \mathfrak{S} + \mathfrak{N}$ is a (Riesz) spectral operator according to Definition 6.5 with

$$\mathfrak{S}\boldsymbol{x} = \sum_{k\in\mathbb{N}} \lambda_k \sum_{j=1}^{r_k^a} \big\langle \boldsymbol{x}, \boldsymbol{\psi}_{k_j} \big\rangle_X \boldsymbol{\phi}_{k_j} \tag{6.13a}$$

[3] Any two elements of $\sigma_p(\mathfrak{A})$ cannot be connected by a segment lying entirely in $\overline{\sigma_p(\mathfrak{A})}$.

$$\mathfrak{N}\boldsymbol{x} = \sum_{k\in\mathbb{N}} \sum_{j=1+r_k^g}^{r_k^a} \left\langle \boldsymbol{x}, \boldsymbol{\psi}_{k_j} \right\rangle_X \boldsymbol{\phi}_{k_{j-1}} \tag{6.13b}$$

for all $\boldsymbol{x} \in \mathcal{D}(\mathfrak{A})$*, where*

$$\mathcal{D}(\mathfrak{A}) = \left\{ \boldsymbol{x} \in X : \sum_{k\in\mathbb{N}} |\lambda_k|^2 \sum_{j=1}^{r_k^a} \left| \left\langle \boldsymbol{x}, \boldsymbol{\psi}_{k_j} \right\rangle_X \right|^2 < \infty \right\}. \tag{6.14}$$

Some remarks to Theorem 6.3 follow. In view of Corollary 6.1, Theorem 6.3 implies that if the set of generalized eigenvectors $((\boldsymbol{\phi}_{k_j})_{j=1,\ldots,r_k^a})_{k\in\mathbb{N}}$ forms a Riesz basis for X, then every $\boldsymbol{x} \in X$ can be uniquely expressed in terms of the Fourier series

$$\boldsymbol{x} = \sum_{k\in\mathbb{N}} \sum_{j=1}^{r_k^a} \langle \boldsymbol{x}, \boldsymbol{\psi}_{k_j} \rangle_X \boldsymbol{\phi}_{k_j}. \tag{6.15}$$

Moreover, it is shown in [24] by a counterexample that the generalized eigenvectors of an operator $\mathfrak{A}$ not necessarily form a Riesz basis for X. As a result, in general the application of one of the criteria provided in Theorem 6.2 is required to verify the Riesz basis property.

The explicit formulation of $\mathfrak{N}$ in (6.13b) holds for the general case of $1 \leq r_k^g \leq r_k^a$ for each eigenvalue λ_k, $k \in \mathbb{N}$. Hence, if $r_k^g = r_k^a$ the operator $\mathfrak{N}$ reduces to the zero operator $\mathfrak{o}$. In addition, a direct evaluation provides in view of the biorthogonality of the Riesz bases $((\boldsymbol{\phi}_{k_j})_{j=1,\ldots,r_k^a})_{k\in\mathbb{N}}$ and $((\boldsymbol{\psi}_{k_j})_{j=1,\ldots,r_k^a})_{k\in\mathbb{N}}$ that

$$\mathfrak{N}^i\boldsymbol{x} = \sum_{k\in\mathbb{N}} \sum_{j=r_k^g+i}^{r_k^a} \left\langle \boldsymbol{x}, \boldsymbol{\psi}_{k_j} \right\rangle_X \boldsymbol{\phi}_{k_{j-i}}, \qquad i \geq 1,$$

which confirms that $\mathfrak{N}$ is nilpotent of rank $n = 1 + r^a - r^g$, where $r^a = \max_{k\in\mathbb{N}}\{r_k^a\} < \infty$ and $r^g = \min_{k\in\mathbb{N}}\{r_k^g\}$, i.e. $\mathfrak{N}^n = \mathfrak{o}$. This observation enables to introduce a closed–form expression of both the resolvent of $\mathfrak{A}$ and the C_0–semigroup generated by $\mathfrak{A}$.

Theorem 6.4. *Let* $\mathfrak{A} = \mathfrak{S} + \mathfrak{N}$ *be a Riesz spectral operator with the scalar operator* $\mathfrak{S}$ *and the finite rank nilpotent operator* $\mathfrak{N}$ *defined in* (6.13)*. Then*

(i) $\lambda \in \rho(\mathfrak{A})$ *if and only if* $\inf_{k\in\mathbb{N}} |\lambda - \lambda_k| > 0$*. In this case,*

$$\begin{aligned}(\lambda\mathfrak{I} - \mathfrak{A})^{-1}\boldsymbol{x} = &\sum_{k\in\mathbb{N}} \frac{1}{\lambda - \lambda_k} \sum_{j=1}^{r_k^a} \langle \boldsymbol{x}, \boldsymbol{\psi}_{k_j} \rangle_X \boldsymbol{\phi}_{k_j} \\ &+ \sum_{k\in\mathbb{N}} \sum_{i=1}^{r_k^a - r_k^g} \frac{1}{(\lambda - \lambda_k)^{i+1}} \sum_{j=r_k^g+i}^{r_k^a} \langle \boldsymbol{x}, \boldsymbol{\psi}_{k_j} \rangle_X \boldsymbol{\phi}_{k_{j-i}}.\end{aligned} \tag{6.16}$$

(ii) The operator $\mathfrak{A}$ generates a C_0–semigroup $\mathfrak{T}(t)$ if and only if $\sup_{k\in\mathbb{N}} \Re\{\lambda_k\} < \infty$. *In this case,*

$$\begin{aligned}\mathfrak{T}(t)\boldsymbol{x} = &\sum_{k\in\mathbb{N}} e^{\lambda_k t} \sum_{j=1}^{r_k^a} \langle \boldsymbol{x}, \boldsymbol{\psi}_{k_j}\rangle_X \boldsymbol{\phi}_{k_j} \\ &+ \sum_{k\in\mathbb{N}} \sum_{i=1}^{r_k^a - r_k^g} \frac{t^i}{i!} e^{\lambda_k t} \sum_{j=r_k^g+i}^{r_k^a} \langle \boldsymbol{x}, \boldsymbol{\psi}_{k_j}\rangle_X \boldsymbol{\phi}_{k_{j-i}}.\end{aligned} \tag{6.17}$$

(iii) The spectrum determined growth condition holds true for $\mathfrak{T}(t)$.

(iv) The operator $\mathfrak{A}$ generates an analytic semigroup if and only if $\sigma_p(\mathfrak{A}) \subset \mathcal{S}_{r,\alpha}$, where $\mathcal{S}_{r,\alpha} = \{z \in \mathbb{C} : \Re\{z\} < r, \ |\arg(z)| > \pi/2 + \alpha\}$ for some $r \in \mathbb{R}^+$ and $\alpha > 0$.

The proof of Theorem 6.4 can be found in [24] for a general quasi–nilpotent operator $\mathfrak{N}$ without providing explicit expressions for resolvent and generated C_0–semigroup[4]. However, these are essential for the solution of the trajectory planning problem. For this, once the Riesz basis of generalized eigenvectors is chosen, it is particularly convenient to exploit the equivalence of both the operator $\mathfrak{A}$ as well as the resolvent $(\lambda\mathfrak{I} - \mathfrak{A})^{-1}$ with infinite–dimensional matrices in the space ℓ^2. Therefore, observe that under the assumptions of Theorem 6.3 any $\boldsymbol{x} \in X$ can be represented by the Fourier series (6.15) with $(\langle \boldsymbol{x}, \boldsymbol{\psi}_{k_j}\rangle_X)_{j=1,\dots,r_k^a,\, k\in\mathbb{N}} \in \ell^2$. This implies that X is isometric isomorph to ℓ^2. Hence, given (6.12) with (6.13), it follows that $\mathfrak{A}$ can be re–formulated as

$$\mathfrak{A} = \operatorname{diag}\{\mathfrak{A}_k\}_{k\in\mathbb{N}}, \tag{6.18}$$

where each sub–matrix is of Jordan canonical form and governed by

$$\mathfrak{A}_k = \lambda_k \mathfrak{I}_k + \mathfrak{N}_k \tag{6.19}$$

Here, $\mathfrak{I}_k$ denotes the $r_k^a \times r_k^a$ identity matrix and $\mathfrak{N}_k$ is the $r_k^a \times r_k^a$ matrix which is nilpotent of rank $n_k = r_k^a - r_k^g$ and given by

$$\big(\mathfrak{N}_k\big)_{l,j} = \sigma\big(j - 1 - r_k^g\big)\delta_{j-1,l}, \quad j,\, l = 1, \dots, r_k^a.$$

Similarly, for all $\lambda \in \rho(\mathfrak{A})$ the resolvent (6.16) can be equivalently represented as

$$(\lambda\mathfrak{I} - \mathfrak{A})^{-1} = \operatorname{diag}\big\{(\lambda\mathfrak{I}_k - \mathfrak{A}_k)^{-1}\big\}_{k\in\mathbb{N}} \tag{6.20}$$

with the $r_k^a \times r_k^a$ matrices

[4] Eqn. (6.16) follows by evaluating $(\lambda\mathfrak{I} - \mathfrak{A})(\lambda\mathfrak{I} - \mathfrak{A})^{-1}\boldsymbol{x} = (\lambda\mathfrak{I} - \mathfrak{A})^{-1}(\lambda\mathfrak{I} - \mathfrak{A})\boldsymbol{x} = \boldsymbol{x}$ for $\lambda \in \rho(\mathfrak{A})$ and $\boldsymbol{x} \in \mathcal{D}(\mathfrak{A})$. In addition, (6.17) can be verified by considering $\partial_t \mathfrak{T}(t)\boldsymbol{x} = \mathfrak{A}\mathfrak{T}(t)\boldsymbol{x} = \mathfrak{T}(t)\mathfrak{A}\boldsymbol{x}$ for $\boldsymbol{x} \in \mathcal{D}(\mathfrak{A})$ and $\mathfrak{T}(0) = \mathfrak{I}$.

$$(\lambda\mathfrak{I}_k - \mathfrak{A}_k)^{-1} = \frac{1}{\lambda - \lambda_k}\mathfrak{I}_k + \overline{\mathfrak{N}}_k, \tag{6.21}$$

where

$$(\overline{\mathfrak{N}}_k)_{l,j} = \sum_{i=1}^{r_k^a - r_k^g} \frac{\sigma\big(j - i - r_k^g\big)}{(\lambda - \lambda_k)^{i+1}}\delta_{j-i,l}, \quad j,\, l = 1, \ldots, r_k^a.$$

Note that Heaviside functions $\sigma(\cdot)$ are introduced to account for the lower summation limits $j \geq 1 + r_k^g$ in (6.13b) and $j \geq i + r_k^g$ in (6.16). By evaluating (6.19) and (6.21) their familiar Jordan canonical forms are obtained, i.e.

$$\mathfrak{A}_k = \left[\begin{array}{\overbrace{ccc}^{r_k^g-1}:\overbrace{cccc}^{r_k^a-r_k^g+1}} \lambda_k & \cdots & 0 & 0 & \cdots & & 0 \\ \vdots & \ddots & \vdots & \vdots & \cdots & & \vdots \\ 0 & \cdots & \lambda_k & 0 & \cdots & & 0 \\ \hdashline 0 & \cdots & 0 & \lambda_k & 1 & \cdots & 0 \\ \vdots & & \vdots & \vdots & \ddots & \ddots & \vdots \\ 0 & \cdots & 0 & 0 & & \lambda_k & 1 \\ 0 & \cdots & 0 & 0 & 0 & 0 & \lambda_k \end{array}\right] \begin{array}{l} \}\, r_k^g - 1 \\ \}\, r_k^a - r_k^g + 1 \end{array}$$

and

$$\big(\lambda\mathfrak{I}_k - \mathfrak{A}_k\big)^{-1} =$$

$$\left[\begin{array}{\overbrace{ccc}^{r_k^g-1}:\overbrace{cccc}^{r_k^a-r_k^g+1}} \frac{1}{\lambda-\lambda_k} & \cdots & 0 & 0 & \cdots & & 0 \\ \vdots & \ddots & \vdots & \vdots & \cdots & & \vdots \\ 0 & \cdots & \frac{1}{\lambda-\lambda_k} & 0 & \cdots & & 0 \\ \hdashline 0 & \cdots & 0 & \frac{1}{\lambda-\lambda_k} & \frac{1}{(\lambda-\lambda_k)^2} & \cdots & \frac{1}{(\lambda-\lambda_k)^{r_k^a-r_k^g+1}} \\ \vdots & & \vdots & \vdots & \ddots & \ddots & \vdots \\ 0 & \cdots & 0 & 0 & & \frac{1}{\lambda-\lambda_k} & \frac{1}{(\lambda-\lambda_k)^2} \\ 0 & \cdots & 0 & 0 & 0 & 0 & \frac{1}{\lambda-\lambda_k} \end{array}\right] \begin{array}{l} \}\, r_k^g - 1 \\ \}\, r_k^a - r_k^g + 1 \end{array}$$

Remark 6.2. The Riesz spectral operator $\mathfrak{A}$ is called diagonalizable if $\mathfrak{A} = \mathfrak{S}$ with $\mathfrak{S}$ as defined in (6.13a). In this case, it follows that the algebraic and geometric multiplicity of each eigenvalue coincide, i.e. $r_k^a = r_k^g$ for all $k \in \mathbb{N}$ such that the operator can be entirely described in terms of its eigenvalues and eigenvectors [66].

Based on these preliminaries, the formal flatness–based state and input parametrization is generically considered for distributed–parameter systems whose system operator is a (Riesz) spectral operator.

6.2 Formal Parametrization of Riesz Spectral Systems

In the following, distributed–parameter systems in abstract form governed by

$$\partial_t \boldsymbol{x}(t) = \mathfrak{A}\boldsymbol{x}(t) + \mathfrak{B}\boldsymbol{u}(t), \quad \boldsymbol{x}(0) = \boldsymbol{x}_0 \in \mathcal{D}(\mathfrak{A}) \tag{6.22a}$$

$$\boldsymbol{y}(t) = \mathfrak{C}\boldsymbol{x}(t) \tag{6.22b}$$

are considered, where $\boldsymbol{x}(t) \in X$, $\mathfrak{A} : \mathcal{D}(\mathfrak{A}) \subset X \to X$ is assumed to be the infinitesimal generator of a C_0–semigroup, $\boldsymbol{u}(t) \in L^2_{\text{loc}}([0,\infty); U)$, and $\mathfrak{B} \in \mathcal{L}(U, X_{-1})$ as well as $\mathfrak{C} \in \mathcal{L}(X_1, Y)$ are assumed to be admissible control and observation operators. Here, X_{-1} and X_1 are as introduced in Lemmas B.3 and B.4. With these preliminaries, (6.22) is well–posed in the sense of Definition 6.3. Furthermore, the following assumptions are imposed.

Assumption 6.1. Given (6.22), then

(i) $\mathfrak{A}$ is assumed to be a (Riesz) spectral operator according to Definition 6.5, i.e. $\mathfrak{A}$ can be decomposed into $\mathfrak{A} = \mathfrak{S} + \mathfrak{N}$ with a scalar operator $\mathfrak{S}$ and a nilpotent operator $\mathfrak{N}$ as defined in (6.13).

(ii) the initial state $\boldsymbol{x}_0$ is assumed to be a stationary state, i.e. $\mathfrak{A}\boldsymbol{x}_0 = \boldsymbol{0}$, $\boldsymbol{x}_0 \in \mathcal{D}(\mathfrak{A})$, such that without loss of generality $\boldsymbol{x}_0 = \boldsymbol{0}$.

By recalling that the resolvent corresponds to the Laplace transform of the C_0–semigroup generated by $\mathfrak{A}$ it hence follows that

$$\hat{\boldsymbol{x}}(s) = \big(s\mathfrak{I} - \mathfrak{A}\big)^{-1}\mathfrak{B}\hat{\boldsymbol{u}}(s), \quad s \in \rho(\mathfrak{A}) \text{ with } s > \sup_{k\in\mathbb{N}} \Re\{\lambda_k\},$$

where $s \in \mathbb{C}$ denotes the Laplace variable and $\hat{\boldsymbol{x}}(s)$ and $\hat{\boldsymbol{u}}(s)$ the Laplace transforms of $\boldsymbol{x}(t)$ and $\boldsymbol{u}(t)$. In view of the explicit expression (6.16) of the resolvent for a Riesz spectral operator this yields for all $s \in \rho(\mathfrak{A})$ with $s > \sup_{k\in\mathbb{N}} \Re\{\lambda_k\}$, that

$$\hat{\boldsymbol{x}}(s) = \sum_{k\in\mathbb{N}} \Bigg(\frac{1}{s-\lambda_k} \sum_{j=1}^{r_k^a} \langle \mathfrak{B}\hat{\boldsymbol{u}}(s), \boldsymbol{\psi}_{k_j} \rangle_X \boldsymbol{\phi}_{k_j} + \sum_{i=1}^{r_k^a - r_k^g} \frac{1}{(s-\lambda_k)^{i+1}} \sum_{j=r_k^g+i}^{r_k^a} \langle \mathfrak{B}\hat{\boldsymbol{u}}(s), \boldsymbol{\psi}_{k_j} \rangle_X \boldsymbol{\phi}_{k_{j-i}} \Bigg).$$

In view of the Riesz basis properties of the generalized eigenvectors of $\mathfrak{A}$ and $\mathfrak{A}^*$, the projection $\langle \cdot, \boldsymbol{\psi}_{k_j} \rangle_X$ onto the k_j–th spectral component

$$\hat{x}_{k_j}(s) := \langle \hat{\boldsymbol{x}}(s), \boldsymbol{\psi}_{k_j} \rangle_X, \qquad j = 1, \ldots, r_k^a,\ k \in \mathbb{N}$$

yields

$$\hat{x}_{k_j}(s) = \frac{1}{s - \lambda_k} \langle \mathfrak{B}\hat{\boldsymbol{u}}(s), \boldsymbol{\psi}_{k_j} \rangle_X + \sum_{i=1}^{r_k^a - r_k^g} \frac{\sigma_{i,j,k}}{(s - \lambda_k)^{i+1}} \langle \mathfrak{B}\hat{\boldsymbol{u}}(s), \boldsymbol{\psi}_{k_{j+i}} \rangle_X \tag{6.23}$$

with $\sigma_{i,j,k} := \sigma(j - r_k^g) - \sigma(j - r_k^a - 1 + i)$ such that $\sigma_{i,j,k} = 1$ for $i = 1, \ldots, r_k^a - j$, $j = r_k^g, \ldots, r_k^a - 1$. Hence, different actuator configurations governed by the operational representation $\mathfrak{B}\boldsymbol{u}(t)$ can be analyzed depending on the dimension, shape, and smoothness of the spatial domain Ω and its boundary $\partial\Omega$. For this, it is shown subsequently that formal state and input parametrizations in terms of a basic output can be determined for both finite–dimensional as well as idealized infinite–dimensional boundary and/or distributed control within the proposed framework.

6.2.1 Finite–Dimensional In–Domain and Boundary Control

For finite–dimensional mixed distributed in–domain and boundary control the input operator $\mathfrak{B}\boldsymbol{u}(t)$ can be in view of (6.7) generically represented as

$$\mathfrak{B}\boldsymbol{u}(t) = \sum_{l=1}^{m} \mathfrak{b}^l u^l(t) \tag{6.24}$$

with the spatial input characteristics $\mathfrak{b}^l = \mathfrak{b}^l(z)$, which implies to introduce

$$b_{k_j}^l = \langle \mathfrak{b}^l, \boldsymbol{\psi}_{k_j} \rangle_X. \tag{6.25}$$

Here, $U = \mathbb{C}^m$, $\mathfrak{b}^l(z) \in \mathcal{L}(U, X_{-1})$, and $u^l(t) \in L^2([0, \infty))$ for all $l = 1, \ldots, m$ such that (6.23) evaluates to

$$\hat{x}_{k_j}(s) = \sum_{l=1}^{m} \left(\frac{1}{s - \lambda_k} b_{k_j}^l + \sum_{i=1}^{r_k^a - r_k^g} \frac{\sigma_{i,j,k}}{(s - \lambda_k)^{i+1}} b_{k_{j+i}}^l \right) \hat{u}^l(s). \tag{6.26}$$

Furthermore, the following assumption has to be imposed to ensure approximate controllability (see, e.g., [3]).

Assumption 6.2. Let $r^g = \max_{k \in \mathbb{N}} \{ r_k^g \} < \infty$. The number m of input components in (6.24) satisfies $m \geq r^g$ and for all $k \in \mathbb{N}$

$$\operatorname{rk}\left(\left[b^l_{k_j}\right]_{\substack{l=1,\dots,m\\ j=1,\dots,r^a_k}}\right) \geq r^g_k.$$

By virtue of the Riesz spectral system description, this assumption allows for a quite intuitive interpretation. The projection of (6.22a) with (6.24) onto the sequence $(\boldsymbol{\psi}_{k_j})_{j=1,\dots,r^a_k}$ for fixed $k \in \mathbb{N}$ results in the r^a_k–dimensional linear system

$$\partial_t \begin{bmatrix} x_{k_1}(t) \\ \vdots \\ x_{k_{r^a_k}}(t) \end{bmatrix} = \mathfrak{A}_k \begin{bmatrix} x_{k_1}(t) \\ \vdots \\ x_{k_{r^a_k}}(t) \end{bmatrix} + \underbrace{\begin{bmatrix} b^1_{k_1} & \dots & b^m_{k_1} \\ \vdots & & \vdots \\ b^1_{k_{r^a_k}} & \dots & b^m_{k_{r^a_k}} \end{bmatrix}}_{=\mathfrak{B}_k} \begin{bmatrix} u^1(t) \\ \vdots \\ u^m(t) \end{bmatrix} \tag{6.27}$$

with $\mathfrak{A}_k$ as introduced in (6.18) and (6.19). Thus, the respective Kalman controllability matrix is non–singular provided that $m \geq r^g_k$ and $\operatorname{rk}(\mathfrak{B}_k) = r^g_k$. By [24, Theorem 3.4], i.e. the Riesz spectral system (6.22a) is approximately controllable if and only if all finite dimensional subsystems (6.27) are controllable, approximate controllability can be deduced from Assumption 6.2.

With these preparations, in the following a formal operational state and input parametrization is systematically introduced in terms of a basic output. For this, it is crucial to note that the expression of the resolvent (6.26) allows a reformulation by introducing so–called Weierstrass primary factors, which are briefly introduced in Appendix B.2.2. This yields an equivalent expression[5] following

$$\begin{aligned}
\hat{x}_{k_j}(s) &= \sum_{l=1}^{m} \left(\left(-\frac{b^l_{k_j}}{\lambda_k} \right) \frac{1}{1-\frac{s}{\lambda_k}} + \sum_{i=1}^{r^a_k - r^g_k} \frac{\sigma_{i,j,k} b^l_{k_{j+i}}}{(-\lambda_k)^{i+1}} \frac{1}{\left(1-\frac{s}{\lambda_k}\right)^{i+1}} \right) \hat{u}^l(s) \\
&= \sum_{l=1}^{m} \left(\left(-\frac{b^l_{k_j}}{\lambda_k} \right) \frac{e^{\theta_k \mathcal{F}\left(\frac{s}{\lambda_k}, g^s\right)} \left(1-\frac{s}{\lambda_k}\right)^{\theta_k - 1} \prod_{\substack{n\in\mathbb{N}\\ n\neq k}} \mathcal{G}^{\theta_n}\left(\frac{s}{\lambda_n}, g^s\right)}{\prod_{n\in\mathbb{N}} \mathcal{G}^{\theta_n}\left(\frac{s}{\lambda_n}, g^s\right)} \right. \\
&\quad \left. + \sum_{i=1}^{r^a_k - r^g_k} \frac{\sigma_{i,j,k} b^l_{k_{j+i}}}{(-\lambda_k)^{i+1}} \frac{e^{\theta_k \mathcal{F}\left(\frac{s}{\lambda_k}, g^s\right)} \left(1-\frac{s}{\lambda_k}\right)^{\theta_k - i - 1} \prod_{\substack{n\in\mathbb{N}\\ n\neq k}} \mathcal{G}^{\theta_n}\left(\frac{s}{\lambda_n}, g^s\right)}{\prod_{n\in\mathbb{N}} \mathcal{G}^{\theta_n}\left(\frac{s}{\lambda_n}, g^s\right)} \right) \hat{u}^l(s)
\end{aligned}$$

with $\theta_k := 1 + r^a_k - r^g_k$. Herein, $\mathcal{G}^{\theta_n}(s, g^s) = (\mathcal{G}(s, g^s))^{\theta_n}$ with the Weierstrass primary factor

$$\mathcal{G}(s, g^s) = \begin{cases} 1-s, & g^s = 0 \\ (1-s)\exp \mathcal{F}(s, g^s), & g^s > 0 \end{cases}, \tag{6.28}$$

[5] The necessity to incorporate Weierstrass primary factors will become apparent in Section 6.3. Until then it is sufficient to formally interpret the infinite products simply as functions of the complex variable s with yet to be determined convergence properties.

where

$$\mathcal{F}(s, g^s) = \sum_{i=1}^{g^s} \frac{s^i}{i}. \tag{6.29}$$

The term g^s is the genus of the sequence of zeros $(\lambda_n)_{n\in\mathbb{N}}$ of the infinite product $\prod_{n\in\mathbb{N}} \mathcal{G}(s/\lambda_n, \gamma)$, see Definition B.4. By formally introducing the new quantity $\hat{\xi}^l(s)$ according to

$$\hat{\xi}^l(s) = \frac{\hat{u}^l(s)}{\prod_{n\in\mathbb{N}} \mathcal{G}^{\theta_n}\left(\frac{s}{\lambda_n}, g^s\right)} \tag{6.30}$$

the formal state and input parametrization

$$\hat{x}_{k_j}(s) = \sum_{l=1}^{m} \left(-\frac{b^l_{k_j}}{\lambda_k} {}^0\hat{\mathcal{D}}^x_k(s) + \sum_{i=1}^{r^a_k - r^g_k} \frac{\sigma_{i,j,k} b^l_{k_{j+i}}}{(-\lambda_k)^{i+1}} {}^i\hat{\mathcal{D}}^x_k(s) \right) \hat{\xi}^l(s) \tag{6.31a}$$

$$\hat{u}^l(s) = \hat{\mathcal{D}}^u(s)\hat{\xi}^l(s). \tag{6.31b}$$

is obtained with the operators ${}^i\hat{\mathcal{D}}^x_k(s)$ and $\hat{\mathcal{D}}^u(s)$ given by

$${}^i\hat{\mathcal{D}}^x_k(s) = e^{\theta_k \mathcal{F}\left(\frac{s}{\lambda_k}, g^s\right)} \left(1 - \frac{s}{\lambda_k}\right)^{\theta_k - i - 1} \prod_{\substack{n\in\mathbb{N} \\ n\neq k}} \mathcal{G}^{\theta_n}\left(\frac{s}{\lambda_n}, g^s\right) \tag{6.32a}$$

$$\hat{\mathcal{D}}^u(s) = \prod_{n\in\mathbb{N}} \mathcal{G}^{\theta_n}\left(\frac{s}{\lambda_n}, g^s\right). \tag{6.32b}$$

Herein, (6.30) implies that the dimensions of $\hat{\xi}^l(s)$ and $\hat{u}^l(s)$, $l = 1, \ldots, m$, necessarily coincide. In accordance with finite–dimensional system's theory, the vector $\hat{\boldsymbol{\xi}}(s) = [\hat{\xi}^1(s), \ldots \hat{\xi}^m(s)]^T$ is called a flat or basic output in the operational domain. Hence, prescribing a suitable desired trajectory for the basic output directly provides the feedforward control by evaluating (6.31b) which realizes the path

$$\hat{\boldsymbol{x}}(s) = \sum_{k\in\mathbb{N}} \sum_{j=1}^{r^a_k} \hat{x}_{k_j}(s; \hat{\boldsymbol{\xi}}(s)) \boldsymbol{\phi}_{k_j}, \tag{6.33}$$

where the notation $\hat{x}_{k_j}(s; \hat{\boldsymbol{\xi}}(s))$ is used to refer to (6.31a).

By formally introducing the inverse Laplace transform of the parametrized Fourier coefficients according to

$$\hat{x}_{k_j}(s; \hat{\boldsymbol{\xi}}(s)) \bullet\!\!-\!\!\circ\, x_{k_j}(\boldsymbol{\xi}(t))$$

the equivalent time–domain formulations of (6.33) and (6.31b) are obtained with

$$\boldsymbol{x}(t) = \sum_{k\in\mathbb{N}} \sum_{j=1}^{r_k^a} x_{k_j}(\boldsymbol{\xi}(t))\boldsymbol{\phi}_{k_j} \tag{6.34a}$$

with $\boldsymbol{\xi}(t) = [\xi^1(t), \ldots, \xi^m(t)]^T$ and

$$\hat{u}^l(s) = \hat{u}^l(s, \hat{\xi}^l(s)) \bullet\!\!-\!\!\circ\, u^l(\xi^l(t)). \tag{6.34b}$$

These conclusions, however, require the convergence of the so far only formal state and input parametrizations, which is analyzed in Sections 6.3.1.3 and 6.3.2.2 depending on the properties of $b_{k_j}^l = \langle \mathfrak{b}^l(z), \boldsymbol{\psi}_{k_j}(z)\rangle_X$ and hence $\mathfrak{b}^l(z)$ as well as $\hat{\xi}^l(s)$ or $\xi^l(t)$, respectively.

Remark 6.3. It is rather obvious that the introduced factorization of the resolvent is not unique. However, by observing that s is the operational equivalent to time differentiation, the proposed set–up ensures that the state and input parametrizations only include derivatives of the basic output with respect to t. This observation is exploited for the convergence analysis and is in addition in strict conformity with the definition of differential flatness for finite–dimensional systems.

Moreover, the number of derivatives, though infinite, can in principle be considered as minimal in the sense that the order of s is exactly chosen so that no time–integration occurs. In order to illustrate this, consider the alternative formal representations

$$\begin{aligned} \hat{x}_{k_j}(s) &= -\frac{1}{\lambda_k}\sum_{l=1}^{m}\left(b_{k_j}^l + \sum_{i=1}^{r_k^a - r_k^g} \frac{\sigma_{i,j,k}}{(s-\lambda_k)^i} b_{k_{j+i}}^l\right)\hat{\mathcal{D}}_k^x(s)\hat{\xi}^l(s) \\ \hat{u}^l(s) &= \hat{\mathcal{D}}^u\hat{\xi}^l(s) \end{aligned} \tag{6.35a}$$

with

$$\hat{\mathcal{D}}_k^x(s) = e^{\mathcal{F}\left(\frac{s}{\lambda_k}, g^s\right)} \prod_{\substack{n\in\mathbb{N}\\ n\neq k}} \mathcal{G}\left(\frac{s}{\lambda_n}, g^s\right) \tag{6.35b}$$

$$\hat{\mathcal{D}}^u(s) = \prod_{n\in\mathbb{N}} \mathcal{G}\left(\frac{s}{\lambda_n}, g^s\right) \tag{6.35c}$$

and

$$\begin{aligned} \hat{x}_{k_j}(s) &= \sum_{l=1}^{m}\left(-\frac{b_{k_j}^l}{\lambda_k}\,{}^0\hat{\mathcal{D}}_k^x(s) + \sum_{i=1}^{r_k^a - r_k^g} \frac{\sigma_{i,j,k} b_{k_{j+i}}^l}{(-\lambda_k)^{i+1}}\,{}^i\hat{\mathcal{D}}_k^x(s)\right)\hat{\xi}^l(s) \\ \hat{u}^l(s) &= \hat{\mathcal{D}}^u(s)\hat{\xi}^l(s) \end{aligned} \tag{6.36a}$$

with

$$ {}^{i}\hat{\mathcal{D}}_k^x(s) = e^{(i+1)\mathcal{F}\left(\frac{s}{\lambda_k},g^s\right)} \prod_{\substack{n\in\mathbb{N}\\ n\neq k}} \mathcal{G}^{i+1}\left(\frac{s}{\lambda_n},g^s\right) \prod_{n\in\mathbb{N}} \mathcal{G}^{\theta-i-1}\left(\frac{s}{\lambda_n},g^s\right) \tag{6.36b} $$

$$ \hat{\mathcal{D}}^u(s) = \prod_{n\in\mathbb{N}} \mathcal{G}^{\theta}\left(\frac{s}{\lambda_n},g^s\right) \tag{6.36c} $$

for $\theta = 1+\max_{k\in\mathbb{N}}(r_k^a - r_k^g)$. While a convolution integral arises in general in (6.35) due to the term $1/(s-\lambda_k)^i$ the principle order in s for (6.36) grows significantly faster than in the proposed setting (6.31).

It is important to note that the assignment of a path $\xi^l(t)$ or $\hat{\xi}^l(s)$, respectively, for the basic output in principle directly yields the feedforward control from the evaluation of (6.31b), which is required to realize the corresponding spatial–temporal path (6.33). While this is the underlying idea of flatness–based trajectory planning its applicability essential relies on the convergence of the state and input parametrizations and hence the determination of suitable paths for the basic output.

Remark 6.4. The determined formal state parametrization in addition allows to express the output (6.22b) in terms of the basic output according to

$$ \boldsymbol{y}(t) = \mathfrak{C}\boldsymbol{x}(t) \tag{6.37} $$

with $\boldsymbol{x}(t)$ from the time–domain equivalent to (6.33) with Fourier coefficients (6.31a). It is thereby obvious that the convergence of the parametrized state directly ensures the convergence of the parametrized output.

Remark 6.5. The parametrization moreover reveals that the basic output in general does not allow a physical interpretation but has to be considered as a computational quantity to enable the formal state and input parametrization. However, as is shown in Section 6.4 below for the admissible trajectory assignment, this does not impose any restriction on the solvability of the considered trajectory planning problems.

6.2.2 *Infinite–Dimensional In–Domain and Boundary Control*

Besides the realizable configuration with a finite–dimensional input operator, given a higher–dimensional spatial domain Ω various input set–ups can be considered, which in general rely on the assumption of an infinite–dimensional input operator. This implies that the input $\mathfrak{B}\boldsymbol{u}(t) = \mathfrak{B}\boldsymbol{u}(\cdot,t)$ is restricted to a subspace of Ω including the boundary $\partial\Omega$ (cf. also the system representation (6.1), which is the basis for the abstract formulation (6.2)). Although these scenarios are primarily of theoretical interest, they on the one hand provide further insight into the principles of the proposed spectral design approach and its limitations. On the other hand and as will be shown in the subsequent sections, the consideration of an idealized input significantly enhances the range of applicability by incorporating methods of interpolation and optimization to approximately realize the infinite–dimensional

control actuation by means of a finite number of suitably placed, shaped, and oriented finite–dimensional actuators.

Due to the explicit dependency of the input on the spatial coordinate, the evaluation of the projection $\langle \mathfrak{B}\hat{\boldsymbol{u}}(s), \boldsymbol{\psi}_{k_j}(z)\rangle_X$ in general can be represented as

$$\langle \mathfrak{B}\hat{\boldsymbol{u}}(s), \boldsymbol{\psi}_{k_j}\rangle_X = \langle \hat{\boldsymbol{u}}(s), \mathfrak{B}^*\boldsymbol{\psi}_{k_j}\rangle_X = \sum_{l=1}^{m} b^l_{k_j}\hat{u}^l_{k_j}(s) \tag{6.38}$$

with m denoting the number of components in the vector $\hat{\boldsymbol{u}}(s)$. With this, (6.23) can be further evaluated to obtain

$$\hat{x}_{k_j}(s) = \sum_{l=1}^{m}\left(\frac{1}{s-\lambda_k}b^l_{k_j}\hat{u}^l_{k_j}(s) + \sum_{i=1}^{r^a_k - r^g_k}\frac{\sigma_{i,j,k}}{(s-\lambda_k)^{i+1}}b^l_{k_{j+i}}\hat{u}^l_{k_{j+i}}(s)\right) \tag{6.39}$$

for all $j = 1,\ldots,r^a_k$, $k \in \mathbb{N}$. Here, $b^l_{k_j}$ denotes a coefficient being constant for each k_j and l while $\hat{u}^l_{k_j}(s)$ can be interpreted as a Fourier coefficient obtained from the projection of $\hat{\boldsymbol{u}}(s)$ onto $\mathfrak{B}^*\boldsymbol{\psi}_{k_j}$. This however implies that the set of functions $\mathfrak{B}^*\boldsymbol{\psi}_{k_j}$ represents a Riesz basis. For higher–dimensional spatial domains and infinite–dimensional control, the application of the adjoint $\mathfrak{B}^*$ to the components of the Riesz basis $((\boldsymbol{\psi}_{k_j})_{j=1,\ldots,r^a_k})_{k\in\mathbb{N}}$ in general results in a linear dependent set of functions $((\mathfrak{B}^*\boldsymbol{\psi}_{k_j})_{j=1,\ldots,r^a_k})_{k\in\mathbb{N}}$, i.e. there exit elements, which can be expressed in terms of linear combinations of the remaining elements in the set. This property is illustrated in the following example.

Example 6.1. It can be easily shown that the sequence $((\psi_{k_j}(z))_{j=1,\ldots,r^a_k})_{k\in\mathbb{N}}$ defined according to

$$\begin{aligned}
&\psi_{1_1} = K\sin(z^1)\sin(z^2)\\
&\psi_{2_1} = K\sin(2z^1)\sin(z^2), && \psi_{2_2} = K\sin(z^1)\sin(2z^2)\\
&\psi_{3_1} = K\sin(2z^1)\sin(2z^2)\\
&\psi_{4_1} = K\sin(3z^1)\sin(z^2), && \psi_{4_2} = K\sin(z^1)\sin(3z^2)\\
&\psi_{5_1} = K\sin(3z^1)\sin(2z^2), && \psi_{5_2} = K\sin(2z^1)\sin(3z^2)\\
&\psi_{6_1} = K\sin(3z^1)\sin(3z^2)\\
&\quad\vdots
\end{aligned} \tag{6.40}$$

with $K = 2/\pi$ is an orthonormal basis and hence a Riesz basis for $L^2(\Omega)$ with $\Omega = \{z \in \mathbb{R}^2 : 0 < z^j < \pi,\ j = 1,2\}$. Let $\mathfrak{B}^*\psi_k(z) = -\partial_{z^2}\psi_{k_j}(z)|_{z^2=\pi}$ such that

$$\begin{aligned}
&\mathfrak{B}^*\psi_{1_1} = K\sin(z^1)\\
&\mathfrak{B}^*\psi_{2_1} = K\sin(2z^1), && \mathfrak{B}^*\psi_{2_2} = -2\mathfrak{B}^*\psi_{1_1}\\
&\mathfrak{B}^*\psi_{3_1} = -2\mathfrak{B}^*\psi_{2_1}
\end{aligned}$$

$$\begin{aligned}
&\mathfrak{B}^*\psi_{4_1} = K\sin(3z^1), && \mathfrak{B}^*\psi_{4_2} = 3\mathfrak{B}^*\psi_{1_1} \\
&\mathfrak{B}^*\psi_{5_1} = -2\mathfrak{B}^*\psi_{4_1}, && \mathfrak{B}^*\psi_{5_2} = 3\mathfrak{B}^*\psi_{2_1} \\
&\mathfrak{B}^*\psi_{6_1} = 3\mathfrak{B}^*\psi_{4_1} \\
&\quad\vdots
\end{aligned} \tag{6.41}$$

It is obvious that the linear independence is lost in the sequence above. However, from (6.41) the sequence $(\chi_k(z^1))_{k\in\mathbb{N}}$ can be extracted according to $\chi_1(z^1) = \mathfrak{B}^*\psi_{1_1}(z),\ \chi_2(z^1) = \mathfrak{B}^*\psi_{2_1}(z),\ \chi_3(z^1) = \mathfrak{B}^*\psi_{4_1}(z),\ \ldots$, which forms an orthonormal basis for $L^2(0,\pi)$. Note that the thus introduced operator $\mathfrak{B}^*$ corresponds to the adjoint of the control operator arising in the boundary control of the heat equation defined on Ω with Dirichlet boundary conditions on all of the boundary of Ω except on the surface $z^2 = \pi$, where the infinite–dimensional input $u(z^1,t)$ is prescribed, i.e.

$$\begin{aligned}
&\partial_t x(z,t) = \Delta x(z,t), && z \in \Omega,\ t > 0 \\
&x(z,t) = 0, && z^1 \in \{0,\pi\} \wedge z^2 = 0 \\
&x(z,t) = u(z^1,t), && z^2 = \pi.
\end{aligned}$$

In this case, (6.40) represents the eigenvectors of the respective system operator.

Hence, in order to address this issue and to enable the reconstruction of $\hat{\boldsymbol{u}}(s)$ from its Fourier coefficients $\hat{u}^l_{k_j}(s)$ the following assumption is imposed.

Assumption 6.3. The sequence $((\mathfrak{B}^*\boldsymbol{\psi}_{k_j})_{j=1,\ldots,r^a_k})_{k\in\mathbb{N}}$ includes a linear independent subsequence $(\boldsymbol{\chi}_k)_{k\in\mathbb{N}}$, which forms a Riesz basis for U. Moreover, the sequence $((\mathfrak{B}\boldsymbol{\phi}_{k_j})_{j=1,\ldots,r^a_k})_{k\in\mathbb{N}}$ includes a linear independent subsequence $(\boldsymbol{\varphi}_k)_{k\in\mathbb{N}}$, which forms a Riesz basis for U biorthogonal to $(\boldsymbol{\chi}_k)_{k\in\mathbb{N}}$.

Note that subsequently, no notational distinction is made between the tuple of independent coordinates z in $\boldsymbol{\phi}_{k_j} = \boldsymbol{\phi}_{k_j}(z)$, $\boldsymbol{\psi}_{k_j} = \boldsymbol{\psi}_{k_j}(z)$ and in $\boldsymbol{\varphi}_{k_j} = \boldsymbol{\varphi}_{k_j}(z)$ and $\boldsymbol{\chi}_{k_j} = \boldsymbol{\chi}_{k_j}(z)$, although Example 6.1 confirms that these do not necessarily coincide.

Remark 6.6. In view of the assumption above, the inner product $\langle\hat{\boldsymbol{u}}, \mathfrak{B}^*\boldsymbol{\psi}_{k_j}\rangle_X$ in (6.38) can be considered as an inner product in U. Hence, subsequently the notation $\langle\hat{\boldsymbol{u}}, \mathfrak{B}^*\boldsymbol{\psi}_{k_j}\rangle_U$ is used to emphasize this property.

Moreover, Assumption 6.3 implies a certain grouping of the spectral input components $\hat{u}^l_{k_j}(s)$, which is formulated in terms of the assumption below.

Assumption 6.4. The spectral components $\hat{u}^l_{k_j}(s)$ are mutually disjoint, i.e. $\nexists k_j$ such that $\hat{u}^{l_1}_{k_j}(s) = \hat{u}^{l_2}_{k_j}(s)$ with[6] $l_1 \neq l_2$. Moreover, there exist countable, densely embedded index sets $S^l_q \subset \mathbb{N}$, $q = 1,2,\ldots$, such that for each $l = 1,\ldots,m$

[6] This property is equivalent to the non–overlapping of the individual actuators, which is a realistic assumption in applications.

(i) $\bigcup_{q\in\mathbb{N}} S_q^l = \{\{k_j\}_{j=1,\dots,r_k^a}\}_{k\in\mathbb{N}}$ while $S_{q_1}^l \cap S_{q_2}^l = \emptyset$ if $q_1 \neq q_2$, and
(ii) for all $k_j \in S_q^l$ it follows that $\hat{u}_{k_j}^l(s) = \hat{u}_q^l(s)$.

These properties are clarified in the following example.

Example 6.2. The eigenvalues of the Laplace operator considered in Example 6.1 corresponding to the eigenvectors (6.40) are given by $\lambda_1 = -2,\ \lambda_2 = -5,\ \lambda_3 = -8,\ \lambda_4 = -10,\ \lambda_5 = -13,\ \lambda_6 = -18,\ \dots$, with $r_k^a = r_k^g$ for all $k \in \mathbb{N}$. By making use of (6.41), the evaluation of (6.39) with $X = L^2(\Omega)$ and $m = 1$ yields

$$
\begin{aligned}
\hat{x}_{1_1}(s) &= \frac{1}{s+2}\langle \hat{u}(s), \chi_1\rangle_{L^2(0,\pi)} \\
\hat{x}_{2_1}(s) &= \frac{1}{s+5}\langle \hat{u}(s), \chi_2\rangle_{L^2(0,\pi)}, \qquad \hat{x}_{2_2}(s) = \frac{-2}{s+5}\langle \hat{u}(s), \chi_1\rangle_{L^2(0,\pi)} \\
\hat{x}_{3_1}(s) &= \frac{-2}{s+8}\langle \hat{u}(s), \chi_2\rangle_{L^2(0,\pi)} \\
\hat{x}_{4_1}(s) &= \frac{1}{s+10}\langle \hat{u}(s), \chi_3\rangle_{L^2(0,\pi)}, \qquad \hat{x}_{4_2}(s) = \frac{3}{s+10}\langle \hat{u}(s), \chi_1\rangle_{L^2(0,\pi)} \\
\hat{x}_{5_1}(s) &= \frac{-2}{s+13}\langle \hat{u}(s), \chi_3\rangle_{L^2(0,\pi)}, \qquad \hat{x}_{5_2}(s) = \frac{3}{s+13}\langle \hat{u}(s), \chi_2\rangle_{L^2(0,\pi)} \\
\hat{x}_{6_1}(s) &= \frac{3}{s+18}\langle \hat{u}(s), \chi_3\rangle_{L^2(0,\pi)}, \qquad \dots
\end{aligned}
$$

Hence, by considering only these first spectral components the three sets $S_1 = \{1_1, 2_2, 4_2\}$, $S_2 = \{2_1, 3_1, 5_2\}$, and $S_3 = \{4_1, 5_1, 6_1\}$ can be identified according to Assumption 6.4. Moreover, the coefficients b_{k_j} follow as $b_{1_1} = b_{2_1} = b_{4_1} = 1$, $b_{2_2} = b_{3_1} = b_{5_1} = -2$, and $b_{4_2} = b_{5_2} = b_{6_1} = 3$. With the orthogonal basis $(\chi_k(z^1))_{k\in\mathbb{N}}$ introduced in Example 6.1 it follows that the boundary input can be represented as $\hat{u}(z^1, s) = \sum_{k\in\mathbb{N}} \hat{u}_k(s)\chi_k(z^1)$ with $\hat{u}_k(s) = \langle \hat{u}(z^1, s), \chi_k(z^1)\rangle_{L^2(0,\pi)}$, which confirms that $U = L^2(0, \pi)$.

If all spectral components $\hat{u}_{k_j}^l(s)$ are identical for all $j = 1, \dots, r_k^a$, $k \in \mathbb{N}$, then the l–th input component is finite–dimensional and the parametrization is obtained as in the previous section. This case is excluded from the analysis.

Subsequently, it is convenient to introduce for each $q \in \mathbb{N}$ the two sets $S_q^{l,1}$ and $S_q^{l,2}$ such that $k \in S_q^{l,1}$ and $j \in S_q^{l,2}$ implies that $k_j \in S_q^l$. Note that the elements of both $S_q^{l,1}$ and $S_q^{l,2}$ are in general not disjoint. As an example consider $S_q^l = \{1_1, 1_2, 2_1\}$, which yields $S_q^{l,1} = \{1, 1, 2\}$ and $S_q^{l,2} = \{1, 2, 1\}$. Let

$$
q^l(k_j) := \{q \in \mathbb{N} : k_j \in S_q^l\}, \tag{6.42}
$$

denote the indicator function, which for given k_j returns the value q such that $k_j \in S_q^l$ and thus $k \in S_{q^l(k_j)}^{l,1}$ as well as $j \in S_{q^l(k_j)}^{l,2}$. With this, the expression for $\hat{x}_{k_j}(s)$ can be re–written as

$$
\hat{x}_{k_j}(s) = \sum_{l=1}^{m}\left(\frac{1}{s-\lambda_k} b_{k_j}^l \hat{u}_{q^l(k_j)}^l(s) + \sum_{i=1}^{r_k^a - r_k^g} \frac{\sigma_{i,j,k}}{(s-\lambda_k)^{i+1}} b_{k_{j+i}}^l \hat{u}_{q^l(k_{j+i})}^l(s)\right).
$$

Moreover, the approximate controllability of the system is assumed based on the conditions summarized below (see, e.g., [3] for related results).

Assumption 6.5. The number m of input components in (6.38) satisfies

$$m \geq \max_{k\in\mathbb{N}} r_k^g$$

while for each $k \in \mathbb{N}$ at least r_k^g coefficients $b_{k_j}^l \hat{u}_{q^l(k_j)}^l$ are non–zero for $l = 1,\ldots,m$ and $j = 1,\ldots,r_k^a$.

With these preliminaries, similar to the previous section a suitable extension of the numerator and denominator of the fraction in terms of Weierstrass primary factors can be introduced for each projected input component $\hat{u}_{k_j}^l(s)$ or $\hat{u}_{q^l(k_j)}^l(s)$, respectively, according to

$$\begin{aligned}
\hat{x}_{k_j}(s) = \sum_{l=1}^{m} e^{\theta_k \mathcal{F}\left(\frac{s}{\lambda_k}, g^s\right)} \times \\
\Bigg\{ \left(-\frac{b_{k_j}^l}{\lambda_k}\right) \frac{\left(1-\frac{s}{\lambda_k}\right)^{\theta_k - 1} \prod_{n\in S_{q^l(k_j)}^{l,1}\setminus\{k\}} \mathcal{G}^{\theta_n}\left(\frac{s}{\lambda_n}, g^s\right)}{\prod_{n\in S_{q^l(k_j)}^{l,1}} \mathcal{G}^{\theta_n}\left(\frac{s}{\lambda_n}, g^s\right)} \hat{u}_{q^l(k_j)}^l(s) \\
+ \sum_{i=1}^{r_k^a - r_k^g} \frac{\sigma_{i,j,k} b_{k_{j+i}}^l}{(-\lambda_k)^{i+1}} \frac{\left(1-\frac{s}{\lambda_k}\right)^{\theta_k - i - 1} \prod_{n\in S_{q^l(k_{j+i})}^{l,1}\setminus\{k\}} \mathcal{G}^{\theta_n}\left(\frac{s}{\lambda_n}, g^s\right)}{\prod_{n\in S_{q^l(k_{j+i})}^{l,1}} \mathcal{G}^{\theta_n}\left(\frac{s}{\lambda_n}, g^s\right)} \hat{u}_{q^l(k_{j+i})}^l(s) \Bigg\}
\end{aligned}$$

with $\theta_k = 1 + r_k^a - r_k^g$. This motivates the formal introduction of the new quantity $\hat{\xi}_q^l(s)$ in terms of

$$\hat{\xi}_q^l(s) = \frac{\hat{u}_q^l(s)}{\prod_{n\in S_q^{l,1}} \mathcal{G}^{\theta_n}\left(\frac{s}{\lambda_n}, g^s\right)}, \tag{6.43}$$

which directly yields the formal state and input parametrization

$$\begin{aligned}
\hat{x}_{k_j}(s) = \sum_{l=1}^{m} \Bigg(\left(-\frac{b_{k_j}^l}{\lambda_k}\right)^0 \hat{\mathcal{D}}_{q^l(k_j),k}^{x,l}(s)\, \hat{\xi}_{q^l(k_j)}^l(s) \\
+ \sum_{i=1}^{r_k^a - r_k^g} \frac{\sigma_{i,j,k} b_{k_{j+i}}^l}{(-\lambda_k)^{i+1}}\, {}^i\hat{\mathcal{D}}_{q^l(k_{j+i}),k}^{x,l}(s)\, \hat{\xi}_{q^l(k_{j+i})}^l(s) \Bigg)
\end{aligned} \tag{6.44a}$$

$$\hat{u}_q^l(s) = \hat{\mathcal{D}}_q^{u,l}(s) \hat{\xi}_q^l(s) \tag{6.44b}$$

in terms of the operators

$$
{}^{i}\hat{\mathcal{D}}^{x,l}_{q^l(k_j),k}(s) = e^{\theta_k \mathcal{F}\left(\frac{s}{\lambda_k}, g^s\right)} \times \left(1 - \frac{s}{\lambda_k}\right)^{\theta_k - i - 1} \prod_{n \in S^{l,1}_{q^l(k_j)} \setminus \{k\}} \mathcal{G}^{\theta_n}\left(\frac{s}{\lambda_n}, g^s\right) \tag{6.45a}
$$

$$
\hat{\mathcal{D}}^{u,l}_{q}(s) = \prod_{n \in S^{l,1}_{q}} \mathcal{G}^{\theta_n}\left(\frac{s}{\lambda_n}, g^s\right) \tag{6.45b}
$$

Similar to the case of a finite–dimensional control for each q the m–tuple $\hat{\xi}^l_q(s)$, $l = 1, \ldots, m$, can be interpreted as the projection of the (now infinite–dimensional) basic output $\hat{\boldsymbol{\xi}}(s) = \hat{\boldsymbol{\xi}}(\cdot, s)$ in the operational domain. For this, recall that the operational state parametrization is obtained by evaluating

$$
\hat{\boldsymbol{x}}(s) = \sum_{k \in \mathbb{N}} \sum_{j=1}^{r^a_k} \hat{x}_{k_j}(s; \hat{\boldsymbol{\xi}}_{q^l(k_j)}(s)) \boldsymbol{\phi}_{k_j} \tag{6.46}
$$

with $\hat{x}_{k_j}(s; \hat{\boldsymbol{\xi}}_{q^l(k_j)}(s))$ referring to the Fourier coefficients (6.44a). In view of Assumptions 6.3 and 6.4, the corresponding operational input parametrizations can be expressed in terms of the Fourier series

$$
\hat{\boldsymbol{u}}(s) = \sum_{l=1}^{m} \sum_{k \in \mathbb{N}} \hat{u}^l_k(s; \hat{\xi}^l_k(s)) \boldsymbol{\varphi}_k \tag{6.47}
$$

with $\hat{u}^l_k(s; \hat{\xi}^l_k(s))$ representing (6.44b) and the Riesz basis $(\boldsymbol{\varphi}_k)_{k \in \mathbb{N}}$ obtained from $((\mathfrak{B}\boldsymbol{\phi}_{k_j})_{j=1,\ldots,r^a_k})_{k \in \mathbb{N}}$. Formally denoting the inverse Laplace transforms of the parametrized Fourier coefficients by

$$
\hat{x}_{k_j}(s; \hat{\boldsymbol{\xi}}_{q^l(k_j)}(s)) \bullet\!\!-\!\!\circ\, x_{k_j}(\boldsymbol{\xi}_{q^l(k_j)}(t)), \qquad \hat{u}^l_k(s; \hat{\xi}^l_k(s)) \bullet\!\!-\!\!\circ\, u^l_k(\xi^l_k(t)),
$$

the equivalent time–domain formulations of (6.46) and (6.47) are given by

$$
\boldsymbol{x}(t) = \sum_{k \in \mathbb{N}} \sum_{j=1}^{r^a_k} x_{k_j}(\boldsymbol{\xi}_{q^l(k_j)}(t)) \boldsymbol{\phi}_{k_j} \tag{6.48a}
$$

with $\boldsymbol{\xi}_\bullet(t) = [\xi^1_\bullet(t), \ldots, \xi^m_\bullet(t)]^T$ and

$$
\boldsymbol{u}(t) = \sum_{l=1}^{m} \sum_{k \in \mathbb{N}} u^l_k(\xi^l_k(t)) \boldsymbol{\varphi}_k. \tag{6.48b}
$$

In addition, note that equality (6.43) and the Riesz basis property introduced in Assumption 6.3 hence imply that the basic output $\hat{\boldsymbol{\xi}}(s) \bullet\!\!-\!\!\circ\, \boldsymbol{\xi}(t) \in \Xi$, with Ξ representing a Hilbert space, can be expressed in terms of the Fourier series

$$\boldsymbol{\xi}(t) = \sum_{l=1}^{m} \sum_{k \in \mathbb{N}} \xi_k^l(t) \boldsymbol{\varphi}_k, \tag{6.49a}$$

where according to Theorem 6.2(iv) it follows that

$$\sum_{k \in \mathbb{N}} |\xi_k^l(t)|^2 < \infty, \tag{6.49b}$$

for each $l = 1, \ldots, m$ and all $t \geq 0$. This immediately illustrates that the domains of $\boldsymbol{u}(t)$ and $\boldsymbol{\xi}(t)$, i.e. U and Ξ, have to coincide such that in the following U and Ξ are used equivalently.

Furthermore, it should be pointed out that the essential difference between the operators introduced in (6.45) and those defined in (6.32) for the case of finite–dimensional in–domain and boundary control is given by the number of components in the product representations. While the products are evaluated in (6.45) over $S^{l,1}_{q^l(k_j)}$ or $S^{l,1}_{q}$, respectively, i.e. a countable dense subset of $\mathbb{N}$, the products in (6.32) are evaluated over $\mathbb{N}$.

Remark 6.7. The determined formal state parametrization in addition allows to express the output (6.22b) in terms of the basic output according to

$$\boldsymbol{y}(t) = \mathfrak{C}\boldsymbol{x}(t) \tag{6.50}$$

with $\boldsymbol{x}(t)$ from (6.48a). It is thereby obvious that the convergence of the parametrized state directly ensures the convergence of the parametrized output.

6.3 Convergence in Gevrey Classes

The determined parametrizations of the projected state and input variables in terms of a basic output are so far only formally valid and their uniform convergence has to be ensured to deduce meaningful expressions in view of the solution of the trajectory planning problem, i.e. the determination of suitable paths for the basic output to solve the transition problem from the initial state to a final state along a prescribed desired spatial–temporal trajectory. For this, it is decisive to observe that the introduced operators $\hat{\mathcal{D}}^u(s)$ for the case of a finite–dimensional control as well as $\hat{\mathcal{D}}^{u,l}_{q^l(k_j)}(s)$ for the case of infinite–dimensional control can be interpreted as Weierstrass canonical products of genus g^s in the sense introduced in Appendix B.2.2 and hence as entire functions. Furthermore, the Hadamard factorization (B.16) of an entire function implies that ${}^i\hat{\mathcal{D}}^x_k(s)$ and ${}^i\hat{\mathcal{D}}^{x,l}_{q^l(k_j),k}(s)$ similarly represent entire functions. Any entire function can be expanded into a MacLaurin series in the Laplace variable s which converges absolutely and uniformly in any disc $|s| < R < \infty$ in the complex domain $\mathbb{C}$. Since s denotes the equivalent to differentiation with respect to the coordinate t the introduced operators can be interpreted as the operational representations of differential operators of infinite order in the sense of [50, 62], i.e.

$$ {}^{i}\mathcal{D}_{k}^{x} \circ \xi^{l}(t) = {}^{i}\hat{\mathcal{D}}_{k}^{x}(\partial_t) \circ \xi^{l}(t) \tag{6.51a} $$

$$ \mathcal{D}^{u} \circ \hat{\xi}^{l}(t) = \hat{\mathcal{D}}^{u}(\partial_t) \circ \xi^{l}(t) \tag{6.51b} $$

or

$$ {}^{i}\mathcal{D}_{q^{l}(k_j),k}^{x,l} \circ \xi_{q^{l}(k_j)}^{l}(t) = {}^{i}\hat{\mathcal{D}}_{q^{l}(k_j),k}^{x,l}(\partial_t) \circ \xi_{q^{l}(k_j)}^{l}(t) \tag{6.52a} $$

$$ \mathcal{D}_{q}^{u,l} \circ \xi_{q}^{l}(t) = \hat{\mathcal{D}}_{q}^{u,l}(\partial_t) \circ \xi_{q}^{l}(t) \tag{6.52b} $$

respectively. Hence, it follows that any trajectory $\xi^{l}(t)$ or $\xi_{q}^{l}(t)$ necessarily has to be a C^{∞}–function. In addition, it is obvious from the definition of the differential operators that their convergence inherently depends on the genus of their zeros and thus the eigenvalue distribution. In order to address these issues, subsequently the operational convergence of the parametrizations in the s–domain is analyzed by exploiting certain properties of entire functions as are summarized in Appendix B.2. With this, general conditions can be determined for the L^2–convergence of the parametrized Fourier series for the state and the input, respectively.

6.3.1 Operational Convergence

In the sequel, the operational convergence of the introduced operators ${}^{i}\hat{\mathcal{D}}_{k}^{x}(s)$ and $\hat{\mathcal{D}}^{u}(s)$ as well as ${}^{i}\hat{\mathcal{D}}_{q^{l}(k_j),k}^{x,l}(s)$ and $\hat{\mathcal{D}}_{q}^{u,l}(s)$ is analyzed in a common framework using results from the theory of entire functions. Thereby, so–called Gevrey–class functions, as introduced in Definition B.1 of Appendix B.1, are incorporated into the convergence analysis.

6.3.1.1 Preliminary Results

By introducing a general differential operator of infinite order, which in the operational domain is given in terms of a Weierstrass canonical product, the main convergence result can be verified, which serves as the basis for the analysis of the operational parametrizations.

Lemma 6.3. *Let* $((\lambda_k)_{j=1,\dots,\theta_k})_{k\in\mathbb{N}}$ *be the sequence of eigenvalues of the Riesz spectral operator* $\mathfrak{A}$ *introduced in* (6.22a) *with each* λ_k *repeated* $(1+r_k^a-r_k^g)=\theta_k$*–times. Assume that* $((\lambda_k)_{j=1,\dots,\theta_k})_{k\in\mathbb{N}}$ *is of convergence exponent* γ *and genus* g^s*. Then, given* $s\in\mathbb{C}$ *and the countable set* $S\subseteq\mathbb{N}$*,*

$$ \hat{\mathcal{D}}(s) = \prod_{n\in S} \mathcal{G}^{\theta_n}\left(\frac{s}{\lambda_n}, g^s\right) = \prod_{n\in S}\prod_{j=1}^{\theta_n} \mathcal{G}\left(\frac{s}{\lambda_n}, g^s\right) \tag{6.53} $$

is an entire function of order $\varrho = \gamma$ and genus $g^f = g^s$. If $\hat{\mathcal{D}}(s)$ is of finite type τ, then

$$f(t) = \hat{\mathcal{D}}(\partial_t) \circ \xi(t) \tag{6.54}$$

satisfies

$$\|f\|_\infty \leq DK(D, \varrho, \tau, \alpha) \tag{6.55a}$$

with the power series

$$K(D, \varrho, \tau, \alpha) = \sum_{n \in \mathbb{N}} (n!)^{\alpha - \frac{1}{\varrho}} \left(\eta_{\varrho,\tau}(D)\right)^n \tag{6.55b}$$

in $\eta_{\varrho,\tau}(D) = (D^\varrho(e\varrho\tau + \epsilon))^{1/\varrho} > 0$, which convergences uniformly for $\xi(t) \in G_{D,\alpha}(\mathbb{R}^+)$ with $\alpha \leq 1/\varrho$.

If S is a finite set, then $\hat{\mathcal{D}}(s)$ is merely a polynomial in s and the claim is trivially satisfied. If S is a countably infinite set, then the proof essentially relies on certain properties of entire functions (see, e.g., the comprehensive treatises in [8, 34, 35] and the brief summary in the Appendix B.2).

Proof. Since $\hat{\mathcal{D}}(s)$ is a Weierstrass canonical product[7] it follows that $\hat{\mathcal{D}}(s)$ is an entire function of order ϱ equal to the convergence exponent γ of the sequence $((\lambda_n)_{j=1,\ldots,\theta_n})_{n \in S}$ of its zeros (cf. Theorem B.2). Moreover, by Theorem B.3 the function $\hat{\mathcal{D}}^u(s)$ is of genus $g^f = g^s$.

If $\hat{\mathcal{D}}(s)$ is an entire function of order ϱ and finite type τ, then it admits a MacLaurin series expansion

$$\hat{\mathcal{D}}(s) = \sum_{n \in \mathbb{N}} c_n s^n,$$

which converges for all $s \in \mathbb{C}$. Since τ is finite by assumption the maximum modulus $M(\eta)$ by the definition of the order and type of an entire function satisfies $M(\eta) < \exp(\tau\eta^\varrho)$ as $\eta \to \infty$. Hence, by [8, Theorem 2.2.10] or [35, Lemma 1] there exists a finite $N(\epsilon) \in \mathbb{N}$ depending on a given $\epsilon > 0$ such that the series coefficients satisfy

$$|c_n| \leq \left(\frac{e\varrho\tau + \epsilon}{n}\right)^{\frac{n}{\varrho}} \tag{6.56}$$

for all $n > N(\epsilon)$. By recalling that s represents the operational equivalent to time differentiation this implies that (6.54) corresponds to

[7] It should be pointed out that the formulation introduced in (6.53) is equivalent to the definition (B.13) of a Weierstrass canonical product since the double product can be re–written in terms of a single product over a new index set.

$$f(t) = \sum_{n\in\mathbb{N}} c_n \partial_t^n \xi(t).$$

Since $\xi(t)$ is Gevrey of order α, i.e. $\xi(t) \in G_{D,\alpha}(\mathbb{R}^+)$, this yields the sequence of bounds

$$\sup_{t\in\mathbb{R}^+} |f(t)| \leq \sum_{n\in\mathbb{N}} |c_n| \sup_{t\in\mathbb{R}^+} |\partial_t^n \xi(t)| \leq \sum_{n\in\mathbb{N}} |c_n| D^{n+1} (n!)^\alpha$$

Taking into account that a finite number of series coefficients does not alter the convergence behavior of the series, it can be assumed without loss of generality that (6.56) holds[8] for all $n \geq 0$. As a result, it follows that

$$\sup_{t\in\mathbb{R}^+} |f(t)| \leq D \sum_{n\in\mathbb{N}} \left(D^\varrho (e\varrho\tau + \epsilon)\right)^{\frac{n}{\varrho}} \frac{(n!)^\alpha}{n^{\frac{n}{\varrho}}} \leq D \sum_{n\in\mathbb{N}} (n!)^{\alpha - \frac{1}{\varrho}} \left(\eta_{\varrho,\tau}(D)\right)^n$$

with finite $\eta_{\varrho,\tau}(D) = \left(D^\varrho (e\varrho\tau + \epsilon)\right)^{1/\varrho} > 0$, where for the latter inequality $1/n^n \leq 1/(n!)$ was used. The resulting bound can be interpreted as a power series in $\eta_{\varrho,\tau}(D)$, whose radius of convergence follows immediately from the Cauchy–Hadamard theorem as

$$\varrho_\eta = \begin{cases} \infty, & \text{if } \alpha < \frac{1}{\varrho} \\ 1, & \text{if } \alpha = \frac{1}{\varrho} \\ 0, & \text{if } \alpha > \frac{1}{\varrho}. \end{cases}$$

Obviously, (6.54) converges uniformly for all $\xi(t) \in G_{D,\alpha}(\mathbb{R}^+)$ with $\alpha \leq 1/\varrho$, which proves the Lemma. □

Based on this result on the operational convergence of the operator (6.53), the following corollary can be deduced.

Corollary 6.2. *Let $((\lambda_k)_{j=1,\dots,\theta_k})_{k\in\mathbb{N}}$ be the sequence of eigenvalues of the Riesz spectral operator $\mathfrak{A}$ introduced in* (6.22a) *with each λ_k repeated $(1+r_k^a-r_k^g) = \theta_k$–times. Assume that $((\lambda_k)_{j=1,\dots,\theta_k})_{k\in\mathbb{N}}$ is of convergence exponent γ and genus g^s. For each $k \in S$ and $i \in \{1, 2, \dots, \theta_k - 1\}$ consider the infinite product*

$$\begin{aligned} {}^i\hat{\mathcal{D}}_k(s) &= e^{\theta_k \mathcal{F}\left(\frac{s}{\lambda_k}, g^s\right)} \left(1 - \frac{s}{\lambda_k}\right)^{\theta_k - i - 1} \prod_{n\in S, n\neq k} \mathcal{G}^{\theta_n}\left(\frac{s}{\lambda_n}, g^s\right) \\ &= e^{\theta_k \mathcal{F}\left(\frac{s}{\lambda_k}, g^s\right)} \left(1 - \frac{s}{\lambda_k}\right)^{\theta_k - i - 1} \prod_{n\in S, n\neq k} \prod_{j=1}^{\theta_n} \mathcal{G}\left(\frac{s}{\lambda_n}, g^s\right) \end{aligned} \tag{6.57}$$

with $s \in \mathbb{C}$ and the countable set $S \subseteq \mathbb{N}$. Then ${}^i\hat{\mathcal{D}}_k(s)$ is an entire function of order $\varrho = \gamma$. If ${}^i\hat{\mathcal{D}}_k(s)$ is of finite type τ, then

[8] Equivalently, ϵ can be chosen sufficiently large until $N(\epsilon) = 0$.

$$f(t) = {}^{i}\hat{\mathcal{D}}_k(\partial_t) \circ \xi(t) \tag{6.58}$$

convergences uniformly for $\xi(t) \in G_{D,\alpha}(\mathbb{R}^+)$ *with* $\alpha \leq 1/\varrho$ *and* $\|f(t)\|_\infty$ *is bounded according to* (6.55)*.*

Proof. By the Hadamard theorem B.3, it follows immediately that ${}^{\theta_k-1}\hat{\mathcal{D}}_k(s)$ is an entire function of finite order ϱ. Since the polynomial degree in $\mathcal{F}(s/\lambda_k, g^s)$ is by definition (cf. Eqn. (6.29)) equal to g^s, the growth order of $\exp\theta_k\mathcal{F}(s/\lambda_k, g^s)$ can be directly determined as $\varrho_{\mathcal{F}} = g^s$. In addition, Theorem B.2 yields that the order $\varrho_{\mathcal{G}}$ of the Weierstrass canonical product $\prod_{n\in S, n\neq k}\mathcal{G}^{\theta_n}(s/\lambda_n, g^s)$ equals the convergence exponent γ of its zeros. Hence, (B.8) provides that the order of the composite function ${}^{\theta_k-1}\hat{\mathcal{D}}_k(s)$ is given by $\varrho = \max\{\varrho_{\mathcal{G}}, \varrho_{\mathcal{F}}\} = \max\{\gamma, g^s\}$. Since Definition B.4 provides $\gamma \geq g^s$, this yields the growth order $\varrho = \gamma$ of ${}^{\theta_k-1}\hat{\mathcal{D}}_k(s)$. Observing that $(1 - s/\lambda_k)^{\theta_k-i-1}$ is only of polynomial degree the growth order of ${}^{i}\hat{\mathcal{D}}_k(s)$ for each $i = \{1, 2, \ldots, \theta_k - 2\}$ equals the growth order of ${}^{\theta_k-1}\hat{\mathcal{D}}_k(s)$, which proves the first part of the claim. With this, the verification of the second part of the corollary follows exactly the lines of the proof of Lemma 6.3 since the orders of growth of $\hat{\mathcal{D}}(s)$ as introduced in (6.53) and ${}^{i}\hat{\mathcal{D}}_k(s)$ coincide. □

The most critical task in the operational convergence analysis is obviously related to the criteria that the infinite product (6.53) is an entire function of finite type and finite order. In view of the operational parametrizations of Riesz spectral systems, this property is essentially determined by the distribution of the eigenvalues $((\lambda_k)_{j=1,\ldots,\theta_k})_{k\in\mathbb{N}}$ of the Riesz spectral system operator with each λ_k repeated $(1 + r_k^a - r_k^g) = \theta_k$–times and thus the particular system under consideration as well as the underlying index set $S \subseteq \mathbb{N}$. Explicit computations involving asymptotic eigenvalue distributions are thereby provided in Section 6.5 based on several application examples.

However, the results obtained above enable to derive explicit results and criteria for operational convergence of the parametrizations (6.31) and (6.44) given either finite–dimensional or infinite–dimensional control inputs, respectively. Therefore, at first the latter case is studied since, as is shown below, the operational convergence of the parametrizations for the finite–dimensional control input can be directly deduced from this configuration.

6.3.1.2 Infinite–Dimensional In–Domain and Boundary Control

By exploiting the relationship between the operator $\hat{\mathcal{D}}_q^{u,l}(s)$ defined in (6.45b) and the operator (6.53), the application of Lemma 6.3 and Corollary 6.2 allows to verify the convergence of the Fourier coefficients $x_{k_j}(t), k \in \mathbb{N}, j = 1, \ldots, r_k^a$, and $u_q^l(t)$, $q \in \mathbb{N}, l = 1, \ldots, m$, parametrized in the operational domain according to (6.44) for the case of an infinite–dimensional control input.

Theorem 6.5. *Assume that* $\hat{\mathcal{D}}_q^{u,l}(s)$ *as defined in* (6.45b) *is an entire function of finite order* ϱ_q^l *and finite type* τ_q^l*. Let* $\xi_q^l(t) \in G_{D_q^l,\alpha_q^l}(\mathbb{R}^+)$ *for each* $l = 1, \ldots, m$

with $\alpha_q^l < 1/\varrho_q^l$. *Then* $x_{k_j}(t) \circ\!\!-\!\!\bullet\, \hat{x}_{k_j}(s)$ *and* $u_q^l(t) \circ\!\!-\!\!\bullet\, \hat{u}_q^l(s)$ *parametrized in terms of* $\xi_q^l(t) \circ\!\!-\!\!\bullet\, \hat{\xi}_q^l(s)$ *as defined in* (6.44) *satisfy the inequalities*

$$\|x_{k_j}\|_\infty \leq \sum_{l=1}^{m} \left(\left| \frac{b_{k_j}^l}{\lambda_k} \right| D_{q^l(k_j)}^l K\left(D_{q^l(k_j)}^l, \varrho_{q^l(k_j)}^l, \tau_{q^l(k_j)}^l, \alpha_{q^l(k_j)}^l \right) + \sum_{i=1}^{r_k^a - r_k^g} \sigma_{i,j,k} \left| \frac{b_{k_{j+i}}^l}{(-\lambda_k)^{i+1}} \right| D_{q^l(k_{j+i})}^l \times K\left(D_{q^l(k_{j+i})}^l, \varrho_{q^l(k_{j+i})}^l, \tau_{q^l(k_{j+i})}^l, \alpha_{q^l(k_{j+i})}^l \right) \right) \tag{6.59a}$$

$$\|u_q^l\|_\infty \leq D_q^l K\left(D_q^l, \varrho_q^l, \tau_q^l, \alpha_q^l \right) \tag{6.59b}$$

with $K(D_q^l, \varrho_q^l, \tau_q^l, \alpha_q^l)$ *as defined in* (6.55b).

As pointed out above, the proof essentially relies on Lemma 6.3.

Proof. By replacing the index set S in (6.53) with $S_q^{l,1}$ the operator $\hat{\mathcal{D}}(s)$ equals $\hat{\mathcal{D}}_q^{u,l}(s)$. Hence, the bound (6.55a) directly carries over with the parameters D, ϱ, τ, and α replaced by D_q^l, ϱ_q^l, τ_q^l, and α_q^l, which together with the uniform convergence of the series $K(D_{q^l(k_j)}^l, \varrho_{q^l(k_j)}^l, \tau_{q^l(k_j)}^l, \alpha_{q^l(k_j)}^l)$ for $\alpha_q^l < 1/\varrho_q^l$ yields (6.59b).

Moreover, the application of Corollary 6.2 with S replaced by $S_q^{l,1}$ implies

$$\left\| {}^i\hat{\mathcal{D}}_{q^l(k_j),k}^{x,l}(\partial_t) \circ \xi_{q^l(k_j)}^l \right\|_\infty \leq D_{q^l(k_j)}^l K\left(D_{q^l(k_j)}^l, \varrho_{q^l(k_j)}^l, \tau_{q^l(k_j)}^l, \alpha_{q^l(k_j)}^l \right)$$

for each $i \in \{1, 2, \ldots, \theta_k - 1\}$ and all k_j with $k \in \mathbb{N}$, $j = 1, \ldots r_k^a$. With this, the evaluation of the norm $\|x_{k_j}\|_\infty$ of $x_{k_j}(t)$ from (6.44a) directly results in (6.59a). □

6.3.1.3 Finite–Dimensional In–Domain and Boundary Control

Similar to the previous paragraph, the relationship between the operator $\hat{\mathcal{D}}^u(s)$ and the operator (6.53) enables to establish the convergence of the parametrized Fourier coefficients $x_{k_j}(t)$ and $u^l(t)$ defined in (6.31) for the case of a finite–dimensional control input by making use of Lemma 6.3 and Corollary 6.2.

Corollary 6.3. *Assume that* $\hat{\mathcal{D}}^u(s)$ *as defined in* (6.32b) *is an entire function of finite order* ϱ *and finite type* τ. *Let* $\xi^l(t) \in G_{D^l,\alpha^l}(\mathbb{R}^+)$ *for each* $l = 1, \ldots, m$ *with* $\alpha^l < 1/\varrho^l$. *Then* $x_{k_j}(t) \circ\!\!-\!\!\bullet\, \hat{x}_{k_j}(s)$ *and* $u^l(t) \circ\!\!-\!\!\bullet\, \hat{u}^l(s)$ *parametrized in terms of* $\xi^l(t) \circ\!\!-\!\!\bullet\, \hat{\xi}^l(s)$ *as defined in* (6.31) *satisfy the inequalities*

$$\|x_{k_j}\|_\infty \leq \sum_{l=1}^{m} \left(\left| \frac{b_{k_j}^l}{\lambda_k} \right| + \sum_{i=1}^{r_k^a - r_k^g} \sigma_{i,j,k} \left| \frac{b_{k_{j+i}}^l}{(-\lambda_k)^{i+1}} \right| \right) D^l K\left(D^l, \varrho^l, \tau^l, \alpha^l \right) \tag{6.60a}$$

$$\|u^l\|_\infty \leq D^l K\big(D^l, \varrho^l, \tau^l, \alpha^l\big) \tag{6.60b}$$

with $K(D^l, \varrho^l, \tau^l, \alpha^l)$ *as defined in* (6.55b)*.*

The proof of thus result follows exactly the lines of the proof of Theorem 6.5 and is hence omitted. Moreover, its should be pointed out that (6.60b) directly represents the convergence result for the input parametrization (6.31b) since $u^l(t)$ is by assumption independent of the tuple z of spatial coordinates.

Having introduced conditions for the convergence of the parametrizations of the Fourier coefficients for the state and input in terms of the basic output and its time–derivatives it is possible to examine the convergence of the respective Fourier series.

6.3.2 Convergence of the Parametrized Fourier Series

In order to deduce meaningful expressions from the (operational) parametrizations of the Fourier coefficients $x_{k_j}(t)$ and $u_k^l(t)$ for the solution of the trajectory planning problem subsequently the convergence of the parametrized Fourier series (6.34a) for finite–dimensional control and (6.48) for infinite–dimensional control are analyzed. Recall that the convergence analysis of the input parametrization (6.34b) arising for finite–dimensional control is completely governed by Corollary 6.3.

Due to the Riesz bases properties of the sequences $((\boldsymbol{\phi}_{k_j})_{j=1,\ldots,r_k^a})_{k\in\mathbb{N}}$ and $(\boldsymbol{\varphi}_k)_{k\in\mathbb{N}}$ (see Assumption 6.3) the functional series convergence thereby requires to verify that

$$\sum_{k\in\mathbb{N}}\sum_{j=1}^{r_k^a}\big|x_{k_j}(t)\big|^2 < \infty, \quad \sum_{k\in\mathbb{N}}\big|u_k^l(t)\big|^2 < \infty \quad \text{for each } l = 1,\ldots,m,$$

which is equivalent to

$$\Big(\big(x_{k_j}\big)_{j=1,\ldots,r_k^a}\Big)_{k\in\mathbb{N}} \in \ell^2(\mathbb{R}^+), \quad (u_k^l)_{k\in\mathbb{N}} \in \ell^2(\mathbb{R}^+).$$

6.3.2.1 Infinite–Dimensional In–Domain and Boundary Control

Similar to the analysis of the operational convergence of the parametrized Fourier coefficients in the following at first the case of an infinite–dimensional control input is considered.

Theorem 6.6. *Assume that* $\hat{\mathcal{D}}_q^{u,l}(s)$ *as defined in* (6.45) *is an entire function of finite order* ϱ_q^l *and finite type* τ_q^l *for each* $q \in \mathbb{N}$*. Let* $\xi_q^l(t) \in G_{D_q^l,\alpha^l}(\mathbb{R}^+)$ *for* $l = 1,\ldots,m$ *with* $\alpha^l < 1/\max_{q\in\mathbb{N}}\{\varrho_q^l\}$*. If* $(D_q^l)_{q\in\mathbb{N}} \in \ell^2$ *and*

$$\sum_{k\in\mathbb{N}}\left(\frac{\max_{i=1,\ldots,r_k^a}\big|b_{k_i}^l\big|^2}{\min_{i=1,\ldots,\theta_k}\big|(-\lambda_k)^i\big|^2}\right) < \infty \tag{6.61}$$

for each $l = 1, \dots, m$, then the Fourier series (6.48a) *and* (6.48b) *with Fourier coefficients parametrized in terms of the basic output converge for all $(z,t) \in \Omega \times \mathbb{R}^+$ and $(z,t) \in \partial\Omega_1 \times \mathbb{R}^+$, respectively.*

Proof. Subsequently, let $\overline{\varrho}^l = \max_{q\in\mathbb{N}}\{\varrho_q^l\}$ and $\overline{\tau}^l = \max_{q\in\mathbb{N}}\{\tau_q^l\}$. With (6.59b), condition $(u_k^l(t))_{k\in\mathbb{N}} \in \ell^2(\mathbb{R}^+)$ is equivalent to $(D_q^l K(D_q^l, \varrho_q^l, \tau_q^l, \alpha^l))_{q\in\mathbb{N}} \in \ell^2$. Under the assumption that $(D_q^l)_{q\in\mathbb{N}} \in \ell^2$ there exists an upper bound $\overline{D}^l$ for each $l = 1, \dots, m$. With this, (6.55b) implies

$$\begin{aligned} K\big(D_q^l, \varrho_q^l, \tau_q^l, \alpha^l\big) &= \sum_{n\in\mathbb{N}} (n!)^{\alpha^l - \frac{1}{\varrho_q^l}} \eta^n_{\varrho_q^l, \tau_q^l}\big(D_q^l\big) \\ &\le \sum_{n\in\mathbb{N}} (n!)^{\alpha^l - \frac{1}{\overline{\varrho}^l}} \eta^n_{\overline{\varrho}^l, \overline{\tau}^l}\big(\overline{D}^l\big) =: \overline{K}^l \end{aligned}$$

since $\alpha^l < 1/\overline{\varrho}^l$, $l = 1, \dots, m$, where $\overline{K}^l \le \overline{K} < \infty$, $\overline{K} = \max_{l=1,\dots,m}\{\overline{K}^l\}$. Hence,

$$\sum_{q\in\mathbb{N}} \Big(D_q^l K\big(D_q^l, \varrho_q^l, \tau_q^l, \alpha^l\big)\Big)^2 \le \overline{K}^2 \sum_{q\in\mathbb{N}} \Big(D_q^l\Big)^2$$

which yields $(u_k^l(t))_{k\in\mathbb{N}} \in \ell^2(\mathbb{R}^+)$ in view of the assumption $(D_q^l)_{q\in\mathbb{N}} \in \ell^2$, $l = 1, \dots, m$.

In order to proceed with the proof of convergence of the parametrized Fourier series for $\boldsymbol{x}(t)$, at first notice that for any finite $m \in \mathbb{N}$, $(\sum_{l=1}^m a_l)^2 \le m \sum_{l=1}^m a_l^2$ given finite $a_l \in \mathbb{R}$. Since $|x_{k_j}(t)|^2 \le \|x_{k_j}\|_\infty^2$ the estimate (6.59a) provides

$$\begin{aligned} &|x_{k_j}(t)|^2 \\ &\le m\overline{K}^2 \sum_{l=1}^m \left(\left|\frac{b_{k_j}^l}{\lambda_k}\right| D^l_{q^l(k_j)} + \sum_{i=1}^{r_k^a - r_k^g} \sigma_{i,j,k} \left| \frac{b^l_{k_{j+i}}}{(-\lambda_k)^{i+1}} \right| D^l_{q^l(k_{j+i})} \right)^2 \\ &\le m\theta_k \overline{K}^2 \sum_{l=1}^m \left(\left|\frac{b_{k_j}^l}{\lambda_k}\right|^2 \Big(D^l_{q^l(k_j)}\Big)^2 + \sum_{i=1}^{r_k^a - r_k^g} \sigma^2_{i,j,k} \left| \frac{b^l_{k_{j+i}}}{(-\lambda_k)^{i+1}} \right|^2 \Big(D^l_{q^l(k_{j+i})}\Big)^2 \right) \\ &\le \underbrace{m\theta_k \overline{K}^2 \left(1 + \sum_{i=1}^{r_k^a - r_k^g} \sigma^2_{i,j,k}\right)}_{= A_{k,j}} \sum_{l=1}^m \left(\frac{\max_{i=1,\dots,r_k^a} \big|b^l_{k_i}\big|^2}{\min_{i=1,\dots,\theta_k} \big|(-\lambda_k)^i\big|^2} \max_{i=1,\dots,r_k^a} \Big(D^l_{q^l(k_i)}\Big)^2 \right), \end{aligned}$$

where $0 < A_{k,j} \le \overline{A} < \infty$ since the coefficients $\sigma_{i,j,k} \in \{0,1\}$, r_k^a, r_k^g, m, and $\overline{K}$ are by assumption finite for all i, j, k. With this, the convergence condition can be reduced to

$$
\begin{aligned}
&\sum_{k\in\mathbb{N}}\sum_{j=1}^{r_k^a}\left|x_{k_j}(t)\right|^2\\
&\leq \overline{A}\sum_{k\in\mathbb{N}}\sum_{j=1}^{r_k^a}\sum_{l=1}^{m}\left(\frac{\max_{i=1,\ldots,r_k^a}\left|b_{k_i}^l\right|^2}{\min_{i=1,\ldots,\theta_k}\left|(-\lambda_k)^i\right|^2}\max_{i=1,\ldots,r_k^a}\left(D_{q^l(k_i)}^l\right)^2\right)\\
&\leq \overline{A}\max_{k\in\mathbb{N}} r_k^a\sum_{l=1}^{m}\sum_{k\in\mathbb{N}}\left(\frac{\max_{i=1,\ldots,r_k^a}\left|b_{k_i}^l\right|^2}{\min_{i=1,\ldots,\theta_k}\left|(-\lambda_k)^i\right|^2}\max_{i=1,\ldots,r_k^a}\left(D_{q^l(k_i)}^l\right)^2\right)\\
&\leq \overline{A}\max_{k\in\mathbb{N}} r_k^a\sum_{l=1}^{m}\left[\sum_{k\in\mathbb{N}}\left(\frac{\max_{i=1,\ldots,r_k^a}\left|b_{k_i}^l\right|^2}{\min_{i=1,\ldots,\theta_k}\left|(-\lambda_k)^i\right|^2}\right)\sum_{k\in\mathbb{N}}\left(\max_{i=1,\ldots,r_k^a}\left(D_{q^l(k_i)}^l\right)^2\right)\right]
\end{aligned}
$$

with the latter estimate following from $\sum_k a_k b_k \leq \sum_k a_k \sum_k b_k$ for $a_k,\, b_k > 0$. Since by assumption $(D_q^l)_{q\in\mathbb{N}} \in \ell^2$ for each $l = 1,\ldots,m$, it follows directly that

$$
\sum_{k\in\mathbb{N}}\left(\max_{i=1,\ldots,r_k^a}\left(D_{q^l(k_i)}^l\right)^2\right) < \infty.
$$

Together with (6.61) this results in $\sum_{k\in\mathbb{N}}\sum_{j=1}^{r_k^a}\left|x_{k_j}(t)\right|^2 < \infty$ which completes the proof. □

Remark 6.8. It should be pointed out that excluding possible pathological cases the condition (6.61) does not impose any restriction. As is shown in Section 6.5 based on different examples, the coefficient $\max_{i=1,\ldots,r_k^a}|b_{k_i}^l|^2$ is at maximum of the order λ_k. Hence, depending on the growth of the eigenvalues λ_k in k the convergence of the series (6.61) can be directly established.

6.3.2.2 Finite–Dimensional In–Domain and Boundary Control

Based on Theorem 6.6, the convergence of the parametrized Fourier series (6.48a) for the case of a finite–dimensional control input can be deduced.

Corollary 6.4. *Assume that* $\hat{\mathcal{D}}^u(s)$ *as defined in* (6.32b) *is an entire function of finite order* ϱ^l *and finite type* τ^l. *Let* $\xi^l(t) \in G_{D^l,\alpha^l}(\mathbb{R}^+)$ *for* $l = 1,\ldots,m$ *with* $\alpha^l < 1/\varrho^l$. *If*

$$
\sum_{k\in\mathbb{N}}\left(\frac{\max_{i=1,\ldots,r_k^a}\left|b_{k_i}^l\right|^2}{\min_{i=1,\ldots,\theta_k}\left|(-\lambda_k)^i\right|^2}\right) < \infty \tag{6.62}
$$

for each $l = 1,\ldots,m$, *then the Fourier series* (6.34a) *with Fourier coefficients* (6.31a) *parametrized in terms of the basic output converges for all* $(z,t) \in \Omega\times\mathbb{R}^+$.

The proof follows exactly the lines of the second part of the proof of Theorem 6.6 and is hence omitted.

6.4 Admissible Trajectory Assignment for the Basic Output

The parametrization and convergence results of the previous section enable the development of a systematic procedure for the realization of finite time transitions between a stationary initial profile $\boldsymbol{x}(0) = \boldsymbol{x}_0$ and a stationary final profile $\boldsymbol{x}(T) = \boldsymbol{x}_T$ for $t \geq T$ within an arbitrarily prescribed transition time $T > 0$. The spatial–temporal transition path $\boldsymbol{x}^*(t)$ connecting $\boldsymbol{x}_0$ and $\boldsymbol{x}_T$ is thereby prescribed by a suitable assignment of a desired trajectory $\boldsymbol{\xi}^*(t)$ for the basic output $\boldsymbol{\xi}(t)$. With this, it is in addition possible to determine a principle approach for the realization of finite time transitions between non–stationary states.

Remark 6.9. It should be pointed out that according to Remarks 6.4 and 6.7 the assignment of admissible trajectories for the basic output can be similarly defined in terms of the system output $\boldsymbol{y}(t)$ such that $\boldsymbol{y}(t) \rightarrow \boldsymbol{y}^*(t)$. However, this approach is inherently covered by the analysis presented below and is hence not treated separately.

6.4.1 Finite Time Transitions between Stationary States

In many applications it is desired to realize finite time transitions between stationary operating profiles. This in particular includes start–up or shutdown processes, which typically arise in thermal or chemical engineering applications, where a plant is either put into operating conditions starting from an initial state or returned into the initial state starting from the operating point.

Given (6.22), stationary states are defined as the solutions $\boldsymbol{x}_s = \boldsymbol{x}_s(z) = \boldsymbol{x}_s(z; \boldsymbol{u}_s(z))$ to the boundary–value problem (BVP)

$$\mathfrak{A}\boldsymbol{x}_s + \mathfrak{B}\boldsymbol{u}_s = \boldsymbol{0}, \qquad \boldsymbol{x}_s \in \mathcal{D}(\mathfrak{A}),\ \boldsymbol{u}_s \in U. \tag{6.63a}$$

$$\boldsymbol{y}_s = \mathfrak{C}\boldsymbol{x}_s. \tag{6.63b}$$

Let the initial stationary state be $\boldsymbol{x}_0 = \boldsymbol{x}_s$. Then it can be assumed without loss of generality that $\boldsymbol{x}(0) = \boldsymbol{0}$, which can be directly achieved by the introduction of the mappings $\boldsymbol{x}(t) \mapsto \boldsymbol{x}(t) + \boldsymbol{x}_s$ and $\boldsymbol{u}(t) \mapsto \boldsymbol{u}(t) + \boldsymbol{u}_s$.

Based on these equations in the following two trajectory planning approaches are presented, depending on either a direct assignment of the basic output or its indirect determination.

6.4.1.1 Direct Trajectory Planning

By making use of the final value theorem, in steady state the operational input parametrizations (6.31b) and (6.44b) for finite– and infinite–dimensional control, respectively, reduce to

$$u_s^l = \lim_{s\to 0} \hat{\mathcal{D}}^u(s)\, s\hat{\xi}^l(s) = \hat{\mathcal{D}}^u(0) \lim_{s\to 0} s\hat{\xi}^l(s) = \xi_s^l \tag{6.64}$$

and

$$u_{s,q}^l = \lim_{s\to 0} \mathcal{D}_q^{u,l}(s)\, s\hat{\xi}_q^l(s) = \mathcal{D}_q^{u,l}(0) \lim_{s\to 0} s\hat{\xi}_q^l(s) = \xi_{s,q}^l \tag{6.65}$$

provided that ξ_s^l and $\xi_{s,q}^l$ exist. Hence, given a stationary input $\boldsymbol{u}_s \in U$ the consistent basic output follows as

$$\xi_s^l = u_s^l \tag{6.66}$$

or

$$\xi_{s,q}^l = \langle \boldsymbol{\xi}_s, \boldsymbol{\chi}_q \rangle_U = \langle \boldsymbol{u}_s, \boldsymbol{\chi}_q \rangle_U = u_{s,q}^l, \tag{6.67}$$

respectively, where, as pointed out in Remark 6.6, the inner product in (6.67) has to be evaluated in the space U. This implies that stationary profiles $\boldsymbol{x}_s$ can be identically determined by

$$\mathfrak{A}\boldsymbol{x}_s + \mathfrak{B}\boldsymbol{\xi}_s = \mathbf{0}, \qquad \boldsymbol{x}_s \in \mathcal{D}(\mathfrak{A}),\ \boldsymbol{\xi}_s \in U. \tag{6.68a}$$

$$\boldsymbol{y}_s = \mathfrak{C}\boldsymbol{x}_s, \tag{6.68b}$$

where[9]

$$\boldsymbol{\xi}_s = \begin{cases} \left[\xi_s^1, \ldots, \xi_s^m\right]^T, & \text{finite–dimensional control} \\ \sum_{l=1}^m \sum_{q\in\mathbb{N}} \xi_{s,q}^l \boldsymbol{\varphi}_q, & \text{infinite–dimensional control} \end{cases}$$

such that subsequently $\boldsymbol{x}_s = \boldsymbol{x}_s(z) = \boldsymbol{x}_s(z;\boldsymbol{\xi}_s)$ refers to a solution of the BVP (6.68). In view of Corollary 6.4 this in particular motivates the following definition of an admissible stationary profile given a finite–dimensional control.

Definition 6.6. The stationary profile $\boldsymbol{x}_s \in X$ satisfying (6.68) with finite–dimensional control according to (6.24) is said to be admissible if (6.62) is fulfilled for each $l = 1, \ldots, m$ with $b_{k_j}^l = \langle \mathfrak{b}^l, \psi_{k_j} \rangle_X$.

In the case of an infinite–dimensional control Theorem 6.6 provides conditions on the convergence of the parametrized Fourier series. Here, the Gevrey constants for the basic output are in addition required to satisfy $(D_q^l)_{q\in\mathbb{N}} \in \ell^2$, which under steady state conditions with vanishing time–derivatives is equivalent to $(\xi_{s,q}^l)_{q\in\mathbb{N}} \in \ell^2$.

Definition 6.7. The stationary profile $\boldsymbol{x}_s \in X$ satisfying (6.68) with infinite–dimensional control is said to be admissible if for each $l = 1, \ldots, m$

(i) (6.61) is fulfilled with $b_{k_j}^l$ as introduced in (6.38) and

[9] Here, the Fourier series representation (6.49a) for the basic output was used for the case of an infinite–dimensional control.

(ii) $(\xi_{s,q}^l)_{q\in\mathbb{N}} \in \ell^2$ with $\xi_{s,q}^l = \langle \boldsymbol{\xi}_s, \boldsymbol{\chi}_q \rangle_U$.

These preparations enable the introduction of a direct approach for the assignment of desired trajectories for the basic output depending on the particular control configuration.

Infinite–Dimensional In–Domain and Boundary Control

The choice of the desired trajectory according to

$$\boldsymbol{\xi}^{*,l}(t) = \sum_{q\in\mathbb{N}} \xi_q^{*,l}(t)\boldsymbol{\varphi}_q, \qquad l = 1,\dots,m \tag{6.69a}$$

with

$$\xi_q^{*,l}(t) = \xi_{T,q}^{*,l}\, g_{T_q^l,\omega_q^l}(t), \tag{6.69b}$$

where $T_q^l \le T$, $g_{T_q^l,\omega_q^l}(t \le 0) = 0$, $g_{T_q^l,\omega_q^l}(t \ge T_q^l) = 1$, and $\partial_t^n g_{T_q^l,\omega_q^l}(t)|_{t=0,T_q^l} = 0$ for all $n \in \mathbb{N}$, exactly realizes the transition from $\boldsymbol{x}_0 = \mathbf{0}$ to the final stationary profile $\boldsymbol{x}_T = \boldsymbol{x}_s(z;\boldsymbol{\xi}^*(z,T))$ along the path

$$\boldsymbol{\xi}^*(t) = \sum_{l=1}^{m}\sum_{q\in\mathbb{N}} \xi_q^{*,l}(t)\boldsymbol{\varphi}_q. \tag{6.70}$$

Obviously, the requirements on $g_{T_q^l,\omega_q^l}(t)$ imply that the function has to be locally non–analytic at $t = 0$ and $t = T_q^l$. An example of a function fulfilling these constraints is provided by (B.3) in Appendix B.1. In view of the Definition B.1 of a Gevrey function this yields on the one hand that necessarily $g_{T_q^l,\omega_q^l}(t) \in G_{D_q^l,\alpha_q^l}(\mathbb{R}^+)$ with $\alpha_q^l > 1$ for all q and $l \in \{1,\dots,m\}$. On the other hand, the convergence conditions determined in Theorem 6.6 require besides the square summability of the Gevrey constants that the Gevrey order α^l of $\boldsymbol{\xi}^{*,l}(t)$ is bounded by the order ϱ_q^l of the entire function $\hat{\mathcal{D}}_q^{u,l}(s)$ according to $\alpha^l < 1/\max_{q\in\mathbb{N}}\{\varrho_q^l\}$. As a result, the trajectory planning problem for the finite time transition between admissible stationary states admits a convergent solution provided that the inequality

$$1 < \alpha^l < \frac{1}{\max_{q\in\mathbb{N}}\{\varrho_q^l\}}, \qquad l = 1,\dots,m \tag{6.71}$$

is satisfied. This implies $\varrho_q^l < 1$ for all $q \in \mathbb{N}$, $l = 1,\dots,m$. The latter condition obviously has to be analyzed individually for each problem setting. However, anticipating the results of Section 6.5 for different application examples, this condition can be satisfied for a rather broad range of distributed–parameter systems. Nevertheless, as is elaborated in further detail in the subsequent paragraph, divergent parametrizations can be similarly integrated into the solution of the trajectory planning problem.

Finite–Dimensional In–Domain and Boundary Control

Similar to the previous paragraph, consider

$$\xi^{*,l}(t) = \xi_T^{*,l} g_{T^l,\omega^l}(t) \tag{6.72}$$

with $0 < T^l \leq T$, $\omega^l > 0$ as the desired trajectory for the basic output with $g_{T,\omega}(t)$ as above. The trajectory (6.72) enables the realization of the finite time transition starting at $\boldsymbol{x}_0 = \mathbf{0}$ to the admissible final stationary profile $\boldsymbol{x}_T = \boldsymbol{x}_s(z;\boldsymbol{\xi}^*(T))$ with $\boldsymbol{\xi}^*(T) = [\xi^{*,1}(T),\ldots,\xi^{*,m}(T)]^T$ for $t \geq T$. In view of Corollary 6.4, the convergence of the state and input parametrizations requires that $\xi^{*,l}(t)$ is of Gevrey order $\alpha^l < 1/\varrho^l$, i.e. $\omega^l > \varrho^l/(1-\varrho^l)$. On the other hand, the required local non–analyticity of $\xi^{*,l}(t)$ imposes the lower bound $1 < \alpha^l < 1/\varrho^l$, which implies that $1/\varrho^l > 1$ or $\varrho^l < 1$ is implicitly necessary for the solution of the finite time transition problem. Hence, configurations might clearly arise, where the trajectory planning problem does not admit a solution. Again anticipating the results of Section 6.5, this condition is mainly satisfied for spatial dimensions $r = 1$ while higher dimensional domains yield entire functions of order greater than unity. Nevertheless, it is shown in the example considered in Section 6.5.3 that computations with divergent parametrizations involving suitable summability methods might provide a promising technique to overcome these limitations.

6.4.1.2 Indirect Trajectory Planning

The direct approach introduced above essentially relies on the solution of either (6.63a) or equivalently (6.68a). However, this imposes certain structural limitations since it is in particular not obvious on how to directly assign a desired stationary profile without the a priori knowledge of the corresponding input. In order to weaken this restriction, subsequently an indirect approach is introduced, which enables the assignment of a final admissible stationary profile, which represents a best approximation in the sense defined below of a prescribed desired profile $\boldsymbol{x}_T \in X$. Note that $\boldsymbol{x}_T$ thereby not necessarily has to satisfy the BVP (6.63a). In addition, this allows to assign a desired spatial state distribution along a certain surface interior to Ω, which can be realized at least approximately, i.e. $\boldsymbol{x}_T|_{\varpi(z)=0}$, where $\varpi(z) = 0$ describes the interior surface.

Infinite–Dimensional In–Domain and Boundary Control

For this, observe from (6.67) that the stationary version of the input parametrization (6.48b) is given by

$$\boldsymbol{u}_s = \sum_{l=1}^{m} \sum_{q\in\mathbb{N}} \xi_{s,q}^l \boldsymbol{\varphi}_k \tag{6.73}$$

Hence, the determination of the input $\boldsymbol{u}_s = \boldsymbol{u}_s(z; \{\xi^l_{s,q}\}_{q\in\mathbb{N},\, l=1,\ldots,m})$ such that

$$\left\|\boldsymbol{x}_s\big(z; \boldsymbol{u}_s\big(z; \{\xi^l_{s,q}\}_{q\in\mathbb{N},\, l=1,\ldots,m}\big)\big) - \boldsymbol{x}_T(z)\right\|_X \leq \epsilon$$

for some $\epsilon > 0$ can be reduced to the following minimization problem for the Fourier coefficients $\{\xi^l_{s,q}\}_{q\in\mathbb{N},\, l=1,\ldots,m}$ for the basic output, i.e.

$$\begin{aligned}\min_{\{\xi^l_{s,q}\}_{q\in\mathbb{N},\, l=1,\ldots,m}} & \left\|\boldsymbol{x}_s\big(z; \boldsymbol{u}_s\big(z; \{\xi^l_{s,q}\}_{q\in\mathbb{N},\, l=1,\ldots,m}\big)\big) - \boldsymbol{x}_T(z)\right\|^2_X \\ \text{subject to (6.63a), (6.73).}\end{aligned} \tag{6.74}$$

Similarly, given $\boldsymbol{x}_T(z)|_{\varpi(z)=0}$ the minimization problem (6.74) reduces to

$$\begin{aligned}\min_{\{\xi^l_{s,q}\}_{q\in\mathbb{N},\, l=1,\ldots,m}} & \left\|\boldsymbol{x}_s\big(z; \boldsymbol{u}_s\big(z; \{\xi^l_{s,q}\}_{q\in\mathbb{N},\, l=1,\ldots,m}\big)\big)|_{\varpi(z)=0}\right. \\ & \qquad \left. - \boldsymbol{x}_T(z)|_{\varpi(z)=0}\right\|^2_X \\ \text{subject to (6.63a), (6.73).}\end{aligned} \tag{6.75}$$

From an implementation point of view it is obvious that only a finite set of Fourier coefficients $\{\xi^l_{s,q}\}_{q\leq\overline{q},\, l=1,\ldots,m}$ with $\overline{q} \ll \infty$ can be determined for the basic output. The corresponding desired trajectory $\boldsymbol{\xi}^*(t)$ for the basic output $\boldsymbol{\xi}(t)$, which realizes the finite time transition from $\boldsymbol{x}_0 = \boldsymbol{0}$ to the final stationary profile $\boldsymbol{x}_s\big(z; \boldsymbol{u}_s\big(z; \{\xi^l_{s,q}\}_{q\in\mathbb{N},\, l=1,\ldots,m}\big)\big)$ approximating $\boldsymbol{x}_T(z)$ follows from (6.70) with (6.69b) for $\xi^{*,l}_{T,q} = \xi^l_{s,q}$, $q = 1,\ldots,\overline{q}$, $l = 1,\ldots,m$. Here, $\xi^l_{s,q}$ denotes the respective element of the solution to (6.74) or (6.75), respectively.

Therefore, it is of course similarly required that the Gevrey orders α^l of $\boldsymbol{\xi}^{*,l}(t)$, $l = 1,\ldots,m$, defined in (6.69a) and hence of $\boldsymbol{\xi}^*(t)$ and the orders of the entire functions $\hat{\mathcal{D}}^{u,l}_q(s)$ have to fulfill (6.71) to ensure the convergence of the parametrized Fourier series for the state and input.

Finite–Dimensional In–Domain and Boundary Control

The above results on the indirect trajectory planning can be applied straight forward to the case of a finite–dimensional control by taking into account that under stationary conditions

$$\boldsymbol{u}_s = \boldsymbol{\xi}_s. \tag{6.76}$$

Here, it is hence required to solve either

$$\min_{\boldsymbol{\xi}_s}\left\|\boldsymbol{x}_s\big(z; \boldsymbol{u}_s(\boldsymbol{\xi}_s)\big) - \boldsymbol{x}_T(z)\right\|^2_X \quad \text{subject to (6.63a), (6.76)} \tag{6.77}$$

or

$$\min_{\boldsymbol{\xi}_s} \left\| \boldsymbol{x}_s\big(z;\boldsymbol{u}_s(\boldsymbol{\xi}_s)\big)|_{\varpi(z)=0} - \boldsymbol{x}_T(z)|_{\varpi(z)=0} \right\|_X^2 \quad \text{subject to (6.63a), (6.76)} \tag{6.78}$$

if $\boldsymbol{x}_T(z)|_{\varpi(z)=0}$ is given. The corresponding paths for the basic output trajectories then follow directly from (6.72) with $\xi_T^{*,l} = \xi_s^l$, $l = 1, \ldots, m$. However, as already pointed out above, the solution of the trajectory planning problem for the case of a finite–dimensional control in general suffers from the loss of convergence when realizing finite time transitions between stationary profiles, which motivates computations with divergent parametrizations as presented for the example considered in Section 6.5.3.

6.4.2 Finite Time Transitions between Non–stationary States

Besides the realization of finite time transitions between stationary profiles, the determined state and input parametrizations in terms of the basic output can be in addition used to approximately achieve finite time transitions between non–stationary profiles. For this, subsequently a principle approach for the determination of suitable desired trajectories for the basic output is proposed, which generalizes the initial results of [32] obtained for trajectory planning using power series given the 1–dimensional heat equation.

Remark 6.10. Note that the subsequent formulation is based on the general case of an infinite–dimensional control input as introduced in Section 6.2.2. The respective equations for the case of a finite–dimensional control input can then be directly deduced. In addition, for the sake of simplicity only the case $r_k^g = r_k^a$ for all $k \in \mathbb{N}$ is considered but it should be pointed out that the provided computations can be similarly extended to the case $r_k^g < r_k^a$ for some $k \in \mathbb{N}$.

Hence, consider an arbitrary initial profile $\boldsymbol{x}_0 = \boldsymbol{x}_0(z) \in X$ and an arbitrary final profile $\boldsymbol{x}_T = \boldsymbol{x}_T(z) \in X$, which is to be achieved at $t = T$ with prescribed $T > 0$. Assume that $((\boldsymbol{\phi}_{k_j})_{j=1,\ldots,r_k^a})_{k\in\mathbb{N}}$ and $((\boldsymbol{\psi}_{k_j})_{j=1,\ldots,r_k^a})_{k\in\mathbb{N}}$ represent orthonormal Riesz bases for X. Then according to Corollary 6.1 both $\boldsymbol{x}_0(z)$ and $\boldsymbol{x}_T(z)$ admit a Fourier representation

$$\boldsymbol{x}_0 = \sum_{k\in\mathbb{N}} \sum_{j=1}^{r_k^a} x_{k_j}^0 \boldsymbol{\phi}_{k_j}, \qquad \boldsymbol{x}_T = \sum_{k\in\mathbb{N}} \sum_{j=1}^{r_k^a} x_{k_j}^T \boldsymbol{\phi}_{k_j} \tag{6.79}$$

with $x_{k_j}^0 = \langle \boldsymbol{x}_0, \boldsymbol{\psi}_{k_j} \rangle_X$ and $x_{k_j}^T = \langle \boldsymbol{x}_T, \boldsymbol{\psi}_{k_j} \rangle_X$. Hence, following [14, Theorem A.2.35] for all $\epsilon > 0$ there exists an $K \in \mathbb{N}$, $K < \infty$ such that

$$\left\| \boldsymbol{x}_0 - \boldsymbol{x}_{0,K} \right\|_X < \epsilon, \qquad \left\| \boldsymbol{x}_T - \boldsymbol{x}_{T,K} \right\|_X < \epsilon,$$

where

$$\boldsymbol{x}_{0,K} = \sum_{k=1}^{K} \sum_{j=1}^{r_k^a} x_{k_j}^0 \boldsymbol{\phi}_{k_j}, \qquad \boldsymbol{x}_{T,K} = \sum_{k=1}^{K} \sum_{j=1}^{r_k^a} x_{k_j}^T \boldsymbol{\phi}_{k_j}.$$

Furthermore, recall from the results of Section 6.3.1.1 (in particular the proof of Lemma 6.3) that the operators (6.45) arising in the formal operational parametrizations (6.44) can be re–written in terms of power series in the Laplace variable s, i.e.

$${}^i\hat{\mathcal{D}}^{x,l}_{q^l(k_j),k}(s) = \sum_{n\in\mathbb{N}} {}^i c^l_{q^l(k_j),n} s^n.$$

In view of Remark 6.10 this enables to re–write the operational state parametrization (6.44a) according to

$$\hat{x}_{k_j}(s) = -\frac{1}{\lambda_k} \sum_{l=1}^{m} \left(b^l_{k_j} \sum_{n\in\mathbb{N}} {}^0 c^l_{q^l(k_j),n} s^n \, \hat{\xi}^l_{q^l(k_j)}(s) \right),$$

whose equivalent in the time–domain evaluates to

$$x_{k_j}(t) = -\frac{1}{\lambda_k} \sum_{l=1}^{m} \left(b^l_{k_j} \sum_{n\in\mathbb{N}} {}^0 c^l_{q^l(k_j),n} \partial_t^n \xi^l_{q^l(k_j)}(t) \right). \tag{6.80}$$

Furthermore, given $g_{T^l_q,\omega^l_q}(t) \in G_{D^l_q,\beta^l_q}(\mathbb{R}^+)$ with $\alpha^l_q = \max_{q\in\mathbb{N}}\{\beta^l_q\}$ introduce the composite function

$$\xi^{*,l}_q(t) = \left(1 - g_{T^l_q,\omega^l_q}(t)\right) \sum_{i=0}^{I} f^{0,l}_{q,i} \frac{t^i}{i!} + g_{T^l_q,\omega^l_q}(t) \sum_{i=0}^{I} f^{T,l}_{q,i} \frac{(t-T)^i}{i!} \tag{6.81}$$

as the desired trajectory for the basic output. It can be directly deduced that $\xi^{*,l}_q(t) \in G_{\overline{D}^l_q,\alpha^l_q}(\mathbb{R}^+)$ with the new Gevrey constant $\bar{D}^l_q = \bar{D}^l_q(D^l_q, \boldsymbol{f}^{0,l}_q, \boldsymbol{f}^{T,l}_q)$ with $\boldsymbol{f}^{0,l}_q = [f^{0,l}_{q,1}, \ldots, f^{0,l}_{q,I}]^T$ and $\boldsymbol{f}^{T,l}_q = [f^{T,l}_{q,1}, \ldots, f^{T,l}_{q,I}]^T$. Moreover, $\xi^{*,l}_q(t)$ fulfills

$$\begin{aligned} &\partial_t^i \xi^{*,l}_q(0) = f^{0,l}_{q,i}, && \partial_t^i \xi^{*,l}_q(T) = f^{T,l}_{q,i}, && 0 \le i \le I \\ &\partial_t^i \xi^{*,l}_q(0) = 0, && \partial_t^i \xi^{*,l}_q(T) = 0, && i > I \end{aligned}$$

for $T^l_q \le T$. The number of derivatives I and hence the upper summation index in (6.81) can thereby vary with q and is subsequently assumed to satisfy $I \le K$. Hence, evaluating (6.80) at $t \in \{0, T\}$ using (6.81) results in two independent linear systems of equations for the coefficients $f^{0,l}_{q^l(k_j),i}$ and $f^{T,l}_{q^l(k_j),i}$, $i = 0, \ldots, I$, i.e.

$$x^0_{k_j} = -\frac{1}{\lambda_k} \sum_{l=1}^{m} \left(b^l_{k_j} \sum_{i=0}^{I} {}^0 c^l_{q^l(k_j),i} f^{0,l}_{q^l(k_j),i} \right) \tag{6.82a}$$

$$x_{k_j}^T = -\frac{1}{\lambda_k}\sum_{l=1}^{m}\left(b_{k_j}^l \sum_{i=0}^{I} {}^0c_{q^l(k_j),i}^l f_{q^l(k_j),i}^{T,l}\right) \tag{6.82b}$$

for $k = 1,\dots,K,\ j = 1,\dots,r_k^a$ with $x_{k_j}^0$ and $x_{k_j}^T$ as introduced in (6.79). Thereby, recall from (6.42) that the indicator function $q^l(k_j)$ provides for each k_j the respective value q such that the index $k_j \in S_q^l$ (see also Assumption 6.4). Let $S^{K,l} = \{q^l(k_j)\}_{k=1,\dots,K,\, j=1,\dots,r_k^a}$, where $\#S^{K,l} = \overline{q} < \infty$ and introduce the vectors

$$\begin{aligned}
\boldsymbol{x}_0^K &= \left[x_{1_1}^0,\dots,x_{1_{r_1^a}}^0,\dots,x_{K_1}^0,\dots,x_{K_{r_K^a}}^0\right]^T\\
\boldsymbol{x}_T^K &= \left[x_{1_1}^T,\dots,x_{1_{r_1^a}}^T,\dots,x_{K_1}^T,\dots,x_{K_{r_K^a}}^T\right]^T\\
\boldsymbol{f}_{K,I}^{0,l} &= \left[f_{q,i}^{0,l}\right]^T_{q\in S^{K,l},\, i=1,\dots,I}\\
\boldsymbol{f}_{K,I}^{T,l} &= \left[f_{q,i}^{T,l}\right]^T_{q\in S^{K,l},\, i=1,\dots,I}.
\end{aligned}$$

As a result, it can be easily deduced that there exist matrices $M_{K,I}^{0,l} \in \mathbb{C}^{\overline{q}\times I}$ and $M_{K,I}^{T,l} \in \mathbb{C}^{\overline{q}\times I}$ such that (6.82) can be re–written as

$$\boldsymbol{x}_0^K = \sum_{l=1}^{m} M_{K,I}^{0,l}\boldsymbol{f}_{K,I}^{0,l}, \qquad \boldsymbol{x}_T^K = \sum_{l=1}^{m} M_{K,I}^{T,l}\boldsymbol{f}_{K,I}^{T,l}. \tag{6.83}$$

If (6.83) admits a solution for $\boldsymbol{f}_{K,I}^{0,l}$ and $\boldsymbol{f}_{K,I}^{T,l}$, then the desired trajectory for the basic output follows as

$$\boldsymbol{\xi}^*(t) = \sum_{l=1}^{m}\sum_{q\in S^{K,l}} \xi_q^{*,l}(t)\boldsymbol{\varphi}_q$$

with $\xi_q^{*,l}(t)$ as introduced in (6.81) and the coefficients $f_{q,i}^{0,l}$ and $f_{q,i}^{T,l}$ substituted accordingly.

However, in order to satisfy the conditions of Theorem 6.6 to ensure the convergence of the parametrized Fourier series, it is besides (6.61) required that $(\bar{D}_q^l)_{q\in\mathbb{N}} \in \ell^2$ as $K \to \infty$. Due to the dependence of $\bar{D}_q^l$ on D_q^l, $\boldsymbol{f}_q^{0,l}$, and $\boldsymbol{f}_q^{T,l}$ and hence $\boldsymbol{f}_{K,I}^{0,l}$ as well as $\boldsymbol{f}_{K,I}^{T,l}$ the latter requirement results in the formulation of a constrained minimization problem for the solution of (6.83), i.e.

$$\begin{aligned}
\min_{\left(\boldsymbol{f}_{K,I}^{0,l},\boldsymbol{f}_{K,I}^{T,l}\right)} &= \left(\left\|\boldsymbol{x}_0^K - \sum_{l=1}^{m} M_{K,I}^{0,l}\boldsymbol{f}_{K,I}^{0,l}\right\|^2 + \left\|\boldsymbol{x}_T^K - \sum_{l=1}^{m} M_{K,I}^{T,l}\boldsymbol{f}_{K,I}^{T,l}\right\|^2\right)\\
\text{subject to } &\left(\bar{D}_q^l\left(D_q^l, \boldsymbol{f}_q^{0,l}, \boldsymbol{f}_q^{T,l}\right)\right)_{q\in S^{K,l}} \in \ell^2.
\end{aligned} \tag{6.84}$$

Note that the slight abuse of notation when referring to the square summability of a sequence of only a finite number of elements is motivated by the desire to emphasize that this condition has to hold in the theoretical limit as $K \to \infty$. For a finite number of elements this can be realized, e.g., by imposing for each $l = 1, \ldots, m$ the constraint

$$\left| \bar{D}_q^l \left(D_q^l, \boldsymbol{f}_q^{0,l}, \boldsymbol{f}_q^{T,l} \right) \right| \leq \frac{\breve{D}^l}{q^{1+\epsilon}} \quad \forall q \in S^{K,l} \tag{6.85}$$

with $\epsilon > 0$ and the finite constants $\breve{D}^l$. Moreover, from an implementation point of view is convenient to decouple the minimization problem into the two individual problems

$$\min_{\boldsymbol{f}_{K,I}^{0,l}} = \left\| \boldsymbol{x}_0^K - \sum_{l=1}^{m} M_{K,I}^{0,l} \boldsymbol{f}_{K,I}^{0,l} \right\|^2 \quad \text{subject to } \left(\boldsymbol{f}_q^{0,l} \right)_{q \in S^{K,l}} \in \ell^2 \tag{6.86a}$$

$$\min_{\boldsymbol{f}_{K,I}^{T,l}} = \left\| \boldsymbol{x}_T^K - \sum_{l=1}^{m} M_{K,I}^{T,l} \boldsymbol{f}_{K,I}^{T,l} \right\|^2 \quad \text{subject to } \left(\boldsymbol{f}_q^{T,l} \right)_{q \in S^{K,l}} \in \ell^2. \tag{6.86b}$$

The notation $(\boldsymbol{f}_q^{j,l})_{q \in S^{K,l}} \in \ell^2$ is thereby used to express $(f_{q,i}^{j,l})_{q \in S^{K,l}, i=1,\ldots I} \in \ell^2$, $j = 0, T$. Assuming that $(D_q^l)_{q \in \mathbb{N}} \in \ell^2$, then as already pointed out above the constraints can be handled similar to (6.85) by imposing for each $l = 1, \ldots, m$ the conditions

$$\left| f_{q,i}^{0,l} \right| \leq \frac{\breve{f}^{0,l}}{q^{1+\epsilon}} \quad \forall q \in S^{K,l},\ i = 0, \ldots, I \tag{6.87}$$

and

$$\left| f_{q,i}^{T,l} \right| \leq \frac{\breve{f}^{T,l}}{q^{1+\epsilon}} \quad \forall q \in S^{K,l},\ i = 0, \ldots, I \tag{6.88}$$

given $\epsilon > 0$ with finite constants $\breve{f}^{0,l}$ and $\breve{f}^{T,l}$. In order to illustrate this, let $\bar{f}_q^{\,l} = \max_{i=0,\ldots,I} \{ |f_{q,i}^{0,l}|, |f_{q,i}^{T,l}| \}$, which in view of (6.86) implies $(\bar{f}_q^l)_{q \in S^{K,l}} \in \ell^2$ for each $l = 1, \ldots, m$. Given $g_{T_q^l, \omega_q^l}(t) \in G_{D_q^l, \beta_q^l}(\mathbb{R}^+)$ it follows from (6.81) that $\sup_{t \in \mathbb{R}^+} |\xi_q^{*,l}(t)| \leq (1 + D_q^l) \bar{f}_q^{\,l} h_T + D_q^l \bar{f}_q^{\,l} h_T = \bar{f}_q^{\,l} h_T + 2 D_q^l \bar{f}_q^{\,l} h_T$ with $h_T = \sum_{i=0}^{I} T^i / i!$. With this estimate the separation introduced into (6.86a) and (6.86b) can be confirmed since under the assumptions above $(\bar{f}_q^{\,l} h_T + 2 D_q^l \bar{f}_q^{\,l} h_T)_{q \in S^{K,l}} \in \ell^2$ and thus $(\bar{D}_q^l (D_q^l, \boldsymbol{f}_q^{0,l}, \boldsymbol{f}_q^{T,l}))_{q \in S^{K,l}} \in \ell^2$.

As already pointed out in the introduction to this section, the presented approach for the realization of finite time transitions between non–stationary profiles has to be evaluated for the particular example under consideration. Moreover, while the results of Section 6.5.3 clearly confirm the applicability of the approach, rather large input amplitudes are obtained, which will in general prevent the evaluation of the solution for a real–world example.

In addition, given a 1–dimensional domain these theoretical results enable to draw a connection between the existence of a basic output and the approximate controllability of the system [31, 32]. This confirms a well–known property for finite–dimensional linear systems. The analytical verification of this connection for spatial dimensions greater than one is still an open question. However, the numerical results presented in the following section provide an initial confirmation of this result.

6.5 Application Examples and Simulation Results

In the following, the spectral solution to the trajectory planning problem is evaluated for different application examples. These include the linear heat and wave equation with in–domain control defined on the line in Section 6.5.1, where it is shown that the parametrization also allow to reflect the finite speed of wave propagation given by a hyperbolic PDE. This is complemented by the analysis of both the finite– and infinite–dimensional boundary control of a linear diffusion–reaction equation on a r–dimensional Riemannian manifold in Section 6.5.2 with a focus on the convergence analysis by making use of the Weyl asymptotic. Finally, results are provided in Section 6.5.3 for a linear diffusion–convection–reaction equation on a parallelepiped domain with finite– and infinite–dimensional boundary control. Here, the applicability of the proposed approach in conjunction with suitable summability techniques in the case of divergent parametrizations as well as the realization of finite time transitions between non–stationary initial and final profiles is presented by means of theoretical and numerical analysis.

6.5.1 Heat and Wave Equation on 1–Dimensional Domain

In order to illustrate the application of the proposed spectral design at first the trajectory planning problem is solved for the linear heat and wave equation defined on a 1–dimensional domain $\Omega = (0,1)$ such that $\partial\Omega = \{0,1\}$. Subsequently, finite–dimensional in–domain control $\mathfrak{b}(z^1)u(t)$ is considered with the spatial characteristic $\mathfrak{b}(z^1) = \sigma(z^1 - a) - \sigma(z^1 - b)$ for $0 < a < b < 1$. With this, it is well–known (see, e.g., [14, 37, 66]) that the heat equation $\partial_t x(z^1,t) = \partial_{z^1}^2 x(z^1,t) + \mathfrak{b}(z^1)u(t)$ with $x(0,t) = x(1,t) = 0$ allows for an operational representation in the state space $X^{(1)} = L^2(\Omega)$ equipped with the standard inner product $\langle x, y\rangle_{X^{(1)}} = \langle x, y\rangle_{L^2(\Omega)}$ and induced norm according to

$$\partial_t x = \mathfrak{A}^{(1)} x + \mathfrak{B}^{(1)} u, \qquad t > 0 \tag{6.89a}$$

$$x(0) = 0 \tag{6.89b}$$

with

$$\mathfrak{A}^{(1)}x = \partial_{z^1}^2 x \tag{6.89c}$$

defined on the domain

$$\mathcal{D}(\mathfrak{A}^{(1)}) = \left\{x \in H^2(\Omega) : \, x(0) = x(1) = 0\right\} \tag{6.89d}$$

and $\mathfrak{B}^{(1)} = \mathfrak{b}(\cdot)$. On the other hand, by introducing the state variables $x^1(z^1,t) = x(z^1,t)$ and $x^2(z^1,t) = \partial_t x(z^1,t)$ the wave equation $\partial_t^2 x(z^1,t) = \partial_{z^1}^2 x(z^1,t) + \mathfrak{b}(z^1)u(t)$ with $x(0,t) = x(1,t) = 0$ can be represented in the state space $X^{(2)} = H^1(\Omega) \times L^2(\Omega)$ equipped with the (energy–like) inner product $\langle \boldsymbol{x}, \boldsymbol{v}\rangle_{X^{(2)}} = \int_0^1 (\partial_{z^1} x^1 \overline{\partial_{z^1}\hat{x}^1} + x^2\overline{\hat{x}^2})\mathrm{d}z^1$ and induced norm $\|\boldsymbol{x}\|_{X^{(2)}} = \sqrt{\langle \boldsymbol{x}, \boldsymbol{x}\rangle_{X^{(2)}}}$ as

$$\boldsymbol{x} = \mathfrak{A}^{(2)}\boldsymbol{x} + \mathfrak{B}^{(2)}u, \qquad t > 0 \tag{6.90a}$$

$$\boldsymbol{x}(0) = \boldsymbol{0} \tag{6.90b}$$

with the operator

$$\mathfrak{A}^{(2)}\boldsymbol{x} = \begin{bmatrix} x^2 \\ \partial_{z^1}^2 x^1 \end{bmatrix} \tag{6.90c}$$

defined on the domain

$$\mathcal{D}(\mathfrak{A}^{(2)}) = \left\{x^1 \in H^2(\Omega),\, x^2 \in L^2(\Omega) : \, x^1(0) = x^1(1) = 0\right\} \tag{6.90d}$$

and $\mathfrak{B}^{(2)} = [0, \mathfrak{b}(\cdot)]^T$. It is a straightforward task to determine the eigenvalues and eigenvectors of the self–adjoint operators $\mathfrak{A}^{(1)}$ and $\mathfrak{A}^{(2)}$, i.e.

$$\lambda_k^{(1)} = -(k\pi)^2 \quad \phi_k^{(1)} = \psi_k^{(1)} = \sqrt{2}\sin(k\pi(z^1)), \qquad k \in \mathbb{N} \tag{6.91}$$

$$\lambda_k^{(2)} = \imath k\pi \qquad \boldsymbol{\phi}_k^{(2)} = \boldsymbol{\psi}_k^{(2)} = \begin{bmatrix} 1 \\ \lambda_k^{(2)} \end{bmatrix} F_k \sin(k\pi z^1) \quad k \in \mathbb{Z}\setminus\{0\} \tag{6.92}$$

with $F_k = 1/(k\pi)$. Note that both sequences $(\phi_k^{(1)})_{k\in\mathbb{N}}$ as well as $(\boldsymbol{\phi}_k^{(2)})_{k\in\mathbb{Z}\setminus\{0\}}$ form orthonormal bases for the respective spaces $X^{(1)}$ and $X^{(2)}$ and hence Riesz bases. Moreover, it is obvious that the algebraic and geometric multiplicity of each eigenvalue coincides and equals one. As a result, $\mathfrak{A}^{(1)}$ and $\mathfrak{A}^{(2)}$ are Riesz spectral operators or scalar operators in the sense of Definition 6.4 and their formal parametrizations are directly obtained from Section 6.2.1 for systems with finite–dimensional in–domain input.

6.5.1.1 Formal Parametrization of the Heat Equation, Trajectory Assignment, and Feedforward Control

With these preparations, it follows for the heat equation (6.89) considered in the operational domain that

$$\hat{x}_k(s) = -\frac{b_k^1}{\lambda_k^{(1)}}\hat{\mathcal{D}}_k^x(s)\hat{\xi}(s), \quad k \in \mathbb{N} \qquad \hat{u}(s) = \hat{\mathcal{D}}^u(s)\hat{\xi}(s) \tag{6.93}$$

with $b_k^{(1)} = \langle \mathfrak{b}, \phi_k^{(1)} \rangle_{X^{(1)}} = \sqrt{2}/(k\pi)(\cos(ak\pi) - \cos(bk\pi))$ and

$$\hat{\mathcal{D}}^u(s) = \prod_{n\in\mathbb{N}} \left(1 - \frac{s}{\lambda_n^{(1)}}\right) = \frac{\sinh(\sqrt{s})}{\sqrt{s}} \tag{6.94}$$

$$\hat{\mathcal{D}}_k^x(s) = \prod_{n\in\mathbb{N}, n\neq k} \left(1 - \frac{s}{\lambda_n^{(1)}}\right) = -\frac{\lambda_k^{(1)}}{s - \lambda_k^{(1)}} \frac{\sinh(\sqrt{s})}{\sqrt{s}}, \tag{6.95}$$

where $\hat{x}_k(s) = \langle \hat{x}(s), \phi_k^{(1)} \rangle_{X^{(1)}}$, $k \in \mathbb{N}$. In particular it is subsequently assumed that $b_k \neq 0$ for all $k \in \mathbb{N}$, which guarantees the approximate controllability of (6.89).

It is a straightforward computation to show that $\hat{\mathcal{D}}^u(s)$ is an entire function of finite type and finite order $\varrho = 1/2$. Hence, the operational convergence of the formal parametrizations (6.93) follows directly from Corollary 6.3 if $\xi(t)$ is a Gevrey function of order $\alpha < 2$. Since the input is independent of z^1, this directly implies the convergence of the input parametrization $u(\xi(t))$. In addition, Corollary 6.4 confirms the convergence of the parametrized Fourier series for the state

$$x(t) = \sum_{k\in\mathbb{N}} x_k(\xi(t))\phi_k^{(1)} \tag{6.96}$$

since obviously

$$\sum_{k\in\mathbb{N}} \frac{\left(b_k^{(1)}\right)^2}{\left(\lambda_k^{(1)}\right)^2} < \infty.$$

Moreover, (6.94) yields the evaluation of $u(t) = \hat{\mathcal{D}}^u(\partial_t) \circ \xi(t)$ in terms of the series

$$u(t) = \sum_{n=0}^{\infty} \frac{\partial_t^n \xi(t)}{(2n+1)!}. \tag{6.97}$$

For the realization of a finite time transition between stationary states, i.e.

$$x_s(u_s) = \left(z^1 \int_0^1 \int_0^\eta \mathfrak{b}(\zeta)\mathrm{d}\zeta\mathrm{d}\eta - \int_0^{z^1} \int_0^\eta \mathfrak{b}(\zeta)\mathrm{d}\zeta\mathrm{d}\eta\right) u_s, \tag{6.98}$$

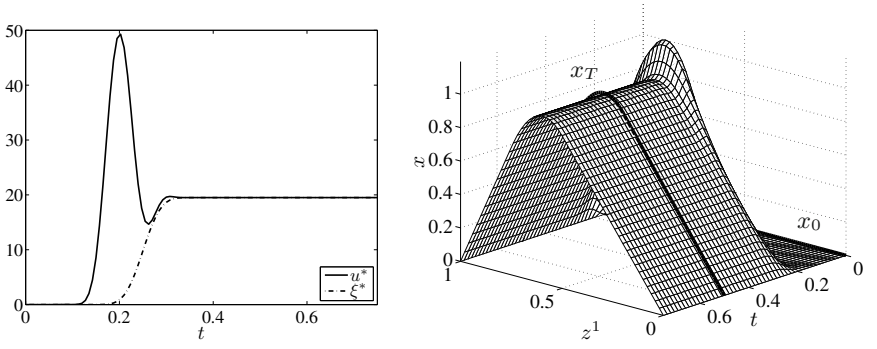

Fig. 6.1 Feedforward control $u^*(t)$ vs. basic output $\xi^*(t)$ (left) and simulated profile in the (z^1, t)–domain (right) for the linear heat equation (6.89) with in–domain actuation.

recall that $u_s = \xi_s$. Hence, the evaluation of (6.97) with the desired trajectory $t \mapsto \xi^*(t)$ for the basic output defined by

$$\xi^*(t) = \xi_{s,0} + (\xi_{s,T} - \xi_{s,0})\mathcal{g}_{T,\omega}(t)$$

with $\mathcal{g}_{T,\omega}(t)$ as introduced in (B.3) and $\omega > 1$ directly provides the feedforward control $u^*(t)$ which is required to achieve the transition starting at the stationary profile $x_s(z^1; \xi_{s,0})$ to the final stationary profile $x_s(z^1; \xi_{s,T})$ within the time interval $t \in [0, T]$. For consistency with the zero initial profile note that necessarily $\xi_{s,0} = 0$.

The resulting transition and the corresponding feedforward control for $\xi_{s,T} = 19.5$, $T = 0.5$, and $\omega = 2$ is shown in Figure 6.1, where the initial and the final stationary profile achieved at $t = T$ are emphasized by the bold lines. The spatial characteristic is restricted to the interval $z^1 \in (1/2, 3/4)$ such that $a = 1/2$ and $b = 3/4$. It is obvious that the determined feedforward control exactly realizes the desired finite time transition. Thereby, initially a rather large input amplitude is required due to the diffusive dynamics of the considered heat equation. In addition, in view of the analysis of the wave equation it should be pointed out that any $0 < T < \infty$ can be assigned as the transition time for the heat equation.

6.5.1.2 Formal Parametrization of the Wave Equation, Trajectory Assignment, and Feedforward Control Design

By proceeding similar to the previous paragraph, the formal operational state and input parametrization for the wave equation (6.90) follows as

$$\hat{x}_k(s) = -\frac{b_k^{(2)}}{\lambda_k^{(2)}}\hat{\mathcal{D}}_k^x(s)\hat{\xi}(s), \quad k \in \mathbb{Z} \setminus \{0\} \qquad \hat{u}(s) = \hat{\mathcal{D}}^u(s)\hat{\xi}(s) \tag{6.99}$$

with $b_k^{(2)} = \int_0^1 \mathfrak{b}(z^1)\overline{\psi_{2,k}^{(2)}(z^1)}\mathrm{d}z^1 = F_k\overline{\lambda_k^{(2)}}/(k\pi)(\cos(ak\pi) - \cos(bk\pi)) \in \mathbb{C}$ and

$$\hat{\mathcal{D}}^u(s) = \prod_{n\in\mathbb{Z}\setminus\{0\}} \left(1 - \frac{s}{\lambda_n^{(2)}}\right) = \prod_{n\in\mathbb{N}} \left(1 + \frac{s^2}{\lambda_n^{(2)}\overline{\lambda_k^{(2)}}}\right)$$
$$= \prod_{n\in\mathbb{N}} \left(1 + \frac{s^2}{(k\pi)^2}\right) = \frac{\sinh(s)}{s} \tag{6.100}$$

$$\hat{\mathcal{D}}_k^x(s) = \prod_{n\in\mathbb{Z}\setminus\{0\}, n\neq k} \left(1 - \frac{s}{\lambda_n^{(2)}}\right) = -\frac{\lambda_k^{(2)}}{s - \lambda_k^{(2)}} \frac{\sinh(s)}{s}, \tag{6.101}$$

where $\hat{x}_k(s) = \langle \hat{\boldsymbol{x}}(s), \boldsymbol{\phi}_k^{(2)} \rangle_{X^{(2)}}$, $k \in \mathbb{N}$. These parametrizations are valid provided that $b_k^{(2)} \neq 0$ for all $k \in \mathbb{Z} \setminus \{0\}$, which ensures the approximate controllability of the distributed–parameter system (6.90). Note that since $\overline{\lambda_k^{(2)}} = -\lambda_k^{(2)}$ and $\lambda_{-k}^{(2)} = -\lambda_k^{(2)}$ this is equivalent to $b_k^{(2)} \neq 0$ for all $k \in \mathbb{N}$.

The function $\hat{\mathcal{D}}^u(s)$ as introduced in (6.101) is entire and of finite type and order $\varrho = 1$. The latter follows directly from the determination of the convergence exponent of the sequence $(\lambda_n^{(2)})_{n\in\mathbb{Z}\setminus\{0\}}$ of zeros of $\hat{\mathcal{D}}^u(s)$, i.e. $\gamma = 1$. Hence, the operational convergence requires that the basic output $\xi(t)$ has to be of Gevrey order[10] $\alpha < 1$. On the other hand, the following relation holds

$$\hat{\mathcal{D}}^u(s)\hat{\xi}(s) = \frac{\sinh(s)}{s}\hat{\xi}(s) = \frac{e^s - e^{-s}}{2s}\hat{\xi} \bullet\!\!-\!\!\circ$$
$$\frac{1}{2}\big(\tilde{\xi}(t+1)\sigma(t+1) - \tilde{\xi}(t-1)\sigma(t-1)\big) = u(t), \tag{6.102}$$

with $\tilde{\xi}(t) = \int_{0^-}^{t} \xi(p)\mathrm{d}p$. This illustrates that the determined parametrization accounts for the wave dynamics expressed in terms of a finite speed of wave propagation along the characteristic curves $\mathrm{d}t/\mathrm{d}z = \pm 1$. In other words, the differential parametrization involving an infinite number of derivatives allows to exactly recover the wave dynamics in such a way that the feedforward control involves advanced and delayed arguments. Moreover, it can be easily deduced that there exists a minimal transition time $T_{\min} = 2$, which corresponds to twice the wave speed. This observation holds similarly for the state parametrization, which can be further evaluated to achieve

$$x_k(t) = b_k^{(2)} e^{\lambda_k^{(2)} t} \star \frac{1}{2}\big(\tilde{\xi}(t+1)\sigma(t+1) - \tilde{\xi}(t-1)\sigma(t-1)\big)$$

where $\star$ denotes the convolution product. Thereby, the definition of $b_k^{(2)}$ and F_k directly implies that $(x_k(t))_{k\in\mathbb{N}} \in \ell^2(\mathbb{R}^+)$. In addition note that since a basic output is not necessarily unique both $\xi(t)$ and $\tilde{\xi}(t)$ can be considered as basic outputs for the wave equation (6.90).

[10] Note that it can be easily shown that $\alpha = 1$ is sufficient.

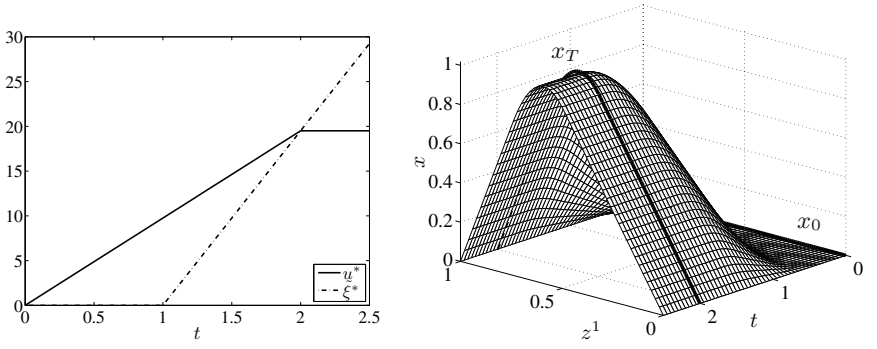

Fig. 6.2 Feedforward control $u^*(t)$ vs. basic output $\tilde{\xi}^*(t)$ (left) and simulated profile in the (z^1, t)–domain (right) for the linear wave equation (6.90) with in–domain actuation.

In view of the realization of finite time transitions between a zero initial steady state and the final steady state determined from (6.98) the connecting desired trajectory for the basic output can be even chosen as a discontinuous function of time since (6.102) does not impose any differentiability conditions. Note that actually also impulsive functions are allowed by the definition of $\tilde{\xi}(t)$. Hence, for the following numerical evaluation the desired trajectory $t \mapsto \xi^*(t)$ is assigned as

$$\xi^*(t) = \xi_{s,0}\delta(t) + (\xi_{s,T} - \xi_{s,0})\sigma(t-1) \tag{6.103}$$

such that

$$\tilde{\xi}^*(t) = \xi_{s,0} + (\xi_{s,T} - \xi_{s,0})(t-1)\sigma(t-1).$$

The shifted argument $t-1$ is thereby introduced for causality purposes to guarantee that $u^*(t) = 0$ for $t < 0$ (cf. (6.102)). For consistency with the zero initial state, subsequently $\xi_{s,0} = 0$. In order to illustrate the resulting transitory behavior, simulation results are depicted in Figure 6.2 for $\xi_{s,T} = 19.5$ and the spatial characteristics being similar to the previous paragraph restricted to the interval $z \in [a, b]$ with $a = 1/2$ and $b = 3/4$. The numerical results confirm the exact realization of the desired finite time transition. Moreover, in contrast to the linear heat equation (cf. Figure 6.1) the feedforward control involves no overshoot compared to the final input value. However, the advancement of the input trajectory compared to the desired trajectory for the basic output (6.103) can be clearly identified as a result of the finite speed of wave propagation. As already pointed out above this also implies the minimal transition time given by $T_{\min} = 2$.

6.5.2 Boundary Controlled Linear Diffusion–Reaction Equation on r–Dimensional Riemannian Manifold

The trajectory planning problem is considered for the linear diffusion–reaction equation

$$\partial_t x(t) = \big(\Delta + c\big)x(t), \qquad (z,t) \in \Omega \times \mathbb{R}^+ \tag{6.104a}$$

defined on the domain $\Omega \subset \mathbb{R}^r$. As illustrated in Figure 6.3, the control is restricted to the boundary according to

$$\epsilon \partial_{\mathbf{n}} x(t) + p^0 x(t) = 0, \qquad (z,t) \in \partial\Omega_0 \times \mathbb{R}^+ \tag{6.104b}$$

$$\epsilon \partial_{\mathbf{n}} x(t) + p^1 x(t) = u_{\partial\Omega}(t), \qquad (z,t) \in \partial\Omega_1 \times \mathbb{R}^+ \tag{6.104c}$$

with $\partial\Omega_1 = \partial\Omega \setminus \partial\Omega_0$. Herein, $\epsilon \in \mathbb{R}$ and p^0, $p^1 > 0$ such that either Dirichlet or Robin boundary conditions can be assigned. Moreover, two control configurations are considered representing infinite–dimensional as well as finite–dimensional actuation, where

$$u_{\partial\Omega}(t) = \begin{cases} v(t), & (B1) \\ \sum_{l=1}^m b^l v^l(t), & (B2). \end{cases} \tag{6.104d}$$

Here, $v(t) = v(\cdot,t) \in L^2(\partial\Omega_1 \times (0,\tau))$ denotes the infinite–dimensional control input while $b^l = b^l(z) \in L^2(\partial\Omega_1^l)$ with $\partial\Omega_1^l$ denoting the subarea of $\partial\Omega$ covered by the l–th actuator such that $\partial\Omega_1 = \cup_{l=1}^m \partial\Omega_1^l$ and $v^l(t) \in L^2(0,\tau)$ for each $l = 1,\dots,m$, represent the spatial actuator characteristics and the respective finite–dimensional control input. The boundary input can be realized, e.g., by means of external sources or sinks which exchange energy with the system along a subset of the domain's boundary. While the infinite–dimensional configuration is primarily of theoretical interest it should be pointed out that in certain applications such as the reheating or selective cooling of slabs in steel processing this assumption is in good accordance with the physical plant configuration.

The initial condition is chosen as

$$x(0) = x_0, \qquad z \in \overline{\Omega}, \tag{6.104e}$$

where, given a stationary initial profile, it can be assumed without loss of generality that $x_0 = x_0(z) = 0$, $z \in \overline{\Omega}$. By applying standard arguments for the analysis of initial–boundary–value problems, given $x_0 \in L^2(\Omega)$ and $u_{\partial\Omega}(t)$ as above the distributed–parameter system (6.104) has a unique weak solution $x(t) \in L^2((0,\tau); H^1(\Omega)) \cap C([0,\tau]; L^2(\Omega))$ for all $\tau > 0$ [68, 15]. In addition, by applying a Lyapunov–type argument together with the Rayleigh principle it can be easily shown that this solution is exponentially stable in the L^2–norm if p^0, $p^1 \geq 0$ and $c < \lambda_{\min}$, where $\lambda_{\min}$ denotes the smallest eigenvalue λ of the Sturm–Liouville problem $\Delta x + \lambda x = 0$ with homogeneous boundary conditions

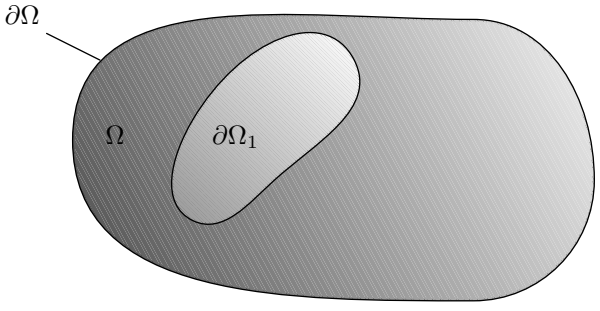

Fig. 6.3 Spatial domain Ω with smooth boundary $\partial\Omega$ and boundary actuation covering the area $\partial\Omega_1$

(6.104b) and (6.104c). However, it should be pointed out that the proposed design approach is independent of the stability properties of the control system and is hence applicable also to the unstable case.

The considered trajectory planning problem concerns the design of an input trajectory $u_{\partial\Omega}(t)$ in order to realize a finite time transition starting at $x_0 = 0$ and reaching a prescribed desired final stationary profile

$$x_0 = x(0) \xrightarrow[t\in[0,T]]{u_{\partial\Omega}(t)} x(T) = x_T, \quad z \in \overline{\Omega} \tag{6.105}$$

along a pre–planned spatial–temporal transition path within the finite time interval $t \in [0, T]$ for a prescribed transition time $T > 0$.

Assumption 6.6. The system (6.104) with spatial domain Ω satisfies the following conditions:

(i) The domain Ω is a smooth Riemannian manifold with oriented smooth boundary $\partial\Omega$.
(ii) The boundary control $u_{\partial\Omega}(t)$ is of compact support in $\partial\Omega$, i.e. $u_{\partial\Omega}(t) = 0$ for $z \in \partial\Omega_0$.

6.5.2.1 Abstract Boundary Control System

By proceeding as outlined generically in Section 6.1.2.1, the boundary controlled diffusion–reaction system (6.104) can be represented as an abstract boundary control system with admissible input operator. For this, take the solution space as $Z = H_R(\Omega)$ with

$$H_R(\Omega) = \left\{x \in H^2(\Omega) : \epsilon\partial_{\mathbf{n}}x + p^0 x = 0\right\}.$$

Moreover, the state space and the input space are chosen as $X = L^2(\Omega)$ and $U = L^2(\partial\Omega_1)$. The operators $\mathfrak{L} \in \mathcal{L}(Z, X)$ and $\mathfrak{K} \in \mathcal{L}(Z, U)$ follow by a direct comparison as

$$\mathfrak{L}x = (\Delta + c)x, \quad \mathfrak{K}x = \epsilon\partial_{\mathbf{n}}x + p^1 x \qquad \forall x \in Z.$$

As in Section 6.1.2.1, introduce the operator $\mathfrak{A} = \mathfrak{L}|_{\mathcal{D}(\mathfrak{A})}$ with domain $\mathcal{D}(\mathfrak{A}) = \ker\mathfrak{K} = \{x \in Z : \epsilon\partial_{\mathbf{n}}x + p^1 x = 0\}$. It is subsequently shown that $\mathfrak{A}$ is the infinitesimal generator of a C_0–semigroup on X. By making use of Green's Theorem it follows for $\phi \in \mathcal{D}(\mathfrak{A})$ and $\psi \in H^2(\Omega)$ that

$$\begin{aligned}
\langle\mathfrak{A}\phi, \psi\rangle_X &= \langle\Delta\phi, \psi\rangle_X + \langle c\phi, \psi\rangle_X \\
&= \langle\phi, (\Delta + c)\psi\rangle_X + \oint_{\partial\Omega} \big(\psi\partial_{\mathbf{n}}\phi - \phi\partial_{\mathbf{n}}\psi\big)\mathrm{d}\partial\Omega \\
&= \langle\phi, (\Delta + c)\psi\rangle_X + \oint_{\partial\Omega_0} \partial_{\mathbf{n}}\phi\left(\psi + \frac{\epsilon}{p^0}\partial_{\mathbf{n}}\psi\right)\mathrm{d}\partial\Omega_0 \\
&\quad + \oint_{\partial\Omega_1} \partial_{\mathbf{n}}\phi\left(\psi + \frac{\epsilon}{p^1}\partial_{\mathbf{n}}\psi\right)\mathrm{d}\partial\Omega_1,
\end{aligned}$$

which yields that $\mathfrak{A}^* = \mathfrak{A}$ with domain $\mathcal{D}(\mathfrak{A}^*) = \mathcal{D}(\mathfrak{A})$, i.e. $\mathfrak{A}$ is self–adjoint. Let now $\mathfrak{A}_0 = -\mathfrak{A}$ with $\mathcal{D}(\mathfrak{A}_0) = \mathcal{D}(\mathfrak{A})$. Then a similar calculation reveals

$$\begin{aligned}
\langle\mathfrak{A}_0 x, x\rangle_X &= \|\nabla x\|_X^2 - c\|x\|_X^2 \\
&\quad + \begin{cases} 0, & \epsilon = 0 \\ -p^0 \oint_{\partial\Omega_0} x^2 \mathrm{d}\partial\Omega_0 - p^1 \oint_{\partial\Omega_1} x^2 \mathrm{d}\partial\Omega_1, & \epsilon = 1 \end{cases} \qquad (6.106) \\
&\geq \left(\frac{1}{K_p^2} - c\right)\|x\|_X^2,
\end{aligned}$$

where the inequality is obtained from the Poincaré inequality [17] with $K_p > 0$ denoting the Poincaré constant. Hence, $\mathfrak{A}_0$ is strictly positive for $1/K_p^2 - c > 0$ such that $-\mathfrak{A}_0 = \mathfrak{A} \leq 0$ and is m–dissipative by [66, Proposition 3.3.5]. Under these conditions $\mathfrak{A}$ is the infinitesimal generator of a C_0–semigroup $\mathfrak{T}(t)$ on X with $\mathfrak{T}(t) \geq 0$ for all $t \geq 0$ [66, Proposition 3.8.5]. If c is finite but such that $1/K_p^2 - c < 0$ the transformation $x(t) \mapsto \exp(ct)x(t)$ enables to deduce a similar result for any finite time interval. Alternatively, $cx(t)$ can be considered as a bounded perturbation of $\Delta x(t)$. Consequently, the conditions (i)–(iv) of Section 6.1.2.1 are directly satisfied such that $(\mathfrak{L}, \mathfrak{K})$ is a boundary control system on U, Z, and X.

Instead of determining the input operator $\mathfrak{B}$ explicitly, subsequently only its adjoint $\mathfrak{B}^*$ is computed by making use of (6.6). For this, let $x \in Z$ and $\psi \in \mathcal{D}(\mathfrak{A}^*) = \mathcal{D}(\mathfrak{A})$, and observe

$$\big\langle\mathfrak{L}x, \psi\big\rangle_X - \big\langle x, \mathfrak{A}^*\psi\big\rangle_X = -\frac{1}{p^1}\oint_{\partial\Omega_1} u_{\partial\Omega}\partial_{\mathbf{n}}\psi \,\mathrm{d}\partial\Omega_1$$

with the right hand side following directly from Green's Theorem together with Assumption 6.6(ii). Together with (6.104c) and (6.104d) this yields for all $\psi \in \mathcal{D}(\mathfrak{A}^*)$ that

$$\mathfrak{B}^*\psi = \begin{cases} -\frac{1}{p^1}\partial_{\mathbf{n}}\psi|_{z\in\partial\Omega_1}, & (B1) \\ -\frac{1}{p^1}\left[b^1\partial_{\mathbf{n}}\psi|_{z\in\partial\Omega_1^1},\dots b^m\partial_{\mathbf{n}}\psi|_{z\in\partial\Omega_1^m}\right], & (B2) \end{cases}. \tag{6.107}$$

It should be pointed out that since $\langle\mathfrak{B}u_{\partial\Omega}(t),\psi\rangle_X = \langle u_{\partial\Omega}(t),\mathfrak{B}^*\psi\rangle_X$ the control operator equals

$$\mathfrak{B} = \begin{cases} \frac{1}{p^1}\partial_{\mathbf{n}}\delta_{\partial\Omega_1}(z), & (B1) \\ \frac{1}{p^1}\left[\partial_{\mathbf{n}}\delta_{\partial\Omega_1^1}(z),\dots,\partial_{\mathbf{n}}\delta_{\partial\Omega_1^m}(z)\right], & (B2) \end{cases}.$$

Here, $\delta_{\partial\Omega_1}(z)$ and $\delta_{\partial\Omega_1^l}(z)$ denote Dirac delta functions with compact support on $z\in\partial\Omega_1$ or $z\in\partial\Omega_1^l$, respectively. Hence, obviously $\mathfrak{B}$ has to be interpreted as a linear functional, i.e. as an element of the dual space X_{-1}.

In order to show that $\mathfrak{B}$ is admissible in the sense of Definition 6.1, subsequently the duality between an admissible control and an admissible observation operator is exploited together with a perturbation argument. By [66, Theorem 4.4.3] given $\mathfrak{B}\in\mathcal{L}(U,X_{-1})$ then $\mathfrak{B}$ is an admissible control operator for the C_0–semigroup $\mathfrak{T}(t)$ if and only if $\mathfrak{B}^*$ is an admissible observation operator for $\mathfrak{T}^*(t)$. The admissibility of an observation operator can be thereby determined using the following proposition [66, Proposition 5.1.3].

Proposition 6.1. *Let $\mathfrak{A}:\mathcal{D}(\mathfrak{A})\to X$ be self–adjoint and $\mathfrak{A}\le 0$. Define $X_{\frac{1}{2}}$ as the completion of $\mathcal{D}(\mathfrak{A})$ with respect to the norm $\|x\|_{\frac{1}{2}}^2 = \langle(\mathfrak{I}-\mathfrak{A})x,x\rangle_X$, $\forall x\in\mathcal{D}(\mathfrak{A})$. If $\mathfrak{C}\in\mathcal{L}(X_{\frac{1}{2}},Y)$, then $\mathfrak{C}$ is an admissible observation operator for the semigroup $\mathfrak{T}(t)$ (of positive operators) generated by $\mathfrak{A}$ on X.*

Hence, $\mathfrak{B}$ is an admissible control operator for $\mathfrak{A}$ if $\mathfrak{B}^*\in\mathcal{L}(X_{\frac{1}{2}},U)$. The verification of this property is carried out for the case of Dirichlet boundary conditions on all of $\partial\Omega$, e.g., in [66, Section 10.6] by introducing the Dirichlet map. In order to express $X_{\frac{1}{2}}$ for the present set–up involving Robin boundary conditions consider first the operator $\mathfrak{A}_0=-\Delta$ with $\mathcal{D}(\mathfrak{A}_0)=\mathcal{D}(\mathfrak{A})$. It can be easily shown that $\mathfrak{A}_0$ is self–adjoint. In addition, $\mathfrak{A}_0$ is positive since

$$\langle\mathfrak{A}_0x,x\rangle_X = \|\nabla x\|_X^2 - \oint_{\partial\Omega} x\partial_{\mathbf{n}}x\,\mathrm{d}\partial\Omega, \qquad \forall x\in\mathcal{D}(\mathfrak{A}_0),$$

where the second term (including the sign) on the right hand side of the equality evaluates to zero if only Dirichlet boundary conditions exist ($\epsilon=0$) and is positive and bounded for Robin boundary conditions ($\epsilon=1$) on $\partial\Omega_0$ with $p^1>0$. Note that in the latter case the Poincaré inequality (applied to the integral over $\partial\Omega$) implies that there exists a constant $K>1$ such that

$$\langle\mathfrak{A}_0x,x\rangle_X \le K^2\|\nabla x\|_X^2, \qquad \forall x\in\mathcal{D}(\mathfrak{A}_0).$$

Consider now the space $H_{\frac{1}{2}} = \mathcal{D}(\mathfrak{A}_0^{\frac{1}{2}})$, which is the completion of $\mathcal{D}(\mathfrak{A}_0)$ with respect to the norm $\|x\|_{\frac{1}{2}} = \sqrt{\langle\mathfrak{A}_0x,x\rangle_X}$, $\forall x\in\mathcal{D}(\mathfrak{A}_0)$ [66, Remark 3.4.4]. With

the previous result, this yields $\|x\|_{\frac{1}{2}} = K\|\nabla x\|_X$, which is for all $x \in \mathcal{D}(\mathfrak{A}_0)$ an equivalent norm to $\|x\|_{H^1(\Omega)} = \sqrt{\|x\|^2_{L^2(\Omega)} + \|\nabla x\|^2_{L^2(\Omega)}}$. By standard density arguments it follows that the closure of $\mathcal{D}(\mathfrak{A}_0)$ in $H^1(\Omega)$ is given by $H_R(\Omega)$. Thus, $H_{\frac{1}{2}} = H_R(\Omega)$. Proceeding similarly for $\mathfrak{I} - \Delta$ instead of $\mathfrak{A}_0$ allows to identify $X_{\frac{1}{2}}$ with $H_{\frac{1}{2}}$ (see the proof of [66, Proposition 5.1.3]). This implies that $\mathfrak{B}^* \in \mathcal{L}(X_{\frac{1}{2}}, U)$ such that $\mathfrak{B}$ is an admissible control operator for C_0–semigroup generated by the operator $-\mathfrak{A}_0 = \Delta$. Since the original operator $\mathfrak{A} = \mathfrak{L}|_{\mathcal{D}(\mathfrak{A})}$ represents a bounded perturbation of $-\mathfrak{A}_0$ the admissibility of the control operator $\mathfrak{B}$ carries over to the perturbed C_0–semigroup [66, Section 10.8].

6.5.2.2 Riesz Spectral System Representation

The previous results are utilized to determine the Riesz spectral system representation of (6.104). For this, certain assumptions are imposed subsequently.

Assumption 6.7. The operator $\mathfrak{A}$ with domain $\mathcal{D}(\mathfrak{A})$ as defined above satisfies the following conditions:

(i) The algebraic and geometric multiplicities r_k^a and r_k^g of each eigenvalue λ_k of $\mathfrak{A}$ coincide.
(ii) The sequences $((\phi_{k_j})_{j=1,\dots,r_k^a})_{k\in\mathbb{N}}$ and $((\psi_{k_j})_{j=1,\dots,r_k^a})_{k\in\mathbb{N}}$ of generalized eigenvectors of the operator $\mathfrak{A}$ and its adjoint $\mathfrak{A}^*$ form biorthogonal Riesz bases for $X = L^2(\Omega)$.
(iii) Zero is not an eigenvalue of $\mathfrak{A}$, i.e. $\{0\} \in \rho(\mathfrak{A})$.

As pointed out above, the operator $\mathfrak{A}$ is self–adjoint, which implies that its eigenvalues $(\lambda_k)_{k\in\mathbb{N}}$ are real. With $\mathfrak{B}^*$ as introduced in (6.107) the above computation in addition provides the Riesz spectral system representation in terms of the Fourier coefficients $x_{k_j}(t) = \langle x(t), \psi_{k_j}\rangle_X$ following

$$\partial_t x_{k_j}(t) = \lambda_k x_{k_j}(t) + u_{k_j}(t), \qquad t > 0 \tag{6.108a}$$

$$x_{k_j}(0) = \langle x_0, \psi_{k_j}\rangle_X = 0 \tag{6.108b}$$

with

$$u_{k_j}(t) = -\frac{1}{p^1}\oint_{\partial\Omega_1} u_{\partial\Omega}(t)\partial_{\mathbf{n}}\psi_{k_j}\,\mathrm{d}\partial\Omega_1. \tag{6.108c}$$

Given (6.104d), the surface integral can be further evaluated to achieve

$$u_{k_j}(t) = \begin{cases} b_{1,k_j} v_{k_j}(t), & (B1) \\ \sum_{l=1}^m b^l_{2,k_j} v^l(t), & (B2) \end{cases} \tag{6.108d}$$

with b_{1,k_j} a constant arising in general from the evaluation of (6.108c) and $b^l_{2,k_j} = \oint_{\partial\Omega_1^l} b^l(z)\partial_{\mathbf{n}}\psi_{k_j}(z)\,\mathrm{d}\partial\Omega_1^l$, $l = 1,\dots,m$. Subsequently it is assumed that system

(6.104) or (6.108), respectively, is approximately controllable, which is equivalent to impose Assumptions 6.2 or 6.5 depending on the considered boundary control configuration. In addition, due to the Riesz basis property of $((\phi_{k_j})_{j=1,\dots,r_k^a})_{k\in\mathbb{N}}$ and $((\psi_{k_j})_{j=1,\dots,r_k^a})_{k\in\mathbb{N}}$ the state $x(t)$ can be re–constructed from the spectral states $x_{k_j}(t)$ in terms of the Fourier series

$$x(t) = \sum_{k\in\mathbb{N}} \sum_{j=1}^{r_k^a} x_{k_j}(t)\phi_{k_j}. \tag{6.109}$$

Remark 6.11. In view of the domain $\mathcal{D}(\mathfrak{A})$ of $\mathfrak{A}$ imposed for the determination of the eigenfunctions ϕ_{k_j}, it follows that in particular the inhomogeneous boundary condition (6.104c) cannot be evaluated pointwise by means of the series representation (6.109) of $x(t)$ but has to be interpreted in the sense of the $L^2(\partial\Omega_1)$–norm, i.e.

$$\left\| u_{\partial\Omega}(t) - \sum_{k=1}^{K} \sum_{j=1}^{r_k^a} x_{k_j}(t)\big(\epsilon\partial_{\mathfrak{n}}\phi_{k_j} + p^1\phi_{k_j}\big) \right\|_{L^2(\partial\Omega_1)} \to 0 \quad \text{as } K\to\infty.$$

6.5.2.3 Formal State and Input Parametrization

Proceeding as in Section 6.2, the spectral system representation (6.108) serves as the basis for determination of a formal state and input parametrization in terms of a basic output. For this, the two scenarios $(B1)$ and $(B2)$ are distinguished corresponding to infinite– and finite–dimensional boundary control. Thereby note that Assumption 6.7(i) implies $\theta_k = 1$ in the (differential) operators (6.32) and (6.45) introduced above.

Case (B1): Infinite–Dimensional Boundary Control

The state and input parametrizations for the case $(B1)$ of an infinite–dimensional boundary control follow directly from (6.44) and (6.45) by taking into account Assumption 6.7(i), which implies that $r_k^a = r_k^g$ for each $k \in \mathbb{N}$. In addition, recall that Assumptions 6.3 and 6.4 have to be satisfied, which impose a certain partitioning and grouping of the Fourier coefficients $v_{k_j}(t)$. This in particular implies that $u_{\partial\Omega}(t)$ admits a Fourier series representation

$$u_{\partial\Omega}(t) = \sum_{q\in\mathbb{N}} v_q(t)\varphi_q \tag{6.110}$$

in terms of the Riesz basis $\{\varphi_q\}_{q\in\mathbb{N}}$ obtained from $((\mathfrak{B}^*\phi_{k_j})_{j=1,\ldots,r_k^a})_{k\in\mathbb{N}}$ (cf. Section 6.2.2). By taking into account the interpretation in terms of differential operators of infinite order according to (6.52), it hence follows that[11]

$$x_{k_j}(t) = -\frac{b_{1,k_j}}{\lambda_k}{}^0\hat{\mathcal{D}}^x_{q(k_j),k}(\partial_t)\circ\xi_{q(k_j)(t)} \tag{6.111}$$

$$v_q(t) = \hat{\mathcal{D}}^u_q(\partial_t)\circ\xi_q(t) \tag{6.112}$$

together with (6.109) and (6.110) denote the formal state and input parametrizations in the case $(B1)$ of an infinite–dimensional boundary control.

Case (B2): Finite–Dimensional Boundary Control

The state and input parametrizations for the case $(B2)$ of a finite–dimensional boundary control follow directly from (6.31) and (6.32) with $r_k^a = r_k^g$ for each $k \in \mathbb{N}$ by Assumption 6.7(i). By making use of the time–domain interpretation introduced in (6.51) this yields

$$x_{k_j}(t) = -\frac{1}{\lambda_k}\sum_{l=1}^{m} b^l_{2,k_j}{}^0\hat{\mathcal{D}}^x_k(\partial_t)\circ\xi^l(t) \tag{6.113}$$

$$v^l(t) = \hat{\mathcal{D}}^u(\partial_t)\circ\xi^l(t), \tag{6.114}$$

which together with (6.109) provides the state and input parametrization in terms of $\xi^l(t)$, $l = 1,\ldots,m$, for the case $(B2)$ of a finite–dimensional boundary control.

6.5.2.4 Convergence of the Parametrized Fourier Series

In order to ensure the convergence of the determined state and input parametrizations it is according to Theorem 6.6 and Corollary 6.4 required to analyze the order and the type of the entire functions $\hat{\mathcal{D}}^u_k(s)$ for $(B1)$ and $\hat{\mathcal{D}}^u(s)$ for $(B2)$. Due to the structure of $\hat{\mathcal{D}}^u_k(s)$ and $\hat{\mathcal{D}}^u(s)$ (see also (6.31b) and (6.44b)) given in terms of Weierstrass canonical products this can be reduced to the determination of the genus of the sequence of their zeros. For this, subsequently the Weyl asymptotics (counting multiplicities) for the counting function and the eigenvalue distribution of the Laplace operator Δ are utilized, i.e.

$$\mathcal{N}^{\Delta}(\eta) \sim \frac{V_r^0 \mathrm{Vol}(\Omega)\eta^{\frac{r}{2}}}{(2\pi)^r} \tag{6.115a}$$

$$(\lambda_k^{\Delta})^{\frac{r}{2}} \sim \frac{(2\pi)^r k}{V_r^0 \mathrm{Vol}(\Omega)}. \tag{6.115b}$$

[11] Recall that by Assumption 6.4 $v_{k_j}(t) = v_q(t)$ for all $k_j \in S_q^l$, $q \in \mathbb{N}$.

as $\eta \to \infty$ or $k \to \infty$, respectively [10]. Here, V_r^0 denotes the volume of the unit disk in $\mathbb{R}^r$. Note that the parameter c in the definition of the considered system operator $\mathfrak{A}$ only introduces a shift in the sense that $\lambda_k = c + \lambda_k^\Delta$ but does not influence the growth of the counting function such that $\mathcal{N}(\eta) = \mathcal{N}^\Delta(\eta)$.

Proposition 6.2. *The convergence exponent of the sequence* $(\lambda_k^\Delta)_{k\in\mathbb{N}}$ *is* $\gamma^\Delta = r/2$ *and its genus is* $g^{s,\Delta} = \lfloor r/2 \rfloor$ *with* $\lfloor\cdot\rfloor$ *denoting the floor function.*

Proof. In order to prove the claim, recall from [35, Section 3.2] that the convergence exponent of a sequence with a countable infinite index set equals the order of its counting function, i.e.

$$\varrho_1^\Delta = \limsup_{\eta\to\infty} \frac{\log \mathcal{N}^\Delta(\eta)}{\log \eta}. \tag{6.116}$$

By making use of (6.115a) a direct computation yields $\varrho_1^\Delta = r/2$, which proves the first part. Moreover, since the genus of the sequence $(\lambda_k^\Delta)_{k\in\mathbb{N}}$ denotes the smallest positive integer $g^{s,\Delta}$ for which $\sum_{k\in\mathbb{N}} |\lambda_k^\Delta|^{-g^{s,\Delta}-1}$ converges $\varrho_1^\Delta = r/2$ implies that $(\lambda_k^\Delta)_{k\in\mathbb{N}}$ is of genus $g^{s,\Delta} = \lfloor r/2 \rfloor$. □

This result enables a systematic convergence analysis for the two boundary control configurations $(B1)$ and $(B2)$. For this, it is however convenient to reverse the order of analysis and to start with $(B2)$, which due to the finite–dimensional control provides the most restrictive convergence conditions. These then serve as an upper bound for the analysis of the infinite–dimensional control setting.

Case (B2): Finite–Dimensional Boundary Control

Let the spatial actuator characteristics $b^l(z)$ be such that

$$\sum_{k\in\mathbb{N}} \left(\frac{\max_{i=1,\dots,r_k^a} \left|b_{2,k_i}^l\right|^2}{\min_{i=1,\dots,\theta_k} \left|(-\lambda_k)^i\right|^2} \right) = \sum_{k\in\mathbb{N}} \left(\frac{\max_{i=1,\dots,r_k^a} \left|b_{2,k_i}^l\right|^2}{\left|(-\lambda_k)\right|^2} \right) < \infty$$

for each $l = 1, \dots, m$. Then, Corollary 6.4 implies convergence of the state and input parametrization for $\xi^l(t) \in G_{D^l,\alpha^l}(\mathbb{R})$ with $\alpha^l < 1/\varrho$, where ϱ denotes the order of the entire function $\hat{\mathcal{D}}^u(s)$ provided that $\hat{\mathcal{D}}^u(s)$ is of finite type τ.

Proposition 6.3. *The Weierstrass canonical product* $\hat{\mathcal{D}}^u(s)$ *is an entire function of order* $1/2 \le \varrho \le r/2$*, which is of mean type* $0 < \tau < \infty$ *if* ϱ *is non–integer and of maximal type* $\tau = \infty$ *if* ϱ *is integer and the series* $\sum_{k\in\mathbb{N}} |\lambda_k|^{-\varrho}$ *diverges.*

Proof. Following [8, Theorem 2.6.5], a Weierstrass canonical product $\mathit{\Pi}(s)$ is an entire function equal to the convergence exponent of its zeros. With this, the order ϱ of $\hat{\mathcal{D}}^u(s)$ follows directly from the convergence exponent of the sequence $(\lambda_k)_{k\in\mathbb{N}}$. Since the Weyl asymptotics (6.115) count all multiple eigenvalues, which are however not included in $\hat{\mathcal{D}}^u(s)$, the order can be only bounded from below and above.

By making use of Proposition 6.2 it follows that $1/2 \leq \varrho \leq r/2$. Here, the lower bound corresponds to the 1–dimensional case with $r = 1$ while the upper bound arises whenever $\Omega \subset \mathbb{R}^r$, $r > 1$, is such that Δ exhibits only discrete eigenvalues λ_k^{Δ} with $r_k^a = 1$.

For the verification of the second part observe that since the order of $\hat{\mathcal{D}}^u(s)$ equals the convergence exponent of its zero set $(\lambda_k)_{k\in\mathbb{N}}$ and hence the order of the counting function (see Proposition 6.2 above) it follows that

$$\mathcal{N}(\eta) = O(\eta^{\varrho}). \tag{6.117}$$

With this, consider first a non–integer order ϱ satisfying $1/2 \leq \varrho \leq r/2$. In this case, following [34, Theorem I.7] the type of $\hat{\mathcal{D}}^u(s)$ can be determined from the upper density of its zero set

$$\Delta_u = \limsup_{\eta\to\infty} \frac{\mathcal{N}(\eta)}{\eta^{\varrho}}.$$

By making use of (6.117) it follows directly that Δ_u is non–zero and finite. Hence, $\hat{\mathcal{D}}^u(s)$ is of mean type $0 < \tau < \infty$ [34, Theorem I.7].

Secondly, if $\hat{\mathcal{D}}^u(s)$ is of integer order ϱ, then no such simple result is available since the order might be larger than the distribution of its zeros might indicate [8, 35]. In order to address this, subsequently Lindelöf's theorem [34, Theorem I.15] is used, which yields that $0 < \tau < \infty$ ($\tau = \infty$) if the quantity $\chi_u = \max(\Delta_u, \delta_u')$ is bounded by $0 < \chi_u < \infty$ ($\chi_u = \infty$), where $\delta_u' = \limsup_{\eta\to\infty} |\delta_u(\eta)|$ with

$$\delta_u(\eta) = \frac{1}{\varrho} \sum_{(\lambda_k)\leq\eta} |\lambda_k|^{-\varrho}.$$

Thus, since $\lambda_1 > \lambda_2 > \ldots > \lambda_K > 0 > \lambda_K > \ldots \downarrow -\infty$ it follows that

$$\delta_u' = \left| \frac{1}{\varrho} \sum_{k\in\mathbb{N}} (\lambda_k)^{-\varrho} \right| = \frac{1}{\varrho} \sum_{k=1}^{K} (\lambda_k)^{-\varrho} + \frac{(-1)^{\varrho \bmod 2}}{\varrho} \sum_{k=K+1}^{\infty} (-\lambda_k)^{-\varrho}.$$

Since a finite number of addends does not change the series convergence, the convergence of the second sum in the expression is equivalent to the convergence of $\sum_{k\in\mathbb{N}} |\lambda_k|^{-\varrho}$. As a result, if $\sum_{k\in\mathbb{N}} |\lambda_k|^{-\varrho} \to \infty$ it follows that $\chi_u = \delta_u' = \infty$, which proves the claim. □

Thus, the convergence result applies if the basic output is of Gevrey order $\alpha^l < 1/\varrho$ with $1/2 \leq \varrho \leq r/2$ provided that $\hat{\mathcal{D}}^u(s)$ is of finite type. It is hence obvious that the convergence of the parametrizations cannot be ensured in general since configurations can arise, where the Gevrey orders ensuring convergence are too small to solve the trajectory planning problem (6.105).

Case (B1): Infinite–Dimensional Boundary Control

Proceeding similar to the previous paragraph, subsequently Proposition 6.2 is used to determine the order and type of $\hat{\mathcal{D}}_k^u(s)$. Thereby, it is a straight forward consequence that Proposition 6.3 also applies to the case $(B1)$ with the major difference arising from the partitioning and the associated grouping of the Fourier coefficients $v_{k_j}(t)$. This is reflected by the respective index set, which determines the set of eigenvalues necessary to evaluate the operators. In addition, with Assumption 6.7 the application of Theorem 6.6 requires that

$$\sum_{k\in\mathbb{N}} \frac{\max_{i=1,\dots,r_k^a} \left|b_{1,k_i}\right|^2}{(-\lambda_k)^2} < \infty.$$

By making use of the Weyl asymptotic (6.115b) it can be easily shown that this condition is in general fulfilled if $\max_{i=1,\dots,r_k^a} \left|b_{1,k_i}\right| = O(k^\beta)$ with $\beta < 2/r - (1+\epsilon)/2$ for some $\epsilon > 0$.

With the previous notation let S_q^l denote the countable infinite index set implying $v_{k_j}^l(t) = v_q^l(t)$ for all $k_j \in S_q^l$, $q \in \mathbb{N}$ (cf. Assumption 6.4). Obviously, for each q the convergence exponent γ_q of the zero set of $\hat{\mathcal{D}}_q^u(s)$, i.e. $(\lambda_n)_{n\in S_q^{l,1}}$, is bounded from above by $\gamma_q \leq r/2$ from Proposition 6.2. In addition, the convergence exponent is bounded from below by $\gamma_q \geq 1/2$. The latter condition follows from the $r = 1$–dimensional setting but, as is illustrated in the example considered in Section 6.5.3 below, arises also in higher–dimensions depending on the structure of Ω and $\partial\Omega_1$. With this, the following result is obtained, whose proof proceeds exactly along the lines of the proof of Proposition 6.3 and is hence omitted.

Proposition 6.4. *The Weierstrass canonical product $\hat{\mathcal{D}}_q^u(s)$ is an entire function of order $1/2 \leq \varrho_q < r/2$, which is of mean type $0 < \tau_q < \infty$ if ϱ_q is non–integer and is of maximal type $\tau_q = \infty$ if ϱ_q is integer and the series $\sum_{k\in S_q^{l,1}} |\lambda_k|^{-\varrho_q}$ diverges.*

Proposition 6.4 is so far the best possible conclusion since the evaluation of the order ϱ_q and hence the type τ_q inherently depends on the particular domain Ω and the boundary $\partial\Omega_1$. Nevertheless, it enables to deduce a rather general convergence result for the case $(B1)$, where according to Theorem 6.6 the basic output $\xi_q(t)$ has to be chosen as a Gevrey function of order $\alpha_q < 1/\varrho_q$ with $(D_q^l)_{q\in\mathbb{N}} \in \ell^2$ provided that ϱ_q is non–integer.

As already pointed out in the discussion for the case $(B2)$, settings can be constructed for which the convergence conditions prevent a convergent solution of the trajectory planning problem (6.105). However, as is shown in the example below also divergent parametrizations can be efficiently utilized, which significantly enhances the domain of applicability of the proposed approach.

6.5.3 Boundary Controlled Linear Diffusion–Convection–Reaction Equation on Parallelepiped Domain

In the sequel, the results of the previous section are used to solve the trajectory planning problem (6.105) for the evolution of the state $x(t)$ governed by the linear diffusion–convection–reaction equation

$$\partial_t x(t) = \sum_{j\in I_r} \left(a_j \partial_{z^j}^2 x(t) + b_j \partial_{z^j} x(t)\right) + cx(t), \quad (z,t) \in \Omega \times \mathbb{R}^+ \tag{6.118a}$$

with orthotropic diffusion and convection and parallelepiped domain $\Omega = \{z \in \mathbb{R}^r : 0 < z^j < L_j,\ j \in I_r\}$ with $I_r = \{1, 2, \ldots, r\}$. Note that Ω is a smooth Riemannian manifold with an oriented but only piecewise smooth boundary $\partial\Omega$. Referring to, e.g., [10], Ω can be also called a normal domain. Nevertheless, the results of Section 6.5.2 determined under the assumption of a smooth boundary, i.e. for a regular domain Ω, can be directly extended to the present case including the divergence theorem and Green's formulas [22]. Due to the geometry of the domain this set–up is appealing since it enables an almost fully analytical evaluation of the arising mathematical formulations [40]. For this, it is convenient to introduce multi–index notation as summarized in Appendix A.2. Moreover, the following assumption is imposed on the parameters of the PDE (6.118a).

Assumption 6.8. The parameters a_j, b_j, and c are assumed to satisfy the following conditions:

(i) For each $j \in I_r$ there exist positive finite constants a_j^l and a_j^u such that $0 < a_j^l \leq a_j \leq a_j^u$, i.e. the PDE (6.118a) is strictly parabolic.
(ii) For each $j \in I_r$ the convection parameter b_j is assumed to be positive and bounded from above, i.e. there exists a finite $b_j^u \in \mathbb{R}^+$ such that $0 \leq b_j \leq b_j^u$.
(iii) The reaction parameter is assumed to be bounded, i.e. there exist finite $c^l,\ c^u \in \mathbb{R}$ such that $c^l \leq c \leq c^u$.

The boundary surface consists of the union of the two subsets $\partial\Omega_1 := \{z \in \partial\Omega : z^r = L_r\}$ and $\partial\Omega_0 = \partial\Omega \backslash \partial\Omega_1$. Thereby, homogeneous Robin boundary conditions are imposed on the $2r-1$ hypersurfaces of $\partial\Omega_0$, i.e.

$$\epsilon_j^0 \partial_{z^j} x(t) - p_j^0 x(t) = 0, \qquad z^j = 0,\ j \in I_r,\ t > 0 \tag{6.118b}$$
$$\epsilon_j^1 \partial_{z^j} x(t) + p_j^1 x(t) = 0, \qquad z^j = L_j,\ j \in I_r^r,\ t > 0 \tag{6.118c}$$

with $I_r^r = I_r \setminus \{r\}$ while the boundary input is restricted to the domain $\partial\Omega_1$, where

$$\epsilon_r^1 \partial_{z^r} x(t) + p_r^1 x(t) = u_{\partial\Omega}(t), \qquad z^r = L_r,\ t > 0. \tag{6.118d}$$

Here, $p_j^0 \neq 0$, $p_j^1 \neq 0$, and the coefficients ϵ_j^0 and ϵ_j^1 can be utilized to impose either Dirichlet or mixed boundary conditions, where $\epsilon_j^0 = 0$ ($\epsilon_j^1 = 0$) or

$\epsilon_j^0 \neq 0$ ($\epsilon_j^1 \neq 0$), respectively. Similar to Section 6.5.2 two boundary control configurations are distinguished, i.e.

$$u_{\partial\Omega}(t) = \begin{cases} v(t), & (B1) \quad (6.118e) \\ \sum_{l=1}^{m} b^l v^l(t), & (B2) \quad (6.118f) \end{cases}$$

with $v(t) = v(\cdot, t)$ acting arbitrarily on the hypersurface $\partial\Omega_1$ for all $t > 0$ and $b^l(z_{(r|)})$, $z_{(r|)} = (z^1, \dots z^{r-1})$, representing the spatial characteristic of the l–th actuator with input $v^l(t)$. The initial condition follows as

$$x(0) = x_0, \qquad z \in \overline{\Omega}. \tag{6.118g}$$

If not stated otherwise the initial profile is assumed to be stationary such that without loss of generality, subsequently a zero initial condition $x_0 = x_0(z) = 0$, $z \in \overline{\Omega}$ is considered, which can be achieved for (6.118) by introducing the transformations $x(z,t) \mapsto x(z,t) + x_0(z)$ and $u(z_{(r|)}, t) \mapsto u(z_{(r|)}, t) + u_s(z_{(r|)})$, where $u_s(z_{(r|)}) \in L^2(\partial\Omega_1)$ denotes the stationary (time–invariant) value of $u(z_{(r|)}, t)$.

In order to distinguish the systems resulting from the two boundary control configurations, in the following the abbreviations

Σ_∞ : (6.118a)–(6.118d), (6.118e), (6.118g)
Σ_m : (6.118a)–(6.118d), (6.118f), (6.118g).

are used to refer to the respective diffusion–reaction system with either infinite–dimensional (Σ_∞) or finite–dimensional (Σ_m) control.

6.5.3.1 Transformation into Standard Form

Without loss of generality, it can be assumed that $a_j = 1$ and $b_j = 0$ for all $j \in I_r$ in the PDE (6.118a). This can be achieved by the following change of variables

$$z^j \mapsto \zeta^j = \frac{z^j}{\sqrt{a_j}}, \quad L_j \mapsto \frac{L_j}{\sqrt{a_j}} \tag{6.119}$$

$$x(z,t) \mapsto x(\zeta,t) \exp\Big(- \sum_{j \in I_r} \frac{b_j}{2\sqrt{a_j}} \zeta^j \Big), \tag{6.120}$$

which transforms the domain Ω according to

$$\Omega \mapsto \left\{ z \in \mathbb{R}^r : 0 < z^j < \frac{L_j}{\sqrt{a_j}},\ j \in I_r \right\}. \tag{6.121}$$

Note that the invertibility of (6.119) and (6.120) is immediately guaranteed by Assumption 6.8. In addition, the set of mappings

$$c \mapsto c - \frac{1}{4}\sum_{j\in I_r}\frac{b_j^2}{a_j}, \tag{6.122a}$$

$$\begin{aligned}&\epsilon_j^0 \mapsto \epsilon_j^0, \quad p_j^0 \mapsto \sqrt{a_j}p_j^0 + \frac{\epsilon_j^0 b_j}{2\sqrt{a_j}},\\ &\epsilon_j^1 \mapsto \epsilon_j^1, \quad p_j^1 \mapsto \sqrt{a_j}p_j^1 - \frac{\epsilon_j^1 b_j}{2\sqrt{a_j}}, \quad \forall j \in I_r\end{aligned} \tag{6.122b}$$

$$u_{\partial\Omega}(z_{(r|)},t) \mapsto \sqrt{a_r}u_{\partial\Omega}(\zeta_{(r|)},t)\exp\left(\sum_{j\in I_r^r}\frac{b_j\zeta^j}{2\sqrt{a_j}} + \frac{b_r L_r}{2\sqrt{a_r}}\right), \tag{6.122c}$$

$$x_0(z) \mapsto x_0(\zeta)\exp\left(-\sum_{j\in I_r}\frac{b_j}{2\sqrt{a_j}}\zeta^j\right) \tag{6.122d}$$

is obtained with $\zeta_{(r|)} = (\zeta^1,\ldots,\zeta^{r-1})$. It should be noticed that both Dirichlet ($\epsilon_j^0 = 0$ or $\epsilon_j^1 = 0$) and Robin boundary conditions ($\epsilon_j^0 \neq 0$ or $\epsilon_j^1 \neq 0$) are preserved under the introduced change of variables. As a result, given the diffusion–convection–reaction system (6.118) it is without loss of generality equivalent to study the boundary controlled diffusion–reaction system

$$\partial_t x(t) = (\Delta + c)x(t), \qquad (z,t) \in \Omega \times \mathbb{R}^+ \tag{6.123a}$$

on the spatial domain (6.121) with the boundary conditions

$$\epsilon_j^0\partial_{z^j}x(t) - p_j^0 x(t) = 0, \qquad z^j = 0,\ j \in I_r,\ t > 0 \tag{6.123b}$$

$$\epsilon_j^1\partial_{z^j}x(t) + p_j^1 x(t) = 0, \qquad z^j = L_j,\ j \in I_r^r,\ t > 0 \tag{6.123c}$$

$$\epsilon_r^1\partial_{z^r}x(t) + p_r^1 x(t) = u_{\partial\Omega}(t), \qquad z^r = L_r,\ t > 0, \tag{6.123d}$$

where $p_j^0 \neq 0$, $p_j^1 \neq 0$, and the initial condition

$$x(0) = 0, \qquad z \in \overline{\Omega}. \tag{6.123e}$$

Standard arguments for the analysis of initial–boundary–value problems imply that the distributed–parameter system (6.123) has a unique weak solution satisfying $x(t) \in L^2((0,\tau);H^1(\Omega)) \cap C([0,\tau];L^2(\Omega))$ for all $\tau > 0$ given $u_{\partial\Omega}(t) \in L^2(\partial\Omega_1\times(0,\tau))$ and $x_0 \in L^2(\Omega)$ [68, 15]. In addition, it follows from a Lyapunov–type argument together with the Rayleigh principle that the solution is exponentially stable in the L^2–norm if $p_j^0, p_j^1 \geq 0$ and $c < \lambda_{\min}$, where $\lambda_{\min}$ denotes the smallest eigenvalue λ of the Sturm–Liouville problem $\Delta x + \lambda x$ with only homogeneous boundary conditions (6.123b)–(6.123d). Nevertheless, the presented solution of the trajectory planning problem is independent of the stability of the distributed–parameter system.

Remark 6.12. Deviating from the general analysis in Section 6.5.2, the parameters p_j^0, p_j^1, ϵ_j^0, and ϵ_j^1 are assumed to differ in each direction z^j. However, the results

of Section 6.5.2 on the abstract formulation of the distributed–parameter system, its Riesz spectral representation, and the formal state and input parametrization directly apply to the present configuration with only minor modifications. This is exploited in the following sections. In particular, the Weyl asymptotics (6.115), which are used to deduce the main results hold for all combinations of Dirichlet, Neumann, and Robin boundary conditions.

6.5.3.2 Abstract Boundary Control System

The representation of (6.123) as an abstract boundary control system follows exactly the lines of Section 6.5.2.1. Hence, take $Z = H^2(\Omega) \cap H_R(\Omega)$, $X = L^2(\Omega)$ and $U = L^2(\partial\Omega_1)$. Due to individual parameters in the boundary conditions for each direction z^j one has $H_R(\Omega) = H_{R,1}(\Omega) \cap H_{R,2}(\Omega)$ with

$$
\begin{aligned}
&H_{R,1}(\Omega) = \\
&\quad \bigcap_{j \in I_r^{D,D}(r)} \big\{ x \in L^2(0, L_j) : \, x(0) = x(L_j) = 0 \big\} \\
&\quad \cap \bigcap_{j \in I_r^{D,R}(r)} \big\{ x \in H^1(0, L_j) : \, x(0) = 0, \, \epsilon_j^1 \partial_{z^j} x(L_j) + p_j^1 x(L_j) = 0 \big\} \\
&\quad \cap \bigcap_{j \in I_r^{R,D}(r)} \big\{ x \in H^1(0, L_j) : \, \epsilon_j^0 \partial_{z^j} x(0) - p_j^0 x(0) = 0, \, x(L_j) = 0 \big\} \\
&\quad \cap \bigcap_{j \in I_r^{R,R}(r)} \left\{ \begin{array}{l} x \in H^1(0, L_j) : \, \epsilon_j^0 \partial_{z^j} x(0) - p_j^0 x(0) = 0, \\ \epsilon_j^1 \partial_{z^j} x(L_j) + p_j^1 x(L_j) = 0 \end{array} \right\}
\end{aligned}
$$

given the index sets $I_r^{D,D}(i) = \{ j \in I_r^i : \, \epsilon_j^0 = 0 \wedge \epsilon_j^1 = 0 \}$, $I_r^{D,R}(i) = \{ j \in I_r^i : \, \epsilon_j^0 = 0 \wedge \epsilon_j^1 \neq 0 \}$, $I_r^{R,D}(i) = \{ j \in I_r^i : \, \epsilon_j^0 \neq 0 \wedge \epsilon_j^1 = 0 \}$, and $I_r^{R,R}(i) = \{ j \in I_r^i : \, \epsilon_j^0 \neq 0 \wedge \epsilon_j^1 \neq 0 \}$ referring to the case of homogeneous Dirichlet–Dirichlet, Dirichlet–Robin, Robin–Dirichlet, and Robin–Robin boundary conditions, respectively, and

$$
\begin{aligned}
&H_{R,2}(\Omega) = \\
&\quad \begin{cases} \big\{ x \in L^2(0, L_r) : \, x(0) = 0 \big\}, & \text{if } \epsilon_r^0 = \epsilon_r^1 = 0 \\ \big\{ x \in H^1(0, L_r) : \, x(0) = 0 \big\}, & \text{if } \epsilon_r^0 = 0 \wedge \epsilon_r^1 \neq 0 \\ \big\{ x \in H^1(0, L_r) : \, \epsilon_r^0 \partial_{z^r} x(0) - p_r^0 x(0) = 0 \big\}, & \text{if } \epsilon_r^0 \neq 0. \end{cases}
\end{aligned}
$$

In view of the geometry of the domain, the adjoint input operator defined in (6.107) can be evaluated as

$$
\mathfrak{B}^* \psi = \begin{cases} -\frac{1}{p_r^1} \partial_{z^r} \psi|_{z^r = L_r}, & (B1) \\ -\frac{1}{p_r^1} \big[b^1, \ldots, b^m \big] \partial_{z^r} \psi|_{z^r = L_r}, & (B2) \end{cases} \qquad \forall \psi \in \mathcal{D}(\mathfrak{A}^*). \tag{6.124}
$$

It should be pointed out that since $\langle \mathfrak{B} u_{\partial\Omega}, \psi \rangle_X = \langle u_{\partial\Omega}, \mathfrak{B}^* \psi \rangle_X$ the control operator can be represented as $\mathfrak{B} = \mathfrak{B}(z^r) = \partial_{z^r} \delta(z^r)/p_r^1$, which has to be interpreted as a linear functional, i.e. in the dual space X_{-1}. Moreover, the analysis in Section 6.5.2.1 reveals that the control operator $\mathfrak{B}$ is admissible in the sense of Definition 6.1.

6.5.3.3 Riesz Spectral System Representation

Having introduced an admissible (boundary) control operator $\mathfrak{B}$, subsequently the previous results are utilized to determine the Riesz spectral system representation of (6.123). For this, the eigenvalues and the set of generalized eigenvectors are determined by considering the eigenproblem

$$\mathfrak{A}\phi = \lambda\phi, \qquad \phi \in \mathcal{D}(\mathfrak{A}) \tag{6.125a}$$

with the operator $\mathfrak{A} = \Delta + c$ defined on the domain

$$\begin{aligned} \mathcal{D}(\mathfrak{A}) &= H^2(\Omega) \cap H_R(\Omega) \\ &\cap \begin{cases} \{x \in L^2(0, L_r) : x(L_r) = 0\}, & \text{if } \epsilon_r^1 = 0 \\ \{x \in H^1(0, L_r) : \epsilon_r^1 \partial_{z^r} x(L_r) + p_r^1 x(L_r) = 0\}, & \text{if } \epsilon_r^1 \neq 0. \end{cases} \end{aligned} \tag{6.125b}$$

Recalling from the analysis in Section 6.5.2.1 that the operator $\mathfrak{A}$ is self–adjoint, the following result is obtained for the eigenvalues and eigenvectors.

Lemma 6.4. *Let ϵ_j^0, ϵ_j^1, p_j^0, and p_j^1 be such that $p_j^0 p_j^1 - ((2l-1)\pi/(2L_j))^2 \epsilon_j^0 \epsilon_j^1 \neq 0$ for all $j \in I_r$ and $l \in \mathbb{N}$. Then, the operator $\mathfrak{A}$ with either Dirichlet ($\epsilon_j^0 = \epsilon_j^1 = 0$) or Robin boundary conditions (ϵ_j^0, $\epsilon_j^1 \neq 0$) has the following spectral properties:*

(i) The eigenvalues $\{\lambda_k\}_{k \in \mathbb{N}^r}$ of $\mathfrak{A}$ are given by

$$\lambda_k = c - \sum_{j=1}^{r} \sigma_{k_j}^2 \tag{6.126}$$

with

$$\sigma_{k_j} \begin{cases} = \frac{k_j \pi}{L_j}, & \text{if } p_j^0 \epsilon_j^1 + p_j^1 \epsilon_j^0 = 0 \qquad (6.127a) \\ \sim_{\downarrow} \frac{k_j \pi}{L_j}, & \text{if } p_j^0 \epsilon_j^1 + p_j^1 \epsilon_j^0 > 0 \wedge \epsilon_j^0 \epsilon_j^1 \neq 0 \\ \sim_{\uparrow} \frac{k_j \pi}{L_j}, & \text{if } p_j^0 \epsilon_j^1 + p_j^1 \epsilon_j^0 < 0 \wedge \epsilon_j^0 \epsilon_j^1 \neq 0 \qquad (6.127b) \\ \sim_{\downarrow} \frac{(2k_j - 1)\pi}{2L_j}, & \text{if } \frac{p_j^0 \epsilon_j^1 + p_j^1 \epsilon_j^0}{p_j^0 p_j^1} > 0 \wedge \epsilon_j^0 \epsilon_j^1 = 0 \\ \sim_{\uparrow} \frac{(2k_j - 1)\pi}{2L_j}, & \text{if } \frac{p_j^0 \epsilon_j^1 + p_j^1 \epsilon_j^0}{p_j^0 p_j^1} < 0 \wedge \epsilon_j^0 \epsilon_j^1 = 0. \qquad (6.127c) \end{cases}$$

Here, $f_n \sim_\downarrow g_n$ and $f_n \sim_\uparrow g_n$ refer to the fact that f_n asymptotically approaches g_n as $n \to \infty$ either from above ($\downarrow$) or from below ($\uparrow$).

(ii) The eigenfunctions $\{\phi_k\}_{k\in\mathbb{N}^r}$ satisfy

$$\phi_k = \prod_{j=1}^{r} \vartheta_{k_j} \tag{6.128}$$

with

$$\vartheta_{k_j} = F_{k_j}\left(\sin(\sigma_{k_j} z^j) + \frac{\epsilon_j^0}{p_j^0}\sigma_{k_j}\cos(\sigma_{k_j} z^j)\right). \tag{6.129}$$

Moreover, given two multi–indexes k, $k' \in \mathbb{N}^r$, then $\langle \phi_k, \phi_{k'}\rangle = \delta_{k,k'}$, where $\delta_{k,k'}$ denotes the Kronecker delta function, if

$$F_{k_j} \begin{cases} = \sqrt{\dfrac{2(p_j^0)^2}{L_j\left((p_j^0)^2+\sigma_{k_j}^2(\epsilon_j^0)^2\right)}}, & \text{if } p_j^0\epsilon_j^1 + p_j^1\epsilon_j^0 = 0 \quad (6.130a) \\ \sim \sqrt{\dfrac{2(p_j^0)^2}{L_j\left((p_j^0)^2+\sigma_{k_j}^2(\epsilon_j^0)^2\right)}}, & \text{if } p_j^0\epsilon_j^1 + p_j^1\epsilon_j^0 \neq 0 \\ & \wedge\, \epsilon_j^0\epsilon_j^1 \neq 0 \quad (6.130b) \\ \sim \sqrt{\dfrac{2(p_j^0)^2}{L_j\left((p_j^0)^2+2\epsilon_j^0 p_j^0/L_j+\sigma_{k_j}^2(\epsilon_j^0)^2\right)}}, & \text{if } p_j^0\epsilon_j^1 + p_j^1\epsilon_j^0 \neq 0 \\ & \wedge\, \epsilon_j^0\epsilon_j^1 = 0 \quad (6.130c) \end{cases}.$$

Proof. The solution of the eigenproblem (6.125) can be directly determined by means of a separation ansatz, which reduces the computation of the eigenfunctions ϕ to the solution of r individual Sturm–Liouville problems in the directions z^j, $j \in I_r$. For this, the substitution of (6.128) into (6.125) yields (6.129) and (6.126) with F_{k_j} a normalization constant to be determined below and σ_{k_j} the solution of the characteristic equation

$$\sigma_{k_j}\cos(\sigma_{k_j}L_j)\left(p_j^0\epsilon_j^1 + \epsilon_j^0 p_j^1\right) + \sin(\sigma_{k_j}L_j)\left(p_j^0 p_j^1 - \sigma_{k_j}^2\epsilon_j^0\epsilon_j^1\right) = 0. \tag{6.131}$$

The root $\sigma_{k_j} = 0$ of (6.131) does not provide a non–trivial solution $\vartheta(z^j)$ and can hence be excluded from the eigenvalue analysis. Furthermore, observe that if there exist $j \in I_r$ and $l \in \mathbb{N}$ such that $p_j^0 p_j^1 = ((2l-1)\pi/(2L_j))^2\epsilon_j^0\epsilon_j^1$, then $\sigma_{k_j} = (2l-1)\pi/(2L_j)$ denotes a single root of (6.131) corresponding to a non–zero solution $\vartheta(z^j)$. Subsequently, this case is similarly excluded from the analysis. With this, the characteristic equation (6.131) can be re–written as

$$\tan(\bar{\sigma}_{k_j}) = \frac{\bar{\sigma}_{k_j}\left(\bar{p}_j^0\epsilon_j^1 + \bar{p}_j^1\epsilon_j^0\right)}{\bar{\sigma}_{k_j}^2\epsilon_j^0\epsilon_j^1 - \bar{p}_j^0\bar{p}_j^1}, \tag{6.132}$$

where $\bar{\sigma}_{k_j} = \sigma_{k_j}L_j$, $\bar{p}_j^0 = p_j^0 L_j$, and $\bar{p}_j^1 = p_j^1 L_j$. Obviously, no general closed–form analytical solution to (6.132) is available. Hence, except for a special case,

subsequently asymptotic results are determined by distinguishing three different configurations:

(i) $\bar{p}_j^0\epsilon_j^1+\bar{p}_j^1\epsilon_j^0=0$: Here, (6.132) reduces to $\tan(\bar{\sigma}_{k_j})=0$, which yields (6.127a)

(ii) $\bar{p}_j^0\epsilon_j^1+\bar{p}_j^1\epsilon_j^0\neq 0$ and $\epsilon_j^0\epsilon_j^1\neq 0$: For this case of Robin boundary conditions at both $z^j=0$ and $z^j=L_j$ an asymptotic solution can be determined for $\bar{\sigma}_{k_j}^2\epsilon_j^0\epsilon_j^1\gg\bar{p}_j^0\bar{p}_j^1$. Therefore, let $h(\bar{\sigma}_{k_j})=\bar{\sigma}_{k_j}(\bar{p}_j^0\epsilon_j^1+\bar{p}_j^1\epsilon_j^0)/(\bar{\sigma}_{k_j}^2\epsilon_j^0\epsilon_j^1-\bar{p}_j^0\bar{p}_j^1)$ such that given $\bar{p}_j^0\epsilon_j^1+\bar{p}_j^1\epsilon_j^0\neq 0$ for increasing $\bar{\sigma}_{k_j}^2\epsilon_j^0\epsilon_j^1>\bar{p}_j^0\bar{p}_j^1$ it follows that $h(\bar{\sigma}_{k_j})$ strictly monotonically approaches zero either from above if $\bar{p}_j^0\epsilon_j^1+\bar{p}_j^1\epsilon_j^0>0$ or from below if $\bar{p}_j^0\epsilon_j^1+\bar{p}_j^1\epsilon_j^0<0$. It is hence a standard procedure from asymptotic analysis to deduce that the roots of (6.132) approach the roots of $\sin(\bar{\sigma}_{k_j})=0$. Thus, $\sigma_{k_j}=\bar{\sigma}_{k_j}/L_j\sim k_j\pi/L_j$ for $k_j\in\mathbb{N}$, $k_j\gg 1$, where $\sim$ denotes that the quotient $\sigma_{k_j}/(k_j\pi/L_j)\to 1$ for increasing k_j. Depending on the sign of the term $\bar{p}_j^0\epsilon_j^1+\bar{p}_j^1\epsilon_j^0$, the asymptotics (6.127b) follow immediately.

(iii) $\bar{p}_j^0\epsilon_j^1+\bar{p}_j^1\epsilon_j^0\neq 0$ and $\epsilon_j^0\epsilon_j^1=0$: In this case of Dirichlet–Robin boundary conditions observe that (6.132) yields $\cot(\bar{\sigma}_{k_j})=-\bar{p}_j^0\bar{p}_j^1/[\bar{\sigma}_{k_j}(\bar{p}_j^0\epsilon_j^1+\bar{p}_j^1\epsilon_j^0)]$. Proceeding as above, the roots of this equation can be asymptotically determined as (6.127c).

Since $\mathfrak{A}$ is self–adjoint the eigenfunctions ϕ and ψ of $\mathfrak{A}$ and $\mathfrak{A}^*$, respectively, coincide. Moreover, $\langle\vartheta_{k_{j_1}},\vartheta_{k_{j_2}}\rangle_{L^2(0,L_j)}=\delta_{k_{j_1},k_{j_2}}$, k_{j_1}, $k_{j_2}\in\mathbb{N}$, the normalization coefficients F_{k_j} in (6.129) follow from the evaluation of $\langle\vartheta_{k_j},\vartheta_{k_j}\rangle_{L^2(0,L_j)}=1$ for σ_{k_j} satisfying the characteristic equation (6.131) or (6.132), respectively. This yields

$$F_{k_j}=\sqrt{\frac{4(\bar{p}_j^0)^2\bar{\sigma}_{k_j}}{L_j\left(\sin(2\bar{\sigma}_{k_j})\left[(\epsilon_j^0\bar{\sigma}_{k_j})^2-(\bar{p}_j^0)^2\right]+2\bar{\sigma}_{k_j}\left[\bar{p}_j^0(\bar{p}_j^0+\epsilon_j^0)+(\epsilon_j^0\bar{\sigma}_{k_j})^2-\epsilon_j^0\bar{p}_j^0\cos(2\bar{\sigma}_{k_j})\right]\right)}}. \tag{6.133}$$

Hence, in view of the determined exact and asymptotic solutions (6.127) for σ_{k_j} or $\bar{\sigma}_{k_j}$, respectively, (6.130) can be directly deduced. □

The separation approach for the solution of the eigenproblem directly illustrates that only simple eigenvalues occur for each individual Sturm–Liouville problem in the coordinate z^j, $j\in I_r$. Hence, it can be easily concluded that the algebraic and the geometric multiplicity of each eigenvalue λ_k governed by (6.126) coincide, which confirms Assumption 6.7 (i). Since each set $\{\vartheta_{k_j}\}_{k_j\in\mathbb{N}}$ represents an orthonormal basis for the space $L^2(0,L_j)$ the separation ansatz implies that ϕ_k as introduced in (6.128) denotes an orthonormal basis for X and hence a Riesz basis [1]. With this, Assumption 6.7 (ii) is fulfilled.

These preliminaries allow the determination of the Riesz spectral system representation. Differing from the general set–up multi–index notation is subsequently used in view of Lemma 6.4. Note first that the application of the adjoint operator $\mathfrak{B}^*$ as defined in (6.124) to the elements of the set $\{\phi_k\}_{k\in\mathbb{N}^r}$ results in

$$\mathfrak{B}^*\phi_k = \begin{cases} -\frac{1}{p_r^1}\varphi_{k_{(r|)}}\partial_{z^r}\vartheta_{k_r}|_{z^r=L_r}, & (B1) \\ -\frac{1}{p_r^1}\varphi_{k_{(r|)}}\left[b^1,\ldots,b^r\right]\partial_{z^r}\vartheta_{k_r}|_{z^r=L_r}, & (B2) \end{cases}$$

with

$$\varphi_{k_{(r|)}} = \varphi_{k_1,\ldots,k_{r-1}} = \prod_{j=1}^{r-1}\vartheta_{k_j}. \tag{6.134}$$

Herein, $\varphi_{k_{(r|)}}$ represents an orthonormal basis for $L^2(\partial\Omega_1)$ such that Assumption 6.3 is satisfied for the case $(B1)$. This in particular implies that the input $v(t)$ can be represented in terms of the Fourier series

$$v(t) = \sum_{k_{(r|)}\in\mathbb{N}^{r-1}} v_{k_{(r|)}}(t)\varphi_{k_{(r|)}}. \tag{6.135}$$

for all $v_{k_{(r|)}}(t) = \langle v, \varphi_{k_{(r|)}}\rangle_{L^2(\partial\Omega_1)} \in \ell^2_{k_{(r|)}}(0,\tau)$. Secondly, Theorem 6.3 yields that $\mathfrak{A}$ is a Riesz spectral operator whose spectral representation can determined in multi–index notation according to

$$\mathfrak{A}x = \sum_{k\in\mathbb{N}^r}\lambda_k\langle x,\phi_k\rangle_X\phi_k, \qquad x\in\mathcal{D}(\mathfrak{A}), \tag{6.136}$$

where

$$\mathcal{D}(\mathfrak{A}) = \left\{x\in X : \sum_{k\in\mathbb{N}^r}|\lambda_k|^2|\langle x,\phi_k\rangle_X|^2 < \infty\right\}. \tag{6.137}$$

Moreover, any $x(t)\in X$ can be represented in terms of the Fourier series

$$x(t) = \sum_{k\in\mathbb{N}^r}\langle x(t),\psi_k\rangle_X\phi_k. \tag{6.138}$$

By making use of the adjoint control operator (6.124) the Riesz spectral system representation of the boundary control system (6.123) according to (6.23), i.e. in the operational domain, can be evaluated using multi–index notation

$$\hat{x}_k(s) = \frac{1}{s-\lambda_k}b_{k_r}\hat{u}_{k_{(r|)}}(s). \tag{6.139a}$$

Here,

$$\hat{u}_{k_{(r|)}}(s) = \begin{cases} \hat{v}_{k_{(r|)}}(s), & (B1) \\ \sum_{l=1}^m b_k^l\hat{v}^l(s), & (B2) \end{cases} \tag{6.139b}$$

with $b_k^l = \langle b^l, \varphi_{k_{(r|)}}\rangle_{L^2(\partial\Omega_1)}/b_{k_r}$ and

$$b_{k_r} = -\frac{\partial_{z^r}\vartheta_{k_r}|_{z^r=L_r}}{p_r^1}. \tag{6.139c}$$

As pointed out during the general treatise, the ability to parametrize state and input in terms of a basic output essentially relies on the (approximate) controllability of the distributed–parameter system according to Assumptions 6.5 and 6.2 for $(B1)$ and $(B2)$, respectively.

Remark 6.13. Since $\mathfrak{A}$ is a Riesz spectral operator approximate controllability of Σ_∞ and Σ_m can be analyzed based on the spectral representation (6.139) by making use of [14, Theorem 4.2.1]:

(i) The system Σ_∞ is approximately controllable since $b_{k_r} \neq 0$ for all $k_r \in \mathbb{N}$. The latter follows immediately from the results on the eigenfunctions in Lemma 6.4. Moreover, consider (6.139a) for $k = (k_{(r|)}, k_r)$ with $k_{(r|)}$ fixed but arbitrary and k_r as the running index. Since λ_k satisfies (6.126) it can be easily deduced that each $k_{(r|)}$ subsystem actuated by $\hat{v}_{k_{(r|)}}(s)$ is approximately controllable, which for the Riesz spectral system Σ_∞ implies approximate controllability.

(ii) Let the algebraic multiplicity r_k^a of the eigenvalue λ_k equal its geometric multiplicity r_k^g and let $r^a = \sup_k r_k^a < \infty$. Then Σ_m is approximately controllable if $m \geq r^a$ and if the spatial characteristics $b^l(z)$, $l = 1, \ldots, m$, are such that

$$\operatorname{rk}\left(\left[\langle b^l, \partial_{z^r}\psi_{k^i}|_{z^r=L_r} \rangle_{L^2(\partial\Omega_1)} \right]_{\substack{l=1,\ldots,m \\ i=1,\ldots,r_k^a}} \right) = r_k^a. \tag{6.140}$$

for all $k \in \mathbb{N}^r$, where $(\psi_{k^i})_{i=1,\ldots,r_k^a}$ is the sequence of generalized eigenvectors to the eigenvalue λ_k. While the finiteness of the algebraic multiplicity and its equality with the geometric multiplicity can be verified for the considered set–up depending on the values of L_j, $j = 1, \ldots, r$, the rank condition (6.140) is assumed to hold subsequently.

Note that similar results are provided, e.g., in [3] for Dirichlet boundary control.

6.5.3.4 Formal State and Input Parametrization

Proceeding as in Section 6.5.2.3 directly reveals the state and input parametrizations in terms of a basic output.

Case (B1): Infinite–Dimensional Boundary Control

In the case of an infinite–dimensional input, (6.111) implies

$$\hat{x}_k(s) = -\frac{b_{k_r 0}}{\lambda_k}\hat{\mathcal{D}}^x_{k_{(r|)}}(s)\hat{\xi}_{k_{(r|)}}(s) \tag{6.141a}$$

$$\hat{v}_{k_{(r|)}}(s) = \hat{\mathcal{D}}^u_{k_{(r|)}}\hat{\xi}_{k_{(r|)}}(s) \tag{6.141b}$$

with the operators as defined in (6.45) re–written using multi–index notation

$$ {}^{0}\hat{\mathcal{D}}^{x}_{k_{(r|)}}(s) = e^{\mathcal{F}(\frac{s}{\lambda_k}, g^{s}_{k_{(r|)}})} \prod_{n \in \mathbb{N}\setminus\{k_r\}} \mathcal{G}\left(\frac{s}{\lambda_{k_{(r|)},n}}, g^{s}_{k_{(r|)}}\right) \tag{6.141c} $$

$$ \hat{\mathcal{D}}^{u}_{k_{(r|)}}(s) = \prod_{n \in \mathbb{N}} \mathcal{G}\left(\frac{s}{\lambda_{k_{(r|)},n}}, g^{s}_{k_{(r|)}}\right). \tag{6.141d} $$

Here, $\lambda_{k_{(r|)},n}$ is used to refer to λ_k with $k_r = n \in \mathbb{N}$ serving as the running index in the product. Moreover, recall that $g^{s}_{k_{(r|)}}$ is used to refer to the genus of the sequence $(s/\lambda_{k_{(r|)},n})_{n\in\mathbb{N}}$. In view of Assumption 6.4 this implies that the introduced index set, for which the projected components of the input coincide, satisfies $S^{l,1}_{q} = S^{1,1}_{q} = \mathbb{N}$. Furthermore, (6.49a) implies that the basic output $\xi(t) = \xi(\cdot, t) = \xi(z_{(r|)}, t)$ can be represented in terms of the Fourier series

$$ \xi(t) = \sum_{k_{(r|)} \in \mathbb{N}^{r-1}} \xi_{k_{(r|)}}(t) \varphi_{k_{(r|)}} \tag{6.142a} $$

with $\varphi_{k_{(r|)}}$ from (6.134) provided that

$$ \sum_{k_{(r|)} \in \mathbb{N}^{r-1}} |\langle \xi(t), \varphi_{k_{(r|)}} \rangle_{L^2(\partial\Omega_1)}|^2 < \infty \tag{6.142b} $$

given $t \in (0, \tau)$ for some $\tau > 0$.

Case (B2): Finite–Dimensional Boundary Control

For the case of a finite–dimensional boundary input it is necessary due to the incorporation of multi–index notation to introduce the two sets

$$ S_\lambda := \bigcap_{k \in \mathbb{N}^r} \{\lambda_k\}, \quad S := \{k \in \mathbb{N}^r : \lambda_k \in S_\lambda\}. \tag{6.143} $$

Obviously, S_λ denotes the set of all disjoint eigenvalues while S represents the corresponding multi–indexes. With these, (6.113) implies

$$ \hat{x}_k(s) = -\sum_{l=1}^{m} \frac{b^l_k}{\lambda_k} {}^{0}\hat{\mathcal{D}}^{x}_{k}(s) \hat{\xi}^l(s) \tag{6.144a} $$

$$ \hat{v}^l(s) = \mathcal{D}^{u}(s) \hat{\xi}^l(s) \tag{6.144b} $$

with the operators (6.32) re–written by making use of (6.143), i.e.

$$ {}^{0}\hat{\mathcal{D}}^{x}_{k}(s) = e^{\mathcal{F}(\frac{s}{\lambda_k}, g^{s})} \prod_{n \in S,\, \lambda_n \neq \lambda_k} \mathcal{G}\left(\frac{s}{\lambda_n}, g^{s}\right) \tag{6.144c} $$

$$\hat{\mathcal{D}}^u(s) = \prod_{n\in S} \mathcal{G}\left(\frac{s}{\lambda_n}, g^s\right). \tag{6.144d}$$

Note that given two different multi–indexes k, $k' \in \mathbb{N}^r$ such that $\lambda_k = \lambda_{k'}$, then the parametrizations of the spectral states $\hat{x}_k(s)$ and $\hat{x}_{k'}(s)$ differ in the coefficients b_k^l due to the rank condition (6.140). Moreover, observe that the main distinction between the formal state and input parametrizations (6.141) and (6.144) is given by the number of elements considered in the Weierstrass canonical products. As pointed out in Remark 6.13, the formal parametrizations (6.141) are evaluated over $\mathbb{N}$ due to the separation of the spectral representation in the case $(B1)$ of an infinite–dimensional control. Since this separation is not valid in the case $(B2)$ of a finite–dimensional control, the resulting formal parametrizations (6.144) have to be evaluated over $S \subseteq \mathbb{N}^r$. This distinction is however crucial for the convergence analysis.

6.5.3.5 Convergence of the Parametrized Fourier Series

In order to ensure the convergence of the parametrizations it is necessary to determine the order and the type of the operator $\hat{\mathcal{D}}^u_{k_{(r|)}}(s)$ for the case $(B1)$ and $\mathcal{D}^u(s)$ for the case $(B2)$.

Case (B1): Infinite–Dimensional Boundary Control

For the analysis of the convergence in the case $(B1)$ it is decisive to observe that (6.126) yields a separation of the eigenvalues according to

$$\lambda_k = \lambda_{k_{(r|)}} + \tilde{\lambda}_{k_r} \tag{6.145}$$

with $\mathbb{R} \ni \lambda_{k_{(r|)}} = c - \sum_{j=1}^{r-1} \sigma^2_{k_j}$ and $\mathbb{R} \ni \tilde{\lambda}_{k_r} = -\sigma^2_{k_r}$. Equation (6.145) hence implies that the order and type of $\hat{\mathcal{D}}^u_{k_{(r|)}}(s)$ are for each fixed but arbitrary multi–index $k_{(r|)} \in \mathbb{N}^{r-1}$ only determined by the sequence $(\tilde{\lambda}_{k_r})_{k_r\in\mathbb{N}}$. Since, the latter is equivalent to the spatially 1–dimensional setting due to the separation utilized for the proof of Lemma 6.4, Proposition 6.2 yields $g^s_{k_{(r|)}} = 0$. With this, Proposition 6.3 provides the order $\varrho_{k_{(r|)}} = 1/2$ while Proposition 6.4 confirms that the type $\tau_{k_{(r|)}}$ is finite.

Remark 6.14. The type of $\hat{\mathcal{D}}^u_{k_{(r|)}}(s)$ can be explicitly computed as

$$\tau_{k_{(r|)}} = \begin{cases} L_r, & \text{if } \left(p^0_r\epsilon^1_r + p^1_r\epsilon^0_r = 0\right) \vee \left(p^0_r\epsilon^1_r + p^1_r\epsilon^0_r \neq 0 \wedge \epsilon^0_r\epsilon^1_r \neq 0\right) \\ \frac{L_r}{2}, & \text{if } \left(p^0_r\epsilon^1_r + p^1_r\epsilon^0_r \neq 0\right) \wedge \left(\epsilon^0_r\epsilon^1_r = 0\right) \end{cases}$$

by making use of the determined asymptotics (6.127). For this, recall from (B.7) that the type $\tau_{k_{(r|)}}$ of $\hat{\mathcal{D}}^u_{k_{(r|)}}(s)$ can be determined by the formula

$$\tau_{k_{(r|)}} = \limsup_{\eta\to\infty} \frac{\log M(\eta)}{\eta^{\varrho_{k_{(r|)}}}},$$

where $M(\eta)$ denotes the maximal modulus of $\hat{\mathcal{D}}^u_{k_{(r|)}}(s)$ (cf. (B.6)). In view of the infinite product representation with genus $g^s_{k_{(r|)}} = 0$ it follows that

$$M(\eta) = \begin{cases} \hat{\mathcal{D}}^u_{k_{(r|)}}(\eta), & \text{if } \lambda_{k_{(r|)}} + \tilde{\lambda}_{k_r} < 0,\ \forall k_r \in \mathbb{N} \\ \displaystyle\prod_{k_r=1}^{N} \left(1 + \frac{\eta}{\lambda_{k_{(r|)}} + \tilde{\lambda}_{k_r}}\right) \times & \text{if } \lambda_{k_{(r|)}} + \tilde{\lambda}_{k_r} > 0 \text{ for} \\ \displaystyle\prod_{k_r=N+1}^{\infty} \left(1 - \frac{\eta}{\lambda_{k_{(r|)}} + \tilde{\lambda}_{k_r}}\right), & k_r \in \{1,\dots,N\} \text{ while} \\ & \lambda_{k_{(r|)}} + \tilde{\lambda}_{k_r} < 0,\ k_r > N. \end{cases} \tag{6.146}$$

Since $\lambda_{k_{(r|)}} \leq \bar{\theta}$ is bounded from above and since $\tilde{\lambda}_{k_r} = -\sigma^2_{k_r} < 0$, for the evaluation of the limit as $\eta \to \infty$ it is sufficient to consider $M(\eta) = \hat{\mathcal{D}}^u_{k_{(r|)}}(\eta)$ for both cases, i.e. $\lambda_{k_{(r|)}} + \tilde{\lambda}_{k_r} < 0$, $\forall k_r \in \mathbb{N}$ and $\lambda_{k_{(r|)}} + \tilde{\lambda}_{k_r} > 0$, $k_r \in \{1,\dots,N\}$ while $\lambda_{k_{(r|)}} + \tilde{\lambda}_{k_r} < 0$, $k_r > N$. Hence, utilizing the determined asymptotics (6.127) for the zeros of $\hat{\mathcal{D}}^u_{k_{(r|)}}(s)$ implies that

$$M(\eta) \sim \begin{cases} \sqrt{\dfrac{\lambda_{k_{(r|)}}}{(\lambda_{k_{(r|)}} + \eta)}} \dfrac{\sinh\big(L_r\sqrt{\lambda_{k_{(r|)}} + \eta}\big)}{\sinh\big(L_r\sqrt{\lambda_{k_{(r|)}}}\big)}, & \text{if } \big(p^0_r\epsilon^1_r + p^1_r\epsilon^0_r = 0\big) \vee \\ & \big(p^0_r\epsilon^1_r + p^1_r\epsilon^0_r \neq 0 \wedge \epsilon^0_r\epsilon^1_r \neq 0\big) \\ \dfrac{\cosh\big(\frac{L_r}{2}\sqrt{\lambda_{k_{(r|)}} + \eta}\big)}{\cosh\big(\frac{L_r}{2}\sqrt{\lambda_{k_{(r|)}}}\big)}, & \text{if } \big(p^0_r\epsilon^1_r + p^1_r\epsilon^0_r \neq 0\big) \wedge \\ & \big(\epsilon^0_r\epsilon^1_r = 0\big) \end{cases}$$

for sufficiently large η. Taking the limit as $\eta \to \infty$ yields $\tau_{k_{(r|)}} = L_r$ or $\tau_{k_{(r|)}} = L_r/2$, respectively.

As a result, the convergence of the parametrizations can be immediately concluded from Theorem 6.6 such that the proof is omitted subsequently.

Proposition 6.5. *If* $\xi_{k_{(r|)}}(t) \in G_{D_{k_{(r|)}},\alpha_{k_{(r|)}}}(\mathbb{R})$ *with* $\alpha_{k_{(r|)}} < 2$ *and if in addition* $(D_{k_{(r|)}})_{k_{(r|)}\in\mathbb{N}^{r-1}} \in \ell^2$*, then the state and input parametrizations* (6.141) *with* (6.138) *and* (6.135) *converge uniformly.*

Remark 6.15. Note that the determined convergence results are fully consistent with the available results for the 1–dimensional case, i.e. $r = 1$, where typically power series are utilized for the determination of the state and input parametrizations (see, e.g., [32, 53, 39, 43]).

Case (B2): Finite–Dimensional Boundary Control

Given the finite–dimensional boundary control, $\hat{\mathcal{D}}^u(s)$ is evaluated over the index set $S \subseteq \mathbb{N}^r$. Hence, Proposition 6.3 applies, which provides a lower and upper bound for the order of the Weierstrass canonical product $\hat{\mathcal{D}}^u(s)$. In addition, the following restriction arises, which refers to the type of $\hat{\mathcal{D}}^u(s)$ being maximal.

Remark 6.16. Since the type of the entire function $\hat{\mathcal{D}}^u(s)$ is maximal for even dimensions r there do not exist finite positive constants A, B such that $|\hat{\mathcal{D}}^u(s)| < A\exp(B|s|^{r/2})$ [34]. However, the validity of this inequality is essential for the operational convergence analysis. Hence, this case has to be excluded from the subsequent analysis for the case of finite–dimensional boundary control.

With these preliminaries, the convergence of the state and input parametrizations in the case $(B2)$ can be deduced from Corollaries 6.3 and 6.4.

Proposition 6.6. *Let r be odd. If $\xi^l(t) \in G_{D^l,\alpha^l}(\mathbb{R})$ with $\alpha^l < 2/r$ and $(b_k^l)_{k\in\mathbb{N}^r} \in \ell^2$ for all $l = 1,\dots,m$, then the state parametrization* (6.138) *with* (6.144a) *and the input parametrization* (6.144b) *converge uniformly.*

Summary

In view of the results determined above, the state and input parametrizations in terms of the basic output for the two boundary control configurations Σ_∞ and Σ_m can be summarized as

$$\Sigma_\infty: \quad x(t) = \sum_{k\in\mathbb{N}^r} x_k(\xi_{k_{(r|)}}(t))\phi_k \tag{6.147}$$

$$v(t) = \sum_{k_{(r|)}\in\mathbb{N}^{r-1}} v_{k_{(r|)}}(\xi_{k_{(r|)}}(t))\varphi_{k_{(r|)}} \tag{6.148}$$

$$\Sigma_m: \quad x(t) = \sum_{k\in\mathbb{N}^r} x_k(\boldsymbol{\xi}(t))\phi_k \tag{6.149}$$

$$v^l(t) = \hat{\mathcal{D}}^u(\partial_t)\circ\xi^l(t) \tag{6.150}$$

with the parametrized Fourier coefficients from (6.141) and (6.144) given in the time–domain by

$$\Sigma_\infty: \quad x_k(\xi_{k_{(r|)}}(t)) = {}^0\hat{\mathcal{D}}^x_{k_{(r|)}}(\partial_t)\circ\xi_{k_{(r|)}}(t)$$

$$v_{k_{(r|)}}(\xi_{k_{(r|)}}(t)) = \hat{\mathcal{D}}^u_{k_{(r|)}}(\partial_t)\circ\xi_{k_{(r|)}}(t)$$

$$\Sigma_m: \quad x_k(\boldsymbol{\xi}(t)) = -\sum_{l=1}^{m}\frac{b_k^l}{\lambda_k}{}^0\hat{\mathcal{D}}^x_k(\partial_t)\circ\xi^l(t),$$

where $\boldsymbol{\xi}(t) = [\xi^1(t),\dots\xi^m(t)]^T$. These expressions serve as the basis for the solution of the considered trajectory planning problem by assigning suitable trajectories

for the basic output towards the determination of feedforward tracking controls for the two boundary control configurations.

6.5.3.6 Constructive Approach to Steady State and Approximate Controllability Analysis

With these results, an explicit solution to the trajectory planning problem can be at least formally determined in a systematic manner. In addition, the presented approach provides a constructive proof of controllability since the feedforward control necessary to reach a desired (admissible) final profile along a prescribed spatial–temporal path starting from a given initial condition is directly obtained.

For this, note that the flatness–based state and input parametrizations (6.147) and (6.148) for the case $(B1)$ by construction represent exact solutions of the respective controllability moment problems (see, e.g., [54, 19]) assuming that the initial and the final profile are stationary. This in particular also confirms the steady state controllability of the considered problem in the sense of [11]. Moreover, the parametrizations for $(B1)$ immediately allow to achieve any spatial–temporal path $x^*(t)$, which can be expressed in terms of basic output trajectories $\xi^*(t)$ ensuring convergence of the Fourier series according to Proposition 6.5. This illustrates the close relationship between (steady state and approximate) controllability and the existence of a basic output, which is well–known for finite–dimensional linear systems. If $r = 1$ it is shown in [32] that this relation holds also for approximate controllability by considering finite time transitions between non–stationary initial and final states. However, for $r > 1$ the general verification of this property is still an open problem.

These results hold at least formally for the case $(B2)$ of a finite–dimensional control, where, as shown above, the determined parametrizations (6.144) might diverge depending on the particular trajectory planning problem and the necessary Gevrey order of the basic output. However, it is shown subsequently that this still allows to compute applicable feedforward controls by incorporating suitable summation techniques towards an approximate solution of the trajectory planning problem. Moreover, the results of Proposition 6.6 yield that any spatial–temporal path $x^*(t)$ can be realized, which is parametrizable in terms of basic output trajectories $\boldsymbol{\xi}^*(t)$ of Gevrey order $\alpha \leq 1/\varrho = 2/r$ for odd dimensions r.

6.5.3.7 Finite time Transition between Stationary Profiles

In the following, the theoretical results of the previous sections are illustrated in simulation scenarios for a cuboid with $r = 3$ and $L_j = 1$, $j = 1, 2, 3$. For this, the diffusion–reaction system (6.123) is discretized with respect to time and space using an implicit and absolutely stable Crank–Nicholson approach. The system parameters are thereby chosen as $c = -10$, $p_j^0 = p_j^1 = 1$, $\epsilon_j^0 = \epsilon_j^1 = 0$ for $j = 1, 2, 3$, i.e. Dirichlet boundary conditions with Dirichlet input. However, Robin

boundary conditions and combinations of Dirichlet and Robin boundary conditions can be considered similarly.

The realization of a finite time transition starting at the initial state $x_0(z) = 0$, $z \in \overline{\Omega}$, to reach a stationary final state $x_T(z)$, $z \in \overline{\Omega}$, for $t \geq T$ with $T = 0.1$ along a prescribed spatial–temporal path is considered following the indirect trajectory planning approach introduced in Section 6.4.1.2. Thereby the final stationary profile is imposed indirectly by prescribing the profile[12]

$$x_T(z)|_{\varpi(z)=0} = \min\{z^1, z^2, L_1 - z^1, L_2 - z^2\} \tag{6.151}$$

on the interior surface $\varpi(z) = z^3 - L_3/2$ of the parallelepipedon Ω.

Case (B1): Infinite–Dimensional Boundary Control

For the solution of the trajectory planning problem the least squares problem (6.75) is solved, which in terms of the considered multi–index notation reads as

$$\min_{\{\xi_{s,k_{(3|)}}\}_{k_{(3|)}\in\mathbb{N}^2}} \left\| x_s(z; v_s(z_{(3|)}; \xi_{s,k_{(3|)}}))|_{\varpi(z)=0} - x_T(z)|_{\varpi(z)=0} \right\|_X^2$$

subject to

$$\begin{aligned}
&(\Delta + c)x_s = 0, && z \in \Omega \\
&\epsilon_j^0 \partial_{z^j} x_s - p_j^0 x_s = 0, && z^j = 0,\ j \in I_r \\
&\epsilon_j^1 \partial_{z^j} x_s + p_j^1 x_s = 0, && z^j = L_j,\ j \in I_r^3 \\
&\epsilon_r^1 \partial_{z^r} x_s + p_r^1 x_s = v_s(z_{(3|)}; \xi_{s,k_{(3|)}}), && z^3 = L_3.
\end{aligned}$$

With this, a solution for the Fourier coefficients $\{\xi_{k_{(3|)}}\}_{k_{(3|)}\in\mathbb{N}^2}$ is obtained in the sense that the solution $x_s = x_s(z; v_s(z_{(3|)}; \xi_{k_{(3|)}}))|_{\varpi(z)=0}$ corresponds to an L^2–approximation of $x_T|_{\varpi(z)=0}$. The resulting profile for $\xi_{k_{(3|)}}$ with $k_{(3|)} \leq (6, 6)$ is shown in Figure 6.4 providing a comparison of $x_T|_{\varpi(z)=0}$ (left) and $x_s|_{\varpi(z)=0}$ (right). Since only a finite number of Fourier coefficients is computable a smoothing of the edges and a small loss of amplitude can be observed, which results in an L^2–error of $\|x_s|_{\varpi(z)=0} - x_T|_{\varpi(z)=0}\|_{L^2(\Omega_\varpi)} = 0.004$ with $\Omega_\varpi = \Omega|_{\varpi(z)=0}$.

In view of these considerations, the spatial–temporal transition path $\xi^*(t) = \xi^*(z_{(3|)}, t)$ for the basic output connecting x_0 and $x_T|_{\varpi(z)=0} = x_s|_{\varpi(z)=0}$ is chosen according to (6.69), which yields using multi–index notation

$$\xi^*(t) = \sum_{k_{(3|)}\in\mathbb{N}^2} \xi_{s,k_{(3|)}} \mathcal{g}_{T,\omega}(t) \varphi_{k_{(3|)}}. \tag{6.152}$$

[12] This set–up partly introduces a 3–dimensional analogon to the finite time transition problem considered within an optimal control setting in [9], where the input $u_{\partial\Omega}(z, t)$ is assumed to act on the complete boundary $\partial\Omega$ of Ω.

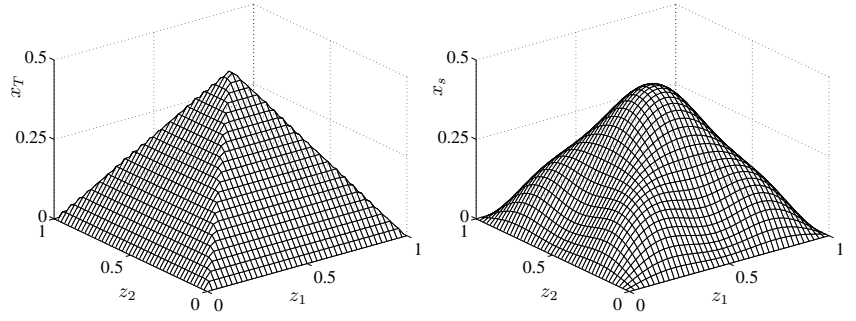

Fig. 6.4 Desired profile (left) determined by (6.151) and its L^2–approximation (right) obtained by solving (6.75)

Here, $g_{T,\omega}(t)$ represents the Gevrey function defined in (B.3) with $\omega = 2$, i.e. $g_{T,\omega}(t)$ is of Gevrey order $\alpha = 3/2$. Note that in particular the transition time $T > 0$ can be freely assigned with small values of T resulting in larger input amplitudes during the transition phase. With this, the corresponding feedforward control $u_{\partial\Omega}(t) = v^*(z_{(3|)}, t)$ follows directly from the evaluation of (6.135) with the Fourier coefficients parametrized in terms of (6.141b).

Simulation results for this scenario are provided in Figure 6.5, where the boundary input $u_{\partial\Omega}(t)$ and the local state profile $x(t)|_{\varpi(z)=0}$ are shown for different instances of time $t \in \{0, 0.02, 0.03, 0.042, 0.053, 0.1\}$. In order to achieve the desired transition within $t \in [0, 0.1]$ a rather non–trivial behaviour of the input is required, which due to the chosen transition time T and trajectory parameter ω yields a rise of $x(t)|_{\varpi(z)=0}$ over the maximal amplitude of the final profile in the initial transition phase (cf. Figure 6.5(d) for $t = 0.042$). For further clarification consider Figure 6.6, where $x(t)|_{\varpi(z)=0}$ evaluated at the center $(z^1, z^2) = (1/2, 1/2)$ is depicted over time t with the markers corresponding to the snapshots of Figure 6.5. Due to the symmetry of the desired final profile (cf. Figure 6.4 (right)) this trajectory describes the evolution of the peak of $x(t)|_{\varpi(z)=0}$. Hence, a highly dynamic behavior is obtained during the transition with an accurate realization of the final profile with an L^2–error $\|x(T)|_{\varpi(z)=0} - x_s|_{\varpi(z)=0}\|_{L^2(\Omega_\varpi)} = 9.736 \times 10^{-4}$. Note that by re–planning $\xi^*(t)$, i.e. in view of (6.152) adjusting T and ω, different spatial–temporal transition paths can be achieved in view of the solution of the trajectory planning problem.

Case (B2): Finite–Dimensional Boundary Control

While the assignment of the basic output trajectory (6.152) with Gevrey order restricted to the interval $\alpha \in (1, 2]$ in the case $(B1)$ of an infinite–dimensional control results in convergent state and input parametrizations it is revealed in Section 6.4 that the corresponding parametrizations in the case $(B2)$ of a finite–dimensional control are inherently divergent for the realization of finite time transitions between

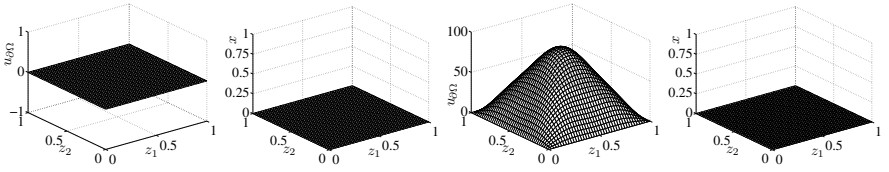

(a) $t = 0$ (b) $t = 0.02$

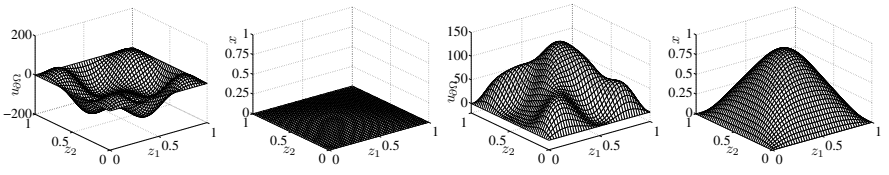

(c) $t = 0.03$ (d) $t = 0.042$

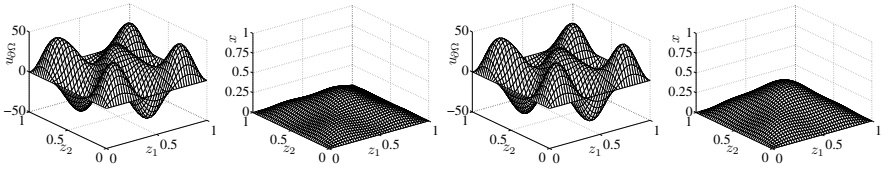

(e) $t = 0.053$ (f) $t = 0.1$

Fig. 6.5 Feedforward control $u_{\partial\Omega}(t)$ and simulated profile $x(t)|_{\varpi(z)=0}$ at different instances of time $t \in \{0, 0.02, 0.03, 0.042, 0.053, 0.1\}$ for the (approximate) realization of the desired final profile (6.151) in the case $(B1)$.

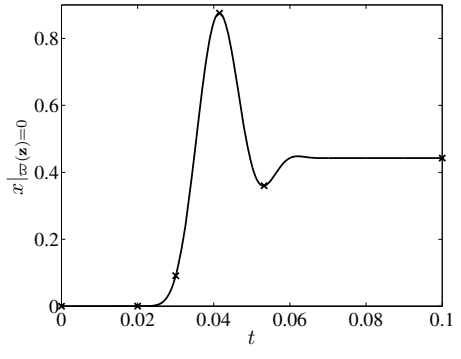

Fig. 6.6 Simulated profile $x(t)|_{\varpi(z)=0}$ evaluated at the center $(z^1, z^2) = (1/2, 1/2)$ in the case $(B1)$

stationary profiles. However, it is shown in [32] by making use of least–term summation as well as [67, 42, 39, 43] by considering more general summability techniques for power series that divergent parametrizations still allow to extract meaningful results, which can be used to solve the trajectory planning problem.

Feedforward control using (N,ξ)–approximate k–summation

In order to evaluate the parametrizations (6.149) and (6.150) for finite–dimensional boundary control, it is necessary to analyze the Weierstrass canonical products ${}^0\hat{\mathcal{D}}_k^x(s)$ and $\hat{\mathcal{D}}^u(s)$ as defined in (6.144c) and (6.144d). Note that subsequently only the results for the input parametrization are provided, which allow an easy deduction of the respective results for the state parametrization. Since ${}^0\hat{\mathcal{D}}_k^x(s)$ and $\hat{\mathcal{D}}^u(s)$ are entire functions of finite order ϱ^l by Proposition 6.3 they admit a MacLaurin series expansion, i.e.

$$\hat{\mathcal{D}}^u(s) = \sum_{j=0}^{\infty} c_j s^j,$$

which converges for all $s \in \mathbb{C}$ [34]. With s denoting the operational equivalent to time differentiation, this yields

$$v^l(\xi^l(t)) = \hat{\mathcal{D}}^u(\partial_t) \circ \xi^l(t) = \sum_{j=0}^{\infty} c_j \partial_t^j \xi^l(t). \tag{6.153}$$

Hence, the input parametrization (6.150) can be alternatively evaluated in terms of a formal series. With the considerations in Section 6.4.1, this series diverges if $\xi^l(t)$ is assigned to realize a finite time transition between stationary states. Moreover, the practical evaluation of (6.153) requires to truncate the series after finite number of addends.

However, following [67, 42, 39, 43] the application of suitable summability techniques still allows to extract a meaningful input trajectory from a finite number of series coefficient of the in general diverging series. Herein, given a power series

$$f(z) = \sum_{j=0}^{\infty} a_j z^j$$

the so–called (N,ξ)–approximate k–summation

$$\left(\mathcal{S}_k^{N,\xi} f\right)(z) = \frac{\sum_{j=0}^{N} s_j(z) \frac{\xi^j}{\Gamma\left(1+\frac{j}{k}\right)}}{\sum_{j=0}^{N} \frac{\xi^j}{\Gamma\left(1+\frac{j}{k}\right)}}, \quad s_j(z) = \sum_{i=0}^{j} a_i z^i \tag{6.154}$$

with $\Gamma(\cdot)$ denoting the Gamma function was introduced and analyzed to approximate the limit of certain slowly converging or even diverging power series $f(z)$ from a finite number of series coefficients $\{a_j\}_{j=0,\ldots,N}$. The summation parameters k and ξ serve as degrees–of–freedom, which have to be chosen appropriately to improve the summation result. For a detailed discussion of the deduction of $\mathcal{S}_k^{N,\xi}$ from the so–called k–summation as considered, e.g., in [47, 4, 5], its properties, and approaches for the determination of the summation parameters k and ξ the interested reader is referred to [39, 42, 43].

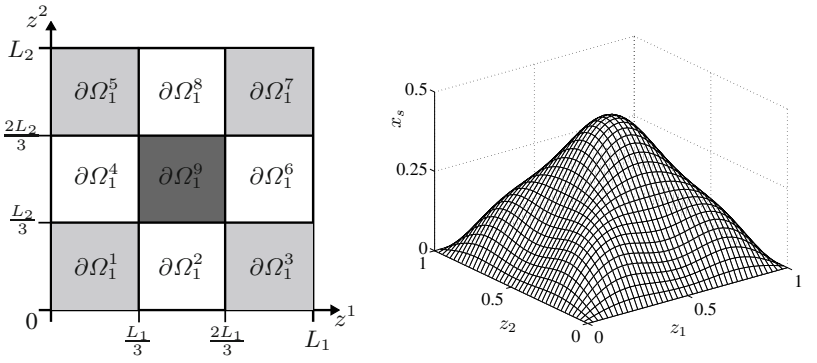

Fig. 6.7 Actuator configuration (left) and resulting L^2–approximation from (6.78) (right) for the profile (6.151) in the case $(B2)$

Hence, subsequently (6.154) is utilized to evaluate the in general diverging series (6.153) such that

$$v^{*,l}(\xi^{*,l}(t)) = \frac{\sum_{j=0}^{N} s_j^*(t)\frac{\xi^j}{\Gamma(1+\frac{j}{\kappa})}}{\sum_{j=0}^{N}\frac{\xi^j}{\Gamma(1+\frac{j}{\kappa})}}, \quad s_j^*(t) = \sum_{i=0}^{j} c_i \partial_t^j \xi^{*,l}(t) \tag{6.155}$$

with the desired trajectory (6.72) is used for the determination of the feedforward tracking control in the case $(B2)$ of a finite–dimensional boundary control.

Numerical results

In order to illustrate the application of (6.155) the actuator configuration depicted in Figure 6.7 (left) is considered, where the plane $z_{(3|)} \in \partial\Omega_1$ is covered with 9 patch actuators. These are a bundled into 3 color–coded spatial input characteristics

$$b^l = \begin{cases} 1, & z_{(3|)} \in \bigcup_{i=0}^{3} \partial\Omega_1^{2i+l} \\ 0, & \text{else} \end{cases}, \quad l = 1,2, \qquad b^3 = \begin{cases} 1, & z_{(3|)} \in \partial\Omega_1^9 \\ 0, & \text{else} \end{cases}$$

with each driven by an input signal $v^l(t)$, $l = 1,2,3$. Similar to the scenario considered for $(B1)$, the indirect trajectory planning approach introduced in Section 6.4.1.2 is applied by solving the least–squares problem (6.78) for $\boldsymbol{\xi}_s$. The resulting smoothed L^2–approximation $x_s = x_s\big(z; v_s(\boldsymbol{\xi}_s)\big)$ with the error $\|x_s|_{\varpi(z)=0} - x_T|_{\varpi(z)=0}\|_{L^2(\Omega_\varpi)} = 0.005$ is shown in Figure 6.7 (right).

In order to connect the initial and final state the desired trajectory $\xi^{*,l}(t)$ according to (6.72) with $\xi_T^{*,l} = \xi_s^l$, $T = 0.1$, and $\omega^l = 2$ for $l = 1,2,3$, is assigned for the basic output $\xi^l(t)$. Hence, $\xi^{*,l}(t)$ is of Gevrey order $\alpha^l = 3/2$. Due to the divergence of the parametrizations the corresponding feedforward controls $v^l(t) = v^{*,l}(\xi^{*,l}(t))$ are determined from (6.155) by making use of the

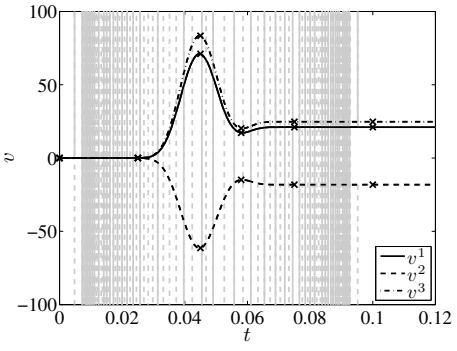

Fig. 6.8 Feedforward controls $v^{*,l}(\xi^{*,l}(t))$, $l = 1, 2, 3$ (black) for the case $(B2)$ obtained from (6.155) in comparison to respective trajectories from the evaluation of the sum (6.153) (gray). The markers correspond the snapshots depicted in Figure 6.9.

(N, ξ)–approximate k–summation. For the following numerical results $N = 71$, which corresponds to the upper limit of derivatives of $\xi^{*,l}(t)$ in the evaluation of $v^{*,l}(\xi^{*,l}(t))$ computable in double precision. The determination of the summation parameter k is motivated by the Gevrey order of $\xi^{*,l}(t)$, which determines the growth of $v^{*,l}(\xi^{*,l}(t))$, such that $k = 3/2$. Moreover, numerical experiments by evaluating (6.155) for N and k fixed with ξ varying motivate the choice of $\xi = 0.145$ for the remaining summation parameter. The resulting input trajectories $v^{*,l}(\xi^{*,l}(t))$, $l = 1, 2, 3$, are depicted in Figure 6.8 in comparison to the respective results obtained from a direct evaluation of the sum (6.153) with $\xi^{*,l}(t)$ substituted for $\xi^l(t)$. The implications of this result are twofold. At first, the application of the (N, ξ)–approximate k–summation obviously allows to extract meaningful input trajectories from the diverging series. Secondly, the feedforward controls involve significant variations in amplitude to realize the desired transition within the time interval $t \in [0, 0.1]$ revealing the transition dynamics.

Simulation results for the application of the feedforward control are provided in Figure 6.9, where the boundary control $u_{\partial\Omega}(t) = \sum_{l=1}^{3} b^l v^{*,l}(\xi^{*,l}(t))$ and the local state profile $x(t)|_{\varpi(z)=0}$ are shown for $t \in \{0, 0.025, 0.045, 0.058, 0.075, 0.1\}$. The temporal snapshots are chosen to cover different transition phases involving both the maximal ($t = 0.045$) and the minimal ($t = 0.058$) input amplitudes within the interval $t \in (0, 0.1)$ (cf. also the markers in Figure 6.8). The deviation between the obtained and desired final state can be quantified in terms of the L^2–error $\|x_s|_{\varpi(z)=0} - x(T)|_{\varpi(z)=0}\|_{L^2(\Omega_\varpi)} = 1.641 \times 10^{-3}$, which is of a magnitude comparable to the error obtained for the infinite–dimensional boundary control. The corresponding transition path for $x(t)|_{\varpi(z)=0}$ evaluated at $(z^1, z^2) = (1/2, 1/2)$ is shown in Figure 6.10 and confirms the realization of the prescribed finite time transition between stationary profiles.

Note that differing from the scenario for the case $(B1)$ no overshoot occurs for $x(t)|_{\varpi(z)=0}$ although both the Gevrey order in the desired trajectory for the basic output and the transition time coincide. This is in particular a result of the boundary

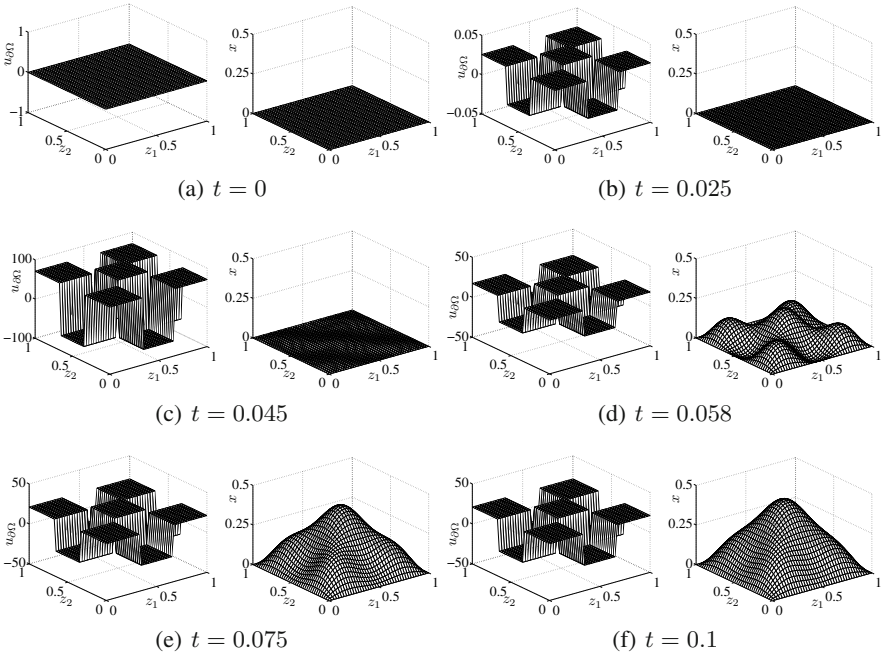

(a) $t = 0$ (b) $t = 0.025$

(c) $t = 0.045$ (d) $t = 0.058$

(e) $t = 0.075$ (f) $t = 0.1$

Fig. 6.9 Feedforward control $u_{\partial\Omega}(t)$ and simulated profile $x(t)|_{\varpi(z)=0}$ at different instances of time $t \in \{0, 0.025, 0.045, 0.058, 0.075, 0.1\}$ for the (approximate) realization of the desired final profile (6.151) in the case $(B2)$

control configuration with a finite number of spatially localized actuators. Nevertheless, these numerical results clearly confirm the applicability of the proposed approach also for the case of a finite–dimensional boundary control, where the inherent divergence of the parametrizations can be addressed by including suitable summation techniques into the solution of the trajectory planning problem.

6.5.3.8 Finite Time Transition between Arbitrary Profiles

Finally, simulation results are presented for the case $(B1)$ of an infinite–dimensional boundary control to realize a finite time transition within $t \in [0, T]$ with $T = 1$ starting at the initial state $x_0(z) = 0$, $z \in \overline{\Omega}$ to reach an ϵ–neighborhood of the non–stationary final profile $x_T(z)$ at $t = T$ depicted in Figure 6.11 (left). Thereby, $x_T(z)$ is given as

$$x_T = \begin{cases} 1, & z \in \Xi\big((\frac{1}{4}, \frac{1}{4}, \frac{1}{4}), \frac{1}{5}\big) \\ -1, & z \in \Xi\big((\frac{3}{4}, \frac{3}{4}, \frac{3}{4}), \frac{1}{5}\big) \\ 0, & \text{else}, \end{cases} \tag{6.156}$$

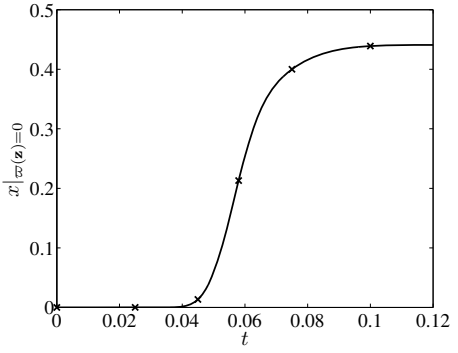

Fig. 6.10 Simulated profile $x(t)|_{\varpi(z)=0}$ evaluated at the center $(z^1, z^2) = (1/2, 1/2)$ in the case $(B2)$

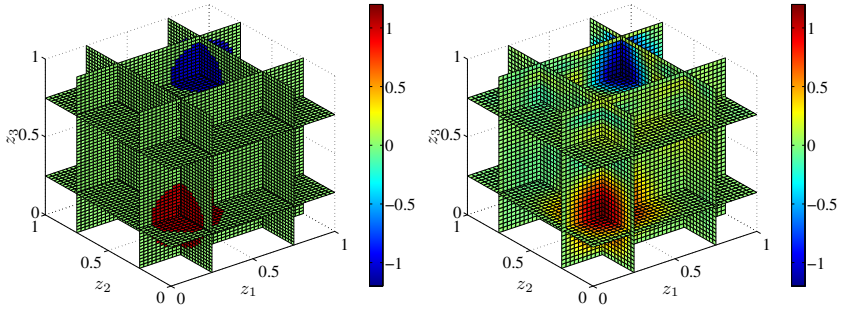

Fig. 6.11 Desired profile $x^*(t)$ (left) and obtained profile $x(t)$ (right) at $t = 1$

with $\Xi(\zeta, R) = \{z \in \Omega : \sum_{j=1}^{3}(z^j - \zeta^j)^2 \leq R^2\}$ denoting the sphere of radius R centered at ζ. Proceeding as proposed in Section 6.4.2, the desired profile (6.156) is projected onto a finite number $k = (6, 6, 40)$ of Fourier coefficients, which are required for the numerical solution of the constrained least–squares problem (6.84) or (6.86a) and (6.86b), respectively. This yields the coefficients $f_{q,i}^{j,l}$ or respectively $f_{k_{(3|)},i}^{j,l}$ in multi–index notation of the desired trajectory (6.81) for the Fourier coefficients $\xi_q^{*,1}$ or $\xi_{k_{(3|)}}^{*,1}$ of the basic output and hence the corresponding spatial–temporal path $\xi^*(z_{(3|)}, t)$ according to (6.70). Subsequently, the function (B.3) is used for $\mathscr{g}_{T_q^l,\omega_q^l}(t) = \mathscr{g}_{T,\omega}(t)$ with $\omega = 2$ chosen for the numerical evaluation of (6.81). By evaluating the input parametrization the respective feedforward control $u_{\partial\Omega}^*(z_{(3|)}, t)$ is obtained as shown in Figure 6.12 for different instances of time $t \in \{0, 1/3, 2/3, 1\}$. Here, rather large variations in both the input amplitude and its spatial distribution can be observed before reaching the final input profile at $t = T$. However, the simulation results indicate that such an input behavior is required to achieve the desired transition along the spatial–temporal transition path determined by $\xi^*(z_{(3|)}, t)$. This is confirmed in Figure 6.11 (right), where a snapshot of the

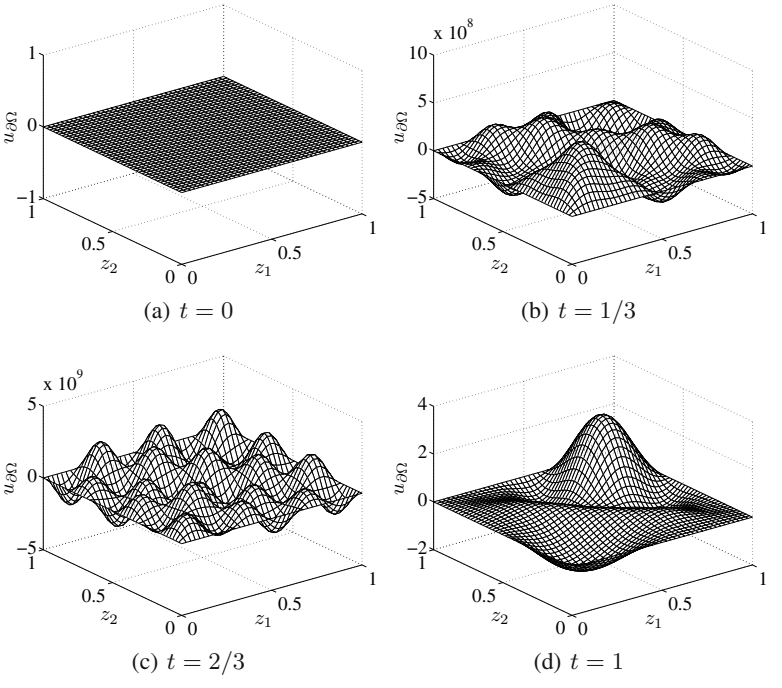

Fig. 6.12 Snapshots of the input $u_{\partial\Omega}(t)$ at different instances of time $t \in \{0, 1/3, 2/3, 1\}$ for the realization of the finite time transition with the final profile depicted in Figure 6.11 (right)

simulated profile $x(z,t)$ due to $u^*_{\partial\Omega}(z_{(3|)}, t)$ is shown at $t = T$. Obviously, a rather accurate tracking is obtained for this rather complicated desired non–stationary profile with only a minor smoothing of the two spheres of positive and negative values of $x(t)$. Due to this smoothing and the non–zero input profile at $t = T$ on the boundary $z^3 = L_3$ (cf. Figure 6.12(d)), only a transition into an ϵ–neighborhood (in an L^2–sense) of x_T can be realized. Of course, it has to be pointed out that the profile $x(T)$ is not holdable for $t > T$. Nevertheless, these results clearly confirm the principle applicability and potential of the proposed solution to the trajectory planning problem.

Notes

The results of Section 6.5.3 are partly based on [40]. Acknowledgement is given to ©2011, Elsevier. Reprinted, with permission, from T. Meurer, "Flatness–based Trajectory Planning for Diffusion–Reaction Systems in a Parallelepipedon — A Spectral Approach", Automatica, 47(5):935–949.

6.6 Experimental Validation for a Flexible Plate with Distributed MFC Actuators

In the following, the spectral design approach is applied to realize desired elastic motion trajectories for the flexible thin plate with spatially distributed MFC actuators introduced in Section 4.2. For the determination of the spectral system representation and hence the formal state and input parametrization, either the strong form of the equations of motion given by (4.41) or the respective weak form (4.48) can be transferred into the operator formulation according to (6.2) with a Riesz spectral operator $\mathfrak{A}$. Based on these results, the solution to the trajectory planning problem is presented and validated by experimental results. For the computationally efficient realization a semi–numeric approach is deduced from the operator theoretic analysis by making use of weighted–residual techniques involving finite element methods for the determination of ansatz functions given a particular spatial domain.

6.6.1 Spectral Properties and Spectral System Representation

In order to be able to cover both the case of $\epsilon > 0$ and $\epsilon = 0$ in the actuator characteristics $\varrho^{\epsilon}(\cdot)$ subsequently the weak form is considered, which is recalled below for the sake of simplicity, i.e.

$$\begin{aligned} &\langle \partial_t^2 w^3(t), \Upsilon \rangle_{\mathcal{V}',\mathcal{V}} + \big(\mathfrak{A}^1 w^3(t)\big)(\Upsilon) + \big(\mathfrak{A}^2 \partial_t w^3(t)\big)(\Upsilon) = f(\Upsilon, t) \\ &w^3(0) = w_0^3,\ \partial_t w^3(0) = w_1^3 \end{aligned} \tag{6.157a}$$

with

$$f(\Upsilon, t) = \sum_{l \in M} \mathcal{b}_l^p(\Upsilon) U_l^p(t) \tag{6.157b}$$

and

$$\begin{aligned} &\mathcal{b}_l^p(\Upsilon) = -\Gamma_l^0 \times \\ &\Bigg(\left\langle \Lambda_l^{\epsilon}, \frac{1}{\rho} \Big[a_{1,l}^{11} \partial_{z^1}^2 \Upsilon + a_{1,l}^{22} \partial_{z^2}^2 \Upsilon + \big(a_{1,l}^{12} + a_{1,l}^{21}\big) \partial_{z^1} \partial_{z^2} \Upsilon \Big] \cos \alpha_l \right\rangle_{\mathcal{H}} + \\ &\left\langle \Lambda_l^{\epsilon}, \frac{1}{\rho} \Big[a_{2,l}^{11} \partial_{z^1}^2 \Upsilon + a_{2,l}^{22} \partial_{z^2}^2 \Upsilon + \big(a_{2,l}^{12} + a_{2,l}^{21}\big) \partial_{z^1} \partial_{z^2} \Upsilon \Big] \sin \alpha_l \right\rangle_{\mathcal{H}} \Bigg). \end{aligned} \tag{6.157c}$$

The Lax–Milgram theorem allows to associate the operators $\mathfrak{A}^1 \in \mathcal{L}(\mathcal{V}, \mathcal{V}')$ and $\mathfrak{A}^2 \in \mathcal{L}(\mathcal{H}, \mathcal{H}')$ with the sesquilinear forms $\varsigma^1(w^3(t), \Upsilon) = \langle \mathfrak{A}^1 w^3(t), \Upsilon \rangle_{\mathcal{V}',\mathcal{V}} = (\mathfrak{A}^1 w^3(t))(\Upsilon)$ and $\varsigma^2(w^3(t), \Upsilon) = \langle \mathfrak{A}^2 w^3(t), \Upsilon \rangle_{\mathcal{H}',\mathcal{H}} = (\mathfrak{A}^2 \partial_t w^3(t))(\Upsilon)$ defined by (4.45) and (4.46). Herein, $\mathcal{V} = H^2_{\partial\Omega_c}(\Omega)$ and $\mathcal{H} = L^2(\Omega)$ is equipped with the inner product (4.43), i.e. $\langle w, \hat{w} \rangle_{\mathcal{H}} = \int_{\Omega} \rho w \overline{\hat{w}} \, \mathrm{d}\Omega$.

Alternatively, (6.157) can be interpreted as an abstract differential equation in the dual space $\mathcal{V}'$ according to

$$\begin{aligned} &\partial_t^2 w^3(t) + \mathfrak{A}^1 w^3(t) + \mathfrak{A}^2 \partial_t w^3(t) = f(t) \\ &w^3(0) = w_0^3,\ \partial_t w^3(0) = w_1^3. \end{aligned} \tag{6.158}$$

6.6.1.1 Undamped Case

For the sake of simplicity viscous damping is at first neglected, i.e. $\mathfrak{A}^2 = \mathfrak{o}$ or $\varsigma^2(\cdot,\cdot) = 0$, respectively. Moreover, recall that $\mathcal{V}$, $\mathcal{H}$, and $\mathcal{V}'$ form a Gelfand triple $\mathcal{V} \hookrightarrow \mathcal{H} = \mathcal{H}' \hookrightarrow \mathcal{V}'$ with continuous and dense embedding.

Lemma 6.5. *$\mathfrak{A}^1$ is self–adjoint.*

Proof. Following [60, Theorem 7.6] the assertion follows if there exist constants $c,\ k > 0$ such that

$$\Re\{\varsigma^1(w,w)\} \geq c\|w\|_{\mathcal{V}}^2 - k\|w\|_{\mathcal{H}}^2 \tag{6.159}$$

for all $w \in \mathcal{V}$. Recall that $\varsigma^1(\cdot,\cdot)$ is real and symmetric and that Lemma 4.1(iii) yields the existence of $k_1 > 0$ with $\Re\{\varsigma^1(w,w)\} = \varsigma^1(w,w) \geq k_1\|w\|_{\mathcal{V}}^2$. Taking into account the Friedrichs inequality, i.e. $\exists K > 0 :\ \|w\|_{\mathcal{H}} \leq \sqrt{K}\|w\|_{\mathcal{V}}$, it follows that $-k\|w\|_{\mathcal{H}}^2 \geq -kK\|w\|_{\mathcal{V}}^2$. As a result, there obviously exist constants $c,\ k > 0$ satisfying $c - kK \leq k_1$, which yields (6.159). □

Alternatively, Lemma 6.5 can be proven by taking into account Gårding's inequality [1] for the quadratic form $\varsigma^1(w,\hat{w})$. With this, the following spectral properties of the operator $\mathfrak{A}^1$ can be deduced.

Lemma 6.6. *Consider the eigenproblem $\mathfrak{A}^1\phi = \lambda\phi$, which in variational form is equivalent to $\varsigma^1(\phi,\Upsilon) = \langle\lambda\phi,\Upsilon\rangle_{\mathcal{H}},\ \forall\Upsilon \in \mathcal{V}$:*

(i) The eigenproblem has only real and positive (countably many) eigenvalues $(\lambda_k)_{k\in\mathbb{N}}$ of finite algebraic multiplicity r_k^a with $\lim_{k\to\infty}\lambda_k \to \infty$. The respective geometric multiplicity r_k^g, i.e. $\dim E(\lambda_k)$ with $E(\lambda_k) = \ker(\mathfrak{A}^1 - \lambda\mathfrak{I})$, is finite.

(ii) For two distinct eigenvalues λ_k and λ_l the eigenspaces $E(\lambda_k)$ and $E(\lambda_l)$ are mutually orthogonal.

(iii) The eigenvectors $((\phi_{k_j})_{j=1,\ldots,r_k^a})_{k\in\mathbb{N}}$ form an orthonormal basis for $\mathcal{V}$ with respect to the inner product $\langle\cdot,\cdot\rangle_{\mathcal{V}_1} = \varsigma^1(\cdot,\cdot)$. Moreover, $\langle\phi_{k_j},\phi_{l_i}\rangle_{\mathcal{H}} = \delta_{k_j,l_i}$ and for any $x \in \mathcal{V}$ the Fourier series

$$x = \sum_{k\in\mathbb{N}}\sum_{j=1}^{r_k^a}\langle x,\phi_{k_j}\rangle_{\mathcal{H}}\phi_{k_j}$$

converges in $\mathcal{V}$.

(iv) The operator $\mathfrak{A}^1$ admits the spectral representation

$$\mathfrak{A}^1 x = \sum_{k\in\mathbb{N}} \lambda_k \sum_{j=1}^{r_k^a} \langle x, \phi_{k_j}\rangle_{\mathcal{H}} \phi_{k_j} + \sum_{k\in\mathbb{N}} \sum_{j=1+r_k^g}^{r_k^a} \big\langle x, \phi_{k_j}\big\rangle_{\mathcal{H}} \phi_{k_{j-1}}.$$

Lemma 6.6 is a direct consequence of Lemma 6.5 and the fact that $(\mathfrak{A}^1)^{-1}$ is a compact operator since the injection $\mathcal{V} \hookrightarrow \mathcal{H}$ is compact by the Sobolev embedding theorem. A proof of Lemma 6.6 can be found, e.g., in [60, Theorem 7.7], [68, Section 12.1, Theorem 17.11] or [36, Theorem 20.12].

Taking into account (6.157a) and (6.157b) with the test function $\Upsilon \in \mathcal{V}$ replaced by ϕ_{k_j} and recalling that $\langle\cdot,\cdot\rangle_{\mathcal{V}',\mathcal{V}}$ is the extension of the inner product $\langle\cdot,\cdot\rangle_{\mathcal{H}}$ from $\mathcal{V}\times\mathcal{H}$ to $\mathcal{V}'\times\mathcal{H}$ hence yields

$$\begin{aligned}\partial_t^2 \big\langle w^3(t), \phi_{k_j}\big\rangle_{\mathcal{H}} + \lambda_k \big\langle w^3(t), \phi_{k_j}\big\rangle_{\mathcal{H}} + \sigma_{j,k} \big\langle w^3(t), \phi_{k_{j+1}}\big\rangle_{\mathcal{H}} \\ = \sum_{l\in M} \mathcal{B}_l^p(\phi_{k_j}) U_l^p(t) \quad (6.160)\end{aligned}$$

for $j = 1,\dots,r_k^a,\ k\in\mathbb{N}$, with $\sigma_{j,k} = \sigma(j - r_k^g) - \sigma(j - r_k^a)$.

Subsequently, let $\lambda_k = \lambda_k' \overline{\lambda_k'}$ with $\lambda_k' = \imath\sqrt{\lambda_k}$ and $\overline{\lambda_k'} = -\imath\sqrt{\lambda_k}$ and introduce the change of coordinates

$$\begin{aligned} x_{k_j}(t) &= \frac{1}{\lambda_k' - \overline{\lambda_k'}} \big(\lambda_k' \big\langle w^3(t), \phi_{k_j}\big\rangle_{\mathcal{H}} - \big\langle \partial_t w^3(t), \phi_{k_j}\big\rangle_{\mathcal{H}}\big) \\ x_{-k_j}(t) &= \frac{1}{\lambda_k' - \overline{\lambda_k'}} \big(\lambda_k' \big\langle w^3(t), \phi_{k_j}\big\rangle_{\mathcal{H}} + \big\langle \partial_t w^3(t), \phi_{k_j}\big\rangle_{\mathcal{H}}\big) \end{aligned} \quad (6.161)$$

for $j = 1,\dots,r_k^a,\ k\in\mathbb{N}$. Differentiation with respect to t and taking into account (6.160) yields

$$\begin{aligned} \partial_t x_{k_j}(t) &= \overline{\lambda_k'} x_{k_j}(t) + \frac{\sigma_{j,k}}{2\lambda_k'}\big(x_{k_{j+1}}(t) + x_{-k_{j+1}}(t)\big) \\ &\quad + \frac{1}{\overline{\lambda_k'} - \lambda_k'} \sum_{l\in M} \mathcal{B}_l^p(\phi_{k_j}) U_l^p(t) \\ \partial_t x_{-k_j}(t) &= \lambda_k' x_{-k_j}(t) - \frac{\sigma_{j,k}}{2\lambda_k'}\big(x_{k_{j+1}}(t) + x_{-k_{j+1}}(t)\big) \\ &\quad - \frac{1}{\overline{\lambda_k'} - \lambda_k'} \sum_{l\in M} \mathcal{B}_l^p(\phi_{k_j}) U_l^p(t) \end{aligned} \quad (6.162)$$

for $j = 1,\dots,r_k^a,\ k\in\mathbb{N}$. Further analysis of (6.162) requires to distinguish two cases depending on the algebraic and geometric multiplicities.

Algebraic and Geometric Multiplicities Coincide

If $r_k^a = r_k^g$ for all $k \in \mathbb{N}$, then with $\mathbb{Z}_1 = \mathbb{Z} \setminus \{0\}$ the ODEs (6.162) are equivalent to

$$\partial_t x_{k_j}(t) = \overline{\lambda'_k} x_{k_j}(t) + \sum_{l \in M} b_{k_j}^{p,l} U_l^p(t), \qquad j = 1, \dots, r_{|k|}^a,\ k \in \mathbb{Z}_1 \tag{6.163a}$$

if $\overline{\lambda'_k}$ is extended to negative indexes by $\overline{\lambda'_{-k}} = \lambda'_k,\ k \in \mathbb{N}$, and

$$b_{k_j}^{p,l} = \frac{\mathcal{B}_l^p(\phi_{|k|_j})}{\overline{\lambda'_k} - \lambda'_k}. \tag{6.163b}$$

Algebraic and Geometric Multiplicities Differ

Let $r_k^g < r_k^a$ for some $k \in \mathbb{N}$. Then it is necessary to introduce a linear transformation $x_{k_j}(t) \mapsto \sum_{i=1}^{r_k^a} T^{ij} x_{k_i}(t)$ to transfer (6.162) for fixed k into its corresponding Jordan normal form. Note that this always possible since r_k^a is finite for all k. By similarly extending $\overline{\lambda'_k}$ to negative indexes, i.e. $\overline{\lambda'_{-k}} = \lambda'_k,\ k \in \mathbb{N}$, and by not distinguishing between $x_{k_j}(t)$ before and after the transformation the spectral representation is finally obtained in the form

$$\partial_t x_{k_j}(t) = \overline{\lambda'_k} x_{k_j}(t) + \sigma_{j,k} x_{k_{j+1}}(t) + \sum_{l \in M} b_{k_j}^{p,l} U_l^p(t) \tag{6.164}$$

for $j = 1, \dots, r_{|k|}^a,\ k \in \mathbb{Z}_1$. Herein, $\sigma_{j,k} = \sigma(j - r_{|k|}^g) - \sigma(j - r_{|k|}^a)$ and $b_{k_j}^{p,l}$ depends on $\mathcal{B}_l^p(\phi_{|k|_j})$, $\overline{\lambda'_k}$, λ'_k, and the elements of the transformation T^{ij}.

As a consequence, the formal parametrization introduced in Section 6.2 can be applied for the spectral system representations (6.163) and (6.164) of the undamped thin plate with distributed MFC actuators with the countable index set $\mathbb{N}$ replaced by $\mathbb{Z}_1$ according to Remark 6.1.

6.6.1.2 Viscously Damped Case – Constant Damping

If $\tilde{\nu}$ is independent of z, then by (4.46) the sesquilinear form $\varsigma^2(w^3, \Upsilon)$ fulfills $\varsigma^2(w^3, \Upsilon) = (\mathfrak{A}^2 w^3)(\Upsilon) = \langle \tilde{\nu} w^3, \Upsilon \rangle_{\mathcal{H}} = \tilde{\nu} \langle w^3, \Upsilon \rangle_{\mathcal{H}}$. Since in addition $\mathcal{H}$ is topologically equivalent to $L^2(\Omega)$ proceeding as in the previous paragraph provides for (6.157a) and (6.157b) with the test function $\Upsilon \in \mathcal{V}$ replaced by ϕ_{k_j} that

$$\begin{aligned} \partial_t^2 \langle w^3(t), \phi_{k_j} \rangle_{\mathcal{H}} + \tilde{\nu} \partial_t \langle w^3(t), \phi_{k_j} \rangle_{\mathcal{H}} + \lambda_k \langle w^3(t), \phi_{k_j} \rangle_{\mathcal{H}} \\ + \sigma_{j,k} \langle w^3(t), \phi_{k_{j+1}} \rangle_{\mathcal{H}} = \sum_{l \in M} \mathcal{B}_l^p(\phi_{k_j}) U_l^p(t), \quad k \in \mathbb{N}. \end{aligned} \tag{6.165}$$

Let subsequently $r_k^a = r_k^g$ for all $k \in \mathbb{N}$ such that $\sigma_{j,k} = 0$ for all j and k. Under weakly damped conditions with $\lambda_k - (\tilde{\nu}/2)^2 > 0,\ \forall k \in \mathbb{N}$, introduce

$$\lambda_k' = -\tilde{\nu}/2 + \imath\sqrt{\lambda_k - (\tilde{\nu}/2)^2}, \quad \overline{\lambda_k'} = -\tilde{\nu}/2 - \imath\sqrt{\lambda_k - (\tilde{\nu}/2)^2}. \tag{6.166}$$

Then the change of coordinates (6.161) results in a representation of (6.165) according to (6.162). By extending $\overline{\lambda_k'}$ to negative indexes with $\overline{\lambda_{-k}'} = \lambda_k',\ k \in \mathbb{N}$, this formulation is equivalent to the spectral representation (6.163).

By proceeding as in the undamped case it can be shown that given $r_k^g < r_k^a$ for some $k \in \mathbb{N}$, then (6.164) can be recovered also for constant viscous damping. Thereby, $\overline{\lambda_k'}$ has to be replaced by (6.166) and extended to negative indexes by $\overline{\lambda_{-k}'} = \lambda_k',\ k \in \mathbb{N}$. As a result, the formal parametrization can be directly applied to the thin plate with constant viscous damping coefficient.

6.6.1.3 Viscously Damped Case – Spatially Varying Damping

Differing from the two previous paragraphs given spatially varying viscous damping the spectral representation of the equations of motion cannot be directly determined from the weak form. Here, the governing equations have to be transferred to a semigroup setting. While physical experience allows to deduce that the eigenvalues occur in conjugated complex pairs, whose real part is strictly less that zero, the spectral properties cannot be established in a way similar to Lemma 6.6. As a result, in this case a semi–numeric realization is proposed below, which makes use of an interpretation of the weak form within a weighted–residual setting.

6.6.2 Formal State and Input Parametrization

The results of the previous section directly enable the determination of a formal state and input parametrization by exploiting the spectral system representations introduced above. In view of the spatially distributed finite–dimensional control input, formula (6.31) applies with the arising operators ${}^i\hat{\mathcal{D}}_k^x(s)$ and $\hat{\mathcal{D}}^u(s)$ defined in (6.32) and the index set $\mathbb{N}$ replaced by $\mathbb{Z}_1$. In particular it follows for the undamped and constant viscously damped thin plate with $r_k^a = r_k^g$ for all $k \in \mathbb{N}$ from (6.163) that

$$\hat{x}_{k_j}(s) = -\sum_{l \in M} \frac{b_{k_j}^{p,l}}{\overline{\lambda_k'}}\, {}^0\hat{\mathcal{D}}_k^x(s)\hat{\xi}^l(s) \tag{6.167a}$$

$$\hat{U}_l^p(s) = \hat{\mathcal{D}}^u(s)\hat{\xi}^l(s). \tag{6.167b}$$

with

$$ {}^{0}\hat{\mathcal{D}}_k^x(s) = e^{\mathcal{F}\left(s/\overline{\lambda'_k}, g^s\right)} \prod_{\substack{n\in\mathbb{Z}_1\\ n\neq k}} \mathcal{G}\left(\frac{s}{\overline{\lambda'_n}}, g^s\right) \tag{6.168a} $$

$$ \hat{\mathcal{D}}^u(s) = \prod_{n\in\mathbb{Z}_1} \mathcal{G}\left(\frac{s}{\overline{\lambda'_n}}, g^s\right) \tag{6.168b} $$

with g^s denoting the genus of the sequence $(\overline{\lambda'_k})_{k\in\mathbb{Z}_1}$, which is identical to the genus of the sequence $(\imath\sqrt{\lambda_k})_{k\in\mathbb{N}}$.

If $r_k^g < r_k^a$ for some $k \in \mathbb{N}$, then, as outlined above, the parametrization reads

$$ \hat{x}_{k_j}(s) = \sum_{l\in M} \left(-\frac{b_{k_j}^{p,l}}{\overline{\lambda'_k}}\, {}^{0}\hat{\mathcal{D}}_k^x(s) + \sum_{i=1}^{r_{|k|}^a - r_{|k|}^g} \frac{\sigma_{i,j,k} b_{k_{j+i}}^{p,l}}{\left(-\overline{\lambda'_k}\right)^{i+1}}\, {}^{i}\hat{\mathcal{D}}_k^x(s) \right) \hat{\xi}^l(s) \tag{6.169a} $$

$$ \hat{U}_l^p(s) = \hat{\mathcal{D}}^u(s)\hat{\xi}^l(s). \tag{6.169b} $$

with the operators ${}^{i}\hat{\mathcal{D}}_k^x(s)$ and $\hat{\mathcal{D}}^u(s)$ given by

$$ {}^{i}\hat{\mathcal{D}}_k^x(s) = e^{\theta_k \mathcal{F}\left(s/\overline{\lambda'_k}, g^s\right)} \left(1 - \frac{s}{\overline{\lambda'_k}}\right)^{\theta_k - i - 1} \prod_{\substack{n\in\mathbb{Z}_1\\ n\neq k}} \mathcal{G}^{\theta_n}\left(\frac{s}{\overline{\lambda'_n}}, g^s\right) \tag{6.170a} $$

$$ \hat{\mathcal{D}}^u(s) = \prod_{n\in\mathbb{Z}_1} \mathcal{G}^{\theta_n}\left(\frac{s}{\overline{\lambda'_n}}, g^s\right) \tag{6.170b} $$

for $\theta_k = 1 + r_{|k|}^a - r_{|k|}^g$. Herein, $\overline{\lambda'_{-k}} = \lambda'_k,\ k \in \mathbb{N}$, with λ'_k and $\overline{\lambda'_k}$ defined in (6.166).

These formal results clearly indicate that convergence of the parametrizations can be guaranteed under the conditions of Corollaries 6.3 and 6.4 by taking into account the index set $\mathbb{Z}_1$. It hence remains to be shown that $\hat{\mathcal{D}}^u(s)$ is an entire function of finite type τ and order ϱ. In view of the desired realization of finite time transitions between stationary deflection profiles, recall that $\varrho < 1$ is required to assign locally non–analytic basic output trajectories of Gevrey order $\alpha > 1$.

6.6.3 Convergence Analysis for Special Plate Configurations

Based on the formal parametrizations determined in the previous paragraph, subsequently convergence is addressed for special plate configurations. Thereby note that contrary to the 1–dimensional setting of a cantilevered Euler–Bernoulli beam model with suitably differentiable spatially varying coefficients (see, e.g., [23]) no analytic or asymptotic solutions to the eigenproblem are available for the considered cantilevered Kirchhoff plate model. Solutions do only exist for certain geometries (circular or rectangular) with special boundary conditions. Hence, no general

convergence analysis can be performed for the considered flexible plate with spatially varying parameters due to the patch–carrier interactions.

Nevertheless, assuming constant parameters $\mu^1 = \mu^2 = \mu^3 > 0$ with $\mu^4 = \mu^5 = \mu^6 = 0$ (isotropic case) in either (4.41a), (4.47), or (4.48), then Weyl's formula for the biharmonic operator Δ^2 yields asymptotic results for the counting function depending on the domain Ω and its boundary $\partial\Omega$. In particular, according to [55] the counting function (counting multiplicities) satisfies

$$\mathcal{N}(\eta) = \frac{A_\Omega}{4\pi}\eta + \frac{cL_{\partial\Omega}}{4\pi}\eta^{\frac{1}{2}} + o\big(\eta^{\frac{1}{2}}\big) \tag{6.171}$$

with A_Ω the surface area of Ω, $L_{\partial\Omega}$ the length of the boundary $\partial\Omega$, and c a dimensionless coefficient depending on the type of boundary condition (see also [12] for the case of purely clamped conditions). Recalling from [35, Section 3.2] that the convergence exponent of a sequence with a countable infinite index set equals the order of its counting function, it follows that

$$\varrho_1 = \gamma = \limsup_{\eta\to\infty} \frac{\log \mathcal{N}(\eta)}{\log \eta} = 1 \tag{6.172}$$

independent of A_Ω, $L_{\partial\Omega}$, and c. In view of Definition B.4 of the genus, Eqn. (6.172) directly implies $g^s = 0$. Moreover, Theorem B.2 yields that the order of $\hat{\mathcal{D}}^u(s)$ given by (6.168b) or (6.170b), respectively[13], is $\varrho = \gamma = 1$. Hence, according to Corollary 6.3, the input parametrizations (6.167b) and (6.169b), respectively, converge for basic output trajectories $\xi^l(t) \in G_{D^l,\alpha^l}(\mathbb{R}^+)$, $l = 1, \ldots, m$, with[14] $\alpha^l < 1$ provided that $\hat{\mathcal{D}}^u(s)$ is of finite type. Differing from the example considered in Section 6.5.3, where an exact analytic expression of the type was determined no such result can be deduced for the thin plate model. However, (6.171) can be utilized by solving

$$\frac{A_\Omega}{4\pi}\eta + \frac{cL_{\partial\Omega}}{4\pi}\eta^{\frac{1}{2}} + o\big(\eta^{\frac{1}{2}}\big) = n$$

with $n \in \mathbb{N}$ for $\eta = \eta_n$, which yields an asymptotic representation of the absolute value of the eigenvalues. Since $g^s = 0$ and recalling that the eigenvalues evolve in complex conjugated pairs, the maximal modulus $M(\eta)$ of $\hat{\mathcal{D}}^u(s)$ can be approximated in the form

$$M(\eta) = \prod_{n\in\mathbb{N}} \left(1 + \frac{\eta^2}{\eta_n^2}\right).$$

With (B.7) the evaluation of

[13] The conclusion holds for both cases since the Weyl asymptotics is counting multiplicities such that $\theta_k \neq 1$ is immediately taken into account.

[14] A straight forward modification of the proof of Lemma 6.3 and hence Corollary 6.3 reveals the sufficiency of $\alpha^l \leq 1$.

$$\tau = \limsup_{\eta\to\infty} \frac{\log M(\eta)}{\eta^{\varrho}} = \limsup_{\eta\to\infty} \frac{\log M(\eta)}{\eta}$$

hence yields $\tau = \infty$, which implies that $\hat{\mathcal{D}}^u(s)$ is of maximal type. Note that this is consistent[15] with the results of Section 6.5.3 for the Laplace operator given a finite–dimensional input. As a result, convergence of can no longer be directly established from the analytic results such that in general summation techniques have to be incorporated to address the divergent character. Nevertheless, different from the results for the linear diffusion–convection–reaction equation, where a highly divergent behavior could be observed, the numerical results presented in Section 6.6.5 below illustrate that meaningful input trajectories can be still directly determined from the evaluation of the determined differential operators.

While the convergence of the parametrizations can be analyzed based on the Weyl asymptotics for the constant parameter isotropic setting, no such result is available for the varying parameter orthotropic setting, in particular if the spatial actuator characteristics approaches superimposed Heaviside functions. An indication that the asymptotic growth of the eigenvalues and hence the counting function is similar to (6.171) can be found in [45], which supports the assertions.

6.6.4 Semi–Numeric Finite–Dimensional Realization and Numerical Convergence Indicator

Besides the incorporation of asymptotic results, which are only available for special cases, the presented spectral design systematics directly admits a semi–numeric realization. With this, an efficient (approximate) solution of the trajectory planning problem becomes available, which can be generalized to rather complex (linear) distributed–parameter systems.

In view of the practical implementation and evaluation of the determined formal state and input parametrization it is particularly useful to utilize the weak formulation in a weighted–residual or Galerkin setting (see, e.g, [38, 15]). To achieve the corresponding finite–dimensional approximation of the equations of motion, recall that (6.157a) is equivalent to (4.44), i.e. given a test function $\Upsilon \in \mathcal{V}$ then $(\mathfrak{A}^1 w^3(t))(\Upsilon) = \varsigma^1(w^3(t), \Upsilon)$ and $(\mathfrak{A}^2 \partial_t w^3(t))(\Upsilon) = \varsigma^2(w^3(t), \Upsilon)$. Hence, with (6.15) let $\mathbb{K} = \{1, 2, \ldots, K\}$ be a finite–dimensional ordered index such that

$$w^3(t) = w^3(\cdot, t) = \sum_{k\in\mathbb{K}} \sum_{j=1}^{r_k^a} \langle w^3(t), \psi_{k_j}\rangle_{\mathcal{V}} \phi_{k_j} = \sum_{k\in\mathbb{K}} \sum_{j=1}^{r_k^a} x_{k_j}(t)\phi_{k_j} \tag{6.173}$$

and consider a sequence of test functions $((\Upsilon_{k_j})_{j=1,\ldots,r_k^a})_{k\in\mathbb{K}}$. Due to the linearity of the sesquilinear forms the substitution of (6.173) into (4.44) yields

[15] Related results for a wave equation with 2– and 3–dimensional spatial domain and finite–dimensional boundary control can be found in [51].

$$\sum_{k\in\mathbb{K}}\sum_{j=1}^{r_k^a}\Big(\partial_t^2 x_{k_j}(t)\big\langle\phi_{k_j},\Upsilon_{l_i}\big\rangle_{\mathcal{V}',\mathcal{V}}+x_{k_j}(t)\varsigma^1(\phi_{k_j},\Upsilon_{l_i})$$
$$+\,\partial_t x_{k_j}(t)\varsigma^2(\phi_{k_j},\Upsilon_{l_i})\Big)=\sum_{l\in M}\mathcal{b}_l^p(\Upsilon_{l_i})U_l^p(t)\tag{6.174}$$

for $i=1,\dots,r_l^a$, $l\in\mathbb{K}$. Thereby, for evaluation purposes $\langle\phi_{k_j},\Upsilon_{l_i}\rangle_{\mathcal{V}',\mathcal{V}}$ can be replaced by the inner product in $\mathcal{H}$, i.e. $\langle\phi_{k_j},\Upsilon_{l_i}\rangle_{\mathcal{H}}$. By introducing the vectors

$$\boldsymbol{x}(t)=\left[x_{1_1}(t),\dots,x_{1_{r_1^a}}(t),\dots x_{\#\mathbb{K}_1}(t),\dots,x_{\#\mathbb{K}_{r_{\#\mathbb{K}}^a}}(t)\right]^T$$
$$\boldsymbol{u}(t)=\left[U_1^p(t),\dots,U_{\#M}^p(t)\right]^T$$

the set of $n=\sum_{k\in\mathbb{K}}r_k^a$ differential equations (6.174) can be re–written in matrix form as a set of first order ODEs according to

$$\underbrace{\begin{bmatrix}\mathfrak{C} & \mathfrak{M}\\ \mathfrak{M} & \mathfrak{o}\end{bmatrix}}_{=\overline{\mathfrak{M}}}\partial_t\overline{\boldsymbol{x}}(t)+\underbrace{\begin{bmatrix}\mathfrak{K} & \mathfrak{o}\\ \mathfrak{o} & -\mathfrak{M}\end{bmatrix}}_{=\overline{\mathfrak{K}}}\overline{\boldsymbol{x}}(t)=\begin{bmatrix}\mathfrak{B}\\ \mathfrak{o}\end{bmatrix}\boldsymbol{u}(t).\tag{6.175}$$

Herein, $\overline{\boldsymbol{x}}(t)=[\boldsymbol{x}^T(t),\partial_t\boldsymbol{x}^T(t)]^T$ and $\overline{\mathfrak{M}}$ as well as $\overline{\mathfrak{K}}$ are symmetric $2n\times 2n$ matrices in terms of the mass, damping, and stiffness matrices $\mathfrak{M},\mathfrak{C},\mathfrak{K}\in\mathbb{R}^{n\times n}$ defined by

$$\mathfrak{M}=\begin{bmatrix}\big\langle\phi_{1_1},\Upsilon_{1_1}\big\rangle_{\mathcal{H}} & \dots & \big\langle\phi_{\#\mathbb{K}_{r_{\#\mathbb{K}}^a}},\Upsilon_{1_1}\big\rangle_{\mathcal{H}}\\ \vdots & & \vdots\\ \big\langle\phi_{1_1},\Upsilon_{\#\mathbb{K}_{\#\mathbb{K}}}\big\rangle_{\mathcal{H}} & \dots & \big\langle\phi_{\#\mathbb{K}_{r_{\#\mathbb{K}}^a}},\Upsilon_{\#\mathbb{K}_{r_{\#\mathbb{K}}^a}}\big\rangle_{\mathcal{H}}\end{bmatrix}$$
$$\mathfrak{C}=\begin{bmatrix}\varsigma^2(\phi_{1_1},\Upsilon_{1_1}) & \dots & \varsigma^2(\phi_{\#\mathbb{K}_{r_{\#\mathbb{K}}^a}},\Upsilon_{1_1})\\ \vdots & & \vdots\\ \varsigma^2(\phi_{1_1},\Upsilon_{\#\mathbb{K}_{\#\mathbb{K}}}) & \dots & \varsigma^2(\phi_{\#\mathbb{K}_{r_{\#\mathbb{K}}^a}},\Upsilon_{\#\mathbb{K}_{r_{\#\mathbb{K}}^a}})\end{bmatrix}$$
$$\mathfrak{K}=\begin{bmatrix}\varsigma^1(\phi_{1_1},\Upsilon_{1_1}) & \dots & \varsigma^1(\phi_{\#\mathbb{K}_{r_{\#\mathbb{K}}^a}},\Upsilon_{1_1})\\ \vdots & & \vdots\\ \varsigma^1(\phi_{1_1},\Upsilon_{\#\mathbb{K}_{\#\mathbb{K}}}) & \dots & \varsigma^1(\phi_{\#\mathbb{K}_{r_{\#\mathbb{K}}^a}},\Upsilon_{\#\mathbb{K}_{r_{\#\mathbb{K}}^a}})\end{bmatrix}$$

The input matrix $\mathfrak{B}\in\mathbb{R}^{n\times\#M}$ follows as

$$\mathfrak{B}=\begin{bmatrix}\mathcal{b}_1^p(\Upsilon_{1_1}) & \dots & \mathcal{b}_{\#M}^p(\Upsilon_{1_1})\\ \vdots & & \vdots\\ \mathcal{b}_1^p(\Upsilon_{\#\mathbb{K}_{r_{\#\mathbb{K}}^a}}) & \dots & \mathcal{b}_{\#M}^p(\Upsilon_{\#\mathbb{K}_{r_{\#\mathbb{K}}^a}})\end{bmatrix}.$$

Based on (6.175), the state and input parametrizations (6.167), (6.169) can be explicitly evaluated by replacing the index set $\mathbb{Z}_1$ with the set $\{-K, \ldots, -1, 1, \ldots K\}$ and by making use of the solution to the algebraic eigenproblem

$$\big(\overline{\mathfrak{M}}\lambda + \overline{\mathfrak{K}}\big)\boldsymbol{\phi} = \mathbf{0}, \tag{6.176}$$

which yields a finite–dimensional approximation to the operator eigenproblem.

With this, on the one hand a very efficient computational evaluation is achieved and on the other hand a high–order approximation can be used to deduce a graphical convergence indicator. For this, observe that the convergence exponent γ of a sequence with countable index set equals the order of its counting function [35, Section 3.2]. Let $\mathcal{N}(\eta)$ denote the counting function of $(\lambda_k)_{k\in\mathbb{N}}$ this yields

$$\gamma = \limsup_{\eta\to\infty} \frac{\log \mathcal{N}(\eta)}{\log(\eta)}.$$

Hence, the graph of $\log \mathcal{N}(\eta)/\log(\eta)$ can be considered as an indicator for γ and hence for the order ϱ provided that a sufficiently large number of eigenvalues can be numerically determined by making use of (6.176). In addition, it should be pointed out that also divergent parametrizations can be used for the solution of the motion planning problem as is shown in Section 6.5.3 and [40], respectively.

6.6.5 Experimental Results for Feedforward and Closed–Loop Tracking Control

The experimental validation of the proposed spectral trajectory planning and feedforward control approach is performed for the flexible plate structure depicted in Figure 6.13. In addition, experimental data is presented for tracking control within the 2DOF control concept.

6.6.5.1 Configuration and System Parameters

The structure is built up of glass fibre composite material with dimensions $L_c^1 = 0.427\,\mathrm{m}$, $L_c^2 = 0.304\,\mathrm{m}$, and $h = 0.001\,\mathrm{m}$. The MFC patches are of the type M8557P1 with an active area of dimension $L_l^{1,p} = 0.085\,\mathrm{m}$, $L_l^{2,p} = 0.057\,\mathrm{m}$, $h_l^p = 3 \times 10^{-4}\,\mathrm{m}$, and electrode spacing $e_l^p = 5 \times 10^{-4}\,\mathrm{m}$ [63]. In the following, only the two patch pairs near the clamped end located at $(z_1^{1,p}, z_1^{2,p}) = (0.023, 0.021)\,\mathrm{m}$ and $(z_2^{1,p}, z_2^{2,p}) = (0.023, 0.223)\,\mathrm{m}$ are utilized for trajectory planning such that $m = \#M = 2$. Prescribed transient deflection profiles for the plate are specified pointwise by

$$y^j(t) = w^3\big(z_j^{1,y}, z_j^{2,y}, t\big), \qquad j = 1, 2 \tag{6.177}$$

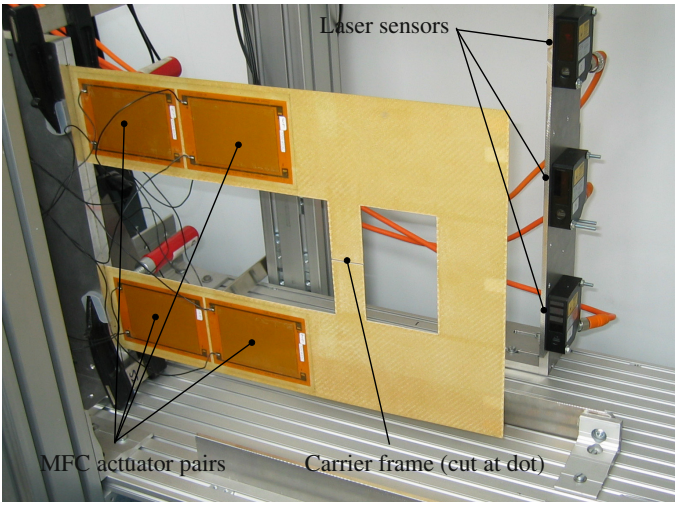

(a) Experimental set–up.

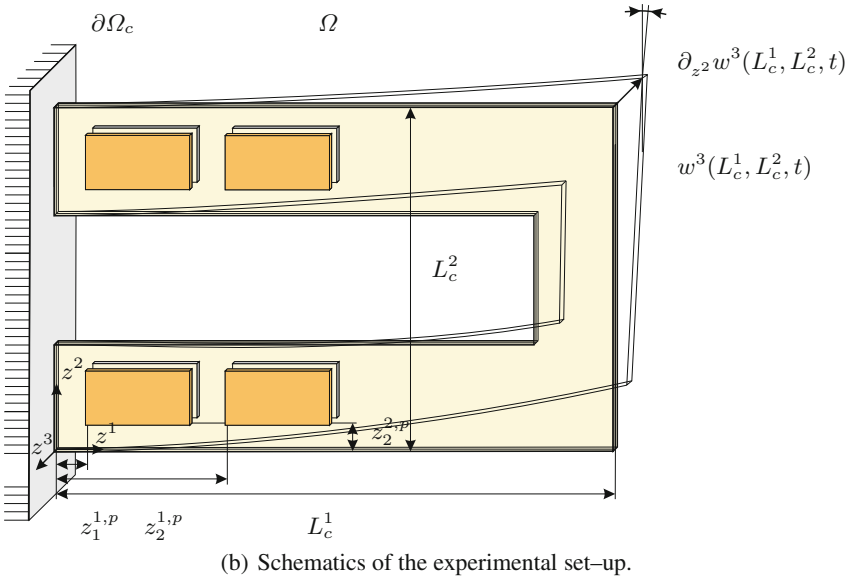

(b) Schematics of the experimental set–up.

Fig. 6.13 Flexible plate structure with distributed MFC actuators [57]

at the two corner locations $(z_1^{1,y}, z_1^{2,y}) = (0.422, 0.012)\,\mathrm{m}$, and $(z_2^{1,y}, z_2^{2,y}) = (0.422, 0.292)\,\mathrm{m}$. For the verification of the resulting tracking behavior three laser sensors are placed at $(z_j^{1,m}, z_j^{2,m}) = (z_j^{1,y}, z_j^{2,y})$, $j = 1, 2$, and in the middle of

the free edge opposite to the clamped boundary at $(z_3^{1,m}, z_3^{2,m}) = (0.422, 0.152)\,\mathrm{m}$ such that

$$y^3(t) = w^3\big(z_3^{1,m}, z_3^{2,m}, t\big). \tag{6.178}$$

The measurements and the implementation of the feedforward control tracking concept are realized using the real–time control board DS1103 of DSPACE with a sampling time of $0.2\,\mathrm{ms}$. The power supply is provided by high-voltage power amplifiers PA05039 of Trek Inc. [63].

Remark 6.17. It is well–known that piezoelectric materials show intrinsic hysteretic behavior and creep effects [46, 27]. However, the application of an appropriate hysteresis and creep compensator allows to cancel out the nonlinear actuator behavior, see, e.g., [29, 30]. In the case of MFC patch actuators, this is verified by detailed experimental investigations in [58] and hence justifies the assumption of linear elastic piezoelectric material behavior.

The remaining system parameters are determined based on an identification procedure making use of the finite–dimensional approximation of the equations of motion (6.175) — for details, the reader is referred to [56]. Thereby, the test functions $((\Upsilon_{k_j})_{j=1,\dots,r_k^a})_{k\in\mathbb{K}}$ are chosen as the eigenfunctions of an undamped orthotropic elastic plate structure of identical geometry and are determined using finite elements. The quality of the approximation can be evaluated from Figure 6.14, where a comparison is provided between the measured output $y^j(t)$ at the measurement locations $(z_j^{1,m}, z_j^{2,m})$, $j = 1, 3$ with the respective trajectories obtained from the numerical simulation. Herein, voltage step excitations are appropriately applied to achieve bending and torsional motion of the plate.

6.6.5.2 Trajectory Planning and Feedforward Control

The desired motion trajectories are assigned as bending and torsion starting from the initial undeformed rest position to reach a prescribed final rest configuration along a specified spatial–temporal path. For this, the determined state and input parametrizations (6.167), (6.169) are utilized and evaluated as outlined in Section 6.6.4. The desired trajectory for the basic output is determined according to the direct trajectory planning approach presented in Section 6.4.1.1, which yields a linear system of equations for $\boldsymbol{\xi}^*(t) = [\xi^{*,1}(t), \xi^{*,2}(t)]^T$ in terms of $\boldsymbol{y}^*(t) = [y^{1,*}(t), y^{2,*}(t)]^T$ at $t = 0$ and $t = T$, respectively. In particular, the first scenario (I) considers rest–to–rest bending motion with

$$\begin{bmatrix} y^1(0) \\ y^2(0) \end{bmatrix} = \begin{bmatrix} 0 \\ 0 \end{bmatrix} \overset{t\in[0,T]}{\longrightarrow} \begin{bmatrix} y^1(T) \\ y^2(T) \end{bmatrix} = \begin{bmatrix} \overline{y}_I \\ \overline{y}_I \end{bmatrix},\ \overline{y}_I \in \{0.005, 0.01\}\,\mathrm{m} \tag{6.179}$$

for while scenario (II) addresses rest–to–rest torsional motion, where

$$\begin{bmatrix} y^1(0) \\ y^2(0) \end{bmatrix} = \begin{bmatrix} 0 \\ 0 \end{bmatrix} \overset{t\in[0,T]}{\longrightarrow} \begin{bmatrix} y^1(T) \\ y^2(T) \end{bmatrix} = \begin{bmatrix} \overline{y}_{II} \\ -\overline{y}_{II} \end{bmatrix},\ \overline{y}_{II} \in \{1.5, 3\} \times 10^{-3}\,\mathrm{m}. \tag{6.180}$$

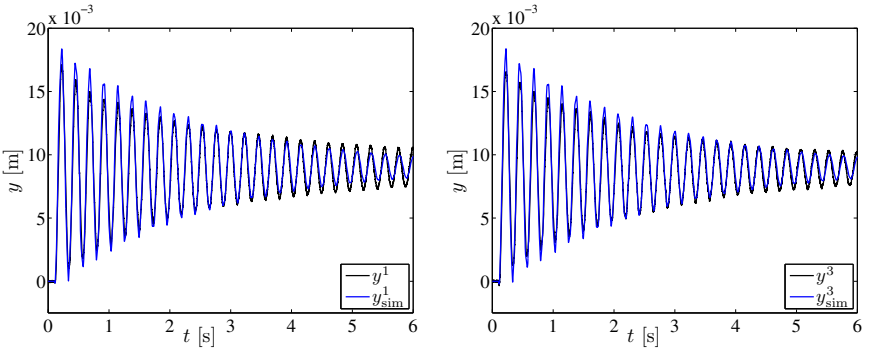

(a) Bending motion.

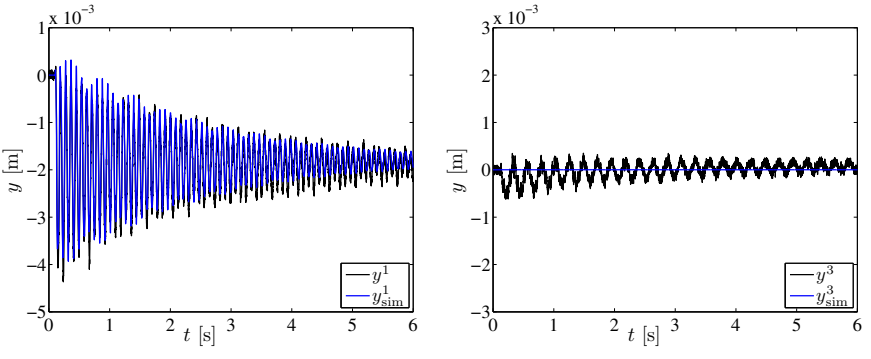

(b) Torsional motion.

Fig. 6.14 Comparison of measured $y^j(t)$ and simulated step response $y^j_{\mathrm{sim}}(t)$ at the measurement locations $(z_j^{1,m}, z_j^{2,m})$, $j = 1, 3$, for bending motion (top) and torsional motion (bottom)

The temporal path for $\boldsymbol{\xi}^*(t)$ is hence assigned in each scenario according to

$$\boldsymbol{\xi}^*(t) = \begin{cases} \boldsymbol{\xi}^*(0), & t \leq 0 \\ \boldsymbol{\xi}^*(0) + \big(\boldsymbol{\xi}^*(T) - \boldsymbol{\xi}^*(0)\big) g_{T,\omega}(t), & t \in (0, T) \\ \boldsymbol{\xi}^*(T), & t \leq T \end{cases} \tag{6.181}$$

with $g_{T,\omega}(t)$ from (B.5) for $T = 0.2\,\mathrm{s}$ and $\omega = 1.8$.

The numerical analysis of the finite–dimensional system approximation (6.175) or (6.176), respectively, for the considered parameter set yields isolated eigenvalues with $r_k^a = 1$. Motivated by the convergence considerations in Section 6.6.3 for different (uniform) thin plate configurations, the genus of the sequence of zeros of the entire functions arising in the operational parametrizations is subsequently set to $g^s = 0$. With this, the convergence of the input parametrization according to (6.167b) is evaluated numerically for different $K \in \{3, 5, 10, 15\}$. The results are

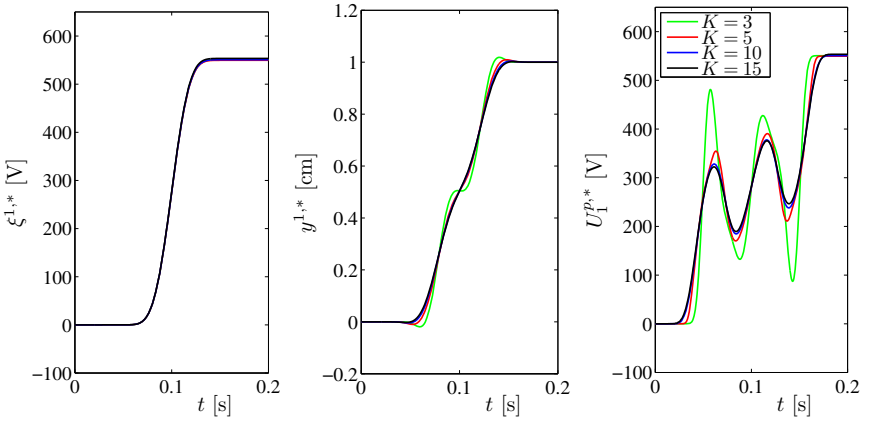

(a) Basic output trajectory. (b) Output trajectory. (c) Feedforward control.

Fig. 6.15 Numerical convergence analysis of the output and input parametrization for scenario (I) by varying $K \in \{3, 5, 10, 15\}$. With (6.179) note that $y^{2,*}(t) = y^{1,*}(t)$ and $U_2^p(t) = U_1^p(t)$.

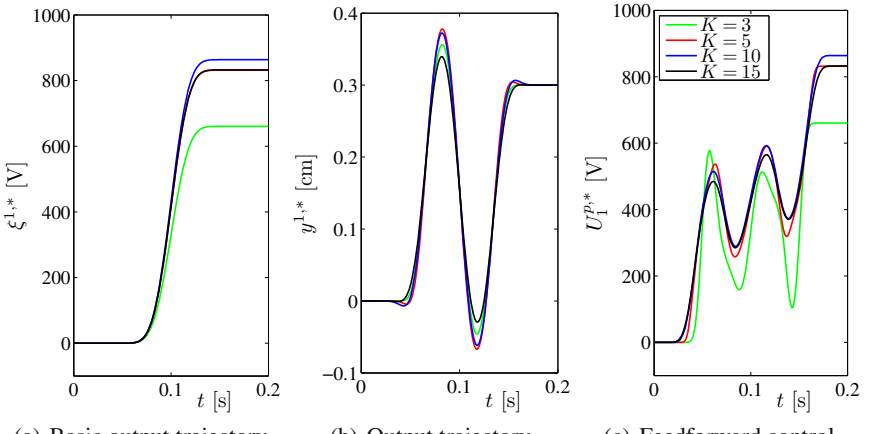

(a) Basic output trajectory. (b) Output trajectory. (c) Feedforward control.

Fig. 6.16 Numerical convergence analysis of the output and input parametrization for scenario (II) by varying $K \in \{3, 5, 10, 15\}$. With (6.180) note that $y^{2,*}(t) = -y^{1,*}(t)$ and $U_2^p(t) = -U_1^p(t)$.

shown in Figure 6.15 for bending motion according to scenario (I) and Figure 6.16 for torsional motion as defined in scenario (II). Herein, the trajectories for $\xi^{*,1}(t)$ and the corresponding output path $y^{1,*}(t)$ are shown additionally. Obviously fast convergence is obtained such that $K = 15$ is used for the experimental validation of the feedforward controls. Moreover, the required voltage signals evolve in a non–trivial manner with phases of acceleration and deceleration. Therefore, the desired

output trajectory $\boldsymbol{y}^*(t)$ is used as a reference path to analyze the open–loop tracking behavior.

Remark 6.18. The theoretical convergence results indicate divergent behaviour due to the violation of the condition $\alpha \leq 1$ by the assigned desired basic output trajectory and the maximal type of $\hat{\mathcal{D}}^u(s)$. These effects, however, may arise by significantly increasing the number K. Thus the presented numerical results can be interpreted in terms of least–term or smallest–term summation, which exploits the fact that certain divergent series converge very fast before diverging [52].

Experimental results for the application of the determined feedforward control are shown in Figures 6.17 and 6.18 for scenario (I) and (II), respectively. Thereby, the voltage signals shown in Figures 6.15(c) and 6.16(c) are applied at the test bench. For comparison purposes, measurement results are provided for the application of voltage trajectories corresponding to the smooth transition function given by (6.181) as shown in Figures 6.15(a) and 6.16(a), respectively. The arising oscillations from the short transition interval clearly confirm the superior tracking behavior of the flatness–based feedforward controllers, where basically no transients occur after reaching the final stationary deflection. It should be once again emphasized that no feedback control is applied throughout these set of experiments.

6.6.5.3 Extension to Tracking Control

Experimental results for tracking control are shown in Figures 6.19 and 6.20 for scenario (I) and (II), respectively. Thereby, flatness–based feedforward control is combined with a passivity–based non–collocated dynamic output error feedback controller with state–observer within the 2DOF control concept to realize trajectory tracking. For details, the reader is referred to [56] and [41, 59, 25] for related results. Note that each MFC actuator is pre–tensioned by a constant voltage of $500\ \mathrm{V}$ to enable the utilization of the available input voltage range of $[-500, 1500]\ \mathrm{V}$. For comparison purposes the respective open–loop measurements are depicted in Figures 6.19(a) and 6.20(a). In particular the spurious oscillations in the output signals arising for the feedforward control are canceled by the 2DOF control, which yields accurate tracking for transition times surpassing the time constant of the structure's first eigenfrequency.

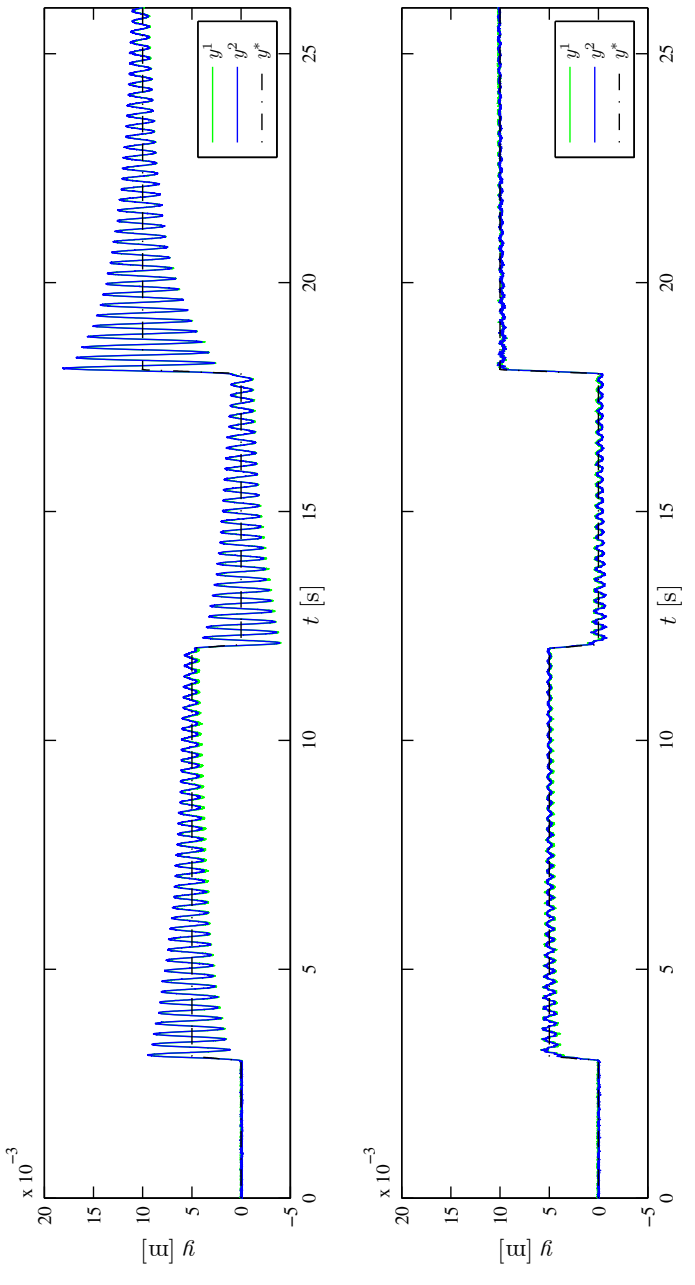

Fig. 6.17 Measurement results for rest–to–rest bending motion according to scenario (I). Comparison of obtained $\boldsymbol{y}(t)$ and desired output $\boldsymbol{y}^*(t)$ for input voltage trajectories in terms of smooth transition function (top) and flatness–based trajectory planning (bottom).

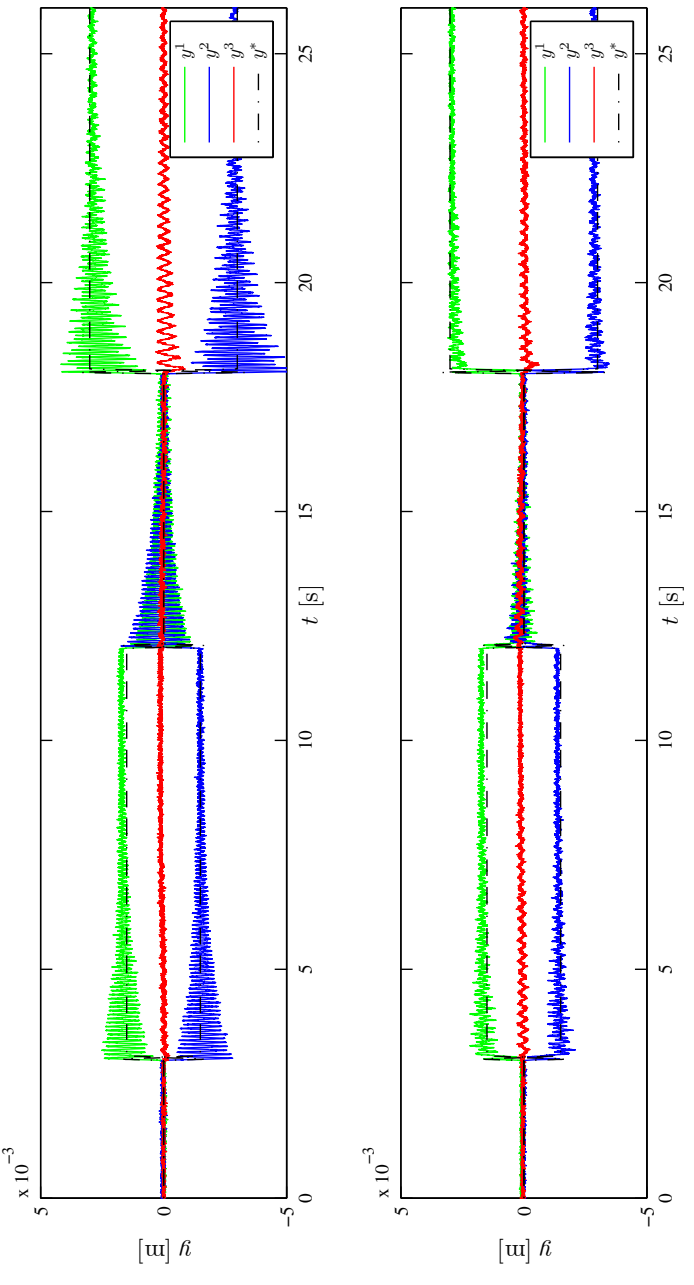

Fig. 6.18 Measurement results for rest–to–rest torsional motion according to scenario (II). Comparison of obtained $\boldsymbol{y}(t)$ and desired output $\boldsymbol{y}^*(t)$ for input voltage trajectories in terms of smooth transition function (top) and flatness–based trajectory planning (bottom).

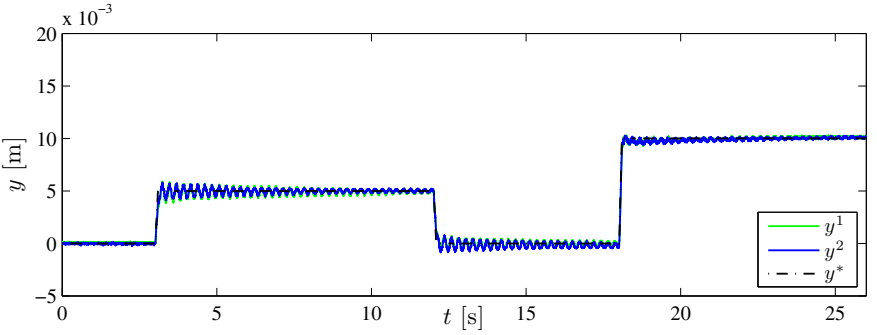

(a) Feedforward control.

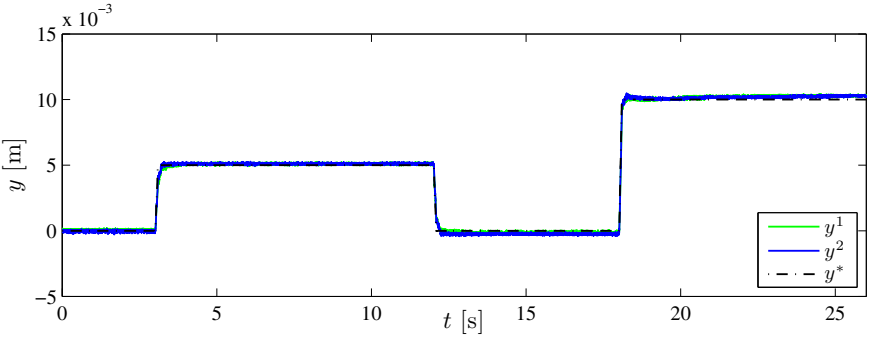

(b) Feedforward and error feedback control.

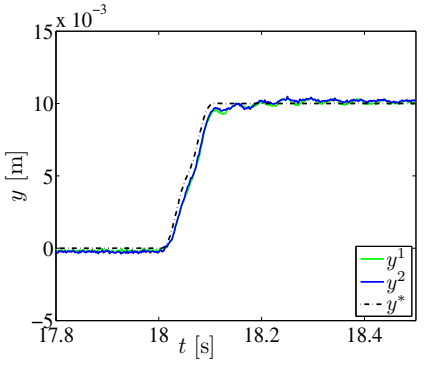

(c) Desired and measured outputs.

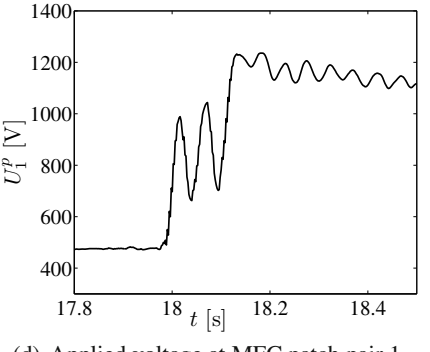

(d) Applied voltage at MFC patch pair 1.

Fig. 6.19 Measurement results for rest–to–rest bending motion according to scenario (I). Comparison of obtained $\boldsymbol{y}(t)$ and desired output $\boldsymbol{y}^*(t)$ for feedforward control (a) and 2DOF tracking control (b). Detail view on output (c) and applied voltage at MFC patch pair 1 (d).

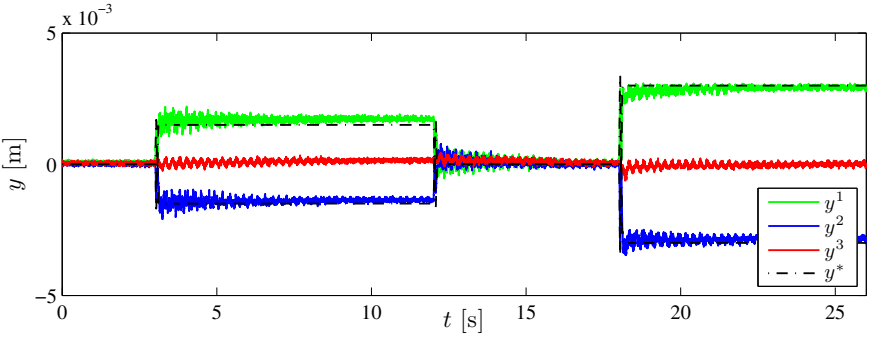

(a) Feedforward control.

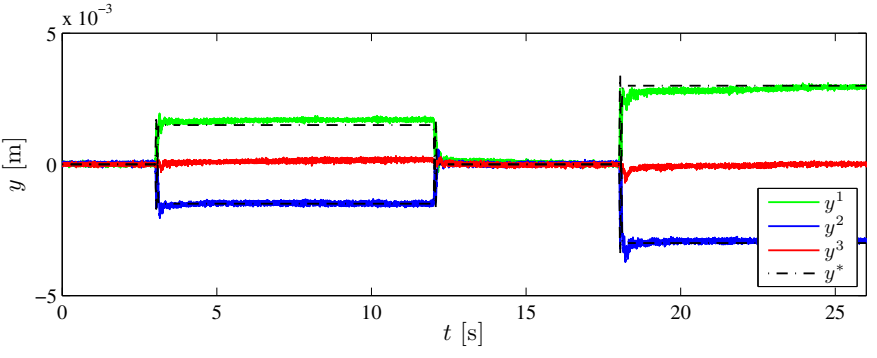

(b) Feedforward and error feedback control.

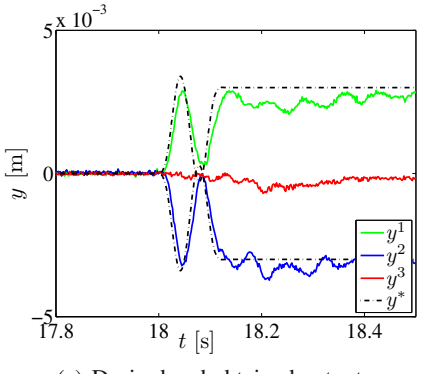

(c) Desired and obtained output.

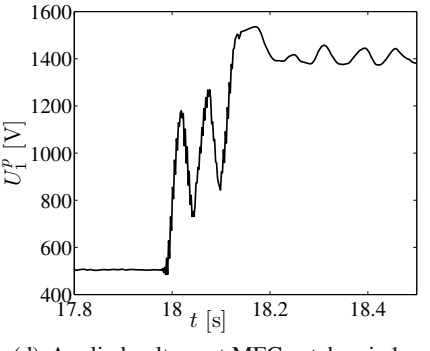

(d) Applied voltage at MFC patch pair 1.

Fig. 6.20 Measurement results for rest–to–rest torsional motion according to scenario (II). Comparison of obtained $\boldsymbol{y}(t)$ and desired output $\boldsymbol{y}^*(t)$ for feedforward control (a) and 2DOF tracking control (b). Detail view on output (c) and applied voltage at MFC patch pair 1 (d).

References

1. Agmon, S.: Lectures on elliptic boundary value problems. Van Nostrand Company Inc., Princeton (1965)
2. Alt, H.: Lineare Funktionalanalysis, 4th edn. Springer, Heidelberg (2000)
3. Avdonin, S., Ivanov, S.: Families of Exponentials. Cambridge University Press, Cambridge (1995)
4. Balser, W.: Formal power series and linear systems of meromorphic ordinary differential equations. Springer, New York (2000)
5. Balser, W., Kostov, V.: Recent progress in the theory of formal solutions for ODE and PDE. Appl. Math. Comput. 141, 113–123 (2003)
6. Bari, N.: Sur les bases dans l'espace de Hilbert. Dokl. Akad. Nauk. SSSR 54, 379–382 (1946)
7. Bari, N.: Biorthogonal systems and bases in Hilbert space. Mathematika 4, 69–107 (1951)
8. Boas, R.: Entire functions. Academic Press, New York (1954)
9. Carthel, C., Glowinski, R., Lions, J.: On Exact and Approximate Boundary Controllabilities for the Heat Equation: A Numerical Approach. J. Optim. Theory and Appl. 82(3), 429–484 (1994)
10. Chavel, I.: Eigenvalues in Riemannian Geometry. Academic Press (1984)
11. Chitour, Y., Coron, J.M., Garavello, M.: On conditions that prevent steady–state controllability of certain linear partial differential equations. Disc. Cont. Dyn. Sys. 14(4), 643–672 (2006)
12. Courant, B.: Über die Schwingungen eingespannter Platten. Math. Z 15, 195–200 (1922)
13. Curtain, R.: On stabilizability of linear spectral systems via state boundary feedback. SIAM J. Control Optim. 23(1), 144–152 (1985)
14. Curtain, R., Zwart, H.: An Introduction to Infinite–Dimensional Linear Systems Theory. Texts in Applied Mathematics, vol. 21, Springer, New York (1995)
15. Dautray, R., Lions, J.: Mathematical Analysis and Numerical Methods for Science and Technology. Evolution Problems I, vol. 5. Springer, Heidelberg (2000)
16. Dunford, N., Schwartz, J.: Linear operators, part III: Spectral operators. Wiley Interscience, New York (1963)
17. Evans, L.: Partial Differential Equations. Graduate Studies in Mathematics, vol. 19. American Mathematical Society, Providence (2002)
18. Fattorini, H.: Boundary control systems. SIAM J. Control 6(3), 349–388 (1968)
19. Fattorini, H.: Boundary control of temperature distributions in a parallelepipedon. SIAM J. Control 13(1), 1–13 (1975)
20. Gilles, E.: Systeme mit verteilten Parametern. R. Oldenbourg Verlag, Wien (1973)
21. Gohberg, I., Krein, M.: Introduction to the Theory of Linear Nonselfadjoint Operators. Translations of Mathematical Monographs, vol. 18. American Mathematical Society, Providence (1969)
22. Grisvard, P.: Elliptic Problems in Non–Smooth Domains. Pitman, Boston (1985)
23. Guo, B.Z.: Riesz basis property and exponential stability of controlled Euler–Bernoulli beam equations with variable coefficients. SIAM J. Control Optim. 40(6), 1905–1923 (2002)
24. Guo, B.Z., Zwart, H.: Riesz spectral systems. Memorandum 1594, Faculty of Mathematical Sciences. University of Twente, The Netherlands (2001)

25. Henikl, J., Schröck, J., Meurer, T., Kugi, A.: Infinit–dimensionaler Reglerentwurf für Euler–Bernoulli Balken mit Macro–Fibre Composite Aktoren. at–Automatisierungstechnik 60(1), 10–19 (2012)
26. Ho, L., Russell, D.: Admissible input elements for systems in Hilbert space and a Carleson measure criterion. SIAM J. Control Optim. 21(4), 614–640 (1983)
27. Janocha, H.: Adaptronics and smart structures: basics, materials, design, and applications, 2nd edn. Springer, Heidelberg (2007)
28. Kato, T.: Perturbation Theory for Linear Operators. Springer, Berlin (1980)
29. Kugi, A., Thull, D., Kuhnen, K.: An infinite–dimensional control concept for piezoelectric structures with complex hysteresis. Struct. Control Health Monit. 13(6), 1099–1119 (2006)
30. Kuhnen, K., Krejci, P.: Compensation of Complex Hysteresis and Creep Effects in Piezoelectrically Actuated Systems — A New Preisach Modeling Approach. IEEE Trans. Autom. Control 54(3), 537–550 (2009)
31. Laroche, B.: Extension de la notion de platitude à des systèmes décrits par des équations aux dérivées partielles linéaires. PhD thesis. École Nationale Supérieure des Mines de Paris (2000)
32. Laroche, B., Martin, P., Rouchon, P.: Motion planning for the heat equation. Int. J. Robust Nonlinear Control 10, 629–643 (2000)
33. Lasiecka, I., Triggiani, R.: Stabilization and structural assignment of Dirichlet boundary feedback parabolic equations. SIAM J. Control Optim 21(5), 766–803 (1983)
34. Levin, B.: Distribution of zeros of entire functions. American Mathematical Society, Providence (1980)
35. Levin, B.: Lectures on Entire Functions. American Mathematical Society, Providence (1996)
36. Lube, G.: Lineare Funktionalanalysis und Anwendungen auf partielle Differentialgleichungen. Lecture Notes. Georg–August–Universität Göttingen (2006)
37. Luo, Z., Guo, B., Morgül, O.: Stability and Stabilization of Infinite Dimensional Systems with Applications. Springer, London (1999)
38. Meirovitch, L.: Principles and Techniques of Vibrations. Prentice Hall, New Jersey (1997)
39. Meurer, T.: Feedforward and Feedback Tracking Control of Diffusion–Convection–Reaction Systems using Summability Methods. Fortschr.–Ber. VDI Reihe 8 Nr. 1081. VDI Verlag, Düsseldorf (2005)
40. Meurer, T.: Flatness–based Trajectory Planning for Diffusion–Reaction Systems in a Parallelepipedon — A Spectral Approach. Automatica 47(5), 935–949 (2011)
41. Meurer, T., Kugi, A.: Tracking control design for a wave equation with dynamic boundary conditions modeling a piezoelectric stack actuator. Int. J. Robust Nonlin. 21(5), 542–562 (2011)
42. Meurer, T., Zeitz, M.: Feedforward and feedback tracking control of nonlinear diffusion–convection–reaction systems using summability methods. Ind. Eng. Chem. Res. 44, 2532–2548 (2005)
43. Meurer, T., Zeitz, M.: Model inversion of boundary controlled parabolic partial differential equations using summability methods. Math. Comp. Model Dyn. Sys (MCMDS) 14(3), 213–230 (2008)
44. Naylor, A., Sell, G.: Linear Operator Theory in Engineering and Science. Applied Mathematical Sciences, vol. 40. Springer, New York (1982)

45. Nazarov, S.: On asymptotics of the spectrum of a problem in elasticity. Sib. Mat. Zh. 41(4), 895–912 (2000)
46. Nowacki, W.: Dynamic Problems of Thermoelasticity. Noordhoff Int. Publ., PWN–Polish Scientific Publ., Warszawa (1975)
47. Ramis, J.P.: Les seriés k–sommables et leurs applications. In: Analysis, Micrological Calculus and Relativistic Quantum Theory. Lecture Notes in Physics, vol. 126, pp. 178–199. Springer (1980)
48. Rebarber, R.: Spectral assignability for distributed parameter systems with unbounded scalar control. SIAM J. Control Optim. 27(1), 148–169 (1989a)
49. Rebarber, R.: Spectral Determination for a Cantilever Beam. IEEE Trans. Automat. Control 34(5), 502–510 (1989b)
50. Ritt, J.: On a general class of linear homogeneous differential equations of infinite order with constant coefficients. Trans. Am. Math. Soc. 18(1), 27–49 (1917)
51. Rouchon, P.: Flatness–based control of oscillators. Z Angew Math Mech. 85(6), 411–421 (2005)
52. Rudin, W.: Principles of mathematical analysis, 3rd edn. McGraw-Hill, New York (1976)
53. Rudolph, J.: Flatness Based Control of Distributed Parameter Systems. Berichte aus der Steuerungs– und Regelungstechnik. Shaker-Verlag, Aachen (2003)
54. Russell, D.: A Unified Boundary Controllability Theory for Hyperbolic and Parabolic Partial Differential Equations. Studies Appl. Math. 52, 189–211 (1973)
55. Safarov, Y., Vassiliev, D.: The Asymptotic Distribution of Eigenvalues of Partial Differential Operators, Translations of Mathematical Monographs. American Mathematical Society, Providence (1997)
56. Schröck, J.: Mathematical Modeling and Tracking Control of Piezo–actuated Flexible Structures. PhD thesis, Automation and Control Institute. Vienna University of Technology (2011)
57. Schröck, J., Meurer, T.: Experimental set–up of a flexible plate with distributed MFC actuators. Automation and Control Institute, Vienna University of Technology (2010/2011)
58. Schröck, J., Meurer, T., Kugi, A.: Control of a flexible beam actuated by macro-fiber composite patches – Part II: Hysteresis and creep compensation, experimental results. Smart Mater Struct. 20(1), article 015016, 11 pages (2011)
59. Schröck, J., Meurer, T., Kugi, A.: Non–collocated Feedback Stabilization of a Non–Uniform Euler–Bernoulli Beam with In–Domain Actuation. In: Proc. IEEE Conference on Decision and Control (CDC), Orlando (FL), USA, pp. 2776–2781 (2011)
60. Showalter, R.: Hilbert Space Methods for Partial Differential Equations. Electron. J. Diff. Eqns. (1994), `http://www.emis.ams.org/journals/EJDE/Monographs/01/toc.html`
61. Shubov, M., Balogh, A.: Asymptotic Distribution of Eigenvalues for Damped String Equation: Numerical Approach. J. Aerosp. Eng. 18(2), 69–83 (2005)
62. Sikkema, P.: Differential operators and differential equations of infinite order with constant coefficients. P. Norrdhoff N.V., Groningen–Djakarta (1953)
63. Smart Material Corp., Datasheet (2010), `http://www.smart-material.com`
64. Staffans, O.: Well–Posed Linear Systems. Cambridge University Press, New York (2005)
65. Triggiani, R.: On the Stabilizability Problem in Banach Spaces. J. Math. Anal. Appl. 52, 383–403 (1975)
66. Tucsnak, M., Weiss, G.: Observation and Control for Operator Semigroups. Birkhäuser, Basel (2009)

67. Wagner, M., Meurer, T., Zeitz, M.: K-summable power series as a design tool for feedforward control of diffusion-convection-reaction systems. In: Proc. 6th IFAC Symposium Nonlinear Control Systems (NOLCOS 2004), Stuttgart (D), pp. 149–154 (2004)
68. Wloka, J.: Partial Differential Equations. Cambridge University Press, Cambridge (1987)
69. Young, R.: An Introduction to Nonharmonic Fourier Series. Academic Press, San Diego (2001)

Chapter 7
Formal Integration Approach for Time Varying Systems with Parallelepiped Spatial Domain

The spectral approach proposed in the previous chapter is essentially restricted to linear time–invariant distributed–parameter trajectory planning problems. In the following a design technique is presented for boundary controlled scalar diffusion–convection–reaction systems with general spatially and time varying parameters defined on a $1 \leq r$–dimensional parallelepipedon. For this, it is assumed that the input relating state and gradient in a general nonlinear fashion is restricted to a $(r-1)$–dimensional hyperplane. The proposed approach is based on the implicit parametrization of the system state and the boundary input in terms of a basic output via a Volterra–type integral equation with operator kernel (IEOK). In order to resolve the implicit description, a series solution to the IEOK is determined, which is based on a recursive computation of the series coefficients. The absolute and uniform series convergence is verified by restricting the system parameters and the basic output to functions of a certain Gevrey class including non–analytic functions. Hence, prescribing a suitably chosen desired profile for the basic output directly yields the corresponding state and input trajectories by evaluating the series solution. The input trajectory thereby represents the feedforward control, which is required to realize the desired spatial–temporal paths for the basic output and state, respectively. For this, compatibility conditions defining admissible trajectories for the basic output are determined, which ensure that the state parametrization is consistent with the system's boundary conditions. In order to prescribe admissible trajectories, finite time transitions are considered between an initial stationary and a prescribed final profile along a pre–planned transition path. As already pointed out in the previous chapters, from a practical point of view this set–up corresponds to the transition between operating points — an import control task in thermal, chemical, and bio–chemical engineering as well as related areas.

The considered trajectory planning problem for diffusion–convection–reaction systems with spatially and time varying parameters and nonlinear boundary input is introduced in Section 7.1. By means of a suitable change of coordinates equivalence to a diffusion–reaction system is provided, whose flatness property is analyzed in Section 7.2. For this, a particular formal integration of the governing PDE is exploited to determine an implicit state and input parametrization in terms of a

T. Meurer: Control of Higher-Dimensional PDEs, CCE, pp. 189–219.
springerlink.com

flat or basic output and its spatial and time derivatives by means of a Volterra–type integral equation. Its explicit solution is obtained by utilizing a functional series ansatz, whose coefficients are computed recursively from the IEOK. The absolute and uniform series convergence is proven in certain Gevrey classes. Based on these results, the suitable assignment of desired trajectories for the basic output is considered in Section 7.3. Moreover, an extension of the formal integration approach to multiple input configurations is proposed in Section 7.4. Simulation results for diffusion–convection–reaction systems with 3–dimensional domain in Section 7.5 finally demonstrate the approach and the feedforward tracking behavior.

Notation. Differing from the previous chapter, where a functional analytic framework was used, subsequently the dependency of the system variables on the independent coordinates z and t is explicitly stated in any expression. This in particular enables a notational distinction, which is necessary for the rigorous formulation of the formal integration approach in view of the time–variant system setting.

7.1 Trajectory Planning Problem

Based on the general problem formulation in Chapter 5, subsequently the trajectory planning is considered for a parabolic diffusion–convection–reaction system with orthotropic diffusion and convection and a spatially and time varying reaction parameter $c(z,t)$, i.e. for $(z,t) \in \Omega \times \mathbb{R}^+_{t_0}$ consider

$$\partial_t x(z,t) = \sum_{j\in I_r} a_j(z^j)\partial^2_{z^j} x(z,t) + \sum_{j\in I_r} b_j(z^j)\partial_{z^j} x(z,t) + c(z,t)x(z,t) \quad (7.1a)$$

with $I_r = \{1,2,\ldots,r\}$, $r \geq 2$. The r–dimensional domain is given by the parallelepipedon

$$\Omega = \left\{ z \in \mathbb{R}^r \mid 0 < z^j < L_j,\ j \in I_r \right\} \quad (7.1b)$$

with positive finite constants L_j and $\mathbb{R}^+_{t_0} = \{t \in \mathbb{R} \mid t > t_0\}$. As pointed out in Section 2, this type of PDE covers a rather large class of systems describing, e.g., unsteady and orthotropic heat conduction in solids, orthotropic convective mass and heat transfer in linear shear flows, and chemical tubular reactors with time varying linear reaction kinetics [1, 2, 3]. General mixed or Robin boundary conditions are imposed according to

$$\epsilon^0_j \partial_{z^j} x(z,t) - p^0_j x(z,t) = 0, \qquad z^j = 0,\ j \in I_r \quad (7.1c)$$

$$\epsilon^1_j \partial_{z^j} x(z,t) + p^1_j x(z,t) = 0, \qquad z^j = L_j,\ j \in I_r \quad (7.1d)$$

for $t > t_0$. The input $u(z_{(i|)},t)$ with $z_{(i|)} = (z^j)_{j\in I^i_r} = (z^1,\ldots,z^{i-1},z^{i+1},\ldots,z^r)$ and $I^i_r = I_r \setminus \{i\}$, is restricted to the hyperplane $\partial\Omega_i = \{z \in \Omega \mid z^i = L_i\}$, i.e.

$$\theta\left(x(z,t), \partial_{z^i} x(z,t)\right) = u(z_{(i|)}, t), \qquad z^i = L_i,\ t > t_0. \tag{7.1e}$$

The consistent initial condition follows as

$$x(z,t_0) = x_0(z), \qquad z \in \overline{\Omega}. \tag{7.1f}$$

Since the PDE (7.1a) is assumed parabolic it follows necessarily that there exist positive finite constants a_j^l, a_j^u such that $a_j^l \leq a_j(z^j) \leq a_j^u$ for all $z^j \in [0, L_j]$, $j \in I_r$. Further assumptions on the system parameters are summarized below.

Assumption 7.1. The system parameters $a_j(z^j)$, $b_j(z^j)$, and $c(z,t)$ satisfy the following conditions:

(i) The parameters are such that $a_j(z^j) \in \mathcal{C}^2([0, L_j])$ and $b_j(z^j) \in \mathcal{C}^1([0, L_j])$ for $j \in I_r$ with $\mathcal{C}^s([0, L_j])$ the space of s–times continuously differentiable functions on the closed interval $[0, L_j]$.

(ii) The parameter $b_j(z^j)$, $j \in I_r$, representing the speed of convection in each direction z^j is assumed to be positive and bounded from above, i.e. $0 \leq b_j(z^j) \leq b_j^u$ for all $z^j \in [0, L_j]$, $j \in I_r$. In this case, the flow is directed in negative z^j–direction while flow reversal is excluded.

(iii) The parameter $c(z,t)$ representing, e.g., a reaction parameter is assumed to be bounded, i.e. $-\infty < c^l \leq c(z,t) \leq c^u < \infty$ for all $z \in \overline{\Omega}$ and $t \geq t_0$. Further requirements on the differentiability of $c(z,t)$ with respect to z and t are introduced below in the course of convergence analysis.

Remark 7.1. Note that the results presented below can be similarly applied to the case of flow reversal with $b_j^l \leq b_j(z^j) \leq b_j^u$ where $b_j^l < 0$ and $b_j^u > 0$. For this configuration an appropriate selection of the location of the input is decisive to be able to influence the flow in a desired fashion. However, this topic is not considered subsequently.

In the following, it is shown that (7.1) can be transformed into a simpler standard form by a suitable change of coordinates and a state transformation.

7.1.1 Transformation into Standard Form

By introducing the change of variables

$$z^j \mapsto \zeta^j = \bar{z}(z^j) := \int_0^{z^j} \frac{1}{\sqrt{a_j(s)}}\,\mathrm{d}s \quad \forall j \in I_r \tag{7.2a}$$

$$L_j \mapsto \bar{z}(L_j) \tag{7.2b}$$

$$x(z,t) \mapsto x(\zeta,t) e^{-\sum_{j\in I_r} g_j(\zeta^j)} \tag{7.2c}$$

where $\zeta = (\zeta^1, \zeta^2, \ldots, \zeta^r)$ and

$$g_j(\zeta^j) = \frac{1}{2}\int_0^{\zeta^j} \Big(a_j(z^j)\partial_{z^j}^2 \bar{z}(z^j) + b_j(z^j)\partial_{z^j}\bar{z}(z^j)\Big)\Big|_{z^j=(\bar{z})^{-1}(s)} \mathrm{d}s, \tag{7.2d}$$

it can be without loss of generality assumed that $a_j(z^j) \equiv 1$ and $b_j(z^j) \equiv 0$. With these transformations the reaction parameter $c(z,t)$ follows as

$$c(z,t) \mapsto c(z,t) - \sum_{j\in I_r} \big[\big(\partial_{\zeta^j} g_j(\zeta^j)\big)^2 + \partial_{\zeta^j}^2 g_j(\zeta^j)\big]. \tag{7.2e}$$

The parameters ϵ_j^0, p_j^0, ϵ_j^1, and p_j^1 for all $j \in I_r$ in the boundary conditions (7.1c), (7.1d) are mapped according to

$$\epsilon_j^0 \mapsto \epsilon_j^0,\ p_j^0 \mapsto \sqrt{a_j(0)}\, p_j^0 + \epsilon_j^0 \partial_{\zeta^j} g_j(\zeta^j)\big|_{\zeta^j=0} \tag{7.2f}$$

$$\epsilon_j^1 \mapsto \epsilon_j^1,\ p_j^1 \mapsto \sqrt{a_j(L_j)}\, p_j^1 - \epsilon_j^1 \partial_{\zeta^j} g_j(\zeta^j)\big|_{\zeta^j=\bar{z}(L_j)}. \tag{7.2g}$$

Only Dirichlet boundary conditions are preserved under the transformation (7.2a), (7.2c) while Neumann and mixed boundary conditions are mapped into mixed boundary conditions with coefficients ϵ_j^0, p_j^0, ϵ_j^1, and p_j^1 as defined in (7.2f) and (7.2g). The nonlinear inhomogeneous boundary condition (7.1e) can be identified from

$$\begin{aligned}
&\theta\big(x(z,t), \partial_{z^i} x(z,t)\big)\big|_{z^i=L_i} \\
&\quad \mapsto \theta\Big(x(\zeta,t)e^{-\sum_{j\in I_r} g_j(\zeta^j)}, \big[\partial_{\zeta^i} x(\zeta,t) - \partial_{\zeta^i} g_i(\zeta^i) x(\zeta,t)\big] \times \\
&\qquad\qquad \partial_{z^i}\bar{z}^i(z^i)|_{z^i=L_i} e^{-\sum_{j\in I_r} g_j(\zeta^j)}\Big)\Big|_{\zeta^i=\bar{z}^i(L_i)}
\end{aligned} \tag{7.2h}$$

$$u(z_{(i|)}, t) \mapsto u(\zeta_{(i|)}, \tau) \tag{7.2i}$$

with $\zeta_{(i|)} = (\zeta^1, \ldots, \zeta^{i-1}, \zeta^{i+1}, \ldots, \zeta^r)$. The transformed initial profile (7.1f) follows as

$$x_0(z) \mapsto x_0(\zeta) e^{-\sum_{j\in I_r} g_j(\zeta^j)}. \tag{7.2j}$$

The invertibility of the transformations as well as the properties of the transformed coefficients is analyzed in the following two remarks.

Remark 7.2. Since $a_j^l \le a_j(z^j) \le a_j^u$ due to the parabolic system character it follows that $\partial_{z^j}\bar{z}(z^j) = 1/\sqrt{a_j(z^j)} > 0$ for all $z^j \in [0, L_j]$, $j \in I_r$. This moreover ensures the invertibility of (7.2a).

Remark 7.3. Continuity and boundedness of the transformed quantities (7.2e)–(7.2j) depend on the properties of $g_j(\zeta^j)$, $j \in I_r$. For this, note that by Assumption 7.1(i) each of the terms

$$\partial_{z^j}\bar{z}(z^j) = \frac{1}{\sqrt{a_j(z^j)}}, \quad \partial_{z^j}^2 \bar{z} = -\frac{1}{2\sqrt[3]{a_j(z^j)}} \partial_{z^j} a_j(z^j)$$

is bounded, continuous, and once continuously differentiable with respect to z^j with bounded derivative. Hence, $g_j(\zeta^j) \in \mathcal{C}^2([0, \bar{z}(L_j)])$, $j \in I_r$, which implies the continuity and boundedness of the introduced mappings.

As a result, the consideration of the diffusion–convection–reaction system (7.1) is equivalent to the analysis of the linear parabolic diffusion–reaction system

$$\partial_t x(z,t) = \Delta x(z,t) + c(z,t)x(z,t), \qquad (z,t) \in \Omega \times \mathbb{R}^+_{t_0}. \tag{7.3a}$$

Since only Dirichlet boundary conditions are preserved under the transformations (7.2) general linear homogeneous boundary conditions

$$\epsilon^0_j \partial_{z^j} x(z,t) - p^0_j x(z,t) = 0, \qquad z^j = 0,\ j \in I_r \tag{7.3b}$$

$$\epsilon^1_j \partial_{z^j} x(z,t) + p^1_j x(z,t) = 0, \qquad z^j = L_j,\ j \in I^i_r \tag{7.3c}$$

with constants $\epsilon^0_j,\ p^0_j,\ \epsilon^1_j,\ p^1_j \in \mathbb{R}$ are considered on the $2r-1$ hyperplanes of the boundary $\partial\Omega$ of Ω to represent Dirichlet ($\epsilon^k_j = 0$, $p^k_j \neq 0$), Neumann ($\epsilon^k_j \neq 0$, $p^k_j = 0$), or Robin ($\epsilon^k_j \neq 0$, $p^k_j \neq 0$) boundary conditions for $t > t_0$. The input $u(z_{(i|)}, t)$ is restricted to the hyperplane $\partial\Omega_i = \{z \in \Omega \mid z^i = L_i\}$ and enters the system in a nonlinear fashion governed by the continuous functional $\theta(\cdot,\cdot)$, which combines the state and the gradient on $\partial\Omega_i$, i.e.

$$\theta\left(x(z,t), \partial_{z^i} x(z,t)\right) = u(z_{(i|)}, t), \qquad z^i = L_i \tag{7.3d}$$

for $t > t_0$ with the coordinate tuple $z_{(i|)} \in \Omega_i$, where

$$\Omega_i := \left\{ z_{(i|)} \in \mathbb{R}^{r-1} \mid 0 < z^j < L_j,\ j = I^i_r \right\} \tag{7.3e}$$

The consistent initial condition follows as

$$x(z, t_0) = x_0(z), \qquad z \in \overline{\Omega}. \tag{7.3f}$$

As pointed out in Section 5.1, for results on the existence and uniqueness of solutions to (7.3), the reader is referred to, e.g., [7, 12, 10, 6].

7.1.2 Boundary Control Problem

The considered boundary control problem is illustrated in Figure 7.1 for the 3–dimensional case, i.e. $r = 3$, with the input being restricted to the surface $z^3 = L_3$, i.e. $i = 3$. It should be pointed out that the considered model represents an idealized scenario with an infinite–dimensional input $u(z_{(i|)}, t)$ acting arbitrarily on the hyperplane $\partial\Omega_i$ for all $t \in \mathbb{R}^+_{t_0}$. However, in certain applications such as

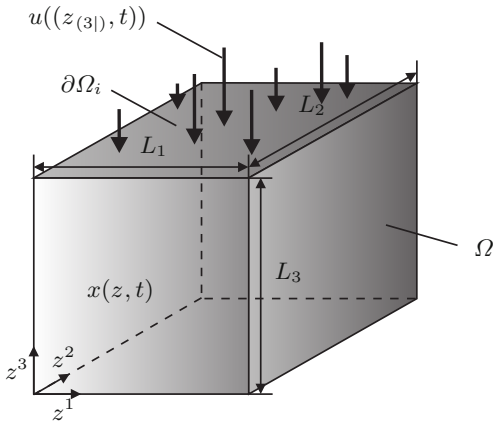

Fig. 7.1 Schematics of the parallelepipedon Ω for $r = 3$ and $i = 3$ with state $x(z,t)$ and boundary input $u((z_{(3|)}, t))$ acting on the surface $z^3 = L_3$

the cooling or reheating of metal slabs in steel industry this assumption is in good accordance with the plant configuration.

According to Section 5.2, the trajectory planning problem addresses the design of a feedforward control $u(z_{(i|)}, t)$ to realize the transition

$$x_0(z) = x(z, t_0) \xrightarrow[t\in[t_0,t_0+T]]{u(z_{(i|)},t)} x(z, t_0 + T) = x_T(z), \quad z \in \overline{\Omega} \tag{7.4}$$

from an initial stationary profile $x_0(z)$ to a desired final profile $x_T(z)$ along a prescribed spatial–temporal transition path within the finite time interval $t \in [t_0, t_0 + T]$. Here, T denotes the specified transition time. This configuration in particular includes the finite time transition problem between stationary profiles, where the final profile is required to satisfy $x(z,t) = x_T(z)$ for $t \geq t_0 + T$ with $x_T(z)$ representing a stationary solution to (7.3).

7.2 Formal State and Input Parametrization

In the following, a basic output $\xi(z_{(i|)}, t)$ is introduced for the diffusion–reaction system (7.3), which allows to formally parametrize the system state $x(z,t)$ and the boundary input $u(z_{(i|)}, t)$. Similar to the previous chapter, the assignment of a suitable trajectory $\xi^*(z_{(i|)}, t)$ for the basic output $\xi(z_{(i|)}, t)$ immediately provides the respective feedforward control $u^*(z_{(i|)}, t)$ to realize the corresponding state trajectory $x^*(z,t)$.

7.2.1 Construction of a Basic Output

In order to provide a systematic extension of the flatness approach to parabolic PDEs with spatially and time varying parameters with r–dimensional parallelepiped domain (7.1b) the appropriate formal integration of the governing PDE is exploited. While the underlying idea of a formal integration with respect to t is typically used for the analysis of the existence and the uniqueness of solutions, the formal integration with respect to a particular spatial coordinate z^i enables to derive an implicit state and input parametrization. For this, the PDE (7.3a) is first solved for $\partial_{z^i}^2 x(z,t)$ and is secondly formally integrated with respect to the z^i–coordinate. This yields a Volterra–type integral equation with operator kernel

$$\begin{aligned} x(z,t) = x(z_{(i|0)},t) + z^i \partial_{z^i} x(z_{(i|0)},t) + \int_0^{z^i} \int_0^{\eta} \Big(\partial_t x(z_{(i|\sigma)},t) \\ - c(z_{(i|\sigma)},t) x(z_{(i|\sigma)},t) - \sum_{j \in I_r^i} \partial_{z^j}^2 x(z_{(i|\sigma)},t) \Big) \mathrm{d}\sigma \mathrm{d}\eta, \end{aligned} \tag{7.5}$$

where $z_{(i|\sigma)} = (z^1, \ldots, z^{i-1}, \sigma, z^{i+1}, \ldots, z^r)$ for $\sigma \in [0, L_i]$. To determine the two constants of integration $x(z_{(i|0)},t)$ and $\partial_{z^i} x(z_{(i|0)},t)$ observe that only a single condition is available from the homogeneous boundary condition (7.3b) for $j = i$. Hence, by introducing an additional variable

$$\xi(z_{(i|)},t) = f_i^0 \partial_{z^i} x(z_{(i|)},t) + f_i^1 x(z_{(i|)},t) \tag{7.6}$$

with the function $\xi(z_{(i|)},t)$ serving as a degree–of–freedom, a linear system of equations is obtained, which can be solved for $x(z_{(i|0)},t)$ and $\partial_{z^i} x(z_{(i|0)},t)$ in terms of $\xi(z_{(i|)},t)$, i.e.

$$\begin{bmatrix} -p_i^0 & \epsilon_i^0 \\ f_i^1 & f_i^0 \end{bmatrix} \begin{bmatrix} x(z_{(i|0)},t) \\ \partial_{z^i} x(z_{(i|0)},t) \end{bmatrix} = \begin{bmatrix} 0 \\ \xi(z_{(i|)},t) \end{bmatrix}.$$

Assuming that $p_i^0 f_i^0 + \epsilon_i^0 f_i^1 \neq 0$, which is equivalent to the condition that the boundary condition (7.3b) for $j = i$ and the imposed condition (7.6) are linearly independent, it follows that

$$x(z_{(i|0)},t) = s_i^0 \xi(z_{(i|)},t) \tag{7.7}$$

$$\partial_{z^i} x(z_{(i|0)},t) = s_i^1 \xi(z_{(i|)},t), \tag{7.8}$$

where $s_i^0 = \epsilon_i^0 / (p_i^0 f_i^0 + \epsilon_i^0 f_i^1)$ and $s_i^1 = p_i^0 / (p_i^0 f_i^0 + \epsilon_i^0 f_i^1)$. Thus, (7.5) evaluates to

$$x(z,t) = \left(s_i^0 + z^i s_i^1\right)\xi(z_{(i|)},t) + \int_0^{z^i}\int_0^{\eta}\Big(\partial_t x(z_{(i|\sigma)},t) - c(z_{(i|\sigma)},t)x(z_{(i|\sigma)},t) - \sum_{j\in I_r^i}\partial_{z^j}^2 x(z_{(i|\sigma)},t)\Big)\mathrm{d}\sigma\mathrm{d}\eta. \tag{7.9}$$

For the explicit solution of the IEOK and the evaluation of the formal parametrization of $x(z,t)$ in terms of $\xi(z_{(i|)},t)$ the solution is expanded into a functional series

$$x(z,t) = \sum_{n=0}^{\infty} x_n(z,t), \tag{7.10a}$$

whose coefficients are determined recursively from (7.9), i.e.

$$x_0(z,t) = \left(s_i^0 + z^i s_i^1\right)\xi(z_{(i|)},t) \tag{7.10b}$$

$$x_n(z,t) = \int_0^{z^i}\int_0^{\eta}\Big(\partial_t x_{n-1}(z_{(i|\sigma)},t) - c(z_{(i|\sigma)},t)x_{n-1}(z_{(i|\sigma)},t) - \sum_{j\in I_r^i}\partial_{z^j}^2 x_{n-1}(z_{(i|\sigma)},t)\Big)\mathrm{d}\sigma\mathrm{d}\eta,\ n\geq 1. \tag{7.10c}$$

The recursion allows to deduce that any series coefficient $x_n(z,t)$, $n\in\mathbb{N}$, depends on $\xi(z_{(i|)},t)$ and its spatial and time derivatives. Hence, formally the relation $x_n(z,t) = x_n(z,t;\xi(z_{(i|)},t))$ is obtained, which in view of (7.10a) implies $x(z,t) = x(z,t;\xi(z_{(i|)},t))$. This property can be immediately exploited for the parametrization of the boundary input in terms of $\xi(z_{(i|)},t)$, which is obtained by formally substituting $x(z,t) = x(z,t;\xi(z_{(i|)},t))$ into (7.3d), i.e.

$$\begin{aligned} u(z_{(i|)},t) &= u(z_{(i|)},t;\xi(z_{(i|)},t)) \\ &= \theta\left(x(z_{(i|L_i)},t;\xi(z_{(i|)},t)), \partial_{z^i}x(z_{(i|L_i)},t;\xi(z_{(i|)},t))\right). \end{aligned} \tag{7.11}$$

In summary, state $x(z,t)$ and boundary input $u(z_{(i|)},t)$ can be formally parametrized in terms of $\xi(z_{(i|)},t)$ and its derivatives, which implies that $\xi(z_{(i|)},t)$ represents a basic output for the diffusion–reaction system (7.3). Nevertheless, the presented computations are so far only formal and their validation requires to ensure uniform convergence of the series (7.10a) with coefficients (7.10b), (7.10c).

7.2.2 Uniform Series Convergence in Gevrey Classes

For the proof of uniform convergence of the parametrized series (7.10) it is assumed that $\xi(z_{(i|)},t)$ is in the Gevrey class $G_{D_\xi,\beta,\alpha}(\Omega\times\mathbb{R}_{t_0}^+)$ of order (β,α) according to Definition B.2. Herein, note that multi–index notation (cf. Appendix A.2) is used to

address different Gevrey orders with respect to the independent coordinates z and t. For the sake of simplicity, all components of $\beta = (\beta^1, \beta^2, \ldots, \beta^r)$ are assumed to coincide.

7.2.2.1 Spatially and Time Varying Gevrey Class Reaction Parameter

If the parameter $c(z,t)$ is a function of the coordinate tuple z and time t, then the main convergence result can be formulated as follows.

Theorem 7.1. *Let* $c(z,t) \in G_{D_c,\beta,\alpha}(\Omega \times \mathbb{R}^+_{t_0})$ *and* $\xi(z_{(i|)},t) \in G_{D_\xi,\beta,\alpha}(\Omega_i \times \mathbb{R}^+_{t_0})$ *with* $\beta \geq 1$ *and* $\alpha \geq 1$. *Then the series coefficients* (7.10b), (7.10c) *satisfy*

$$\begin{aligned} &\sup_{(z_{(i|)},t)\in\Omega_i\times\mathbb{R}^+_{t_0}} \left|\partial^l_{z_{(i|)}}\partial^k_t x_n(z,t)\right| \\ &\leq D^{k+|l|+2n+1}(l+2n)!^\beta (k+n)!^\alpha M_n^{\beta,\alpha,D}\left(s_i^0\frac{(z^i)^{2n}}{(2n)!}+s_i^1\frac{(z^i)^{2n+1}}{(2n+1)!}\right) \end{aligned} \tag{7.12}$$

with $D = \max\{D_c, D_\xi\}$, $l = (l^1, l^2, \ldots, l^{i-1}, l^{i+1}, \ldots, l^r) \in \mathbb{N}^{r-1}$, $(l+2n)! = ((l^1+2n)!, \ldots, (l^{i-1}+2n)!, (l^{i+1}+2n)!, \ldots, (l^r+2n)!) \in \mathbb{N}^{r-1}$, $k \in \mathbb{N}$, *and*

$$M_n^{\beta,\alpha,D} = \begin{cases} 1, & n = 0 \\ \prod_{p=1}^n \left[\frac{1}{D\,(2p(2p-1))^{\beta(r-1)}}\left(1+\frac{1}{p^\alpha}\right)\right. & \\ \quad \left. +\frac{1}{p^\alpha}\frac{r-1}{(2p(2p-1))^{\beta(r-2)}}\right], & n > 0. \end{cases} \tag{7.13}$$

In particular, the series (7.10a) *converges absolutely and uniformly if* $\beta = 1$ *and* $1 \leq \alpha \leq 2$ *for all* $z \in \Omega$ *with* $|z^i| < \rho$, *where*

$$\rho = \begin{cases} \frac{1}{D\sqrt{r-1+\frac{1}{4}\delta_{\alpha,2}}}, & D \geq 1 \\ \frac{1}{\sqrt{D(r-1+\frac{1}{4}\delta_{\alpha,2})}}, & D < 1. \end{cases} \tag{7.14}$$

Obviously, the radius of convergence is proportional to the inverse of the square root of the problem dimension r and depends on the constant D of the Gevrey estimate for the reaction term $c(z,t)$ and the trajectory for the basic output $\xi(z_{(i|)},t)$.

Proof. The proof of Theorem 7.1 follows by induction. Due to the dependence of the recursion (7.10c) on z and t and the appearance of derivatives of $x_{n-1}(z,t)$ with respect to $z_{(i|)}$ and t, the convergence analysis of the series (7.10a) requires to analyze the growth of the derivatives of each $x_n(z,t)$, $n \in \mathbb{N}$ up to an arbitrary order, say $l \in \mathbb{N}^r$ with respect to $z_{(i|)}$ and $k \in \mathbb{N}$ with respect to t. Once this is obtained, the absolute and uniform convergence of the series (7.10a) can be evaluated by taking $l = 0$ and $k = 0$ in the upper bound for $|\partial^l_{z_{(i|)}}\partial^k_t x_n(z,t)|$. Since $D = \max\{D_c, D_\xi\}$, without loss of generality $D_c = D_\xi = D$ can be substituted in the Gevrey estimates. Hence, observe that for $n = 0$, (7.12) yields

$$\sup_{(z_{(i|)},t)\in\Omega_i\times\mathbb{R}^+_{t_0}} \left|\partial^l_{z_{(i|)}}\partial^k_t x_0(z,t)\right| \le D^{k+|l|+1}(l)!^\beta(k)!^\alpha \left(s_i^0+s_i^1 z^i\right),$$

which directly corresponds to the starting condition (7.10b) given by $\xi(z_{(i|)},t)\in G_{D,\beta,\alpha}(\Omega_i\times\mathbb{R}^+_{t_0})$. Assuming that (7.12) holds for all $n=0,1,\ldots,N-1$, $N\ge 1$, it follows from (7.10c) that

$$\begin{aligned}
&\sup_{(z_{(i|)},t)\in\Omega_i\times\mathbb{R}^+_{t_0}} \left|\partial^l_{z_{(i|)}}\partial^k_t x_N(z,t)\right| \\
&\le \sup_{(z_{(i|)},t)\in\Omega_i\times\mathbb{R}^+_{t_0}} \int_0^{z^i}\int_0^{\eta}\Big(\left|\partial^l_{z_{(i|)}}\partial^{k+1}_t x_{N-1}(z,t)\right| \\
&\qquad + \left|\partial^l_{z_{(i|)}}\partial^k_t\left[c(z,t)x_{N-1}(z,t)\right]\right| \\
&\qquad + \left|\partial^l_{z_{(i|)}}\partial^k_t\sum_{j\in I^i_r}\partial^2_{z^j}x_{N-1}(z,t)\right|\Big)\Big|_{z^i=\sigma}\mathrm{d}\sigma\mathrm{d}\eta.
\end{aligned} \tag{7.15}$$

Since by assumption $c(z,t)\in G_{D,\beta,\alpha}(\Omega\times\mathbb{R}^+_{t_0})$ the successive differentiation of the product $c(z,t)x_{N-1}(z,t)$ can be majorized utilizing (7.12) together with (B.18) and (B.23) introduced in Lemmas B.6 and B.7 of Appendix B.4 to obtain

$$\begin{aligned}
&\sup_{(z_{(i|)},t)\in\Omega_i\times\mathbb{R}^+_{t_0}} \left|\partial^l_{z_{(i|)}}\partial^k_t\left[c(z,t)x_{N-1}(z,t)\right]\right| \\
&\le D^{k+|l|+2N}M^{\beta,\alpha,D}_{N-1}\left(\frac{s_i^0(z^i)^{2N-2}}{(2N-2)!}+\frac{s_i^1(z^i)^{2N-1}}{(2N-1)!}\right)\times \\
&\quad\sum_{\gamma_0=0}^{k}\binom{k}{\gamma_0}\sum_{\gamma=0}^{l}\binom{l}{\gamma}(l-\gamma)!^\beta(k-\gamma_0)!^\alpha(\gamma+2N-2)!^\beta(\gamma_0+N-1)!^\alpha \\
&\overset{(B.18)}{\le} D^{k+|l|+2N}M^{\beta,\alpha,D}_{N-1}\left(\frac{s_i^0(z^i)^{2N-2}}{(2N-2)!}+\frac{s_i^1(z^i)^{2N-1}}{(2N-1)!}\right)\times \\
&\quad\left(\frac{(k+N)!}{N}\right)^\alpha\prod_{j\in I^i_r}\left(\frac{(l^j+2N-1)!}{2N-1}\right)^\beta.
\end{aligned}$$

Here, $\gamma=(\gamma^1,\ldots,\gamma^{i-1},\gamma^{i+1},\ldots,\gamma^r)$ and $(\gamma+2N-2)!=((\gamma^1+2N-2)!,\ldots,(\gamma^{i-1}+2N-2)!,(\gamma^{i+1}+2N-2)!,\ldots,(\gamma^r+2N-2)!)$ are multi–indexes of the same dimension as l and the inequality $\sum_j a_j^\kappa\le(\sum_j a_j)^\kappa$ for $\kappa\ge 1$ and $a_j\ge 0$ was used (see, e.g., [8]) since $\beta\ge 1$ by assumption. Together with (B.19) Eqn. (7.15) can be evaluated to obtain

$$\begin{aligned}
&\sup_{(z_{(i|)},t)\in\Omega_i\times\mathbb{R}^+_{t_0}} \left|\partial^l_{z_{(i|)}}\partial^k_t x_N(z,t)\right| \le M^{\beta,\alpha,D}_{N-1}\left(\frac{s_i^0(z^i)^{2N}}{(2N)!}+\frac{s_i^1(z^i)^{2N+1}}{(2N+1)!}\right)\times \\
&\quad\Big\{D^{k+|l|+2N}((l+2N-2)!)^\beta(k+N)!^\alpha
\end{aligned}$$

$$+ D^{k+|l|+2N} \left(\frac{(k+N)!}{N} \right)^{\alpha} \prod_{j \in I_r^i} \left(\frac{(l^j + 2N - 1)!}{2N-1} \right)^{\beta}$$

$$+ D^{k+|l|+2N+1} (k+N-1)!^{\alpha} \sum_{j \in I_r^i} \prod_{p \in I_r i} (l^p + 2(N-1) + 2\delta_{p,j})!^{\beta} \Bigg\}$$

and hence

$$\sup_{(z_{(i|)},t) \in \Omega_i \times \mathbb{R}_{t_0}^+} \left| \partial_{z_{(i|)}}^l \partial_t^k x_N(z,t) \right| \leq$$

$$D^{k+|l|+2N+1} (l+2N)!^{\beta} (k+N)!^{\alpha} M_{N-1}^{\beta,\alpha,D} \left(\frac{s_i^0 (z^i)^{2N}}{(2N)!} + \frac{s_i^1 (z^i)^{2N+1}}{(2N+1)!} \right) \times$$

$$\Bigg\{ \frac{1}{D} \Bigg(\prod_{j \in I_r^i} \frac{1}{[(l^j + 2N)(l^j + 2N - 1)]^{\beta}}$$

$$+ \frac{1}{(2N-1)^{\beta(r-1)} N^{\alpha}} \prod_{j \in I_r^i} \frac{1}{(l^j + 2N)^{\beta}} \Bigg)$$

$$+ \frac{1}{(k+N)^{\alpha}} \sum_{j \in I_r^i} \prod_{p \in I_r^i} \left(\frac{(l^p + 2(N-1) + 2\delta_{p,j})!}{(l^p + 2N)!} \right)^{\beta} \Bigg\}.$$

Since $k \geq 0$ and $l^j \geq 0$ for all $j \in I_r i$, the latter expression simplifies to

$$\sup_{(z_{(i|)},t) \in \Omega_i \times \mathbb{R}_{t_0}^+} \left| \partial_{z_{(i|)}}^l \partial_t^k x_N(z,t) \right|$$

$$\leq D^{k+|l|+2N+1} (l+2N)!^{\beta} (k+N)!^{\alpha} \left(\frac{s_i^0 (z^i)^{2N}}{(2N)!} + \frac{s_i^1 (z^i)^{2N+1}}{(2N+1)!} \right) \times$$

$$M_{N-1}^{\beta,\alpha,D} \left(\frac{1}{D \left(2N(2N-1)\right)^{\beta(r-1)}} \left[1 + \frac{1}{N^{\alpha}} \right] \right.$$

$$\left. + \frac{1}{N^{\alpha}} \frac{r-1}{(2N(2N-1))^{\beta(r-2)}} \right)$$

$$= D^{k+|l|+2N+1} (l+2N)!^{\beta} (k+N)!^{\alpha} M_N^{\beta,\alpha,D} \left(\frac{s_i^0 (z^i)^{2N}}{(2N)!} + \frac{s_i^1 (z^i)^{2N+1}}{(2N+1)!} \right),$$

which is identical to (7.12) for $n = N$ and hence proves the first result.

For the determination of the radius of convergence of the respective series note that

$$M_N^{\beta,\alpha,D} \leq \begin{cases} M_N^{\beta,\alpha}, & D \geq 1 \\ \frac{1}{D^N} M_N^{\beta,\alpha}, & D < 1, \end{cases}$$

where $M_N^{\beta,\alpha} = M_N^{\beta,\alpha,1}$. Depending on D, the series (7.10a) can thus be majorized using the bound (7.12) evaluated for $l = 0$ and $k = 0$, i.e.

$$\begin{aligned}|x(z,t)| \leq \sum_{n=0}^{\infty} |x_n(z,t)| \leq \sum_{n=0}^{\infty} D^{2n+1}(2n)!^{\beta(r-1)}(n)!^{\alpha} M_n^{\beta,\alpha,D} \times \\ \left(\frac{s_i^0 (z^i)^{2n}}{(2n)!} + \frac{s_i^1 (z^i)^{2n+1}}{(2n+1)!}\right) \\ \leq D\big(|s_i^0| + L_i |s_i^1|\big) \sum_{n=0}^{\infty} a_n \left(\eta^2\right)^n, \end{aligned} \tag{7.16}$$

where

$$a_n = (2n)!^{\beta(r-1)-1}(n)!^{\alpha} M_n^{\beta,\alpha}$$

and $\eta = Dz^i$ if $D \geq 1$ and $\eta = \sqrt{D} z^i$ if $D < 1$. Since (7.16) constitutes a power series in η^2 its radius of convergence ρ can be determined explicitly. From (7.13) it follows for $n \geq 1$ that

$$\begin{aligned} M_n^{\beta,\alpha} &= \prod_{p=1}^{n} \frac{1}{(2p(2p-1))^{\beta(r-2)}} \prod_{p=1}^{n} \frac{1}{p^{\alpha}} \left(r - 1 + \frac{1+p^{\alpha}}{(2p(2p-1))^{\beta}}\right) \\ &= \frac{1}{(2n)!^{\beta(r-2)}} \frac{1}{(n)!^{\alpha}} \prod_{p=1}^{n} \left(r - 1 + \frac{1+p^{\alpha}}{(2p(2p-1))^{\beta}}\right). \end{aligned} \tag{7.17}$$

With this, the series coefficient a_n evaluates to

$$a_n = \begin{cases} 1, & n = 0 \\ (2n)!^{\beta-1} \prod_{p=1}^{n} \left(r - 1 + \frac{1+p^{\alpha}}{(2p(2p-1))^{\beta}}\right), & n \geq 1 \end{cases}$$

such that the quotient a_n / a_{n-1} is given by

$$\frac{a_n}{a_{n-1}} = \begin{cases} 2^{\beta-1}(r-1) + 1, & n = 1 \\ \frac{r-1}{(2n(2n-1))^{1-\beta}} + \frac{1+n^{\alpha}}{2n(2n-1)}, & n \geq 2 \end{cases} \tag{7.18}$$

As $n \to \infty$ the first term of the quotient can be only bounded if $1 - \beta \geq 0$, which in view of the assumption that $\beta \geq 1$ yields that $\beta = 1$. In addition, since the denominator of the second term of the quotient is of the order n^2, boundedness restricts α to the interval $1 \leq \alpha \leq 2$. In this case, it follows for $n \geq 2$ that $b_n = (1 + n^{\alpha})/(2n(2n-1)) < 1$ with $\lim_{n\to\infty} b_n = 0$ if $1 \leq \alpha < 2$ and $\lim_{n\to\infty} b_n = 1/4$ if $\alpha = 2$. Hence, $a_1/a_0 = r$ while $a_n/a_{n-1} < r$ for $n \geq 2$, which implies that $a_n \leq r^n$ with equality only in the cases $n = 0,\ 1$. As a result, the majorization $\sum_{n=0}^{\infty} a_n \left(\eta^2\right)^n < \sum_{n=0}^{\infty} \left(r\eta^2\right)^n$ implies the absolute convergence of the series (7.10a) with coefficients (7.10b), (7.10c) given $\beta = 1$ and $1 \leq \alpha \leq 2$.

The respective radius of convergence ρ_{η^2} with respect to η^2 is obtained from the quotient criterion

$$\rho_{\eta^2} = \lim_{n\to\infty} \frac{a_{n-1}}{a_n} = \lim_{n\to\infty} \frac{2n(2n-1)}{(2n(2n-1))^{\beta}(r-1)+1+n^{\alpha}},$$

which for $\beta = 1$ and $1 \leq \alpha \leq 2$ yields

$$\rho_{\eta^2} = \lim_{n\to\infty} \frac{1}{r-1+\frac{1+n^{\alpha}}{2n(2n-1)}} = \begin{cases} \frac{1}{r-1}, & 1 \leq \alpha < 2 \\ \frac{1}{r-\frac{3}{4}}, & \alpha = 2. \end{cases}$$

Recalling that $\eta = Dz^i$ if $D \geq 1$ and $\eta = \sqrt{D}z^i$ if $D < 1$, the radius of convergence in z^i follows according to (7.14), which proves Theorem 7.1. □ □

Remark 7.4. Theorem 7.1 includes the case $c(z,t) \in G_{D_c,\beta,\alpha_c}(\Omega \times \mathbb{R}^+_{t_0})$ and $\xi(z_{(i|)},t) \in G_{D_\xi,\beta,\alpha_\xi}(\Omega \times \mathbb{R}^+_{t_0})$ for different Gevrey orders $0 \leq \alpha_c \leq 2$ and $0 \leq \alpha_\xi \leq 2$. In order to apply Theorem 7.1 the condition on the Gevrey order α transfers to $\max\{1, \alpha_c, \alpha_\xi\} \leq \alpha \leq 2$.

Remark 7.5. The proof of Theorem 7.1 implies that $c(z,t)$ has to be only continuous in the coordinate z^i. This is due to the fact that the parametrization (7.9) or (7.10), respectively, only involves differentiations with respect to z^j, $j \in I^i_r$.

7.2.2.2 Time Varying Gevrey Class Reaction Parameter

In addition, if the reaction term $c(z,t)$ is only a function of time, i.e. $c(z,t) = c(t)$, an infinite radius of convergence of the parametrization (7.9), (7.10) can be deduced provided that $\xi(z_{(i|)},t)$ is an entire function in Ω_i.

Proposition 7.1. *Let* $c(z,t) \equiv c(t) \in G_{D_c,0,\alpha}(\mathbb{R}^+_{t_0})$ *and* $\xi(z_{(i|)},t) \in G_{D_\xi,\beta,\alpha}(\Omega_i \times \mathbb{R}^+_{t_0})$ *with* $0 \leq \beta < 1$ *and* $\alpha \geq 1$. *Then the series coefficients* (7.10b), (7.10c) *satisfy* (7.12), (7.13). *In particular, the series* (7.10a) *converges absolutely and uniformly if* $1 \leq \alpha \leq 2$ *for all* $z \in \Omega$ *with* $|z^i| < \rho$, *where*

$$\rho = \begin{cases} \infty, & 1 \leq \alpha < 2,\ \forall D \\ \frac{4}{D}, & \alpha = 2,\ D \geq 1 \\ \frac{4}{\sqrt{D}}, & \alpha = 2,\ D < 1. \end{cases} \tag{7.19}$$

The proof of Proposition 7.1 is subsequently only briefly sketched since it follows in principle directly the lines of the proof of Theorem 7.1.

Proof. Since the evaluation of (7.12), (7.13) for $n = 0$ corresponds to the assumption $\xi(z_{(i|)},t) \in G_{D_\xi,\beta,\alpha}(\Omega_i \times \mathbb{R}^+_{t_0})$ proceed by induction. Given $c(z,t) \equiv c(t) \in G_{D_c,0,\alpha}(\mathbb{R}^+_{t_0})$, it follows with (B.18), $D = \max\{D_c, D_\xi\}$, and $\alpha \geq 1$ that

$$
\begin{aligned}
&\sup_{(z_{(i|)},t)\in\Omega_i\times\mathbb{R}^+_{t_0}} \left|\partial^l_{z_{(i|)}}\partial^k_t\left[c(t)x_{N-1}(z,t)\right]\right| \\
&\leq D^{k+|l|+2N}(l+2N-2)!^{\beta} M^{\beta,\alpha,D}_{N-1}\left(\frac{s^0_i(z^i)^{2N-2}}{(2N-2)!}+\frac{s^1_i(z^i)^{2N-1}}{(2N-1)!}\right)\times \\
&\quad \sum_{\gamma_0=0}^{k}\binom{k}{\gamma_0}(k-\gamma_0)!^{\alpha}(\gamma_0+N-1)!^{\alpha} \\
&\leq D^{k+|l|+2N}(l+2N-2)!^{\beta}\left(\frac{(k+N)!}{N}\right)^{\alpha}\times \\
&\quad M^{\beta,\alpha,D}_{N-1}\left(\frac{s^0_i(z^i)^{2N-2}}{(2N-2)!}+\frac{s^1_i(z^i)^{2N-1}}{(2N-1)!}\right).
\end{aligned}
$$

By proceeding along the proof of the first part of Theorem 7.1 the bound (7.12) on the composite derivatives of the series coefficients $x_n(z,t)$, $n\in\mathbb{N}$ can be directly determined.

For the investigation of the convergence behavior of the series (7.10a) with coefficients (7.10b), (7.10c) parametrized in terms of $\xi(z_{(i|)},t)$, recall that (7.16) holds similarly if $c(z,t)\equiv c(t)$. Hence the quotient criterion can be applied to deduce the respective radius of convergence. For this, recall from the proof of Theorem 7.1 that by (7.18) the quotient $a_n/a_{n-1}\leq r$ for $n\geq 1$ given $\beta<1$ and $1\leq\alpha\leq 2$. Thus, the majorization $\sum_{n=0}^{\infty}a_n\left(\eta^2\right)^n<\sum_{n=0}^{\infty}\left(r\eta^2\right)^n$ is obtained, which proves the absolute convergence of the series (7.10a). With $\beta<1$, the respective radius of convergence ρ_{η^2} with respect to η^2 follows as

$$
\begin{aligned}
\rho_{\eta^2} &= \lim_{n\to\infty}\frac{a_{n-1}}{a_n}=\lim_{n\to\infty}\frac{2n(2n-1)}{(2n(2n-1))^{\beta}(r-1)+1+n^{\alpha}} \\
&= \begin{cases}\infty, & 1\leq\alpha<2\\ 4, & \alpha=2.\end{cases}
\end{aligned}
$$

Since $\eta=Dz^i$ if $D\geq 1$ and $\eta=\sqrt{D}z^i$ if $D<1$, the radius of convergence in z^i is given by (7.19), which proves the proposition. □

7.2.2.3 Reduction to the 1–Dimensional Setting

Besides the multi–dimensional case with $r>1$, the obtained parametrization and convergence results can be similarly applied to the 1–dimensional case. For this, let $r=1$ and $z=z^i=z^1$, $I^i_r=\emptyset$, and $\Omega=(0,L)$. Thus, the following result holds.

Corollary 7.1. *Let $r=1$, $c(z,t)\in G_{D_c,\beta,\alpha}(\Omega\times\mathbb{R}^+_{t_0})$, and $\xi(t)\in G_{D_\xi,\alpha}(\mathbb{R}^+_{t_0})$ with $\beta\geq 0$ and $\alpha\geq 1$, then the series coefficients* (7.10b)*,* (7.10c) *satisfy*

$$\begin{aligned}&\sup_{t\in\mathbb{R}^+_{t_0}}\left|\partial_t^k x_n(z,t)\right|\\&\leq D^{k+n+1}(k+n)!^\alpha\prod_{p=0}^{n}\left(1+\frac{1-\delta_{p,0}}{\delta_{p,0}+p^\alpha}\right)\left(s_i^0\frac{z^{2n}}{(2n)!}+s_i^1\frac{z^{2n+1}}{(2n+1)!}\right)\end{aligned}\tag{7.20}$$

with $D=\max\{D_c,D_\xi\}$. *In particular, the series* (7.10a) *converges uniformly for arbitrary* $\beta\geq 0$ *for all* $|z|<\rho$, *where*

$$\rho=\begin{cases}\infty, & 1\leq\alpha<2\\ \frac{1}{2\sqrt{D}}, & \alpha=2.\end{cases}\tag{7.21}$$

Proof. Since $I_r^i=\emptyset$, i.e. the recursion (7.10c) does not involve differentiations with respect to spatial coordinate, the first result (7.20) can be directly deduced from the respective proof of Theorem 7.1 by substituting $r=1$ and $\beta=0$. The valuation of (7.20) for $k=0$ yields

$$\begin{aligned}|x(z,t)|&\leq\sum_{n=0}^{\infty}|x_n(z,t)|\\&\leq\sum_{n=0}^{\infty}D^{n+1}(n)!^\alpha\prod_{p=0}^{n}\left(1+\frac{1-\delta_{p,0}}{\delta_{p,0}+p^\alpha}\right)\left(\frac{s_i^0z^{2n}}{(2n)!}+\frac{s_i^1z^{2n+1}}{(2n+1)!}\right)\\&\leq D\big(|s_i^0|+L_i|s_i^1|\big)\underbrace{\sum_{n=0}^{\infty}\frac{(n)!^\alpha}{(2n)!}\prod_{p=0}^{n}\left(1+\frac{1-\delta_{p,0}}{\delta_{p,0}+p^\alpha}\right)}_{=a_n}\big(\eta^2\big)^n,\end{aligned}\tag{7.22}$$

where $\eta=\sqrt{D}z$. Noting

$$\begin{aligned}&\prod_{p=0}^{n}\left(1+\frac{1-\delta_{p,0}}{\delta_{p,0}+p^\alpha}\right)=\prod_{p=1}^{n}\frac{1}{p^\alpha}\prod_{p=1}^{n}(1+p^\alpha)=(n!)^{-\alpha}\prod_{p=1}^{n}(1+p^\alpha)\\&\quad\leq(n)!^{-\alpha}(n+1)!^\alpha\end{aligned}$$

for $n\geq 1$, it follows that $a_n\leq(n+1)!^\alpha/(2n)!$. With these preparations the asserted radius of convergence (7.21) of the power series (7.22) can be directly determined by making use of the Cauchy–Hadamard theorem. □

7.2.2.4 Remarks

It has to be emphasized that the convergence result for the 1–dimensional case is independent of any additional analyticity property of $c(z^1,t)$. With this, an extensions of the results proposed, e.g., in [11, 13] is achieved, where the parameter $c(z^1,t)$ is restricted to analytic functions in z^1.

Furthermore, a comparison of Theorem 7.1 for the $2 \leq r$–dimensional case with Corollary 7.1 for the 1–dimensional case clearly reveals the appearance of an additional analyticity restriction on the system parameter $c(z,t)$ and the basic output $\xi(z_{(i|)},t)$ if $r \geq 2$. This is in particular due to the necessity to study differentiations of the variables with respect to the coordinate set $z_{(i|)}$.

With the verification of absolute and uniform convergence of the series solution (7.10) to the IEOK (7.9) in terms of the basic output $\xi(z_{(i|)},t)$ a solution to the trajectory planning problem of Section 7.1 is obtained. In addition, the analysis provides a constructive proof of controllability since it directly yields the input required to reach a certain final profile starting from a given initial condition. As illustrated below, for this additional restrictions on the basic output arising from the remaining homogeneous boundary conditions (7.3b) and (7.3c) have to be taken into account.

7.3 Admissible Trajectory Assignment for the Basic Output

The explicit evaluation of the determined parametrizations requires the assignment of suitable trajectories for the basic output satisfying the conditions of Theorem 7.1 or Proposition 7.1, respectively. In order to address their proper determination, subsequently the realization of finite time transitions between a stationary initial profile $x(z,t_0) = x_0(z)$ and a final possibly time varying profile $x(z,t) = x_T(z,t)$ for $t \geq t_0 + T$ with arbitrary prescribed transition time T is considered. Herein, the spatial–temporal transition path $x^*(z,t)$ is assigned in terms of a suitably planned desired trajectory $\xi^*(z_{(i|)},t)$ for the basic output $\xi(z_{(i|)},t)$. In view of (7.6), this immediately determines the evolution of $\xi(z_{(i|)},t) = f_i^0 \partial_{z^i} x(z,t)|_{z^i=0} + f_i^1 x(z,t)|_{z^i=0}$ on the hyperplane $z^i = 0$, which is crucial for trajectory planning.

7.3.1 Stationary Profiles

Differing from PDEs with time–invariant parameters the analysis of stationary profiles for the time varying case becomes more involved. Hence, given (7.3) a stationary profile at $t = t_s \geq t_0$ requires that the following equations are satisfied for all $t \geq t_s$, i.e.

$$\Delta x_s(z) + c(z,t)x_s(z) = 0, \qquad z \in \Omega \tag{7.23a}$$

$$\epsilon_j^0 \partial_{z^j} x_s(z) - p_j^0 x_s(z) = 0, \qquad z^j = 0,\ j \in I_r \tag{7.23b}$$

$$\epsilon_j^1 \partial_{z^j} x_s(z) + p_j^1 x_s(z) = 0, \qquad z^j = L_j,\ j \in I_r^i \tag{7.23c}$$

$$f_i^0 \partial_{z^i} x_s(z) + f_i^1 x_s(z) = \xi_s^*(z_{(i|)}), \qquad z^i = 0, \tag{7.23d}$$

where $\xi_s^*(z_{(i|)})$ denotes the time–invariant stationary profile for $\xi^*(z_{(i|)},t)$ and $c(z,t) = c_s(z)$ for all $t \geq t_s$ if $x_s(z) \neq 0$. If $\xi_s^*(z_{(i|)}) = 0$, then $x_s(z) = 0$ is a

stationary profile independent of $c(z,t)$. Otherwise, the demands on both $\xi^*(z_{(i|)},t)$ and $c(z,t)$ imply that both functions are locally non–analytic with respect to the time coordinate at $t = t_s$. Hence if $c(z,t) \in G_{D_c,\beta,\alpha}(\Omega \times \mathbb{R}^+_{t_0})$ with $\alpha \leq 1$, no stationary solution exists.

Subsequently, $x_s(z;\xi^*_s(z_{(i|)})) = x_s(z)$ is called a stationary profile depending on $\xi^*_s(z_{(i|)})$ if it fulfills the BVP (7.23). Due to the parametrization property introduced in Section 7.2.1, it is possible to express stationary profiles in terms of $\xi^*_s(z_{(i|)})$. Hence, different choices for $\xi^*_s(z_{(i|)})$ result in different stationary profiles $x_s(z;\xi^*_s(z_{(i|)}))$. Thereby, the corresponding input for $t \geq t_s$ follows directly from the evaluation of (7.3d) with $x(z,t)$ replaced by $x_s(z;\xi^*_s(z_{(i|)}))$, i.e.

$$u_s(z_{(i|)}) = \theta\left(x_s(z_{(i|L_i)};\xi^*_s(z_{(i|)})), \partial_{z^i} x_s(z_{(i|L_i)};\xi^*_s(z_{(i|)}))\right). \tag{7.24}$$

7.3.2 Admissible Trajectories for the Basic Output

In the following, so–called admissible trajectories for the basic output are introduced, which rely on the assumption below.

Assumption 7.2. The initial profile (7.3f) is stationary, i.e. $x_0(z) = x_s(z;\xi^*_0(z_{(i|)}))$, and is parametrizable in terms of $\xi^*(z_{(i|)},t_0) = \xi^*_0(z_{(i|)})$. Furthermore, $\xi^*(z_{(i|)},t)$ and $c(z,t)$ satisfy the convergence conditions of Theorem 7.1, i.e. $\xi(z_{(i|)},t) \in G_{D_\xi,1,\alpha}(\Omega_i \times \mathbb{R}^+_{t_0})$ and $c(z,t) \in G_{D_c,1,\alpha}(\Omega \times \mathbb{R}^+_{t_0})$ with $1 < \alpha \leq 2$.

As pointed out above, $1 < \alpha \leq 2$ ensures that $\xi(z_{(i|)},t)$ and $c(z,t)$ are non–analytic in t, which is necessary for the existence of a stationary solution. With these preparations, the notion of an admissible trajectory can be introduced.

Definition 7.1 (Admissible trajectory). The desired trajectory $\xi^*(z_{(i|)},t)$ for the basic output $\xi(z_{(i|)},t)$ is said to be admissible if it satisfies the two compatibility conditions

$$\begin{aligned} C_1: \quad & \xi^*(z_{(i|)},t_0) = \xi^*_0(z_{(i|)}) \\ & \partial^k_t \xi^*(z_{(i|)},t)|_{t=t_0} = 0, \quad \forall k \in \mathbb{N}. \end{aligned} \tag{7.25}$$

$$\begin{aligned} C_2: \quad & \epsilon^0_j \partial_{z^j} x^*_n(z,t) - p^0_j x^*_n(z,t) = 0, \quad z^j = 0,\ j \in I_r \\ & \epsilon^1_j \partial_{z^j} x^*_n(z,t) + p^1_j x^*_n(z,t) = 0, \quad z^j = L_j,\ j \in I^i_r \end{aligned} \tag{7.26}$$

for each $n \in \mathbb{N}$ and $t \geq t_0$, where $x^*_n(z,t)$ denotes the series coefficient $x_n(z,t)$ determined recursively according to (7.10b), (7.10c) with $\xi(z_{(i|)},t)$ replaced by $\xi^*(z_{(i|)},t)$.

Condition C_1 ensures that $\xi^*(z_{(i|)},t)$ connects smoothly to the initial stationary profile $x_0(z) = x_s(z;\xi^*_0(z_{(i|)}))$. In addition, due to Liouville's theorem C_1 implies that if $\xi^*(z_{(i|)},t)$ is non–constant for $t > t_0$ it has to be non–analytic at $t = t_0$. Condition C_2 ensures consistency in the sense that the parametrization (7.9) in terms

of the basic output has to satisfy the homogeneous boundary conditions (7.3b) and (7.3c). Note that by construction any coefficient $x_n(z,t)$, $n \in \mathbb{N}$, parametrized in terms of $\xi(z_{(i|)},t)$ satisfies (7.26) for $j = i$ (cf. (7.9)). In order to satisfy C_1 and C_2 simultaneously, admissible trajectories $\xi^*(z_{(i|)},t)$ for the basic output $\xi(z_{(i|)},t)$ have to be determined appropriately.

7.3.3 Construction of Admissible Trajectories for the Basic Output

This is subsequently addressed provided that the reaction parameter can be decomposed into a time–invariant part depending only on $z_{(i|)}$ and a time varying part depending on z^i, i.e.[1]

$$c(z,t) = c_0(z_{(i|)}) + c_1(z^i,t).$$

In this case, the following result can be verified, which, besides ensuring the admissibility of the trajectory $\xi^*(z_{(i|)},t)$, provides a systematic and computationally efficient approach to compute the respective series coefficients $x_n(z,t)$ of the series ansatz (7.10a).

Proposition 7.2. *Given the reaction parameter $c(z,t) \in G_{D_c,1,\alpha}(\Omega \times \mathbb{R}^+_{t_0})$ with $1 < \alpha \leq 2$ where $c(z,t) = c_0(z_{(i|)}) + c_1(z^i,t)$ and the desired trajectory for the basic output $\xi^*(z_{(i|)},t) = \phi(t)\psi(z_{(i|)})$ with $\phi(t)$ a Gevrey function of order $1 < \alpha \leq 2$ satisfying $\phi(t_0) = \phi_0$ while $\partial_t^k \phi(t)|_{t=t_0} = 0$ and $\psi(z_{(i|)})$ determined as a solution to the boundary–value problem*

$$\Delta\psi(z_{(i|)}) = \big(\lambda - c_0(z_{(i|)})\big)\,\psi(z_{(i|)}), \qquad z_{(i|)} \in \Omega_i \tag{7.27a}$$

$$\epsilon_j^0 \partial_{z^j}\psi(z_{(i|)}) - p_j^0 \psi(z_{(i|)}) = 0, \qquad z^j = 0,\ j \in I_r^i \tag{7.27b}$$

$$\epsilon_j^1 \partial_{z^j}\psi(z_{(i|)}) + p_j^1 \psi(z_{(i|)}) = 0, \qquad z^j = L_j,\ j \in I_r^i \tag{7.27c}$$

with $\lambda \in \mathbb{R}$. Then the conditions C_1 and C_2 of Definition 7.1 are satisfied.

Proof. Since $\xi^*(z_{(i|)},t)$ is by assumption of Gevrey order $\alpha > 1$ with $\phi(t_0) = \phi_0$ and $\partial_t^k \phi(t)|_{t=t_0} = 0$ condition C_1 is directly fulfilled. By substituting $\xi^*(z_{(i|)},t) = \phi(t)\psi(z_{(i|)})$ into (7.10b), (7.10c) with $c(z,t) = c_0(z_{(i|)}) + c_1(z^i,t)$ it can be shown that any coefficient $x_n(z,t)$ can be parametrized schematically as $x_n(z,t) = \upsilon_n(z^i,t)\psi(z_{(i|)})$. For this, consider first $n = 0$, where (7.10b) yields $x_0(z,t) = (s_i^0 + z^i s_i^1)\phi(t)\psi(z_{(i|)})$ such that $\upsilon_0(z^i,t) = (s_i^0 + z^i s_i^1)\phi(t)$. Hence, assume that $x_n(z,t) = \upsilon_n(z^i,t)\psi(z_{(i|)})$ holds for all $n = 0,1,\ldots,N-1$. Then it follows from the recursion (7.10c) that

[1] Note that in view of the transformations introduced in Section 7.1.1 for the general diffusion–convection–reaction equation (7.1a) with spatially varying diffusion and convection parameter, this assumption is satisfied provided that the original reaction parameter $c(z,t)$ in (7.1a) can be decomposed as $c(z,t) = c_0(z_{(i|)}) + c_1(z^i,t)$.

$$
\begin{aligned}
x_N(z,t) = \int_0^{z^i}\int_0^{\eta} \Big(& \partial_t \upsilon_{N-1}(\sigma,t)\psi(z_{(i|)}) - \upsilon_{N-1}(\sigma,t) \sum_{j\in I_r^i} \partial_{z^j}^2 \psi(z_{(i|)}) \\
& - c(z_{(i|\sigma)},t)\upsilon_{N-1}(\sigma,t)\psi(z_{(i|)}) \Big) \mathrm{d}\sigma \mathrm{d}\eta \\
\overset{(7.27a)}{=} & \underbrace{\int_0^{z^i}\int_0^{\eta} \big(\partial_t \upsilon_{N-1}(\sigma,t) - \upsilon_{N-1}(\sigma,t)[\lambda + c_1(\sigma,t)] \big) \mathrm{d}\sigma \mathrm{d}\eta}_{= \upsilon_N(z^i,t)} \psi(z_{(i|)}),
\end{aligned}
$$

which by induction proves the assertion. Since $\psi(z_{(i|)})$ by definition satisfies the boundary conditions (7.27b) it follows that each $x_n(z,t)$, $n \in \mathbb{N}$ fulfills the compatibility condition C_2. □

The BVP (7.27) corresponds to the eigenproblem for the distributed–parameter system (7.3a)–(7.3c) defined on the $(r-1)$–dimensional subspace $\Omega_i \subset \Omega$. Here, λ denotes the eigenvalue corresponding to the eigenfunction $\psi(z_{(i|)})$. Since (7.27) is of Sturm–Liouville type there exists an ordered set of eigenvalues $\{\lambda_k\}_{k\in\mathbb{N}}$ with corresponding eigenfunctions $\psi_k(z_{(i|)})$, $k \in \mathbb{N}$, which form a basis for the Hilbert space $X = \{\psi(z_{(i|)}) \in L^2(\Omega_i) \mid \sum_{j\in I_r^i} \partial_{z^j}^2 \psi(z_{(i|)}) \in L^2(\Omega_i),\ \psi(z_{(i|)}) \text{ satisfies (7.27b) and (7.27c)}\}$. As a result, any linear combination of eigenfunctions $\xi^*(z_{(i|)},t) = \sum_{k\in I_{\xi^*}\subset\mathbb{N}} \phi_k(t)\psi_k(z_{(i|)})$ can be utilized to assign admissible trajectories for the basic output. This property can be exploited in terms of a projection–based construction of admissible trajectories.

7.3.3.1 Projection–Based Trajectory Construction

Let $\bar{\xi}^*(z_{(i|)}) \in X$ denote a desired profile for the basic output $\xi^*(z_{(i|)},t)$ at a fixed but arbitrary instance of time $t \geq t_0$. Recalling the basis property of $\psi_k(z_{(i|)})$, $k \in \mathbb{N}$, for X it follows that

$$
\bar{\xi}^*(z_{(i|)}) = \sum_{k=1}^{\infty} \langle \bar{\xi}^*(z_{(i|)}), \psi_k(z_{(i|)}) \rangle \psi_k(z_{(i|)}),
$$

where $\langle \cdot,\cdot \rangle$ denotes the inner product in $L^2(\Omega_i)$. In view of [4, Theorem A.2.35], this in particular implies that the finite series

$$
\hat{\bar{\xi}}^*(z_{(i|)}) = \sum_{k=1}^{K} \langle \bar{\xi}^*(z_{(i|)}), \psi_k(z_{(i|)}) \rangle \psi_k(z_{(i|)}), \quad K \in \mathbb{N} \tag{7.28}
$$

yields an approximation of the profile $\bar{\xi}^*(z_{(i|)})$ in an L^2–sense with the error decreasing for increasing K. This observation can be exploited for a projection–based profile assignment by constructing a basic output trajectory $\xi^*(z_{(i|)},t)$ fulfilling both conditions of Definition 7.1. Let $\bar{\xi}_0^*(z_{(i|)})$ and $\bar{\xi}_T^*(z_{(i|)})$ represent desired

initial and final profiles at $t = t_0$ and $t = t_0 + T$. With Proposition 7.2 and (7.28) the choice

$$\xi^*(z_{(i|)},t) = \sum_{k=1}^{K} \langle \bar{\xi}_0^*(z_{(i|)}), \psi_k(z_{(i|)})\rangle \psi_k(z_{(i|)}) + \phi(t) \sum_{k=1}^{K} \big(\langle \bar{\xi}_T^*(z_{(i|)}), \psi_k(z_{(i|)})\rangle - \langle \bar{\xi}_0^*(z_{(i|)}), \psi_k(z_{(i|)})\rangle \big) \psi_k(z_{(i|)})$$

yields an admissible desired trajectory, which allows an approximate realization of the transition from $\bar{\xi}_0^*(z_{(i|)})$ to $\bar{\xi}_T^*(z_{(i|)})$ along the temporal path $\phi(t)$. As outlined above, this requires the local non–analyticity of $\phi(t)$ at $t = t_0$ and $t = t_0 + T$. For this, the function $\phi(t) = g_{T,\omega}(t - t_0)$ introduced in (B.3) is subsequently assigned, which is a Gevrey function of order $\alpha = 1 + 1/\omega$.

For more general situations, where the reaction parameter $c(z,t)$ cannot be decomposed according to Proposition 7.2, so far no general approach is available to systematically determine an admissible trajectory for the basic output in the sense of Definition 7.1 to realize finite time transitions between stationary operating profiles. In order to overcome this, the use of a desired trajectory $\xi^*(z_{(i|)},t)$ being non–analytic at the respective boundary hyperplanes seems to be an interesting option, which would further enhance the applicability of the proposed approach. Nevertheless, in this case convergence can no longer be guaranteed since the respective function $\xi^*(z_{(i|)},t)$ would be of Gevrey order $\beta > 1$ in $z_{(i|)}$ (cf. Theorem 7.1).

7.3.3.2 Generalized Constructions

It should be pointed out that admissible trajectories according to Definition 7.1 can be also determined if more general transitions are considered by dropping the restriction to initial and final stationary profiles. For this, consider $c(z,t) \in G_{D_c,1,\alpha}(\Omega \times \mathbb{R}^+_{t_0})$, $1 < \alpha \leq 2$, and assume

$$c(z,t) = c_0(z_{(i|)},t) + c_1(z^i,t).$$

Moreover, let $\xi^*(z_{(i|)},t) = \phi(t)\psi(z_{(i|)},t)$ denote the desired trajectory for the basic output with $\phi(t)$ a Gevrey function of order $1 < \alpha \leq 2$ satisfying $\phi(t_0) = \phi_0$ while $\partial_t^k \phi(t)|_{t=t_0} = 0$ and $\psi(z_{(i|)},t)$ determined as a solution to

$$\partial_t \psi(z_{(i|)},t) = \sum_{j \in I_r^i} \partial_{z^j}^2 \psi(z_{(i|)},t) - \big(\lambda(t) - c_0(z_{(i|)},t)\big)\, \psi(z_{(i|)},t) \tag{7.29a}$$

for $(z_{(i|)},t) \in \Omega_i \times \mathbb{R}^+_{t_0}$ and $\lambda(t) \in \mathbb{R}$ with

$$\epsilon_j^0 \partial_{z^j} \psi(z_{(i|)},t) - p_j^0 \psi(z_{(i|)},t) = 0, \qquad z^j = 0,\ j \in I_r^i \tag{7.29b}$$

$$\epsilon_j^1 \partial_{z^j} \psi(z_{(i|)},t) + p_j^1 \psi(z_{(i|)},t) = 0, \qquad z^j = L_j,\ j \in I_r^i \tag{7.29c}$$

$$\psi(z_{(i|)}, t_0) = \psi_0(z_{(i|)}), \qquad z_{(i|)} \in \overline{\Omega_i}. \tag{7.29d}$$

Then condition C_2 of Definition 7.1 is satisfied. This assertion can be proven using induction by verifying that any coefficient $x_n(z,t)$ can be parametrized schematically according to $x_n(z,t) = \upsilon_n(z^i,t)\psi(z_{(i|)},t)$. Consider first $n = 0$, where (7.10b) yields $x_0(z,t) = (s_i^0 + z^i s_i^1)\phi(t)\psi(z_{(i|)},t)$ such that $\upsilon_0(z^i,t) = (s_i^0 + z^i s_i^1)\phi(t)$. Hence, assume that $x_n(z,t) = \upsilon_n(z^i,t)\psi(z_{(i|)},t)$ holds for all $n = 0, 1, \ldots, N-1$. Then it follows from recursion (7.10c) that

$$\begin{aligned}
&x_N(z,t)\\
&= \int_0^{z^i}\int_0^{\eta}\Big(\partial_t \upsilon_{N-1}(\sigma,t)\psi(z_{(i|)},t) + \upsilon_{N-1}(\sigma,t)\partial_t\psi(z_{(i|)},t)\\
&\quad - \upsilon_{N-1}(\sigma,t)\sum_{j\in I_r^i}\partial_{z^j}^2\psi(z_{(i|)},t) - c(z_{(i|\sigma)},t)\upsilon_{N-1}(\sigma,t)\psi(z_{(i|)},t)\Big)\mathrm{d}\sigma\mathrm{d}\eta\\
&\overset{(7.29a)}{=} \underbrace{\int_0^{z^i}\int_0^{\eta}\big(\partial_t\upsilon_{N-1}(\sigma,t) - \upsilon_{N-1}(\sigma,t)[\lambda(t) + c_1(\sigma,t)]\big)\mathrm{d}\sigma\mathrm{d}\eta}_{=\upsilon_N(z^i,t)}\,\psi(z_{(i|)},t)
\end{aligned}$$

which proves the claim. Since $\psi(z_{(i|)},t)$ by definition satisfies boundary conditions (7.29b), (7.29c) it follows that each $x_n(z,t)$, $n \in \mathbb{N}$, fulfills the compatibility condition C_2.

However, the verification of compatibility condition C_1 relies on the Gevrey order of $\xi^*(z_{(i|)},t)$. For this, recall that Gevrey class functions form a ring with respect to the arithmetic product of functions [15, 9]. Thus, the Gevrey order of $\xi^*(z_{(i|)},t) = \phi(t)\psi(z_{(i|)},t)$ can be deduced from the properties of $\phi(t)$, which is a Gevrey function of order $1 < \alpha \leq 2$ being locally non–analytic at $t = t_0$, and $c(z,t) \in G_{D_c,1,\alpha}(\Omega \times \mathbb{R}_{t_0}^+)$ determining $\psi(z_{(i|)},t)$ by means of (7.29).

7.3.3.3 Remarks

The above analysis reveals that prescribing a trajectory $\xi^*(z_{(i|)},t)$ satisfying the conditions of Proposition 7.2 enables to realize trajectory tracking $\xi(z_{(i|)},t) \to \xi^*(z_{(i|)},t)$ with $\xi(z_{(i|)},t)$ as defined in (7.6). If $\xi(z_{(i|)},t)$ represents the system output, this immediately allows to realize desired output trajectories. In addition, the proposed set–up implicitly realizes the tracking of $x(z,t) \to x^*(z,t)$, where $x^*(z,t)$ is determined by evaluating the state parametrization (7.9) with $\xi(z_{(i|)},t)$ replaced by $\xi^*(z_{(i|)},t)$. Thereby, starting at an initial stationary state $x(z,t_0) = x^*(z,t_0) = x_0(z)$, the system not necessarily has to reach a new stationary state solution but can rather evolve along the spatial–temporal path $x^*(z,t)$ parametrized in terms of $\xi^*(z_{(i|)},t)$. Hence, by construction a characterization of (certain) reachable (transient) states starting at $x_0(z)$ is achieved.

7.4 Extension to Multiple Input Configurations

The results above can be directly extended to the case of multiple inputs located on opposite sides of the parallelepipedon. For this, consider the distributed–parameter system (7.3) modified according to

$$\partial_t x(z,t) = \Delta x(z,t) + c(z,t)x(z,t), \qquad (z,t) \in \Omega \times \mathbb{R}^+_{t_0} \tag{7.30a}$$

with

$$\epsilon^0_j \partial_{z^j} x(z,t) - p^0_j x(z,t) = 0, \qquad z^j = 0,\ j \in I^i_r \tag{7.30b}$$
$$\epsilon^1_j \partial_{z^j} x(z,t) + p^1_j x(z,t) = 0, \qquad z^j = L_j,\ j \in I^i_r \tag{7.30c}$$
$$\theta_0\left(x(z,t), \partial_{z^i} x(z,t)\right) = u^{i_0}(z_{(i|)},t), \qquad z^i = 0 \tag{7.30d}$$
$$\theta_1\left(x(z,t), \partial_{z^i} x(z,t)\right) = u^{i_1}(z_{(i|)},t), \qquad z^i = L_i \tag{7.30e}$$

for $t > t_0$ and

$$x(z,t_0) = x_0(z), \qquad z \in \overline{\Omega}. \tag{7.30f}$$

Proceeding similar to Section 7.2.1, the PDE (7.30a) is formally integrated twice in the z^i–direction starting at an arbitrary $\bar{z}^i \in (0, L_i)$, which yields

$$\begin{aligned} x(z,t) = {} & x(z_{(i|\bar{z}^i)},t) + \left(z^i - \bar{z}^i\right)\partial_{z^i} x(z_{(i|\bar{z}^i)},t) \\ & + \int_{\bar{z}^i}^{z^i} \int_{\bar{z}^i}^{\eta} \Big(\partial_t x(z_{(i|\sigma)},t) - c(z_{(i|\sigma)},t)x(z_{(i|\sigma)},t) \\ & \qquad - \sum_{j \in I^i_r} \partial^2_{z^j} x(z_{(i|\sigma)},t) \Big) \mathrm{d}\sigma \mathrm{d}\eta. \end{aligned} \tag{7.31}$$

The IEOK resembles (7.5) with the distinction in the domain of integration and the two constants of integration

$$\xi^{i_0}(z_{(i|)},t) = x(z_{(i|\bar{z}^i)},t) \tag{7.32a}$$
$$\xi^{i_1}(z_{(i|)},t) = \partial_{z^i} x(z_{(i|\bar{z}^i)},t). \tag{7.32b}$$

It can be directly deduced that the tuple $\boldsymbol{\xi}(z_{(i|)},t) = [\xi^{i_0}(z_{(i|)},t), \xi^{i_1}(z_{(i|)},t)]^T$ is a basic output for (7.30) parametrizing the state variable $x(z,t) = x(z,t;\boldsymbol{\xi}(z_{(i|)},t))$ according to

$$
\begin{aligned}
x(z,t;\boldsymbol{\xi}(z_{(i|)},t)) &= \xi^{i_0}(z_{(i|)},t) + \left(z^i-\bar{z}^i\right)\xi^{i_1}(z_{(i|)},t) \\
&+ \int_{\bar{z}^i}^{z^i}\int_{\bar{z}^i}^{\eta}\Big(\partial_t x(z_{(i|\sigma)},t) - c(z_{(i|\sigma)},t)x(z_{(i|\sigma)},t) \\
&\qquad - \sum_{j\in I_r^i}\partial_{z^j}^2 x(z_{(i|\sigma)},t)\Big)\mathrm{d}\sigma\mathrm{d}\eta
\end{aligned}
\tag{7.33}
$$

and the input tuple by

$$
u^{i_0}(z_{(i|)},t) = \theta_0\left(x(z,t;\boldsymbol{\xi}(z_{(i|)},t)),\partial_{z^i}x(z,t;\boldsymbol{\xi}(z_{(i|)},t))\right) \tag{7.34a}
$$

$$
u^{i_1}(z_{(i|)},t) = \theta_1\left(x(z,t;\boldsymbol{\xi}(z_{(i|)},t)),\partial_{z^i}x(z,t;\boldsymbol{\xi}(z_{(i|)},t))\right). \tag{7.34b}
$$

In order to resolve the implicit parametrization (7.33), proceed as in Section 7.2.1 by introducing a successive series approximation following

$$
x(z,t) = \sum_{n=0}^{\infty} x_n(z,t), \tag{7.35a}
$$

with the recursively computed series coefficients

$$
x_0(z,t) = \xi^{i_0}(z_{(i|)},t) + \left(z^i-\bar{z}^i\right)\xi^{i_1}(z_{(i|)},t) \tag{7.35b}
$$

$$
\begin{aligned}
x_n(z,t) = \int_{\bar{z}^i}^{z^i}\int_{\bar{z}^i}^{\eta}\Big(&\partial_t x_{n-1}(z_{(i|\sigma)},t) - c(z_{(i|\sigma)},t)x_{n-1}(z_{(i|\sigma)},t) \\
&- \sum_{j\in I_r^i}\partial_{z^j}^2 x_{n-1}(z_{(i|\sigma)},t)\Big)\mathrm{d}\sigma\mathrm{d}\eta,\ n\geq 1.
\end{aligned}
\tag{7.35c}
$$

Obviously, any series coefficient depends on successive derivatives of $\boldsymbol{\xi}(z_{(i|)},t)$ with respect to t and $(z^j)_{j\in I_r^i}$ such that convergence has to be analyzed in appropriate Gevrey classes. Thus, let $\xi^{i_0}(z_{(i|)},t)\in G_{D_\xi^0,\beta,\alpha}(\Omega_i\times\mathbb{R}_{t_0}^+)$ and $\xi^{i_1}(z_{(i|)},t)\in G_{D_\xi^1,\beta,\alpha}(\Omega_i\times\mathbb{R}_{t_0}^+)$ and choose $D=\max\{D_\xi^0,D_\xi^1\}$, then the results of Theorem 7.1, Proposition 7.1, and Corollary 7.1 can be applied to ensure the uniform convergence of the parametrized series (7.35) in the considered multiple input setting.

In addition, the assignment of admissible trajectories $(z_{(i|)},t)\mapsto\boldsymbol{\xi}^*(z_{(i|)},t)$ for the basic output $\boldsymbol{\xi}(z_{(i|)},t)$ can be performed in a way similar to Section 7.3 by assuming that $c(z,t)$ is locally non–analytic with respect to t. The main distinction arises from the fact that the components of $\boldsymbol{\xi}(z_{(i|)},t)$ no longer correspond to boundary values but to the state and its spatial derivative at $z^i=\bar{z}^i$ with $\bar{z}^i\in(0,L_i)$, fixed but arbitrary, as introduced in (7.32). Hence, differing from the stationary state analysis in terms of the basic output considered in Section 7.3.1 it is required to pursue a direct approach by assigning stationary input values for $u_s^{i_0}(z_{(i|)})$ and $u_s^{i_1}(z_{(i|)})$. Alternatively, interior conditions by means of a stationary version of (7.32) can be introduced, which, however, significantly complicates the solution procedure.

In the first case, the corresponding stationary state $x_s(z)$ follows from the solution of the boundary–value problem

$$\begin{aligned}
&\Delta x_s(z) + c(z,t)x_s(z) = 0, && z \in \Omega && \text{(7.36a)}\\
&\epsilon_j^0 \partial_{z^j} x_s(z) - p_j^0 x_s(z) = 0, && z^j = 0,\ j \in I_r^i && \text{(7.36b)}\\
&\epsilon_j^1 \partial_{z^j} x_s(z) + p_j^1 x_s(z) = 0, && z^j = L_j,\ j \in I_r^i && \text{(7.36c)}\\
&\theta_0\left(x_s(z), \partial_{z^i} x_s(z)\right) = u_s^{i_0}(z_{(i|)}), && z^i = 0, && \text{(7.36d)}\\
&\theta_1\left(x_s(z), \partial_{z^i} x_s(z)\right) = u_s^{i_1}(z_{(i|)}), && z^i = L_i. && \text{(7.36e)}
\end{aligned}$$

Let $x_0(z)$ and $x_T(z)$ denote two solutions to (7.36) representing stationary profiles at $t = t_0$ and $t = T$, respectively. In order to determine a spatial–temporal path $\boldsymbol{\xi}^*(z_{(i|)}, t)$ realizing the finite time transition from $x_0(z)$ to $x_T(z)$ within $t \in (t_0, t_0 + T)$ evaluate (7.32), which yields

$$\begin{aligned}
\xi_0^{*,i_0}(z_{(i|)}) &= \xi^{*,i_0}(z_{(i|)}, t_0) = x_0(z_{(i|\bar{z}^i)})\\
\xi_T^{*,i_0}(z_{(i|)}) &= \xi^{*,i_0}(z_{(i|)}, t_0 + T) = x_T(z_{(i|\bar{z}^i)})
\end{aligned} \qquad \text{(7.37a)}$$

and

$$\begin{aligned}
\xi_0^{*,i_1}(z_{(i|)}) &= \xi^{*,i_1}(z_{(i|)}, t_0) = \partial_{z^i} x_0(z_{(i|\bar{z}^i)})\\
\xi_T^{*,i_1}(z_{(i|)}) &= \xi^{*,i_1}(z_{(i|)}, t_0 + T) = \partial_{z^i} x_T(z_{(i|\bar{z}^i)}).
\end{aligned} \qquad \text{(7.37b)}$$

Using, e.g., the Gevrey class function (B.3) introduced in Appendix B.1, the transition paths for the basic output components can be assigned in the form

$$\begin{aligned}
\xi^{*,i_0}(z_{(i|)}, t) &= \xi_0^{*,i_0}(z_{(i|)}) + \left(\xi_T^{*,i_0}(z_{(i|)}) - \xi_0^{*,i_0}(z_{(i|)})\right) g_{T,\omega}(t - t_0)\\
\xi^{*,i_1}(z_{(i|)}, t) &= \xi_0^{*,i_1}(z_{(i|)}) + \left(\xi_T^{*,i_1}(z_{(i|)}) - \xi_0^{*,i_1}(z_{(i|)})\right) g_{T,\omega}(t - t_0).
\end{aligned} \qquad \text{(7.38)}$$

In particular, $\boldsymbol{\xi}^*(z_{(i|)}, t)$ is a Gevrey class function of order $\alpha = 1 + 1/\omega$.

As a second option, the steady state problem can be formulated in an indirect manner by considering interior conditions according to

$$\begin{aligned}
&\Delta x_s(z) + c(z,t)x_s(z) = 0, && z \in \Omega && \text{(7.39a)}\\
&\epsilon_j^0 \partial_{z^j} x_s(z) - p_j^0 x_s(z) = 0, && z^j = 0,\ j \in I_r^i && \text{(7.39b)}\\
&\epsilon_j^1 \partial_{z^j} x_s(z) + p_j^1 x_s(z) = 0, && z^j = L_j,\ j \in I_r^i && \text{(7.39c)}\\
&x_s(z) = \xi_s^{*,i_0}(z_{(i|)}), && z^i = \bar{z}^i && \text{(7.39d)}\\
&\partial_{z^i} x_s(z) = \xi_s^{*,i_1}(z_{(i|)}), && z^i = \bar{z}^i && \text{(7.39e)}
\end{aligned}$$

with $\xi_s^{*,i_0}(z_{(i|)})$ and $\xi_s^{*,i_1}(z_{(i|)})$ representing stationary profiles for $\xi^{*i_0}(z_{(i|)}, t)$ and $\xi^{*i_1}(z_{(i|)}, t)$, respectively. While this set–up enables a solution only in terms of the basic output, its implementation is significantly complicated due to the interior conditions (7.39d), (7.39e). Replacing the initial and final values in (7.38) with the

assigned stationary values for $\boldsymbol{\xi}^*(z_{(i|)}, t)$ introduced in (7.39) hence determines the spatial–temporal transition path by solving (7.35). Once the recursion is solved, the respective feedforward controls follow immediately from the input parametrization (7.34).

According to Section 7.3, desired trajectories for the basic output have to fulfill additional constraints to ensure admissibility and thus to guarantee that the parametrized series coefficients (7.35b), (7.35c) are consistent with the remaining boundary conditions (7.30b), (7.30c). By construction, consistency is directly imposed in the first case involving the solution of (7.36). In the second case, special emphasis is required for the proper introduction of $\xi_s^{*,i_0}(z_{(i|)})$ and $\xi_s^{*,i_1}(z_{(i|)})$ in the boundary–value problem (7.39). Here, Proposition 7.2 can be applied to exploit projection–based trajectory assignment to guarantee admissibility. With these considerations, flatness–based trajectory planning can be addressed by means of formal integration also in the case of multiple inputs acting on opposing boundary surfaces of the parallelepiped domain. An application of this technique is provided in Section 9.8.2, where trajectory planning and backstepping are combined for the synchronization of a large scale multi–agent network.

7.5 Application Examples and Simulation Results

In order to illustrate the proposed trajectory planning approach and to apply the theoretical results determined above, in the following, a simulation scenario is considered for a cuboid with $r = 3$ and $L_j = 1$, $j = 1, 2, 3$ in (7.1b) and a single input on the boundary $L_3 = 1$, i.e. $i = 3$. As outlined above, the focus is on the realization of a finite time transition from a zero stationary initial profile $x_0(z) = 0$ at $t = t_0$ to a prescribed final time varying profile $x_T(z, t)$ for $t \geq t_0 + T$. For this, the reaction parameter in the diffusion–reaction equation (7.3a) is considered to take the form

$$c(z,t) = c_1(t) - \frac{1}{4}\sum_{j=1}^{3} \frac{a_{1,j}\left(\cosh\left(\sqrt{a_{1,j}}z^j\right)^2 + 1\right)}{\cosh\left(\sqrt{a_{1,j}}z^j\right)^2} \tag{7.40}$$

with constants $a_{1,j} \geq 0$, $j = 1, 2, 3$. With this, $c(z, t)$ is an entire and hence analytic function with respect to z for all $z \in \mathbb{R}^3$. Hence, the convergence of the recursive parametrization (7.10) is ensured by Theorem 7.1 with at least a radius of convergence given by (7.14).

Remark 7.6. Note that by the change of coordinates introduced in Section 7.1.1, this choice of $c(z, t)$ corresponds to the study of the diffusion–convection–reaction equation (7.1a) with the parameters $a_j(z^j) = a_{0,j} + a_{1,j}(z^j)^2$ and $b_j(z^j) = \partial_{z^j} a_j(z^j) = 2a_{1,j}z^j$ for $a_{0,j} > 0$ and $a_{1,j} > 0$ and $c(z, t) = c_1(t)$. The domain is herein given by the parallelepipedon (7.1b) with $L_j = \operatorname{arcsinh}(\sqrt{a_{1,j}/a_{0,j}})/\sqrt{a_{1,j}}$. Hence, the diffusion parameters $a_j(z^j)$ increase with $(z^j)^2$ while the choice of

$b_j(z^j)$ implies that the diffusion–convection part in (7.1a) can be summarized as $\sum_{j=1}^{3} \partial_{z^j}(a_j(z^j)\partial_{z^j} x(z,t))$.

Without loss of generality, the time varying part $c_1(t)$ in (7.40) is exemplarily chosen as

$$c_1(t) = 2g_{1,2}(t-t_0)\Phi_{2,1}(t-t_0)\sin(2\pi(t-t_0)), \tag{7.41}$$

with $g_{T,\omega}(t-t_0)$ defined in (B.3). In view of (7.41) it can be easily verified that the initial condition $x_0(z) = 0$ represents a stationary profile. Hence, with (7.23) the desired trajectory $\xi^*(z_{(3|)},t)$ for the basic output has to satisfy $\xi^*(z_{(3|)},t_0) = \xi_0^*(z_{(3|)}) = 0$.

The remaining system parameters in the boundary conditions (7.3b) and (7.3c) are chosen as $\epsilon_j^0 = 1$, $p_j^0 = 0$ for $j = 1,2,3$ and $\epsilon_j^1 = 1$, $p_j^1 = 0$ for $j = 1,2$, i.e. Neumann boundary conditions referring to adiabatic conditions are imposed on all sides of the cuboid except for $z^3 = 1$. There, for the sake of simplicity, a Dirichlet input is considered with $u(z_{(3|)},t) = x(z_{(3|1)},t)$. However, as illustrated above a (nonlinear) Neumann– or Robin–type boundary input can be addressed similarly. The parameters f_3^0 and f_3^1 defining the basic output according to (7.6) are in view of the condition $p_3^0 f_3^0 + \epsilon_3^0 f_3^1 \neq 0$ determined as $f_3^0 = 0$ and $f_3^1 = 1$, i.e. subsequently the basic output corresponds to the state on the surface $z^3 = 0$ such that $\xi(z_{(3|)},t) = x(z_{(3|0)},t)$.

In the considered simulation scenarios, the desired spatial–temporal path $x^*(z,t)$ is parametrized by the desired trajectory $\xi^*(z_{(3|)},t)$ for the basic output $\xi(z_{(3|)},t)$ to exemplarily realize $x(z_{(3|0)},t) = 0$ for $t \leq t_0$ while $x(z_{(3|0)},t) = 1$ uniformly for $t \geq t_0 + T$. With this, the respective state $x(z,t)$ evolves along the profile $x^*(z,t)$ determined by substituting $\xi^*(z_{(3|)},t)$ into (7.10). The required feedforward control $u^*(z_{(3|)},t)$ follows from the evaluation of (7.11) with $\xi(z_{(3|)},t)$ replaced by $\xi^*(z_{(3|)},t)$. Therefore, depending on either isotropic or orthotropic material properties with $a_{1,j} = 0$ or $a_{1,j} \neq 0$, $j = 1,2,3$, in (7.40), respectively, different desired trajectories $\xi^*(z_{(3|)},t)$ have to be determined to obtain the desired uniform distribution of $x(z,t)$ on the surface $z^3 = 0$.

For the simulations, the governing equations (7.3) are discretized using an implicit and numerically absolutely stable Crank–Nicholson approach (see, e.g., [16]). The required matrix factorization(s) in order to solve the resulting linear system of equations for the spatially and temporally discretized state variables were performed using the UMFPACK library [5]. Although being computationally rather expensive, for the considered problem this approach has proven to yield significantly better results than the related but theoretically computationally less expensive alternating direction approach or finite–element solution techniques.

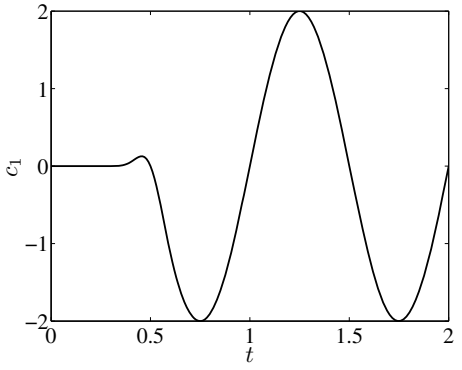

Fig. 7.2 Reaction parameter $c(z,t) \equiv c_1(t)$ defined in (7.40) for scenario (I) with $a_{1,j} = 0$, $j = 1,2,3$; ©2009, IEEE

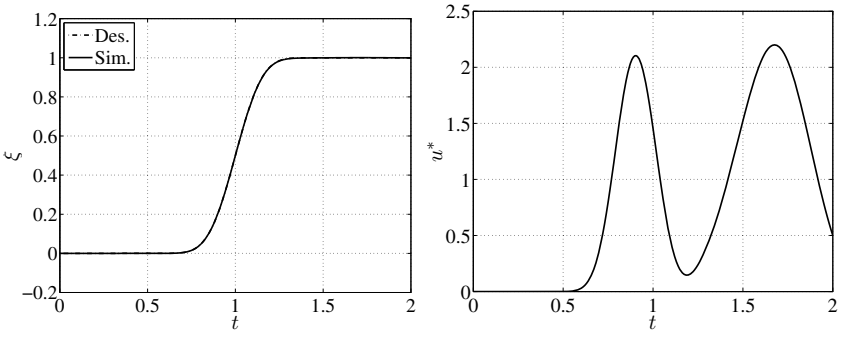

Fig. 7.3 Trajectory planning for the basic output and simulation results for scenario (I) with $a_{1,j} = 0$. Left: comparison of the desired and the obtained spatially uniform trajectories $\xi^*(z_{(3|)},t)$ and $\xi(z_{(3|)},t)$, respectively; right: corresponding feedforward control $u^*(z_{(3|)},t)$; ©2009, IEEE.

7.5.1 Isotropic Diffusion and Reaction

In the first scenario (I), an isotropic material is considered with $a_{1,j} = 0$, $j = 1,2,3$ in (7.40). The only time varying parameter $c(z,t) \equiv c_1(t)$ defined in (7.40) is depicted in Figure 7.2. In view of Proposition 7.1, an infinite radius of convergence is obtained for the recursively determined state and input parametrizations provided that $\xi^*(z_{(3|)},t)$ is an entire function with respect to $z_{(3|)}$. In view of Proposition 7.2 and the transition problem specified above, observe that for the considered set of system parameters the function $\psi(z_{(3|)}) = 1$ with $\lambda = 0$ is a solution to the boundary–value problem (7.27). Hence, by making use of the projection–based trajectory construction, the desired trajectory

$$\xi^*(z_{(3|)},t) = g_{T,\omega}(t - t_0) \tag{7.42}$$

for the basic output $\xi(z_{(3|)},t) = x(z_{(3|0)},t)$ with $g_{T,\omega}(t-t_0)$ from (B.3) ensures $x(z_{(3|0)},t) = 0$ for $t \leq t_0$ while $x(z_{(3|0)},t) = 1$ for $t \geq t_0+T$. Furthermore, (7.42) is entire in $z_{(3|)}$ and is an admissible trajectory in the sense that both compatibility conditions (7.25) and (7.26) are satisfied.

The choice (7.42) implies that $\xi^*(z_{(3|)},t)$ and thus the feedforward control $u^*(z_{(3|)},t)$ only vary with time t. The corresponding temporal behavior is shown in Figure 7.3, where the desired trajectory (7.42) for $\omega = 2$, $T = 2$, and $t_0 = 0$ is depicted (left) compared to the time–evolution of the simulation result for $\xi(z_{(3|)},t) = x(z_{(3|0)},t)$ obtained from applying the feedforward control $u^*(z_{(3|)},t)$ (right) to the surface $z^3 = 1$. Clearly, almost no deviation between the desired and the resulting trajectory appears. The emerging periodic behavior in $u^*(z_{(3|)},t)$ is thereby due to the periodic character of $c_1(t)$ according to (7.41). In particular, rather large variations in $u^*(z_{(3|)},t)$ can be observed after an initial phase (cf. Figure 7.3).

7.5.2 Orthotropic Diffusion and Reaction

In the second scenario (II), an orthotropic material is considered with $a_{1,j} = 20$, $j = 1,2,3$, in (7.40). Differing from the previous section, the respective profile $c(z,t)$ as defined in (7.40) is now a function of all independent coordinates. Due to the dependency of $c(z,t)$ on z, $\psi(z_{(3|)}) = 1$ is no longer a solution to the eigenproblem (7.27). Hence, in order to (approximately) realize the desired uniform state profile $\xi^*(z_{(3|)},t) = x(z_{(3|0)},t) = 1$, Eqn. (7.28) is subsequently considered for $\bar{\xi}^*(z_{(3|)}) = 1$. In view of the initial condition $\xi^*(z_{(3|)},t_0) = 0$, an admissible trajectory for the basic output realizing the transition from $x(z_{(3|0)},t) = 0$ for $t \leq t_0$ into a neighborhood of $x(z_{(3|0)},t) = 1$ for $t \geq t_0 + T$ is given by

$$\xi^*(z_{(3|)},t) = g_{T,\omega}(t-t_0)\sum_{k=1}^{K}\langle 1,\psi_k(z_{(3|)})\rangle\psi_k(z_{(3|)}). \tag{7.43}$$

Herein, the number of addends K can be, e.g., determined by imposing an upper bound $\epsilon > 0$ on the $L^2(\Omega_3)$–norm of the difference $\bar{\xi}^*(z_{(3|)}) - \xi^*(z_{(3|)},t_0+T)$, i.e. $\|\bar{\xi}^*(z_{(3|)}) - \xi^*(z_{(3|)},t_0+T)\| < \epsilon$. The resulting trajectory $\xi^*(z_{(3|)},t)$ for $\omega = 2$, $T = 2$, $t_0 = 0$, and $K = 10$ as well as the corresponding feedforward control $u^*(z_{(3|)},t)$ obtained from evaluating (7.11) with $\xi(z_{(3|)},t)$ replaced by $\xi^*(z_{(3|)},t)$ are shown in Figure 7.4 (left) and (middle), respectively, for $t \in \{0.8, 1.0, 1.7, 2.0\}$. Obviously, the desired value $x(z_{(3|0)},t) = 1$ for $t \geq 2$ is only obtained approximately but with minor deviations from uniformity. However, increasing K in (7.43) allows to further decrease the difference at the cost of an increasing input amplitude due to the necessity to excite higher order modes $\psi_k(z_{(3|)})$, $k > 10$. For the determination of the evolving tracking error $e(z_{(3|)},t) = \xi^*(z_{(3|)},t) - x(z_{(3|0)},t)$ as shown in Figure 7.4 (right), the diffusion–reaction system (7.3) is solved numerically with the Dirichlet input $u^*(z_{(3|)},t)$ imposed on the surface $z^3 = 1$. Similar to the first scenario, a highly accurate tracking behavior is obtained also in the presence of a

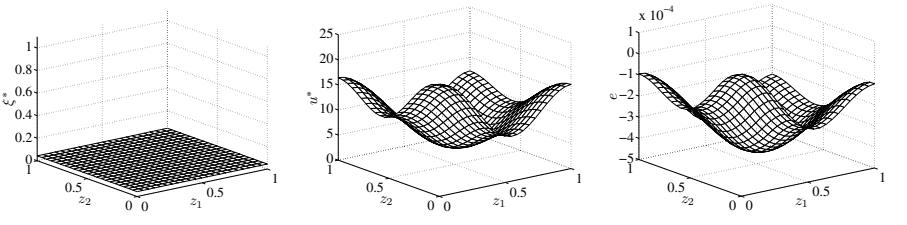

(a) $t = 0.8$

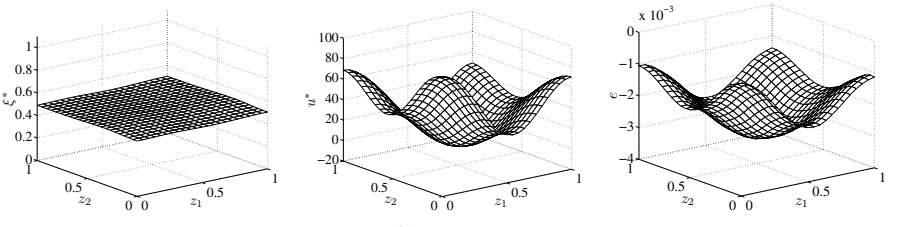

(b) $t = 1.0$

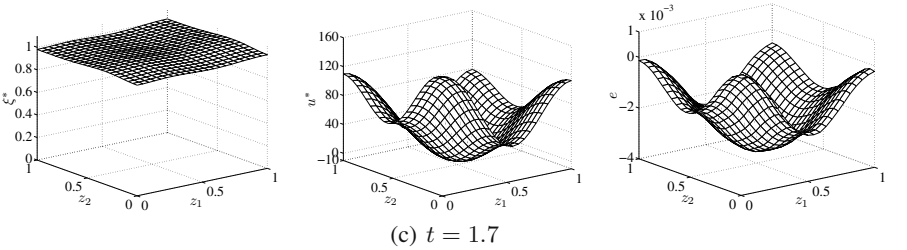

(c) $t = 1.7$

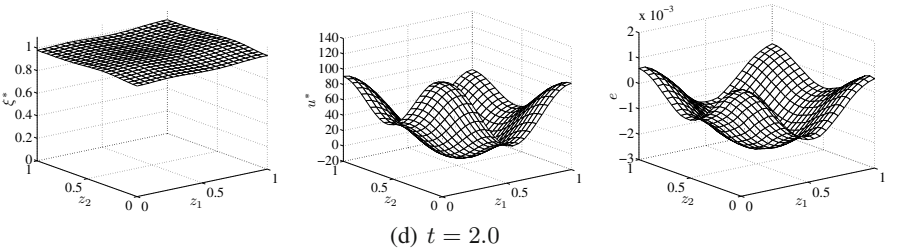

(d) $t = 2.0$

Fig. 7.4 Trajectory planning for the basic output and simulation results for scenario (II) with $a_{1,j} = 20$, $j = 1, 2, 3$. Left: desired trajectory $\xi^*(z_{(3|)}, t)$ for the basic output in the (z^1, z^2)–domain; middle: corresponding feedforward control $u^*(z_{(3|)}, t)$; right: tracking error $e(z_{(3|)}, t) = \xi^*(z_{(3|)}, t) - x(z_{(3|0)}, t)$; ©2009, IEEE.

spatially and time varying reaction parameter. The respective spatial–temporal evolution of $x(z, t)$ is depicted in Figure 7.5, where the emerging profiles in the cuboid are shown at $t \in \{0, 0.8, 1.0, 1.2, 1.7, 2.0\}$. Differing from the isotropic case considered in Section 7.5.1, the simulation results illustrate the spatially non–uniform state distribution within the cuboid due to the spatially and time varying reaction

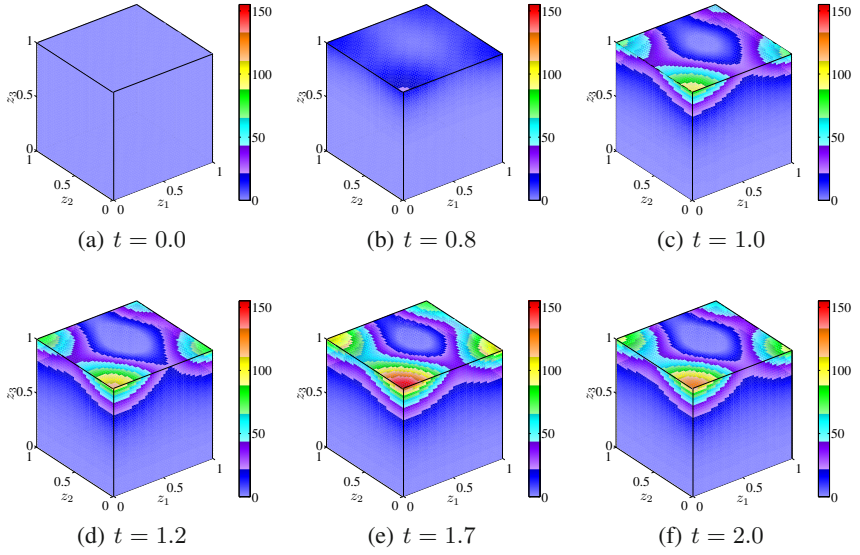

Fig. 7.5 Snapshots of the spatial–temporal evolution of $x(z,t)$ in scenario (II) for $a_{1,j} = 20$, $j = 1,2,3$, at $t \in \{0, 0.8, 1.0, 1.2, 1.7, 2.0\}$ with $u^*(z_{(3|)}, t)$ applied to the surface $z^3 = 1$; ©2009, IEEE.

parameter (7.40) for $a_{1,j} = 20$, $j = 1,2,3$. Nevertheless, although rather large variations in the input on the surface $z^3 = 1$ are required throughout the transition, the state $x(z,t)$ on the surface $z^3 = 0$ accurately follows the prescribed spatial–temporal path $\xi^*(z_{(3|)}, t)$. In particular, (7.43) yields that $x(z_{(3|0)}, t)$ evolves according to $x^*(z_{(3|0)}, t) = \sum_{k=1}^{K} \langle 1, \psi_k(z_{(3|)}) \rangle \psi_k(z_{(3|)})$ for $t \geq 2$ while the overall profile $x(z,t)$ varies periodically with the input $u^*(z_{(3|)}, t)$.

Notes

The results of this chapter are partly based on [14]. Acknowledgement is given to ©2009, IEEE. Reprinted, with permission, from T. Meurer and A. Kugi, "Trajectory planning for boundary controlled parabolic PDEs with varying parameters on higher-dimensional spatial domains", IEEE Transactions on Automatic Control, 54(8):1854–1868.

References

1. Atkinson, B.: Biochemical Reactors. Pion Limited (1974)
2. Baehr, H., Stephan, K.: Heat and Mass Transfer, 2nd edn. Springer, Berlin (2006)
3. Bird, R., Stewart, W., Lightfoot, E.: Transport Phenomena. John Wiley & Sons, Inc., New York (2002)
4. Curtain, R., Zwart, H.: An Introduction to Infinite–Dimensional Linear Systems Theory. Texts in Applied Mathematics, vol. 21. Springer, New York (1995)
5. Davis, T.: UMFPACK (2009), `http://www.cise.ufl.edu/research/sparse/umfpack`
6. Evans, L.: Partial Differential Equations. Graduate Studies in Mathematics, vol. 19. American Mathematical Society, Providence (2002)
7. Friedman, A.: Partial differential equations of parabolic type. Prentice–Hall, Englewood Cliffs (1964)
8. Gevrey, M.: Sur la nature analytique des solutions des équations aux dérivées partielles. Annales Scientifiques de l'Ecole Normale Superieure 25, 129–190 (1918)
9. Hua, C., Rodino, L.: General theory of PDE and Gevrey classes. In: Min-You, Q., Rodino, L. (eds.) General Theory of PDEs and Microlocal Analysis, pp. 6–81. Addison Wesley (1996)
10. Ladyženskaja, O., Solonnikov, V., Ural'ceva, N.: Linear and Quasi–linear Equations of Parabolic Type. Translations of Mathematical Monographs, 5th edn., vol. 23. American Mathematical Society, Providence (1998)
11. Laroche, B., Martin, P., Rouchon, P.: Motion planning for the heat equation. Int. J. Robust Nonlinear Control 10, 629–643 (2000)
12. Lions, J., Magenes, E.: Non–Homogeneous Boundary Value Problems and Applications, vol. 3. Springer, Berlin (1973)
13. Lynch, A., Rudolph, J.: Flatness–based boundary control of a class of quasilinear parabolic distributed parameter systems. Int. J. Control 75(15), 1219–1230 (2002)
14. Meurer, T., Kugi, A.: Trajectory planning for boundary controlled parabolic PDEs with varying parameters on higher-dimensional spatial domains. IEEE T. Automat. Contr. 54(8), 1854–1868 (2009)
15. Rodino, L.: Linear Partial Differential Operators in Gevrey Spaces. World Scientific Publishing Co. Pte. Ltd., Singapore (1993)
16. Thomas, J.: Numerical Partial Differential Equations: Finite Difference Methods. Texts in Applied Mathematics, vol. 22. Springer, New York (1998)

Chapter 8
Backstepping for Linear Diffusion–Convection–Reaction Systems with Varying Parameters on 1–Dimensional Domains

For finite–dimensional (nonlinear) systems backstepping yields a powerful recursive technique for feedback stabilization [13]. The approach relies on the application of a Lyapunov–based or passivation design to a part of the system followed by a successive reapplication by augmenting the subsystem at each step to finally recover the whole system [27, 11].

Initial results for the application of backstepping to linear distributed–parameter systems trace back to [5, 6], where the recursive design is applied to a semi–discretization of the governing PDEs using finite differences. Herein, weak convergence results are established for vanishing discretization stepsize in the limit as the semi–discrete formulation approaches the continuous limit. In view of the late lumping approach, where the distributed–parameter system description is explicitly considered for control design, subsequent extensions [19, 28, 4, 29] motivate the utilization of a Volterra integral equation to achieve a one–to–one correspondence between the possibly unstable plant dynamics and a suitably selected exponentially stable target system. For this, it is required to solve a BVP with higher–dimensional domain governing the evolution of the kernel. This enables to compute the state–feedback control, which realizes the desired transformation [31, 14, 12, 15, 32, 7, 33]. Moreover, backstepping can be similarly applied for the state–observer design [30, 14]. In combination with state–feedback control this results in dynamic output feedback control for the exponential stabilization of the distributed–parameter system. Besides linear systems with constant or spatially varying parameters results are available for time varying reaction parameters [31], spatially and time varying coefficients [22] and nonlinearities in terms of Volterra series [34, 35].

Based on these results, in the following a unique combination of backstepping and differential flatness is considered to develop an integrated trajectory planning and tracking control design approach for unstable boundary controlled parabolic distributed–parameter systems defined on a 1–dimensional spatial domain with spatially and time varying parameters. For this, backstepping by means of a Volterra integral transformation is used in Section 8.2 to determine a state–feedback control, which maps the original distributed–parameter system into an exponentially stable target distributed–parameter system of a significantly simpler structure. Differing

T. Meurer: Control of Higher-Dimensional PDEs, CCE, pp. 223–267.
springerlink.com

from classical PDE–backstepping the time variance induces that the integral kernel is also a function of time and is governed by an IBVP with triangular spatial domain [22, 23]. For its solution the method of integral operators is applied together with a successive approximation, which yields a functional series representation of the kernel. Series convergence thereby relies on certain Gevrey class properties of the system parameters. Together with the inverse backstepping transformation these considerations enable to deduce the exponential stabilization of the governing distributed–parameter system under the determined state–feedback control with the decay behavior being defined by the target system.

Since the state–feedback control essentially relies on the complete knowledge of the system state the control–loop has to be extended by a suitable state–observer to estimate the spatial–temporal evolution of the system state. For its design it is shown in Section 8.3 that backstepping can be similarly applied for the determination of the output injection gains of a Luenberger–type observer consisting of a system copy and the correction by means of the measured output. By combining the backstepping–based state–feedback control and state–observer a separation principle is deduced, which enables to verify the exponential stability of the composite distributed–parameter system.

Finally, it is shown in Section 8.4 that a reformulation of the target system allows to introduce an additional degree–of–freedom. The latter can be exploited for the flatness–based trajectory planning and feedforward control design to realize the tracking of suitably prescribed desired trajectories for the output of the original system with varying parameters. The combination of flatness–based trajectory planning with backstepping–based state–feedback control and state–observer design hence results in a systematics for the integrated design of exponentially stabilizing tracking control given parabolic distributed–parameter systems. This is confirmed by simulation studies in Section 8.5, which confirm the applicability of the introduced concepts and the achievable tracking performance.

Notation. Throughout this chapter $z = z^1$ is used to simplify the presentation for the spatially 1–dimensional setting. Moreover, the dependency of the system variables on the independent coordinates z and t is explicitly stated in any expression.

8.1 Stabilization and Tracking Control Problem

Subsequently, a scalar linear diffusion–convection–reaction system with spatially and time varying parameters and nonlinear boundary input is considered. The PDE reads as

$$\partial_t x(z,t) = a(z)\partial_z^2 x(z,t) + b(z)\partial_z x(z,t) + c(z,t)x(t) \tag{8.1a}$$

with domain $(z,t) \in (0,L) \times \mathbb{R}^+_{t_0}$, where $\mathbb{R}^+_{t_0} := \{t \in \mathbb{R}^+ : t > t_0\}$. Mixed boundary conditions are considered with

$$-\epsilon^0 \partial_z x(0,t) + p^0 x(0,t) = 0, \qquad t > t_0 \tag{8.1b}$$

$$\theta(x(L,t), \partial_z x(L,t)) = u(t), \qquad t > t_0 \tag{8.1c}$$

while the consistent initial condition follows as

$$x(z,t_0) = x_0(z), \qquad z \in [0,L]. \tag{8.1d}$$

Depending on the values of $\epsilon^0 \geq 0$, $p^0 \geq 0$, a Dirichlet ($\epsilon^0 = 0$, $p^0 = 1$), a Neumann ($\epsilon^0 = 1$, $p^0 = 0$), or a mixed boundary condition ($\epsilon^0 \neq 0$, $p^0 \neq 0$) is obtained at $z = 0$. Furthermore note that the boundary input $u(t)$ at $z = L$ enters the system in a general nonlinear fashion governed by the continuous but not necessarily bounded functional $\theta(\cdot,\cdot)$, which combines the state and its gradient at the outlet. For results on the existence and uniqueness of solutions to (8.1) with the input $u(t)$ from a certain Banach space, the interested reader is referred to, e.g., [18, 2, 1, 16]. Note that in general the existence of a solution is restricted to a certain finite time–interval due to the time–dependence of $c(z,t)$. In addition, depending on the growth of the functional $\theta(\cdot,\cdot)$, the nonlinear boundary condition (8.1c) might introduce a finite time blow–up of the solution. The system output $y(t)$ is assumed as

$$y(t) = h^0 \partial_z x(0,t) + h^1 x(0,t), \qquad t \geq t_0 \tag{8.1e}$$

with h^0, h^1 fulfilling the condition $h^0 p^0 + h^1 \epsilon^0 \neq 0$ so that (8.1b) and (8.1e) are linearly independent.

Since (8.1a) represents a parabolic PDE $0 < a_l \leq a(z) \leq a_u$ has to hold for all $z \in [0,L]$ with positive finite constants a_l and a_u. Further properties concerning differentiability of $a(z)$, $b(z)$, and $c(z,t)$ are summarized below.

Assumption 8.1. The system parameters satisfy the following conditions:

(i) The parameters fulfill $a(z) \in \mathcal{C}^2([0,L])$, $b(z) \in \mathcal{C}^1([0,L])$.
(ii) Convective flow is directed in the negative z–direction while flow reversal is excluded, i.e. $0 \leq b(z) \leq b_u$ for all $z \in [0,L]$.
(iii) The reaction parameter is a Gevrey class function in t and satisfies $c(z,t) \in \mathcal{C}^0([0,L]) \times G_{D,\alpha}(\mathbb{R}^+_{t_0})$ for $\alpha \leq 2$.

The considered stabilization and tracking control problem

$$x(z,t) \xrightarrow{u(t)} x^*(z,t) \text{ with } \|x(z,t) - x^*(z,t)\|_X \leq M e^{-\beta(t-t_0)},\ \beta > 0 \tag{8.2a}$$

is concerned with the design of an exponentially stabilizing controller $u(t)$ to realize the tracking $y(t) \to y^*(t)$ of suitably prescribed trajectories $y^*(t)$ for the output $y(t)$. Note that this problem implicitly includes the realization of finite time transitions between an initial stationary profile $x_0(z)$ and a final stationary profile $x_T(z)$ along the desired output path $y^*(t)$, i.e.

$$x_0(z) = x(z,t_0) \xrightarrow[t\in[t_0,t_0+T]]{u(t)} x(z,t_0+T) = x_T(z), \quad z \in \overline{\Omega}. \tag{8.2b}$$

For the solution of the tracking problem, in the following an integrated approach is proposed by combining backstepping and differential flatness.

Remark 8.1. The considered system formulation (8.1) covers a large class of examples arising in thermal or chemical engineering (cf. also the exposition in Chapter 2). Thereby, spatially varying parameters are obtained for anisotropic materials such as heat conduction or diffusion through multi–layered or porous media or built–in components influencing the convective flow. Furthermore, ageing effects as well as varying sources or sinks depending linearly on the state are generically represented by the reaction parameter $c(z,t)$ depending on the coordinates z and t. Typically, the parameters ϵ^0 and p^0 introduced in the boundary condition (8.1b) are related to the parameters $a(z)$ and $b(z)$ of the PDE (8.1a) by $\epsilon^0 = a(0)$ and $p^0 = Pb(0)$ with a constant $P > 0$. For thermal problems, the parameter p^0 typically represents the heat transfer coefficient (see, e.g., [3]) while for systems arising in chemical engineering p^0 is a function of the convection speed $b(0)$ (see, e.g., [25]). Moreover, as is shown in Chapter 3, interconnected multi–agent networks can be similarly embedded into the mathematical framework of diffusion–convection–reaction systems.

By proceeding identical to Section 7.1.1, an invertible change of coordinates can be introduced in such a way that the consideration of the distributed–parameter system (8.1) is equivalent to the analysis of the linear diffusion–reaction system with a single varying parameter governed by

$$\partial_t x(z,t)(z,t) = \partial_z^2 x(z,t)(z,t) + c(z,t)x(z,t) \tag{8.3a}$$

defined on $z \in (0,1),\ t \in \mathbb{R}_{t_0}^+$ with boundary conditions

$$-\epsilon^0 \partial_z x(0,t) + p^0 x(0,t) = 0, \qquad t > t_0 \tag{8.3b}$$

$$\theta\left(x(1,t), \partial_z x(1,t)\right) = u(t), \qquad t > t_0, \tag{8.3c}$$

and initial condition

$$x(z,t_0) = x_0(z), \qquad z \in [0,1]. \tag{8.3d}$$

The structure of the output (8.1e) remains unchanged, i.e.

$$y(t) = h^0 \partial_z x(0,t) + h^1 x(0,t), \qquad t \geq t_0. \tag{8.3e}$$

Subsequently, in a first step a backstepping–based boundary controller is designed in order to exponentially stabilize the possibly unstable parabolic diffusion–reaction system (8.3) and hence the diffusion–convection–reaction system (8.1).

8.2 Exponentially Stabilizing State–Feedback Control

In the following, the kernel of a Volterra integral transformation is determined to transform the diffusion–reaction system (8.3) into a prescribed exponentially stable target distributed–parameter system. It is thereby shown that the kernel has to satisfy a particular linear PDE with a spatially and time varying parameter defined on a triangular spatial domain. For its solution the method of integral operators together with a successive series approximation is applied and convergence is verified for a varying parameter of a certain Gevrey order.

8.2.1 Selection of the Target System

PDE–backstepping crucially relies on the appropriate choice of a target system to ensure asymptotic or exponential stability of the closed–loop control system. For the subsequent analysis and for the determination of the PDE governing the backstepping kernel, the following lemma is utilized.

Lemma 8.1. *The parabolic PDE*

$$\partial_t w(z,t) = \partial_z^2 w(z,t) - \mu(t) w(z,t), \qquad z \in (0,1),\ t > t_0 \tag{8.4a}$$

$$w(z,t_0) = w_0(z), \qquad z \in [0,1] \tag{8.4b}$$

is exponentially stable in the L^2–norm for any combination of Dirichlet, Neumann, and mixed boundary conditions

$$-\epsilon_w^0 \partial_z w(0,t) + p_w^0 w(0,t) = 0, \qquad t > t_0 \tag{8.4c}$$

$$\epsilon_w^1 \partial_z w(1,t) + p_w^1 w(1,t) = 0 \qquad t > t_0 \tag{8.4d}$$

if $\mu(t) + \lambda_{\min} > \epsilon > 0,\ \forall t \in \mathbb{R}_{t_0}^+$ for some $\epsilon > 0$, where $\lambda_{\min}$ denotes the smallest eigenvalue λ of the Sturm–Liouville problem $\partial_z^2 w(z,t) + \lambda w(z,t) = 0$ with BCs (8.4c)*,* (8.4d)*.*

The proof of Lemma 8.1 follows directly from a Lyapunov–type argument together with the Rayleigh principle.

Proof. Let $X = L^2(0,1)$ and consider the change of the positive semi–definite Lyapunov functional $V(t) = 1/2\|w(t)\|_X^2$ along a solution trajectory of (8.4), i.e.

$$\begin{aligned}\partial_t V(t) &= \int_0^1 \partial_z^2 w(z,t) w(z,t) \mathrm{d}z - \mu(t)\|w(t)\|_X^2 \\ &= -\|\partial_z w(t)\|_X + \left[\partial_z w(z,t) w(z,t)\right]_{z=0}^{z=1} - \mu(t)\|w(t)\|_X^2.\end{aligned}$$

Moreover, it is a classical result that the Sturm–Liouville problem consisting of the PDE $\partial_z^2 w(z,t) + \lambda w(z,t) = 0$ with boundary conditions (8.4c) and (8.4d) possesses

a purely discrete and simple set of eigenvalues, which can be arranged according to $0 \leq \lambda_1 < \lambda_2 < \ldots$. Hence, it follows that

$$\begin{aligned} 0 &= \int_0^1 w(z,t)\partial_z^2 w(z,t)\mathrm{d}z + \lambda \|w(t)\|_X^2 \\ &= -\|\partial_z w(t)\|_X^2 + \left[\partial_z w(z,t) w(z,t)\right]_{z=0}^{z=1} + \lambda \|w(t)\|_X^2 \end{aligned}$$

such that

$$-\|\partial_z w(t)\|_X^2 + \left[\partial_z w(z,t) w(z,t)\right]_{z=0}^{z=1} = -\lambda \|w(t)\|_X^2 \leq -\lambda_1 \|w(t)\|_X^2. \quad (8.5)$$

Let $\lambda_{\min} = \lambda_1$, then $\partial_t V(t) = 1/2\, \partial_t \|w(t)\|_X^2 \leq -(\lambda_{\min} + \mu(t))\|w(t)\|_X^2$ or equivalently

$$\|w(t)\|_X \leq e^{-\int_{t_0}^t (\lambda_{\min} + \mu(\tau))\mathrm{d}\tau} \|w_0\|_X.$$

Thus, $\|w(t)\|_X \to 0$ exponentially if there exists an $\epsilon > 0$ such that $\lambda_{\min} + \mu(t) > \epsilon$ for all $t \in \mathbb{R}_{t_0}^+$. □

Given Dirichlet or Neumann boundary conditions, a further improvement is possible to verify that $\sup_{z\in[0,1]} |w(z,t)|$ decays exponentially in t.

Lemma 8.2. *The parabolic PDE* (8.4) *is exponentially stable in the* H^1*–norm and the* sup*–norm* $\|w(t)\|_\infty = \sup_{z\in[0,1]} |w(z,t)|$ *for boundary conditions satisfying*

$$w(z,t)\partial_z w(z,t) = 0 \text{ at } z \in \{0,1\} \quad (8.6)$$

if $\mu(t) + \lambda_{\min} > \epsilon > 0,\ \forall t \in \mathbb{R}_{t_0}^+$ *for some* $\epsilon > 0$. *Herein,*

$$\lambda_{\min} = \begin{cases} \pi^2, & \text{if } w(0,t) = w(1,t) = 0 \\ \frac{\pi^2}{4}, & \text{if } w(0,t) = \partial_z w(1,t) = 0 \ \vee\ \partial_z w(0,t) = w(1,t) = 0 \\ 0, & \text{if } \partial_z w(0,t) = \partial_z w(1,t) = 0. \end{cases}$$

This result follows in a way rather analogous to the proof of Lemma 8.1 by considering the change of the positive semi–definite Lyapunov functional $V(t) = 1/2 \int_0^1 (w^2(z,t) + (\partial_z w(z,t))^2 \mathrm{d}z$ along a solution trajectory of (8.4) with (8.6) together with the Rayleigh principle and the Agmon inequality.

Proof. Consider the positive semi–definite Lyapunov functional

$$V(t) = \frac{1}{2}\|w(t)\|_{H^1}^2 = \frac{1}{2}\int_0^1 w^2(z,t)\mathrm{d}z + \frac{1}{2}\int_0^1 (\partial_z w(z,t))^2 \mathrm{d}z$$

such that

$$\partial_t V(t) = \int_0^1 \partial_z^2 w(z,t) w(z,t)\mathrm{d}z - \mu(t)\|w(t)\|_{L^2}^2$$

$$
\begin{aligned}
&\quad + \int_0^1 \partial_t \partial_z w(z,t) \partial_z w(z,t) \mathrm{d}z \\
&= -\|\partial_z w(t)\|_{L^2} + \left[\partial_z w(z,t) w(z,t)\right]_{z=0}^{z=1} - \mu(t)\|w(t)\|_{L^2}^2 \\
&\quad - \|\partial_z^2 w(t)\|_{L^2} + \left[\partial_z^2 w(z,t) \partial_z w(z,t)\right]_{z=0}^{z=1} - \mu(t)\|\partial_z w(t)\|_{L^2}^2 \\
&\overset{(8.4)}{\underset{(8.6)}{=}} -\|\partial_z w(t)\|_{L^2} - \mu(t)\|w(t)\|_{L^2}^2 - \|\partial_z^2 w(t)\|_{L^2} - \mu(t)\|\partial_z w(t)\|_{L^2}^2.
\end{aligned}
$$

Proceeding as in the proof of Lemma 8.1 by exploiting the Sturm–Liouville properties of the PDE $\partial_z^2 w(z,t) + \lambda w(z,t) = 0$ it follows that

$$
\begin{aligned}
0 &= \int_0^1 \partial_z^2 w(z,t) \partial_z^2 w(z,t) \mathrm{d}z + \lambda \int_0^1 \partial_z^2 w(z,t) w(z,t) \mathrm{d}z \\
&= \|\partial_z^2 w(t)\|_{L^2}^2 - \lambda \|\partial_z w(t)\|_{L^2}^2
\end{aligned}
$$

and hence

$$
-\|\partial_z^2 w(t)\|_{L^2}^2 = -\lambda \|\partial_z w(t)\|_{L^2}^2 \leq -\lambda_1 \|\partial_z w(t)\|_{L^2}^2.
$$

Here, $\lambda_{\min} = \lambda_1$ denotes the smallest eigenvalue λ of $\partial_z^2 w(z,t) + \lambda w(z,t) = 0$ with homogeneous Dirichlet or Neumann boundary conditions. An explicit computation easily yields the values provided in the lemma. Together with (8.5) this implies $\partial_t V(t) \leq -2(\lambda_{\min} + \mu(t)) V(t)$ or equivalently

$$
\|w(t)\|_{H^1} \leq e^{-\int_0^t (\lambda_{\min} + \mu(\tau)) \mathrm{d}\tau} \|w_0\|_{H^1}.
$$

Moreover, this yields

$$
\begin{aligned}
2\|w(t)\|_{L^2} \|\partial_z w(t)\|_{L^2} &\leq \|w(t)\|_{L^2}^2 + \|\partial_z w(t)\|_{L^2}^2 \\
&\leq e^{-\int_0^t (\lambda_{\min} + \mu(\tau)) \mathrm{d}\tau} \left(\|w_0\|_{L^2}^2 + \|\partial_z w_0\|_{L^2}^2 \right),
\end{aligned}
$$

which in view of the Agmon inequality implies

$$
\|w(t)\|_{\infty} \leq e^{-\int_0^t (\lambda_{\min} + \mu(\tau)) \mathrm{d}\tau} \left(\|w_0\|_{L^2}^2 + \|\partial_z w_0\|_{L^2}^2 \right).
$$

Thus, both $\|w(t)\|_{H^1} \to 0$ and $\|w(t)\|_{\infty} \to 0$ exponentially if there exists an $\epsilon > 0$ such that $\lambda_{\min} + \mu(t) > \epsilon$ for all $t \in \mathbb{R}_{t_0}^+$. □

With these preparations the kernel of a backstepping–like integral transformation can be determined relating the possibly unstable diffusion–reaction system (8.3) and the exponentially stable target system (8.4).

8.2.2 Determination of the Kernel–PDE

The fundamental idea of the backstepping approach for distributed–parameter systems (see, e.g., [31]) is related to the introduction of a Volterra–type integral transformation

$$w(z,t) = x(z,t) - \int_0^z k(z,\zeta,t)x(\zeta,t)\mathrm{d}\zeta, \tag{8.7}$$

which traces back to [8], to transform (8.3a)–(8.3d) into the exponentially stable target system (8.4). For this, observe that the integral kernel $k(z,\zeta,t)$ has to be chosen as a function of t to deal with the time varying parameter $c(z,t)$ of the diffusion–reaction system (8.3a)–(8.3d). This in particular constitutes a major difference to the backstepping approach for distributed–parameter systems with constant or spatially varying parameters[1] [29, 31, 12].

Differentiation of (8.7) with respect to z and t yields

$$\begin{aligned}
\partial_z w(z,t) &= \partial_z x(z,t) - k(z,z,t)x(z,t) - \int_0^z \partial_z k(z,\zeta,t)x(\zeta,t)\mathrm{d}\zeta \qquad (8.8)\\
\partial_z^2 w(z,t) &= \partial_z^2 x(z,t) - \mathrm{d}_z k(z,z,t)x(z,t) - k(z,z,t)\partial_z x(z,t)\\
&\quad - \partial_z k(z,z,t)x(z,t) - \int_0^z \partial_z^2 k(z,\zeta,t)x(\zeta,t)\mathrm{d}\zeta\\
\partial_t w(z,t) &= \partial_t x(z,t) - \int_0^z \big[\partial_t k(z,\zeta,t)x(\zeta,t) + k(z,\zeta,t)\partial_t x(\zeta,t)\big]\mathrm{d}\zeta,
\end{aligned}$$

where $\mathrm{d}_z k(z,z,t) = \partial_z k(z,z,t) + \partial_\zeta k(z,z,t)$ is the total differential. The latter equation can be further evaluated by substituting (8.3a) and integrating by parts such that

$$\begin{aligned}
\partial_t w(z,t) &= \partial_z^2 x(z,t) + c(z,t)x(z,t)\\
&\quad - \big[k(z,\zeta,t)\partial_\zeta x(\zeta,t) - \partial_\zeta k(z,\zeta,t)x(\zeta,t)\big]_{\zeta=0}^{\zeta=z}\\
&\quad - \int_0^z \big[\partial_t k(z,\zeta,t) + \partial_\zeta^2 k(z,\zeta,t) + c(\zeta,t)k(z,\zeta,t)\big]x(\zeta,t)\mathrm{d}\zeta.
\end{aligned}$$

As a result, given the target system (8.4a) it follows that the kernel $k(z,\zeta,t)$ has to satisfy the equation

[1] Note that in [31] besides spatially varying parameters a series solution for the backstepping kernel is determined if $c(z,t) = c(t)$ with a Dirichlet BC. However, this result cannot be extended to the considered case of a general non–separable parameter $c(z,t) \in \mathcal{C}^0([0,1]) \times G_{D,\alpha}(\mathbb{R}_{t_0}^+)$ with either Dirichlet, Neumann or mixed BC.

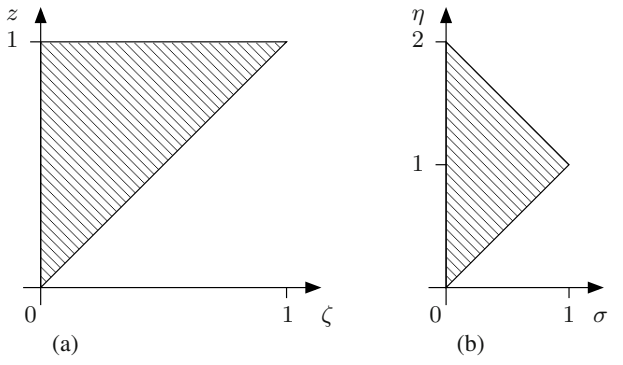

Fig. 8.1 Domains of integration of the kernel–PDE: in the (z,ζ)–domain with $\zeta \in (0,1)$, $z \in (\zeta,1)$ (left) and in the (η,σ)–domain as defined in (8.11) with $\sigma \in (0,1)$, $\eta \in (\sigma, 2-\sigma)$ (right).

$$\begin{aligned} 0 = \int_0^z \big[&\partial_t k(z,\zeta,t) + \partial_\zeta^2 k(z,\zeta,t) - \partial_z^2 k(z,\zeta,t) \\ &+ \gamma(\zeta,t) k(z,\zeta,t)\big] x(\zeta,t)\mathrm{d}\zeta - x(z,t)\big(\gamma(z,t) + 2\mathrm{d}_z k(z,z,t)\big) \\ &- k(z,0,t)\partial_z x(0,t) + \partial_\zeta k(z,0,t) x(0,t), \end{aligned} \tag{8.9}$$

where

$$\gamma(z,t) = c(z,t) + \mu(t).$$

From this, the so–called kernel–PDE can be deduced, i.e.

$$\partial_t k(z,\zeta,t) = \partial_z^2 k(z,\zeta,t) - \partial_\zeta^2 k(z,\zeta,t) - \gamma(\zeta,t) k(z,\zeta,t) \tag{8.10a}$$

defined on the triangular domain $\zeta \in (0,1)$, $z \in (\zeta,1)$ depicted in Figure 8.1(a). The respective boundary condition along $\zeta = z$ follows immediately as

$$\gamma(z,t) + 2\mathrm{d}_z k(z,z,t) = 0. \tag{8.10b}$$

The determination of the remaining boundary condition requires to distinguish between the specification of a Dirichlet or a mixed boundary condition at $z = 0$ for the PDE (8.3a). Moreover, observe that the boundary condition at $z = 0$ for the target system (8.4a) cannot be assigned independently but follows directly from the respective boundary condition for $x(z,t)$. In order to illustrate this, consider a Dirichlet condition for $x(z,t)$ at $z = 0$, i.e. $\epsilon^0 = 0$, $p^0 = 1$ in (8.3b). Hence from (8.7) one obtains that $w(0,t) = 0$ while from (8.9) with (8.10a), (8.10b) it follows that the kernel has to satisfy $k(z,0,t) = 0$. Proceeding similarly for a mixed boundary condition, the following relations can be determined:

(i) For a Dirichlet condition at $z = 0$, i.e. $\epsilon^0 = 0$, $p^0 \neq 0$ in (8.3b), the kernel has to satisfy

$$k(z,0,t) = 0 \tag{8.10c}$$

while the target system is restricted to

$$w(0,t) = 0. \tag{8.10d}$$

(ii) For a mixed condition at $z = 0$, i.e. $\epsilon^0 \neq 0,\ p^0 \neq 0$ in (8.3b), the kernel has to satisfy

$$-\partial_\zeta k(z,0,t) + \bar{p}^0 k(z,0,t) = 0, \tag{8.10e}$$

where $\bar{p}^0 = p^0/\epsilon^0$. In this case, the target system is restricted to

$$-\epsilon_w^0 \partial_z w(0,t) + p_w^0 w(0,t) = 0 \tag{8.10f}$$

with ϵ_w^0 and p_w^0 chosen to ensure stability of the target system (cf. Lemma 8.1 and 8.2). Thereby, the kernel has to fulfill the additional constraint

$$k(0,0,t) = \bar{p}^0 - \frac{p_w^0}{\epsilon_w^0}. \tag{8.10g}$$

The initial conditions at $t = t_0$ for $x(z,t)$, $w(z,t)$, and $k(z,\zeta,t)$ have to satisfy the constraint

$$\int_0^z k(z,\zeta,t_0) x_0(\zeta) \mathrm{d}\zeta = x_0(z) - w_0(z), \qquad z \in [0,1]. \tag{8.10h}$$

Hence, if $x_0(z) = w_0(z)$ this yields $k(z,\zeta,t_0) = 0$. The presentation reveals that in general a closed–form analytical solution of the kernel–PDE (8.10a) with boundary conditions (8.10b) as well as (8.10c) or (8.10e), (8.10g) and initial condition (8.10h) is hardly available. This is in particular due to the unusual type of PDE (8.10a), whose spatial operator, i.e. its right–hand side, is hyperbolic while only a first order derivative of $k(z,\zeta,t)$ with respect to t appears. Hence, standard solution approaches such as the finite–difference method cannot be directly applied. For the special case of $\gamma(\zeta,t) = \gamma(t)$ and Dirichlet boundary condition at $z = 0$, a series solution to the kernel–PDE is obtained in [31]. Nevertheless, this approach is based on a specific transformation involving the only time varying parameter $\gamma(t)$ and cannot be extended to the general case of a spatially and time varying parameter $\gamma(\zeta,t)$. In the subsequent section, the so–called method of integral operators as introduced in [8] is considered in order to determine a solution to the kernel equations.

8.2.3 Solution of the Kernel–PDE

Under the assumption that $\gamma(\zeta,t)$ is analytic in t, the existence of a solution to the kernel–PDE is studied in [8] along the lines of the Cauchy–Kovalevskaya theorem.

In [26] it is pointed out that a general existence result is so far not available. For the special case of $\gamma(z,t) = \gamma(z) \in \mathcal{C}^1([0,1])$, a strong solution is obtained in [19].

In the following a strong solution of the kernel–PDE is determined under the assumption that $\gamma(\zeta,t) \in \mathcal{C}^0([0,1]) \times G_{D,\alpha}(\mathbb{R}^+_{t_0})$ for $\alpha \in [1,2]$ by applying the so–called method of integral operators. The kernel is thereby recursively computed by a successive approximation technique. For this, scattering coordinates are introduced

$$\eta = z + \zeta, \qquad \sigma = z - \zeta, \tag{8.11}$$

such that $k(z,\zeta,t) = \bar{k}(\eta(z,\zeta),\sigma(z,\zeta),t)$. In view of (8.10a), (8.10b) this yields that $\bar{k}(\eta,\sigma,t)$ has to satisfy the PDE

$$\partial_t \bar{k}(\eta,\sigma,t) = 4\partial_\eta \partial_\sigma \bar{k}(\eta,\sigma,t) - \gamma\Big(\frac{\eta-\sigma}{2},t\Big)\bar{k}(\eta,\sigma,t) \tag{8.12a}$$

with the boundary condition

$$\gamma\left(\frac{\eta}{2},t\right) + 4\partial_\eta \bar{k}(\eta,0,t) = 0 \tag{8.12b}$$

since (8.11) implies that $\zeta = z$ is equivalent to $\sigma = 0$. Note that the transformed kernel–PDE (8.12a) is defined on the new domain $\sigma \in (0,1)$, $\eta \in (\sigma, 2-\sigma)$ depicted in Figure 8.1(b). In addition, depending on either a Dirichlet (8.10c) or a mixed boundary condition (8.10e), (8.10g) the following constraints are obtained at $\sigma = \eta$:

(i) For the Dirichlet condition (8.10c) it follows that

$$\bar{k}(\eta,\eta,t) = 0. \tag{8.12c}$$

(ii) For the mixed boundary condition (8.10e), (8.10g) the two relations

$$\partial_\sigma \bar{k}(\eta,\eta,t) - \partial_\eta \bar{k}(\eta,\eta,t) + \bar{p}^0 \bar{k}(\eta,\eta,t) = 0 \tag{8.12d}$$

$$\bar{k}(0,0,t) = \bar{p}^0 - \frac{p^0_w}{\epsilon^0_w} \tag{8.12e}$$

are imposed.

In order to determine a solution to (8.12a), (8.12b) with either (8.12c) or (8.12d), (8.12e), a formal integration with respect to σ and η is performed. This yields an implicit formal solution for $\bar{k}(\eta,\sigma,t)$, i.e.

$$\begin{aligned}\bar{k}(\eta,\sigma,t) = A(\eta,\sigma,t) + \int_0^\sigma \Bigg[& B_{\bar{k}}(\sigma,s,t) \\ & + \frac{1}{4}\int_\sigma^\eta \big(\partial_t \bar{k}(r,s,t) + \gamma\Big(\frac{r-s}{2},t\Big)\bar{k}(r,s,t)\big)\mathrm{d}r\Bigg]\mathrm{d}s,\end{aligned} \tag{8.13a}$$

where

$$A(\eta,\sigma,t)=\begin{cases}-\frac{1}{4}\int_\sigma^\eta \gamma\left(\frac{s}{2},t\right)\mathrm{d}s, & \text{Dirichlet BC}\\ \left(\bar{p}^0-\frac{p_w^0}{\epsilon_w^0}\right)e^{-\bar{p}^0\sigma}-\frac{1}{4}\int_\sigma^\eta \gamma\left(\frac{s}{2},t\right)\mathrm{d}s & \\ -\frac{1}{2}\int_0^\sigma e^{-\bar{p}^0(\sigma-r)}\gamma\left(\frac{r}{2},t\right)\mathrm{d}r, & \text{mixed BC}\end{cases} \tag{8.13b}$$

and

$$B_{\bar{k}}(\sigma,s,t)=\begin{cases}0, & \text{Dirichlet BC},\\ e^{-\bar{p}^0(\sigma-s)}C_{\bar{k}}(s,t), & \text{mixed BC}\end{cases} \tag{8.13c}$$

with

$$C_{\bar{k}}(s,t)=\frac{1}{2}\int_0^s\Big(\partial_t\bar{k}(s,v,t)+\gamma\Big(\frac{s-v}{2},t\Big)\bar{k}(s,v,t)\Big)\mathrm{d}v. \tag{8.13d}$$

For the explicit computation of the kernel $\bar{k}(\eta,\sigma,t)$ the method of successive approximation is applied to determine a solution of (8.13) in terms of the functional series

$$\bar{k}(\eta,\sigma,t)=\sum_{n=1}^{\infty}\bar{k}_n(\eta,\sigma,t). \tag{8.14}$$

Substituting (8.14) into (8.13a) yields that the coefficients $\bar{k}_n(\eta,\sigma,t)$, $n\geq 1$ are obtained recursively from

$$\bar{k}_1(\eta,\sigma,t)=A(\eta,\sigma,t) \tag{8.15a}$$

$$\bar{k}_n(\eta,\sigma,t)=\int_0^\sigma\Bigg[B_{\bar{k}_{n-1}}(\sigma,s,t)+\frac{1}{4}\int_\sigma^\eta\big(\partial_t\bar{k}_{n-1}(r,s,t)+\gamma\Big(\frac{r-s}{2},t\Big)\bar{k}_{n-1}(r,s,t)\big)\mathrm{d}r\Bigg]\mathrm{d}s,\quad n\geq 2. \tag{8.15b}$$

The convergence of the successive approximation is subsequently analyzed depending on the type of boundary conditions.

8.2.3.1 Dirichlet Conditions

For Dirichlet boundary conditions, convergence follows from the theorem below.

Theorem 8.1. *Given* $\gamma(z,t)\in\mathcal{C}^0([0,1])\times G_{D,\alpha}(\mathbb{R}^+_{t_0})$ *with* $\alpha\in[1,2]$*, then the series coefficients* (8.15) *obtained for the boundary condition* (8.12c) *satisfy*

$$\sup_{t\in\mathbb{R}^+_{t_0}} \left|\partial_t^l \bar{k}_n(\eta,\sigma,t)\right| \le \frac{D^{l+n}}{4^n}\left(\frac{(l+n-1)!}{(n-1)!}\right)^{\alpha} \times (\eta\sigma)^{n-1}(\eta-\sigma)\prod_{j=0}^{n-1}\frac{(1+j^{\alpha})}{(j+1)(j+\delta_{j,0})}, \quad n\ge 1. \tag{8.16}$$

In particular, the series (8.14) *converges absolutely and uniformly in the domain* $\sigma\in[0,1]$, $\eta\in[\sigma,2-\sigma]$ *for* $\alpha\in[1,2)$ *independent of* D *and for* $\alpha=2$ *if* $D<4$.

Proof. For the proof of Theorem 8.1 at first an induction argument is used to verify condition (8.16). Due to the explicit time–dependence of the recursion formula (8.15a), (8.15b) and the appearance of the time–derivative of $\bar{k}_n(\eta,\sigma,t)$, the convergence analysis of the functional series solution (8.14) requires to consider the growth of successive time–derivatives of each $\bar{k}_n(\eta,\sigma,t)$, $n\in\mathbb{N}$, up to an arbitrary order $l\in\mathbb{N}$. Once this is obtained, the absolute convergence of the series (8.14) can be evaluated by taking $l=0$.

With[2] $\gamma(z,t)\in\mathcal{C}^0([0,1])\times G_{D,\alpha}(\mathbb{R}^+_{t_0})$ for $\alpha\ge 1$, it follows for $n=1$ from (8.15a) with (8.13b)–(8.13d) given a Dirichlet boundary condition that

$$\sup_{t\in\mathbb{R}^+_{t_0}} |\partial_t^l \bar{k}_1(\eta,\sigma,t)| \le \sup_{t\in\mathbb{R}^+_{t_0}} \frac{1}{4}\int_\sigma^\eta \left|\partial_t^l\gamma(s/2,t)\right|\mathrm{d}s \le \frac{D^{l+1}}{4}(l!)^{\alpha}(\eta-\sigma),$$

which is equal to (8.16) for $n=1$. Assuming that (8.16) holds for all $n=1,2,\ldots,N-1$, $N>2$, one has

$$\begin{aligned}
&\sup_{t\in\mathbb{R}^+_{t_0}} \left|\partial_t^l \bar{k}_N(\eta,\sigma,t)\right| \\
&\le \sup_{t\in\mathbb{R}^+_{t_0}} \frac{1}{4}\int_\sigma^\eta\int_0^\sigma \Big(\left|\partial_t^{l+1}\bar{k}_{N-1}(r,s,t)\right| \\
&\quad + \sum_{j=0}^{l}\binom{l}{j}\left|\partial_t^j\gamma\Big(\frac{r-s}{2},t\Big)\right|\left|\partial_t^{l-j}\bar{k}_{N-1}(r,s,t)\right|\Big)\mathrm{d}s\mathrm{d}r \\
&\overset{(8.16)}{\le} \frac{D^{l+N}}{4^N((N-2)!)^{\alpha}}\prod_{j=0}^{N-2}\frac{(1+j^{\alpha})}{(j+1)(j+\delta_{j,0})}\int_\sigma^\eta\int_0^\sigma (rs)^{N-2}(r-s)\mathrm{d}s\mathrm{d}r\times \\
&\quad \left(((l+N-1)!)^{\alpha}+\sum_{j=0}^{l}\binom{l}{j}(j!)^{\alpha}((l+N-2-j)!)^{\alpha}\right) \\
&\overset{\substack{(B.18)\\(B.21)}}{\le} \frac{D^{l+N}}{4^N}\left(\frac{(l+N-1)!}{(N-1)!}\right)^{\alpha}(\eta\sigma)^{N-1}(\eta-\sigma)\prod_{j=0}^{N-1}\frac{(1+j^{\alpha})}{(j+1)(j+\delta_{j,0})}
\end{aligned}$$

[2] This implies $\sup_{t\in\mathbb{R}^+_{t_0}}|\partial_t^l\gamma(z,t)|\le D^{l+1}(l)^{\alpha}$ for all $z\in[0,1]$.

Thereby, the inequality $\sum_j a_j^\kappa \leq (\sum_j a_j)^\kappa$ for $\kappa \geq 1$ and $a_j \geq 0$ was used (see, e.g., [10]). In particular the obtained expression is identical to (8.16) for $n = N$, which proves the first result.

With this, the series (8.14) can be majorized using (8.16) evaluated at $l = 0$ since

$$\left|\bar{k}(\eta,\sigma,t)\right| =\leq \sum_{n=1}^{\infty}\left|\bar{k}_n(\eta,\sigma,t)\right| \leq \frac{D}{4}(\eta-\sigma)\sum_{n=0}^{\infty} a_{n+1}\left(\frac{D\eta\sigma}{4}\right)^n, \tag{8.17}$$

where

$$a_n = \prod_{j=0}^{n-1}\frac{(1+j^\alpha)}{((j+1)(j+\delta_{j,0}))}.$$

Given $\alpha = 1$ it follows immediately that $a_n = 1/(n-1)!$ such that $|\bar{k}(\eta,\sigma,t)| \leq D/4(\eta-\sigma)\exp(D\eta\sigma/4)$, which is bounded since $\sigma \in [0,1]$, $\eta \in [\sigma, 2-\sigma]$. Furthermore, note that the right hand side of (8.17) constitutes a power series in $D\eta\sigma/4$ whose radius of convergence ϱ can be determined from

$$\varrho = \lim_{n\to\infty}\left|\frac{a_{n+1}}{a_{n+2}}\right| = \lim_{n\to\infty}\frac{(n+1)(n+2)}{((n+1)^\alpha+1)}.$$

This yields

$$\varrho = \begin{cases}\infty, & \text{for } \alpha \in [1,2)\\ 1, & \text{for } \alpha = 2\\ 0, & \text{for } \alpha > 2.\end{cases}$$

As a result, the series converges with infinite radius of convergence if $\alpha \in [1,2)$. In addition if $\alpha = 2$, convergence requires that $D\eta\sigma/4 < 1$, which is equivalent to $D < 4$ since $\eta\sigma \leq 1$ in the considered domain $\sigma \in [0,1]$, $\eta \in [\sigma, 2-\sigma]$. □

8.2.3.2 Neumann and Mixed Conditions

Given mixed boundary conditions the convergence of the successive approximation can be guaranteed under the conditions formulated below.

Theorem 8.2. *Given* $\gamma(z,t) \in \mathcal{C}^0([0,1]) \times G_{D,\alpha}(\mathbb{R}^+_{t_0})$ *with* $\alpha \in [1,2]$*, then the series coefficients* (8.15) *obtained for the boundary conditions* (8.12d)*,* (8.12e) *satisfy*

$$\begin{aligned}\sup_{t\in\mathbb{R}^+_{t_0}}\left|\partial_t^l\bar{k}_n(\eta,\sigma,t)\right| \leq \left(\frac{\nu}{4}\right)^n D^{l+n}\left(\frac{(l+n-1)!}{(n-1)!}\right)^\alpha \times \\ (\eta\sigma)^{n-1}(\eta+\sigma)\prod_{j=0}^{n-1}\frac{(1+j^\alpha)}{(j+1)(j+\delta_{j,0})}, \quad n \geq 1\end{aligned} \tag{8.18}$$

if $\bar{p}^0 = p^0/\epsilon^0 = p_w^0/\epsilon_w^0$. *Herein,* $\nu = 1$ *if* $\bar{p}^0 \geq 0$ *while* $\nu = \exp(-\bar{p}^0)$ *if* $\bar{p}^0 < 0$. *If* $\bar{p}^0 \neq p_w^0/\epsilon_w^0$, *then* $\bar{k}_n(\eta,\sigma,t) = \bar{k}_n^1(\eta,\sigma,t) + \bar{k}_n^2(\eta,\sigma,t)$ *where* $\bar{k}_n^1(\eta,\sigma,t)$ *satisfies* (8.18) *and* $\bar{k}_n^2(\eta,\sigma,t)$ *is bounded by*

$$\sup_{t\in\mathbb{R}_{t_0}^+}\left|\partial_t^l \bar{k}_n^2(\eta,\sigma,t)\right| \leq \begin{cases} \nu\beta\delta_{l,0}, & n=1 \\ \beta D^{l+n-1}\nu^n\left(\frac{\eta\sigma}{4}\right)^{n-1}\left(\frac{(l+n-2)!}{(n-2)!}\right)^{\alpha}\times & \\ ((n-1)!)^{\alpha-2}, & n\geq 2 \end{cases} \tag{8.19}$$

with $\beta = |\bar{p}^0 - p_w^0/\epsilon_w^0|$. *In particular, the series* (8.14) *converges absolutely and uniformly in the domain* $\sigma \in [0,1]$, $\eta \in [\sigma, 2-\sigma]$ *for* $\alpha \in [1,2)$ *independent of* D *and* ν *and for* $\alpha = 2$ *if* $D\nu < 4$.

Proof. Similar to the proof of Theorem 8.1, the convergence analysis requires to analyze the growth of successive time–derivatives of the series coefficients $\bar{k}_n(\eta,\sigma,t)$, $n \in \mathbb{N}$, up to an arbitrary order $l \in \mathbb{N}$. For this, observe first that due to the time–independence of the exponential terms in (8.15a) with (8.13b)–(8.13d) evaluated for the case of a mixed boundary condition it holds that

$$\left|\partial_t^l \int_0^\sigma e^{-\bar{p}^0(\sigma-r)}\gamma(r/2,t)\mathrm{d}r\right| \leq \begin{cases} \int_0^\sigma |\partial_t^l\gamma(\frac{r}{2},t)|\mathrm{d}r, & \text{if } \bar{p}^0 \geq 0 \\ e^{-\bar{p}^0\sigma}\int_0^\sigma |\partial_t^l\gamma(\frac{r}{2},t)|\mathrm{d}r, & \text{if } \bar{p}^0 < 0. \end{cases}$$

Similarly, it follows that

$$\left|\partial_t^l \int_0^\sigma e^{-\bar{p}^0(\sigma-s)}C_{\bar{k}_{n-1}}(s,t)\mathrm{d}s\right| \leq \begin{cases} \int_0^\sigma |\partial_t^l C_{\bar{k}_{n-1}}(s,t)|\mathrm{d}s, & \text{if } \bar{p}^0 \geq 0 \\ e^{-\bar{p}^0\sigma}\int_0^\sigma |\partial_t^l C_{\bar{k}_{n-1}}(s,t)|\mathrm{d}s, & \text{if } \bar{p}^0 < 0. \end{cases}$$

Observing that $\exp(-\bar{p}^0\sigma) \leq \exp(-\bar{p}^0)$ for $\bar{p}^0 \geq 0$ since $\sigma \in [0,1]$, the abbreviation $\nu = 1$ for $\bar{p}^0 \geq 0$ and $\nu = \exp(-\bar{p}^0) > 1$ for $\bar{p}^0 < 0$ is used subsequently.

The case $\bar{p}^0 = p_w^0/\epsilon_w^0$

Assuming that $\gamma(z,t) \in \mathcal{C}^0([0,1]) \times G_{D,\alpha}(\mathbb{R}_{t_0}^+)$ with $\alpha \geq 1$ it follows for $n = 1$ from (8.15a), (8.13b)–(8.13d) that

$$\begin{aligned}\sup_{t\in\mathbb{R}_{t_0}^+}\left|\partial_t^l \bar{k}_1(\eta,\sigma,t)\right| &\leq \sup_{t\in\mathbb{R}_{t_0}^+}\left\{\frac{1}{4}\int_\sigma^\eta \left|\partial_t^l\gamma\Big(\frac{s}{2},t\Big)\right|\mathrm{d}s + \frac{\nu}{2}\int_0^\sigma \left|\partial_t^l\gamma\Big(\frac{r}{2},t\Big)\right|\mathrm{d}r\right\} \\ &\leq D^{l+1}(l!)^\alpha\left(\frac{\eta-\sigma}{4} + \nu\frac{\sigma}{2}\right) \leq D^{l+1}\frac{\nu}{4}(l!)^\alpha(\eta+\sigma),\end{aligned}$$

which equals (8.18) for $n = 1$. Hence assume that (8.18) holds for all $n = 1, 2, \ldots, N-1$, $N > 2$. Then it follows that

$$
\begin{aligned}
&\sup_{t\in\mathbb{R}^+_{t_0}} \left|\partial_t^l \bar{k}_N(\eta,\sigma,t)\right| \\
&\leq \sup_{t\in\mathbb{R}^+_{t_0}} \Bigg\{ \frac{1}{4}\int_\sigma^\eta \int_0^\sigma \Bigg(\left|\partial_t^{l+1}\bar{k}_{N-1}(r,s,t)\right| \\
&\qquad + \sum_{j=0}^{l} \binom{l}{j} \left|\partial_t^j \gamma\Big(\frac{r-s}{2},t\Big)\right| \left|\partial_t^{l-j}\bar{k}_{N-1}(r,s,t)\right| \Bigg) \mathrm{d}s\mathrm{d}r \\
&\quad + \frac{\nu}{2}\int_0^\sigma \int_0^s \Bigg(\left|\partial_t^{l+1}\bar{k}_{N-1}(s,q,t)\right| \\
&\qquad + \sum_{j=0}^{l} \binom{l}{j} \left|\partial_t^j \gamma\Big(\frac{s-q}{2},t\Big)\right| \left|\partial_t^{l-j}\bar{k}_{N-1}(s,q,t)\right| \Bigg) \mathrm{d}q\mathrm{d}s \Bigg\} \\
&\overset{(8.18)}{\leq} \frac{D^{l+N}\left(\frac{\nu}{4}\right)^{N-1}}{((N-2)!)^\alpha} \Bigg(((l+N-1)!)^\alpha + \sum_{j=0}^{l} \binom{l}{j} (j!)^\alpha ((l+N-2-j)!)^\alpha \Bigg) \times \\
&\quad \prod_{j=0}^{N-2} \frac{(1+j^\alpha)}{(j+1)(j+\delta_{j,0})} \Bigg(\frac{1}{4}\int_\sigma^\eta \int_0^\sigma (rs)^{N-2}(r+s)\mathrm{d}s\mathrm{d}r \\
&\qquad + \frac{\nu}{2}\int_0^\sigma \int_0^s (sq)^{N-2}(s+q)\mathrm{d}q\mathrm{d}s \Bigg) \\
&\overset{\substack{(B.18)\\(B.20)\\(B.22)}}{\leq} D^{l+N}\left(\frac{\nu}{4}\right)^N \left(\frac{(l+N-1)!}{(N-1)!} \right)^\alpha (\eta\sigma)^{N-1}(\eta+\sigma) \prod_{j=0}^{N-1} \frac{(1+j^\alpha)}{(j+1)(j+\delta_{j,0})}.
\end{aligned}
$$

Here again the inequality $\sum_j a_j^\kappa \leq (\sum_j a_j)^\kappa$ for $\kappa \geq 1$ and $a_j \geq 0$ was used together with

$$
\frac{1}{4}(\eta\sigma)^{N-1}(\eta+\sigma) + \frac{(\nu-1)}{2}\sigma^{2N-1} \leq \frac{\nu}{4}(\eta\sigma)^{N-1}(\eta+\sigma),
$$

which holds since $\sigma \leq \eta \leq 2-\sigma$ and $\nu \geq 1$ such that $\sigma^{2N-1}/2 \leq (\eta\sigma)^{N-1}(\eta+\sigma)/4$. In particular the obtained expression is identical to (8.18) for $n = N$, which proves the first result. Majorizing the series (8.14) using (8.18) for $l = 0$ yields

$$
\left|\bar{k}(\eta,\sigma,t)\right| \leq \sum_{n=1}^{\infty} \left|\bar{k}_n(\eta,\sigma,t)\right| \leq \frac{D\nu}{4}(\eta+\sigma) \sum_{n=0}^{\infty} a_{n+1} \Big(\frac{D\nu\eta\sigma}{4}\Big)^n, \tag{8.20}
$$

where

$$
a_n = \prod_{j=0}^{n-1} \frac{(1+j^\alpha)}{((j+1)(j+\delta_{j,0}))}.
$$

The radius of convergence ϱ of the power series (8.20) in $D\nu\eta\sigma/4$ can be determined from

$$\varrho = \lim_{n\to\infty} \left|\frac{a_{n+1}}{a_{n+2}}\right| = \lim_{n\to\infty} \frac{(n+1)(n+2)}{((n+1)^\alpha + 1)},$$

which yields

$$\varrho = \begin{cases} \infty, & \text{for } \alpha \in [1,2) \\ 1, & \text{for } \alpha = 2 \\ 0, & \text{for } \alpha > 2. \end{cases}$$

Hence the series converges with infinite radius of convergence if $\alpha \in [1,2)$. In addition if $\alpha = 2$, convergence requires that $D\nu\eta\sigma/4 < 1$, which is equivalent to $D\nu < 4$ since $\eta\sigma \leq 1$ in the considered domain $\sigma \in [0,1]$, $\eta \in [\sigma, 2-\sigma]$. This completes the proof of the first part.

The case $\bar{p}^0 \neq p_w^0/\epsilon_w^0$

If $\bar{p}^0 \neq p_w^0/\epsilon_w^0$ it follows from (8.13b) that an additional time–invariant term appears in the coefficient $\bar{k}_1(\eta,\sigma,t)$. Since the recursion (8.15b) is linear in $\bar{k}_n(\eta,\sigma,t)$, the convergence analysis can be split into two parts, i.e. $\bar{k}_n(\eta,\sigma,t) = \bar{k}_n^1(\eta,\sigma,t) + \bar{k}_n^2(\eta,\sigma,t)$, where $\bar{k}_n^1(\eta,\sigma,t)$ is treated in the previous paragraph and $\bar{k}_n^2(\eta,\sigma,t)$ describes the recursive processing of $\bar{k}_1^2(\eta,\sigma,t) = (\bar{p}^0 - p_w^0/\epsilon_w^0)\exp(-\bar{p}^0\sigma)$. With ν as defined before the bound in (8.19) for $n = 1$ follows immediately. Under the assumption that $\gamma(z,t) \in \mathcal{C}^0([0,1]) \times G_{D,\alpha}(\mathbb{R}_{t_0}^+)$ with $\alpha \geq 1$, the bound for $n \geq 2$ can be easily proven by induction following the lines of the proof for $\bar{p}^0 = p_w^0/\epsilon_w^0$ and utilizing the estimate

$$\frac{\nu}{2}\int_0^\sigma \int_0^s (sr)^n \mathrm{d}r\mathrm{d}s + \frac{1}{4}\int_\sigma^\eta \int_0^\sigma (sr)^n \mathrm{d}r\mathrm{d}s \leq \frac{\nu}{(4(n+1)^2)}(\eta\sigma)^{n+1},\ n \in \mathbb{N}$$

since $\nu \geq 1$ by definition and $\sigma \leq \eta \leq 2-\sigma$. Due to its formal relation to the previous result, an explicit verification is omitted. For the proof of absolute and uniform series convergence note that

$$\left|\bar{k}(\eta,\sigma,t)\right| = \left|\sum_{n=1}^\infty \bar{k}_n(\eta,\sigma,t)\right| \leq \sum_{n=1}^\infty \left|\bar{k}_n^1(\eta,\sigma,t)\right| + \sum_{n=1}^\infty \left|\bar{k}_n^2(\eta,\sigma,t)\right|.$$

Convergence of the series involving $\bar{k}_n^1(\eta,\sigma,t)$ is ensured by the results of the paragraph above. Proceeding similarly for the series over $\bar{k}_n^2(\eta,\sigma,t)$ yields

$$\sum_{n=1}^\infty \left|\bar{k}_n^2(\eta,\sigma,t)\right| \leq \beta \sum_{n=0}^\infty \left(\frac{D\nu\eta\sigma}{4}\right)^n (n!)^{\alpha-2}.$$

The radius of convergence of the majorizing power series in $D\nu\eta\sigma/4$ can be easily determined as $\varrho = \infty$ for $\alpha \in [1, 2)$. If $\alpha = 2$ convergence requires that $D\nu\eta\sigma/4 < 1$, which, as outlined above, is equivalent to $D\nu < 4$. □

Notably, the analysis above generalizes the results of [8], where convergence of the successive approximation is verified under the assumption that $\gamma(z, t)$ is analytic with respect to t and that $\bar{p}^0 = 0$. Observing that

$$\partial_\eta \partial_\sigma \bar{k}_n(\eta, \sigma, t) = \frac{1}{4}\Big[\partial_t \bar{k}_{n-1}(\eta, \sigma, t) + \gamma\Big(\frac{\eta - \sigma}{2}, t\Big)\bar{k}_{n-1}(\eta, \sigma, t)\Big], \;\; n \geq 2,$$

with $\partial_\eta \partial_\sigma \bar{k}_1(\eta, \sigma, t) = 0$, the absolute and uniform convergence of the series $\sum_{n=1}^{\infty} \partial_\eta \partial_\sigma \bar{k}_n(\eta, \sigma, t)$ can be easily verified under the assumptions of Theorems 8.1 and 8.2 provided that the bounds (8.16) and (8.18), (8.19), respectively, hold. As a result, it follows from the series expression (8.14) that the determined $\bar{k}(\eta, \sigma, t)$ is of Gevrey–order $\alpha \leq 2$ with respect to t and is a strong solution to the kernel–PDE (8.12a) with (8.12b) and (8.12c) or (8.12d), (8.12e), respectively. In view of (8.11) this implies that $k(z, \zeta, t)$ is of Gevrey–order $\alpha \leq 2$ with respect to t and is a strong solution to the kernel–PDE (8.10a) with (8.10b) and (8.10c) or (8.10e), (8.10g), respectively.

With these preparations it is now possible to explicitly compute the state–feedback control, which realizes the desired transformation from the possibly unstable diffusion–reaction system (8.3) into the exponentially stable target system (8.4).

8.2.4 Backstepping–Based State–Feedback Controller

The state–feedback controller requires suitable expressions for $x(1, t)$ and $\partial_z x(1, t)$ in terms of the kernel $k(z, \zeta, t)$. From (8.7), (8.8), it follows that

$$w(1, t) = x(1, t) - \int_0^1 k(1, \zeta, t)x(\zeta, t)\mathrm{d}\zeta$$

$$\partial_z w(1, t) = \partial_z x(1, t) - k(1, 1, t)x(1, t) - \int_0^1 \partial_z k(1, \zeta, t)x(\zeta, t)\mathrm{d}\zeta.$$

Hence, given the boundary condition (8.4d) of the target system at $z = 1$, the respective backstepping–based state–feedback controller can be evaluated depending on ϵ_w^1 and p_w^1:

(i) For $\epsilon_w^1 = 0$, i.e. $w(1, t) = 0$, with

$$x(1, t) = \int_0^1 k(1, \zeta, t)x(\zeta, t)\mathrm{d}\zeta =: \Xi_D(x(z, t))$$

the state–feedback controller (8.3c) evaluates to

$$u(t) = \theta\big(\Xi_D(x(z,t)), \partial_z x(1,t)\big). \tag{8.21a}$$

(ii) For $p_w^1 = 0$, i.e. $\partial_z w(1,t) = 0$, with

$$\partial_z x(1,t) = k(1,1,t)x(1,t) + \int_0^1 \partial_z k(1,\zeta,t)x(\zeta,t)\mathrm{d}\zeta =: \Xi_N(x(z,t))$$

the state–feedback controller (8.3c) takes the form

$$u(t) = \theta\big(x(1,t), \Xi_N(x(z,t))\big). \tag{8.21b}$$

(iii) For $\epsilon_w^1 > 0,\ p_w^1 > 0$, i.e. $\epsilon_w^1 \partial_z w(1,t) + p_w^1 w(1,t) = 0$, with

$$\partial_z x(1,t) = x(1,t)\left(k(1,1,t) - \frac{p_w^1}{\epsilon_w^1}\right) + \int_0^1 \left(\partial_z k(1,\zeta,t) + \frac{p_w^1}{\epsilon_w^1} k(1,\zeta,t)\right) x(\zeta,t)\mathrm{d}\zeta =: \Xi_M(x(z,t))$$

the state–feedback controller (8.3c) reads as

$$u(t) = \theta\big(x(1,t), \Xi_M(x(z,t))\big). \tag{8.21c}$$

Here, it should be noticed for the case (i) that the choice of a Dirichlet boundary condition at $z = 1$ for the target system requires to additionally evaluate the derivative $\partial_z x(1,t)$. This disadvantage can be avoided by the choice of either a Neumann or mixed boundary condition at $z = 1$ for the target system.

8.2.5 Inverse Backstepping–Transformation and Exponential Stability of the Closed–Loop System

The analysis of the exponential stability of the closed–loop system involving the backstepping–based state–feedback controller determined above requires the analysis of the inverse backstepping–transformation, i.e. the transformation from the target system into the original diffusion–reaction system. Instead of considering the invertibility conditions for Volterra integral transformations of the form (8.7) the inverse is determined explicitly. Hence, consider

$$x(z,t) = w(z,t) + \int_0^z g(z,\zeta,t)w(\zeta,t)\mathrm{d}\zeta \tag{8.22}$$

and proceed as in Section 8.2.2, i.e. differentiate (8.22) with respect to t, twice with respect to z, and substitute the obtained expressions into the equations (8.3) for the diffusion–reaction system in $x(z,t)$. This yields that the kernel–PDE for the inverse transformation $g(z,\zeta,t)$ is identical to the original kernel–PDE (8.10) except for

the coefficient $\gamma(\zeta,t)$ in (8.10a) replaced by $-\gamma(z,t)$ and the coefficients $\epsilon^0,\ p^0$ in (8.10e) exchanged with $\epsilon_w^0,\ p_w^0$, i.e.

$$\partial_t g(z,\zeta,t) = \partial_z^2 g(z,\zeta,t) - \partial_\zeta^2 g(z,\zeta,t) + \gamma(z,t) g(z,\zeta,t) \tag{8.23a}$$

$$\gamma(z,t) + 2\mathrm{d}_z g(z,z,t) = 0 \tag{8.23b}$$

and

$$\begin{cases} g(z,0,t) = 0 & \text{if } \epsilon_w^0 = 0,\ p_w^0 \neq 0 \\ -\partial_\zeta g(z,0,t) + \frac{p_w^0}{\epsilon_w^0} g(z,0,t) = 0, & \\ \quad g(0,0,t) = \bar{p}^0 - \frac{p_w^0}{\epsilon_w^0} & \text{if } \epsilon_w^0 \neq 0,\ p_w^0 \neq 0. \end{cases} \tag{8.23c}$$

Hence the solution procedure using the method of integral operators followed by a successive approximation as well as the proof of uniform and absolute convergence can be identically applied to the inverse kernel $g(z,\zeta,t)$. This result in particular allows to conclude exponential stability of the closed–loop system with the backstepping–based state–feedback controller.

Theorem 8.3. *Consider the diffusion–reaction system* (8.3) *with state–feedback control* (8.21a)*,* (8.21b)*, or* (8.21c) *depending on the boundary condition at* $z = 0$*. Then the equilibrium* $x(z,t) \equiv 0$ *is exponentially stable for all* $t \in \mathbb{R}_{t_0}^+$ *in the* L^2*–norm for the target system* (8.4) *and in the* H^1*–norm for the target system governed by* (8.4a)*,* (8.4b) *with* (8.6)*.*

The proof of this result follows directly from the exponential stability of the target system (cf. Lemma 8.1 and 8.2) and the boundedness of the kernels $k(z,\zeta,t)$ and $g(z,\zeta,t)$ by Theorem 8.1 and 8.2.

Proof. Let $\Omega = (0,1)$, let X be either $L^2(\Omega)$ or $H^1(\Omega)$, and assume $x_0(z), w_0(z) \in X$. Moreover, denote $\Theta_0 = \{(z,\zeta) : \zeta \in \Omega,\ z \in [\zeta,1]\}$ and $\Theta = \{(z,\zeta,t) : \zeta \in \Omega,\ z \in [\zeta,1],\ t \in \mathbb{R}_{t_0}^+\}$. Applying the Minkowski inequality yields

$$\begin{aligned} \|w_0\|_X &= \left\| x_0(z) - \int_0^z k(z,\zeta,t_0)\, x_0(\zeta)\mathrm{d}\zeta \right\|_X \\ &\leq \|x_0\|_X + \left\| \int_0^z k(z,\zeta,t_0)\, x_0(\zeta)\mathrm{d}\zeta \right\|_X . \end{aligned}$$

Recalling from the convergence analysis that the kernel $k(z,\zeta,t)$ and the inverse kernel $g(z,\zeta,t)$ are bounded with bounded derivative with respect to z for all $(z,\zeta,t) \in \Theta_0$ the Cauchy–Schwarz inequality implies the existence if a constant $C_0 > 0$ such that

$$\|w_0\|_X \leq C_0 \|x_0\|_X,$$

where

$$C_0 = 1 + \begin{cases} \sup_{(z,\zeta)\in\Theta_0} |k(z,\zeta,t_0)|, & \text{if } X = L^2(\Omega) \\ \sqrt{2}\sup_{(z,\zeta)\in\Theta_0} |k(z,\zeta,t_0)| & \\ + \sup_{(z,\zeta)\in\Theta_0} |\partial_z k(z,\zeta,t_0)|, & \text{if } X = H^1(\Omega). \end{cases}$$

In order to illustrate this, consider $X = H^1(\Omega)$. With the definition of $\|\cdot\|_{H^1(\Omega)}$ the last term in the estimate for $\|w_0\|_X$ above evaluates according to

$$\begin{aligned} &\left\| \int_0^z k(z,\zeta,t_0)\, x_0(\zeta) \mathrm{d}\zeta \right\|^2_{H^1(\Omega)} \\ &= \int_0^1 \left(\int_0^z k(z,\zeta,t_0)\, x_0(\zeta) \mathrm{d}\zeta \right)^2 \mathrm{d}z \\ &\quad + \int_0^1 \left(k(z,z,t_0)\, x_0(z) + \int_0^z \partial_z k(z,\zeta,t_0)\, x_0(\zeta) \mathrm{d}\zeta \right)^2 \mathrm{d}z. \end{aligned}$$

By the Cauchy–Schwarz inequality

$$\int_0^1 \left(\int_0^z k(z,\zeta,t_0)\, x_0(\zeta) \mathrm{d}\zeta \right)^2 \mathrm{d}z \le \left(\sup_{(z,\zeta)\in\Theta_0} |k(z,\zeta,t_0)| \right)^2 \|x_0\|^2_{L^2}$$

and similarly taking into account the triangle inequality

$$\begin{aligned} &\int_0^1 \left(k(z,z,t_0)\, x_0(z) + \int_0^z \partial_z k(z,\zeta,t_0)\, x_0(\zeta) \mathrm{d}\zeta \right)^2 \mathrm{d}z \\ &\le \left(\sup_{(z,\zeta)\in\Theta_0} |k(z,\zeta,t_0)| + \sup_{(z,\zeta)\in\Theta_0} |\partial_z k(z,\zeta,t_0)| \right)^2 \|x_0\|^2_{L^2} \end{aligned}$$

provides the constant C_0 utilizing $\sqrt{a^2 + (a+b)^2} \le \sqrt{2}a + b$ for $a,\ b \ge 0$. In view of Lemma 8.1 for $X = L^2(\Omega)$ and Lemma 8.2 for $X = H^1(\Omega)$ this implies

$$\|w(t)\|_X \le e^{-\kappa(t)} \|w_0\|_X \le C_0 e^{-\kappa(t)} \|x_0\|_X$$

with $\kappa(t) = \int_{t_0}^t (\mu(s) + \lambda_{\min}) \mathrm{d}s > \epsilon(t - t_0)$ with $\epsilon > 0$. Taking the norm of $x(z,t)$ defined by the inverse backstepping transformation (8.22) in terms of $w(z,t)$ a similar argumentation yields that there exists a constant $C_1 > 0$ such that

$$\|x(t)\|_X \le C_1 \|w(t)\|_X \le C_0 C_1 e^{-\kappa(t)} \|x_0\|_X$$

with

$$C_1 = 1 + \begin{cases} \sup_{(z,\zeta,t)\in\Theta} |g(z,\zeta,t)|, & \text{if } X = L^2(\Omega) \\ \sqrt{2}\sup_{(z,\zeta,t)\in\Theta} |g(z,\zeta,t)| & \\ + \sup_{(z,\zeta,t)\in\Theta} |\partial_z g(z,\zeta,t)|, & \text{if } X = H^1(\Omega). \end{cases}$$

Hence, the state $x(z,t)$ of the closed–loop system decays exponentially with t in both the $L^2(\Omega)$– and the $H^1(\Omega)$–norm. □

Remark 8.2. Besides its importance for the verification of the exponential stability of the closed–loop system for the diffusion–reaction system (8.3) with the state–feedback control according to (8.21) the inverse backstepping–transformation proves to be an essential tool for trajectory planning as is outlined in Section 8.4.

Obviously, all three feedback controllers require the knowledge of $x(z,t)$ for all $z \in [0,1]$ and $t \in \mathbb{R}_{t_0}^+$. Therefore, the control–loop has to be amended by a suitable observer. This can be again performed by means of a backstepping approach.

8.3 State–Observer with Exponentially Stable Error Dynamics

Since the implementation of (8.21) essentially relies on the knowledge of $x(z,t)$ for all $(z,t) \in [0,1] \times \mathbb{R}_{t_0}^+$ a state–observer is required to provide a model–based estimation $\hat{x}(z,t)$ of $x(z,t)$ from the available measurement information such that $\|\hat{x}(z,t) - x(z,t)\| \to 0$ in some suitable norm. For this, it is subsequently assumed that the output $y(t)$ is measured. Moreover, it is desired to prescribe an exponential decay of the observation error. In order to solve these tasks, given (8.3) a distributed–parameter state–observer of Luenberger type is set–up according to

$$\partial_t \hat{x}(z,t) = \partial_z^2 \hat{x}(z,t) + c(z,t)\hat{x}(z,t) + l_1(z,t)[y(t) - \hat{y}(t)], \tag{8.24a}$$

for $(z,t) \in (0,1) \times \mathbb{R}_{t_0}^+$ with the boundary conditions

$$-\epsilon^0 \partial_z \hat{x}(0,t) + p^0 \hat{x}(0,t) = l_{10}(t)[y(t) - \hat{y}(t)], \qquad t > t_0 \tag{8.24b}$$

$$\theta\left(\hat{x}(1,t), \partial_z \hat{x}(1,t)\right) = u(t), \qquad t > t_0, \tag{8.24c}$$

the initial condition

$$\hat{x}(z,t_0) = \hat{x}_0(z), \qquad z \in [0,1], \tag{8.24d}$$

and

$$\hat{y}(t) = h^0 \partial_z \hat{x}(0,t) + h^1 \hat{x}(0,t), \qquad t \geq t_0. \tag{8.24e}$$

Here, $l_1(z,t)$ and $l_{10}(t)$ denote the observer gains, which have to be determined such that the norm of the observer error state $\tilde{x}(z,t) = x(z,t) - \hat{x}(z,t)$ decays exponentially. By comparing (8.3) with (8.24) it follows that $\tilde{x}(z,t)$ is governed by

$$\begin{aligned}\partial_t \tilde{x}(z,t) = {} & \partial_z^2 \tilde{x}(z,t) + c(z,t)\tilde{x}(z,t) \\ & - l_1(z,t)[h^0 \partial_z \tilde{x}(0,t) + h^1\, \tilde{x}(0,t)],\end{aligned} \tag{8.25a}$$

for $(z,t) \in (0,1) \times \mathbb{R}_{t_0}^+$ with the boundary conditions

$$(l_{10}(t)h^0 - \epsilon^0)\partial_z\tilde{x}(0,t) + (l_{10}(t)h^1 + p^0)\,\tilde{x}(0,t) = 0, \qquad t > t_0 \tag{8.25b}$$

$$\theta\left(\tilde{x}(1,t) + \hat{x}(1,t), \partial_z\tilde{x}(1,t) + \partial_z\hat{x}(1,t)\right) - \theta\left(\tilde{x}(1,t), \partial_z\tilde{x}(1,t)\right) = 0, \qquad t > t_0, \tag{8.25c}$$

and the initial condition

$$\tilde{x}(z,t_0) = \tilde{x}_0(z) = x_0(z) - \hat{x}_0(z), \qquad z \in [0,1]. \tag{8.25d}$$

Differing from the determination of an exponentially stabilizing state–feedback control the nonlinear input characteristics $\theta(\cdot,\cdot)$ results in a nonlinear stabilization problem for the design of the respective state–observer. Hence, subsequently the nonlinear boundary condition (8.25c) is replaced by a linear boundary condition.

Assumption 8.2. The functional $\theta(\cdot,\cdot)$ is linear and is given by

$$\theta(x(1,t), \partial_z x(1,t)) = \epsilon^1\partial_z x(1,t) + p^1 x(1,t) \tag{8.25e}$$

with constants ϵ^1 and p^1.

In view of (8.25e) the boundary condition (8.25c) simplifies to

$$\epsilon^1\partial_z\tilde{x}(1,t) + p^1\tilde{x}(1,t) = 0, \qquad t > t_0. \tag{8.25f}$$

It should be emphasized that the state–feedback control can be determined for a rather general nonlinear input characteristics. However, the state–observer design essentially relies on linear boundary control.

Similar to Section 8.2 the backstepping approach is utilized and extended to determine the observer gains $l_1(z,t)$ and $l_{10}(t)$ to exponentially stabilize the observer error dynamics (8.25). For this, a Volterra integral transformation is determined to transform (8.25) into a target system with prescribed stability properties.

8.3.1 Selection of the Target System

As pointed out above, one of the crucial parts of the backstepping approach is related to the choice of a suitable target system. Therefore, with the results of Section 8.2.1 consider

$$\partial_t\tilde{w}(z,t) = \partial_z^2\tilde{w}(z,t) - \tilde{\mu}(t)\tilde{w}(z,t), \qquad z \in (0,1),\ t > t_0 \tag{8.26a}$$

$$\tilde{w}(z,t_0) = \tilde{w}_0(z), \qquad z \in [0,1] \tag{8.26b}$$

with boundary conditions

$$-\tilde{\epsilon}_w^0\partial_z\tilde{w}(0,t) + \tilde{p}_w^0\tilde{w}(0,t) = 0, \qquad t > t_0 \tag{8.26c}$$

$$\tilde{\epsilon}_w^1\partial_z\tilde{w}(1,t) + \tilde{p}_w^1\tilde{w}(1,t) = 0 \qquad t > t_0. \tag{8.26d}$$

The exponential stability of (8.26) in both the L^2– and the H^1–norm depending on $\tilde{\mu}(t)$, $\tilde{\epsilon}_w^0$, $\tilde{p}_w^0$, $\tilde{\epsilon}_w^1$, and $\tilde{p}_w^1$ is thereby guaranteed under the conditions imposed by Lemmas 8.1 and 8.2. With this, the kernel of a backstepping–like integral transformation can be determined, which relates the possibly unstable observer error dynamics (8.25) and the exponentially stable target system (8.26).

8.3.2 Determination of the Kernel–PDE and the Observer Gains

Differing from the approach introduced in Section 8.2.2 for the determination of the observer gains the Volterra integral transformation is set–up to transform the target system (8.26) into the observer error system (8.25), i.e.

$$\tilde{x}(z,t) = \tilde{w}(z,t) - \int_0^z l(z,\zeta,t)\tilde{w}(\zeta,t)\mathrm{d}\zeta. \tag{8.27}$$

Proceeding as in Section 8.2.2, i.e. differentiating $\tilde{x}(z,t)$ in (8.27) with respect to z and t in view of (8.26a) and substituting the expressions into (8.25a), yields after some intermediate computations

$$\begin{aligned} 0 = &\int_0^z \big[\partial_t l(z,\zeta,t) + \partial_\zeta^2 l(z,\zeta,t) - \partial_z^2 l(z,\zeta,t) - \tilde{\gamma}(z,t) l(z,\zeta,t)\big]\tilde{w}(\zeta,t)\mathrm{d}\zeta \\ &- \tilde{w}(z,t)\big[2\mathrm{d}_z l(z,z,t) - \tilde{\gamma}(z,t)\big] - \big[h^0 l_1(z,t) + l(z,0,t)\big]\partial_z\tilde{w}(0,t) \\ &- \big[(h^1 - h^0 l(0,0,t))l_1(z,t) - \partial_\zeta l(z,0,t)\big]\tilde{w}(0,t) \end{aligned} \tag{8.28}$$

with

$$\tilde{\gamma}(z,t) = c(z,t) + \tilde{\mu}(t).$$

From this, the kernel–PDE follows as

$$\partial_t l(z,\zeta,t) = \partial_z^2 l(z,\zeta,t) - \partial_\zeta^2 l(z,\zeta,t) + \tilde{\gamma}(z,t) l(z,\zeta,t) \tag{8.29a}$$

with the triangular spatial domain $\zeta \in (0,1)$, $z \in (\zeta,1)$ shown in Figure 8.1(a). Moreover, the kernel has to satisfy the condition

$$2\mathrm{d}_z l(z,z,t) - \tilde{\gamma}(z,t) = 0 \tag{8.29b}$$

along $\zeta = z$. The remaining boundary conditions have to be determined from (8.25f) and (8.26d) in view of (8.27). Depending on the individual parameter set–up of the observer error dynamics and the target system this results in:

(i) For Dirichlet boundary conditions at $z = 1$ in (8.25f), i.e. $\epsilon^1 = 0$, $p^1 \neq 0$ the kernel has to satisfy

$$l(1,\zeta,t) = 0 \tag{8.29c}$$

while the target system has to fulfill

$$\tilde{w}(1,t) = 0, \tag{8.29d}$$

and hence $\tilde{\epsilon}_w^1 = 0$.

(ii) For Neumann or mixed boundary conditions at $z = 1$ in (8.25f), i.e. $\epsilon^1 \neq 0$, the kernel is restricted to the conditions

$$\partial_z l(1,\zeta,t) + \bar{p}^1 l(1,\zeta,t) = 0 \tag{8.29e}$$

$$l(1,1,t) = \bar{p}^1 - \frac{\tilde{p}_w^1}{\tilde{\epsilon}_w^1} \tag{8.29f}$$

with $\bar{p}^1 = p^1/\epsilon^1$. This in particular implies that the boundary condition (8.26d) of the target system has to possess a similar structure with $\tilde{\epsilon}_w^1 \neq 0$.

The initial condition at $t = t_0$ for $\tilde{x}(z,t)$, $\tilde{w}(z,t)$, and $l(z,\zeta,t)$ in addition has to satisfy the constraint

$$\int_0^z l(z,\zeta,t_0)\tilde{w}_0(\zeta)\mathrm{d}\zeta = \tilde{w}_0(z) - \tilde{x}_0(z), \qquad z \in [0,1]. \tag{8.29g}$$

Hence, if $\tilde{w}_0(z) = \tilde{x}_0(z)$ this yields $l(z,\zeta,t_0) = 0$. Once $l(z,\zeta,t)$ is computed, the observer gains $l_1(z,t)$ and $l_{10}(t)$ can be determined accordingly from (8.28) in view of (8.29), i.e.

$$\begin{aligned} 0 = &- \left[h^0 l_1(z,t) + l(z,0,t)\right]\partial_z\tilde{w}(0,t) \\ &- \left[(h^1 - h^0 l(0,0,t))l_1(z,t) - \partial_\zeta l(z,0,t)\right]\tilde{w}(0,t) \end{aligned}$$

and (8.26c) evaluated with (8.27), i.e.

$$\begin{aligned} 0 = &\left[l_{10}(t)h^0 - \epsilon^0\right]\partial_z\tilde{w}(0,t) \\ &+ \left[l_{10}(t)h^1 + p^0 - (l_{10}(t)h^0 - \epsilon^0)l(0,0,t)\right]\tilde{w}(0,t) \end{aligned}$$

by making use of the boundary condition (8.26c). Comparison hence yields

$$l_1(z,t) = \begin{cases} -\dfrac{l(z,0,t)}{h^0}, & \text{if } \tilde{\epsilon}_w^0 = 0 \wedge h^0 \neq 0 \\ -\dfrac{\partial_\zeta l(z,0,t) - \frac{\tilde{p}_w^0}{\tilde{\epsilon}_w^0} l(z,0,t)}{h^0\left(l(0,0,t) - \frac{\tilde{p}_w^0}{\tilde{\epsilon}_w^0}\right) - h^1}, & \text{if } \tilde{\epsilon}_w^0 \neq 0 \wedge \\ & h^0\left(l(0,0,t) - \frac{\tilde{p}_w^0}{\tilde{\epsilon}_w^0}\right) - h^1 \neq 0 \end{cases} \tag{8.30}$$

and

$$l_{10}(t) = \begin{cases} \dfrac{\epsilon^0}{h^0}, & \text{if } \tilde{\epsilon}_w^0 = 0 \wedge h^0 \neq 0 \\ \dfrac{p^0 + \epsilon^0\Big(l(0,0,t) - \frac{\tilde{p}_w^0}{\tilde{\epsilon}_w^0}\Big)}{h^0\Big(l(0,0,t) - \frac{\tilde{p}_w^0}{\tilde{\epsilon}_w^0}\Big) - h^1}, & \text{if } \tilde{\epsilon}_w^0 \neq 0 \wedge \\ & h^0\Big(l(0,0,t) - \frac{\tilde{p}_w^0}{\tilde{\epsilon}_w^0}\Big) - h^1 \neq 0. \end{cases} \tag{8.31}$$

Remark 8.3. It has to be pointed out that the arising conditionals, i.e. $\tilde{\epsilon}_w^0 = 0 \wedge h^0 \neq 0$ or $\tilde{\epsilon}_w^0 \neq 0 \wedge h^0(l(0,0,t) - \tilde{p}_w^0/\tilde{\epsilon}_w^0) - h^1 \neq 0$, for the computation of the observer gains can be easily fulfilled by a suitable choice of the parameters of the target system. In particular, since $\tilde{\gamma}(z,t)$ is apriori known and since the kernel $l(z,\zeta,t)$ is independent of $\tilde{\epsilon}_w^0$ and $\tilde{p}_w^0$ the quotient $\tilde{p}_w^0/\tilde{\epsilon}_w^0$ can be assigned to guarantee $h^0(l(0,0,t) - \tilde{p}_w^0/\tilde{\epsilon}_w^0) - h^1 \neq 0$ for given values of h^0 and h^1.

The main difficulty arises from the necessary solution of the distributed–parameter system (8.29) governing the evolution of the kernel, where a closed–form analytical solution is unlikely except for certain special and simplified cases (see, e.g., the results in [31, 30, 12] for distributed–parameter system with constant and only time varying parameters). Moreover, a numerical solution using standard approaches such as finite differences is complicated due to the unusual character of the PDE, which combines a hyperbolic spatial operator with a first order time differentiation. Hence, proceeding as in Section 8.2.3 in the following the method of integral operators is considered to determine a solution to the kernel equations.

8.3.3 Solution of the Kernel–PDE

Consider the change of coordinates according to

$$\tilde{\eta} = 2 - z - \zeta, \qquad \tilde{\sigma} = z - \zeta, \tag{8.32}$$

which maps the spatial domain $\zeta \in (0,1)$, $z \in (\zeta, 1)$ into the domain shown in Figure 8.1(b) (replacing η and σ with $\tilde{\eta}$ and $\tilde{\sigma}$, respectively) and denote $l(z,\zeta,t) = \bar{l}(\tilde{\eta}(z,\zeta), \tilde{\sigma}(z,\zeta), t)$. Hence, (8.29) reduces to

$$-\partial_t \bar{l}(\tilde{\eta},\tilde{\sigma},t) = 4\partial_{\tilde{\eta}}\partial_{\tilde{\sigma}}\bar{l}(\tilde{\eta},\tilde{\sigma},t) - \tilde{\gamma}\Big(1 - \frac{\tilde{\eta}-\tilde{\sigma}}{2}, t\Big)\bar{l}(\tilde{\eta},\tilde{\sigma},t) \tag{8.33a}$$

with the boundary condition

$$\tilde{\gamma}\Big(1 - \frac{\tilde{\eta}}{2}, t\Big) + 4\partial_{\tilde{\eta}}\bar{l}(\tilde{\eta},0,t) = 0 \tag{8.33b}$$

while for $z = 1$ and hence $\tilde{\sigma} = \tilde{\eta}$ the following distinction has to be taken into account:

(i) For the Dirichlet condition (8.29c) it follows that

$$\bar{l}(\tilde{\eta},\tilde{\eta},t)=0. \tag{8.33c}$$

(ii) For the mixed boundary condition (8.29e), (8.29f) the subsequent conditions are imposed

$$\partial_{\tilde{\sigma}}\bar{l}(\tilde{\eta},\tilde{\eta},t)-\partial_{\tilde{\eta}}\bar{l}(\tilde{\eta},\tilde{\eta},t)+\bar{p}^1\bar{l}(\tilde{\eta},\tilde{\eta},t)=0 \tag{8.33d}$$

$$\bar{l}(0,0,t)=\bar{p}^1-\frac{\tilde{p}_w^1}{\tilde{\epsilon}_w^1}. \tag{8.33e}$$

Of course, it should be pointed out that the restrictions on the target system formulated for (8.29d), (8.29f) have to be fulfilled similarly.

A comparison of (8.33) and (8.12) reveals that the only differences between the two sets of equations are given by the sign on the left hand side of the kernel–PDE (8.33a) and the arguments of $\tilde{\gamma}(\cdot,t)$ and $\gamma(\cdot,t)$. This, however, implies that the results obtained for the successive approximation of the kernel $k(z,\zeta,t)$ or $\bar{k}(\eta,\sigma,t)$ directly carry over to the kernel $l(z,\zeta,t)$ or $\bar{l}(\tilde{\eta},\tilde{\sigma},t)$, respectively. In particular, let

$$\bar{l}(\tilde{\eta},\tilde{\sigma},t)=\sum_{n=1}^{\infty}\bar{l}_n(\tilde{\eta},\tilde{\sigma},t). \tag{8.34}$$

Then proceeding as in Section 8.2.3 provides that the series coefficients $\bar{l}_n(\tilde{\eta},\tilde{\sigma},t)$ can be determined recursively from

$$\bar{l}_1(\tilde{\eta},\tilde{\sigma},t)=\tilde{A}(\tilde{\eta},\tilde{\sigma},t) \tag{8.35a}$$

$$\begin{aligned}\bar{l}_n(\tilde{\eta},\tilde{\sigma},t)=\int_0^{\tilde{\sigma}}\Bigg[&\tilde{B}_{\bar{l}_{n-1}}(\tilde{\sigma},s,t)+\frac{1}{4}\int_{\tilde{\sigma}}^{\tilde{\eta}}\big(-\partial_t\bar{l}_{n-1}(r,s,t)\\&+\tilde{\gamma}\Big(1-\frac{r-s}{2},t\Big)\bar{l}_{n-1}(r,s,t)\big)\mathrm{d}r\Bigg]\mathrm{d}s,\quad n\geq 2,\end{aligned} \tag{8.35b}$$

where

$$\tilde{A}(\tilde{\eta},\tilde{\sigma},t)=\begin{cases}-\frac{1}{4}\int_{\tilde{\sigma}}^{\tilde{\eta}}\tilde{\gamma}\big(1-\frac{s}{2},t\big)\mathrm{d}s, & \text{Dirichlet BC}\\ \Big(\bar{p}^1-\frac{\tilde{p}_w^1}{\tilde{\epsilon}_w^1}\Big)e^{-\bar{p}^1\tilde{\sigma}}-\frac{1}{4}\int_{\tilde{\sigma}}^{\tilde{\eta}}\tilde{\gamma}\big(1-\frac{s}{2},t\big)\mathrm{d}s & \\ -\frac{1}{2}\int_0^{\tilde{\sigma}}e^{-\bar{p}^1(\tilde{\sigma}-r)}\tilde{\gamma}\big(1-\frac{r}{2},t\big)\mathrm{d}r, & \text{mixed BC}\end{cases} \tag{8.36}$$

and

$$\tilde{B}_{\bar{l}_{n-1}}(\tilde{\sigma},s,t)=\begin{cases}0, & \text{Dirichlet BC},\\ e^{-\bar{p}^1(\tilde{\sigma}-s)}\tilde{C}_{\bar{l}_{n-1}}(s,t), & \text{mixed BC}\end{cases} \tag{8.37}$$

with

$$\tilde{C}_{\bar{l}_{n-1}}(s,t) = \frac{1}{2}\int_0^s \Big(-\partial_t \bar{l}_{n-1}(s,v,t) + \tilde{\gamma}\Big(1-\frac{s-v}{2},t\Big)\bar{l}_{n-1}(s,v,t)\Big)\mathrm{d}v. \tag{8.38}$$

The convergence of the successive approximation can be guaranteed provided that $\tilde{\gamma}(z,t)$ is a Gevrey function with respect to t of a certain order.

8.3.3.1 Dirichlet Conditions

Given a Dirichlet boundary condition, then convergence can be ensured under the conditions determined below.

Theorem 8.4. *Given $\tilde{\gamma}(z,t) \in \mathcal{C}^0([0,1]) \times G_{D,\alpha}(\mathbb{R}^+_{t_0})$ with $\alpha \in [1,2]$, then the series coefficients* (8.35) *obtained for the boundary condition* (8.33c) *satisfy*

$$\sup_{t\in\mathbb{R}^+_{t_0}} \left|\partial_t^l \bar{l}_n(\tilde{\eta},\tilde{\sigma},t)\right| \leq \frac{D^{l+n}}{4^n}\left(\frac{(l+n-1)!}{(n-1)!}\right)^{\alpha} \times (\tilde{\eta}\tilde{\sigma})^{n-1}(\tilde{\eta}-\tilde{\sigma})\prod_{j=0}^{n-1}\frac{(1+j^\alpha)}{(j+1)(j+\delta_{j,0})}, \quad n \geq 1. \tag{8.39}$$

In particular, the series (8.34) *converges absolutely and uniformly in the domain $\tilde{\sigma} \in [0,1]$, $\tilde{\eta} \in [\tilde{\sigma}, 2-\tilde{\sigma}]$ for $\alpha \in [1,2)$ independent of D and for $\alpha = 2$ if $D < 4$.*

8.3.3.2 Neumann and Mixed Conditions

In the case of Neumann or mixed boundary condition the successive approximation procedure converges uniformly depending on certain Gevrey properties.

Theorem 8.5. *Given $\tilde{\gamma}(z,t) \in \mathcal{C}^0([0,1]) \times G_{D,\alpha}(\mathbb{R}^+_{t_0})$ with $\alpha \in [1,2]$, then the series coefficients* (8.35) *obtained for the boundary conditions* (8.33d), (8.33e) *satisfy*

$$\sup_{t\in\mathbb{R}^+_{t_0}} \left|\partial_t^l \bar{l}_n(\tilde{\eta},\tilde{\sigma},t)\right| \leq \left(\frac{\nu}{4}\right)^n D^{l+n}\left(\frac{(l+n-1)!}{(n-1)!}\right)^{\alpha} \times (\tilde{\eta}\tilde{\sigma})^{n-1}(\tilde{\eta}+\tilde{\sigma})\prod_{j=0}^{n-1}\frac{(1+j^\alpha)}{(j+1)(j+\delta_{j,0})}, \quad n \geq 1 \tag{8.40}$$

if $\bar{p}^1 = p^1/\epsilon^1 = \tilde{p}^1_w/\tilde{\epsilon}^1_w$. Herein, $\nu = 1$ if $\bar{p}^1 \geq 0$ while $\nu = \exp(-\bar{p}^1)$ if $\bar{p}^1 < 0$. If $\bar{p}^1 \neq \tilde{p}^1_w/\tilde{\epsilon}^1_w$, then $\bar{l}_n(\tilde{\eta},\tilde{\sigma},t) = \bar{l}^1_n(\tilde{\eta},\tilde{\sigma},t) + \bar{l}^2_n(\tilde{\eta},\tilde{\sigma},t)$ where $\bar{l}^1_n(\tilde{\eta},\tilde{\sigma},t)$ satisfies (8.40) *and $\bar{l}^2_n(\tilde{\eta},\tilde{\sigma},t)$ is bounded by*

$$\sup_{t\in\mathbb{R}^+_{t_0}} \left|\partial_t^l \bar{l}_n^2(\tilde{\eta},\tilde{\sigma},t)\right| \leq \begin{cases} \nu\beta\delta_{l,0}, & n=1 \\ \beta D^{l+n-1}\nu^n \left(\frac{\tilde{\eta}\tilde{\sigma}}{4}\right)^{n-1} \times \\ \left(\frac{(l+n-2)!}{(n-2)!}\right)^{\alpha} ((n-1)!)^{\alpha-2}, & n\geq 2 \end{cases} \tag{8.41}$$

with $\beta = |\bar{p}^1 - \tilde{p}_w^1/\bar{\epsilon}_w^1|$. *In particular, the series* (8.34) *converges absolutely and uniformly in the domain* $\tilde{\sigma}\in[0,1]$, $\tilde{\eta}\in[\tilde{\sigma},2-\tilde{\sigma}]$ *for* $\alpha\in[1,2)$ *independent of* D *and* ν *and for* $\alpha=2$ *if* $D\nu<4$.

The proofs of these results follow exactly the lines of the proofs of Theorems 8.1 and 8.2 by observing that the negative sign for the term $-\partial_t \bar{l}_n(\tilde{\eta},\tilde{\sigma},t)$ in (8.35b) and (8.38) can be neglected for the convergence analysis, where only absolute values are considered.

8.3.4 Inverse Backstepping–Transformation and Exponential Stability of the Observer Error Dynamics

Similar to the analysis of the state–feedback control in Section 8.2.5 when applied to the diffusion–reaction system (8.3), the verification of the exponential stability of the observer error dynamics with the observer gains $l_1(z,t)$ and $l_{10}(t)$ requires to analyze the inverse backstepping–transformation from the original diffusion–reaction system to the target system. For this, consider

$$\tilde{w}(z,t) = \tilde{x}(z,t) + \int_0^z m(z,\zeta,t)\tilde{x}(\zeta,t)\mathrm{d}\zeta, \tag{8.42}$$

differentiate with respect to t and z, and substitute the obtained equations into (8.26a). This yields after some intermediate computations

$$\begin{aligned} 0 &= \tilde{x}(z,t)\big(-2\mathrm{d}_z m(z,\zeta,t) + \tilde{\gamma}(z,t)\big) \\ &+ \tilde{x}(0,t)\left[\partial_\zeta m(z,0,t) - h^1\left(l_1(z,t) + \int_0^z m(z,\zeta,t)l_1(\zeta,t)\mathrm{d}\zeta\right)\right] \\ &- \partial_z\tilde{x}(0,t)\left[m(z,0,t) + h^0\left(l_1(z,t) + \int_0^z m(z,\zeta,t)l_1(\zeta,t)\mathrm{d}\zeta\right)\right] \\ &+ \int_0^z \big[\partial_t m(z,\zeta,t) + \partial_\zeta^2 m(z,\zeta,t) - \partial_z^2 m(z,\zeta,t) + \tilde{\gamma}(\zeta,t)m(z,\zeta,t)\big]\tilde{x}(\zeta,t)\mathrm{d}\zeta. \end{aligned} \tag{8.43}$$

As a result the inverse kernel $m(z,\zeta,t)$ has to satisfy the PDE

$$\partial_t m(z,\zeta,t) = \partial_z^2 m(z,\zeta,t) - \partial_\zeta^2 m(z,\zeta,t) - \tilde{\gamma}(\zeta,t)m(z,\zeta,t) \tag{8.44a}$$

for $\zeta\in(0,1)$, $z\in(\zeta,1)$ with

$$2\mathrm{d}_z m(z,z,t) - \tilde{\gamma}(z,t) = 0. \tag{8.44b}$$

Moreover, observe that substituting (8.27) into (8.42) implies the relation

$$\begin{aligned}
&\int_0^z \big(m(z,\zeta,t) - l(z,\zeta,t)\big)\tilde{w}(\zeta,t)\mathrm{d}\zeta \\
&= \int_0^z m(z,\zeta,t)\bigg(\int_0^\zeta l(\zeta,s,t)\tilde{w}(s,t)\mathrm{d}s\bigg)\mathrm{d}\zeta \\
&= \int_0^z \tilde{w}(s,t)\bigg(\int_s^z m(z,\zeta,t)l(\zeta,s,t)\mathrm{d}\zeta\bigg)\mathrm{d}s,
\end{aligned}$$

where the latter equation is obtained by changing the order of integration. Hence,

$$m(z,s,t) - l(z,s,t) = \int_s^z m(z,\zeta,t)l(\zeta,s,t)\mathrm{d}\zeta,$$

which by direct substitution in particular implies together with (8.30) that the right–hand side of (8.43) is identical to zero for all combinations of $\tilde{x}(0,t)$ and $\partial_z\tilde{x}(0,t)$.

The remaining boundary conditions are finally obtained by evaluating (8.26d) with (8.42) in view of (8.25f):

(i) For a Dirichlet boundary condition at $z = 1$ in (8.26d), i.e. $\tilde{\epsilon}_w^1 = 0$, $\tilde{p}_w^1 \neq 0$, the kernel has to satisfy

$$m(1,\zeta,t) = 0 \tag{8.44c}$$

while necessarily $\epsilon^1 = 0$ and $p^1 \neq 0$.

(ii) For a Neumann or mixed boundary condition at $z = 1$, i.e. $\tilde{\epsilon}_w^1 \neq 0$, the kernel is restricted to

$$\partial_z m(1,\zeta,t) - \frac{\tilde{p}_w^1}{\tilde{\epsilon}_w^1} m(1,\zeta,t) = 0 \tag{8.44d}$$

$$m(1,1,t) = \bar{p}^1 - \frac{\tilde{p}_w^1}{\tilde{\epsilon}_w^1}. \tag{8.44e}$$

Thereby it is required that $\epsilon^1 \neq 0$.

Obviously, the distributed–parameter system (8.44) for the inverse kernel $m(z,\zeta,t)$ is structurally identical to (8.29). Hence, the solution approach presented in Section 8.3.3 can be applied and convergence is induced by Theorems 8.4 and 8.5, respectively. This in particular illustrates that a strong solution to (8.44) can be determined, which is of Gevrey order $\alpha \leq 2$ in t. As a result, exponential stability of the observer error dynamics can be immediately guaranteed following the lines of the proof of Theorem 8.3.

Corollary 8.1. *Consider the observer error dynamics* (8.25) *with observer gains* $l_1(z,t)$ *and* $l_{10}(t)$ *according to* (8.30) *and* (8.31)*. Then the equilibrium* $\tilde{x}(z,t) \equiv 0$ *is exponentially stable for all* $t \in \mathbb{R}_{t_0}^+$ *in the* L^2*–norm for the target system* (8.26)

and in the H^1–norm for the target system (8.26a)*,* (8.26b) *with boundary conditions satisfying* (8.6)*.*

Corollary 8.1 in addition enables to deduce a separation principle, which illustrates that the dynamics of the state–feedback controlled system and of the state–observer can be assigned independently.

8.3.5 Separation Principle and Exponential Stability of the Closed–Loop System

For the realization of the state–feedback controller (8.21) the state $x(z,t)$ has to be replaced by the estimated quantity $\hat{x}(z,t)$ obtained from the solution of (8.25) with (8.30) and (8.31). As pointed out in [30, 12] for the case of time–invariant distributed–parameter system this is equivalent to the evaluation of the backstepping–transformation (8.7) with $x(z,t)$ replaced by $\hat{x}(z,t) = x(z,t) - \tilde{x}(z,t)$, i.e.

$$\begin{aligned} w(z,t) &= \hat{x}(z,t) - \int_0^z k(z,\zeta,t)\hat{x}(\zeta,t)\mathrm{d}\zeta \\ &= x(z,t) - \int_0^z k(z,\zeta,t)x(\zeta,t)\mathrm{d}\zeta \\ &\quad - \left(\tilde{x}(z,t) + \int_0^z k(z,\zeta,t)\tilde{x}(\zeta,t)\mathrm{d}\zeta\right) \end{aligned} \tag{8.45}$$

With Assumption 8.2 and proceeding along the lines of the determination of the kernel–PDEs, this provides in view of (8.3) and (8.25) that the corresponding target systems in $w(z,t)$ and $\tilde{w}(z,t)$ read as

$$\partial_t \begin{bmatrix} w(z,t) \\ \tilde{w}(z,t) \end{bmatrix} = \begin{bmatrix} \partial_z^2 w(z,t) - \mu(t)w(z,t) \\ \partial_z^2 \tilde{w}(z,t) - \tilde{\mu}(t)\tilde{w}(z,t) \end{bmatrix} + \begin{bmatrix} q(z,t) \\ 0 \end{bmatrix} \tilde{y}(t) \tag{8.46a}$$

with the forcing term

$$\begin{aligned} q(z,t) &= \left(l_1(z,t) - \int_0^z k(z,\zeta,t)l_1(\zeta,t)\mathrm{d}\zeta\right) \\ &\quad - \begin{cases} \frac{l_{10}(t)}{p^0}\partial_\zeta k(z,0,t), & \epsilon^0 = 0 \wedge p^0 \neq 0 \\ \frac{l_{10}(t)}{\epsilon^0}k(z,0,t), & \epsilon^0 \neq 0 \end{cases} \end{aligned} \tag{8.46b}$$

and

$$\tilde{y}(t) = h^0\partial_z\tilde{w}(0,t) + (h^1 - h^0 l(0,0,t))\tilde{w}(0,t).$$

The boundary conditions are given by

$$\begin{aligned}
-\epsilon_w^0 \partial_z w(0,t) + p_w^0 w(0,t) &= \tilde{y}(t) \times \begin{cases} \frac{p_w^0}{p^0} l_{10}(t), & \epsilon_w^0 = 0 \wedge p_w^0 \neq 0 \\ \frac{\epsilon_w^0}{\epsilon^0} l_{10}(t), & \epsilon_w^0 \neq 0 \end{cases} \\
\epsilon_w^1 \partial_z w(1,t) + p_w^1 w(1,t) &= 0 \\
-\tilde{\epsilon}_w^0 \partial_z \tilde{w}(0,t) + \tilde{p}_w^0 \tilde{w}(0,t) &= 0 \\
\tilde{\epsilon}_w^1 \partial_z \tilde{w}(1,t) + \tilde{p}_w^1 \tilde{w}(1,t) &= 0,
\end{aligned} \tag{8.46c}$$

together with the initial conditions

$$\begin{bmatrix} w(z,t_0) \\ \tilde{w}(z,t_0) \end{bmatrix} = \begin{bmatrix} w_0(z) \\ \tilde{w}_0(z) \end{bmatrix}. \tag{8.46d}$$

Obviously, the incorporation of the estimated state yields a one–sided coupling of the target system for the state–feedback in $w(z,t)$ with the target system for the observer error dynamics in $\tilde{w}(z,t)$. Given a finite–dimensional linear system the separation principle implies that the dynamics of the feedback part and the observer part can be assigned independently. In terms of the backstepping approach similar results are presented in [30, 12] for diffusion–reaction systems with constant and spatially varying parameters. Thereby, a Lyapunov–type argument is considered in [12], which however relies on a particular set of boundary conditions and is hence not applicable for the general linear setting above. For this, the exponential stability follows from the Theorem below.

Theorem 8.6. *Let $k(z,\zeta,t)$ and $l(z,\zeta,t)$ be the solutions to* (8.10) *and* (8.29)*, let the target systems* (8.4) *and* (8.26) *satisfy the assumptions of Lemma 8.1, and let Assumption 8.2 hold. Then for any $x_0(z),\ \hat{x}_0(z) \in L^2([0,1])$ the composite system consisting of the plant* (8.3) *and the observer* (8.24) *with state–feedback control* (8.21) *evaluated in terms of the observer state $\hat{x}(z,t)$ is exponentially stable in the L^2–norm.*

Proof. The coordinate transformations (8.45) and (8.27) map the original diffusion–reaction system (8.3) and the observer error dynamics (8.25) into (8.46). The $\tilde{w}$–subsystem of (8.46) and the homogeneous w–subsystem (with $q(z,t) = 0$ and the right–hand side in (8.46c) equal to zero) are by assumption exponentially stable. The interconnected $(w,\tilde{w})$–system is a cascade with the forcing by means of bounded functions with bounded derivative in z (cf. Theorem 8.3). This in particular implies the exponential stability of the $(w,\tilde{w})$–system. Due to the invertibility of $k(z,\zeta,t)$ and $l(z,\zeta,t)$ (cf. Sections 8.2.5 and 8.3.4) and the relation $\tilde{x}(z,t) = x(z,t) - \hat{x}(z,t)$ this yields the exponential stability of the closed–loop $(x,\hat{x})$–system under the state–feedback controls (8.21) evaluated with the observer state $\hat{x}(z,t)$. □

8.4 Tracking Control Using Backstepping and Differential Flatness

The fundamental idea of the backstepping approach relies on the transformation of the possibly unstable linear diffusion–reaction system (8.3) into the exponentially stable linear target distributed–parameter system (8.4). Subsequently, it is crucial to note that the stability of the target system is preserved if the boundary condition (8.4d) is modified according to

$$\epsilon_w^1 \partial_z w(1,t) + p_w^1 w(1,t) = u_w(t), \tag{8.47}$$

where $u_w(t)$ denotes an arbitrary function of time. This degree–of–freedom can be utilized as a feedforward controller to realize the tracking of suitable trajectories $t \mapsto \xi^*(t)$ for the output (8.3e) and hence to solve the tracking control problem. For this, flatness–based methods are incorporated, which allow a systematic solution of trajectory planning problems for distributed–parameter systems as presented in Part III for various system and control configurations.

8.4.1 Flatness–Based Trajectory Planning

In order to solve the trajectory planning problem given the target system (8.4a)–(8.4c) with (8.47), the formal integration approach presented in Chapter 7 can be directly applied. Here, Corollary 7.1 guarantees the convergence of the resulting state and input parametrizations under certain Gevrey conditions for the parameter $\mu(t)$ as well as the basic output.

However, since the parameter in the PDE of the target system depends solely on time t, alternatively formal power series can be applied for the solution of the trajectory planning problem. As is shown below, this in particular allows to deduce rather explicit and easily implementable representations for the state and input parametrizations. Following, e.g., [17, 20, 24, 21], a parametrization of the state $w(z,t)$ of the inhomogeneous target system (8.4a)–(8.4c), (8.47) is sought in terms of

$$\hat{w}(z,t) = \sum_{n=0}^{\infty} \hat{w}_n(t) \, \frac{(z)^n}{n!}, \tag{8.48}$$

For the application of the formal power series (8.48), observe first that the output (8.3e) in terms of $x(z,t)$ can be re–written as a function of $w(z,t)$ using (8.7) and (8.8), i.e.

$$y(t) = h^0 \partial_z w(0,t) + \bar{h}^1 w(0,t), \tag{8.49}$$

where $\bar{h}^1 = h^1 + h^0 k(0,0,t)$. Here, $k(0,0,t)$ can be replaced by either (8.10c) or (8.10g) depending on the type of boundary condition at $z = 0$.

For the computation of the series coefficients $\hat{w}_n(t)$ formally substitute (8.48) into the PDE (8.4a) for the target system. After sorting terms of equal degree in z a differential recursion is obtained for the series coefficients, i.e.

$$\hat{w}_n(t) = \partial_t \hat{w}_{n-2}(t) + \mu(t)\hat{w}_{n-2}(t), \qquad n \geq 2 \tag{8.50}$$

Obviously, two starting conditions for $\hat{w}_0(t)$ and $\hat{w}_1(t)$ are required to uniquely determine $\hat{w}_n(t)$ for all $n \geq 2$. For this, the evaluation of (8.4c) and (8.49) with the formal power series ansatz (8.48) yields

$$-\epsilon_w^0 \hat{w}_1(t) + p_w^0 \hat{w}_0(t) = 0 \tag{8.51}$$

$$h^0 \hat{w}_1(t) + \bar{h}^1 \hat{w}_0(t) = y(t). \tag{8.52}$$

Assuming that $h^0 p_w^0 + \bar{h}^1 \epsilon_w^0 \neq 0$, which is equivalent to require that (8.4c) and (8.49) are linearly independent with respect to $w(0,t)$ and $\partial_z w(0,t)$, it follows that

$$\hat{w}_0(t) = s^0 y(t),\ \hat{w}_1(t) = s^1 y(t) \tag{8.53}$$

where $s^0 = \epsilon_w^0/(h^0 p_w^0 + \bar{h}^1 \epsilon_w^0)$ and $s^1 = p_w^0/(h^0 p_w^0 + \bar{h}^1 \epsilon_w^0)$. In view of (8.50) it is obvious that any series coefficient $\hat{w}_n(t)$ can be parametrized in terms of $y(t)$ and its time–derivatives. In particular it follows that

$$\hat{w}_{2n}(t) = s^0 \mathcal{D}^n\{y(t)\},\ \hat{w}_{2n+1}(t) = s^1 \mathcal{D}^n\{y(t)\} \tag{8.54}$$

for $n \geq 0$ with $\mathcal{D}^n\{y(t)\} = \mathcal{D}\{\mathcal{D}^{n-1}\{y(t)\}\}$, $\mathcal{D}^0\{y(t)\} = y(t)$ with the operator $\mathcal{D} = \partial_t + \mu(t)$. Obviously any series coefficient $\hat{w}_n(t)$, $n \in \mathbb{N}$, can be expressed in terms of $y(t)$ and its time–derivatives. As a result, the state and input parametrization can be determined from (8.47), (8.48), and (8.54), i.e.

$$\hat{w}(z,t) = \sum_{n=0}^{\infty} \mathcal{D}^n\{y(t)\} \left(s^0 \frac{(z)^{2n}}{(2n)!} + s^1 \frac{(z)^{2n+1}}{(2n+1)!} \right) \tag{8.55}$$

$$\hat{u}_w(t) = \epsilon_w^1 \partial_z \hat{w}(1,t) + p_w^1 \hat{w}(1,t). \tag{8.56}$$

Hence, $\xi(t) = y(t) = h^0 \partial_z w(0,t) + \bar{h}^1 w(0,t)$ can be called a basic or flat output. In order to guarantee that $\hat{w}(z,t) \to w(z,t)$ and $\hat{u}_w(t) \to u_w(t)$ it is required to ensure uniform convergence of (8.55) with at least a unit radius of convergence.

Theorem 8.7. *Let* $\xi(t) \in G_{D_\xi,\alpha}(\mathbb{R}_{t_0}^+)$ *and let* $\mu(t) \in G_{D_\mu,\alpha}(\mathbb{R}_{t_0}^+)$ *with* $\alpha \in [1,2)$. *Then the series* (8.55) *converges to the solution of* (8.4a)–(8.4c), (8.47) *with an infinite radius of convergence.*

The proof of Theorem 8.7 follows basically the lines proposed in [20] and is provided below for the sake of completeness.

Proof. As proposed in [20] it is shown by induction that under the assumptions of Theorem 8.7, i.e. $\xi(t) \in G_{D_\xi,\alpha}(\mathbb{R}_{t_0}^+)$, $\mu(t) \in G_{D_\mu,\alpha}(\mathbb{R}_{t_0}^+)$, the series coefficients $\hat{w}_n(t)$ defined in (8.50), (8.51), and (8.53) can be majorized according to

$$\sup_{t\in\mathbb{R}^+_{t_0}} \left|\partial_t^l \hat{w}_n(t)\right| \leq D^{l+1}\varepsilon^n \frac{((l+n)!)^\alpha}{(n!)^{\frac{\alpha}{2}}}, \qquad n \geq 0 \tag{8.57}$$

for any $l \in \mathbb{N}$ and $\alpha \in [1,2]$. Here $D = \max\{D_\xi, D_\mu\} \times \max\{s^0, s^1\}$ and ε is a constant to be determined below. Given $n = 0$, (8.57) yields

$$\sup_{t\in\mathbb{R}^+_{t_0}} |\partial_t^l \hat{w}_0(t)| \leq D^{l+1}(l!)^\alpha,$$

which is equivalent to the fact that $\hat{w}_0(t) = s^0\xi(t)$ and $\xi(t) \in G_{D_\xi,\alpha}(\mathbb{R}^+_{t_0})$. Similarly for $n = 1$ one obtains $\sup_{t\in\mathbb{R}^+_{t_0}} |\partial_t^l \hat{w}_1(t)| \leq D^{l+1}\varepsilon((l+1)!)^\alpha$, which majorizes $\hat{w}_1(t) = s^1\xi(t)$. Hence assuming that (8.57) holds for $n = 0, 1, \ldots, N-1$, $N \geq 2$ it follows from (8.50) that

$$\sup_{t\in\mathbb{R}^+_{t_0}} \left|\partial_t^l \hat{w}_N(t)\right| \leq \sup_{t\in\mathbb{R}^+_{t_0}} \left|\partial_t^{l+1}\hat{w}_{N-2}(t) + \sum_{j=0}^{l} \binom{l}{j} \partial_t^j \mu(t) \partial_t^{l-j} \hat{w}_{N-2}(t)\right|.$$

Substituting the bounds for the Gevrey functions $\xi(t)$ and $\mu(t)$, the inequality reduces to

$$\sup_{t\in\mathbb{R}^+_{t_0}} \left|\partial_t^l \hat{w}_N(t)\right| \leq \frac{D^{l+1}\varepsilon^N((l+N)!)^\alpha}{(N!)^{\frac{\alpha}{2}}} \left(\frac{2D}{\varepsilon^2} \frac{(N(N-1))^{\frac{\alpha}{2}}}{(N+l)^\alpha}\right),$$

which for all $N \geq 2$ and $l \geq 0$ implies

$$\sup_{t\in\mathbb{R}^+_{t_0}} \left|\partial_t^l \hat{w}_N(t)\right| \leq \frac{D^{l+1}\varepsilon^N((l+N)!)^\alpha}{(N!)^{\frac{\alpha}{2}}} f(\varepsilon)$$

with $f(\varepsilon) := 2D/\varepsilon^2$. Here (B.18) and the property $\sum_j a_j^\alpha \leq (\sum_j a_j)^\alpha$ for $\alpha \geq 1$ and $a_j \geq 0$ were used. Solving $f(\varepsilon) = 1$ for ε, i.e. $\varepsilon = \sqrt{2D}$, yields the desired result (8.57). With this, the radius of convergence ϱ of the parametrized series (8.55) can be determined using the Cauchy–Hadamard formula such that $\varrho = \infty$ if $\alpha \in [1,2)$, $\varrho = 1/\varepsilon$ if $\alpha = 2$, and $\varrho = 0$ for $\alpha > 2$. □

As a result, assigning suitable desired trajectories $t \mapsto \xi^*(t) = y^*(t)$ from the Gevrey class of order $\alpha \in [1,2)$ for the output $\xi(t) = y(t)$, the respective state and input trajectories $w^*(z,t)$ and $u_w^*(t)$ follow directly from the evaluation of (8.55) and (8.56) with $\xi(t)$ replaced by $\xi^*(t)$. Since the target system is by definition exponentially stable, the application of the determined input trajectory $u_w^*(t)$ to the system (8.4a)–(8.4c), (8.47) directly ensures that $\xi(t) \to \xi^*(t)$ while $w(z,t) \to w^*(z,t)$.

However, recall that the considered tracking control task (8.2) is provided in terms of the state $x(z,t)$ of the governing diffusion–convection–reaction system and hence has to be transformed to a trajectory planning problem for the state $w(z,t)$ of

the target system. It is hence required to re–formulate the tracking control problem, which, as is shown in the subsequent section, results in the planning of appropriate trajectories $\xi^*(t)$ for the basic output $\xi(t)$.

Remark 8.4. Note that the original diffusion–reaction system (8.3) is flat with $\xi(t) = y(t)$ as a basic output (see, e.g, [20] for the case of linear diffusion–convection–reaction system with spatially dependent coefficients). However, it should be pointed out that the approach of [20] cannot be extended to the case of a varying parameter $c(z,t)$ without imposing further assumptions. On the other hand, as illustrated above, the flatness property is preserved under the backstepping transformation. This provides the great advantage that flatness–based trajectory planning can be performed by means of the equations of the target system (8.4a)–(8.4c), (8.47), (8.49), which are of a significantly simpler structure than the original diffusion–reaction system in view of the spatially and time varying parameter $c(z,t)$. Besides the determination of the respective differential recursion, the proof of uniform convergence of the parametrized series is similarly simplified using the presented approach.

8.4.2 Trajectory Assignment in Gevrey Classes Using the Backstepping Transformation

For trajectory planning, in the following the focus is on the realization of finite time transitions between a stationary initial profile $x(z,t_0) = x_0(z)$ and a final possibly time varying profile $x(z,t)$ for $t \geq t_0 + T$ with prescribed transition time $T > 0$ along a prescribed trajectory $\xi^*(t)$ for the (basic) output $\xi(t)$. However, differing from the discussion in Chapter 7 the introduced backstepping transformation allows to simplify the trajectory planning task since stationary profiles can be either considered for the x–system or equivalently for the w–system.

8.4.2.1 Steady State Analysis

Due to the time–variance of the governing PDE (8.3a) the analysis of stationary profiles becomes more involved compared to time–invariant PDEs. In particular, stationarity at $t = t_s \geq t_0$ requires that for all $t \geq t_s$ the following equations are satisfied

$$\partial_z^2 x_s(z) + c(z,t)x_s(z) = 0, \qquad z \in (0,1) \tag{8.58a}$$

$$-\epsilon^0 \partial_z x_s(0) + p^0 x_s(0) = 0 \tag{8.58b}$$

$$h^0 \partial_z x_s(0) + h^1 x_s(0) = \xi_s^*, \tag{8.58c}$$

where ξ_s^* denotes the constant desired stationary value of $\xi^*(t)$ and for $x_s(z) \neq 0$ the parameter $c(z,t) = c_s(z)$ for all $t \geq t_s$. Note that if $\xi_s^* = 0$, then $x_s(z) = 0$ is a solution to (8.58) independent of $c(z,t)$. Subsequently, if the equations (8.58) of

the BVP are satisfied, $x_s(z;\xi_s^*) = x_s(z)$ is called a stationary profile depending on ξ_s^*. Observe that due to the flatness property of (8.3) (see Remark 8.4) and (8.4a)–(8.4c), (8.47), (8.49) it is possible to express stationary profiles in terms of the basic output ξ_s^*. Obviously, a different choice for ξ_s^* results in different stationary profiles $x_s(z)$. The corresponding constant input for $t \geq t_s$ follows from the evaluation of (8.3c) with $x(z,t)$ replaced by $x_s(z;\xi_s^*)$, i.e.

$$u_s(\xi_s^*) = \theta(x_s(1;\xi_s^*), \partial_z x_s(1;\xi_s^*)). \tag{8.59}$$

Proceeding similarly for the target system (8.4a)–(8.4c), (8.47), (8.49) the stationary profile $w_s(z;\xi_s) = w(z)$ for $w(z,t)$ necessarily has to satisfy the BVP

$$\partial_z^2 w(z) - \mu(t) w(z) = 0, \qquad z \in (0,1) \tag{8.60a}$$

$$-\epsilon_w^0 \partial_z w(0) + p_w^0 w(0) = 0 \tag{8.60b}$$

$$h^0 \partial_z w(0) + \bar{h}^1 w(0) = \xi_s^*. \tag{8.60c}$$

Herein, given $\xi_s^* \neq 0$ and hence $w(z) \neq 0$ the parameter $\mu(t)$ has to fulfill $\mu(t) = \mu_s$ for all $t \geq t_s$. The corresponding constant input follows from (8.47) with $w(z,t)$ replaced by $w_s(z;\xi_s)$. In particular, $x_s(z;\xi_s^*)$ and $w_s(z;\xi_s)$ are interconnected by the backstepping transformation (8.7), i.e.

$$w_s(z;\xi_s) = x_s(z;\xi_s^*) - \int_0^z k_s(z,\zeta) x_s(\zeta;\xi_s^*) \mathrm{d}\zeta \tag{8.61}$$

with $k_s(z,\zeta)$ the stationary solution to the kernel–PDE (8.10a) for $\gamma(\zeta,t) = \gamma_s(\zeta) = c_s(z) + \mu_s$ and $\partial_t^l \gamma(\zeta,t) = 0$ for all $l \geq 1$ and $t \geq t_s$.

These results serve as the basis for the determination of suitable trajectories $\xi^*(t)$ for the basic output $\xi(t)$ to solve the considered tracking control problem.

8.4.2.2 Finite Time Transitions between Stationary Profiles

Subsequently, it is assumed that the initial profile (8.3d) represents a stationary profile for the diffusion–reaction system (8.3), i.e. a solution $x_0(z) = x_s(z;\xi_s^*)$ to the BVP (8.58) with $\xi_s^* = \xi_{s,0}^*$. As is outlined above, evaluation of (8.61) yields the corresponding stationary initial profile $w_0(z) = w_s(z,\xi_{s,0}^*)$ for the target system. Note that due to the equivalence of the original diffusion–reaction system and the target system induced by the backstepping transformation as well as the mapped output (8.49), trajectory planning can be performed in terms of either $x(z,t)$ or $w(z,t)$.

In view of the stationarity of the initial profile $x_0(z) = x_s(z;\xi_{s,0}^*)$ any trajectory for the basic output has to satisfy $\xi^*(t_0) = \xi_{s,0}^*$ while $\partial_t^l \xi^*(t_0) = 0$ for all $l \geq 1$. This in particular illustrates that $\xi^*(t)$ cannot be analytic at $t = t_0$. Thus, the basic output is chosen as

$$\xi^*(t) = \xi_{s,0}^* + \big(\xi_{s,T}^* - \xi_{s,0}^*\big) g_{T,\omega}(t - t_0) \tag{8.62}$$

with the locally non–analytic function $g_{T,\omega}(\cdot)$ of Gevrey order $\alpha = 1 + 1/\omega$ introduced in (B.3). Note that for all $t \geq t_0 + T$ the desired trajectory satisfies $\xi^*(t) = \xi^*_{s,T}$ while $\partial_t^l \xi^*(t) = 0$ for $l \geq 1$. Assuming that for all $t \geq t_0 + T$ the parameter $\mu(t)$ in the target system fulfills $\mu(t) = \mu_s$, $\partial_t^l \mu(t) = 0$ for $l \geq 1$, it follows from (8.60) that the target system reaches the stationary profile $w_s(z; \xi^*_{s,T})$ for $t \geq t_0 + T$. Since $\mu_s > 0$, this equilibrium is exponentially stable. As a result, substitution of (8.62) into the input parametrization (8.56) yields the feedforward control $u^*_w(t)$, which allows to realize the transition from the initial stationary profile $w_s(z; \xi^*_{s,0})$ to the final stationary profile $w_s(z; \xi^*_{s,T})$ within the prescribed finite time interval $t \in [t_0, t_0 + T]$, $T > 0$. By utilizing the transformation (8.61) and the inverse backstepping transformation (8.22) this result is equivalent to the transition from the initial stationary profile $x_s(z; \xi^*_{s,0})$ to the final (not necessarily stationary) profile

$$x(z,t) = w_s(z; \xi^*_{s,T}) + \int_0^z g(z,\zeta,t) w_s(\zeta; \xi^*_{s,T}) \mathrm{d}\zeta \tag{8.63}$$

for $t \geq t_0 + T$ along the desired trajectory (8.62) for the (basic) output (8.3e).

Remark 8.5. In addition to the realization of a finite time transition from a stationary initial profile to the final profile defined in (8.63) it is possible to solve more general tracking control tasks. As an example consider the tracking of a periodic trajectory for the (basic) output $\xi^*(t)$ for the case of a stationary initial profile. The choice of

$$\xi^*(t) = \xi^*_{s,0} + (A_1 \sin(\omega_1 t) + A_2 \cos(\omega_2 t)) g_{T,\omega}(t - t_0)$$

provides a smooth and at $t = t_0$ non–analytic desired trajectory, which is consistent with the stationary initial profile $x_0(z) = x_s(z; \xi^*_{s,0})$. Substitution of $\xi^*(t)$ into the input parametrization (8.56) provides the feedforward control $u^*_w(t)$ to realize the periodic trajectory $\xi^*(t) = \xi^*_{s,0} + A_1 \sin(\omega_1 t) + A_2 \cos(\omega_2 t)$ for $t \geq t_0$ for the output (8.3e) or (8.49). In addition, the approach above can be suitably extended to perform trajectory planning for a non–stationary initial profile following, e.g., the approach considered in [17, 9] or the treatise in Section 6.4.2.

These simple examples clearly illustrate the wide applicability of the considered approach, where the trajectory planning is performed on the basis of the exponentially stable target system, which has a significantly simpler structure compared to the original problem.

8.4.3 *Combining Backstepping and Differential Flatness for Exponentially Stabilizing Tracking Control*

By combining the backstepping–based state–feedback controller introduced in Section 8.2.4 with the flatness–based feedforward controller determined above, an exponentially stabilizing tracking controller is obtained, which solves the tracking

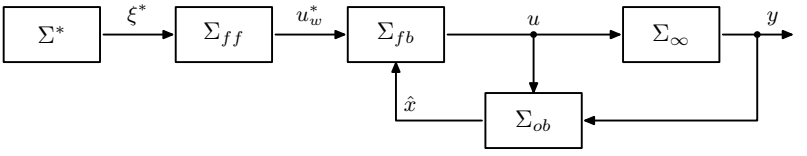

Fig. 8.2 Block diagram of state–feedback tracking controller with state–observer combining backstepping and flatness. The control structure consists of a trajectory generator Σ^* for the basic output, the feedforward control Σ_{ff}, the backstepping–based state–feedback control Σ_{fb} and state–observer Σ_{ob}, and the distributed–parameter system (8.3).

control problem for the diffusion–reaction system (8.3). For this, a simple modification of the state–feedback controllers (8.21) is required in terms of (8.47). Depending on the values of ϵ_w^1 and p_w^1 this yields:

(i) For $\epsilon_w^1 = 0$, i.e. $w(1,t) = u_w^*(t)/p_w^1$, with (8.21a) the tracking controller evaluates to

$$u(t) = \theta\bigg(\Xi_D(x(z,t)) + \frac{u_w^*(t)}{p_w^1}, \partial_z x(1,t) \bigg). \tag{8.64a}$$

(ii) For $p_w^1 = 0$, i.e. $\partial w/\partial z(1,t) = u_w^*(t)/\epsilon_w^1$, with (8.21b) the tracking controller reads as

$$u(t) = \theta\bigg(x(1,t), \Xi_N(x(z,t)) + \frac{u_w^*(t)}{\epsilon_w^1} \bigg). \tag{8.64b}$$

(iii) For $p_w^1,\ \epsilon_w^1 > 0$, i.e. $\epsilon_w^1 \partial w/\partial z(1,t) + p_w^1 w(1,t) = u_w^*(t)$, with (8.21c) the tracking controller follows as

$$u(t) = \theta\bigg(x(1,t), \Xi_M(x(z,t)) + \frac{u_w^*(t)}{\epsilon_w^1} \bigg). \tag{8.64c}$$

In view of the application of the determined tracking control, the state $x(z,t)$ has to be replaced in (8.64) by the observer state $\hat{x}(z,t)$ obtained from the evaluation of the distributed–parameter state–observer (8.24) with the observer gains according to (8.30), (8.31). This results in a dynamics output feedback tracking control scheme, which ensures the exponentially stable tracking of suitably designed output trajectories. The corresponding block diagram, which schematically illustrates the proposed tracking control concept, is shown in Figure 8.2.

8.5 Application Examples and Simulation Results

In order to evaluate the performance of the determined tracking control, simulation results are presented for the transition starting from an initial stationary profile to

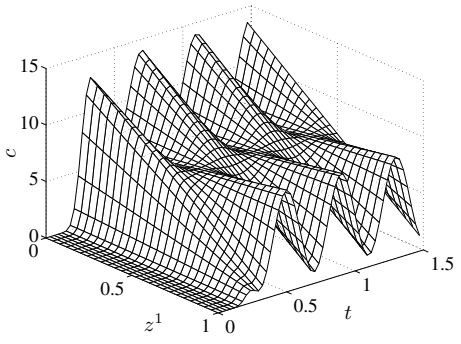

Fig. 8.3 Spatially and time varying parameter $c(z,t)$ as defined in (8.65)

reach a final stationary profile along a prescribed output path. Thereby, a mixed boundary condition (8.3b) is considered with the system parameters $\epsilon^0 = p^0 = 1$. The output (8.3e) is determined by the parameters $h^0 = 0$ and $h^1 = 1$ such that $\xi(t) = x(0,t)$. For the sake of simplicity, the initial time t_0 is chosen as $t_0 = 0$.

As an example, the varying parameter $c(z,t)$ in the PDE (8.3a) is chosen as

$$c(z,t) = g_{T_c,\omega_c}(t-t_0)\big(a_1(t) + z a_2(t)\big) \tag{8.65}$$

with $a_1(t) = 10 + 4\cos(5\pi t + \pi/2)$, $a_2(t) = 5 - a_1(t) + 4\sin(5\pi t)$ and $\omega_c = 3/2$ and $T_c = 1/2$. Note that due to the choice (8.65), the parameter $c(z,t)$ satisfies $c(z,t_0) = 0$, $\partial_t^l c(z,t_0) = 0$ for $l \geq 1$ while $c(z,t) = a_1(t) + z a_2(t)$ for $t \geq t_0 + T_c$. The resulting evolution of $c(z,t)$ in the (z,t)–domain with amplitudes changing periodically for $t \geq t_0 + T_c$ between the extrema $\min_{z\in[0,1],t\geq t_0+T_c} c(z,t) = 1$ and $\max_{z\in[0,1],t\geq t_0+T_c} c(z,t) = 14$ is illustrated in Figure 8.3. The parameters for the target system are chosen as $\epsilon_w^0 = \epsilon_w^1 = 1$, $p_w^0 = p_w^1 = 0$ while two different parameters $\mu(t)$ are considered, i.e.

$$\mu_1(t) = \mu_1 = 10$$
$$\mu_2(t) = 20 - 10 g_{T_\mu,\omega_\mu}(t-t_0)$$

with $\omega_\mu = 2$ and $T_\mu = 0.4$. The latter choice with a time varying $\mu(t)$ is thereby included in order to illustrate the different possibilities when defining the target system and the resulting consequences on the tracking behavior. With these parameters, exponential stability of the target system in the L^2– and H^1–norm is guaranteed by Lemma 8.1 and 8.2.

8.5.1 Trajectory Planning

The desired output trajectory $t \mapsto \xi^*(t)$ is assigned as defined in (8.62) with $\xi^*_{s,0} = -2$, $\xi^*_{s,T} = 2$, $T = 1$, and $\omega = 2$. Hence, the desired trajectory is of Gevrey order $\alpha = 3/2 < 2$ such that convergence of the formal power series parametrizations of the state and the input of the target system is ensured by Theorem 8.7. As outlined in Section 8.4.2.2, for the choice of the desired trajectory $\xi^*(t)$ and the ansatz for $c(z,t)$, the trajectory planning problem corresponds to the realization of a transition starting from the initial stationary profile $x_s(z;\xi^*_{s,0}) = (1+z)\xi^*_{s,0}$, i.e. $x_0(z) = x_s(z;\xi^*_{s,0})$, to the non–stationary profile defined by (8.63) for $t \geq t_0 + T$. Here, the final stationary profile $w_s(z;\xi^*_{s,T})$ for the target system is obtained by solving (8.60), which yields for the considered set of parameters and $\mu_s = \mu_1 = \mu_2(T_\mu)$ that $w_s(z;\xi^*_{s,T}) = \xi^*_{s,T}\,{}_0F_1(;2/3;{\mu_s}^3(z)/9)$, where ${}_0F_1(;\cdot;\cdot)$ denotes the confluent hypergeometric function.

This is illustrated in Figure 8.4, where the evolution of $w^*(z,t)$ as defined in (8.55) with $\xi(t)$ replaced by $\xi^*(t)$ is shown for $\mu_1(t)$ (Figure 8.4(a)) and $\mu_2(t)$ (Figure 8.4(b)). By making use of the inverse backstepping transformation (8.22) the corresponding profiles $x^*(z,t)$ of the original system can be directly determined as shown in Figures 8.4(c) and 8.4(d). With this, a design systematics can be derived, which correlates trajectory planning in the w–system with trajectory planning in the x–system by means of an invertible transformation. As a result, a direct validation of the desired dynamics is available, which can be exploited in an iterative process to suitably assign $\xi^*(t)$ towards the fulfillment and offline evaluation of possible state and input constraint or additional desired dynamical process features.

8.5.2 Stabilization and Tracking

Since (8.65) is of Gevrey order $\alpha = 5/3$ and since $\mu(t)$ is constant or of Gevrey order $\alpha = 3/2 < 2$, the uniform convergence of the successive approximation for the determination of the kernel $k(z,\zeta,t)$ is ensured by Theorem 8.2. In order to illustrate this, Figure 8.5(a) and 8.5(b) depict the kernel $k(z,\zeta,t)$ in the (z,ζ)–domain for $t \in \{0, 0.5, 1.0, 1.5\}$ computed with 6 series coefficients in (8.14). Significant differences between the result for $\mu(t) = \mu_1$ and $\mu(t) = \mu_2(t)$ can be observed for $t < T_\mu$ due to the time–variance of $\mu_2(t)$ while both kernels coincide for $t \geq T_\mu$. As an example a nonlinear boundary condition (8.3c) of the form

$$\theta\big(x(1,t), \partial_z x(1,t)\big) = \partial_z x(1,t) + \sinh(x(1,t)) \tag{8.66}$$

is considered, which involves an exponential growth in $x(1,t)$. Note that due to the nonlinear boundary condition (8.66) and in particular due to the time varying parameter $c(z,t)$ in the PDE (8.3a) the eigenvalue analysis is not applicable for the stability analysis. However, open–loop simulations directly reveal the instability of the uncontrolled system. On the other hand, highly accurate trajectory tracking

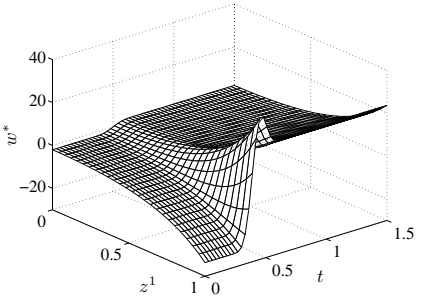

(a) Desired profile $w^*(z,t)$ for $\mu_1(t)$.

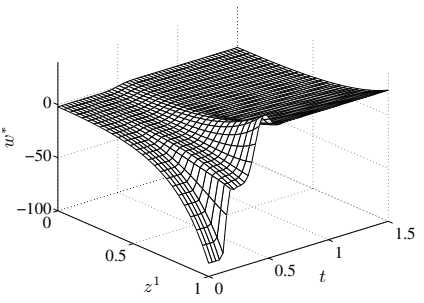

(b) Desired profile $w^*(z,t)$ for $\mu_2(t)$.

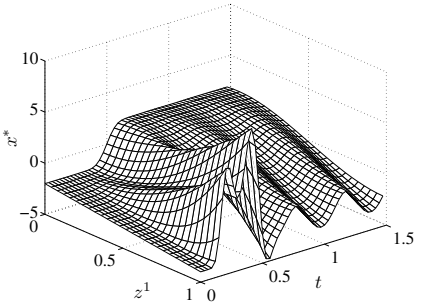

(c) Corresponding profile $x^*(z,t)$ for $\mu_1(t)$.

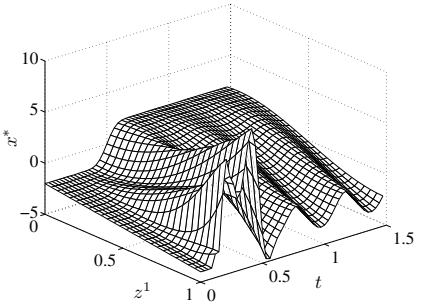

(d) Corresponding profile $x^*(z,t)$ for $\mu_2(t)$.

Fig. 8.4 Trajectory planning for target and original system

can be achieved by applying the determined tracking controller (8.64c) for mixed boundary conditions. This is shown in Figures 8.5(c)–8.5(f). Here, the evolution of the controlled state $x(z,t)$ (Figure 8.5(c)) is depicted in the (z,t)–domain for $\mu(t) = \mu_1$ in order to illustrate the transition behavior with the state $x(z,t)$ satisfying (8.63) for $t \geq t_0 + T = 1$. Obviously, after an initial transition phase the obtained profile changes periodically with time t over the spatial domain. For the evaluation of the tracking performance, a comparison between the obtained output $\xi(t) = x(0,t)$ and the desired output $\xi^*(t)$ is provided in Figure 8.5(d). Here, the achievable almost perfect tracking behavior is illustrated for both choices of $\mu(t)$. The effect of the time varying parameter $\mu(t) = \mu_2(t)$ can by directly evaluated in Figures 8.5(e) and 8.5(f) where the input is shown for $\mu(t) = \mu_1$ and $\mu(t) = \mu_2(t)$, respectively. The feedforward control $u_w^*(t)$ determined from (8.56) computed using 20 series coefficients and the respective tracking controls $u(t)$ as defined in (8.64c) are thereby depicted for comparison reasons. Due to the different choice of $\mu(t)$, a rather significant change in both the feedforward part $u_w^*(t)$ and the tracking controller $u(t)$ can be observed. Note that detailed simulation studies reveal that the evolving peaks in $u(t)$ at $t \approx 0.2$ and $t \approx 0.4$ are a direct consequence of the nonlinear boundary condition (8.66) and are hence necessary to stabilize the system.

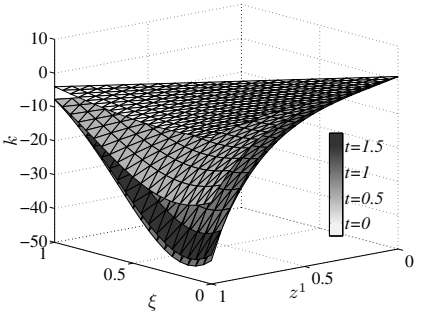

(a) Kernel $k(z,\zeta,t)$ for $\gamma(z,t) = c(z,t) + \mu_1$ at $t \in \{0, 0.5, 1.0, 1.5\}$.

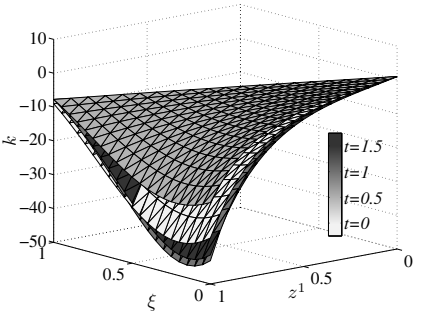

(b) Kernel $k(z,\zeta,t)$ for $\gamma(z,t) = c(z,t) + \mu_2(t)$ at $t \in \{0, 0.5, 1.0, 1.5\}$.

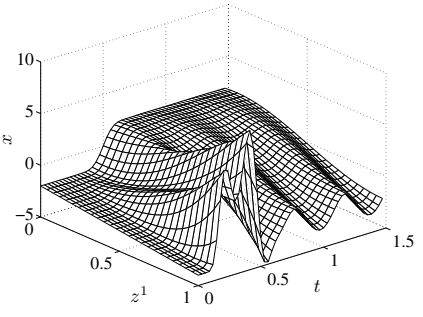

(c) Profile $x(z,t)$ in (z,t)–domain with tracking controller (8.64c) for $\mu(t) = \mu_1$.

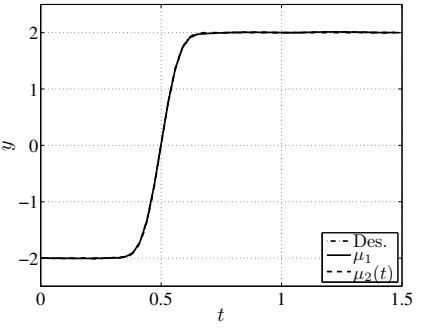

(d) Comparison of the output $y(t)$ for $\mu(t) = \mu_1$ (bold) and $\mu(t) = \mu_2(t)$ (dashed) with $\xi^*(t)$ (8.62).

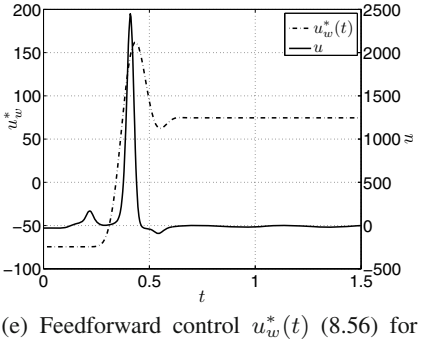

(e) Feedforward control $u_w^*(t)$ (8.56) for $\mu(t) = \mu_1$ and tracking control $u(t)$ (8.64c).

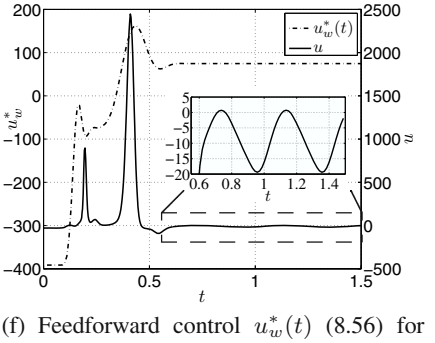

(f) Feedforward control $u_w^*(t)$ (8.56) for $\mu(t) = \mu_2(t)$, tracking control $u(t)$ (8.64c), and magnification of $u(t)$.

Fig. 8.5 Feedback stabilization and tracking control

In summary, the obtained simulation results clearly illustrate the feasibility and the achievable high tracking performance of the proposed exponentially stabilizing tracking control concept for boundary controlled linear diffusion–reaction and diffusion–convection–reaction systems with varying parameters.

Notes

The results of Section 8.5 are partly based on [23]. Acknowledgement is given to ©2009, Elsevier. Reprinted, with permission, from T. Meurer and A. Kugi, "Tracking control for boundary controlled parabolic PDEs with varying parameters: combining backstepping and flatness", Automatica, 45(5):1182–1194.

References

1. Ahmed, N., Xiang, X.: Nonlinear Boundary Control of Semilinear Parabolic Systems. SIAM J. Control Optim. 34(2), 473–490 (1996)
2. Amann, H.: Parabolic Evolution Equations and Nonlinear Boundary Conditions. J. Diff. Eqns. 72, 201–269 (1988)
3. Baehr, H., Stephan, K.: Heat and Mass Transfer, 2nd edn. Springer, Berlin (2006)
4. Balogh, A., Krstic, M.: Stability of partial difference equations governing control gains in infinite–dimensional backstepping. Systems & Control Letters 51, 151–164 (2004)
5. Bošković, D., Krstic, M.: Backstepping control of chemical tubular reactors. Comp. Chem. Eng. 26, 1077–1085 (2002)
6. Bošković, D., Balogh, A., Krstic, M.: Backstepping in infinite dimension for a class of parabolic distributed parameter systems. Math. Control. Signal. 16, 44–75 (2003)
7. Cochran, J., Krstic, M.: Motion planning and trajectory tracking for three–dimensional Poiseuille flow. J. Fluid Mech. 626, 307–332 (2009)
8. Colton, D.: The Solution of Initial–Boundary Value Problems for Parabolic Equations by the Method of Integral Operators. J. Diff. Eqns. 26, 181–190 (1977)
9. Dunbar, W., Petit, N., Rouchon, P., Martin, P.: Motion Planning for a nonlinear Stefan Problem. ESAIM Contr. Optim. Ca. 9, 275–296 (2003)
10. Gevrey, M.: Sur la nature analytique des solutions des équations aux dérivées partielles. Annales Scientifiques de l'Ecole Normale Superieure 25, 129–190 (1918)
11. Khalil, H.: Nonlinear Systems, 3rd edn. Prentice-Hall, New Jersey (2002)
12. Krstic, M., Smyshlyaev, A.: Boundary Control of PDEs: A Course on Backstepping Designs. SIAM, Philadelphia (2008)
13. Krstić, M., Kanellakopoulos, I., Kokotović, P.: Nonlinear and Adaptive Control Design. John Wiley & Sons, New York (1995)
14. Krstic, M., Guo, B., Balogh, A., Smyshlyaev, A.: Output–feedback stabilization of an unstable wave equation. Automatica 44(1), 63–74 (2008)
15. Krstic, M., Magnis, L., Vazquez, R.: Nonlinear Stabilization of Shock–Like Unstable Equilibria in the Viscous Burgers PDE. IEEE Trans. Automat. Control 53(7), 1678–1683 (2008)

16. Ladyženskaja, O., Solonnikov, V., Ural'ceva, N.: Linear and Quasi–linear Equations of Parabolic Type. Translations of Mathematical Monographs, 5th edn., vol. 23. American Mathematical Society, Providence (1998)
17. Laroche, B., Martin, P., Rouchon, P.: Motion planning for the heat equation. Int. J. Robust Nonlinear Control 10, 629–643 (2000)
18. Lions, J.: Optimal Control of Systems Governed by Partial Differential Equations. Springer, Heidelberg (1971)
19. Liu, W.: Boundary feedback stabilization of an unstable heat equation. SIAM J. Control Optim. 42(3), 1033–1043 (2003)
20. Lynch, A., Rudolph, J.: Flatness–based boundary control of a class of quasilinear parabolic distributed parameter systems. Int. J. Control 75(15), 1219–1230 (2002)
21. Meurer, T.: Feedforward and Feedback Tracking Control of Diffusion–Convection–Reaction Systems using Summability Methods. Fortschr.–Ber. VDI Reihe 8 Nr. 1081. VDI Verlag, Düsseldorf (2005)
22. Meurer, T., Kugi, A.: Tracking control for a diffusion–convection–reaction system: combining flatness and backstepping. In: Proc. 7th IFAC Symposium Nonlinear Control Systems (NOLCOS 2007), Pretoria (SA), pp. 583–588 (2007)
23. Meurer, T., Kugi, A.: Tracking control for boundary controlled parabolic PDEs with varying parameters: combining backstepping and flatness. Automatica 45(5), 1182–1194 (2009)
24. Meurer, T., Zeitz, M.: Feedforward and feedback tracking control of nonlinear diffusion–convection–reaction systems using summability methods. Ind. Eng. Chem. Res. 44, 2532–2548 (2005)
25. Ray, W.: Advanced Process Control. McGraw–Hill, New York (1981)
26. Seidman, T.I.: Two Results on Exact Boundary Control of Parabolic Equations. Appl. Math Optim. 11, 145–152 (1984)
27. Sepulchre, R., Janković, M., Kokotović, P.: Constructive Nonlinear Control. Springer, London (1997)
28. Smyshlyaev, A., Krstic, M.: Regularity of hyperbolic PDEs governing backstepping gain kernels for parabolic PDEs. In: Proc. American Control Conference, Denver (CO), USA, vol. 3, pp. 2634–2639 (2003)
29. Smyshlyaev, A., Krstic, M.: Closed–Form Boundary State Feedbacks for a Class of 1–D Partial Integro–Differential Equations. IEEE Trans. Automat. Control 49(12), 2185–2202 (2004)
30. Smyshlyaev, A., Krstic, M.: Backstepping observers for a class of parabolic PDEs. Systems & Control Letters 54, 613–625 (2005a)
31. Smyshlyaev, A., Krstic, M.: On control design for PDEs with space–dependent diffusivity or time–dependent reactivity. Automatica 41, 1601–1608 (2005b)
32. Smyshlyaev, A., Guo, B.Z., Krstic, M.: Arbitrary decay rate for Euler–Bernoulli beam by backstepping boundary feedback. IEEE Trans. Autom. Control 54(5), 1134–1141 (2009)
33. Smyshlyaev, A., Cerpa, E., Krstic, M.: Boundary stabilization of a 1–D wave equation with in–domain anti–damping. SIAM J. Control Optim. 48(6), 4014–4031 (2010)
34. Vazquez, R., Krstic, M.: Control of 1-D parabolic PDEs with Volterra nonlinearities – Part I: Design. Automatica 44, 2778–2790 (2008a)
35. Vazquez, R., Krstic, M.: Control of 1-D parabolic PDEs with Volterra nonlinearities – Part II: Analysis. Automatica 44, 2791–2803 (2008b)

Chapter 9
Backstepping for Linear Diffusion–Convection–Reaction Systems with Varying Parameters on Parallelepiped Domains

The backstepping approach presented in the previous chapter for boundary controlled distributed–parameter systems defined on a 1–dimensional domain with a single control and output located at the boundary is subsequently extended to linear diffusion–convection–reaction systems with orthotropic diffusion and convection defined on an r–dimensional parallelepipedon. Initial results towards the generalization of the backstepping concept can be, e.g., found in [12, 11], where the linearized equations of Hartmann flow are considered in a double semi–infinite domain. The system of linear PDEs with 3–dimensional domain is thereby reduced to a PDE system with 1–dimensional domain in the wave number space by making use of Fourier transformation techniques. Similar approaches are addressed in [6] for the Navier–Stokes equations linearized around a parabolic Poiseuille profile.

Differing from these results, in the following the backstepping–based design of state–feedback controllers and state–observers is considered for distributed–parameter systems with bounded domain of dimension larger than one and multiple inputs and outputs on the domain's boundary. Starting with the general problem formulation in Section 9.1 this at first comprises the analysis of the single input and single output case in Sections 9.2 and 9.3. In addition to the study of the separation property this is complemented in Section 9.4 by supplementing the control–loop with flatness–based trajectory planning towards the determination of exponentially stabilizing tracking controllers. Based on these results, multiple input and output configurations are addressed in Sections 9.5 and 9.6, where multi–linear backstepping transformations are introduced to solve the stabilization and state estimation problem. Following a discussion of the possible extensions to exponentially stabilizing tracking control by means of flatness–based methods in Section 9.7, the applicability as well as the control and observer performance is finally analyzed by numerical simulations for two application examples in Section 9.8.

Notation. Subsequently, the dependency of the system variables on the independent coordinates $z = (z^1, \ldots, z^r)$ and t is explicitly stated in any expression. This notational distinction is necessary for the proper representation of the individual actuation and sensing configurations, which are reflected in the formulation of the respective backstepping techniques.

T. Meurer: Control of Higher-Dimensional PDEs, CCE, pp. 269–346.
springerlink.com

9.1 Stabilization and Tracking Control Problem

The trajectory tracking problem is considered for a linear parabolic diffusion–convection–reaction system with orthotropic diffusion and convection and a spatially and time varying reaction parameter $c(z,t)$, i.e. for $(z,t) \in \Omega \times \mathbb{R}^+_{t_0}$ consider

$$\partial_t x(z,t) = \sum_{j\in I_r} a_j(z^j)\partial^2_{z^j} x(z,t) + \sum_{j\in I_r} b_j(z^j)\partial_{z^j} x(z,t) + c(z,t)x(z,t) \quad (9.1a)$$

defined on the r–dimensional parallelepipedon

$$\Omega = \left\{ z \in \mathbb{R}^r \mid 0 < z^j < L_j,\ j \in I_r \right\} \quad (9.1b)$$

with $I_r = \{1, 2, \ldots, r\}$. The PDE (9.1a) is assumed to be parabolic, which implies that there exist positive finite constants a^l_j, a^u_j such that $a^l_j \leq a_j(z^j) \leq a^u_j$ for all $z^j \in [0, L_j]$, $j \in I_r$.

Assumption 9.1. The following conditions hold for the system parameters $a_j(z^j)$, $b_j(z^j)$, and $c(z,t)$:

(i) The parameters fulfill $a_j(z^j) \in \mathcal{C}^2([0, L_j])$ and $b_j(z^j) \in \mathcal{C}^1([0, L_j])$ for $j \in I_r$.
(ii) The parameter $b_j(z^j)$, $j \in I_r$, is assumed to be positive and bounded from above, i.e. $0 \leq b_j(z^j) \leq b^u_j$ for all $z^j \in [0, L_j]$, $j \in I_r$ such that flow reversal is excluded.
(iii) The parameter $c(z,t)$ representing, e.g., a reaction parameter is assumed to be bounded, i.e. $-\infty < c^l \leq c(z,t) \leq c^u < \infty$ for all $z \in \overline{\Omega}$ and $t \geq t_0$. Additional structural constraints and differentiability conditions for $c(z,t)$ with respect to z and t are introduced below.

As pointed out in Part II, this type of PDE covers a rather large class of systems describing, e.g., unsteady and orthotropic heat conduction in solids, orthotropic convective mass and heat transfer in linear shear flows, and chemical tubular reactors with time varying linear reaction kinetics [1, 2, 3]. In addition, as shown in Chapter 3 interconnected multi–agent systems allow a corresponding PDE representation.

General mixed or Robin boundary conditions are imposed for $t > t_0$, i.e.

$$-\epsilon^0_j \partial_{z^j} x(z,t) + p^0_j x(z,t) = 0, \qquad z^j = 0,\ j \in I_r \quad (9.1c)$$

$$\epsilon^1_j \partial_{z^j} x(z,t) + p^1_j x(z,t) = 0, \qquad z^j = L_j,\ j \in I_r^{I_m} \quad (9.1d)$$

with constants $\epsilon^0_j,\ p^0_j,\ \epsilon^1_j,\ p^1_j \in \mathbb{R}$ and the index set $I_m \subset I_r$, $\#I_m = m$. With this configuration, Dirichlet ($\epsilon^k_j = 0$, $p^k_j \neq 0$), Neumann ($\epsilon^k_j \neq 0$, $p^k_j = 0$), or Robin ($\epsilon^k_j \neq 0$, $p^k_j \neq 0$) boundary conditions are obtained. The m boundary inputs $u^i(z_{(i|)}, t)$, $i \in I_m$ are restricted to hyperplanes $\partial\Omega_i = \{z \in \Omega : z^i = L_i\}$ and enter the system in a nonlinear fashion governed by the continuous functional $\theta^i(\cdot,\cdot)$, which combines the state and the gradient on $\partial\Omega_i$, i.e.

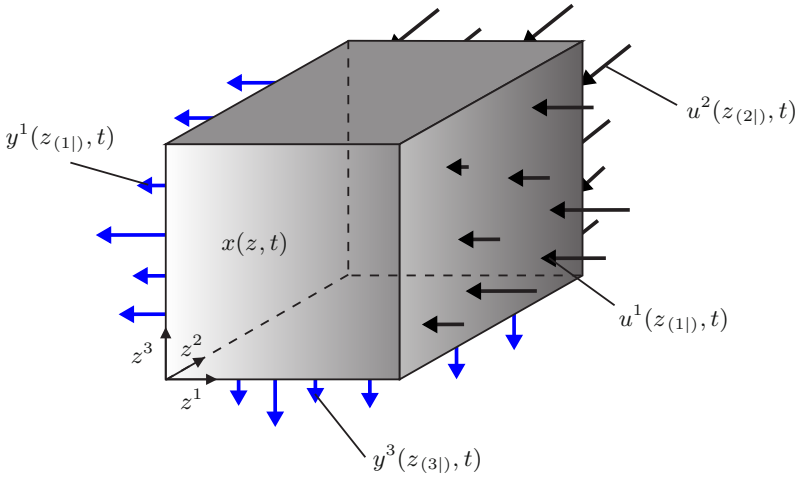

Fig. 9.1 Schematics of the boundary control and output configuration for the parallelepipedon Ω with $r = 3$ and $I_m = \{1, 2\}$ and $I_p = \{1, 3\}$

$$\theta^i\left(x(z,t), \partial_{z^i} x(z,t)\right) = u^i(z_{(i|)}, t), \qquad z^i = L_i,\ i \in I_m \tag{9.1e}$$

for $t > t_0$ with $z_{(i|)} = (z^j)_{j \in I_r^i} = (z^1, \ldots, z^{i-1}, z^{i+1}, \ldots, z^r)$. The consistent initial condition is given by

$$x(z, t_0) = x_0(z), \qquad z \in \overline{\Omega}. \tag{9.1f}$$

The system outputs $y^i(z_{(i|)}, t)$ are considered for $t \geq t_0$ in the form

$$y^i(z_{(i|)}, t) = h_i^0 \partial_{z^i} x(z,t) + h_i^1 x(z,t), \qquad z^i = 0,\ i \in I_p \tag{9.1g}$$

with the index set $I_p \subset I_r$, $\#I_p = p$. The constants h_i^0, h_i^1 are assumed to fulfill $h_i^0 p_i^0 + h_i^0 \epsilon_i^0 \neq 0$, which implies that (9.1c) for $j \in I_p$ and (9.1g) are linearly independent.

The boundary control and output configuration is exemplary illustrated in Figure 9.1 for a 3–dimensional setting with the sets $I_m = \{1, 2\}$ and $I_p = \{1, 3\}$ corresponding to inputs acting on the surfaces $z^i = L_i$, $i \in I_m$, and outputs along $z^i = 0$, $i \in I_p$.

Remark 9.1. Subsequently, it is assumed that any input (output) is located on a plane $z^i = L_i$ ($z^i = 0$). This can be achieved in general by introducing the mapping $z^i \mapsto L_i - z^i$ for those inputs (outputs) acting on the plane $z^i = 0$ ($z^i = L_i$).

9.1.1 Transformation into Standard Form

With Assumptions 9.1(i) and (ii) it is shown in Section 7.1.1 that a suitable invertible change of coordinates and variables exists such that (9.1) can be transferred to a linear diffusion–reaction system with constant and normalized diffusion parameter. As a result, instead of considering (9.1) it is equivalent to analyze

$$\partial_t x(z,t) = \Delta x(z,t) + c(z,t)x(z,t) \tag{9.2a}$$

defined on $(z,t) \in \Omega \times \mathbb{R}^+_{t_0}$. Since only Dirichlet boundary conditions are preserved under the presented transformations and Neumann boundary conditions are transformed into mixed or Robin boundary conditions general linear homogeneous boundary conditions

$$-\epsilon_j^0 \partial_{z^j} x(z,t) + p_j^0 x(z,t) = 0, \qquad z^j = 0,\ j \in I_r \tag{9.2b}$$

$$\epsilon_j^1 \partial_{z^j} x(z,t) + p_j^1 x(z,t) = 0, \qquad z^j = L_j,\ j \in I_r^{I_m} \tag{9.2c}$$

are considered for $t > t_0$ together with nonlinear boundary inputs

$$\theta^i\left(x(z,t), \partial_{z^i} x(z,t)\right) = u^i(z_{(i|)},t), \qquad z^i = L_i,\ i \in I_m, \tag{9.2d}$$

and the initial condition

$$x(z,t_0) = x_0(z), \qquad z \in \overline{\Omega}. \tag{9.2e}$$

The structure of the outputs (9.1g) remains unchanged, i.e.

$$y^i(z_{(i|)},t) = h_i^0 \partial_{z^i} x(z,t) + h_i^1 x(z,t), \qquad z^i = 0,\ i \in I_p \tag{9.2f}$$

for $t \geq t_0$. Note that results on the existence and uniqueness of solutions to (9.2) can be, e.g., found in [9].

Throughout this chapter the following condition is assumed to hold for the structure of the spatially and time varying parameter $c(z,t)$ in the PDE (9.2a).

Assumption 9.2. Depending on the design task, the parameter $c(z,t)$ allows for a decomposition according to

$$c(z,t) \begin{cases} c_0(z_{(I_m|)},t) + \displaystyle\sum_{n \in I_m} c_1^n(z^n,t), & \text{state–feedback design} \quad (9.3a) \\ c_0(z_{(I_p|)},t) + \displaystyle\sum_{n \in I_p} c_1^n(z^n,t), & \text{state–observer design} \quad (9.3b) \\ c_0(z_{(I_m \cap I_p|)},t) + \displaystyle\sum_{n \in I_m \cap I_p} c_1^n(z^n,t), & \text{merging state–feedback with state–observer} \quad (9.3c) \end{cases}$$

Herein, $c_1^n(z^n,t) \in C^0([0,L_n]) \times G_{D,\alpha}(\mathbb{R}_{t_0}^+)$ with $\alpha \in [1,2]$ for each n from the respective index set.

This in particular implies that $c(z,t)$ is separable in the individual directions of the control actuation and output sensing. Moreover, (9.3c) refers to the evaluation of the state–feedback control with the observer states. Nevertheless, these conditions only include the dependency of $c(z,t)$ on the tuple of spatial coordinates. Constant or time dependent $c(z,t)$ can be covered completely without any structural assumptions except those on the differentiability in t determined below, which are required for the computation of the backstepping kernels.

Remark 9.2. The considered boundary control and output configurations represent idealized settings with the infinite–dimensional control $u^i(z_{(i|)},t)$, $i \in I_m$, as well as the infinite–dimensional output $y^i(z_{(i|)},t)$, $i \in I_p$, being restricted to hyperplanes. Although this preliminary can be assumed fulfilled in particular examples the configuration is primarily of theoretical interest in view of the methodic extension of the backstepping approach to distributed–parameter systems with higher–dimensional domains. In order to overcome this restriction, in the course of this chapter approximation approaches are introduced for both state–feedback and state–observer design, which allow the approximate realization of the determined results by means of a finite number of suitably placed actuators and sensors.

9.1.2 Boundary Control Problem

With these preliminary considerations, the boundary stabilization and tracking control problem

$$x(z,t) \xrightarrow{\{u^i(z_{(i|)},t)\}_{i\in I_m}} x^*(z,t) \tag{9.4a}$$

with

$$\|x(z,t) - x^*(z,t)\|_X \leq Me^{-\beta(t-t_0)},\ \beta > 0 \tag{9.4b}$$

is concerned with the design of an exponentially stabilizing controller $u^i(z_{(i|)},t)$, $i \in I_m$, to realize the tracking $y^i(z_{(i|)},t) \to y^{i,*}(z_{(i|)},t)$, $i \in I_p$, of suitably prescribed output trajectories $y^{i,*}(z_{(i|)},t)$. Note that this problem implicitly includes the realization of finite time transitions between an initial stationary profile $x_0(z)$ and a final stationary profile $x_T(z)$, i.e.

$$x_0(z) = x(z,t_0) \xrightarrow[t\in[t_0,t_0+T]]{\{u^i(z_{(i|)},t)\}_{i\in I_m}} x(z,t_0+T) = x_T(z), \quad z \in \overline{\Omega}. \tag{9.4c}$$

Similar to the previous chapters herein special attention is paid to achieve finite time transitions between stationary profiles along desired spatial–temporal output paths

$y^{i,*}(z_{(i|)},t)$. In order to solve this control problem subsequently an extension of the backstepping approach to higher–dimensional domains is provided and merged with the results of Chapter 7 on flatness–based trajectory planning for diffusion–reaction systems of the form (9.2). Thereby, single and multiple boundary control and output configurations are addressed for the design of the exponentially stabilizing tracking control with distributed–parameter state–observer.

9.2 Exponentially Stabilizing State–Feedback Control — The Single Input Case

In order to motivate the generalization of the backstepping approach to distributed–parameter systems with multiple boundary controls at first the solution to the feedback stabilization problem is determined for the diffusion–reaction system (9.2) with parallelepiped domain and a single boundary input located on the hypersurface $z^i = L_i$ such that[1] $I_m = \{i\}$, $\#I_m = m = 1$ and $u^i(z_{(i|)},t) = u(z_{(i|)},t)$. For this, it is shown that the results obtained in Section 8 for the 1–dimensional case can be directly applied to achieve the transformation of the possibly unstable original distributed–parameter system into a target distributed–parameter system with prescribed desired stability properties. However, differing from the approach of Section 8.2 in the following the appropriate choice of the target system is motivated from the integral transformation.

9.2.1 Determination of the Kernel–PDE and Selection of the Target System

Let $w(z,t)$ denote the state of the target system and consider the linear Volterra–type integral transformation

$$w(z,t) = x(z,t) - \int_0^{z^i} k(z^i,\zeta,t)\, x(z_{(i|\zeta)},t)\mathrm{d}\zeta \tag{9.5}$$

for $i \in I_m$ and $z_{(i|\zeta)} = (z^1,\ldots,z^{i-1},\zeta,z^{i+1},\ldots,z^r)$. The successive differentiation of (9.5) with respect to z^j, $j \in I_r$, i.e.

$$\partial_{z^j} w(z,t) = \begin{cases} \partial_{z^j} x(z,t) - \int_0^{z^i} k(z^i,\zeta,t)\partial_{z^j} x(z_{(i|\zeta)},t)\mathrm{d}\zeta, & j \neq i \\ \partial_{z^i} x(z,t) - k(z^i,z^i,t)x(z,t) & \\ \quad - \int_0^{z^i} \partial_{z^i} k(z^i,\zeta,t)x(z_{(i|\zeta)},t)\mathrm{d}\zeta, & j = i \end{cases} \tag{9.6}$$

[1] Observe from (9.2d) that only a single nonlinear BC arises for this configuration with all remaining BCs governed by (9.2b) and (9.2c).

$$\partial^2_{z^j} w(z,t) = \begin{cases} \partial^2_{z^j} x(z,t) - \int_0^{z^i} k(z^i,\zeta,t)\partial^2_{z^j} x(z_{(i|\zeta)},t)\mathrm{d}\zeta, & j \neq i \\ \partial^2_{z^i} x(z,t) - \mathrm{d}_{z^i} k(z^i,z^i,t)x(z,t) & \\ -k(z^i,z^i,t)\partial_{z^i} x(z,t) - \partial_{z^i} k(z^i,z^i,t)x(z,t) & \\ -\int_0^{z^i} \partial^2_{z^i} k(z^i,\zeta,t)x(z_{(i|\zeta)},t)\mathrm{d}\zeta, & j = i \end{cases} \tag{9.7}$$

yields the Laplacian of (9.5)

$$\begin{aligned} \Delta w(z,t) = \Delta x(z,t) &- \sum_{j\in I_r^i} \int_0^{z^i} k(z^i,\zeta,t)\partial^2_{z^j} x(z_{(i|\zeta)},t)\mathrm{d}\zeta \\ &- \mathrm{d}_{z^i} k(z^i,z^i,t)x(z,t) - k(z^i,z^i,t)\partial_{z^i} x(z,t) \\ &- \partial_{z^i} k(z^i,z^i,t)x(z,t) - \int_0^{z^i} \partial^2_{z^i} k(z^i,\zeta,t)x(z_{(i|\zeta)},t)\mathrm{d}\zeta \end{aligned} \tag{9.8}$$

Differentiating $w(z,t)$ with respect to t results in

$$\begin{aligned} \partial_t w(z,t) = \partial_t x(z,t) &\\ - \int_0^{z^i} &\big[\partial_t k(z^i,\zeta,t)x(z_{(i|\zeta)},t) + k(z^i,\zeta,t)\partial_t x(z_{(i|\zeta)},t)\big]\mathrm{d}\zeta, \end{aligned}$$

which can be further evaluated by making use of (9.2a), i.e.

$$\begin{aligned} \partial_t w(z,t) = \Delta x(z,t) &+ c(z,t)x(z,t) \\ &- \big[k(z^i,\zeta,t)\partial_\zeta x(z_{(i|\zeta)},t) - \partial_\zeta k(z^i,\zeta,t)x(z_{(i|\zeta)},t)\big]_{\zeta=0}^{\zeta=z^i} \\ &- \sum_{j\in I_r^i} \int_0^{z^i} k(z^i,\zeta,t)\partial^2_{z^j} x(z_{(i|\zeta)},t)\mathrm{d}\zeta \\ &- \int_0^{z^i} \big[\partial_t k(z^i,\zeta,t) + \partial^2_\zeta k(z^i,\zeta,t) + c(z_{(i|\zeta)},t)k(z^i,\zeta,t)\big]x(z_{(i|\zeta)},t)\mathrm{d}\zeta. \end{aligned} \tag{9.9}$$

The second integral in the previous equation already illustrates the necessity to impose Assumption 9.2 for the structural dependency of $c(z,t)$ on z and t since the ansatz for $k(z^i,\zeta,t)$ only involves the coordinate z^i. In order to verify this, evaluate

$$\partial_t w(z,t) = \Delta w(z,t) - d(z,t)w(z,t) \tag{9.10}$$

together with (9.5)–(9.9), which yields

$$
\begin{aligned}
0 = \int_0^{z^i} & \big[\partial_t k(z^i,\zeta,t) + \partial_\zeta^2 k(z^i,\zeta,t) - \partial_{z^i}^2 k(z^i,\zeta,t) \\
& \qquad + (c(z_{(i|\zeta)},t) + d(z,t))k(z^i,\zeta,t)\big] x(z_{(i|\zeta)},t)\mathrm{d}\zeta \\
& - x(z,t)\Big[c(z,t) + d(z,t) + 2\mathrm{d}_{z^i} k(z^i,z^i,t)\Big] \\
& + \big[\partial_\zeta k(z^i,0,t)x(z_{(i|0)},t) - k(z^i,0,t)\partial_{z^i} x(z_{(i|0)},t)\big].
\end{aligned} \tag{9.11}
$$

9.2.1.1 Determination of the Kernel Equations

With (9.3a) from Assumption 9.2 for $I_m = \{i\}$, the choice of the parameter $d(z,t) = \mu(t) - c_0(z_{(i|)},t)$ yields the kernel–PDE

$$
\partial_t k(z^i,\zeta,t) = \partial_{z^i}^2 k(z^i,\zeta,t) - \partial_\zeta^2 k(z^i,\zeta,t) - \gamma(\zeta,t)k(z^i,\zeta,t), \tag{9.12a}
$$

where $\gamma(\zeta,t) = c_1^i(\zeta,t) + \mu(t)$. The PDE is defined on the triangular domain $\zeta \in (0,z^i)$, $z^i \in (0,L_i)$ with the boundary condition

$$
2\mathrm{d}_{z^i} k(z^i,z^i,t) + \gamma(z^i,t) = 0. \tag{9.12b}
$$

Note that (9.12a) and (9.12b) directly correspond to the equations obtained for the kernel in the case of a single spatial dimension in Section 8.2.2. With this, the remaining conditions for $k(z^i,\zeta,t)$ to fulfill (9.11) follow exactly from (8.10c)–(8.10g) and are hence provided below for the sake of completeness:

(i) For a Dirichlet condition at $z^i = 0$, i.e. $\epsilon_i^0 = 0$, $p_i^0 \neq 0$ in (9.2b), the kernel has to satisfy

$$
k(z^i,0,t) = 0 \tag{9.12c}
$$

while the target system is restricted to

$$
w(z_{(i|0)},t) = 0. \tag{9.12d}
$$

(ii) For a Neumann or mixed condition at $z^i = 0$, i.e. $\epsilon_i^0 \neq 0$ in (9.2b), the kernel has to satisfy

$$
-\partial_\zeta k(z^i,0,t) + \bar{p}_i^0 k(z^i,0,t) = 0, \tag{9.12e}
$$

where $\bar{p}_i^0 = p_i^0/\epsilon_i^0$. In this case, the target system is constrained to a corresponding boundary condition

$$
-\epsilon_{w,i}^0 \partial_{z^i} w(z_{(i|0)},t) + p_{w,i}^0 w(z_{(i|0)},t) = 0. \tag{9.12f}
$$

Moreover, the kernel has to fulfill

$$k(0,0,t) = \bar{p}_i^0 - \frac{p_{w,i}^0}{\epsilon_{w,i}^0}. \tag{9.12g}$$

In addition, evaluating (9.5) for $t = t_0$ provides the constraint

$$\int_0^{z^i} k(z^i, \zeta, t_0) x_0(z) \mathrm{d}\zeta = x_0(z) - w(z, t_0), \qquad z \in \overline{\Omega}. \tag{9.12h}$$

Hence, if $x_0(z) = w(z, t_0) = w_0(z)$ the kernel has to fulfill

$$k(z^i, \zeta, t_0) = 0. \tag{9.12i}$$

9.2.1.2 Construction of the Target System

In view of the previous results, the target system can be deduced as

$$\partial_t w(z,t) = \Delta w(z,t) - d(z,t) w(z,t), \qquad (z,t) \in \Omega \times \mathbb{R}_{t_0}^+ \tag{9.13a}$$

for $d(z,t) = \mu(t) - c_0(z_{(i|)}, t)$ with the boundary conditions

$$\begin{aligned}
&- \epsilon_{w,i}^0 \partial_{z^i} w(z,t) + p_{w,i}^0 w(z,t) = 0, && z^i = 0,\ i \in I_m && \text{(9.13b)}\\
&- \epsilon_j^0 \partial_{z^j} w(z,t) + p_j^0 w(z,t) = 0, && z^j = 0,\ j \in I_r^{I_m} && \text{(9.13c)}\\
&\epsilon_{w,i}^1 \partial_{z^i} w(z,t) + p_{w,i}^1 w(z,t) = 0, && z^i = L_i,\ i \in I_m && \text{(9.13d)}\\
&\epsilon_j^1 \partial_{z^j} w(z,t) + p_j^1 w(z,t) = 0, && z^j = L_j,\ j \in I_r^{I_m} && \text{(9.13e)}
\end{aligned}$$

for $t > t_0$ and the initial condition

$$w(z, t_0) = w_0(z), \qquad z \in \overline{\Omega}. \tag{9.13f}$$

In particular, the Volterra integral transformation only allows to impose the boundary conditions (9.13b) and (9.13d) in z^i–direction while the remaining boundary conditions are invariant under the transformation. Moreover, the applicability for the feedback stabilization requires that (9.13) is exponentially stable in some normed linear space.

Lemma 9.1. *The parabolic distributed–parameter system* (9.13) *is exponentially stable in the L^2–norm for any combination of Dirichlet, Neumann, or mixed boundary conditions if $\mu(t) + \lambda_{\min} - \bar{c}_0(t) > \epsilon > 0\ \forall t \in \mathbb{R}_{t_0}^+$ for some $\epsilon > 0$. Here,*

$$\bar{c}_0(t) = \sup_{z_{(i|)} \in \bigtimes_{j \in I_r \setminus I_m} [0, L_j]} c_0(z_{(i|)}, t)$$

and $\lambda_{\min}$ denotes the smallest eigenvalue λ of $\Delta w(z,t) + \lambda w(z,t) = 0$ with boundary conditions (9.13b)–(9.13e).

Proof. Consider the positive definite functional $V(t) = 1/2\|w(t)\|^2_{L^2(\Omega)}$ and consider the rate of change of $V(t)$ along a solution trajectory, i.e.

$$\begin{aligned}\partial_t V(t) = &\int_\Omega w(z,t)\Delta w(z,t)\mathrm{d}\Omega + \int_\Omega c_0(z_{(i|)},t)w^2(z,t)\mathrm{d}\Omega \\ &- \mu(t)\int_\Omega w^2(z,t)\mathrm{d}\Omega\end{aligned}$$

Together with Green's Theorem this evaluates to

$$\begin{aligned}\partial_t V(t) &= -\int_\Omega \nabla w(z,t)\cdot\nabla w(z,t)\mathrm{d}\Omega + \oint_{\partial\Omega} w(z,t)\nabla w(z,t)\cdot\mathbf{n}\mathrm{d}\partial\Omega \\ &\quad + \int_\Omega (c_0(z_{(i|)},t)-\mu(t))w^2(z,t)\mathrm{d}\Omega \\ &\leq -\int_\Omega \nabla w(z,t)\cdot\nabla w(z,t)\mathrm{d}\Omega + \oint_{\partial\Omega} w(z,t)\nabla w(z,t)\cdot\mathbf{n}\mathrm{d}\partial\Omega \\ &\quad + \big(\bar{c}_0(t)-\mu(t)\big)\|w(t)\|^2_{L^2(\Omega)}.\end{aligned}$$

It is well–known that $\Delta w(z,t)+\lambda w(z,t)=0$ with boundary conditions (9.13b)–(9.13e) possesses a purely discrete set of eigenvalues (cf. Lemma 6.4), which can be arranged as $0\leq\lambda_1\leq\lambda_2\leq\ldots$ with each λ_k repeated according to its multiplicity. Multiplying $\Delta w(z,t)+\lambda w(z,t)=0$ with $w(z,t)$ and integrating over Ω results in

$$\begin{aligned}0 &= \int_\Omega w(z,t)\Delta w(z,t)\mathrm{d}\Omega + \lambda\|w(t)\|^2_{L^2(\Omega)} \\ &= -\int_\Omega \nabla w(z,t)\cdot\nabla w(z,t)\mathrm{d}\Omega + \oint_{\partial\Omega} w(z,t)\nabla w(z,t)\cdot\mathbf{n}\mathrm{d}\partial\Omega \\ &\quad + \lambda\|w(t)\|^2_{L^2(\Omega)}\end{aligned}$$

and hence

$$\begin{aligned}-\int_\Omega \nabla w(z,t)\cdot\nabla w(z,t)\mathrm{d}\Omega + \oint_{\partial\Omega} w(z,t)\nabla w(z,t)\cdot\mathbf{n}\mathrm{d}\partial\Omega \\ = -\lambda\|w(t)\|^2_{L^2(\Omega)} \leq -\lambda_1\|w(t)\|^2_{L^2(\Omega)}.\end{aligned}$$

Let $\lambda_{\min}=\lambda_1$ then it follows that

$$\partial_t V(t) \leq -\big(\mu(t)+\lambda_{\min}-\bar{c}_0(t)\big)\|w(t)\|^2_{L^2(\Omega)}.$$

Recalling $V(t)=1/2\,\|w(t)\|^2_{L^2(\Omega)}$ the latter result implies

$$\|w(t)\|_{L^2(\Omega)} \leq e^{-\int_{t_0}^t(\mu(\tau)+\lambda_{\min}-\bar{c}_0(\tau))\mathrm{d}\tau}\,\|w_0\|_{L^2(\Omega)},$$

which proves the claim if there exists an $\epsilon > 0$ such that $\mu(t) + \lambda_{\min} - \bar{c}_0(t) > \epsilon > 0$ for all $t \in \mathbb{R}^+_{t_0}$. □

Remark 9.3. The analysis above reveals that the varying parameter $c(z,t)$ has to be separable in the direction z^i, $i \in I_m$, i.e. in the directions actuated by the input $u(z_{(i|)},t)$, while the non–separable part $c_0(z_{(i|)},t)$ of $c(z,t)$ is compensated by means of the target system.

Remark 9.4. Exponential stability subsequently refers to stability in the L^2–norm. Extensions by considering the analysis in the H^1– and hence the sup–norm require to impose additional restrictions on the derivatives of $d(z,t)$ and thus $c_0(z_{(i|)},t)$ with respect to z.

Summarizing the above results provides that (9.5) enables the transformation of the possibly unstable diffusion–reaction system (9.2) into the target system (9.13), which is exponentially stable under the conditions of Lemma 9.1. This however requires the solution of the distributed–parameter system (9.12) for the kernel $k(z^i,\zeta,t)$.

9.2.2 Solution of the Kernel–PDE

Since the equations for the determination of the kernel $k(z^i,\zeta,t)$, $i \in I_m$, directly correspond to those for the 1–dimensional case, their explicit solution by introducing scattering coordinates, applying the method of integral operators, and determining a recursive solution by means of a successive approximation is subsequently omitted and the reader is referred to Section 8.2.3. However, due to the geometry of the domain $\zeta \in (0, z^i)$, $z^i \in (0, L_i)$ a one–to–one correspondence between the results requires to introduce the change of coordinates

$$z^i \mapsto \frac{z^i}{L_i}, \quad \zeta \mapsto \frac{\zeta}{L_i}, \quad t \mapsto \frac{t}{L_i^2} \tag{9.14a}$$

together with

$$\begin{aligned} &\gamma(z^i,t) \mapsto L_i^2 \gamma(z^i,t), \quad k(z^i,\zeta,t) \mapsto L_i k(z^i,\zeta,t) \\ &\bar{p}_i^0 \mapsto L_i \bar{p}_i^0, \quad \frac{p_{w,i}^0}{\epsilon_{w,i}^0} \mapsto L_i \frac{p_{w,i}^0}{\epsilon_{w,i}^0}. \end{aligned} \tag{9.14b}$$

Thus, the kernel can be computed in terms of the functional series

$$k(z^i,\zeta,t) = \sum_{n \in \mathbb{N}} \bar{k}_n(\eta,\sigma,t)\big|_{\eta^i = \frac{z^i+\zeta}{L_i},\, \sigma^i = \frac{z^i-\zeta}{L_i}} \tag{9.15}$$

with the series coefficients $\bar{k}_n(\eta,\sigma,t)$ determined recursively from (8.15) in view of (9.14). Moreover, convergence of (9.15) follows from Theorems 8.1 and 8.2,

respectively, provided that $\gamma(z^i,t)\in C^0([0,L_i])\times G_{D,\alpha}(\mathbb{R}^+_{t_0})$ with $\alpha\in[1,2]$. The convergence results in particular imply that $k(z^i,\zeta,t)$ is of Gevrey order $\alpha\leq 2$ in t and a strong solution to (9.12). Hence, the backstepping–based state–feedback control can be determined depending on the particular boundary conditions of the target system at $z^i=L_i$ as is summarized below.

9.2.3 Backstepping–Based State–Feedback Controller

The state–feedback control, which is required to realize the desired transformation into the exponentially stable target system, is determined analogous to Section 8.2.4 with the essential difference that the boundary control $u(z_{(i|)},t)$ is a function of both $z_{(i|)}$ and t. For this, consider

$$\begin{aligned} w(z_{(i|L_i)},t) &= x(z_{(i|L_i)},t)-\int_0^{L_i} k(L_i,\zeta,t)x(z_{(i|\zeta)},t)\mathrm{d}\zeta\\ \partial_{z^i}w(z_{(i|L_i)},t) &= \partial_{z^i}x(z_{(i|L_i)},t)-k(L_i,L_i,t)x(z_{(i|L_i)},t)\\ &\quad -\int_0^{L_i}\partial_{z^i}k(L_i,\zeta,t)x(z_{(i|\zeta)},t)\mathrm{d}\zeta. \end{aligned}$$

In view of (9.2d) and (9.13d) this yields:

(i) For $\epsilon^1_{w,i}=0$, i.e. $w(z_{(i|L_i)},t)=0$, with

$$x(z_{(i|L_i)},t)=\int_0^{L_i}k(L_i,\zeta,t)x(z_{(i|\zeta)},t)\mathrm{d}\zeta=:\Xi_D(x(z_{(i|)},t))$$

the state–feedback controller (9.2d) evaluates to

$$u(z_{(i|)},t)=\theta\big(\Xi_D(x(z_{(i|)},t)),\partial_{z^i}x(z_{(i|L_i)},t)\big). \tag{9.16a}$$

(ii) For $p^1_{w,i}=0$, i.e. $\partial_{z^i}w(z_{(i|L_i)},t)=0$, with

$$\begin{aligned}\partial_{z^i}x(z_{(i|L_i)},t) &= k(L_i,L_i,t)x(z_{(i|L_i)},t)\\ &\quad+\int_0^{L_i}\partial_{z^i}k(L_i,\zeta,t)x(z_{(i|\zeta)},t)\mathrm{d}\zeta=:\Xi_N(x(z_{(i|)},t))\end{aligned}$$

the state–feedback controller (9.2d) is obtained as

$$u(z_{(i|)},t)=\theta\big(x(z_{(i|L_i)},t),\Xi_N(x(z_{(i|)},t))\big). \tag{9.16b}$$

(iii) For $\epsilon^1_{w,i},\ p^1_{w,i}\neq 0$, i.e. $\epsilon^1_{w,i}\partial_{z^i}w(z_{(i|L_i)},t)+p^1_{w,i}w(z_{(i|L_i)},t)=0$, where

$$\partial_{z^i} x(z_{(i|L_i)},t) = x(z_{(i|L_i)},t)\left(k(L_i,L_i,t) - \frac{p^1_{w,i}}{\epsilon^1_{w,i}}\right)$$
$$+\int_0^{L_i}\left(\partial_{z^i} k(L_i,\zeta,t) + \frac{p^1_{w,i}}{\epsilon^1_{w,i}} k(L_{i,\zeta,t})\right) x(z_{(i|\zeta)},t)\mathrm{d}\zeta =: \Xi_M(x(z_{(i|)},t))$$

the state–feedback controller (9.2d) evolves as

$$u(z_{(i|)},t) = \theta\big(x(z_{(i|L_i)},t), \Xi_M(x(z_{(i|)},t))\big). \tag{9.16c}$$

Note that the evaluation of the derivative $\partial_{z^i} x(z_{(i|L_i)},t)$ in (9.16a) can be avoided by replacing the Dirichlet boundary condition of the target system at $z^i = L_i$ with a Neumann or mixed boundary condition.

9.2.4 *Inverse Backstepping–Transformation and Exponential Stability of the Closed–Loop System*

The verification of the exponential stability of the closed–loop system consisting of (9.2) and the corresponding state–feedback control (9.16) relies on the analysis of the inverse backstepping–transformation, i.e. the transformation from the target system into the original diffusion–reaction system. Instead of considering the invertibility conditions for Volterra integral transformations of the form (9.5), the inverse transformation is determined explicitly. For this, consider

$$x(z,t) = w(z,t) + \int_0^{z^i} g(z^i,\zeta,t)\, w(z_{(i|\zeta)},t)\mathrm{d}\zeta \tag{9.17}$$

and proceed as in Section 9.2.1 by determining $\Delta x(z,t)$ and evaluating $\partial_t x(z,t)$ in view of (9.13). The substitution of the resulting expressions into (9.2) yields that the governing equations for each inverse kernel $g(z^i,\zeta,t)$ correspond to those for $k(z^i,\zeta,t)$ with the exceptions that $\gamma(\zeta,t)$ is replaced by $-\gamma(z^i,t)$ and the coefficients $p^0_i,\ \epsilon^0_i$ in (9.12e) are exchanged with $p^0_{w,i},\ \epsilon^0_{w,i}$ (cf. (8.23)). However, the solution procedure as well as the convergence analysis are in principle identical. This in particular enables the stability analysis of the closed–loop system with the determined backstepping–based state–feedback controller.

Theorem 9.1. *Consider the diffusion–reaction system* (9.2) *with state–feedback control* (9.16a), (9.16b), *or* (9.16c) *depending on the boundary condition at* $z^i = L_i$. *Then the equilibrium* $x(z,t) \equiv 0$ *is exponentially stable for all* $t \in \mathbb{R}^+_{t_0}$ *in the* L^2*–norm if the corresponding target system* (9.13) *satisfies the conditions of Lemma 9.1.*

The proof follows exactly the lines of the proof of Theorem 8.3 and is hence only briefly sketched for the sake of completeness.

Proof. Let $X = L^2(\Omega)$, assume $x_0(z),\, w_0(z) \in X$, and denote $\Theta_0^i = \{(z^i, \zeta) : \zeta \in [0, L_i],\, z^i \in [\zeta, L_i]\}$ and $\Theta^i = \{(z^i, \zeta, t) : \zeta \in [0, L_i],\, z^i \in [\zeta, L_i],\, t \in \mathbb{R}_{t_0}^+\}$. Moreover, recall that both $k(z^i, \zeta, t)$ and $g(z^i, \zeta, t)$ are bounded strong solutions to the respective kernel–PDEs. At first, consider

$$\begin{aligned}\|w_0\|_X &= \left\| x_0(z) - \int_0^{z^i} k(z^i, \zeta, t_0) x_0(z_{(i|\zeta)}) \mathrm{d}\zeta \right\|_X \\ &\leq \|x_0\|_X + \left\| \int_0^{z^i} k(z^i, \zeta, t_0) x_0(z_{(i|\zeta)}) \mathrm{d}\zeta \right\|_X ,\end{aligned}$$

where the upper bound follows from the Minkowski inequality. The application of the Cauchy–Schwarz inequality hence implies

$$\begin{aligned}&\left\| \int_0^{z^i} k(z^i, \zeta, t_0) x_0(z_{(i|\zeta)}) \mathrm{d}\zeta \right\|_X^2 \\ &\quad = \int_\Omega \left(\int_0^{z^i} k(z^i, \zeta, t_0) x_0(z_{(i|\zeta)}) \mathrm{d}\zeta \right)^2 \mathrm{d}\Omega \\ &\quad \leq \int_\Omega \left(\int_0^{z^i} k^2(z^i, \zeta, t_0) \mathrm{d}\zeta \int_0^{z^i} x_0^2(z_{(i|\zeta)}) \mathrm{d}\zeta \right) \mathrm{d}\Omega \\ &\quad \leq L_i \left(\sup_{(z^i,\zeta)\in\Theta_0^i} |k(z^i, \zeta, t_0)| \right)^2 \int_\Omega \left(\int_0^{z^i} x_0^2(z_{(i|\zeta)}) \mathrm{d}\zeta \right) \mathrm{d}\Omega \\ &\quad = L_i^2 \left(\sup_{(z^i,\zeta)\in\Theta_0^i} |k(z^i, \zeta, t_0)| \right)^2 \|x_0\|_X^2\end{aligned}$$

such that

$$\|w_0\|_X \leq \underbrace{\left(1 + L_i \sup_{(z^i,\zeta)\in\Theta_0^i} |k(z^i, \zeta, t_0)| \right)}_{=C_0} \|x_0\|_X .$$

In addition, Lemma 9.1 on the stability of the target system and its proof provide

$$\|w(t)\|_X \leq e^{-\kappa(t)} \|w_0\|_X \leq C_0 e^{-\kappa(t)} \|x_0\|_X$$

for $\kappa(t) = \int_{t_0}^t (\mu(s) + \lambda_{\min} - \bar{c}_0(s)) \mathrm{d}s$. Proceeding as for the determination of the upper bound for $\|w_0\|_X$, the norm of $x(z, t)$ can be bounded from above by taking into account the boundedness of the inverse backstepping kernel $g(z^i, \zeta, t)$, i.e.

$$\|x(t)\|_X \leq \underbrace{\left(1 + L_i \sup_{(z^i,\zeta,t)\in\Theta^i} |g(z^i,\zeta,t)|\right)}_{=C_1} \|w(t)\|_X \leq C_0 C_1 e^{-\kappa(t)} \|x_0\|_X,$$

which proves the exponential stability of the closed–loop system under the backstepping–based state–feedback control. □

9.2.5 *Approximate Finite–Dimensional Realization of Backstepping–Based State–Feedback Control*

As already pointed out in Remark 9.2, the considered boundary control configuration represents an idealized setting with an infinite–dimensional input $u(z_{(i|)}, t)$, which can be assigned arbitrarily for all $(z_{(i|)}, t)$. However, in view of applications the control is typically realized by means of a finite number m of finite–dimensional actuators suitably placed on the i–th hyperplane $z^i = L_i$ such that

$$u(z_{(i|)}, t) = \sum_{l=1}^{m} \mathfrak{b}^l(z_{(i|)}) u^l(t), \tag{9.18}$$

where $\mathfrak{b}^l(z_{(i|)})$ denotes the spatial actuator characteristics. Nevertheless, it is obvious from the determined state–feedback controllers (9.16) for the different types of boundary conditions of the target system that (9.18) cannot be fulfilled exactly. This is due to the fact that the backstepping transformation into the target system inherently requires an infinite–dimensional boundary control, which serves as the basis for the exponential stabilization of the closed–loop system as illustrated in the previous section.

In order to address this, subsequently an approximate realization of the backstepping–based state–feedback control is proposed to provide an approximate (in a sense to be defined below) realization of (9.16). For this, it is crucial to assume that

(i) the state $x(z,t)$ is known, e.g., by means of a distributed–parameter state–observer

and to notice that

(ii) for implementation the state–feedback control is evaluated and applied to the system at discrete instances of time t_k, $k \in \mathbb{N}$.

Let $u_k(z_{(i|)}) = u(z_{(i|)}, t_k)$ with the respective state–feedback strategy according to (9.16) for $x(z,t)$ replaced by $x_k(z) = x(z,t_k)$, i.e.

$$u_k(z_{(i|)}) = \begin{cases} \theta\big(\Xi_D(x(z_{(i|)},t_k)), \partial_{z^i} x(z_{(i|L_i)},t_k)\big), & \epsilon^1_{w,i} = 0 \\ \theta\big(x(z_{(i|L_i)},t_k), \Xi_N(x(z_{(i|)},t_k))\big), & p^1_{w,i} = 0 \\ \theta\big(x(z_{(i|L_i)},t_k), \Xi_M(x(z_{(i|)},t_k))\big), & \epsilon^0_{w,i},\ p^0_{w,i} \neq 0. \end{cases}$$

Hence, in view of (i) and (ii) it is obvious that (9.18) reduces to a static equation for each t_k. With this, introduce the least–squares problem

$$\min_{\{u_k^l\}_{l=1,\dots,m}} \left\| u_k(z_{(i|)}) - \sum_{l=1}^{m} \mathfrak{b}^l(z_{(i|)}) u_k^l \right\|^2_{L^2(\partial\Omega_i)} \tag{9.19}$$

with $u_k^l = u^l(t_k)$, $l = 1, \dots, m$. By solving (9.19) consecutively for each $k \in \mathbb{N}$ an L^2–approximation of the infinite–dimensional state–feedback controller is obtained in terms of the spatial characteristics $\mathfrak{b}^l(z_{(i|)})$ and the discrete input values u_k^l for $l = 1, \dots, m$. Obviously, the quality of the approximation and hence the capability of the finite–dimensional state–feedback control to stabilize the possibly unstable diffusion–reaction system (9.2) essentially depends on $\mathfrak{b}^l(z_{(i|)})$, i.e. the actuator shape and location, and the number m of actuators, which have to be adjusted to the particular problem under consideration.

Remark 9.5. In view of the approximation approach proposed above it is crucial to observe that the proof of exponential stability of the closed–loop control is violated by means of the finite–dimensional actuator configuration. Although simulation results presented in Section 9.8 still confirm the exponential stabilization property of the approximated finite–dimensional state–feedback control the theoretical stability analysis of the closed–loop system remains an open problem.

Since the state–feedback control essentially relies on the availability of the state profile $x(z,t)$ a distributed–parameter state–observer is required to estimate the state evolution from the available output (9.2f). For its design, backstepping is similarly applied for the exponential stabilization of the observer error dynamics.

9.3 State–Observer with Exponentially Stable Error Dynamics — The Single Output Case

In order to determine an estimate of the spatial–temporal evolution of the state $x(z,t)$ from the knowledge of the available output subsequently a distributed–parameter state–observer is designed for the single output case, i.e. $I_p = \{i\}$, $\#I_p = 1$, and $y^i(z_{(i|)}, t) = y(z_{(i|)}, t)$. For this, similar to Section 8.3, the backstepping–approach is considered to determine the observer gains to achieve an exponentially stable observer error dynamics. The state–observer is set–up in a Luenberger–type structure according to

$$\partial_t \hat{x}(z,t) = \Delta\hat{x}(z,t) + c(z,t)\hat{x}(z,t) + l_1(z^i,t)\big[y(z_{(i|)},t) - \hat{y}(z_{(i|)},t)\big] \tag{9.20a}$$

for $(z,t) \in \Omega \times \mathbb{R}^+_{t_0}$ with the boundary conditions

$$-\epsilon_j^0 \partial_{z^j}\hat{x}(z,t) + p_j^0 \hat{x}(z,t) = 0, \qquad z^j = 0,\ j \in I_r^{I_p} \tag{9.20b}$$

$$
\begin{aligned}
&-\epsilon_i^0 \partial_{z^i}\hat{x}(z,t) + p_i^0 \hat{x}(z,t) = \\
&\qquad l_{10}(t)\big[y(z_{(i|)},t) - \hat{y}(z_{(i|)},t)\big], && z^i = 0,\ i \in I_p && \text{(9.20c)}\\
&\epsilon_j^1 \partial_{z^j}\hat{x}(z,t) + p_j^1 \hat{x}(z,t) = 0, && z^j = L_j,\ j \in I_r^{I_m} && \text{(9.20d)}\\
&\theta^i\left(\hat{x}(z,t), \partial_{z^i}\hat{x}(z,t)\right) = u^i(z_{(i|)},t), && z^i = L_i,\ i \in I_m && \text{(9.20e)}
\end{aligned}
$$

for $t > t_0$, the initial condition

$$
\hat{x}(z,t_0) = \hat{x}_0(z), \qquad z \in \overline{\Omega}, \qquad \text{(9.20f)}
$$

and

$$
\hat{y}(z_{(i|)},t) = h_i^0 \partial_{z^i}\hat{x}(z,t) + h_i^1 \hat{x}(z,t), \qquad z^i = 0,\ i \in I_p,\ t \geq t_0. \qquad \text{(9.20g)}
$$

Here, $l_1(z^i,t)$ and $l_{10}(t)$ denote the observer gains, which have to be determined such that the observer error $\tilde{x}(z,t) = x(z,t) - \hat{x}(z,t)$ decays exponentially in a suitable norm. Comparing (9.2) and (9.20) yields

$$
\begin{aligned}
\partial_t \tilde{x}(z,t) = \Delta\tilde{x}(z,t) + c(z,t)\tilde{x}(z,t)& \\
- l_1(z^i,t)\big[h_i^0 \partial_{z^i}\tilde{x}(z_{(i|0)},t) + h_i^1 \tilde{x}(z_{(i|0)},t)\big]& \qquad \text{(9.21a)}
\end{aligned}
$$

for $(z,t) \in \Omega \times \mathbb{R}_{t_0}^+$ with the boundary conditions

$$
\begin{aligned}
&-\epsilon_j^0 \partial_{z^j}\tilde{x}(z,t) + p_j^0 \tilde{x}(z,t) = 0, && z^j = 0,\ j \in I_r^{I_p} && \text{(9.21b)}\\
&\big(l_{10}(t)h_i^0 - \epsilon_i^0\big)\partial_{z^i}\tilde{x}(z,t) \\
&\qquad + \big(l_{10}(t)h_i^1 + p_i^0\big)\tilde{x}(z,t) = 0, && z^i = 0,\ i \in I_p && \text{(9.21c)}\\
&\epsilon_j^1 \partial_{z^j}\tilde{x}(z,t) + p_j^1 \tilde{x}(z,t) = 0, && z^j = L_j,\ j \in I_r^{I_m} && \text{(9.21d)}\\
&\theta^i\left(\hat{x}(z,t) + \tilde{x}(z,t), \partial_{z^i}(\hat{x}(z,t) + \tilde{x}(z,t))\right) \\
&\qquad - \theta^i\left(\hat{x}(z,t), \partial_{z^i}\hat{x}(z,t)\right) = 0, && z^i = L_i,\ i \in I_m && \text{(9.21e)}
\end{aligned}
$$

for $t > t_0$ and the initial condition

$$
\tilde{x}(z,t_0) = \tilde{x}_0(z) = x_0(z) - \hat{x}_0(z), \qquad z \in \overline{\Omega}. \qquad \text{(9.21f)}
$$

Due to the nonlinear input characteristics the resulting observer error dynamics is nonlinear and cannot be directly addressed by means of the backstepping approach. Hence, subsequently the following assumption is imposed.

Assumption 9.3. The functional $\theta^i(\cdot,\cdot)$, $i \in I_m$, is linear and satisfies

$$
\theta^i\left(x(z,t), \partial_{z^i}x(z,t)\right) = \epsilon_i^1 \partial_{z^i}x(z,t) + p_i^1 x(z,t), \qquad z^i = L_i
$$

with constants ϵ_i^1 and p_i^1.

As a result, (9.21e) reduces to

$$\epsilon_i^1 \partial_{z^j} \tilde{x}(z,t) + p_i^1 \tilde{x}(z,t) = 0. \tag{9.21g}$$

Note that while the state–feedback control can be determined for a rather general nonlinear input characteristics the state–observer design requires a linear input combination of gradient and state.

In order to achieve the exponential stabilization of the observer error dynamics (9.21) a Volterra integral transformation is subsequently determined to realize the dynamic equivalence to a target system with prescribed stability properties.

9.3.1 Selection of the Target System

Referring to the analysis in Section 9.2.1, the target system is chosen as

$$\partial_t \tilde{w}(z,t) = \Delta \tilde{w}(z,t) - \tilde{d}(z,t)\tilde{w}(z,t), \qquad (z,t) \in \Omega \times \mathbb{R}^+_{t_0} \tag{9.22a}$$

for $\tilde{d}(z,t) = \tilde{\mu}(t) - c_0(z_{(i|)},t)$ (cf. (9.3b) of Assumption 9.2) with the boundary conditions

$$-\epsilon_j^0 \partial_{z^j} \tilde{w}(z,t) + p_j^0 \tilde{w}(z,t) = 0, \qquad z^j = 0,\ j \in I_r^{I_p} \tag{9.22b}$$

$$-\tilde{\epsilon}_{w,i}^0 \partial_{z^i} \tilde{w}(z,t) + \tilde{p}_{w,i}^0 \tilde{w}(z,t) = 0, \qquad z^i = 0,\ i \in I_p \tag{9.22c}$$

$$\epsilon_j^1 \partial_{z^j} \tilde{w}(z,t) + p_j^1 \tilde{w}(z,t) = 0, \qquad z^j = L_j,\ j \in I_r^{I_p} \tag{9.22d}$$

$$\tilde{\epsilon}_{w,i}^1 \partial_{z^i} \tilde{w}(z,t) + \tilde{p}_{w,i}^1 \tilde{w}(z,t) = 0, \qquad z^i = L_i,\ i \in I_p \tag{9.22e}$$

for $t > t_0$ and the initial condition

$$\tilde{w}(z,t_0) = \tilde{w}_0(z), \qquad z \in \overline{\Omega}. \tag{9.22f}$$

By applying Lemma 9.1 the exponential stability of (9.22) in the L^2–norm can be guaranteed depending on $\tilde{\mu}(t)$ and provided that

$$\tilde{c}_0(t) = \sup_{z_{(i|)} \in \mathsf{X}_{j \in I_r \setminus I_p}[0,L_j]} c_0(z_{(i|)},t)$$

exits and is bounded for all $t \in \mathbb{R}^+_{t_0}$. Proceeding as in Section 9.2.1 allows to compute the kernel of a Volterra integral transformation, which enables the determination of the observer gains $l_1(z^i,t)$ and $l_{10}(t)$ to exponentially stabilize (9.21).

9.3.2 Determination of the Kernel–PDE and the Observer Gains

Subsequently, consider the Volterra integral equation

$$\tilde{x}(z,t) = \tilde{w}(z,t) - \int_0^{z^i} l(z^i,\zeta,t)\,\tilde{w}(z_{(i|\zeta)},t)\mathrm{d}\zeta \tag{9.23}$$

to transform the target system (9.22) into the observer error system (9.21). Applying the Laplace operator to both sides of (9.23) and evaluating the derivative of (9.23) with respect to t in view of (9.22) after some intermediate computations result in

$$\begin{aligned}
\Delta\tilde{x}(z,t) &= \Delta\tilde{w}(z,t) - \sum_{j\in I_r^i}\int_0^{z^i} l(z^i,\zeta,t)\partial_{z^j}^2\tilde{w}(z_{(i|\zeta)},t)\mathrm{d}\zeta \\
&\quad - \Big(\mathrm{d}_{z^i}l(z^i,z^i,t)\tilde{w}(z,t) + l(z^i,z^i,t)\partial_{z^i}\tilde{w}(z,t) + \partial_{z^i}l(z^i,z^i,t)\tilde{w}(z,t) \\
&\qquad + \int_0^{z^i}\partial_{z^i}^2 l(z^i,\zeta,t)\tilde{w}(z_{(i|\zeta)},t)\mathrm{d}\zeta\Big) \\
\partial_t\tilde{x}(z,t) &= \Delta\tilde{w}(z,t) - \tilde{d}(z,t)\tilde{w}(z,t) \\
&\quad - \Big(\big[l(z^i,\zeta,t)\partial_\zeta\tilde{w}(z_{(i|\zeta)},t) - \partial_\zeta l(z^i,\zeta,t)\tilde{w}(z_{(i|\zeta)},t)\big]_{\zeta=0}^{\zeta=z^i} \\
&\quad + \int_0^{z^i}\big[\partial_t l(z^i,\zeta,t) + \partial_\zeta^2 l(z^i,\zeta,t) - \tilde{d}(z_{(i|\zeta)},t)l(z^i,\zeta,t)\big]\tilde{w}(z_{(i|\zeta)},t)\mathrm{d}\zeta\Big) \\
&\quad - \sum_{j\in I_r^i}\int_0^{z^i} l(z^i,\zeta,t)\partial_{z^j}^2\tilde{w}(z_{(i|\zeta)},t)\mathrm{d}\zeta.
\end{aligned}$$

Substituting the above expressions into (9.21a) hence yields

$$\begin{aligned}
0 = \int_0^{z^i} &\big[\partial_t l(z^i,\zeta,t) + \partial_\zeta^2 l(z^i,\zeta,t) - \partial_{z^i}^2 l(z^i,\zeta,t) \\
&\quad - (\tilde{d}(z_{(i|\zeta)},t) + c(z,t))l(z^i,\zeta,t)\big]\tilde{w}(z_{(i|\zeta)},t)\mathrm{d}\zeta \\
&- \tilde{w}(z,t)\Big[-(\tilde{d}(z,t)+c(z,t)) + 2\mathrm{d}_{z^i}l(z^i,z^i,t)\Big] \\
&- \big[\partial_\zeta l(z^i,0,t)\tilde{w}(z_{(i|0)},t) - l(z^i,0,t)\partial_{z^i}\tilde{w}(z_{(i|0)},t) \\
&\quad + l_1(z^i,t)\big(h_i^0\partial_{z^i}\tilde{x}(z_{(i|0)},t) + h_i^1\tilde{x}(z_{(i|0)},t)\big)\big].
\end{aligned} \tag{9.24}$$

The implications of the equality are twofold. At first, it can be directly deduced in view of Assumption 9.2 that $l(z^i,\zeta,t)$ has to satisfy the kernel–PDE

$$\partial_t l(z^i,\zeta,t) = \partial_{z^i}^2 l(z^i,\zeta,t) - \partial_\zeta^2 l(z^i,\zeta,t) + \tilde{\gamma}(z^i,t)l(z^i,\zeta,t) \tag{9.25a}$$

with $\tilde{\gamma}(z^i,t) = c_1^i(z^i,t) + \tilde{\mu}(t)$ and the triangular domain $\zeta \in (0, z^i)$, $z^i \in (0, L_i)$. In addition, the boundary condition

$$2\mathrm{d}_{z^i} l(z^i, z^i, t) - \tilde{\gamma}(z^i, t) = 0 \tag{9.25b}$$

follows from the third line of (9.24). The remaining boundary conditions for the backstepping kernel $l(z^i, \zeta, t)$ can be determined from the evaluation of (9.21g) with (9.23), i.e.

$$\begin{aligned} 0 = {} & \epsilon_i^1 \partial_{z^i} \tilde{w}(z_{(i|L_i)}, t) + \big[p_i^1 - \epsilon_i^1 l(L_i, L_i, t)\big] w(z_{(i|L_i)}, t) \\ & - \int_0^{L_i} \big[\epsilon_i^1 \partial_{z^i} l(L_i, \zeta, t) + p_i^1 l(L_i, \zeta, t)\big] \tilde{w}(z_{(i|\zeta)}, t) \mathrm{d}\zeta. \end{aligned}$$

In view of the respective boundary conditions (9.22e) for the target system, i.e. $\tilde{\epsilon}_{w,j}^1 \partial_{z^i} \tilde{w}(z,t) + \tilde{p}_{w,j}^1 \tilde{w}(z,t) = 0,\ z^i = L_i$, the remaining boundary conditions for the kernel $l(z^i, \zeta, t)$ are obtained together with the corresponding relations between the parameters ϵ_i^1, p_i^1, $\tilde{\epsilon}_{w,j}^1$, and $\tilde{p}_{w,j}^1$ according to:

(i) For a Dirichlet boundary condition at $z^i = L_i$ in (9.21g), i.e. $\epsilon_i^1 = 0$, $p_i^1 \neq 0$, the respective boundary condition (9.22e) of the target has to satisfy $\tilde{\epsilon}_{w,i}^1 = 0$, $\tilde{p}_{w,i}^1 \neq 0$ while the kernel is restricted to

$$l(L_i, \zeta, t) = 0. \tag{9.25c}$$

(ii) For a Neumann or mixed boundary condition at $z^i = L_i$ in (9.21g), i.e. $\epsilon_i^1 \neq 0$, the respective boundary condition (9.22e) of the target has to satisfy $\tilde{\epsilon}_{w,i}^1 \neq 0$ while the kernel is restricted to

$$\partial_{z^i} l(L_i, \zeta, t) + \bar{p}_i^1 l(L_i, \zeta, t)] = 0 \tag{9.25d}$$

$$l(L_i, L_i, t) = \bar{p}_i^1 - \frac{\tilde{p}_{w,i}^1}{\tilde{\epsilon}_{w,i}^1} \tag{9.25e}$$

with $\bar{p}_i^1 = p_i^1 / \epsilon_i^1$.

In addition, considering (9.23) for $t = t_0$ yields the constraint

$$\int_0^{z^i} l(z^i, \zeta, t_0) \tilde{w}_0(z_{(i|\zeta)}, t) \mathrm{d}\zeta = \tilde{w}_0(z) - \tilde{x}_0(z), \qquad z^i \in [0, L_i]. \tag{9.25f}$$

Hence, assuming $\tilde{w}_0(z) = \tilde{x}_0(z)$ the initial condition for each kernel follows as

$$l(z^i, \zeta, t_0) = 0.$$

The observer gains realizing the transformation into the target system are obtained by evaluating the last two lines of (9.24) in view of (9.25a) and (9.25b). For this, recall from (9.23) that

$$\begin{aligned}\tilde{x}(z_{(i|0)},t) &= \tilde{w}(z_{(i|0)},t)\\ \partial_{z^i}\tilde{x}(z_{(i|0)},t) &= \partial_{z^i}\tilde{w}(z_{(i|0)},t) - l(0,0,t)\tilde{w}(z_{(i|0)},t).\end{aligned} \tag{9.26}$$

With this, the remainder can be re–written as

$$\begin{aligned}0 = \big[l(z^i,0,t) + h_i^0 l_1(z^i,t)\big]\partial_{z^i}\tilde{w}(z_{(i|0)},t) + \\ \big[l_1(z^i,t)\big(h_i^1 - h_i^0 l(0,0,t)\big) - \partial_\zeta l(z^i,0,t)\big]\tilde{w}(z_{(i|0)},t)\end{aligned}$$

By taking into account the respective boundary conditions (9.22c) for the target system, the observer gain $l_1(z^i,t)$ can be determined as

$$l_1(z^i,t) = \begin{cases} -\dfrac{l(z^i,0,t)}{h_i^0}, & \text{if } \tilde{\epsilon}_{w,i}^0 = 0 \wedge h_i^0 \neq 0 \\ -\dfrac{\partial_\zeta l(z^i,0,t) - \frac{\tilde{p}_{w,i}^0}{\tilde{\epsilon}_{w,i}^0} l(z^i,0,t)}{h_i^0\Big(l(0,0,t) - \frac{\tilde{p}_{w,i}^0}{\tilde{\epsilon}_{w,i}^0}\Big) - h_i^1}, & \text{if } \tilde{\epsilon}_{w,i}^0 \neq 0 \wedge \\ & h_i^0\Big(l(0,0,t) - \frac{\tilde{p}_{w,i}^0}{\tilde{\epsilon}_{w,i}^0}\Big) - h_i^1 \neq 0. \end{cases} \tag{9.27}$$

Proceeding similarly for the evaluation of the boundary conditions (9.21c) in view of (9.26) and (9.22c) provides the observer gain $l_{10}(t)$ in the form

$$l_{10}(t) = \begin{cases} \dfrac{\epsilon_i^0}{h_i^0}, & \text{if } \tilde{\epsilon}_{w,i}^0 = 0 \wedge h_i^0 \neq 0 \\ \dfrac{p_i^0 + \epsilon_i^0\Big(l(0,0,t) - \frac{\tilde{p}_{w,i}^0}{\tilde{\epsilon}_{w,i}^0}\Big)}{h_i^0\Big(l(0,0,t) - \frac{\tilde{p}_{w,i}^0}{\tilde{\epsilon}_{w,i}^0}\Big) - h_i^1}, & \text{if } \tilde{\epsilon}_{w,i}^0 \neq 0 \wedge \\ & h_i^0\Big(l(0,0,t) - \frac{\tilde{p}_{w,i}^0}{\tilde{\epsilon}_{w,i}^0}\Big) - h_i^1 \neq 0. \end{cases} \tag{9.28}$$

As is pointed out in Remark 8.3, the arising conditionals for the computation of $l_1(z^i,t)$ and $l_{10}(t)$ can be easily fulfilled to guarantee a unique solution by a suitable parametrization of the target system.

9.3.3 Solution of the Kernel–PDE

Comparing the equations governing the evolution of the kernel $l(z^i,\zeta,t)$ reveals consistency with the kernel equations (8.29) for the 1–dimensional setting. Hence, proceeding as in Section 8.3.3, the solution to (9.25), (9.25c), or (9.25d), (9.25e), respectively, can be determined by first evaluating the change of coordinates (9.14) to map the domain to the triangle $\zeta \in (0,z^i)$, $z^i \in (0,1)$ and secondly by introducing scattering coordinates to evaluate the formal integral solution by means of a successive approximation. Moreover, the convergence results in Theorems 8.4 and 8.5 can be directly applied by imposing that $\tilde{\gamma}(z^i,t) \in C^0([0,L_i]) \times G_{D,\alpha}(\mathbb{R}_{t_0}^+)$ holds for $\tilde{\gamma}(z^i,t) = c_1^i(z^i,t) + \tilde{\mu}(t)$ with $\alpha \in [1,2]$. In view of Assumption 9.2 the latter condition is fulfilled provided that $\tilde{\mu}(t) \in$ with α as above.

9.3.4 Inverse Backstepping–Transformation and Exponential Stability of the Observer Error Dynamics

As already pointed out in Section 8.3.4 for the 1–dimensional setting and Section 9.2.4 for the state–feedback control, the stability analysis of the observer error dynamics with the determined backstepping–based observer gains $l_1(z^i,t)$ and $l_{10}(t)$ relies on the consideration of the inverse to (9.23), i.e.

$$\tilde{w}(z,t) = \tilde{x}(z,t) + \int_0^{z^i} m(z^i,\zeta,t)\,\tilde{x}(z_{(i|\zeta)},t)\mathrm{d}\zeta, \tag{9.29}$$

where $m(z^i,\zeta,t)$ denotes the inverse backstepping kernel. For its determination proceed as above by evaluating the Laplacian applied to both sides of the equality and by computing the time derivative of $\tilde{w}(z,t)$ in view of the equations of the observer error system (9.21). This yields after some intermediate computations

$$\begin{aligned}
0 = &\int_0^{z^i} \big[\partial_t m(z^i,\zeta,t) + \partial_\zeta^2 m(z^i,\zeta,t) - \partial_{z^i}^2 m(z^i,\zeta,t) \\
&\qquad + \tilde{\gamma}(\zeta,t) m(z^i,\zeta,t)\big]\tilde{x}(z_{(i|\zeta)},t)\mathrm{d}\zeta \\
&+ \tilde{x}(z,t)\big[-2\mathrm{d}_{z^i} m(z^i,z^i,t) + \tilde{\gamma}(z^i,t)\big] \\
&- \partial_{z^i}\tilde{x}(z,t)(z_{(i|0)},t)\Big[m(z^i,0,t) \\
&\qquad + h_i^0\Big(l_1(z^i,t) + \int_0^{z^i} m(z^i,\zeta,t) l_1(\zeta,t)\mathrm{d}\zeta\Big)\Big] \\
&+ \tilde{x}(z_{(i|0)},t)\Big[\partial_\zeta m(z^i,0,t) - h_i^1\Big(l_1(z^i,t) + \int_0^{z^i} m(z^i,\zeta,t) l_1(\zeta,t)\mathrm{d}\zeta\Big)\Big].
\end{aligned} \tag{9.30}$$

Hence, it follows that

$$\partial_t m(z^i,\zeta,t) = \partial_{z^i}^2 m(z^i,\zeta,t) - \partial_\zeta^2 m(z^i,\zeta,t) - \tilde{\gamma}(\zeta,t) m(z^1,\zeta,t) \tag{9.31a}$$

for $\zeta \in (0, L_i)$, $z^i \in (\zeta, L_i)$ and

$$2\mathrm{d}_{z^i} m(z^i,\zeta,t) - \tilde{\gamma}(z^1,t) = 0, \tag{9.31b}$$

which is obviously identical to (8.44a) and (8.44b) for the 1–dimensional set–up. This implies that the remaining results of Section 8.3.4 directly carry over to the considered setting with the difference that the arguments in (8.44c)–(8.44e) have to be adjusted for the non–unit length L_i. Thus, the remaining boundary conditions are obtained from the evaluation of (9.22e) and (9.21g) in view of (9.29) according to:

(i) For a Dirichlet boundary condition at $z^i = L_i$ in (9.22e), i.e. $\tilde{\epsilon}_{w,i}^1 = 0, \tilde{p}_{w,i}^1 \neq 0$, the kernel has to satisfy

$$m(L_i, \zeta, t) = 0 \tag{9.31c}$$

while necessarily $\epsilon_i^1 = 0$ and $p_i^1 \neq 0$.

(ii) For a Neumann or mixed boundary condition at $z^i = L_i$, i.e. $\tilde{\epsilon}_{w,i}^1 \neq 0$, the kernel is restricted to

$$\partial_{z^i} m(L_i, \zeta, t) - \frac{\tilde{p}_{w,i}^1}{\tilde{\epsilon}_{w,i}^1} m(L_i, \zeta, t) = 0 \tag{9.31d}$$

$$m(L_i, L_i, t) = \bar{p}_i^1 - \frac{\tilde{p}_{w,i}^1}{\tilde{\epsilon}_{w,i}^1}. \tag{9.31e}$$

In this case it is required that $\epsilon_i^1 \neq 0$.

By making use of the change of coordinates (9.14), the solution approach presented in Section 8.2.3 can be directly applied to compute a functional series representation of the kernel $m(z^i, \zeta, t)$. Moreover, the respective convergence conditions for the successive approximation directly follow from Theorems 8.1 and 8.2. This in addition confirms that the thus determined $m(z^i, \zeta, t)$ represents a strong solution to (9.31) of Gevrey order $\alpha \leq 2$ in t, which is bounded with bounded derivative with respect to the tuple (z^i, ζ). Hence, the exponential stability of the observer error dynamics with the observer gains $l_1(z^i, t)$ and $l_{10}(t)$ of (9.27) and (9.28) can be deduced from Corollary 8.1.

Corollary 9.1. *Consider the observer error dynamics* (9.21) *with observer gains* $l_1(z^1, t)$ *and* $l_{10}(t)$ *according to* (9.27) *and* (9.28)*. Then the equilibrium* $\tilde{x}(z^1, t) \equiv 0$ *is exponentially stable for all* $t \in \mathbb{R}_{t_0}^+$ *in the* L^2*–norm if the target system* (9.22) *satisfies the conditions of Lemma 9.1.*

9.3.5 Separation Principle and Exponential Stability of the Closed–Loop System

The realization of the state–feedback control (9.16) requires to replace the state $x(z, t)$ by the observer state $\hat{x}(z, t)$ determined by (9.20) with observer gains according to (9.27) and (9.28). This implies the evaluation of the backstepping transformation (9.5) in terms of $\hat{x}(z, t) = x(z, t) - \tilde{x}(z, t)$, i.e.

$$\begin{aligned} w(z, t) &= \hat{x}(z, t) - \int_0^{z^i} k(z^i, \zeta, t) \hat{x}(z_{(i|\zeta)}, t) \mathrm{d}\zeta \\ &= x(z, t) - \int_0^{z^i} k(z^i, \zeta, t) x(z_{(i|\zeta)}, t) \mathrm{d}\zeta \\ &\quad - \left(\tilde{x}(z, t) - \int_0^{z^i} k(z^i, \zeta, t) \tilde{x}(z_{(i|\zeta)}, t) \mathrm{d}\zeta \right). \end{aligned} \tag{9.32}$$

Similar to the analysis in Section 8.3.5, this results in a cascaded structure with an inhomogeneous distributed–parameter system in $w(z,t)$, which depends on the state $\tilde{w}(z,t)$ of the target system for the observer error dynamics. For this, Assumption 9.3 implying linear boundary conditions is imposed to evaluate (9.13) with (9.32) in view of (9.2), (9.21) and (9.22). Herein note that the system cascade arises from the mapping of $\tilde{x}(z,t)$ governed by (9.21) under the transformation (9.32), which reduces the necessary analysis to the mapping of the $\tilde{x}(z,t)$ part. Thereby, two configurations have to be distinguished depending on the location of the boundary input and the boundary output and hence the index sets I_m and I_p.

9.3.5.1 Boundary Control and Boundary Output on Opposite Surfaces

In the following, let the boundary input $u(z_{(i|)},t)$ and the output $y(z_{(i|)},t)$ be located on opposing sides of the domain Ω along the z^i–coordinate such that $I_m = I_p$. With this, target systems in $w(z,t)$ and $\tilde{w}(z,t)$ are interconnected according to

$$\partial_t \begin{bmatrix} w(z,t) \\ \tilde{w}(z,t) \end{bmatrix} = \begin{bmatrix} \Delta w(z,t) - d(z,t)w(z,t) \\ \Delta \tilde{w}(z,t) - \tilde{d}(z,t)\tilde{w}(z,t) \end{bmatrix} + \begin{bmatrix} q(z^i,t)\tilde{y}(z_{(i|)},t) \\ 0 \end{bmatrix} \tag{9.33a}$$

with the forcing term

$$\begin{aligned} q(z^i,t) = &\left(l_1(z^i,t) - \int_0^{z^i} k(z^i,\zeta,t) l_1(\zeta,t) \mathrm{d}\zeta \right) \\ &- \begin{cases} \frac{l_{10}(t)}{p_i^0} \partial_\zeta k(z^i,0,t), & \epsilon_i^0 = 0 \wedge p_i^0 \neq 0 \\ \frac{l_{10}(t)}{\epsilon_i^0} k(z^i,0,\zeta), & \epsilon_i^0 \neq 0, \end{cases} \end{aligned}$$

where

$$\tilde{y}(z_{(i|)},t) = h_i^0 \partial_{z^i} \tilde{w}(z_{(i|0)},t) + \big(h_i^1 - h_i^0 l(0,0,t)\big)\tilde{w}(z_{(i|0)},t).$$

Herein, the boundary conditions (9.12c), (9.12e), and (9.12g) for $k(z^i,\zeta,t)$ were used to simplify the expressions. By recalling that (9.5) maps homogeneous boundary conditions for $z^j \in \{0, L_j\}$, $j \in I_r^i$, into homogeneous boundary conditions, it follows from (9.12c)–(9.12g) for $k(z^i,\zeta,t)$, (9.13b)–(9.13e) for $w(z,t)$, (9.21b)–(9.21e) for $\tilde{x}(z,t)$, and (9.22b)–(9.22e) for $\tilde{w}(z,t)$ that

$$-\epsilon_j^0 \partial_{z^j} w(z,t) + p_j^0 w(z,t) = 0, \qquad z^j = 0,\ j \in I_r^{I_m} \tag{9.33b}$$

$$\begin{aligned} &-\epsilon_{w,i}^0 \partial_{z^i} w(z,t) + p_{w,i}^0 w(z,t) \\ &\quad = \tilde{y}(z_{(i|)},t) \times \begin{cases} \frac{p_{w,i}^0}{p_i^0} l_{10}(t), & \epsilon_i^0 = 0 \wedge p_i^0 \neq 0 \\ \frac{\epsilon_{w,i}^0}{\epsilon_i^0} l_{10}(t), & \epsilon_i^0 \neq 0 \end{cases}, \qquad z^i = 0,\ i \in I_m \end{aligned} \tag{9.33c}$$

$$\epsilon_j^1 \partial_{z^j} w(z,t) + p_j^1 w(z,t) = 0, \qquad z^j = L_j,\ j \in I_r^{I_m} \tag{9.33d}$$

$$\epsilon^1_{w,i}\partial_{z^i} w(z,t) + p^1_{w,i} w(z,t) = 0, \qquad z^i = L_i,\ i \in I_m \tag{9.33e}$$
$$-\epsilon^0_j \partial_{z^j} \tilde{w}(z,t) + p^0_j \tilde{w}(z,t) = 0, \qquad z^j = 0,\ j \in I_r^{I_p} \tag{9.33f}$$
$$-\tilde{\epsilon}^0_{w,i}\partial_{z^i} \tilde{w}(z,t) + \tilde{p}^0_{w,i} \tilde{w}(z,t) = 0, \qquad z^i = 0,\ i \in I_p \tag{9.33g}$$
$$\epsilon^1_j \partial_{z^j} \tilde{w}(z,t) + p^1_j \tilde{w}(z,t) = 0, \qquad z^j = L_j,\ j \in I_r^{I_p} \tag{9.33h}$$
$$\tilde{\epsilon}^1_{w,i}\partial_{z^i} \tilde{w}(z,t) + \tilde{p}^1_{w,i} \tilde{w}(z,t) = 0, \qquad z^i = L_i,\ i \in I_p \tag{9.33i}$$

for $t > t_0$ and $I_r^{I_m} = I_r^{I_p} = I_r^i$. With these preparations, the stability of the closed–loop system follows from the result below.

Theorem 9.2. *The closed–loop system* (9.33) *is exponentially stable in the* L^2*–norm if* $\mu(t)$ *and* $\tilde{\mu}(t)$ *are such that* $\mu(t) + \lambda_{\min} - \bar{c}_0(t) > \epsilon$ *and* $\tilde{\mu}(t) + \tilde{\lambda}_{\min} - \tilde{c}_0(t) > \tilde{\epsilon}$ *for some* $\epsilon,\ \tilde{\epsilon} > 0$*. Here,* $\lambda_{\min}$ *and* $\tilde{\lambda}_{\min}$ *denote the minimal eigenvalue of the PDE* $\Delta w(z) + \lambda w(z) = 0$ *with boundary conditions* (9.13b)–(9.13e) *and* (9.22b)–(9.22e)*, respectively.*

The proof of this claim is subsequently omitted since it can be directly deduced from the general MIMO setting considered in Section 9.6.5 by exploiting the cascaded structure of the exponentially stable $\tilde{w}$– system and the w–system.

9.3.5.2 Boundary Control and Boundary Output on Non–Opposite Surfaces

Subsequently, let the boundary input $u(z_{(i|)}, t)$ be located on the surface $z^i = L_i$ with the output $y(z_{(k|)}, t)$ being restricted to the surface $z^k = 0$ with $i \neq k$. In view of Assumption 9.2, which is imposed for the design of both the state–feedback control and the state–observer, it can be deduced that the analysis of $I_m = \{i\} \neq \{k\} = I_p$ essentially relies on the separability of the varying system parameter $c(z,t)$ with respect to z^i and z^k. With this preliminary, the evaluation of (9.32) in view of the respective distributed–parameter systems (9.2), (9.20), and (9.21) yields

$$\partial_t \begin{bmatrix} w(z,t) \\ \tilde{w}(z,t) \end{bmatrix} = \begin{bmatrix} \Delta w(z,t) - d(z,t) w(z,t) \\ \Delta \tilde{w}(z,t) - \tilde{d}(z,t) \tilde{w}(z,t) \end{bmatrix} + \begin{bmatrix} q(z,t) \\ 0 \end{bmatrix} \tag{9.34a}$$

with the forcing term

$$q(z,t) = l_1(z^k, t) \left(\tilde{y}(z_{(k|)}, t) - \int_0^{z^i} k(z^i, \zeta, t) \tilde{y}(z_{(k|,i|\zeta)}, t) \mathrm{d}\zeta \right), \tag{9.34b}$$

where $(z_{(k|,i|\zeta)}, t) = (z^1, \ldots, z^{k-1}, z^{k+1}, \ldots, z^{i-1}, \zeta, z^{i+1}, \ldots, z^r)$ and

$$\tilde{y}(z_{(k|)}, t) = h^0_k \partial_{z^k} \tilde{w}(z_{(k|0)}, t) + \big(h^1_k - h^0_k l(0,0,t)\big) \tilde{w}(z_{(k|0)}, t).$$

Herein, (9.3c) implies

$$d(z,t) = \mu(t) - \big(c_0(z_{(i|,k|)}, t) + c^k_1(z^k, t)\big)$$

$$\tilde{d}(z,t) = \tilde{\mu}(t) - \big(c_0(z_{(i|,k|)},t) + c_1^i(z^i,t)\big).$$

The boundary conditions for $w(z,t)$ and $\tilde{w}(z,t)$ can be determined similarly to those in (9.33) with the essential difference in the location and the structure of the output injection, i.e.

$$\begin{aligned}
&-\epsilon_j^0 \partial_{z^j} w(z,t) + p_j^0 w(z,t) = 0, && z^j = 0,\ j \in I_r^{I_m \cup I_p} && \text{(9.34c)}\\
&-\epsilon_{w,i}^0 \partial_{z^i} w(z,t) + p_{w,i}^0 w(z,t) = 0, && z^i = 0,\ i \in I_m && \text{(9.34d)}\\
&-\epsilon_k^0 \partial_{z^k} w(z,t) + p_k^0 w(z,t) && && \\
&\quad = l_{10}(t)\Bigg(\tilde{y}(z_{(k|)},t) && && \\
&\qquad - \int_0^{z^i} k(z^i,\zeta,t)\tilde{y}(z_{(k|,i|\zeta)},t)\mathrm{d}\zeta\Bigg), && z^k = 0,\ k \in I_p && \text{(9.34e)}\\
&\quad \epsilon_j^1 \partial_{z^j} w(z,t) + p_j^1 w(z,t) = 0, && z^j = L_j,\ j \in I_r^{I_m} && \text{(9.34f)}\\
&\quad \epsilon_{w,i}^1 \partial_{z^i} w(z,t) + p_{w,i}^1 w(z,t) = 0, && z^i = L_i,\ i \in I_m && \text{(9.34g)}\\
&-\epsilon_j^0 \partial_{z^j} \tilde{w}(z,t) + p_j^0 \tilde{w}(z,t) = 0, && z^j = 0,\ j \in I_r^{I_p} && \text{(9.34h)}\\
&-\tilde{\epsilon}_{w,k}^0 \partial_{z^k} \tilde{w}(z,t) + \tilde{p}_{w,k}^0 \tilde{w}(z,t) = 0, && z^k = 0,\ i \in I_p && \text{(9.34i)}\\
&\quad \epsilon_j^1 \partial_{z^j} \tilde{w}(z,t) + p_j^1 \tilde{w}(z,t) = 0, && z^j = L_j,\ j \in I_r^{I_p} && \text{(9.34j)}\\
&\quad \tilde{\epsilon}_{w,i}^1 \partial_{z^i} \tilde{w}(z,t) + \tilde{p}_{w,i}^1 \tilde{w}(z,t) = 0, && z^i = L_i,\ i \in I_p && \text{(9.34k)}
\end{aligned}$$

for $t > t_0$. Similar to the previous paragraph, the stability of the closed–loop system follows from the theorem below, whose proof is omitted but can be directly obtained from the generalized MIMO setting considered in Section 9.6.5.

Theorem 9.3. *The closed–loop system* (9.34) *is exponentially stable in the* L^2*–norm if* $\mu(t)$ *and* $\tilde{\mu}(t)$ *are such that* $\mu(t) + \lambda_{\min} - \bar{c}_0(t) > \epsilon$ *and* $\tilde{\mu}(t) + \tilde{\lambda}_{\min} - \tilde{c}_0(t) > \tilde{\epsilon}$ *for some* $\epsilon,\ \tilde{\epsilon} > 0$*. Here,* $\lambda_{\min}$ *and* $\tilde{\lambda}_{\min}$ *denote the minimal eigenvalue of the PDE* $\Delta w(z) + \lambda w(z) = 0$ *with boundary conditions* (9.13b)–(9.13e) *and* (9.22b)–(9.22e)*, respectively.*

9.3.6 Approximate Realization of the State–Observer by means of Spatial Output Interpolation

As pointed out in Remark 9.2, the considered set–up presents an idealized configuration with an infinite–dimensional output $y(z_{(i|)},t)$ capturing the state and its derivative according to (9.2f) for all $(z_{(i|)},t)$ on the hypersurface $z^i = 0,\ i \in I_p$. However, in applications only localized finite–dimensional measurements are available, which can be in general represented as

$$y^l(t) = \int_{\partial\Omega_i^0} \left[\mathfrak{c}_1^l(z_{(i|)})\partial_{z^i} x(z_{(i|0)}, t) + \mathfrak{c}_0^l(z_{(i|)}) x(z_{(i|0)}, t)\right] \mathrm{d}\partial\Omega_i^0 \tag{9.35}$$

for $l = 1, \ldots, p$, where $\partial\Omega_i^0 = \{z \in \Omega : z^i = 0\}$ and $\mathfrak{c}_0^l(z_{(i|)})$ and $\mathfrak{c}_1^l(z_{(i|)})$ denote the spatial characteristics of the measurement device. Clearly, $\{y^l(t)\}_{l=1,\ldots,p}$ is not of the structure (9.2f), which is required for the state–observer design with exponentially stable error dynamics.

For implementation of the state–observer it is hence required to obtain an approximation of $y(z_{(i|)}, t)$ by making use of $\{y^l(t)\}_{l=1,\ldots,p}$. In order to achieve this, subsequently spatial interpolation is considered to approximately recover $y(z_{(i|)}, t)$ from a finite number of measurements. Therefore, consider at first the class of trial functions, e.g., in terms of a Fourier series

$$x_N(z) = \sum_{n=1}^{N} F_n \phi_n(z) \tag{9.36}$$

with the linear independent ansatz functions $\{\phi_n(z)\}_{n\in\{1,\ldots,N\}}$ chosen so that

$$-\epsilon_i^0 \partial_{z^i} x_N(z_{(i|0)}) + p_i^0 x_N(z_{(i|0)}) = 0$$

is fulfilled for $i \in I_p$. Note that also the remaining boundary conditions (9.2b)–(9.2d) may be partially imposed on the ansatz functions to achieve further consistency. Secondly, note that the state–observer is implemented in discrete time. Hence, measurements are only available at the respective samples t_k, $k \in \mathbb{N}$. With this, introduce the least–squares (interpolation) problem

$$\min_{\{F_n\}_{n=1,\ldots,N}} \left\| \boldsymbol{y}(t_k) - \boldsymbol{y}_N(t_k) \right\|_2^2 \tag{9.37a}$$

with

$$\begin{aligned} \boldsymbol{y}(t_k) &= \left[y^1(t_k), \ldots, y^p(t_k)\right]^T \\ \boldsymbol{y}_N(t_k) &= \left[y_N^1(t_k), \ldots, y_N^p(t_k)\right]^T, \end{aligned} \tag{9.37b}$$

where $y_N^l(t_k)$ refers to the evaluation of (9.35) with $x(z,t)$ replaced by (9.36) at $t = t_k$. The consecutive solution of the spatial interpolation problem (9.37) in each time step $k \in \mathbb{N}$ yields an L^2–approximation

$$y_N(z_{(i|)}, t_k) = h_i^0 \partial_{z^i} x_N(z_{(i|0)}) + h_i^1 x_N(z_{(i|0)})$$

of the infinite–dimensional output $y(z_{(i|)}, t_k)$. The quality of the approximation essentially relies on the choice of $\{\phi_n(z)\}_{n\in\{1,\ldots,N\}}$ as well as the suitable location of the measurement devices and eventually increases for large p [8].

Remark 9.6. It has to be noted that the application of the spatial interpolation to determine an approximation of $y(z_{(i|)}, t)$ violates the stability analysis of the observer error dynamics under the observer gains $l_1(z^i, t)$ and $l_{10}(t)$. This is however a

well–known problem in the control and the observer design for distributed–parameter systems for which a satisfactory analysis approach is so far not available. Nevertheless, the simulation results in Section 9.8.1 confirm the applicability of the approach. Moreover, the idea of spatial interpolation includes observer design techniques, where the observer gain is determined by means of physical considerations (see, e.g., [14, 13, 5]) in such a way that the state profile is approximately recovered from the available system outputs. While this is in general only applicable to spatially 1–dimensional distributed–parameter systems, the available experimental results, e.g., in [4], illustrate the estimation capability.

9.4 Tracking Control Combining Backstepping and Differential Flatness — The Single Input and Output Case

The extension of the backstepping–based feedback stabilization approach to exponentially stable tracking control for higher–dimensional domains in principle follows the systematics introduced in Section 8.4. However, differing from the 1–dimensional setting, the results of Chapter 7 are applied for the solution of the trajectory planning problem given boundary controlled diffusion–reaction systems of the form (9.2). For this, recall that the idea underlying the backstepping approach originates in the transformation of the possibly unstable diffusion–reaction system (9.2) into the target system (9.13) with prescribed dynamics. Moreover, observe that the stability properties of (9.13) remain unchanged if the homogeneous boundary condition for $w(z,t)$ at $z^i = L_i$ for $i \in I_m$ with $\#I_m = 1$ is replaced by

$$\epsilon^1_{w,i}\partial_{z^i} w(z,t) + p^1_{w,i} w(z,t) = u_w(z_{(i|)},t), \qquad z^i = L_i,\ t > t_0, \tag{9.38}$$

where $u_w(z_{(i|)},t)$ denotes an arbitrary function of time. This degree–of–freedom can be utilized as a feedforward controller to realize the tracking of suitable trajectories $t \mapsto y^*(z_{(k|)},t)$ for the output $y(z_{(k|)},t)$ at $z^k = 0$, $k \in I_p$ and hence to solve the tracking control problem. Proceeding as in Section 7.2.1, the function

$$\xi(z_{(i|)},t) = f^0_i \partial_{z^i} w(z,t) + f^1_i w(z,t), \qquad z^i = 0,\ i \in I_m,\ t > t_0 \tag{9.39}$$

represents a basic output and thus parametrizing the state $w(z,t)$ and the input $u_w(z_{(i|)},t)$ provided that the condition $p^0_i f^0_i + \epsilon^0_i f^1_i \neq 0$ is fulfilled. Hence, the formal integration of (9.13) with (9.39) yields an implicit state parametrization

$$\begin{aligned} w(z,t) &= \left(s^0_i + z^i s^1_i\right)\xi(z_{(i|)},t) \\ &+ \int_0^{z^i}\int_0^{\eta}\left(\partial_t w(z_{(i|\sigma)},t) + d(z,t) w(z_{(i|\sigma)},t) - \sum_{j\in I^i_r} \partial^2_{z^j} w(z_{(i|\sigma)},t)\right)\mathrm{d}\sigma\mathrm{d}\eta \end{aligned}$$

with $s^0_i = \epsilon^0_i/(p^0_i f^0_i + \epsilon^0_i f^1_i)$ and $s^1_i = p^0_i/(p^0_i f^0_i + \epsilon^0_i f^1_i)$. This IEOK allows for a explicit solution in terms of an infinite series

$$w(z,t) = \sum_{n=0}^{\infty} w_n(z,t), \tag{9.40}$$

whose coefficients can be computed recursively according to

$$w_0(z,t) = \left(s_i^0 + z^i s_i^1\right) \xi(z_{(i|)},t) \tag{9.41a}$$

$$\begin{aligned} w_n(z,t) = \int_0^{z^i}\int_0^{\eta}\Big(&\partial_t w_{n-1}(z_{(i|\sigma)},t) + d(z,t) w_{n-1}(z_{(i|\sigma)},t) \\ &- \sum_{j\in I_r^i} \partial_{z^j}^2 w_{n-1}(z_{(i|\sigma)},t)\Big)\mathrm{d}\sigma\mathrm{d}\eta, \quad n \geq 1. \end{aligned} \tag{9.41b}$$

Uniform convergence of the series (9.40) with coefficients (9.41) is guaranteed by Theorem 7.1 if $d(z,t) \in G_{D_d,\beta,\alpha_d}(\Omega \times \mathbb{R}_{t_0}^+)$ and $\xi(z_{(i|)},t) \in G_{D_\xi,\beta,\alpha_\xi}(\Omega_i \times \mathbb{R}_{t_0}^+)$ are analytic or entire functions in z and Gevrey functions of appropriate order in t.

Hence, let $w_n(z,t) = w_n(z,t;\xi(z_{(i|)},t))$ formally denote the solution to the recursion (9.41) and let $w(z,t) = w(z,t;\xi(z_{(i|)},t))$ represent the substitution of $w_n(z,t;\xi(z_{(i|)},t))$ into (9.40). In view of (9.38) this implies the parametrization of the boundary input $u_w(z_{(i|)},t)$ following

$$u_w(z_{(i|)},t) = \epsilon_{w,i}^1 \partial_{z^i} w(z,t;\xi(z_{(i|)},t)) + p_{w,i}^1 w(z,t;\xi(z_{(i|)},t)) \tag{9.42}$$

for $z^i = L_i$. By prescribing a suitable spatial–temporal path $\xi^*(z_{(i|)},t)$ for the basic output $\xi(z_{(i|)},t)$ this yields the feedforward control $u_w^*(z_{(i|)},t)$, which is required to track the corresponding path (9.39) in open–loop. For admissible trajectory planning for the basic output towards the realization of finite time transitions between steady states along pre–defined paths, the reader is referred to Section 7.3, in particular Proposition 7.2, and the deduced approaches for the construction of admissible desired trajectories. The combination of (9.38) with (9.16) hence yields an exponentially stabilizing tracking control depending on the values of $\epsilon_{w,i}^1$ and $p_{w,i}^1$ following

$$u^i(z_{(i|)},t) = \begin{cases} \theta\Big(\Xi_D(x(z_{(i|)},t)) + \frac{u_w^*(z_{(i|)},t)}{p_{w,i}^1}, \partial_{z^i} x(z_{(i|L_i)},t)\Big), & \epsilon_{w,i}^1 = 0 \\ \theta\Big(x(z_{(i|L_i)},t), \Xi_N(x(z_{(i|)},t)) + \frac{u_w^*(z_{(i|)},t)}{\epsilon_{w,i}^1}\Big), & p_{w,i}^1 = 0 \\ \theta\Big(x(z_{(i|L_i)},t), \Xi_M(x(z_{(i|)},t)) + \frac{u_w^*(z_{(i|)},t)}{\epsilon_{w,i}^1}\Big), & \epsilon_{w,i}^1,\ p_{w,i}^1 \neq 0 \end{cases} \tag{9.43}$$

Moreover, the backstepping transformation (9.5) and its inverse (9.17) provide a one–to–one relation between $x(z,t)$ and $w(z,t)$ and hence between the respective steady states. This can be directly utilized for the assignment of admissible desired trajectories for the basic output, i.e. steady states in $x(z,t)$ are mapped into steady states in $w(z,t)$ by means of (9.5) while the inverse is obtained utilizing (9.17). Thus, trajectory assignment can be equivalently performed for the original diffusion–reaction system or the target system. In view of the realization of desired

output trajectories $y(z_{(k|)},t) \to y^*(z_{(k|)},t)$, $k \in I_p$, observe from (9.2f) by making use of (9.17) that

$$\begin{aligned} y(z_{(k|)},t) = {} & h_k^0 \partial_{z^k} w(z_{(k|0)},t;\xi(z_{(i|,k|0)},t)) + h_k^1 w(z_{(k|0)},t;\xi(z_{(i|,k|0)},t)) \\ & + \int_0^{z^i} g^i(z^i,\zeta^i,t)\big[h_k^0 \partial_{z^k} w(z_{(k|0)},t;\xi(z_{(i|,k|0)},t)) \\ & \qquad + h_k^1 w(z_{(k|0)},t;\xi(z_{(i|,k|0)},t))\big]\,\mathrm{d}\zeta. \end{aligned}$$

This expression denotes the parametrization of the output in terms of the basic output such that re–planning $\xi(z_{(i|)},t) = \xi^*(z_{(i|)},t)$ results in different output paths. If $I_p = I_m$, i.e. $i = k$ in the notation above, then the expression simplifies to

$$\begin{aligned} y(z_{(i|)},t) = {} & h_i^0 \partial_{z^i} w(z_{(i|0)},t;\xi(z_{(i|)},t)) \\ & + \big(h_i^1 + h_i^0 g(0,0,t)\big) w(z_{(i|0)},t;\xi(z_{(i|)},t)) \end{aligned}$$

With this, a systematic and integrated approach is obtained for the solution of the tracking control problem given the diffusion–reaction system (9.2) with varying reaction parameters. Nevertheless, as pointed out above, the realization of the tracking control essentially relies on the availability of the state profile $x(z,t)$ such that the control–loop has to be amended by the state–observer designed in Section 9.3.

9.5 Exponentially Stabilizing State–Feedback Control — The Multiple Input Case

The results for the single input case can be directly utilized for the extension of the backstepping–based state–feedback control design to the multi input case. For this, it is crucial to observe that given the set I_m with $\#I_m = m > 1$, then for a single fixed $i \in I_m$ the application of the backstepping–transformation (9.5) in z^i–direction maps the diffusion–reaction system (9.2) into the target system (9.13) but with the boundary conditions split into

$$-\epsilon_{w,i}^0 \partial_{z^i} w(z,t) + p_{w,i}^0 w(z,t) = 0, \qquad z^i = 0 \tag{9.44a}$$

$$-\epsilon_j^0 \partial_{z^j} w(z,t) + p_j^0 w(z,t) = 0, \qquad z^j = 0,\ j \in I_r^i \tag{9.44b}$$

$$\epsilon_j^1 \partial_{z^j} w(z,t) + p_j^1 w(z,t) = 0, \qquad z^j = L_j,\ j \in I_r^{I_m} \tag{9.44c}$$

$$\epsilon_{w,i}^1 \partial_{z^i} w(z,t) + p_{w,i}^1 w(z,t) = 0, \qquad z^i = L_i \tag{9.44d}$$

and

$$\theta^j\left(x(z_{(j|L_j)},t), \partial_{z^j} x(z_{(j|L_j)},t)\right) = u^j(z_{(j|)},t), \qquad j \in I_m^i \tag{9.44e}$$

for $t > t_0$. Equations (9.44a) and (9.44d) thereby follow directly from the transformation and the state–feedback control while (9.44b) and (9.44c) are a consequence

of the invariance of linear boundary conditions under the transformation (9.5). Finally, (9.44e) follows from the property that all inhomogeneous boundary conditions for $j \in I_m^i$ are mapped into inhomogeneous boundary conditions for the target system. Herein, the inverse backstepping transformation $g(z^i, \zeta, t)$ can be used to express $x(z_{(j|L_j)}, t)$ and $\partial_{z^j} x(z_{(j|L_j)}, t)$ for $j \in I_m^i$ in terms of the target state in the form

$$x(z_{(j|L_j)}, t) = w(z_{(j|L_j)}, t) + \int_0^{z^i} g(z^i, \zeta, t)\, w(z_{(i|\zeta, j|L_j)}, t)\mathrm{d}\zeta$$

$$\partial_{z^j} x(z_{(j|L_j)}, t) = \partial_{z^j} w(z_{(j|L_j)}, t) + \int_0^{z^i} g(z^i, \zeta, t)\, \partial_{z^j} w(z_{(i|\zeta, j|L_j)}, t)\mathrm{d}\zeta.$$

9.5.1 Multi–linear Backstepping–Transformation

Given multiple inputs $u^i(z_{(i|)}, t)$, $i \in I_m$, the results above motivate the introduction of a sequence of $\#I_m$ transformations with each determining one boundary control. Therefore, it is convenient to introduce the operator

$$\mathfrak{K}^i(z^i, t) \circ x(z, t) = x(z, t) - \int_0^{z^i} k^i(z^i, \zeta^i, t)\, x(z_{(i|\zeta^i)}, t)\mathrm{d}\zeta^i$$

and to assume that the index set I_m is sorted ascendingly with $I_m = \{i_1, \ldots, i_m\}$. With this, introduce the sequence of transformations

$$\begin{aligned}
w^{i_1}(z, t) &= \mathfrak{K}^{i_1}(z^{i_1}, t) \circ x(z, t) \\
w^{i_2}(z, t) &= \mathfrak{K}^{i_2}(z^{i_2}, t) \circ w^{i_1}(z, t) \\
&\vdots \\
w(z, t) &= \mathfrak{K}^{i_m}(z^{i_m}, t) \circ w^{i_{m-1}}(z, t) \\
&= \underbrace{\mathfrak{K}^{i_m}(z^{i_m}, t) \circ \mathfrak{K}^{i_{m-1}}(z^{i_{m-1}}, t) \circ \cdots \circ \mathfrak{K}^{i_1}(z^{i_1}, t)}_{=\bar{\mathfrak{K}}^{I_m}(z_{(I_r \setminus I_m|)}, t)} \circ x(z, t).
\end{aligned} \tag{9.45}$$

It can be easily deduced that the last line determining $w(z, t)$ is equivalent to a multi–linear Volterra–type integral transformation, i.e.

$$\begin{aligned}
w(z, t) &= \bar{\mathfrak{K}}^{I_m}(z_{(I_r^{I_m}|)}, t) \circ x(z, t) \\
&= x(z, t) - \sum_{k=1}^{m} \int_0^{z^{i_k}} k^{i_k}(z^{i_k}, \zeta^{i_k}, t)\, x(z_{(i_k|\zeta^{i_k})}, t)\mathrm{d}\zeta^{i_k} \\
&\quad + \int_0^{z^{i_1}} \int_0^{z^{i_2}} k^{i_1}(z^{i_1}, \zeta^{i_1}, t) k^{i_2}(z^{i_2}, \zeta^{i_2}, t) x(z_{(i_1|\zeta^{i_1}, i_2|\zeta^{i_2})}, t)\mathrm{d}\zeta^{i_2}\mathrm{d}\zeta^{i_1}
\end{aligned}$$

$$
\begin{aligned}
&+\cdots+\int_0^{z^{i_{m-1}}}\int_0^{z^{i_m}} k^{i_{m-1}}(z^{i_{m-1}},\zeta^{i_{m-1}},t)k^{i_m}(z^{i_m},\zeta^{i_m},t)\times\\
&\qquad x(z_{(i_{m-1}|\zeta^{i_{m-1}},i_m|\zeta^{i_m})},t)\mathrm{d}\zeta^{i_m}\mathrm{d}\zeta^{i_{m-1}}\\
&+\cdots+(-1)^{\#I_m}\int_0^{z^{i_1}}\cdots\int_0^{z^{i_m}} k^{i_1}(z^{i_1},\zeta^{i_1},t)\cdots k^{i_m}(z^{i_m},\zeta^{i_m},t)\times\\
&\qquad x(z_{(i_1|\zeta^{i_1},\cdots,i_m|\zeta^{i_m})},t)\mathrm{d}\zeta^{i_m}\cdots\mathrm{d}\zeta^{i_1}.
\end{aligned}
\tag{9.46}
$$

In view of the introductory remarks, it is obvious from (9.45) that each transformation $\mathfrak{K}^{i_k}(z^{i_k},t)$, $i_k\in I_m$, determines the corresponding state–feedback control $u^{i_k}(z_{(i_k|)},t)$, which is required for the implementation of the transformation. This particularly illustrates that each $\mathfrak{K}^{i_k}(z^{i_k},t)$ results in a homogeneous boundary condition at $z^{i_k}=L_{i_k}$ in the target system $w^{i_k}(z,t)$ such that after m steps the desired realization of the overall target system $w(z,t)$ with purely homogeneous boundary conditions is obtained. Moreover, it can directly deduced by the construction of the sequence that the evolution of each $\mathfrak{K}^{i_k}(z^{i_k},t)$ is governed by the equations for a 1–dimensional kernel given by (9.12) depending on the particular boundary conditions of the diffusion–reaction system (9.2) and the individual target system $w^{i_k}(z,t)$ as well as the separability of the parameter $c(z,t)$ with respect to the independent coordinates z^{i_k}, $i_k\in I_m$, according to Assumption 9.2.

9.5.2 Determination and Solution of the Kernel–PDEs

In order to verify these assertions, let $w^{i_0}(z,t)=x(z,t)$, $w(z,t)=w^{i_m}(z,t)$, $d^{i_0}(z,t)=-c(z,t)$, and consider for the moment the transformation of the PDE $\partial_t w^{i_{k-1}}(z,t)-\Delta w^{i_{k-1}}(z,t)+d^{i_{k-1}}(z,t)w^{i_{k-1}}(z,t)=0$ into $\partial_t w^{i_k}(z,t)-\Delta w^{i_k}(z,t)+d^{i_k}(z,t)w^{i_k}(z,t)=0$ for one arbitrary $i_k\in I_m$ using (9.45). After some intermediate computations this provides

$$
\begin{aligned}
&\partial_t w^{i_k}(z,t)-\Delta w^{i_k}(z,t)+d^{i_k}(z,t)w^{i_k}(z,t)\\
&=\big[2\mathrm{d}_{z^{i_k}}k^{i_k}(z^{i_k},z^{i_k},t)+d^{i_k}(z,t)-d^{i_{k-1}}(z,t)\big]w^{i_{k-1}}(z,t)\\
&\quad+k^{i_k}(z^{i_k},0,t)\partial_{z^{i_k}}w^{i_{k-1}}(z_{(i_k|0)},t)\\
&\quad-\partial_{\zeta^{i_k}}k^{i_k}(z^{i_k},0,t)w^{i_{k-1}}(z_{(i_k|0)},t)\\
&\quad-\int_0^{z^{i_k}}\Big(\partial_t k^{i_k}(z^{i_k},\zeta^{i_k},t)+\partial^2_{\zeta^{i_k}}k^{i_k}(z^{i_k},\zeta^{i_k},t)-\partial^2_{z^{i_k}}k^{i_k}(z^{i_k},\zeta^{i_k},t)\\
&\qquad+\big[d^{i_k}(z,t)-d^{i_{k-1}}(z_{(i_k|\zeta^{i_k})},t)\big]k^{i_k}(z^{i_k},\zeta^{i_k},t)\Big)\times\\
&\qquad w^{i_{k-1}}(z_{(i_k|\zeta^{i_k})},t)\mathrm{d}\zeta^{i_k}.
\end{aligned}
\tag{9.47}
$$

Due to the relationship between the obtained expression and the equations determining the backstepping kernel and the target system in the single input setting, these computations motivate the choice of the individual target systems in the form

$$\partial_t w^{i_k}(z,t) = \Delta w^{i_k}(z,t) - d^{i_k}(z,t) w^{i_k}(z,t), \qquad (z,t) \in \Omega \times \mathbb{R}^+_{t_0} \tag{9.48a}$$

with $d^{i_k}(z,t)$ determined below. Boundary conditions are imposed by

$$\begin{aligned}
&-\epsilon^0_j \partial_{z^j} w^{i_k}(z,t) + p^0_j w^{i_k}(z,t) = 0, && z^j = 0,\ j \in I_r^{\{i_1,\ldots,i_k\}} && (9.48b)\\
&-\epsilon^0_{w,j} \partial_{z^j} w^{i_k}(z,t) + p^0_{w,j} w^{i_k}(z,t) = 0, && z^j = 0,\ j \in \{i_1,\ldots,i_k\} && (9.48c)\\
&\epsilon^1_j \partial_{z^j} w^{i_k}(z,t) + p^1_j w^{i_k}(z,t) = 0, && z^j = L_j,\ j \in I_r^{I_m} && (9.48d)\\
&\epsilon^1_{w,j} \partial_{z^j} w^{i_k}(z,t) + p^1_{w,j} w^{i_k}(z,t) = 0, && z^j = L_j,\ j \in \{i_1,\ldots,i_k\} && (9.48e)
\end{aligned}$$

for $t > t_0$ and the initial condition is assumed as

$$w^{i_k}(z,t_0) = w_0^{i_k}(z), \qquad z \in \overline{\Omega}. \tag{9.48f}$$

Differing from the single input set–up, note that for $k < m$ in addition $m-k$ inhomogeneous boundary conditions at $z^j = L_j$, $j \in \{i_{k+1},\ldots,i_m\}$ arise from the undetermined boundary controls. Due to the nonlinearity in terms of $\theta^i(\cdot,\cdot)$ for $i \in I_m$, which relates the boundary control $u^i(z_{(i|)},t)$ and the state along the respective hypersurface, the successive transformation from the nonlinear expressions in $w^{i_{k-1}}(z,t)$ into $w^{i_k}(z,t)$ requires to consider the corresponding inverse to $k^{i_k}(z^{i_k},\zeta^{i_k},t)$ (see also the introductory remarks to this section). Since the explicit determination of these inhomogeneous boundary conditions is here only of minor interest their evaluation is omitted. Nevertheless, it is crucial to observe that in each step i_k one boundary control is eliminated by means of the corresponding transformation. By means of a consecutive application of the m individual transformations this enables a complete determination of the state–feedback controls for all $i \in I_m$. Hence, stability of the target system can be only deduced after the evaluation of the final transformation $\mathfrak{K}^{i_m}(z^{i_m},t)$, which requires to determine each kernel $k^{i_k}(z^{i_k},\zeta^{i_k},t)$.

With (9.3a) of Assumption 9.2, each $d^{i_k}(z,t)$, $k = 1,\ldots,m$, can be determined[2] according to

$$d^{i_k}(z,t) = \sum_{j=1}^{k} \mu^{i_j}(t) - c_0(z_{(I_m|)},t) - \sum_{j=k+1}^{m} c_1^{i_j}(z^{i_j},t). \tag{9.49}$$

By introducing $\gamma^{i_k}(z^{i_k},t) := d^{i_k}(z,t) - d^{i_{k-1}}(z,t) = \mu^{i_k}(t) + c_1^{i_k}(z^{i_k},t)$, Eqn. (9.47) implies that the i_k–th kernel is governed by the PDE

$$\begin{aligned}
\partial_t k^{i_k}(z^{i_k},\zeta^{i_k},t) = {} & \partial^2_{z^i} k^{i_k}(z^{i_k},\zeta^{i_k},t) - \partial^2_{\zeta} k^{i_k}(z^{i_k},\zeta^{i_k},t)\\
& - \gamma^{i_k}(\zeta^{i_k},t) k^{i_k}(z^{i_k},\zeta^{i_k},t)
\end{aligned} \tag{9.50a}$$

[2] Equivalently, $\mu^{i_j}(t)$ can be replaced by $\mu^{i_j}(z^{i_j},t)$. This, however, requires to reanalyze the stability of the resulting target system according to the proof of Lemma 9.1.

defined on the triangular domain $\zeta^{i_k} \in (0, z^{i_k})$, $z^{i_k} \in (0, L_{i_k})$ with the boundary condition

$$2\mathrm{d}_{z^{i_k}} k^{i_k}(z^{i_k}, z^{i_k}, t) + \gamma^{i_k}(z^{i_k}, t) = 0. \tag{9.50b}$$

In view of (9.47) and the structure of the individual target systems (9.48) it can be easily deduced that the remaining boundary conditions for $k^{i_k}(z^{i_k}, \zeta^{i_k}, t)$ are identical to those for the 1–dimensional case. These are hence provided below for the sake of completeness:

(i) For a Dirichlet condition at $z^{i_k} = 0$, i.e. $\epsilon^0_{i_k} = 0$, $p^0_{i_k} \neq 0$ in (9.48c), the kernel has to satisfy

$$k^{i_k}(z^{i_k}, 0, t) = 0 \tag{9.50c}$$

while the target system is restricted to $\epsilon^0_{w,i_k} = 0$, i.e.

$$w^{i_k}(z_{(i_k|0)}, t) = 0. \tag{9.50d}$$

(ii) For a Neumann or mixed condition at $z^{i_k} = 0$, i.e. $\epsilon^0_{i_k} \neq 0$ in (9.48c), the kernel has to satisfy

$$-\partial_{\zeta^{i_k}} k^{i_k}(z_{(i_k|0)}, t) + \bar{p}^0_{i_k} k^{i_k}(z_{(i_k|0)}, t) = 0, \tag{9.50e}$$

where $\bar{p}^0_{i_k} = p^0_{i_k}/\epsilon^0_{i_k}$. Thereby, the target system is restricted to the boundary condition

$$-\epsilon^0_{w,i_k} \partial_{z^i} w^{i_k}(z_{(i_k|0)}, t) + p^0_{w,i_k} w^{i_k}(z_{(i_k|0)}, t) = 0. \tag{9.50f}$$

In addition, the kernel has to fulfill the additional constraint

$$k^{i_k}(0, 0, t) = \bar{p}^0_{i_k} - \frac{p^0_{w,i_k}}{\epsilon^0_{w,i_k}}. \tag{9.50g}$$

These results furthermore imply that the solution approach considered in Section 9.2.2 by means of introducing suitable scattering coordinates for the application of the method of integral operators and the solution of the resulting expression using a successive approximation can be directly applied to determine the solution for the integral kernels $k^{i_k}(z^{i_k}, \zeta^{i_k}, t)$ for all $i_k \in I_m$. In particular, with this a strong solution for $k^{i_k}(z^{i_k}, \zeta^{i_k}, t)$ is obtained, which is bounded with bounded derivatives with respect to (z^{i_k}, ζ^{i_k}) and is of Gevrey order $\alpha \in [1, 2]$ in t provided that the conditions of Theorems 8.1 and 8.2 on the system parameters are fulfilled.

Hence, it follows from (9.48) and Assumption 9.2 that after the m–th transformation $w(z, t) = w^{i_m}(z, t)$ satisfies

$$\partial_t w(z, t) = \Delta w(z, t) - d(z, t) w(z, t), \qquad (z, t) \in \Omega \times \mathbb{R}^+_{t_0} \tag{9.51a}$$

with

$$d(z,t) = d^{i_m}(z,t) = \sum_{j=1}^{m} \mu^{i_j}(t) - c_0(z_{(I_m|)},t), \tag{9.51b}$$

the boundary conditions

$$\begin{aligned}
&-\epsilon_j^0 \partial_{z^j} w(z,t) + p_j^0 w(z,t) = 0, && z^j = 0,\ j \in I_r^{I_m} && \text{(9.51c)}\\
&-\epsilon_{w,j}^0 \partial_{z^j} w(z,t) + p_{w,j}^0 w(z,t) = 0, && z^j = 0,\ j \in I_m && \text{(9.51d)}\\
&\epsilon_j^1 \partial_{z^j} w(z,t) + p_j^1 w(z,t) = 0, && z^j = L_j,\ j \in I_r^{I_m} && \text{(9.51e)}\\
&\epsilon_{w,j}^1 \partial_{z^j} w(z,t) + p_{w,j}^1 w(z,t) = 0, && z^j = L_j,\ j \in I_m && \text{(9.51f)}
\end{aligned}$$

for $t > t_0$, and the initial condition

$$w(z,t_0) = w_0(z), \qquad z \in \overline{\Omega}. \tag{9.51g}$$

The stability properties of the overall target system hence depend on $d(z,t)$ and the selection of the degrees–of–freedom $\mu^{i_j}(t)$.

Lemma 9.2. *The parabolic distributed–parameter system* (9.51) *is exponentially stable in the L^2–norm for any combination of Dirichlet, Neumann, or mixed boundary conditions if $\sum_{j=1}^{m} \mu^{i_j}(t) + \lambda_{\min} - \bar{c}_0(t) > \epsilon > 0\ \forall t \in \mathbb{R}_{t_0}^+$ for some $\epsilon > 0$. Here,*

$$\bar{c}_0(t) = \sup_{z_{(I_r|)} \in \mathsf{X}_{j \in I_r \setminus I_m}[0,L_j]} c_0(z_{(I_m|)},t)$$

and $\lambda_{\min}$ denotes the smallest eigenvalue λ of $\Delta w(z,t) + \lambda w(z,t) = 0$ with boundary conditions (9.51c)–(9.51f)*.*

The proof of this result follows directly along the lines of the proof of Lemma 9.1. Hence, the exponential stability of (9.51) in the L^2–norm can be guaranteed provided that $\mu(t) = \sum_{j=1}^{m} \mu^{i_j}(t)$ as introduced in (9.49) is chosen appropriately.

9.5.3 Backstepping–Based State–Feedback Controller

The results on the multi–linear backstepping–transformation enable the determination of the respective state–feedback control to achieve the exponential stabilization of the diffusion–reaction system (9.2). For this, it is crucial to note the following two properties of (9.45), i.e.

$$\begin{aligned}
w(z_{(i_k|L_{i_k})},t) = {} & \mathfrak{K}^{i_m}(z^{i_m},t) \circ \cdots \circ \mathfrak{K}^{i_{k+1}}(z^{i_{k+1}},t) \circ \mathfrak{K}^{i_{k-1}}(z^{i_{k-1}},t) \circ \\
& \cdots \circ \mathfrak{K}^{i_1}(z^{i_1},t) \circ \big(\mathfrak{K}^{i_k}(L_{i_k},t) \circ x(z,t)\big)
\end{aligned} \tag{9.52a}$$

$$\partial_{z^{i_k}} w(z_{(i_k|L_{i_k})},t) = \mathfrak{K}^{i_m}(z^{i_m},t)\circ\cdots\circ\mathfrak{K}^{i_{k+1}}(z^{i_{k+1}},t)\circ\mathfrak{K}^{i_{k-1}}(z^{i_{k-1}},t)\circ \cdots\circ\mathfrak{K}^{i_1}(z^{i_1},t)\circ\partial_{z^{i_k}}\big(\mathfrak{K}^{i_k}(L_{i_k},t)\circ x(z,t)\big), \tag{9.52b}$$

where

$$\mathfrak{K}^{i_k}(L_{i_k},t)\circ x(z,t) = x(z_{(i_k|L_{i_k})},t) - \int_0^{L_{i_k}} k^{i_k}(L_{i_k},\zeta^{i_k},t)x(z_{(i_k|\zeta^{i_k})},t)\mathrm{d}\zeta^{i_k}$$

$$\partial_{z^{i_k}}\big(\mathfrak{K}^{i_k}(L_{i_k},t)\circ x(z,t)\big) = \partial_{z^{i_k}} x(z_{(i_k|L_{i_k})},t)$$

$$-k^{i_k}(L_{i_k},L_{i_k},t)x(z_{(i_k|L_{i_k})},t) - \int_0^{L_{i_k}} \partial_{z^{i_k}} k^{i_k}(L_{i_k},\zeta^{i_k},t)x(z_{(i_k|\zeta^{i_k})},t)\mathrm{d}\zeta^{i_k}.$$

Proceeding as in Section 9.2.3, the state–feedback control can be determined depending on the parameters ϵ^1_{w,i_k} and p^1_{w,i_k}. With (9.2d) and (9.51f) this yields for each $i_k \in I_m$, $k = 1,\dots,m$:

(i) For $\epsilon^1_{w,i_k} = 0$, i.e. $w(z_{(i_k|L_{i_k})},t) = 0$, (9.52a) implies

$$\begin{aligned} 0 &= \mathfrak{K}^{i_m}(z^{i_m},t)\circ\cdots\circ\mathfrak{K}^{i_{k+1}}(z^{i_{k+1}},t)\circ\mathfrak{K}^{i_{k-1}}(z^{i_{k-1}},t)\circ \\ &\quad \cdots\circ\mathfrak{K}^{i_1}(z^{i_1},t)\circ\big(\mathfrak{K}^{i_k}(L_{i_k},t)\circ x(z,t)\big) \\ &= \mathfrak{K}^{i_m}(z^{i_m},t)\circ\cdots\circ\mathfrak{K}^{i_{k+1}}(z^{i_{k+1}},t)\circ\mathfrak{K}^{i_{k-1}}(z^{i_{k-1}},t)\circ\cdots\circ\mathfrak{K}^{i_1}(z^{i_1},t)\circ \\ &\quad \left(x(z_{(i_k|L_{i_k})},t) - \int_0^{L_{i_k}} k^{i_k}(L_{i_k},\zeta^{i_k},t)x(z_{(i_k|\zeta^{i_k})},t)\mathrm{d}\zeta^{i_k}\right). \end{aligned}$$

Since the latter expression has to hold for all $z_{(i_k|)} \in \mathsf{X}_{j\in I_m^{i_k}}[0,L_j]$ it follows that necessarily

$$\begin{aligned} x(z_{(i_k|L_{i_k})},t) &= \int_0^{L_{i_k}} k^{i_k}(L_{i_k},\zeta^{i_k},t)x(z_{(i_k|\zeta^{i_k})},t)\mathrm{d}\zeta^{i_k} \\ &=: \Xi_D(x(z_{(i_k|)},t)). \end{aligned}$$

As a result, the state–feedback control is obtained as

$$u^{i_k}(z_{(i_k|)},t) = \theta^{i_k}\big(\Xi_D(x(z_{(i_k|)},t)),\partial_{z^{i_k}} x(z_{(i_k|L_{i_k})},t)\big). \tag{9.53a}$$

(ii) For $p^1_{w,i_k} = 0$, i.e. $\partial_{z^{i_k}} w(z_{(i_k|L_{i_k})},t) = 0$, proceeding as above by making use of (9.52b) results in

$$\begin{aligned} \partial_{z^{i_k}} x(z_{(i_k|L_{i_k})},t) &= k^{i_k}(L_{i_k},L_{i_k},t)x(z_{(i_k|L_{i_k})},t) \\ &\quad + \int_0^{L_{i_k}} \partial_{z^{i_k}} k^{i_k}(L_{i_k},\zeta^{i_k},t)x(z_{(i_k|\zeta^{i_k})},t)\mathrm{d}\zeta^{i_k} \\ &=: \Xi_N(x(z_{(i_k|)},t)). \end{aligned}$$

With this, the state–feedback control follows as

$$u^{i_k}(z_{(i_k|)},t) = \theta^{i_k}\big(x(z_{(i_k|L_{i_k})},t), \Xi_N(x(z_{(i_k|)},t))\big). \tag{9.53b}$$

(iii) If $\epsilon^1_{w,i_k},\ p^1_{w,i_k} \neq 0$ a similar argument yields

$$\begin{aligned}
&\partial_{z^{i_k}} x(z_{(i_k|L_{i_k})},t) = x(z_{(i_k|L_{i_k})},t)\left(k^{i_k}(L_{i_k},L_{i_k},t) - \frac{p^1_{w,i_k}}{\epsilon^1_{w,i_k}}\right)\\
&+\int_0^{L_{i_k}}\left(\partial_{z^{i_k}} k^{i_k}(L_{i_k},\zeta^{i_k},t) + \frac{p^1_{w,i_k}}{\epsilon^1_{w,i_k}} k^{i_k}(L_{i_k},\zeta^{i_k},t)\right) x(z_{(i_k|\zeta^{i_k})},t)\mathrm{d}\zeta^{i_k}\\
&=: \Xi_M(x(z_{(i_k|)},t))
\end{aligned}$$

such that the state–feedback control can be schematically represented as

$$u^{i_k}(z_{(i_k|)},t) = \theta^{i_k}\big(x(z_{(i_k|L_{i_k})},t), \Xi_M(x(z_{(i_k|)},t))\big). \tag{9.53c}$$

9.5.4 Inverse Multi–linear Backstepping–Transformation and Exponential Stability of the Closed–Loop System

As already outlined in Section 8.2.5 for the 1–dimensional setting and in Section 9.2.4 for the case of a single boundary control it is necessary to analyze the inverse backstepping transformation to verify the exponential stability of the diffusion–reaction system under the action of the determined state–feedback control. By introducing

$$\mathfrak{G}^i(z^i,t)\circ w(z,t) = w(z,t) + \int_0^{z^i} g^i(z^i,\zeta^i,t)\, w(z_{(i|\zeta^i)},t)\mathrm{d}\zeta^i$$

the results of Section 9.2.4 imply that the sequence of transformations

$$\begin{aligned}
x^{i_{m-1}}(z,t) &= \mathfrak{G}^{i_m}(z^{i_m},t)\circ w(z,t)\\
x^{i_{m-2}}(z,t) &= \mathfrak{G}^{i_{m-1}}(z^{i_{m-1}},t)\circ x^{i_{m-1}}(z,t)\\
&\vdots\\
x(z,t) &= \mathfrak{G}^{i_1}(z^{i_1},t)\circ x^{i_1}(z,t)\\
&= \underbrace{\mathfrak{G}^{i_1}(z^{i_1},t)\circ \mathfrak{G}^{i_2}(z^{i_2},t)\circ\cdots\circ \mathfrak{G}^{i_m}(z^{i_m},t)}_{=\bar{\mathfrak{G}}^{I_m}(z_{(I_r\setminus I_m|)},t)}\circ w(z,t).
\end{aligned} \tag{9.54}$$

inverts the multi–linear Volterra–type transformation (9.45). The determination of the individual kernels $g^{i_k}(z^{i_k},\zeta^{i_k},t)$, $k=1,\ldots,m$, thereby follows exactly the lines of Section 9.5.2 and hence yields that the governing equations for the inverse kernel $g^{i_k}(z^{i_k},\zeta^{i_k},t)$ correspond to those for $k^{i_k}(z^{i_k},\zeta^{i_k},t)$ with $\gamma^{i_k}(\zeta^{i_k},t)$ replaced by $-\gamma^{i_k}(z^{i_k},t)$ and the coefficients $p^0_{i_k},\ \epsilon^0_{i_k}$ in (9.50e) interchanged with

p^0_{w,i_k}, ϵ^0_{w,i_k}. Hence, the solution procedure in terms of the method of integral operators and successive approximations as well as the convergence proof are identical. This in particular ensures that each $g^{i_k}(z^{i_k},\zeta^{i_k},t)$ is bounded with bounded derivative with respect to (z^{i_k},ζ^{i_k}) and is of Gevrey order $\alpha\in[1,2]$ in t under the conditions of Theorems 8.1 and 8.2.

Theorem 9.4. *Consider the diffusion–reaction system* (9.2) *with state–feedback control* (9.53a)*,* (9.53b)*, or* (9.53c) *for $i_k\in I_m$ depending on the boundary condition at $z^{i_k}=L_{i_k}$. Then the equilibrium $x(z,t)\equiv 0$ is exponentially stable for all $t\in\mathbb{R}^+_{t_0}$ in the L^2–norm if the target system* (9.51) *satisfies the conditions of Lemma 9.2.*

The proof follows basically the lines of the proof of Theorem 9.1.

Proof. Let $X=L^2(\Omega)$ and assume $x_0(z)$, $w_0(z)\in X$. Since $k^{i_k}(z^{i_k},\zeta^{i_k},t)$ and $g^{i_k}(z^{i_k},\zeta^{i_k},t)$ are strong bounded solutions to the respective kernel–PDEs for all $k=1,\ldots,m$, it follows by the Minkowski and Cauchy–Schwarz inequalities that

$$\|w_0^{i_k}\|_X\le C_0^{i_k}\|w_0^{i_{k-1}}\|_X$$

with $C_0^{i_k}=1+L_{i_k}\sup_{(z^{i_k},\zeta^{i_k})\in\Theta_0^{i_k}}|k^{i_k}(z^{i_k},\zeta^{i_k},t)|$, where $\Theta_0^{i_k}=\{(z^{i_k},\zeta^{i_k}):\zeta^{i_k}\in[0,L_{i_k}],\ z^{i_k}\in[\zeta^{i_k},L_{i_k}]\}$. Thus, since $w_0(z)=w^{i_m}(z,t_0)$ and $x_0(z)=w^{i_0}(z,t_0)$ the estimate

$$\|w_0\|_X\le C_0\|x_0\|_X$$

holds with $C_0=\prod_{k=1}^m C_0^{i_k}$. With Lemma 9.2 for (9.51) one obtains

$$\|w(t)\|_X\le e^{-\kappa(t)}\|w_0\|_X\le C_0e^{-\kappa(t)}\|x_0\|_X$$

for $\kappa(t)=\int_{t_0}^t(\sum_{j=1}^m\mu^{i_j}(s)+\lambda_{\min}-\bar c_0(s))\mathrm{d}s$. In view of (9.54), proceeding similarly provides in view of the boundedness of $g^{i_k}(z^{i_k},\zeta^{i_k},t)$ that there exists a constant C_1 such that

$$\|x(t)\|_X\le C_1\|w(t)\|_X\le C_0C_1e^{-\kappa(t)}\|x_0\|_X.$$

Hence, exponential stability of the closed–loop system follows if $\kappa(t)>\epsilon>0$. □

9.5.5 Approximate Finite–Dimensional Realization of Backstepping–Based State–Feedback Control

In order to deal with the considered idealized boundary control configuration with infinite–dimensional inputs $u^i(z_{(i|)},t)$, $i\in I_m$, their implementation requires to approximate each $u^i(z_{(i|)},t)$ by a set of finite–dimensional actuators, which are suitably placed on the input surfaces $\partial\Omega_i$. For this, a realization approach is presented

in Section 9.2.5 based on the single input configuration. The proposed approach can be directly applied to the multiple input configuration by proceeding as outlined for each actuator $u^i(z_{(i|)}, t)$, $i \in I_m$, i.e. let

$$u^i(z_{(i|)}, t) = \sum_{l=1}^{m_i} \mathfrak{b}^{l,i}(z_{(i|)}) u^{l,i}(t)$$

where $\mathfrak{b}^{l,i}(z_{(i|)})$ denotes the spatial actuator characteristics of the m_i finite–dimensional actuators. Then, given a discrete time implementation the solution of the sequence of $\#I_m$ least–squares problems

$$\min_{\{u_k^{l,i}\}_{l=1,\ldots,m_i}} \left\| u^i(z_{(i|)}, t_k) - \sum_{l=1}^{m_i} \mathfrak{b}^{l,i}(z_{(i|)}) u_k^{l,i} \right\|^2_{L^2(\partial\Omega_i)}, \qquad i \in I_m$$

at each sampling instance t_k provides the discrete time input values $u^{l,i}(t_k) = u_k^{l,i}$, $l = 1, \ldots, m_i$, for each input surface $i = 1, \ldots, m$. While this yields a practical (approximate) implementation technique the stability analysis for the closed–loop control system cannot be easily transferred to the finite–dimensional actuator setting as is pointed out in Remark 9.5. Nevertheless, the simulation results provided in Section 9.8 confirm the applicability and the stabilization property of the proposed realization approach.

Obviously, the realization of the state–feedback control relies on the knowledge of the state $x(z,t)$ and its derivatives $\partial_{z^i} x(z,t)$, $i \in I_m$. For this, a distributed–parameter state–observer design is subsequently developed by extending the backstepping technique to multiple output configurations.

9.6 State–Observer with Exponentially Stable Error Dynamics — The Multiple Output Case

The state–observer design in Section 9.3 is based on the weighted feedback of a single output variable. Subsequently, this approach is extended to determine an estimate of the evolution of the state $x(z,t)$ from the knowledge of p outputs $y^i(z_{(i|)}, t)$, $i \in I_p$, $\#I_p = p > 1$. For this, similar to Section 9.5, multi–linear Volterra–type integral transformations are considered for the systematic determination of observer gains to achieve an exponentially stable observer error dynamics.

Assumption 9.4. The functionals $\theta^i(\cdot,\cdot)$, $i \in I_m$, are linear and satisfy

$$\theta^i\left(x(z,t), \partial_{z^i} x(z,t)\right) = \epsilon_i^1 \partial_{z^i} x(z,t) + p_i^1 x(z,t), \quad z^i = L_i, \ \forall i \in I_m \tag{9.55}$$

with constants ϵ_i^1 and p_i^1.

Contrary to the state–feedback design, which is applicable for rather general nonlinear input characteristics, the state–observer design relies on a linear boundary input.

With this preliminary a Luenberger–type observer is considered, i.e.

$$\partial_t \hat{x}(z,t) = \Delta \hat{x}(z,t) + c(z,t)\hat{x}(z,t) \tag{9.56a}$$
$$+ \sum_{i \in I_p} l_1^i(z^i,t)\big[y^i(z_{(i|)},t) - \hat{y}^i(z_{(i|)},t)\big] \tag{9.56b}$$

for $(z,t) \in \Omega \times \mathbb{R}^+_{t_0}$ with the boundary conditions

$$-\epsilon_j^0 \partial_{z^j}\hat{x}(z,t) + p_j^0 \hat{x}(z,t) = 0, \qquad z^j = 0,\ j \in I_r^{I_p} \tag{9.56c}$$
$$-\epsilon_i^0 \partial_{z^i}\hat{x}(z,t) + p_i^0 \hat{x}(z,t) = l_{10}^i(t)\big[y^i(z_{(i|)},t) - \hat{y}^i(z_{(i|)},t)\big], \qquad z^i = 0,\ i \in I_p \tag{9.56d}$$
$$\epsilon_j^1 \partial_{z^j}\hat{x}(z,t) + p_j^1 \hat{x}(z,t) = 0, \qquad z^j = L_j,\ j \in I_r^{I_m} \tag{9.56e}$$
$$\epsilon_j^1 \partial_{z^j}\hat{x}(z,t) + p_j^1 \hat{x}(z,t) = u^j(z_{(i|)},t), \qquad z^j = L_j,\ j \in I_m, \tag{9.56f}$$

for $t > t_0$, the initial condition

$$\hat{x}(z,t_0) = \hat{x}_0(z), \qquad z \in \overline{\Omega}, \tag{9.56g}$$

and

$$\hat{y}^i(z_{(i|)},t) = h_i^0 \partial_{z^i}\hat{x}(z,t) + h_i^1 \hat{x}(z,t), \qquad z^i = 0,\ i \in I_p,\ t \geq t_0. \tag{9.56h}$$

Here, $l_1^i(z^i,t)$ and $l_{10}^i(t)$, $i \in I_p$, denote the observer gains, which are determined to achieve the exponential decay of the observer error $\tilde{x}(z,t) = x(z,t) - \hat{x}(z,t)$. Comparing (9.2) with (9.56) in view of (9.55) results in the PDE

$$\partial_t \tilde{x}(z,t) = \Delta \tilde{x}(z,t) + c(z,t)\tilde{x}(z,t)$$
$$- \sum_{i \in I_p} l_1^i(z^i,t)\big[h_i^0 \partial_{z^i}\tilde{x}(z_{(i|0)},t) + h_i^1 \tilde{x}(z_{(i|0)},t)\big] \tag{9.57a}$$

for $(z,t) \in \Omega \times \mathbb{R}^+_{t_0}$ with the boundary conditions

$$-\epsilon_j^0 \partial_{z^j}\tilde{x}(z,t) + p_j^0 \tilde{x}(z,t) = 0, \qquad z^j = 0,\ j \in I_r^{I_p} \tag{9.57b}$$
$$\big(l_{10}^i(t)h_i^0 - \epsilon_i^0\big)\partial_{z^i}\tilde{x}(z,t) + \big(l_{10}^i(t)h_i^1 + p_i^0\big)\tilde{x}(z,t) = 0, \qquad z^i = 0,\ i \in I_p \tag{9.57c}$$
$$\epsilon_j^1 \partial_{z^j}\tilde{x}(z,t) + p_j^1 \tilde{x}(z,t) = 0, \qquad z^j = L_j,\ j \in I_r \tag{9.57d}$$

for $t > t_0$ and the initial condition

$$\tilde{x}(z,t_0) = \tilde{x}_0(z) = x_0(z) - \hat{x}_0(z), \qquad z \in \overline{\Omega}. \tag{9.57e}$$

9.6.1 Multi–linear Backstepping–Transformation

Differing from the case of a single output in Section 9.3, in the following an alternative approach is presented by considering the transformation from the observer error dynamics into a suitable target system. Pursuing this path in particular allows to systematically motivate and to constructively deduce the structure of the target system and to determine structural restrictions on the considered class of systems. For this, it is convenient to introduce the operator

$$\mathfrak{M}^i(z^i,t)\circ\tilde{x}(z,t)=\tilde{x}(z,t)+\int_0^{z^i} m^i(z^i,\zeta^i,t)\,\tilde{x}(z_{(i|\zeta^i)},t)\mathrm{d}\zeta^i \tag{9.58}$$

and to assume that the index set I_p is ordered ascendingly with $I_p=\{i_1,\ldots,i_p\}$. Moreover, consider the sequence of transformations

$$\begin{aligned}
\tilde{w}^{i_1}(z,t)&=\mathfrak{M}^{i_1}(z^{i_1},t)\circ\tilde{x}(z,t)\\
\tilde{w}^{i_2}(z,t)&=\mathfrak{M}^{i_2}(z^{i_2},t)\circ\tilde{w}^{i_1}(z,t)\\
&\vdots\\
\tilde{w}(z,t)&=\mathfrak{M}^{i_p}(z^{i_p},t)\circ\tilde{w}^{i_{p-1}}(z,t)\\
&=\underbrace{\mathfrak{M}^{i_p}(z^{i_p},t)\circ\mathfrak{M}^{i_{p-1}}(z^{i_{p-1}},t)\circ\cdots\circ\mathfrak{M}^{i_1}(z^{i_1},t)}_{=\bar{\mathfrak{M}}^{I_p}(z_{(I_r\setminus I_p|)},t)}\circ\tilde{x}(z,t).
\end{aligned} \tag{9.59}$$

Sequential evaluation of the multi–linear Volterra–type operator $\bar{\mathfrak{M}}^{I_p}(z_{(I_r^{I_p}|)},t)$ yields

$$\begin{aligned}
\tilde{w}(z,t)=\tilde{x}(z,t)&+\sum_{k=1}^{p}\int_0^{z^{i_k}} m^{i_k}(z^{i_k},\zeta^{i_k},t)\,\tilde{x}(z_{(i_k|\zeta^{i_k})},t)\mathrm{d}\zeta^{i_k}\\
&+\int_0^{z^{i_1}}\int_0^{z^{i_2}} m^{i_1}(z^{i_1},\zeta^{i_1},t)m^{i_2}(z^{i_2},\zeta^{i_2},t)\times\\
&\quad\tilde{x}(z_{(i_1|\zeta^{i_1},i_2|\zeta^{i_2})},t)\mathrm{d}\zeta^{i_2}\mathrm{d}\zeta^{i_1}+\cdots\\
&+\int_0^{z^{i_{p-1}}}\int_0^{z^{i_p}} m^{i_{p-1}}(z^{i_{p-1}},\zeta^{i_{p-1}},t)m^{i_p}(z^{i_p},\zeta^{i_p},t)\times\\
&\quad\tilde{x}(z_{(i_{p-1}|\zeta^{i_{p-1}},i_p|\zeta^{i_p})},t)\mathrm{d}\zeta^{i_p}\mathrm{d}\zeta^{i_{p-1}}+\cdots\\
&+\int_0^{z^{i_1}}\cdots\int_0^{z^{i_p}} m^{i_1}(z^{i_1},\zeta^{i_1},t)\,\cdots\,m^{i_p}(z^{i_p},\zeta^{i_p},t)\times\\
&\quad\tilde{x}(z_{(i_1|\zeta^{i_1},\cdots,i_p|\zeta^{i_p})},t)\mathrm{d}\zeta^{i_p}\,\cdots\,\mathrm{d}\zeta^{i_1}.
\end{aligned} \tag{9.60}$$

Subsequently, it is shown that the transformation $\mathfrak{M}^{i_k}(z^{i_k},t)$ mapping $\tilde{w}^{i_{k-1}}(z,t)$ invertibly into $\tilde{w}^{i_k}(z,t)$ uniquely determines the corresponding observer gains

$l_1^{i_k}(z^{i_k},t)$ and $l_{10}^{i_k}(t)$. As a result, the consecutive application for all $k=1,\dots,p$ provides the transformation and the observer parametrization to achieve the exponential stability of the observer error dynamics.

In order to motivate the development, the individual analysis and solution steps are presented in detail for the application of $\mathfrak{M}^{i_1}(z^{i_1},t)$. Thereby, both the evolution of the corresponding integral kernel and the structure of the target system are deduced to conclude with the formulation of the corresponding observer gains. The sequential application of these individual steps finally yields the observer components to realize the transformation into the final target system.

9.6.2 Determination of the Kernel–PDEs and the Observer Gains

By making use of the multi–linear backstepping transformation introduced in (9.58) and (9.59) the equations governing the kernels and the observer gains can be determined simultaneously. This, however, requires an appropriate choice of the sequence of target systems. To illustrate this, in the following the expressions are evaluated for the transformation of $\tilde{x}(z,t)$ into $w^{i_1}(z,t)$. Similar to the state–feedback control design in Section 9.5, where inhomogeneous boundary conditions arise until the final m–th transformation, for the state–observer design inhomogeneous PDEs emerge up to the p–th transformation. Proceeding gradually enables to deduce the individual observer gains and the equations governing the sequence of target systems. Hence, consider first the evaluation of the ansatz $\partial_t\tilde{w}^{i_1}(z,t)-\Delta\tilde{w}^{i_1}(z,t)+\tilde{d}^{i_1}(z,t)\tilde{w}^{i_1}(z,t)$ for the i_1–th target system in view of (9.57) and (9.58). This yields after some intermediate computations that

$$
\begin{aligned}
&\partial_t\tilde{w}^{i_1}(z,t)-\Delta\tilde{w}^{i_1}(z,t)+\tilde{d}^{i_1}(z,t)\tilde{w}^{i_1}(z,t)\\
&=\big[c(z,t)+\tilde{d}^{i_1}(z,t)-2\mathrm{d}_{z^{i_1}}m^{i_1}(z^{i_1},z^{i_1},t)\big]\tilde{x}(z,t)\\
&\quad+\partial_{\zeta^{i_1}}m^{i_1}(z^{i_1},0,t)\tilde{x}(z_{(i_1|0)},t)-m^{i_1}(z^{i_1},0,t)\partial_{z^{i_1}}\tilde{x}(z_{(i_1|0)},t)\\
&\quad+\int_0^{z^{i_1}}\Big(\partial_t m^{i_1}(z^{i_1},\zeta^{i_1},t)+\partial_{\zeta^{i_1}}^2m^{i_1}(z^{i_1},\zeta^{i_1},t)-\partial_{z^{i_1}}^2m^{i_1}(z^{i_1},\zeta^{i_1},t)\\
&\qquad+\big[c(z_{(i_1|\zeta^{i_1})},t)+\tilde{d}^{i_1}(z,t)\big]m^{i_1}(z^{i_1},\zeta^{i_1},t)\Big)\tilde{x}(z_{(i_1|\zeta^{i_1})},t)\mathrm{d}\zeta^{i_1}\\
&\quad-\tilde{y}^{i_1}(z_{(i_1|)},t)\,\mathfrak{M}^{i_1}(z^{i_1},t)\circ l_1^{i_1}(z^{i_1},t)\\
&\quad-\sum_{k\in I_p^{i_1}}l_1^k(z^k,t)\,\mathfrak{M}^{i_1}(z^{i_1},t)\circ\tilde{y}^k(z_{(k|)},t)
\end{aligned}
\tag{9.61}
$$

with

$$
\tilde{y}^i(z_{(i|)},t)=h_i^0\partial_{z^i}\tilde{x}(z_{(i|0)},t)+h_i^1\tilde{x}(z_{(i|0)},t),\qquad i\in I_p. \tag{9.62}
$$

Herein, $\mathfrak{M}^{i_1}(z^{i_1},t)\circ\tilde{y}^k(z_{(k|)},t)$ can be interpreted as the mapping of $\tilde{y}^k(z_{(k|)},t) = y^k(z_{(k|)},t) - \hat{y}^k(z_{(k|)},t)$, $k \in I_r^{i_1}$, by $\mathfrak{M}^{i_1}(z^{i_1},t)$. Based on (9.61), the equations governing the kernel as well as the observer gains can be successively constructed. Differing from the procedure of 9.3, where the target system was imposed apriori and where the transformation from target system to observer error dynamics was considered, subsequently an alternative approach is proposed, which makes use the relation between $\mathfrak{M}^{i_k}(z^{i_k},t)$ and its inverse.

9.6.2.1 Determination of the Kernel–PDE

In view of condition (9.3b) of Assumption 9.2 impose

$$\tilde{d}^{i_1}(z,t) = \tilde{\mu}^{i_1}(t) - c_0(z_{(I_p|)},t) - \sum_{k=2}^{p} c_1^{i_k}(z^{i_k},t).$$

With this, the integral term in (9.61) evaluates to zero for $m^{i_1}(z^{i_1},\zeta^{i_1},t)$ satisfying

$$\begin{aligned}\partial_t m^{i_1}(z^{i_1},\zeta^{i_1},t) = \partial_{z^{i_1}}^2 m^{i_1}(z^{i_1},\zeta^{i_1},t) - \partial_{\zeta^{i_1}}^2 m^{i_1}(z^{i_1},\zeta^{i_1},t)\\ - \tilde{\gamma}^{i_1}(\zeta^{i_1},t) m^{i_1}(z^{i_1},\zeta^{i_1},t),\end{aligned} \tag{9.63a}$$

for $\tilde{\gamma}^{i_1}(\zeta^{i_1},t) := c^{i_1}(\zeta^{i_1},t) + \tilde{\mu}^{i_1}(t)$ and the domain $\zeta^{i_1} \in (0,z^{i_1})$, $z^{i_1} \in (0,L_{i_1})$. The boundary condition along $\zeta^{i_1} = z^{i_1}$ thereby follows as

$$2\mathrm{d}_{z^{i_1}} m^{i_1}(z^{i_1},z^{i_1},t) - \tilde{\gamma}^{i_1}(z^{i_1},t) = 0. \tag{9.63b}$$

Equation (9.61) hence reduces to

$$\begin{aligned}&\partial_t \tilde{w}^{i_1}(z,t) - \Delta\tilde{w}^{i_1}(z,t) + \tilde{d}^{i_1}(z,t)\tilde{w}^{i_1}(z,t)\\ &= \partial_{\zeta^{i_1}} m^{i_1}(z^{i_1},0,t)\tilde{x}(z_{(i_1|0)},t) - m^{i_1}(z^{i_1},0,t)\partial_{z^{i_1}}\tilde{x}(z_{(i_1|0)},t)\\ &\quad - \tilde{y}^{i_1}(z_{(i_1|)},t)\,\mathfrak{M}^{i_1}(z^{i_1},t)\circ l_1^{i_1}(z^{i_1},t)\\ &\quad - \sum_{k\in I_p^{i_1}} l_1^k(z^k,t)\,\mathfrak{M}^{i_1}(z^{i_1},t)\circ\tilde{y}^k(z_{(k|)},t)\end{aligned} \tag{9.64}$$

Note that the last term is independent of $l_1^{i_1}(z^{i_1},t)$ and hence represents the remaining contribution to be successively eliminated in each further transformation $\mathfrak{M}^{i_k}(z^{i_k},t)$, $k = 2,\ldots,p$. Moreover, note the following relations

$$\tilde{w}^{i_1}(z,t) = \tilde{x}(z,t) + \int_0^{z^{i_1}} m^{i_1}(z^{i_1},\zeta^{i_1},t)\,\tilde{x}(z_{(i_1|\zeta^{i_1})},t)\mathrm{d}\zeta^{i_1} \tag{9.65a}$$

$$\begin{aligned}&\partial_{z^j}\tilde{w}^{i_1}(z,t) = \partial_{z^j}\tilde{x}(z,t)\\ &\quad + \int_0^{z^{i_1}} m^{i_1}(z^{i_1},\zeta^{i_1},t)\,\partial_{z^j}\tilde{x}(z_{(i_1|\zeta^{i_1})},t)\mathrm{d}\zeta^{i_1}, \qquad j \in I_r^{i_1}\end{aligned} \tag{9.65b}$$

$$\partial_{z^{i_1}}\tilde{w}^{i_1}(z,t) = \partial_{z^{i_1}}\tilde{x}(z,t) + m^{i_1}(z^{i_1},z^{i_1},t)\tilde{x}(z,t) + \int_0^{z^{i_1}} \partial_{z^{i_1}} m^{i_1}(z^{i_1},\zeta^{i_1},t)\,\partial_{z^j}\tilde{x}(z_{(i_1|\zeta^{i_1})},t)\mathrm{d}\zeta^{i_1}, \quad i_1 \in I_p, \tag{9.65c}$$

which are frequently applied in the subsequent computations.

9.6.2.2 Determination of the Observer Gains

The degrees–of–freedom in terms of the boundary conditions for $\tilde{w}^{i_1}(z,t)$ can be suitably exploited to determine $l_1^{i_1}(z^{i_1},t)$ and $l_{10}^{i_1}(t)$. Therefore, consider (9.64) and let

$$0 = \partial_{\zeta^{i_1}} m^{i_1}(z^{i_1},0,t)\tilde{x}(z_{(i_1|0)},t) - m^{i_1}(z^{i_1},0,t)\partial_{z^{i_1}}\tilde{x}(z_{(i_1|0)},t) - \tilde{y}^{i_1}(z_{(i_1|)},t)\,\mathfrak{M}^{i_1}(z^{i_1},t)\circ l_1^{i_1}(z^{i_1},t). \tag{9.66}$$

In order to obtain a unique expression for $l_1^{i_1}(z^{i_1},t)$ or $\mathfrak{M}^{i_1}(z^{i_1},t)\circ l_1^{i_1}(z^{i_1},t)$, respectively, introduce the boundary condition

$$-\tilde{\epsilon}_{w,i_1}^0\partial_{z^{i_1}}\tilde{w}^{i_1}(z,t) + \tilde{p}_{w,i_1}^0\tilde{w}^{i_1}(z,t) = 0, \qquad z^{i_1} = 0,\ t > t_0. \tag{9.67}$$

With (9.62) and (9.65), this yields the linear system of equations

$$\begin{bmatrix} a_{11} & a_{12} \\ a_{21} & a_{22} \end{bmatrix} \begin{bmatrix} \partial_{z^{i_1}}\tilde{x}(z_{(i_1|0)},t) \\ \tilde{x}(z_{(i_1|0)},t) \end{bmatrix} = \begin{bmatrix} 0 \\ 0 \end{bmatrix} \tag{9.68}$$

with the matrix elements

$$\begin{aligned} a_{11} &= -h_{i_1}^0\,\mathfrak{M}^{i_1}(z^{i_1},t)\circ l_1^{i_1}(z^{i_1},t) - m^{i_1}(z^{i_1},0,t) \\ a_{12} &= \partial_{\zeta^{i_1}} m^{i_1}(z^{i_1},0,t) - h_{i_1}^1\,\mathfrak{M}^{i_1}(z^{i_1},t)\circ l_1^{i_1}(z^{i_1},t) \\ a_{21} &= -\tilde{\epsilon}_{w,i_1}^0 \\ a_{22} &= \tilde{p}_{w,i_1}^0 - \tilde{\epsilon}_{w,i_1}^0 m^{i_1}(0,0,t). \end{aligned}$$

A non–zero solution of (9.68) is obtained provided that

$$\mathfrak{M}^{i_1}(z^{i_1},t)\circ l_1^{i_1}(z^{i_1},t) = \begin{cases} -\dfrac{m^{i_1}(z^{i_1},0,t)}{h_{i_1}^0}, & \text{if } \tilde{\epsilon}_{w,i_1}^0 = 0 \wedge h_{i_1}^0 \neq 0 \\ -\dfrac{\left\{\begin{array}{l}\partial_{\zeta^{i_1}} m^{i_1}(z^{i_1},0,t) \\ +m^{i_1}(z^{i_1},0,t)\left(m^{i_1}(0,0,t) - \frac{\tilde{p}_{w,i_1}^0}{\tilde{\epsilon}_{w,i_1}^0}\right)\end{array}\right\}}{q_m^{i_1}(t)}, & \text{if } \tilde{\epsilon}_{w,i_1}^0 \neq 0 \wedge q_m^{i_1}(t) \neq 0. \end{cases} \tag{9.69}$$

with

$$q_m^{i_1}(t) = h_{i_1}^0 \left(m^{i_1}(0,0,t) - \frac{\tilde{p}_{w,i_1}^0}{\tilde{\epsilon}_{w,i_1}^0} \right) - h_{i_1}^1 .$$

For the computation of $l_{10}^{i_1}(t)$ note that the evaluation of (9.67) and (9.57c) for $i = i_1$ with (9.65) and (9.62) results in the linear (2×2)–system

$$\begin{bmatrix} l_{10}^{i_1}(t) h_{i_1}^0 - \epsilon_{i_1}^0 & l_{10}^{i_1}(t) h_{i_1}^1 + p_{i_1}^0 \\ -\tilde{\epsilon}_{w,i_1}^0 & \tilde{p}_{w,i_1}^0 - \tilde{\epsilon}_{w,i_1}^0 m^{i_1}(0,0,t) \end{bmatrix} \begin{bmatrix} \partial_{z^{i_1}} \tilde{x}(z_{(i_1|0)}, t) \\ \tilde{x}(z_{(i_1|0)}, t) \end{bmatrix} = \begin{bmatrix} 0 \\ 0 \end{bmatrix},$$

which only allows for a non–trivial solution if

$$l_{10}^{i_1}(t) = \begin{cases} \dfrac{\epsilon_{i_1}^0}{h_{i_1}^0}, & \text{if } \tilde{\epsilon}_{w,i_1}^0 = 0 \wedge h_{i_1}^0 \neq 0 \\ \dfrac{p_{i_1}^0 + \epsilon_{i_1}^0 \left(m^{i_1}(0,0,t) - \frac{\tilde{p}_{w,i_1}^0}{\tilde{\epsilon}_{w,i_1}^0} \right)}{q_m^{i_1}(t)}, & \text{if } \tilde{\epsilon}_{w,i_1}^0 \neq 0 \ \wedge \ q_m^{i_1}(t) \neq 0. \end{cases} \tag{9.70}$$

9.6.2.3 Kernel Relations

In order to determine $l_1^{i_1}(z^{i_1}, t)$ from (9.69) it is necessary to consider the inverse to $\mathfrak{M}^{i_1}(z^{i_1}, t)$. Similar to Section 9.4, it is known that the operator $\mathfrak{L}^{i_k}(z^{i_k}, t)$ defined according to

$$\begin{aligned} \mathfrak{L}^{i_k}(z^{i_k}, t) \circ \tilde{w}^{i_k}(z, t) = \tilde{w}^{i_k}(z_{(i_k|z^{i_k})}, t) \\ - \int_0^{z^{i_k}} l^{i_k}(z^{i_k}, \zeta^{i_k}, t) \tilde{w}^{i_k}(z_{(i_k|\zeta^{i_k})}, t) \mathrm{d}\zeta^{i_k} \end{aligned} \tag{9.71}$$

with a suitable kernel $l^{i_k}(z^{i_k}, \zeta^{i_k}, t)$ inverts $\mathfrak{M}^{i_k}(z^{i_k}, t)$. This in addition confirms the following relation.

Lemma 9.3. *Let $\mathfrak{L}^{i_k}(z^{i_k}, t)$ denote the inverse to $\mathfrak{M}^{i_k}(z^{i_k}, t)$. Then the kernels $l^{i_k}(z^{i_k}, \zeta^{i_k}, t)$ and $m^{i_k}(z^{i_k}, \zeta^{i_k}, t)$ satisfy the equality*

$$m^{i_k}(z^{i_k}, \zeta^{i_k}, t) - l^{i_k}(z^{i_k}, \zeta^{i_k}, t) = \int_{\zeta^{i_k}}^{z^{i_k}} l^{i_k}(z^{i_k}, s, t) m^{i_k}(s, \zeta^{i_k}, t) \mathrm{d}s. \tag{9.72}$$

Proof. The proof relies on the substitution of

$$\tilde{w}^{i_k}(z, t) = \mathfrak{M}^{i_k}(z^{i_k}, t) \circ \tilde{w}^{i_{k-11}}(z, t)$$

into (9.71), i.e.

$$\tilde{w}^{i_{k-1}}(z, t) = \mathfrak{L}^{i_k}(z^{i_k}, t) \circ \mathfrak{M}^{i_k}(z^{i_k}, t) \circ \tilde{w}^{i_{k-1}}(z, t)$$

$$
\begin{aligned}
&= \tilde{w}^{i_{k-1}}(z,t) + \int_0^{z^{i_k}} m^{i_k}(z^{i_k},\zeta^{i_k},t)\tilde{w}^{i_{k-1}}(z_{(i_k|\zeta^{i_k})},t)\mathrm{d}\zeta^{i_k} \\
&\quad - \int_0^{z^{i_k}} l^{i_k}(z^{i_k},\zeta^{i_k},t)\tilde{w}^{i_{k-1}}(z_{(i_k|\zeta^{i_k})},t)\mathrm{d}\zeta^{i_k} \\
&\quad - \int_0^{z^{i_k}} l^{i_k}(z^{i_k},\zeta^{i_k},t)\int_0^{\zeta^{i_k}} m^{i_k}(\zeta^{i_k},s,t)\tilde{w}^{i_{k-1}}(z_{(i_k|s)},t)\mathrm{d}s\,\mathrm{d}\zeta^{i_k}.
\end{aligned}
$$

This implies

$$
\begin{aligned}
0 &= \int_0^{z^{i_k}} \Big(m^{i_k}(z^{i_k},\zeta^{i_k},t) - l^{i_k}(z^{i_k},\zeta^{i_k},t)\Big)\tilde{w}^{i_{k-1}}(z_{(i_k|\zeta^{i_k})},t)\mathrm{d}\zeta^{i_k} \\
&\quad - \int_0^{z^{i_k}} l^{i_k}(z^{i_k},\zeta^{i_k},t)\int_0^{\zeta^{i_k}} m^{i_k}(\zeta^{i_k},s,t)\tilde{w}^{i_{k-1}}(z_{(i_k|s)},t)\mathrm{d}s\,\mathrm{d}\zeta^{i_k}. \qquad (9.73)
\end{aligned}
$$

By an interchange of the order of integration, the last integral fulfills

$$
\begin{aligned}
&\int_0^{z^{i_k}} l^{i_k}(z^{i_k},\zeta^{i_k},t)\int_0^{\zeta^{i_k}} m^{i_k}(\zeta^{i_k},s,t)\tilde{w}^{i_{k-1}}(z_{(i_k|s)},t)\mathrm{d}s\,\mathrm{d}\zeta^{i_k} \\
&\qquad = \int_0^{z^{i_k}} \tilde{w}^{i_{k-1}}(z_{(i_k|\zeta^{i_k})},t)\int_{\zeta^{i_k}}^{z^{i_k}} l^{i_k}(z^{i_k},s,t)m^{i_k}(s,\zeta^{i_k},t)\mathrm{d}s\,\mathrm{d}\zeta^{i_k},
\end{aligned}
$$

which together with (9.73) yields (9.72) since $\tilde{w}^{i_{k-1}}(z,t)$ is arbitrary. □

By making use of (9.72), expression (9.69) can be re–formulated in terms of the kernel $l^{i_1}(z^{i_1},\zeta^{i_1},t)$, which after some intermediate computations results in

$$
\begin{aligned}
l_1^{i_1}(z^{i_1},t) &= \mathfrak{L}^{i_1}(z^{i_1},t)\circ\mathfrak{M}^{i_1}(z^{i_1},t)\circ l_1^{i_1}(z^{i_1},t) \\
&= \begin{cases} -\dfrac{l^{i_1}(z^{i_1},0,t)}{h_{i_1}^0}, & \text{if } \tilde{\epsilon}_{w,i_1}^0 = 0 \wedge h_{i_1}^0 \neq 0 \\ -\dfrac{\partial_{\zeta^{i_1}} l^{i_1}(z^{i_1},0,t) - \frac{\tilde{p}_{w,i_1}^0}{\tilde{\epsilon}_{w,i_1}^0} l^{i_1}(z^{i_1},0,t)}{q_l^{i_1}(t)}, & \text{if } \tilde{\epsilon}_{w,i_1}^0 \neq 0 \ \wedge\ q_l^{i_1}(t) \neq 0. \end{cases} \qquad (9.74)
\end{aligned}
$$

with

$$
q_l^{i_1}(t) = h_{i_1}^0\left(l^{i_1}(0,0,t) - \frac{\tilde{p}_{w,i_1}^0}{\tilde{\epsilon}_{w,i_1}^0}\right) - h_{i_1}^1.
$$

The correspondence to (9.27) for the single output case is hence clearly visible. It is thereby remarked that the determination of (9.74) requires

(i) to evaluate the application of $\mathfrak{L}^{i_1}(z^{i_1},t)$ to (9.69) and to take into account that (9.67) can be re–written as

$$-\tilde{\epsilon}^0_{w,i_1}\Big(\partial_{z^{i_1}}\tilde{x}(z,t)+m^{i_1}(0,0,t)\tilde{x}(z,t)\Big)+\tilde{p}^0_{w,i_1}\tilde{x}(z,t)=0,\quad z^{i_1}=0$$

using (9.65);

(ii) to substitute (9.72) as well as its obvious corollary

$$\partial_{\zeta^{i_k}}l^{i_k}(z^{i_k},0,t)-\partial_{\zeta^{i_k}}m^{i_k}(z^{i_k},0,t)-l^{i_k}(z^{i_k},0,t)m^{i_k}(0,0,t)+\int_0^{z^{i_k}}l^{i_k}(z^{i_k},s,t)\partial_{\zeta^{i_k}}m^{i_k}(s,0,t)\mathrm{d}s=0.$$

Finally, sorting terms for the two cases $\tilde{\epsilon}^0_{w,i_1}=0$ or $\tilde{\epsilon}^0_{w,i_1}\neq 0$ provides (9.74).

In addition, taking into account (9.72) and hence $m^{i_1}(0,0,t)=l^{i_1}(0,0,t)$ an equivalent formulation for $l^{i_1}_{10}(t)$ defined in (9.70) is obtained satisfying

$$l^{i_1}_{10}(t)=\begin{cases}\dfrac{\epsilon^0_{i_1}}{h^0_{i_1}}, & \text{if } \tilde{\epsilon}^0_{w,i_1}=0\wedge h^0_{i_1}\neq 0\\[2ex] \dfrac{p^0_{i_1}+\epsilon^0_{i_1}\Big(l^{i_1}(0,0,t)-\frac{\tilde{p}^0_{w,i_1}}{\tilde{\epsilon}^0_{w,i_1}}\Big)}{q^{i_1}_l(t)}, & \text{if}\tilde{\epsilon}^0_{w,i_1}\neq 0\ \wedge\ q^{i_1}_l(t)\neq 0.\end{cases}\tag{9.75}$$

In particular observe that (9.75) is, as expected, identical to (9.28) with $l(0,0,t)$ replaced by $l^{i_1}(0,0,t)$.

9.6.2.4 Determination of the Boundary Conditions for the Target System

In view of (9.65), it can be easily shown using (9.57b)–(9.57d) that the boundary conditions for $\tilde{w}^{i_1}(z,t)$ at $z^j\in\{0,L_j\},\ j\in I^{i_1}_r$ follow as

$$-\epsilon^0_j\partial_{z^j}\tilde{w}^{i_1}(z,t)+p^0_j\tilde{w}^{i_1}(z,t)=0,\qquad z^j=0,\ j\in I^{I_p}_r\tag{9.76a}$$

$$-\epsilon^0_j\partial_{z^j}\tilde{w}^{i_1}(z,t)+p^0_j\tilde{w}^{i_1}(z,t)=-l^j_{10}(t)\,\mathfrak{M}^{i_1}(z^{i_1},t)\circ\tilde{y}^j(z_{(j|)},t),\qquad z^j=0,\ j\in I^{i_1}_p\tag{9.76b}$$

$$\epsilon^1_j\partial_{z^j}\tilde{w}^{i_1}(z,t)+p^1_j\tilde{w}^{i_1}(z,t)=0,\qquad z^j=L_j,\ j\in I^{i_1}_r\tag{9.76c}$$

for $t>t_0$ with

$$\mathfrak{M}^{i_1}(z^{i_1},t)\circ\tilde{y}^j(z_{(j|)},t)=h^0_j\partial_{z^j}\tilde{w}^{i_1}(z_{(j|0)},t)+h^1_j\tilde{w}^{i_1}(z_{(j|0)},t).\tag{9.77}$$

The latter equation confirms that $\mathfrak{M}^{i_1}(z^{i_1},t)\circ\tilde{y}^j(z_{(j|)},t)$, $j\in I^{i_1}_r$, is identical to $\tilde{y}^j(z_{(j|)},t)$ with $\tilde{x}(z,t)$ replaced by $\tilde{w}^{i_1}(z,t)$.

Similar to (9.67) the boundary condition for $\tilde{w}^{i_1}(z,t)$ at $z^{i_1}=L_{i_1}$ can be considered as a degree–of–freedom and is subsequently imposed in the form

$$\tilde{\epsilon}^1_{w,i_1}\partial_{z^{i_1}}\tilde{w}^{i_1}(z,t)+\tilde{p}^1_{w,i_1}\tilde{w}^{i_1}(z,t)=0,\qquad z^{i_1}=L_{i_1},\ t>t_0.\tag{9.78}$$

Additional constraints on the parameters $\tilde{\epsilon}^1_{w,i_1}$ and $\tilde{p}^1_{w,i_1}$ arise from the substitution of (9.65) in view of the respective boundary condition (9.57d) for the observer error. This simultaneously yields the remaining boundary condition for the integral kernel $m^{i_1}(z^{i_1}, \zeta^{i_1}, t)$.

9.6.2.5 Determination of the Remaining Boundary Conditions for the Kernel

The joint evaluation of (9.78) and (9.57d) for $i = i_1 \in I_p$ with (9.65) yields the following conditions:

(i) If $\epsilon^1_{i_1} = 0$, $p^1_{i_1} \neq 0$, then

$$m^{i_1}(L_{i_1}, \zeta^{i_1}, t) = 0 \tag{9.79}$$

while the target boundary condition (9.78) is restricted to satisfy $\tilde{\epsilon}^1_{w,i_1} = 0$, i.e. $\tilde{w}^{i_1}(z_{(i_1|L_i)}, t) = 0$.

(ii) If $\epsilon^1_{i_1} \neq 0$, then the kernel is restricted to

$$\partial_{z^{i_1}} m^{i_1}(L_{i_1}, \zeta^{i_1}, t) + \frac{\tilde{p}^1_{w,i_1}}{\tilde{\epsilon}^1_{w,i_1}} m^{i_1}(L_{i_1}, \zeta^{i_1}, t) = 0 \tag{9.80a}$$

$$m^{i_1}(L_{i_1}, L_{i_1}, t) = \frac{p^1_{i_1}}{\epsilon^1_{i_1}} - \frac{\tilde{p}^1_{w,i_1}}{\tilde{\epsilon}^1_{w,i_1}} \tag{9.80b}$$

with the target system being required to fulfill $\tilde{\epsilon}^1_{w,i_1} \neq 0$.

These computations for the transformation of $\tilde{x}(z,t)$ into $\tilde{w}^{i_1}(z,t)$ are subsequently exploited to deduce the structure of the individual target systems, which are realized by the consecutive application of the individual backstepping transformations according to (9.59).

9.6.2.6 Sequential Evaluation of the Multi–linear Backstepping–Transformation

As a result of the presented procedure, the dynamics of the target system $\tilde{w}^{i_1}(z,t)$ is obtained from (9.64) according to

$$\begin{aligned}\partial_t \tilde{w}^{i_1}(z,t) = {} & \Delta \tilde{w}^{i_1}(z,t) - \tilde{d}^{i_1}(z,t)\tilde{w}^{i_1}(z,t) \\ & - \sum_{k \in I_p^{i_1}} l_1^k(z^k,t)\left[h_k^0 \partial_{z^k} \tilde{w}^{i_1}(z_{(k|0)},t) + h_k^1 \tilde{w}^{i_1}(z_{(k|0)},t)\right], \end{aligned} \tag{9.81a}$$

where the latter term follows from (9.77) and the domain is given by $(z,t) \in \Omega \times \mathbb{R}^+_{t_0}$. Herein, the spatially and time varying coefficient satisfies

$$\tilde{d}^{i_1}(z,t) = \tilde{\mu}^{i_1}(t) - c_0(z_{(I_p|)},t) - \sum_{k=2}^{p} c_1^{i_k}(z^{i_k},t)$$

with the boundary conditions from (9.67), (9.76), and (9.78), i.e.

$$\begin{aligned}
&-\epsilon_j^0 \partial_{z^j}\tilde{w}^{i_1}(z,t) + p_j^0 \tilde{w}^{i_1}(z,t) = 0, && z^j = 0,\ j \in I_r^{I_p} && \text{(9.81b)}\\
&-\epsilon_j^0 \partial_{z^j}\tilde{w}^{i_1}(z,t) + p_j^0 \tilde{w}^{i_1}(z,t) = \\
&\qquad - l_{10}^j(t)\big[h_j^0 \partial_{z^j}\tilde{w}^{i_1}(z,t) + h_j^1 \tilde{w}^{i_1}(z,t)\big], && z^j = 0,\ j \in I_p^{i_1} && \text{(9.81c)}\\
&-\tilde{\epsilon}_{w,i_1}^0 \partial_{z^{i_1}}\tilde{w}^{i_1}(z,t) + \tilde{p}_{w,i_1}^0 \tilde{w}^{i_1}(z,t) = 0, && z^{i_1} = 0 && \text{(9.81d)}\\
&\epsilon_j^1 \partial_{z^j}\tilde{w}^{i_1}(z,t) + p_j^1 \tilde{w}^{i_1}(z,t) = 0, && z^j = L_j,\ j \in I_r^{i_1} && \text{(9.81e)}\\
&\tilde{\epsilon}_{w,i_1}^1 \partial_{z^{i_1}}\tilde{w}^{i_1}(z,t) + \tilde{p}_{w,i_1}^1 \tilde{w}^{i_1}(z,t) = 0, && z^{i_1} = L_{i_1} && \text{(9.81f)}
\end{aligned}$$

for $t > t_0$ and the initial condition

$$\tilde{w}^{i_1}(z,t_0) = \tilde{w}_0^{i_1}(z), \qquad z \in \overline{\Omega}. \qquad \text{(9.81g)}$$

In this setting the observer observer gains $l_1^{i_1}(z^{i_1},t)$ and $l_{10}^{i_1}(t)$ are determined by (9.74) and (9.75).

Proceeding as above for $i_2,\ i_3, \ldots, i_p$, i.e. mapping $\tilde{w}^{i_{k-1}}(z,t)$ into $\tilde{w}^{i_k}(z,t)$, $k = 2,\ 3, \ldots, p$, by means of $\mathfrak{M}^{i_k}(z^{i_k},t)$, directly provides the evaluation of the multi–linear backstepping–transformation into the target system $\tilde{w}(z,t)$. The previous analysis illustrates that each transformation determines the corresponding observer gains[3] $l_1^{i_k}(z^{i_k},t)$ and $l_{10}^{i_k}(t)$ according to (9.74) and (9.75) with i_1 replaced by i_k, i.e.

$$l_1^{i_k}(z^{i_k},t) = \begin{cases} -\dfrac{l^{i_k}(z^{i_k},0,t)}{h_{i_k}^0}, & \text{if } \tilde{\epsilon}_{w,i_k}^0 = 0 \wedge h_{i_k}^0 \neq 0 \\ -\dfrac{\partial_{\zeta^{i_k}} l^{i_k}(z^{i_k},0,t) - \frac{\tilde{p}_{w,i_k}^0}{\tilde{\epsilon}_{w,i_k}^0} l^{i_k}(z^{i_k},0,t)}{q_l^{i_k}(t)}, & \text{if } \tilde{\epsilon}_{w,i_k}^0 \neq 0 \wedge q_l^{i_k}(t) \neq 0 \end{cases} \qquad \text{(9.82a)}$$

$$l_{10}^{i_k}(t) = \begin{cases} \dfrac{\epsilon_{i_k}^0}{h_{i_k}^0}, & \text{if } \tilde{\epsilon}_{w,i_k}^0 = 0 \wedge h_{i_k}^0 \neq 0 \\ \dfrac{p_{i_k}^0 + \epsilon_{i_k}^0\left(l^{i_k}(0,0,t) - \frac{\tilde{p}_{w,i_k}^0}{\tilde{\epsilon}_{w,i_k}^0}\right)}{q_l^{i_k}(t) \neq 0}, & \text{if } \tilde{\epsilon}_{w,i_k}^0 \neq 0 \wedge q_l^{i_k}(t) \neq 0, \end{cases} \qquad \text{(9.82b)}$$

where

[3] Similar to the 1–dimensional and the single output case the arising conditionals for the computation of $l_1^{i_k}(z^{i_k},t)$ and $l_{10}^{i_k}(t)$ can be fulfilled by a suitable choice of the parameters of the target system by taking into account Remark 8.3.

$$q_l^{i_k}(t) = h_{i_k}^0\left(l^{i_k}(0,0,t) - \frac{\tilde{p}_{w,i_k}^0}{\tilde{\epsilon}_{w,i_k}^0}\right) - h_{i_k}^1,$$

in such a way that after $\#I_p = p$ consecutive transformations the distributed–parameter system governing $\tilde{w}(z,t)$ is homogeneous. The corresponding transformation kernels $m^{i_k}(z^{i_k},\zeta^{i_k},t)$, $i_k \in I_p$, are thereby governed by (9.63) with either (9.79) or (9.80) for i_1 replaced by i_k, i.e.

$$\begin{aligned}\partial_t m^{i_k}(z^{i_k},\zeta^{i_k},t) = \partial_{z^{i_k}}^2 m^{i_k}(z^{i_k},\zeta^{i_k},t) - \partial_{\zeta^{i_k}}^2 m^{i_k}(z^{i_k},\zeta^{i_k},t)\\ - \tilde{\gamma}^{i_k}(\zeta^{i_k},t) m^{i_k}(z^{i_k},\zeta^{i_k},t)\end{aligned} \tag{9.83a}$$

with $\zeta^{i_k} \in (0, z^{i_k})$, $z^{i_k} \in (0, L_{i_k})$, $t > t_0$ and

$$2\mathrm{d}_{z^{i_k}} m^{i_k}(z^{i_k},z^{i_k},t) - \tilde{\gamma}^{i_k}(z^{i_k},t) = 0 \tag{9.83b}$$

$$\begin{cases} m^{i_k}(L_{i_k},\zeta^{i_k},t) = 0, & \text{if } \epsilon_{i_k}^1 = 0 \wedge p_{i_k}^1 \neq 0 \wedge \tilde{\epsilon}_{w,i_k}^1 = 0 \\ \begin{cases} \partial_{z^{i_k}} m^{i_k}(L_{i_k},\zeta^{i_k},t) \\ \quad + \frac{\tilde{p}_{w,i_k}^1}{\tilde{\epsilon}_{w,i_k}^1} m^{i_k}(L_{i_k},\zeta^{i_k},t) = 0 \\ m^{i_k}(L_{i_k},L_{i_k},t) = \frac{p_{i_k}^1}{\epsilon_{i_k}^1} - \frac{\tilde{p}_{w,i_k}^1}{\tilde{\epsilon}_{w,i_k}^1} \end{cases}, & \text{if } \epsilon_{i_k}^1 \neq 0 \ \wedge\ \tilde{\epsilon}_{w,i_k}^1 \neq 0 \end{cases} \tag{9.83c}$$

and $\tilde{\gamma}^{i_k}(\cdot,t) := c^{i_k}(\cdot,t) + \tilde{\mu}^{i_k}(t)$. The verification of this property can be directly obtained by means of an induction argument, which is however omitted subsequently due to the straight forward technical procedure.

As a result, it is a trivial consequence of the previous analysis that the target system $\tilde{w}(z,t) := \tilde{w}^{i_p}(z,t)$ fulfills

$$\partial_t \tilde{w}(z,t) = \Delta\tilde{w}(z,t) - \tilde{d}(z,t)\tilde{w}(z,t) \tag{9.84a}$$

with domain $(z,t) \in \Omega \times \mathbb{R}_{t_0}^+$ and $\tilde{d}(z,t) = \tilde{d}^{i_p}(z,t)$, where[4]

$$\tilde{d}^{i_k}(z,t) = \sum_{j=1}^{k} \tilde{\mu}^{i_j}(t) - c_0(z_{(I_p|)},t) - \sum_{j=k+1}^{p} c_1^{i_j}(z^{i_j},t) \tag{9.84b}$$

in view of Assumption 9.2. The boundary conditions thereby follow as

$$-\epsilon_j^0 \partial_{z^j}\tilde{w}(z,t) + p_j^0 \tilde{w}(z,t) = 0, \qquad z^j = 0,\ j \in I_r^{I_p} \tag{9.84c}$$

$$-\tilde{\epsilon}_{w,j}^0 \partial_{z^j}\tilde{w}(z,t) + \tilde{p}_{w,j}^0 \tilde{w}(z,t) = 0, \qquad z^j = 0,\ j \in I_p \tag{9.84d}$$

$$\epsilon_j^1 \partial_{z^j}\tilde{w}(z,t) + p_j^1 \tilde{w}(z,t) = 0, \qquad z^j = L_j,\ j \in I_r^{I_p} \tag{9.84e}$$

[4] Equivalently, $\tilde{\mu}^{i_j}(t)$ can be replaced by $\tilde{\mu}^{i_j}(z^{i_j},t)$. This, however, requires to reanalyze the stability of the resulting target system by suitably extending Lemma 9.2.

$$\tilde{\epsilon}^1_{w,j}\partial_{z^j}\tilde{w}(z,t)+\tilde{p}^1_{w,j}\tilde{w}(z,t)=0, \qquad z^j=L_j,\ j\in I_p \tag{9.84f}$$

for $t>t_0$ and the initial condition

$$\tilde{w}(z,t_0)=\tilde{w}_0(z), \qquad z\in\overline{\Omega}. \tag{9.84g}$$

The exponential stability of (9.84) in the L^2–norm can be directly ensured for a suitable choice of $\tilde{\mu}(t)=\sum_{j=1}^{p}\tilde{\mu}^{i_j}(t)$ by Lemma 9.2 provided that

$$\tilde{c}_0(t)=\sup_{z_{(I_p|)}\in\bigtimes_{j\in I_r\setminus I_p}[0,L_j]} c_0(z_{(I_p|)},t)$$

exists and is bounded for all $t\in\mathbb{R}^+_{t_0}$.

9.6.3 Solution of the Kernel–PDEs

Due to the equivalence of the equations (9.83) governing $m^{i_k}(z^{i_k},\zeta^{i_k},t)$ for each $i_k\in I_p$, and the equations (9.25) for the case of a single observer gain, the solution of the kernel–PDE follows exactly the presentation in Section 9.3.3 and is hence omitted. However, it is crucial to recall that the convergence of the successive approximations can be ensured under the conditions of Theorems 8.4 and 8.5. In addition, this confirms that $m^{i_k}(z^{i_k},\zeta^{i_k},t)$ for each $i_k\in I_p$ is a strong solution to the kernel–PDE, which is of Gevrey order $\alpha\in[1,2]$ in t and bounded with bounded derivative with respect to z^{i_k} and ζ^{i_k}.

9.6.4 Inverse Backstepping–Transformation and Exponential Stability of the Observer Error Dynamics

In the course of the procedure presented in Section 9.6.2, the inverse transformation (9.71) is used to determine the observer gain (9.74). Hence, generalizing this approach it can be easily seen that the consecutive application of (9.71) in terms of the transformation sequence

$$\begin{aligned}
\tilde{x}^{i_{p-1}}(z,t)&=\mathfrak{L}^{i_p}(z^{i_p},t)\circ\tilde{w}(z,t)\\
\tilde{x}^{i_{p-2}}(z,t)&=\mathfrak{L}^{i_{p-1}}(z^{i_{p-1}},t)\circ\tilde{x}^{i_{p-1}}(z,t)\\
&\vdots\\
\tilde{x}(z,t)&=\mathfrak{L}^{i_1}(z^{i_1},t)\circ\tilde{x}^{i_1}(z,t)\\
&=\underbrace{\mathfrak{L}^{i_1}(z^{i_1},t)\circ\mathfrak{L}^{i_2}(z^{i_2},t)\circ\cdots\circ\mathfrak{L}^{i_p}(z^{i_p},t)}_{=\bar{\mathfrak{L}}^{p}(z_{(I_r\setminus I_p|)},t)}\circ\tilde{w}(z,t)
\end{aligned} \tag{9.85}$$

inverts the multi–linear Volterra–type transformation (9.59). The individual kernels $l^{i_k}(z^{i_k},\zeta^{i_k},t)$, $k=1,\ldots,p$ can be determined by proceeding in principle as in

Section 9.6.2 by making use of (9.74), (9.75), and the relationship (9.72) between the integral kernels. This shows after some tedious intermediate computations that the governing equations for the inverse kernel $l^{i_k}(z^{i_k},\zeta^{i_k},t)$ correspond to those (9.83) for $m^{i_k}(z^{i_k},\zeta^{i_k},t)$ with $\tilde{\gamma}^{i_k}(\zeta^{i_k},t)$ replaced by $-\tilde{\gamma}^{i_k}(z^{i_k},t)$ and $\tilde{p}^1_{w,i_k}$, $\tilde{\epsilon}^1_{w,i_k}$ in (9.83c) exchanged with $p^1_{i_k}$, $\epsilon^1_{i_k}$. As a result, the solution procedure in terms of the method of integral operators and successive approximations as well as the convergence proof can be applied. The solution approach in addition yields that each $l^{i_k}(z^{i_k},\zeta^{i_k},t)$ is bounded with bounded derivative with respect to z^{i_k} and ζ^{i_k} and is of Gevrey order $\alpha\in[1,2]$ in t under the conditions of Theorems 8.1 and 8.2.

Theorem 9.5. *Consider the observer error dynamics* (9.57) *with the observer gains* (9.82a) *and* (9.82b)*. Then the equilibrium* $\tilde{x}(z,t)\equiv 0$ *is exponentially stable for all* $t\in\mathbb{R}^+_{t_0}$ *in the* L^2*–norm if the target system* (9.84) *satisfies the conditions of Lemma 9.2.*

The proof follows exactly the lines of the proof of Theorem 9.4.

Proof. Let $X=L^2(\Omega)$ and assume $\tilde{x}_0(z)$, $\tilde{w}_0(z)\in X$. Since both $l^{i_k}(z^{i_k},\zeta^{i_k},t)$ and $m^{i_k}(z^{i_k},\zeta^{i_k},t)$ are strong and bounded solutions to the respective kernel–PDEs for all $k=1,\ldots,p$ it follows by the Minkowski and Cauchy–Schwarz inequality that

$$\|\tilde{w}_0^{i_k}\|_X\le C_0^{i_k}\|\tilde{w}_0^{i_{k-1}}\|_X$$

with $C_0^{i_k}=1+L_{i_k}\sup_{(z^{i_k},\zeta^{i_k})\in\Theta_0^{i_k}}|m^{i_k}(z^{i_k},\zeta^{i_k},t)|$ for the set $\Theta_0^{i_k}=\{(z^{i_k},\zeta^{i_k}):\zeta^{i_k}\in[0,L_{i_k}],\ z^{i_k}\in[\zeta^{i_k},L_{i_k}]\}$. Thus, $\|\tilde{w}_0\|_X\le C_0\|\tilde{x}_0\|_X$ for $C_0=\prod_{i_k\in I_m}C_0^{i_k}$, which in view of (9.84) and Lemma 9.2 yields

$$\|\tilde{w}(t)\|_X\le e^{-\kappa(t)}\|\tilde{w}_0\|_X\le C_0e^{-\kappa(t)}\|\tilde{x}_0\|_X$$

for $\kappa(t)=\int_{t_0}^t(\sum_{j=1}^p\tilde{\mu}^{i_j}(s)+\lambda_{\min}-\tilde{c}_0(s))\mathrm{d}s$. In view of (9.85), a similar procedure provides in view of the boundedness of $l^{i_k}(z^{i_k},\zeta^{i_k},t)$ that there exists a constant C_1 such that

$$\|\tilde{x}(t)\|_X\le C_1\|\tilde{w}(t)\|_X\le C_0C_1e^{-\kappa(t)}\|\tilde{x}_0\|_X.$$

Hence, $\kappa(t)>\epsilon>0$ implies exponential stability of the closed–loop system. □

9.6.5 Separation Principle and Exponential Stability of the Closed–Loop System

In a way similar to Section 9.3.5 the stability analysis of the closed–loop MIMO system consisting of the state–feedback control (9.53) and the state–observer (9.56) requires to analyze the target system in $[w(z,t),\tilde{w}(z,t)]^T$ obtained from[5]

[5] For the sake of simplicity the arguments of $\bar{\mathfrak{K}}^{I_m}$ and $\bar{\mathfrak{M}}^{I_p}$ are dropped throughout this section.

$$\begin{bmatrix} w(z,t) \\ \tilde{w}(z,t) \end{bmatrix} = \begin{bmatrix} \bar{\mathfrak{K}}^{I_m} \circ \hat{x}(z,t) \\ \bar{\mathfrak{M}}^{I_p} \circ \tilde{x}(z,t) \end{bmatrix}$$

with $\bar{\mathfrak{K}}^{I_m}$ and $\bar{\mathfrak{M}}^{I_p}$ as introduced in (9.45) and (9.59), respectively. For this, it is subsequently assumed that the number m of inputs and p of outputs coincide with $I_m = I_p$, i.e. each input is located opposite to an output[6]. The main difference in the analysis of the MIMO system arises in the evaluation of the transformation into $w(z,t)$ in terms of the observer state $\hat{x}(z,t) = x(z,t) - \tilde{x}(z,t)$ such that

$$w(z,t) = \bar{\mathfrak{K}}^{I_m} \circ x(z,t) - \bar{\mathfrak{K}}^{I_m} \circ \tilde{x}(z,t). \tag{9.86}$$

As is shown below, this induces a coupling of the resulting target systems. Here, the first term serves as the basis for the determination of the state–feedback control in Section 9.5. It hence suffices to evaluate the second term, for which after some intermediate computations the following two relations

$$\begin{aligned}
\Delta\big(\bar{\mathfrak{K}}^{I_m} \circ \tilde{x}(z,t)\big) &= \bar{\mathfrak{K}}^{I_m} \circ \sum_{j \in I_r^{I_m}} \partial_{z^j}^2 \tilde{x}(z,t) \\
&\quad + \sum_{k=1}^{m} \bar{\mathfrak{K}}_{i_k}^{I_m} \circ \Big(\partial_{z^{i_k}}^2 \tilde{x}(z,t) - \mathrm{d}_{z^{i_k}} k^{i_k}(z^{i_k}, z^{i_k}, t) \tilde{x}(z,t) \\
&\qquad - k^{i_k}(z^{i_k}, z^{i_k}, t) \partial_{z^{i_k}} \tilde{x}(z,t) - \partial_{z^{i_k}} k^{i_k}(z^{i_k}, z^{i_k}, t) \tilde{x}(z,t) \\
&\qquad - \int_0^{z^{i_k}} \partial_{z^{i_k}}^2 k^{i_k}(z^{i_k}, \zeta^{i_k}, t) \tilde{x}(z_{(i_k|\zeta^{i_k})}, t) \mathrm{d}\zeta^{i_k} \Big)
\end{aligned} \tag{9.87a}$$

$$\begin{aligned}
\partial_t\big(\bar{\mathfrak{K}}^{I_m} \circ \tilde{x}(z,t)\big) &= \bar{\mathfrak{K}}^{I_m} \circ \partial_t \tilde{x}(z,t) \\
&\qquad - \sum_{k=1}^{m} \bar{\mathfrak{K}}_{i_k}^{I_m} \circ \int_0^{z^{i_k}} \partial_t k^{i_k}(z^{i_k}, \zeta^{i_k}, t) \tilde{x}(z_{(i_k|\zeta^{i_k})}, t) \mathrm{d}\zeta^{i_k} \\
&= \bar{\mathfrak{K}}^{I_m} \circ \sum_{j \in I_r^{I_m}} \partial_{z^j}^2 \tilde{x}(z,t) + \bar{\mathfrak{K}}^{I_m} \circ \big(c(z,t)\tilde{x}(z,t)\big) \\
&\quad - \bar{\mathfrak{K}}^{I_m} \circ \sum_{i \in I_p} l_1^i(z^i, t) \big[h_i^0 \partial_{z^i} \tilde{x}(z_{(i|0)}, t) + h_i^1 \tilde{x}(z_{(i|0)}, t)\big] \\
&\quad + \sum_{k=1}^{m} \bar{\mathfrak{K}}_{i_k}^{I_m} \circ \Big(\partial_{z^{i_k}}^2 \tilde{x}(z,t) - \big[k^{i_k}(z^{i_k}, \zeta^{i_k}, t) \partial_{\zeta^{i_k}} \tilde{x}(z_{(i_k|\zeta^{i_k})}, t) \\
&\qquad - \partial_{\zeta^{i_k}} k^{i_k}(z^{i_k}, \zeta^{i_k}, t) \tilde{x}(z_{(i_k|\zeta^{i_k})}, t)\big]_{\zeta^{i_k}=0}^{z^{i_k}} \\
&\quad - \int_0^{z^{i_k}} \big[\partial_t k^{i_k}(z^{i_k}, \zeta^{i_k}, t) + \partial_{\zeta^{i_k}}^2 k^{i_k}(z^{i_k}, \zeta^{i_k}, t)\big] \tilde{x}(z_{(i_k|\zeta^{i_k})}, t) \mathrm{d}\zeta^{i_k} \Big)
\end{aligned} \tag{9.87b}$$

[6] The more general situation with $I_m \neq I_p$ is briefly discussed at the end of this section.

can be verified by making use of the PDE (9.57a) of the observer error dynamics and by recalling that $\bar{\mathfrak{K}}^{I_m}$ is a linear, commutative, and associative operator. Herein, the abbreviation

$$\bar{\mathfrak{K}}^{I_m}_{i_k} = \mathfrak{K}^{i_m}(z^{i_m},t) \circ \cdots \circ \mathfrak{K}^{i_{k+1}}(z^{i_{k+1}},t) \circ \mathfrak{K}^{i_{k-1}}(z^{i_{k-1}},t) \circ \cdots \circ \mathfrak{K}^{i_1}(z^{i_1},t)$$

is used. With this, the evaluation of the target–PDE (9.51a) yields

$$\begin{aligned}
&\partial_t w(z,t) - \Delta w(z,t) + d(z,t)w(z,t)\\
&= \partial_t\big(\bar{\mathfrak{K}}^{I_m} \circ x(z,t)\big) - \Delta\big(\bar{\mathfrak{K}}^{I_m} \circ x(z,t)\big) + d(z,t)\bar{\mathfrak{K}}^{I_m} \circ x(z,t)\\
&\quad - \Big(\partial_t\big(\bar{\mathfrak{K}}^{I_m} \circ \tilde{x}(z,t)\big) - \Delta\big(\bar{\mathfrak{K}}^{I_m} \circ \tilde{x}(z,t)\big) + d(z,t)\bar{\mathfrak{K}}^{I_m} \circ \tilde{x}(z,t)\Big).
\end{aligned}$$

While the terms involving $x(z,t)$ by construction (cf. Section 9.5) equal zero the last line represents the interconnection between the $w(z,t)$ and the $\tilde{w}(z,t)$ dynamics. To clarify this, consider (9.87), which in view of Assumption 9.2 implies

$$\begin{aligned}
&\partial_t w(z,t) - \Delta w(z,t) + d(z,t)w(z,t)\\
&= \sum_{k=1}^{m} \bar{\mathfrak{K}}^{I_m}_{i_k} \circ \Bigg(\int_0^{z^{i_k}} \big[\partial_t k^{i_k}(z^{i_k},\zeta^{i_k},t) + \partial^2_{\zeta^{i_k}} k^{i_k}(z^{i_k},\zeta^{i_k},t)\\
&\qquad\qquad - \partial^2_{z^{i_k}} k^{i_k}(z^{i_k},\zeta^{i_k},t) + \big[c_1^i(\zeta^{i_k},t) + \mu^{i_k}(t)\big)\big]\tilde{x}(z_{(i_k|\zeta^{i_k})},t)\mathrm{d}\zeta^{i_k}\\
&\qquad + \big[\mathrm{d}_{z^{i_k}} k^{i_k}(z^{i_k},z^{i_k},t) + c_1^{i_k}(z^{i_k},t) + \mu^{i_k}(t)\big]\tilde{x}(z,t)\\
&\qquad - k^{i_k}(z^{i_k},0,t)\partial_{z^{i_k}}\tilde{x}(z_{(i_k|0)},t) + \partial_{\zeta^{i_k}} k^{i_k}(z^{i_k},0,t)\tilde{x}(z_{(i_k|0)},t)\Bigg)\\
&\qquad + \bar{\mathfrak{K}}^{I_m} \circ \sum_{i\in I_p} l_1^i(z^i,t)\big[h_i^0\partial_{z^i}\tilde{x}(z_{(i|0)},t) + h_i^1\tilde{x}(z_{(i|0)},t)\big].
\end{aligned} \tag{9.88}$$

Thereby, given $d(z,t) = d^{i_m}(z,t)$ with (9.49) the sequence of equalities

$$\begin{aligned}
&\bar{\mathfrak{K}}^{I_m} \circ \big(c(z,t)\tilde{x}(z,t)\big) + d(z,t)\bar{\mathfrak{K}}^{I_m} \circ \tilde{x}(z,t)\\
&= \bar{\mathfrak{K}}^{I_m} \circ \Bigg(\sum_{k=1}^{m} c_1^i(z^{i_k},t)\tilde{x}(z,t)\Bigg) + \sum_{k=1}^{m} \mu^{i_k}(t)\bar{\mathfrak{K}}^{I_m} \circ \tilde{x}(z,t)\\
&= \sum_{k=1}^{m} \bar{\mathfrak{K}}^{I_m}_{i_k} \circ \Bigg(\big(c_1^i(z^{i_k},t) + \mu^{i_k}(t)\big)\tilde{x}(z,t)\\
&\qquad\qquad - \int_0^{z^{i_k}} k^{i_k}(z^{i_k},\zeta^{i_k},t)\big(c_1^i(\zeta^{i_k},t) + \mu^{i_k}(t)\big)\tilde{x}(z_{(i_k|\zeta^{i_k})},t)\mathrm{d}\zeta^{i_k}\Bigg)
\end{aligned}$$

is used to properly collect terms. In view of the kernel–PDE (9.50), the first two lines on the right–hand side of (9.88) evaluate to zero such that

$$\partial_t w(z,t) - \Delta w(z,t) + d(z,t)w(z,t)$$

$$= \sum_{k=1}^{m} \bar{\mathfrak{K}}_{i_k}^{I_m} \circ \Big(-k^{i_k}(z^{i_k},0,t)\partial_{z^{i_k}}\tilde{x}(z_{(i_k|0)},t) + \partial_{\zeta^{i_k}} k^{i_k}(z^{i_k},0,t)\tilde{x}(z_{(i_k|0)},t) \Big)$$
$$+ \bar{\mathfrak{K}}^{I_m} \circ \sum_{i\in I_p} l_1^i(z^i,t)\big[h_i^0 \partial_{z^i}\tilde{x}(z_{(i|0)},t) + h_i^1 \tilde{x}(z_{(i|0)},t)\big]. \tag{9.89}$$

Recalling the assumption $I_m = I_p$ and by making use of the boundary conditions (9.57c) for $\tilde{x}(z,t)$ at $z^{i_k} = 0$, $i_k \in I_p$, as well as the boundary conditions (9.50c) for $k^{i_k}(z^{i_k},\zeta^{i_k},t)$ along $\zeta^{i_k} = 0$ for $\epsilon_{i_k}^0 = 0 \wedge p_{i_k}^0 \neq 0$ or (9.50e), (9.50g) if $\epsilon_{i_k}^0 \neq 0$, $i_k \in I_m$, introduce

$$q(z,t) = \sum_{k=1}^{m} \bar{\mathfrak{K}}_{i_k}^{I_m} \circ \Big(-k^{i_k}(z^{i_k},0,t)\partial_{z^{i_k}}\tilde{x}(z_{(i_k|0)},t) + \partial_{\zeta^{i_k}} k^{i_k}(z^{i_k},0,t)\tilde{x}(z_{(i_k|0)},t) \Big), \tag{9.90a}$$

which hence evaluates to

$$q(z,t) = \sum_{j=1}^{m} \bar{\mathfrak{K}}_{i_k}^{I_m} \circ \begin{cases} -\frac{l_{10}^{i_k}(t)}{p_{i_k}^0}\partial_{\zeta^{i_k}} k^{i_k}(z^{i_k},0,t)\tilde{y}^{i_k}(z_{(i_k|)},t), & \epsilon_{i_k}^0 = 0 \wedge p_{i_k}^0 \neq 0 \\ -\frac{l_{10}^{i_k}(t)}{\epsilon_{i_k}^0} k^{i_k}(z^{i_k},0,t)\tilde{y}^{i_k}(z_{(i_k|)},t), & \epsilon_{i_k\neq 0}^0. \end{cases} \tag{9.90b}$$

In addition, with (9.85) the terms involving $\tilde{x}(z_{(i|0)},t)$ and $\partial_{z^i}\tilde{x}(z_{(i|0)},t)$, $i \in I_p$, or equivalently $\tilde{x}(z_{(i_k|0)},t)$ and $\partial_{z^i}\tilde{x}(z_{(i_k|0)},t)$, $i_k \in I_p$, $k = 1,\dots,p$, can be expressed in terms of $\tilde{w}(z,t)$ according to[7]

$$\begin{aligned} \tilde{x}(z_{(i_k|0)},t) &= \bar{\mathfrak{L}}_{i_k}^{I_p} \circ \tilde{w}(z_{(i_k|0)},t) \\ \partial_{z^{i_k}}\tilde{x}(z_{(i_k|0)},t) &= \bar{\mathfrak{L}}_{i_k}^{I_p} \circ \big(\partial_{z^{i_k}}\tilde{w}(z_{(i_k|0)},t) - l^{i_k}(0,0,t)\tilde{w}(z_{(i_k|0)},t)\big), \end{aligned} \tag{9.91}$$

where

$$\bar{\mathfrak{L}}_{i_k}^{I_p} = \mathfrak{L}^{i_1}(z^{i_1},t) \circ \cdots \circ \mathfrak{L}^{i_{k-1}}(z^{i_{k-1}},t) \circ \mathfrak{L}^{i_{k+1}}(z^{i_{k+1}},t) \circ \cdots \circ \mathfrak{L}^{i_p}(z^{i_p},t).$$

As a result, the PDE governing the evolution of $w(z,t)$ is given by (9.89) with (9.90) and (9.91), i.e.

$$\begin{aligned} &\partial_t w(z,t) - \Delta w(z,t) + d(z,t)w(z,t) \\ &= q(z,t) + \bar{\mathfrak{K}}^{I_m} \circ \sum_{k=1}^{p} l_1^{i_k}(z^{i_k},t)\big[h_{i_k}^0 \bar{\mathfrak{L}}_{i_k}^{I_p} \circ \partial_{z^{i_k}}\tilde{w}(z_{(i_k|0)},t) \\ &\qquad + \big(h_{i_k}^1 - h_{i_k}^0 l^{i_k}(0,0,t)\big)\bar{\mathfrak{L}}_{i_k}^{I_p} \circ \tilde{w}(z_{(i_k|0)},t)\big]. \end{aligned} \tag{9.92a}$$

[7] Similar to the convention for $\bar{\mathfrak{K}}^{I_m}$ the arguments for $\bar{\mathfrak{L}}^{p}$ are subsequently dropped for the sake of simplicity.

The boundary conditions for this forced target–PDE can be directly determined from the evaluation of (9.51c)–(9.51f) in view of (9.86) by making use[8] of the boundary conditions (9.2b)–(9.2d) for $x(z,t)$ and (9.57b)–(9.57d) for $\tilde{x}(z,t)$. It is thereby crucial to incorporate the determined conditions for each integral kernel $k^{i_k}(z^{i_k},\zeta^{i_k},t)$ governed by (9.50c)–(9.50g) and their relationship with the boundary conditions for the target system $w(z,t)$. Since $I_m = I_p$, this implies that it is only necessary to further evaluate boundary conditions at $z^{i_k} = 0$ for $i_k \in I_m$ — any other boundary condition remains unchanged by the definition of the individual transformations comprising $\bar{\mathfrak{K}}^{I_m}$. This yields after some intermediate computations

$$-\epsilon_j^0 \partial_{z^j} w(z,t) + p_j^0 w(z,t) = 0, \qquad z^j = 0,\ j \in I_r^{I_m} \tag{9.92b}$$

$$-\epsilon_{w,i_k}^0 \partial_{z^{i_k}} w(z,t) + p_{w,i_k}^0 w(z,t) = \bar{\mathfrak{K}}_{i_k}^{I_m} \circ \begin{cases} \frac{p_{w,i_k}^0}{p_{i_k}^0} l_{10}^{i_k}(t) \tilde{y}^{i_k}(z_{(i_k|)},t), & \epsilon_{i_k}^0 = 0 \\ \frac{\epsilon_{w,i_k}^0}{\epsilon_{i_k}^0} l_{10}^{i_k}(t) \tilde{y}^{i_k}(z_{(i_k|)},t), & \epsilon_{i_k}^0 \neq 0 \end{cases}, \quad z^{i_k} = 0,\ i_k \in I_m \tag{9.92c}$$

$$\epsilon_j^1 \partial_{z^j} w(z,t) + p_j^1 w(z,t) = 0, \qquad z^j = L_j,\ j \in I_r^{I_m} \tag{9.92d}$$

$$\epsilon_{w,j}^1 \partial_{z^j} w(z,t) + p_{w,j}^1 w(z,t) = 0, \qquad z^j = L_j,\ j \in I_m \tag{9.92e}$$

for $t > t_0$. Note that herein $\tilde{y}^{i_k}(z_{(i_k|)},t)$ arising in (9.92c) has to be replaced in terms of $\tilde{w}(z,t)$ by making use of (9.91). In addition, the initial condition follows as

$$w(z,t_0) = w_0(z) = \bar{\mathfrak{K}}^{I_m} \circ x_0(z) - \bar{\mathfrak{K}}^{I_m} \circ \tilde{x}_0(z), \qquad z \in \overline{\Omega}. \tag{9.92f}$$

Since the application of the multi–linear backstepping–transformation $\bar{\mathfrak{M}}^{I_p} \circ \tilde{x}(z,t)$ by definition results in the target system (9.84) for the observer error dynamics, which is independent of $w(z,t)$, the closed–loop system is given in a cascaded structure, where the $w(z,t)$ dynamics is driven by the autonomous $\tilde{w}(z,t)$ dynamics. Similar to the previous consideration this one–sided coupling proves to be crucial for the stability analysis of the closed–loop system.

Theorem 9.6. *The closed–loop system* (9.92)*,* (9.84) *is exponentially stable in the* L^2*–norm if* $\mu(t)$ *and* $\tilde{\mu}(t)$ *are such that* $\mu(t) + \lambda_{\min} - \bar{c}_0(t) > \epsilon > 0$ *and* $\tilde{\mu}(t) + \tilde{\lambda}_{\min} - \tilde{c}_0(t) > \tilde{\epsilon} > 0$ *for some* $\epsilon,\ \tilde{\epsilon}$*. Here,*

$$\mu(t) = \sum_{j=1}^{m} \mu^{i_j}(t), \quad \tilde{\mu}(t) = \sum_{j=1}^{p} \tilde{\mu}^{i_j}(t)$$

and $\lambda_{\min}$ *as well as* $\tilde{\lambda}_{\min}$ *denote the minimal eigenvalue of the PDE* $\Delta w(z) + \lambda w(z) = 0$ *with boundary conditions* (9.48b)–(9.48e) *and* (9.84c)–(9.84f)*, respectively.*

[8] Assumption 9.3 has to be taken into account to reduce (9.1e) to a linear inhomogeneous BC.

Proof. Note first that the target system in $\tilde{w}(z,t)$ is autonomous such that Lemma 9.2 ensures that $\tilde{\mu}(t)$ can be chosen appropriately to ensure its exponential stability, i.e. $\exists C > 0,\ \tilde{\epsilon} > 0 : \|\tilde{w}(t)\|_{L^2(\Omega)} \leq C\exp\left(-\tilde{\kappa}(t)\right)\|\tilde{w}_0\|_{L^2(\Omega)}$ with $\tilde{\kappa}(t) = \int_{t_0}^{t}(\tilde{\mu}(\tau) + \tilde{\lambda}_{\min} - \tilde{c}_0(\tau))\mathrm{d}\tau$ and $(\tilde{\mu}(t) + \tilde{\lambda}_{\min} - \tilde{c}_0(t)) > \tilde{\epsilon}$ for all $t \in \mathbb{R}_{t_0}^{+}$. As a result, the stability analysis reduces to the consideration of the $w(z,t)$–system, which is driven by the $\tilde{w}(z,t)$–system via the terms on the right–hand of the PDE (9.92a) as well as in the boundary conditions (9.92c).

For this, it is convenient to introduce a homogenization of the inhomogeneous boundary conditions (9.92c) by introducing the change of variables

$$w(z,t) \mapsto w(z,t) + v(z,t),$$

where $v(z,t)$ simultaneously satisfies the sets of homogeneous and inhomogeneous boundary conditions (9.92b)–(9.92e). Hence, the PDE (9.92a) can be re–formulated according to

$$\partial_t w(z,t) = \Delta w(z,t) - d(z,t)w(z,t) + Q(z,t) \tag{9.93}$$

with

$$\begin{aligned} Q(z,t) = & -\partial_t v(z,t) + \Delta v(z,t) - d(z,t)v(z,t) + q(z,t) \\ & + \bar{\mathfrak{K}}^{I_m} \circ \sum_{k=1}^{p} l_1^{i_k}(z^{i_k},t)\big[h_{i_k}^0\, \bar{\mathfrak{L}}_{i_k}^{I_p} \circ \partial_{z^{i_k}} \tilde{w}(z_{(i_k|0)},t) \\ & \qquad + \big(h_{i_k}^1 - h_{i_k}^0 l^{i_k}(0,0,t)\big)\bar{\mathfrak{L}}_{i_k}^{I_p} \circ \tilde{w}(z_{(i_k|0)},t)\big], \end{aligned} \tag{9.94}$$

homogeneous boundary conditions

$$-\epsilon_j^0 \partial_{z^j} w(z,t) + p_j^0 w(z,t) = 0, \qquad z^j = 0,\ j \in I_r^{I_m} \tag{9.95a}$$

$$-\epsilon_{w,i_k}^0 \partial_{z^{i_k}} w(z,t) + p_{w,i_k}^0 w(z,t) = 0, \qquad z^{i_k} = 0,\ i_k \in I_m \tag{9.95b}$$

$$\epsilon_j^1 \partial_{z^j} w(z,t) + p_j^1 w(z,t) = 0, \qquad z^j = L_j,\ j \in I_r^{I_m} \tag{9.95c}$$

$$\epsilon_{w,j}^1 \partial_{z^j} w(z,t) + p_{w,j}^1 w(z,t) = 0, \qquad z^j = L_j,\ j \in I_m, \tag{9.95d}$$

and the initial condition

$$w(z,t_0) = w_0(z) + v(z,t_0).$$

Hence, multiplying both sides of (9.93) with $w(z,t)$ and integrating over Ω yields

$$\begin{aligned} \frac{1}{2}\partial_t \|w(t)\|_X^2 = & \int_\Omega w(z,t)\Delta w(z,t)\mathrm{d}\Omega - \int_\Omega d(z,t)w^2(z,t)\mathrm{d}\Omega \\ & + \int_\Omega Q(z,t)w(z,t)\mathrm{d}\Omega, \end{aligned}$$

where $X = L^2(\Omega)$. By considering the Rayleigh principle, as in the proof of Lemmas 9.1 and 9.2, it follows that

$$\frac{1}{2}\partial_t \|w(t)\|_X^2 \leq -\big(\mu(t) + \lambda_{\min} - \bar{c}_0(t)\big)\|w(t)\|_X^2 + \int_\Omega Q(z,t)w(z,t)\mathrm{d}\Omega,$$

where $\lambda_{\min}$ as in the formulation of the theorem. In addition, using Hölder's and Cauchy's inequality implies

$$\begin{aligned}\int_\Omega Q(z,t)w(z,t)\mathrm{d}\Omega &\leq \int_\Omega |Q(z,t)w(z,t)|\mathrm{d}\Omega \\ &\leq \|Q(t)\|_X\|w(t)\|_X \leq \eta\|w(t)\|_X^2 + \frac{\|Q(t)\|_X^2}{4\eta}\end{aligned}$$

for $\eta > 0$. With this, the evolution of $\|w(t)\|_X^2$ can be bounded by

$$\partial_t \|w(t)\|_X^2 \leq -2\big(\mu(t) + \lambda_{\min} - \bar{c}_0(t) - \eta\big)\|w(t)\|_X^2 + \frac{\|Q(t)\|_X^2}{2\eta}$$

such that Gronwall's inequality implies

$$\|w(t)\|_X^2 \leq e^{-2\int_0^t (\mu(\tau)+\lambda_{\min}-\bar{c}_0(\tau)-\eta)\mathrm{d}\tau}\left[\|w_0\|_X^2 + \int_{t_0}^t \frac{\|Q(\tau)\|_X^2}{2\eta}\mathrm{d}\tau\right].$$

Hence, the stability of the closed–loop system essentially relies on the properties of $\|Q(t)\|_X$. In order to evaluate this term, recall from (9.94) that $Q(z,t)$ is linear and non–affine in $\tilde{w}(z,t)$, i.e. any term depends linearly on $\tilde{w}(z,t)$. Moreover, recalling the boundedness of each kernel $k^{i_k}(z^{i_k}, \zeta^{i_k}, t)$ arising in the integral operators $\mathfrak{K}^{i_k}(z^{i_k}, t)$ the exponential stability of the $\tilde{w}$–system allows to deduce by successively making use of the Cauchy–Schwarz inequality that there exists a constant $C' > 0$ such that $\|Q(t)\|_X \leq C'\|\tilde{w}_0\|_X \exp(-\int_{t_0}^t \tilde{\kappa}(\tau)\mathrm{d}\tau) \leq C'\|\tilde{w}_0\|_X \exp(-\tilde{\epsilon}(t-t_0))$, $\tilde{\epsilon} > 0$. This yields

$$\begin{aligned}\|w(t)\|_X^2 \leq\ & e^{-2\int_0^t (\mu(\tau)+\lambda_{\min}-\bar{c}_0(\tau)-\eta)\mathrm{d}\tau} \times \\ & \left[\|w_0\|_X^2 + \frac{(C'\|\tilde{w}_0\|_X)^2}{4\tilde{\epsilon}\eta}\Big(1 - e^{-2\tilde{\epsilon}(t-t_0)}\Big)\right].\end{aligned}$$

As a result, if $\mu(t)$ is such that $\mu(t) + \lambda_{\min} - \bar{c}_0(t) - \eta > \epsilon > 0$ for all $t \in \mathbb{R}_{t_0}^+$, then

$$\|w(t)\|_X^2 \leq e^{-2\epsilon(t-t_0)}\|w_0\|_X^2 + e^{-2\epsilon(t-t_0)}\frac{(C'\|\tilde{w}_0\|_X)^2}{4\tilde{\epsilon}\eta}\Big(1 - e^{-2\tilde{\epsilon}(t-t_0)}\Big).$$

Taking into account $\|\tilde{w}(t)\|_X \leq C\exp(-\tilde{\kappa}(t))\|\tilde{w}_0\|_X \leq C\exp(-\tilde{\epsilon}(t-t_0)\|\tilde{w}_0\|_X$ implies the exponential stability of the cascaded structure since $0 < \eta < \infty$ can be chosen arbitrarily small. □

Remark 9.7. In principle the determined stability properties of the closed–loop control can be directly extended to the situation where I_m and I_p contain disjoint elements. This results in rather tedious computations and the necessity to distinguish various special cases depending on the sets I_m and I_p, which are omitted subsequently. However, the procedure to prove the stability assertion is identical to the presentation above. Moreover, the theoretical analysis is supported by the application examples considered in Section 9.8, which confirm the separation property also in this general setting.

9.6.6 Approximate Realization of the State–Observer by means of Spatial Output Interpolation

As pointed out above, the considered design scenario represents an idealized configuration with infinite–dimensional system outputs. In view of the realization of the state–observer it is hence required to introduce an approximation to be able to (approximately) re–construct the spatially distributed output variables from a finite number of suitable placed finite–dimensional measurement devices. For this, a spatial output interpolation approach is proposed in Section 9.3.6 above, which can be directly applied to the considered multi output scenario by proceeding as outlined for each output $y^i(z_{(i|)},t)$, $i \in I_p$. Hence, let

$$y^{l,i}(t) = \int_{\partial\Omega_i^0} \left[\mathfrak{c}_1^{l,i}(z_{(i|)})\partial_{z^i} x(z_{(i|0)},t) + \mathfrak{c}_0^{l,i}(z_{(i|)})x(z_{(i|0)},t)\right] \mathrm{d}\partial\Omega_i^0$$

for $l = 1,\dots,p_i$, $i \in I_p$, denote the finite–dimensional measurements, where $\partial\Omega_i^0 = \{z \in \Omega : z^i = 0\}$ and $\mathfrak{c}_0^{l,i}(z_{(i|)})$ and $\mathfrak{c}_1^{l,i}(z_{(i|)})$ denote the spatial characteristics of the measurement device. In a discrete time setting, consider the least–squares problem

$$\min_{\{F_{n,i}\}_{n=1,\dots,N}} \left\| \boldsymbol{y}^i(t_k) - \boldsymbol{y}_N^i(t_k) \right\|_2^2$$

with

$$\boldsymbol{y}^i(t_k) = \left[y^{1,i}(t_k),\dots,y^{p_i,i}(t_k)\right]^T, \quad \boldsymbol{y}_N^i(t_k) = \left[y_N^{1,i}(t_k),\dots,y_N^{p_i,i}(t_k)\right]^T,$$

where $y_N^{l,i}(t_k)$ refers to the evaluation of $y^{l,i}(t)$ with $x(z,t)$ evaluated at $t = t_k$ replaced by the ansatz

$$x_N(z) = \sum_{n=1}^{N} F_n \phi_n(z).$$

Herein, $(\phi_n(z))_{n\in\{1,\dots,N\}}$ denotes the set of linear independent ansatz functions fulfilling

$$-\epsilon_i^0 \partial_{z^i} x_N(z_{(i|0)}) + p_i^0 x_N(z_{(i|0)}) = 0, \qquad i \in I_p.$$

By consecutively solving the spatial interpolation problem in each time step $k \in \mathbb{N}$ an L^2–approximation with

$$y_N^i(z_{(i|)}, t_k) = h_i^0 \partial_{z^i} x_N(z) + h_i^1 x_N(z), \qquad z^i = 0,\ i \in I_p$$

can be deduced for the infinite–dimensional output $y^i(z_{(i|)}, t)$. Note that also global spatial ansatz functions can be incorporated into the approach, which simultaneously satisfy the homogeneous boundary conditions of the $x(z,t)$ systems along the output boundary surfaces.

As pointed out before, the utilization of spatial interpolation does in general not enable to conclude exponential stability of the observer error dynamics by means of the backstepping approach. However, the simulation results presented in the following confirm that the theoretical analysis holds also for the finite–dimensional output approximation.

9.7 Tracking Control Combining Backstepping and Differential Flatness — The Multiple Input and Output Case

It is revealed in Section 8.4 and 9.4 that backstepping–based feedback stabilization can be systematically combined with flatness–based trajectory planning and feedforward control to realize an exponentially stable tracking controller. Proceeding similar to the single input case addressed in Section 9.4 in view of the formal integration technique introduced in Chapter 7 enables to extend the presentation to the multiple input scenario for distributed–parameter systems with higher–dimensional parallelepiped domain. Herein, different configurations can be considered, where either all inputs of the set I_m or only a subset of I_m are exploited for feedforward control. The principle procedure thereby follows exactly the lines of Section 9.4 by taking into account the notes provided in Section 7.4 on the extension of the formal integration approach to the case of multiple inputs. For this, an application is presented below to achieve consensus and synchronization in a multi–agent network.

Moreover, if the system parameters allow to render $d(z,t)$ time–invariant, i.e. if $\sum_{j=1}^{m} \mu^{i_j}(t) - c_0(z_{(I_m|)}, t)$ is independent of time t, then the spectral design approach introduced in Chapter 6 can be applied to solve the trajectory planning and feedforward control problem. As outlined, this approach in particular enables a systematic consideration of the multiple input case and provides techniques to realize admissible transitions between stationary and non–stationary profiles.

9.8 Application Examples and Simulation Results

In order to evaluate the performance of the determined backstepping–based state–feedback control with state–observer numerical results are presented subsequently for two simulation scenarios. At first, the exponential stabilization of a diffusion–reaction system with a 3–dimensional spatial domain is analyzed in a MIMO configuration with $I_m \neq I_p$. Secondly, the deployment of a network of interconnected agents along prescribed desired spatial–temporal paths is considered by combining flatness and backstepping as outlined above. For the sake of simplicity, the initial time t_0 is chosen as $t_0 = 0$ throughout the examples.

9.8.1 Exponential Feedback Stabilization and State Estimation for an Unstable Time Varying Diffusion–Reaction System

In the following, a 3–dimensional extension of the simulation scenario of Section 8.5 is considered on the parallelepiped domain $\Omega = \times_{j=1}^{3}(0,1)$ in a MIMO configuration according to Figure 9.1. The reaction coefficient $c(z,t)$ in the distributed–parameter system (9.2) is assumed as

$$c(z,t) = \sum_{i=1}^{3} c_1^i(z^i,t) \tag{9.96}$$

with

$$c_1^i(z^i,t) = g_{\bar{T},\bar{\omega}}(t-t_0)\big(a_1^i(t) + z^i a_2^i(t)\big),$$

where $g_{\bar{T},\bar{\omega}}(\cdot)$ is given by (B.3) for $\bar{\omega} = 3/2$, $\bar{T} = 1/2$ and

$$\begin{aligned}
a_1^1(t) &= 12 + 4\cos(8\pi t + \pi/2), & a_2^1(t) &= 5 - a_1(t) + 4\sin(8\pi t)\\
a_1^2(t) &= 10 + 4\cos(5\pi t + \pi/2), & a_2^2(t) &= 5 - a_1(t) + 4\sin(5\pi t)\\
a_1^3(t) &= 8 + 4\cos(3\pi t + \pi/2), & a_2^3(t) &= 5 - a_1(t) + 4\sin(3\pi t).
\end{aligned}$$

Thus, $c(z,t)$ satisfies $c(z,t_0) = 0$, $\partial_t^n c(z,t_0) = 0$ for $n \geq 1$ while $c(z,t) = \sum_{i=1}^{3}(a_1^i(t) + z^i a_2^i(t))$ for $t \geq t_0 + \bar{T}$. The evolution of $c_{\max}(t) = \max_{z\in\Omega} c(z,t)$ and $c_{\min}(t) = \min_{z\in\Omega} c(z,t)$ is shown in Figure 9.2. The remaining system parameters are chosen as $\epsilon_j^0 = p_j^0 = \epsilon_j^1 = p_j^1 = 1$ for all $j \in I_r$, i.e. Robin boundary conditions are imposed on the boundary $\partial\Omega$ of Ω and Assumption 9.4 holds, which yields linear boundary conditions on the input boundary surfaces. The initial condition is assigned as

$$x(z,t_0) = \begin{cases} 5 & \text{for } z^1 \in (0.1,0.9) \wedge z^2 \in (0.2,0.8) \wedge z^3 \in (0.3,0.7) \\ 0 & \text{else} \end{cases}$$

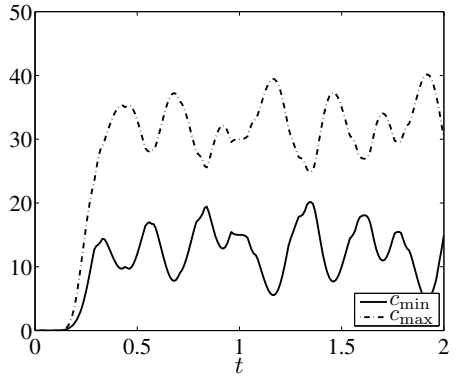

Fig. 9.2 Transients of the reaction coefficient $c(z,t)$ governed by (9.96). Here, $c_{\max}(t) = \max_{z\in\Omega} c(z,t)$ and $c_{\min}(t) = \min_{z\in\Omega} c(z,t)$.

and is shown in Figure 9.5(a) (left column). By making use of a Lyapunov–type argument, it can be easily shown in view of the reaction coefficient $c(z,t)$ that the uncontrolled distributed–parameter system (9.2) with (9.96) is unstable for the considered parameter set.

9.8.1.1 Backstepping–Based State–Feedback Control with State–Observer

Subsequently, two state–feedback controllers $u^i(z_{(i|)},t)$, $i \in I_m$ with $I_m = \{1,2\}$ are applied on the boundary surfaces $z^1 = 1$ and $z^2 = 1$. For their design, backstepping according to the treatise in Section 9.5 is considered with the target system chosen according to (9.51) parametrized by $\mu^{i_1}(t) = \mu^{i_2}(t) = 8$ such that $d(z,t) = \mu^1(t) + \mu^2(t) - c_1^3(z^3,t) = 16 - c_1^3(z^3,t) > 0$ and $\epsilon^0_{w,i} = \epsilon^1_{w,i} = 1$, $p^0_{w,i} = p^1_{w,i} = 0, i = 1,2$. Hence, the state–feedback control is governed by (9.53b), where successive approximation is applied to compute 7 series coefficients for the determination of the kernels $k^i(z^i,\zeta^i,t)$, $i = 1,2$.

The infinite–dimensional state–feedback controls obtained from the backstepping technique are implemented by making use of the approximation approach suggested in Section 9.2.5 or 9.5.5, respectively, in terms of 9 finite–dimensional actuators covering each of the two boundary surfaces $z^1 = 1$ and $z^2 = 1$, i.e.

$$u^i(z_{(i|)},t) = \sum_{l=1}^{9} \mathfrak{b}^{i,l}(z_{(i|)}) u^{i,l}(t)$$

with the spatial actuator characteristics $\mathfrak{b}^{i,l}(z_{(i|)}) = 1$ for $z_{(i|)} \in \partial\Omega^i_l$ and zero elsewhere (cf. Figure 9.3).

The realization of the state–feedback control is subsequently achieved by incorporating a state–observer as presented in Section 9.6 with the measurements

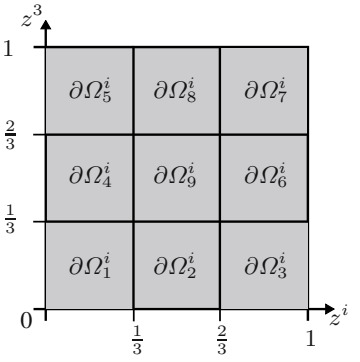

Fig. 9.3 Finite–dimensional actuator configuration for the approximate implementation of the backstepping–based state–feedback control

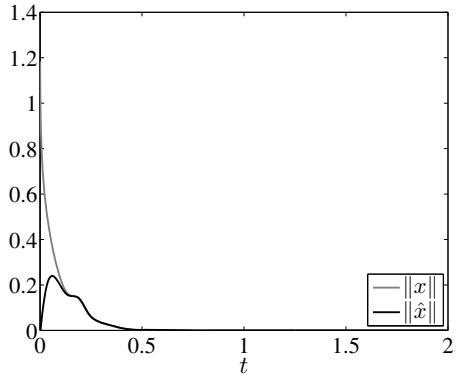

Fig. 9.4 Time evolution of the closed–loop system state $\|x(t)\|_{L^2(\Omega)}$ and the observer state $\|\hat{x}(t)\|_{L^2(\Omega)}$ in a sample–hold configuration with sampling time $\Delta t = 0.0025$

corresponding to the spatial–temporal evolution of $x(z,t)$ along the boundary surfaces $z^1 = 0$ and $z^3 = 0$, i.e. $y^i(z_{(i|)},t) = x(z_{(i|0)},t)$, $i = 1,3$, and $I_p = \{1,3\}$. For this, the state–observer is set–up following (9.56) with the observer gains determined to exponentially stabilize the observer error dynamics (9.57). The respective target system (9.84) for the observer error is parametrized by $\tilde{d}(z,t) = \tilde{\mu}^1(t) + \tilde{\mu}^3(t) - c_1^2(z^2,t)$ with $\tilde{\mu}^1(t) = \tilde{\mu}^3(t) = 14$ such that $\tilde{d}(z,t) = 28 - c_1^2(z^2,t) > 0$. The remaining parameters are herein chosen as $\tilde{\epsilon}_{w,i}^0 = \tilde{\epsilon}_{w,i}^1 = 1$ and $\tilde{p}_{w,i}^0 = \tilde{p}_{w,i}^1 = 0$ for $i = 1,3$. For the determination of the kernels $m^i(z^i,\zeta^i,t)$, $i = 1,3$, and hence the observer gains $l_1^i(z^i,t)$ and $l_{10}^i(t)$ according to (9.82) successive approximation is used to compute 7 addends of the functional series for the kernels. The initial condition for the observer is chosen as $\hat{x}(z,t_0) = 0$, $z \in \overline{\Omega}$, which imposes an initial observer error $\tilde{x}(z,t_0) = x(z,t_0)$ (cf. also Figure 9.5(a) (middle and right column)).

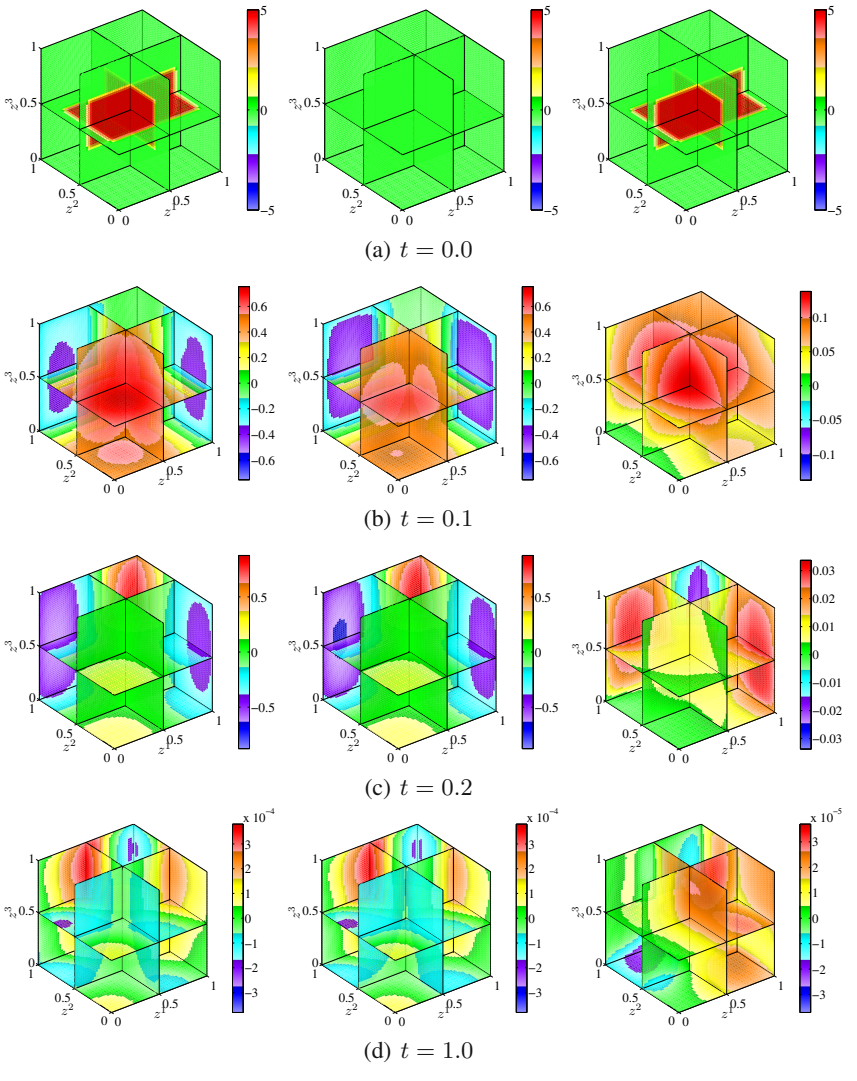

Fig. 9.5 Snapshots of the spatial–temporal evolution of $x(z,t)$ (left column), $\hat{x}(z,t)$ (middle column), and $\tilde{x}(z,t)$ (right column) for at $t \in \{0, 0.1, 0.2, 1.0\}$

9.8.1.2 Simulation Results

As pointed out in Remark 9.7, the stability analysis of Theorem 9.6 for the combination of state–feedback control with state–observer in the case $I_m = I_p$ can be extended to the presently considered scenario with $I_m \neq I_p$. This is confirmed by the numerical results in Figure 9.4 for the time–evolution of the norms $\|x(t)\|_{L^2(\Omega)}$ and $\|\hat{x}(t)\|_{L^2(\Omega)}$, respectively, which clearly confirm the exponential convergence

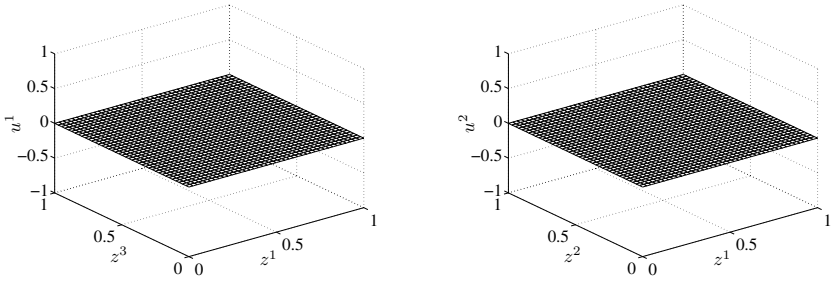

(a) $t = 0.0$

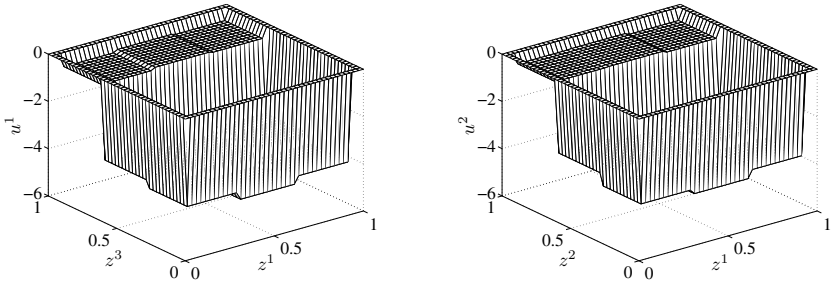

(b) $t = 0.1$

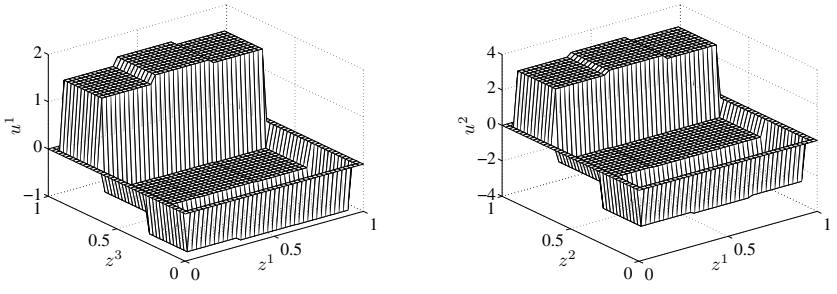

(c) $t = 0.2$

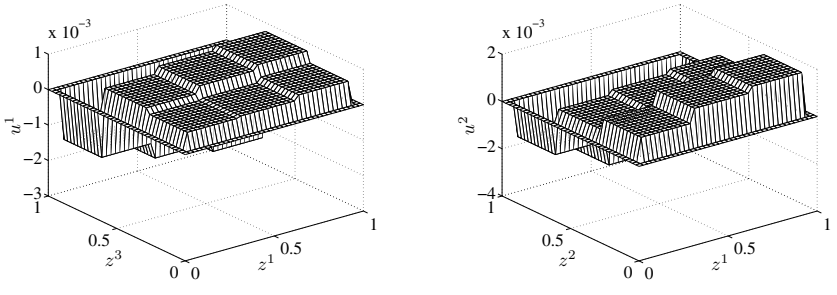

(d) $t = 1.0$

Fig. 9.6 Snapshots of the spatial–temporal evolution of the state–feedback controls $u^1(z_{(1|)}, t)$ (left column) and $u^2(z_{(2|)}, t)$ (right column) for at $t \in \{0, 0.1, 0.2, 1.0\}$

of both the observer in view of the initial observer error as well as the state evolution. Thereby, it should be pointed out that the simulation is set–up in a sample–hold configuration to reflect the effect of sampling times in the control–loop. Due to the instability of the open–loop system, the sampling time has to be adjusted properly. In view of the assigned dynamics of the target systems for the state–feedback control and the state–observer a sampling time of $\Delta t = 0.0025$ is chosen subsequently. The distributed–parameter systems governing the diffusion–reaction system as well as the state–observer are discretized using a 3–dimensional implicit and absolutely stable Crank–Nicholson scheme with a spatial grid size of $\Delta z^j = 0.05$, $j = 1, 2, 3$. The numerical solution is implemented using MATLAB with the necessary matrix factorizations being realized using UMFPACK [7].

In order to obtain further insight into the dynamics of the closed–loop control system with state–observer consider Figure 9.5, where snapshots of the spatial–temporal evolution of $x(z,t)$, $\hat{x}(z,t)$, and $\tilde{x}(z,t) = x(z,t) - \hat{x}(z,t)$ in the cuboid are shown at $t \in \{0.0, 0.1, 0.2, 1.0\}$. The corresponding state–feedback controls computed using the observer state are shown in Figure 9.6. Here, the convergence of the state–observer to the actual state after the initial transients due to the imposed observer error at $t = t_0$ can be directly visualized. Moreover, a rather non–trivial behavior of the state–feedback controls evaluated using the state–observer can be observed in the considered finite–dimensional actuator configuration. However, the periodically varying reaction coefficient $c(z,t)$ yields a non–stationary state–feedback control, which is required to maintain the exponential stability properties of the closed–loop system in terms of the assigned target distributed–parameter systems.

9.8.2 Synchronization of Large Scale Multi–Agent Network

As is outlined in Chapter 3, PDEs can be exploited for the mathematical formulation and control of multi–agent networks. In order to illustrate this, in the following the active synchronization of a large scale multi–agent network is considered, whose interconnected dynamics is governed by (3.11) for $a_i^{j_i} = 1$, $b_i^{j_i} = 0$, $u_\Omega^k(\mathtt{n}_j, t) = 0$, $r = 3$, and $n = 1$, i.e.

$$\begin{aligned}\partial_t x(\mathtt{n}_j, t) = \sum_{i=1}^{r} \frac{1}{(\mathrm{d}z^i)^2}\left[x(\mathtt{n}_{(j_i|j_i+1)}, t) - 2x(\mathtt{n}_j, t) + x(\mathtt{n}_{(j_i|j_i-1)}, t)\right] \\ + c(t)x(\mathtt{n}_j, t)\end{aligned} \tag{9.97a}$$

with boundary conditions

$$x(\mathtt{n}_{(j_i|0)}, t) = x(\mathtt{n}_{(j_i|1)}, t), \qquad i \in \{2, 3\} \tag{9.97b}$$

$$x(\mathtt{n}_{(j_i|N_{i+1})}, t) = x(\mathtt{n}_{(j_i|N_i)}, t), \qquad i \in \{2, 3\} \tag{9.97c}$$

$$x(\mathtt{n}_j, t) = u^{1_0}(\mathtt{n}_{(j_1|)}, t), \qquad j_1 = 1 \tag{9.97d}$$

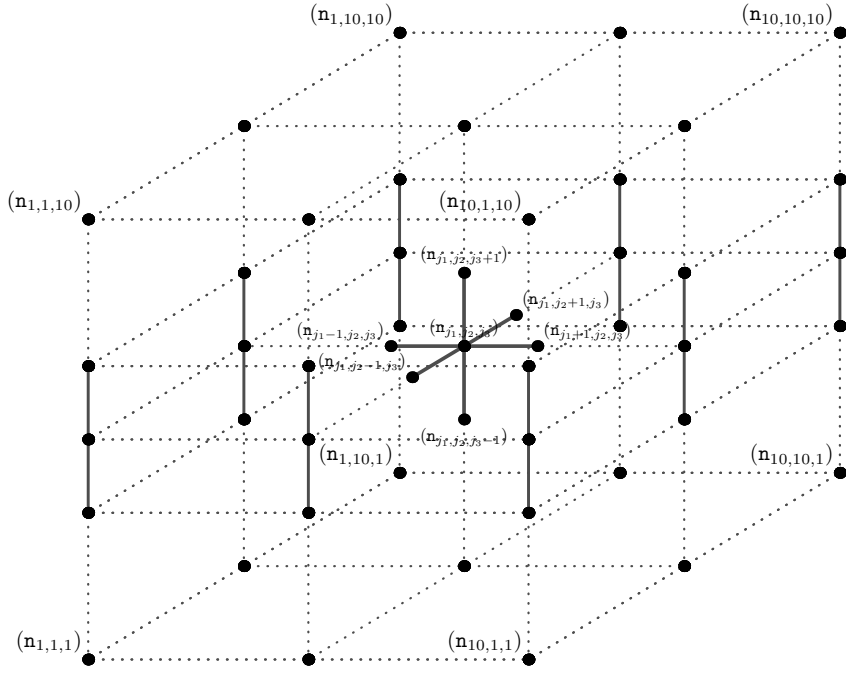

Fig. 9.7 Communication topology with agents $\mathtt{n}_j$ represented by the dots. The graph is build up of individual octahedral subgraphs as is shown in the center of the interior.

$$x(\mathtt{n}_j, t) = u^{1_1}(\mathtt{n}_{(j_1|)}, t), \qquad j_1 = N_1 \tag{9.97e}$$

initial condition

$$x(\mathtt{n}_j, t_0) = x_0(\mathtt{n}_j, t_0) \tag{9.97f}$$

and output

$$y(\mathtt{n}_{(j_3|)}, t) = x(\mathtt{n}_{(j_3|0)}, t). \tag{9.97g}$$

Herein, the nodes are given by $\mathtt{n}_j \equiv ((j_1-1)\mathrm{d}z^1, (j_2-1)\mathrm{d}z^2, (j_3-1)\mathrm{d}z^3)$ with $\mathrm{d}z^i = 1/(N_i-1)$ and $N_i = 10$. Hence, a network of 1000 agents is considered with $x(\mathtt{n}_j, t)$ representing the individual agent states, which could represent temperature, oscillation phase, or location. The corresponding communication topology with the individual nodes is shown in Figure 9.7 with the octahedral subgraph emphasized in the interior of the domain motivating the introduction of the Laplacian in the continuous formulation. Note that the inhomogeneous boundary conditions (9.97d), (9.97e) represent the leader agents with $u^{1_0}(\mathtt{n}_{(j_1|)}, t)$, $u^{1_1}(\mathtt{n}_{(j_1|)}, t)$ used to actuate the network. In addition, the nodes $y(\mathtt{n}_{(j_3|)}, t)$ according to (9.97g) denote sensor agents, whose states are available for processing.

Proceeding as in Sections 3.1.1 and 3.1.2, the multi–agent system (9.97) can be similarly considered in a distributed–parameter systems framework according to (9.2), which for the present case results in

$$\partial_t x(z,t) = \Delta x(z,t) + c(t)x(z,t) \tag{9.98a}$$

defined on $(z,t) \in \Omega \times \mathbb{R}^+_{t_0}$ for $\Omega = \bigtimes_{j=1}^{3}(0,1)$ with[9] boundary conditions

$$\partial_{z^j} x(z,t) = 0, \qquad z^j = 0,\ j \in \{2,3\},\ t > t_0 \tag{9.98b}$$

$$\partial_{z^j} x(z,t) = 0, \qquad z^j = 1,\ j \in \{2,3\},\ t > t_0 \tag{9.98c}$$

$$x(z,t) = u^{1_0}(z_{(1|)},t), \qquad z^1 = 0,\ t > t_0, \tag{9.98d}$$

$$x(z,t) = u^{1_1}(z_{(1|)},t), \qquad z^1 = 1,\ t > t_0, \tag{9.98e}$$

and the initial condition

$$x(z,t_0) = x_0(z), \qquad z \in \overline{\Omega}. \tag{9.98f}$$

The output moreover follows as

$$y(z_{(3|)},t) = x(z,t), \qquad z^3 = 0,\ t > t_0. \tag{9.98g}$$

The time varying parameter $c(t)$ is assumed to be a Gevrey class function

$$c(t) = c_0 + (c_1 - c_0)\mathcal{g}_{T,\omega}(t) \tag{9.99}$$

with $\mathcal{g}_{T,\omega}(t)$ as introduced in (B.3) for $\omega > 1$ and constants $c_0 = 10$, $c_1 = 15$. With this $c(t) \in G_{D,\alpha}(\mathbb{R})$ for $\alpha = 1 + 1/\omega < 2$.

Based on (9.98), trajectory planning and state feedback control design with observer are subsequently addressed to realize the finite time synchronization of the multi–agent network (9.97) starting from a random initial state (9.97f) or (9.98f), respectively. Differing from the presentation in Section 9.7 for this at first flatness–based techniques are applied to determine a spatial–temporal reference path $x^*(z,t)$ and the necessary feedforward controls $(u^{*,1_0}(z_{(1|)},t), u^{*,1_1}(z_{(1|)},t))$ to realize a desired dynamics. Secondly, backstepping is applied for the feedback stabilization of the tracking error dynamics in $x_e(z,t) = x(z,t) - x^*(z,t)$.

Remark 9.8. It should be pointed out that this yields an alternative to the tracking control design presented in Section 9.4, where trajectory planning and feedforward control are based on the target distributed–parameter system. While both approaches are equivalent for linear systems certain nonlinear PDEs can be addressed by the reverse design sequence as is shown in [10] for the 1–dimensional case.

[9] A direction comparison yields $\epsilon_1^0 = \epsilon_1^1 = 0$, $p_1^0 = p_1^1 = 1$ and $\epsilon_j^0 = \epsilon_j^1 = 1$, $p_j^0 = p_j^1 = 0$ for $j = 2,3$, $\theta^i(x(z,t), \partial_{z^i} x(z,t)) = x(z,t)$ as well as $h_i^0 = 0$, $i = 1,2,3$, and $h_i^1 = 0$, $i = 1,2$, but $h_3^1 = 1$.

9.8.2.1 Flatness–Based Trajectory Planning

For the present multi input scenario, the formal integration approach of Section 7.4 is applied for the solution of the trajectory planning problem. Therefore, the recursive parametrization (7.35) is solved with the desired trajectories $\boldsymbol{\xi}^*(z_{(1|)},t)$ for the basic output $\boldsymbol{\xi}(z_{(1|)},t)$ assigned similar to (7.38), i.e.

$$\begin{aligned}\xi^{*,1_0}(z_{(1|)},t) &= \xi_0^{*,1_0}(z_{(1|)}) \\ &\quad + \big(\xi_T^{*,1_0}(z_{(1|)}) - \xi_0^{*,1_0}(z_{(1|)})\big)g_{T,\omega}(t-t_0-\bar{t}) \qquad (9.100a)\\ \xi^{*,1_1}(z_{(1|)},t) &= \xi_0^{*,1_1}(z_{(1|)}) \\ &\quad + \big(\xi_T^{*,1_1}(z_{(1|)}) - \xi_0^{*,1_1}(z_{(1|)})\big)g_{T,\omega}(t-t_0-\bar{t}) \qquad (9.100b)\end{aligned}$$

with $T=0.5$, $\omega=2.0$, and $\bar{t}=0.5$. Note that $\bar{t}$ is used to infer a delayed transition (cf. (B.3)), which is required to address the non–stationary and random initial condition as is further elaborated below. The terms $\xi_0^{*,1_j}(z_{(1|)})$ and $\xi_T^{*,1_j}(z_{(1|)})$, $j=0,1$, are thereby evaluated using (7.37) for $\bar{z}^1=0.5$. Herein, stationary profiles are assumed at $t=t_0$ and $t=t_0+T+\bar{t}$ governed by the boundary–value problem (7.36) with $c(z,t)$ replaced by c_0 and c_1 at $t=t_0$ and $t=t_0+T+\bar{t}$, respectively. In this direct approach[10], the stationary inputs are chosen as $u_s^{1_0}(z_{(1|)})=u_s^{1_1}(z_{(1|)})=0$ at $t=t_0$ and $u_s^{1_0}(z_{(1|)})=1$ and $u_s^{1_1}(z_{(1|)})=-1$ at $t=t_0+T+\bar{t}$. With this, the desired initial stationary profile is given by $x_0^*(z)=0$ while the desired final stationary profile is obtained as $x_T^*(z)=\sin(\sqrt{15}(1/2-z^1))/\sin(\sqrt{15}/2)$. By making use of (9.100), the state parametrization $x^*(z,t)$ follows from the evaluation of (7.35). Hence, the feedforward controls $(u^{*,1_0}(z_{(1|)},t),u^{*,1_1}(z_{(1|)},t))$ can be computed by utilizing the input parametrizations (7.34a), (7.34b). Their application in particular enables to realize the finite time transition from $x_0^*(z)$ to $x_T^*(z)$ in the nominal case. Note that due to the special structure of the stationary profiles depending only on z^1, the feedforward controls are uniform in $z_{(1|)}$ and vary only in t.

Subsequently, it is however assumed that the initial state $x_0(z)$ is random (normally distributed) and unknown. In order to address this, backstepping is used for the exponential stabilization of the tracking error dynamics.

9.8.2.2 Backstepping–Based State–Feedback Control with State–Observer

Since $x^*(z,t)$ by construction satisfies (9.98) with $u^{1_0}(z_{(1|)},t)$ and $u^{1_1}(z_{(1|)},t)$ replaced by $u^{*,1_0}(z_{(1|)},t)$ and $u^{*,1_1}(z_{(1|)},t)$), the dynamics of the tracking error $x_e(z,t)=x(z,t)-x^*(z,t)$ is given by

$$\partial_t x_e(z,t) = \Delta x_e(z,t) + c(t)x_e(z,t), \qquad (z,t)\in\Omega\times\mathbb{R}_{t_0}^+ \qquad (9.101a)$$

[10] As pointed out in Section 7.4, this set–up ensures the admissibility of the basic output trajectories.

$$\partial_{z^j} x_e(z,t) = 0, \qquad z^j = 0,\ j \in \{2,3\} \tag{9.101b}$$
$$\partial_{z^j} x_e(z,t) = 0, \qquad z^j = 1,\ j \in \{2,3\} \tag{9.101c}$$
$$x_e(z,t) = u^{1_0}(z_{(1|)},t) - u^{*,1_0}(z_{(1|)},t), \qquad z^1 = 0 \tag{9.101d}$$
$$x_e(z,t) = u^{1_1}(z_{(1|)},t) - u^{*,1_1}(z_{(1|)},t), \qquad z^1 = 1 \tag{9.101e}$$
$$x_e(z,t_0) = x_0(z) - x_0^*(z), \qquad z \in \overline{\Omega}. \tag{9.101f}$$

In addition, the error output follows as

$$y_e(z_{(3|)},t) = x_e(z,t), \qquad z^3 = 0,\ t > t_0. \tag{9.101g}$$

Hence, taking $u^{1_0}(z_{(1|)},t) = u^{*,1_0}(z_{(1|)},t)$ and $u^{1_1}(z_{(1|)},t) = u^{*,1_1}(z_{(1|)},t) + u_e^{1_1}(z_{(1|)},t)$ with $u_e^{1_1}(z_{(1|)},t)$ denoting a state–feedback control to stabilize the tracking error dynamics, (9.101) is in the elementary form (cf. (9.2)) for backstepping. Since only the SISO case is considered, subsequently the results of Sections 9.2 and 9.3 apply to determine an exponentially stabilizing state–feedback with state–observer. It should be thereby pointed out that only error variables are fed back contrary to the classical state–feedback, which, in combination with trajectory planning, is consistent with the 2DOF control concept (see also Figure 1.1).

In view of the boundary conditions (9.101d), (9.101e) the target system (9.13) is parametrized with $d(z,t) \equiv d(t) = c(t) + \mu$ for $\mu = 1$, $\epsilon_{w,1}^0 = \epsilon_{w,1}^1 = 0$, and $p_{w,1}^0 = p_{w,1}^1 = 1$. With this, the exponential stability of the target system is ensured by Lemma 9.1. Hence, the Dirichlet–type state–feedback $u_e^{1_1}(z_{(1|)},t)$ is determined from (9.16a) and reads

$$u_e^{1_1}(z_{(1|)},t) = \int_0^1 k(1,\zeta,t) x_e(z_{(1|\zeta)},t)\mathrm{d}\zeta. \tag{9.102}$$

The kernel $k(z^1,\zeta,t)$ is thereby computed using the method of integral operators and successive approximation with 7 series coefficients as outlined in Section 9.2.2. For the realization of (9.102), the error state $x_e(z,t)$ has to be re–constructed from the output variable $y_e(z_{(3|)},t)$ by means of a state–observer, i.e.

$$\begin{aligned}\partial_t \hat{x}_e(z,t) &= \Delta \hat{x}_e(z,t) + c(t)\hat{x}_e(z,t) \\ &\quad + l_1(z^1,t)\big[y_e(z_{(3|)},t) - \hat{y}_e(z_{(3|)},t)\big], \qquad (z,t) \in \Omega \times \mathbb{R}_{t_0}^+\end{aligned} \tag{9.103a}$$

with

$$\partial_{z^2} \hat{x}_e(z,t) = 0, \qquad z^2 = 0 \tag{9.103b}$$
$$\partial_{z^3} \hat{x}_e(z,t) = l_{10}(t)\big[y_e(z_{(3|)},t) - \hat{y}_e(z_{(3|)},t)\big], \quad z^3 = 0 \tag{9.103c}$$
$$\partial_{z^2} \hat{x}_e(z,t) = 0, \qquad z^2 = 1 \tag{9.103d}$$
$$\partial_{z^3} \hat{x}_e(z,t) = 0, \qquad z^3 = 1 \tag{9.103e}$$
$$\hat{x}_e(z,t) = 0, \qquad z^1 = 0 \tag{9.103f}$$

$$\hat{x}_e(z,t) = u_e^{1_1}(z_{(1|)},t), \qquad z^1 = 1 \tag{9.103g}$$

$$\hat{x}_e(z,t_0) = \hat{x}_{e,0}(z), \qquad z \in \overline{\Omega}. \tag{9.103h}$$

Thereby, backstepping is applied following the treatise in Section 9.3 to exponentially stabilize the target system (9.22) assigned for the observer error dynamics in $\tilde{x}_e(z,t) = x_e(z,t) - \hat{x}_e(z,t)$. With the choice of $\tilde{d}(z,t) \equiv \tilde{d}(t) = c(t) + \tilde{\mu}$ for $\tilde{\mu} = 4$, $\tilde{\epsilon}^0_{w,3} = \tilde{\epsilon}^1_{w,3} = 1$, and $\tilde{p}^0_{w,3} = \tilde{p}^1_{w,3} = 0$, the exponential stability of target system is guaranteed by Lemma 9.1. The observer gains $l_1(z^1,t)$ and $l_{10}(t)$ herein follow from (9.27), (9.28) with the kernel $l(z^1,\zeta,t)$ computed by means of the method of integral operators and successive approximation with 7 series coefficients according to the comments in Section 9.3.3. Hence, the state–feedback is subsequently evaluated in terms of $\hat{x}_e(z,t)$, i.e.

$$u_e^{1_1}(z_{(1|)},t) = \int_0^1 k(1,\zeta,t)\hat{x}_e(z_{(1|\zeta)},t)\mathrm{d}\zeta$$

with the distributed–parameter system (9.103) for the observer being solved numerically using an absolutely stable Crank–Nicholson scheme. The resulting state values $x(\mathtt{n}_j,t)$ at the nodes $\mathtt{n}_j$ hence follow directly by interpolation. Alternatively, (9.103) could be spatially discretized according to Section 3.1.2.

Remark 9.9. Note that differing from the previous example, both the input and output are assumed idealized. Nevertheless, the procedures discussed in Sections 9.2.5, 9.3.6 can be applied to achieve a finite–dimensional realization in terms of suitably placed actuator and sensor agents.

9.8.2.3 Simulation Results

In the following, the feedforward and state–feedback control with state–observer are applied to the multi–agent system governed by (9.97). The simulation is set–up in a sample–hold configuration with a sampling time of $\Delta t = 0.002$. Hence, the state–observer and the state–feedback are consecutively evaluated with updates in terms of measurements at any $t_k = k\Delta t$, $k = 1,\ldots,1000$. The observer is initialized by $\hat{x}_{e,0}(z) = 0$, $z \in \overline{\Omega}$, imposing an initial deviation in view of the randomly assigned $x_0(z)$ and $x_0^*(z) = 0$.

The resulting evolution of the agent state $x(\mathtt{n}_j,t)$, the observed agent state $x^*(\mathtt{n}_j,t) + \hat{x}_e(\mathtt{n}_j,t)$, and the desired state $x^*(\mathtt{n}_j,t)$ at different nodes $\mathtt{n}_j$ is shown in Figure 9.8. Here, in each subfigure nodes are selected by considering the subgraph building an octahedral interconnection according to Figure 9.7. In other words, Figure 9.8(a) illustrates the evolution of the nodes $\mathtt{n}_j$, $\mathtt{n}_{(j_1|j_1+1)}$, $\mathtt{n}_{(j_1|j_1-1)}$, $\mathtt{n}_{(j_2|j_2+1)}$, $\mathtt{n}_{(j_2|j_2-1)}$, $\mathtt{n}_{(j_3|j_3+1)}$ as well as $\mathtt{n}_{(j_3|j_3-1)}$ surrounding the center node $j_1 = j_2 = j_3 = 6$. Similarly, the nodes neighboring the center nodes with $j_1 = j_2 = j_3 = 8$ and $j_1 = j_2 = j_3 = 3$ are depicted in Figures 9.8(b) and 9.8(c), respectively. Starting from the randomly assigned initial states convergence to the desired states is achieved corresponding to consensus with a zero state. This is followed by the accurate realization of the transition to the final stationary state

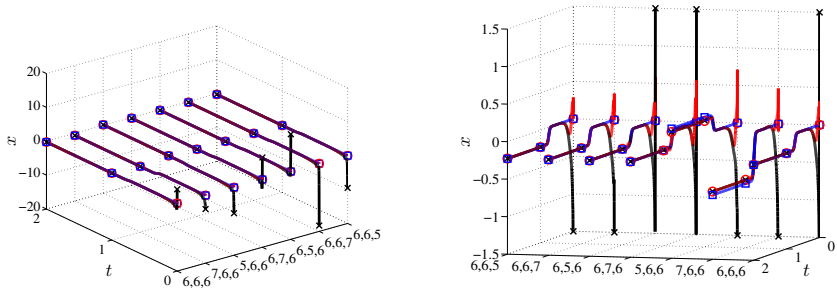

(a) Octahedral with center node $\mathtt{n}_{6,6,6}$

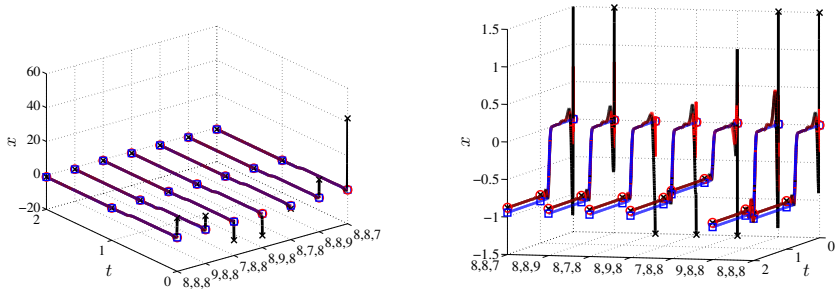

(b) Octahedral with center node $\mathtt{n}_{8,8,8}$

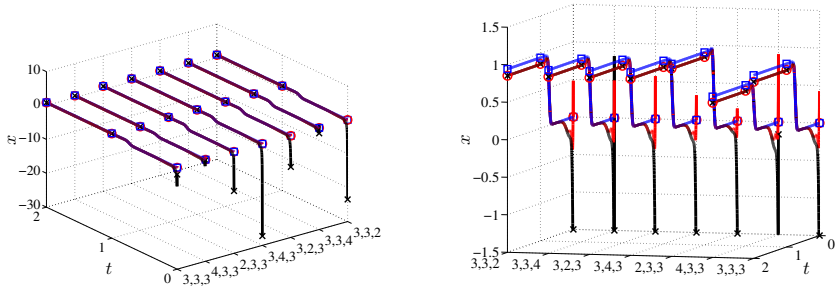

(c) Center node $\mathtt{n}_{3,3,3}$

Fig. 9.8 Simulation scenario with 1000 nodes. Evolution of the nodes synthesizing the octahedral subgraph centered as indicated (see also Figure 9.7) with the left and right column corresponding to two different perspectives and vertical axes limits. The vertical axis in the figures on the left shows the full amplitude while the figures on the right are cut–off. The markers correspond to the agents state $x(\mathtt{n}_j, t)$ (black line marked $\times$), the observed agent state $x^*(\mathtt{n}_j, t) + \hat{x}_e(\mathtt{n}_j, t)$ (red line marked $\circ$), and the desired state $x^*(\mathtt{n}_j, t)$ (blue line marked $\square$) at the individual nodes.

along the prescribed paths. However, some minor deviations from the desired paths can be observed in Figures 9.8(b) and 9.8(c), i.e. the nodes extending to the boundaries. These are due to the approximation error induced by the discretization of the feedforward and the state–feedback control with state–observer.

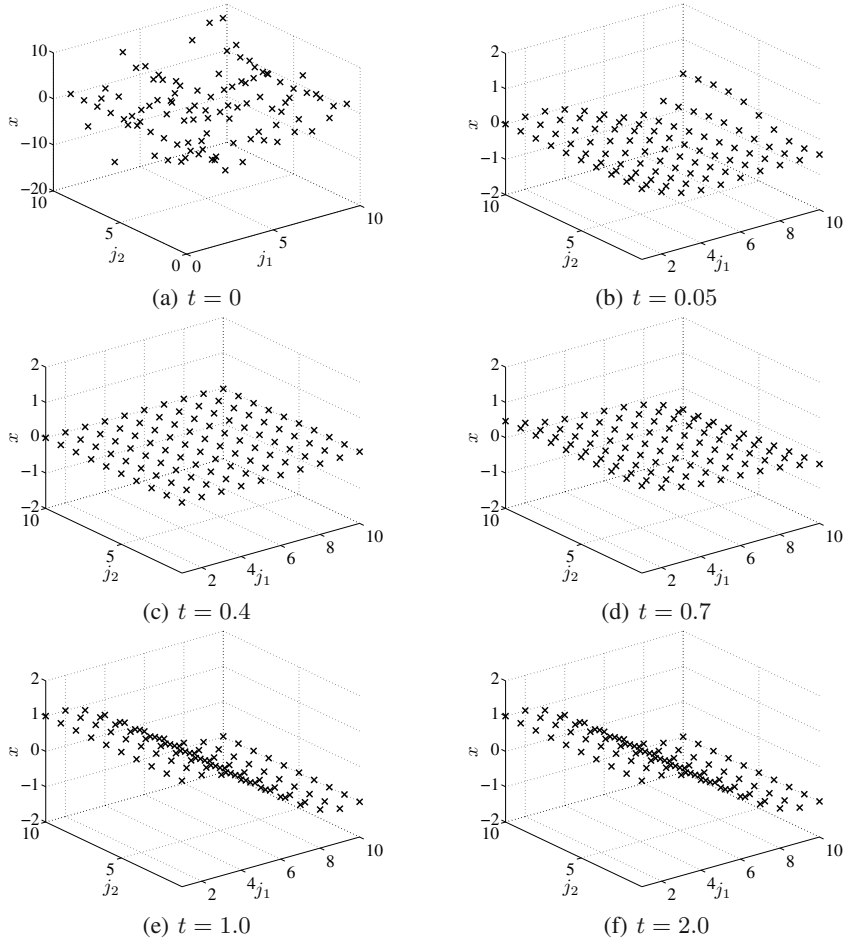

(a) $t = 0$ (b) $t = 0.05$

(c) $t = 0.4$ (d) $t = 0.7$

(e) $t = 1.0$ (f) $t = 2.0$

Fig. 9.9 Simulation scenario with 1000 nodes. Snapshots of $x(\mathtt{n}_{(j_3|10)}, t)$ at $t \in \{0, 0.05, 0.4, 0.7, 1.0, 2.0\}$.

The synchronization is moreover confirmed by Figure 9.9, where the spatial–temporal evolution of $x(\mathtt{n}_{(j_3|10)}, t)$ in the center plane $\mathtt{n}_{(j_3|10)}$ is shown at different instances of time $t \in \{0, 0.05, 0.4, 0.7, 1.0, 2.0\}$. Thereby, in particular the convergence to the final stationary state $x_T(\mathtt{n}_{(j_3|10)}, t)$ is visualized at $t = T$. Note that the final profile is identical in any plane parallel to $\mathtt{n}_{(j_3|10)}$ as outlined above.

The input trajectories consisting of the feedforward control $u^{1_0}(\mathtt{n}_{(j_1|)}, t) = u^{*,1_0}(\mathtt{n}_{(j_1|)}, t)$ and the tracking control $u^{1_1}(\mathtt{n}_{(j_1|)}, t)$ combining feedforward and state–feedback control are shown in Figure 9.10 over time $t \in [0, 2]$. Here, the values at different nodes are plotted successively, which illustrates that the relative motion of most leader nodes is rather small. Moreover, the tracking control $u^{1_1}(\mathtt{n}_{(j_1|)}, t)$ is dominated by the feedforward path after the initial transients, which

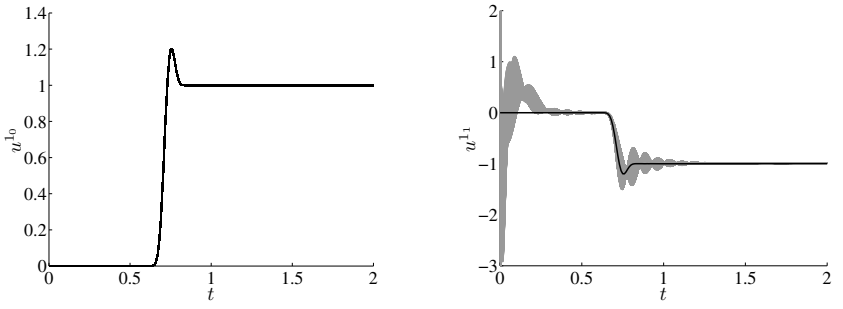

Fig. 9.10 Simulation scenario with 1000 nodes. Time evolution of the inputs $u^{1_0}(\mathtt{n}_{(j_1|)}, t)$ (left, gray) and $u^{1_1}(\mathtt{n}_{(j_1|)}, t)$ (right, gray) compared to the respective feedforward controls $u^{*,1_0}(\mathtt{n}_{(j_1|)}, t)$ (left, black) and $u^{*,1_1}(\mathtt{n}_{(j_1|)}, t)$ (right, black). The values of all nodes $\mathtt{n}_{(j_1|)}$, $j_2 = 1, \ldots, N_2$, $j_3 = 1, \ldots N_3$ are plotted successively.

is a common characteristics of the 2DOF control concept, where the state–feedback control only stabilizes the tracking error dynamics. As a result, this examples clearly illustrates that distributed–parameter systems and control theory can be efficiently exploited to analyze synchronization and related control problems for large scale multi–agent networks. In particular, it should be pointed out that the state–observer can be also utilized for monitoring purposes since, as is shown in Figure 9.8, the states of any agent can be re–constructed solely by means of the sensor nodes $y(\mathtt{n}_{(j_3|)}, t)$. Here, $N_1 \times N_2 = 100$ nodes are used to determine the state of the remaining 800 agents ($N_1 \times N_2 \times N_3$ minus the leader nodes). Nevertheless, the number of sensor agents can be reduced by considering the procedure presented in Section 9.3.6 for the approximation of $y(\mathtt{n}_{(j_3|)}, t)$ by means of only a low number of suitably assigned sensor agents.

Moreover, note that the presented approach is independent of the number[11] of agents considered in the network. In order to illustrate this, results for an identical simulation scenario as depicted in Figures 9.8–9.10 are shown in Figures 9.11–9.13 with the difference that $N_1 = 20$, i.e. 8000 agents are covered with 800 leader agents and 400 sensor agents. The design approach can be hereby applied without any modification, which confirms the scale–up capabilities of the developed methods for multi–agent systems. Since the initial condition is assumed to be random but normally distributed, the transients between the scenario with 1000 agents and those with 8000 differ. In addition, spurious oscillations emerge in Figure 9.11(b). These are due to the fact that the final profile corresponds to an unstable profile whose eigenvalues are computed with much higher accuracy as in the scenario with 1000 agents. In order to address this, it would be required to properly adjust the sampling time Δt, which is, however, kept as before to ensure the comparability of the results.

[11] Obviously, the discretization error has to be considered as pointed out in Section 3.1.2, which decreases as the number of agents increases and approaches the continuous formulation used for the design.

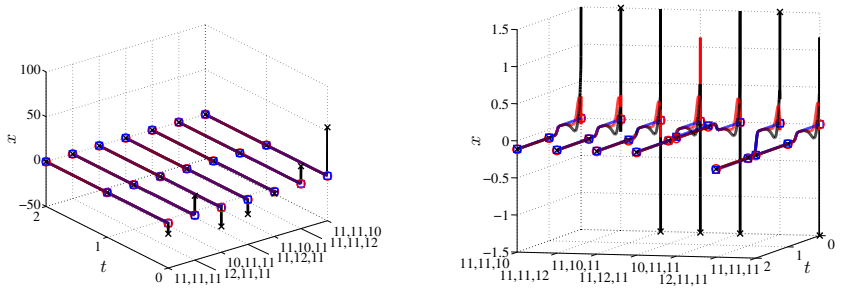

(a) Octahedral with center node $\mathtt{n}_{11,11,11}$

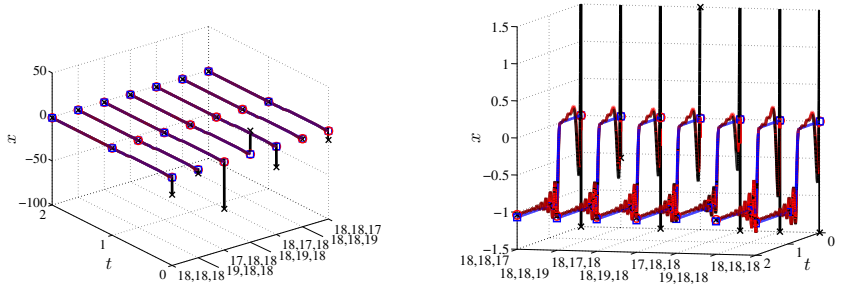

(b) Octahedral with center node $\mathtt{n}_{18,18,18}$

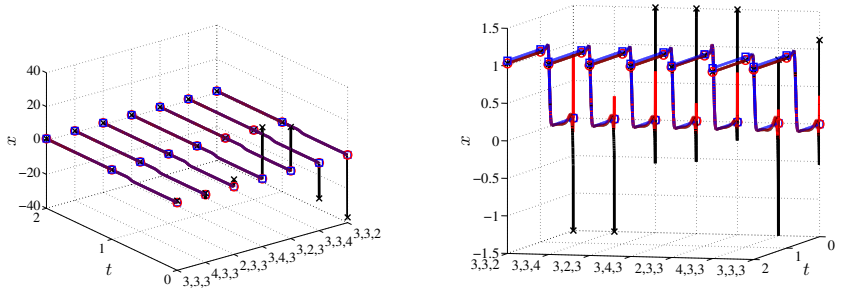

(c) Center node $\mathtt{n}_{3,3,3}$

Fig. 9.11 Simulation scenario with 8000 nodes. Evolution of the nodes synthesizing the octahedral subgraph centered as indicated (see also Figure 9.7) with the left and right column corresponding to two different perspectives and vertical axes limits. The vertical axis in the figures on the left shows the full amplitude while the figures on the right are cut–off. The markers correspond to the agents state $x(\mathtt{n}_j, t)$ (black line marked $\times$), the observed agent state $x^*(\mathtt{n}_j, t) + \hat{x}_e(\mathtt{n}_j, t)$ (red line marked $\circ$), and the desired state $x^*(\mathtt{n}_j, t)$ (blue line marked $\square$) at the individual nodes.

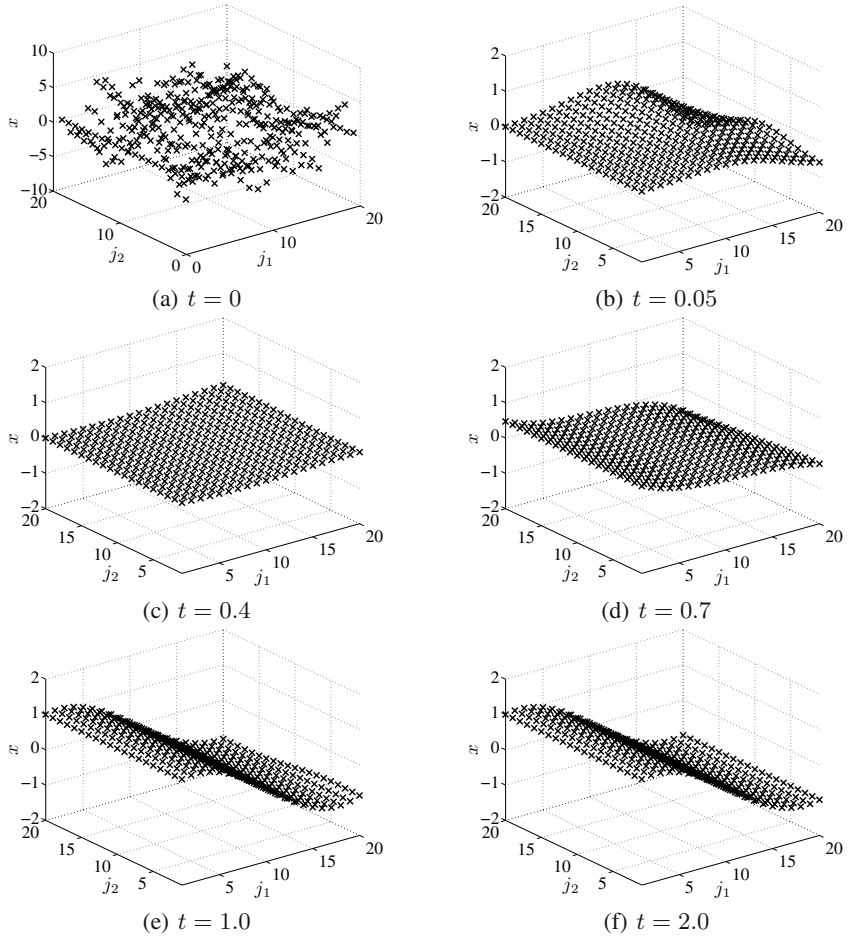

(a) $t = 0$ (b) $t = 0.05$

(c) $t = 0.4$ (d) $t = 0.7$

(e) $t = 1.0$ (f) $t = 2.0$

Fig. 9.12 Simulation scenario with 8000 nodes. Snapshots of $x(\mathtt{n}_{(j_3|10)}, t)$ at $t \in \{0, 0.05, 0.4, 0.7, 1.0, 2.0\}$

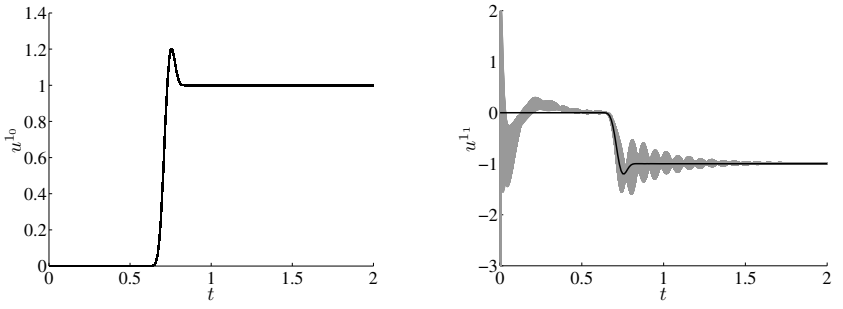

Fig. 9.13 Simulation scenario with 8000 nodes. Time evolution of the inputs $u^{1_0}(\mathtt{n}_{(j_1|)}, t)$ (left, gray) and $u^{1_1}(\mathtt{n}_{(j_1|)}, t)$ (right, gray) compared to the respective feedforward controls $u^{*,1_0}(\mathtt{n}_{(j_1|)}, t)$ (left, black) and $u^{*,1_1}(\mathtt{n}_{(j_1|)}, t)$ (right, black). The values of all nodes $\mathtt{n}_{(j_1|)}$, $j_2 = 1, \ldots, N_2$, $j_3 = 1, \ldots N_3$ are plotted successively.

References

1. Atkinson, B.: Biochemical Reactors. Pion Limited (1974)
2. Baehr, H., Stephan, K.: Heat and Mass Transfer, 2nd edn. Springer, Berlin (2006)
3. Bird, R., Stewart, W., Lightfoot, E.: Transport Phenomena. John Wiley & Sons, Inc., New York (2002)
4. Bitzer, M.: Model-based Nonlinear Tracking Control of Pressure Swing Adsorption Plants. In: Meurer, T. (ed.) Control and Observer Design for Nonlinear Finite and Infinite Dimensional Systems. LNCIS, vol. 322, pp. 403–418. Springer, Berlin (2005)
5. Bitzer, M., Zeitz, M.: Design of a nonlinear distributed parameter observer for a pressure swing adsorption plant. Journal of Process Control 12(4), 533–543 (2002)
6. Cochran, J., Krstic, M.: Motion planning and trajectory tracking for three–dimensional Poiseuille flow. J. Fluid. Mech. 626, 307–332 (2009)
7. Davis, T.: UMFPACK (2009), `http://www.cise.ufl.edu/research/sparse/umfpack`
8. Jadachowski, L., Meurer, T., Kugi, A.: State estimation for parabolic PDEs with varying parameters on 3–dimensional spatial domains. In: Proc. 18th IFAC World Congress, Milan, vol. (I), pp. 13,338–13,343 (2011)
9. Ladyženskaja, O., Solonnikov, V., Ural'ceva, N.: Linear and Quasi–linear Equations of Parabolic Type, Translations of Mathematical Monographs, 5th edn., vol. 23. American Mathematical Society, Providence (1998)
10. Meurer, T., Kugi, A.: Tracking control for a diffusion–convection–reaction system: combining flatness and backstepping. In: Proc. 7th IFAC Symposium Nonlinear Control Systems (NOLCOS 2007), Pretoria (SA), pp. 583–588 (2007)
11. Vazquez, R., Krstic, M.: Control of Turbulent and Magnetohydrodynamic Channel Flow. Birkhäuser, Boston (2008)
12. Vazquez, R., Schuster, E., Krstic, M.: Magnetohydrodynamic state estimation with boundary sensors. Automatica 44(10), 2517–2527 (2008)
13. Wouwer, A.V., Zeitz, M.: Parameter estimation in distributed parameter systems. In: Unbehauen, H. (ed.) Encyclopedia of Life Support Systems (EOLSS), chap. Control Systems, Robotics and Automation, article No. 6.43.19.3, EOLSS Publishers, Oxford, UK (2001)
14. Zeitz, M.: Nichtlineare Beobachter für chemische Reaktoren. Fortschr.–Ber. VDI Reihe 8 Nr. 27, VDI Verlag, Düsseldorf (1977)

Part V
Appendix

Appendix A
Notation

A.1 Einstein Summation Convention

In Part II of this monograph, the Einstein summation convention referring to the summation over repeated indexes is used, i.e.

$$a^{ij}b_j = \sum_{j=1}^{J} a^{ij}b_j.$$

The multiplication of two matrices A and B can be hence represented as $C = AB$ with $C^k_j = A^i_j B^k_i$ denoting the respective matrix elements.

Einstein's notation can be used to distinguish between co– and contravariant tensors and hence between vectors and covectors. Let the sets $\{\boldsymbol{e}_k\}_{k=1,\ldots,r}$ and $\{\boldsymbol{e}^k\}_{k=1,\ldots,r}$ represent the co– and contravariant bases of a Cartesian coordinate system satisfying the orthogonality relations $\boldsymbol{e}_k\boldsymbol{e}_l = \delta_{kl}$, $\boldsymbol{e}^k\boldsymbol{e}^l = \delta^{kl}$, and $\boldsymbol{e}_k\boldsymbol{e}^l = \delta^l_k$ with the Kronecker delta function

$$\delta^{l\ldots q}_{k\ldots p} = \begin{cases} 1, & \text{if } k = l = \ldots = p = q \\ 0, & \text{else} \end{cases}.$$

Depending on the context, also the notation

$$\delta^{l\ldots q}_{k\ldots p} = \delta^{l,\ldots,q}_{k,\ldots,p}$$

is used for the sake of clarity. An arbitrary tensor $\boldsymbol{A}$ with Cartesian components[1] $A^{l\ldots q}_{k\ldots p}$ is represented as

$$\boldsymbol{A} = A^{l\ldots q}_{k\ldots p}\boldsymbol{e}_k \otimes \cdots \otimes \boldsymbol{e}_p \otimes \boldsymbol{e}^l \otimes \cdots \otimes \boldsymbol{e}^q$$

[1] While it is not necessary to distinguish between co– and contravariant tensors in Cartesian coordinate systems in $\mathbb{R}^r$ the notation is used for the clarity of presentation in view of the proper introduction of tensor transformations in Section 4.

with respect to the basis $\{\boldsymbol{e}_k \otimes \cdots \otimes \boldsymbol{e}_p \otimes \boldsymbol{e}^l \otimes \cdots \otimes \boldsymbol{e}^q\}$, where $\otimes$ denotes the tensor product. The identity tensor is given by $\boldsymbol{\delta}$ with components $\delta^{l\ldots q}_{k\ldots p}$ defined above. First rank contravariant tensors correspond to column vectors and first rank covariant tensors to row vectors [1].

A.2 Multi–Index Notation

Multi–index notation is used in various parts of the text. Let $r,\, l \in \mathbb{N}$ and let the r–tuples $k = (k_1, \ldots, k_r) \in \mathbb{N}^r$ and $K = (K_1, \ldots, K_r) \in \mathbb{N}^r$ denote two multi–indexes. Then the length or the order of k is given by

$$|k| = k_1 + \ldots + k_r.$$

Throughout this contribution sub–tuples are denotes as

$$k_{(l|)} = (k_1, \ldots, k_{l-1}, k_{l+1}, \ldots, k_r) \in \mathbb{N}^{r-1}.$$

The notion $k \leq K$ is used to express that $k_j < K_j$ for all $j \in I_r = \{1, 2, \ldots, r\}$. Sums and products over a multi–index are defined as

$$\sum_{k \in \mathbb{N}^r} f_k = \sum_{k_1=1}^{\infty} \cdots \sum_{k_r=1}^{\infty} f_{k_1,\ldots,k_r}, \qquad \prod_{k \in \mathbb{N}^r} f_k = \prod_{k_1=1}^{\infty} \cdots \prod_{k_r=1}^{\infty} f_{k_1,\ldots,k_r}$$

while

$$\sum_{k=1}^{K} f_k = \sum_{k_1=1}^{K_1} \cdots \sum_{k_r=1}^{K_r} f_{k_1,\ldots,k_r}, \qquad \prod_{k=1}^{K} f_k = \prod_{k_1=1}^{K_1} \cdots \prod_{k_r=1}^{K_r} f_{k_1,\ldots,k_r}.$$

In addition, factorials are defined according to

$$(k+K)! = \prod_{i=1}^{r} (k_i + K_i)!, \qquad (k+l)! = \prod_{i=1}^{r} (k_i + l)!.$$

Reference

1. Simmonds, J.: A Brief on Tensor Analysis, 2nd edn. Springer, New York (1994)

Appendix B
Mathematical Background

B.1 Complex Analysis

In the following, selected results from complex analysis are summarized, which are used throughout the presentation.

Definition B.1 (Gevrey class). The function $y(t)$ is in $G_{D,\alpha}(\Lambda)$, the Gevrey class of order α in $\Lambda \subseteq \mathbb{R}$, if $y(t) \in C^\infty(\Lambda)$ and for every closed subset $\bar{\Lambda}$ of Λ, there exists a positive constant D such that for all $j \in \mathbb{N}$

$$\sup_{t\in\bar{\Lambda}} \left|\partial_t^j y(t)\right| \leq D^{j+1}(j!)^\alpha. \tag{B.1}$$

Similarly, Gevrey classes can be defined for functions of several arguments and functions which are of different order with respect to the arguments.

Definition B.2 (Gevrey class for functions of several arguments). The function $y(z,t)$ is in $G_{D,\beta,\alpha}(\Lambda)$, $\Lambda = \Omega \times \mathbb{R}$ with $\Omega \subseteq \mathbb{R}^r$, the Gevrey class of order $\beta = (\beta_1, \ldots, \beta_r)$ in z and order α in t, if $y(z,t) \in C^\infty(\Lambda)$ and for every closed subset $\bar{\Lambda}$ of Λ, there exists a positive constant D such that for all $j \in \mathbb{N}^r$ and $k \in \mathbb{N}$

$$\begin{aligned}\sup_{(z,t)\in\bar{\Lambda}} \left|\partial_z^j \partial_t^k y(z,t)\right| &= \sup_{(z,t)\in\bar{\Lambda}} \left|\partial_{z^1}^{j_1} \cdots \partial_{z^r}^{j_r} \partial_t^k y(z,t)\right| \\ &\leq D^{|j|+k+1}(k!)^\alpha \prod_{i=1}^{r} (j_i!)^{\beta_i}.\end{aligned} \tag{B.2}$$

Note that both $G_{D,\alpha}(\Lambda)$ and $G_{D,\beta,\alpha}(\Lambda)$ form a linear vector space and a ring with respect to the arithmetic product of functions, which is closed under the standard rules of differentiation [14, 8]. In particular, it can be easily verified that functions of Gevrey order $\beta < 1$ ($\alpha < 1$) are entire and analytic in the case $\beta = 1$ ($\alpha = 1$).

Two examples of Gevrey class functions [2, 16] are given by

$$\mathcal{g}^1_{T,\omega}(t) = \begin{cases} 0, & t \leq 0 \\ \dfrac{\int_0^t \hbar_{T,\omega}(p)\mathrm{d}p}{\int_0^T \hbar_{T,\omega}(p)\mathrm{d}p}, & t \in (0,T) \\ 1, & t \geq T, \end{cases} \tag{B.3}$$

where

$$\hbar_{T,\omega}(t) = \begin{cases} \exp\left(-\left(\left[1-\dfrac{t}{T}\right]\dfrac{t}{T}\right)^{-\omega}\right), & t \in (0,T) \\ 0, & t \neq (0,T) \end{cases} \tag{B.4}$$

and

$$\mathcal{g}^2_{T,\omega}(t) = \begin{cases} 0, & t \leq 0 \\ \dfrac{1}{2} + \dfrac{1}{2}\tanh\left(\dfrac{2\left(2\frac{t}{T}-1\right)}{\left(\frac{4t}{T}\left(1-\frac{t}{T}\right)\right)^{\omega}}\right), & t \in (0,T) \\ 1, & t \geq T, \end{cases} \tag{B.5}$$

It can be shown that $\mathcal{g}^1_{T,\omega}(t)$ and $\mathcal{g}^2_{T,\omega}(t)$ are in the Gevrey class of order $\alpha = 1+1/\omega$ (see, e.g., [8] for (B.3) and [15] given (B.5)).

B.2 Entire Functions

Subsequently, a selection of results is presented addressing entire functions and their properties following the comprehensive treatises in [4, 11, 12]. Thereby, certain asymptotic inequalities are considered, where the notation $f(\eta) <_{\text{as}} g(\eta)$ is used to express that $f(\eta) < g(\eta)$ holds for sufficiently large η. Similarly, if $f(\eta) < g(\eta)$ holds for some sequence of values $(\eta_n)_n$ with $\eta_n \to \infty$, then the notation $f(\eta) <_n g(\eta)$ is used.

B.2.1 Fundamental Notions

Given an entire function $\hat{f}(s)$ its maximal modulus $M(\eta)$ is defined as

$$M(\eta) = \max_{|s|=\eta} |\hat{f}(s)|. \tag{B.6}$$

This enables to characterize the growth of the entire function $\hat{f}(s)$. In particular the entire function $\hat{f}(s)$ is of finite order if $M(\eta) <_{\text{as}} \exp(\eta^k)$ for some $k > 0$. The order ϱ is then given as the infimum of those k for which the asymptotic inequality is fulfilled. With this, it follows that

$$e^{\eta^{\varrho-\epsilon}} <_n M(\eta) <_{\text{as}} e^{\eta^{\varrho+\epsilon}}$$

and hence by taking the logarithm twice one can conclude that

$$\varrho = \limsup_{\eta\to\infty} \frac{\log\log M(\eta)}{\log\eta}.$$

The function $\hat{f}(s)$ has a finite type if for some $A > 0$ the inequality $M(\eta) <_{\text{as}} \exp(A\eta^{\varrho})$ holds. The type τ is then determined as the infimum of those A for which the asymptotic inequality is satisfied. Moreover, this implies the inequalities

$$e^{(\tau-\epsilon)\eta^{\varrho}} <_n M(\eta) <_{\text{as}} e^{(\tau+\epsilon)\eta^{\varrho}}$$

and hence

$$\tau = \limsup_{\eta\to\infty} \frac{\log M(\eta)}{\eta^{\varrho}}. \tag{B.7}$$

If for a given ϱ the type of $\hat{f}(s)$ is infinite, then the function is of maximal type. If $0 < \tau < \infty$, then the type is normal while for $\tau = 0$ the type is minimal. Note that entire functions of order $\varrho = 1$ and normal type are called entire functions of exponential type.

Let $\hat{f}(s)$ and $\hat{g}(s)$ denote two entire functions of order ϱ_f, ϱ_g and type τ_f, τ_g, respectively. Subsequently, let ϱ_{fg}, ϱ_{f+g} and τ_{fg}, τ_{f+g} denote the order and type of the product $\hat{f}(s)\hat{g}(s)$ and the sum $\hat{f}(s) + \hat{g}(s)$. As pointed out in [12, Section 1.2] it can be shown that

$$\varrho_{fg} \le \max(\varrho_f, \varrho_g), \qquad \varrho_{f+g} \le \max(\varrho_f, \varrho_g) \tag{B.8}$$

$$\tau_{fg} \le \tau_f + \tau_g, \qquad \tau_{f+g} \le \max(\tau_f, \tau_g). \tag{B.9}$$

In addition, given a non–decreasing sequence $(a_n)_{n\in\mathbb{N}}$ of complex numbers the so–called counting function $\mathcal{N}(\eta)$, i.e., the number of elements of the sequence not exceeding η, can be introduced according to

$$\mathcal{N}(\eta) = \#\{a_n,\, n \in \mathbb{N} :\, |a_n| \le \eta\}. \tag{B.10}$$

Moreover, the order ϱ_1 of the counting function $\mathcal{N}(\eta)$ [4, Theorem 2.5.8] can be defined as

$$\varrho_1 = \limsup_{\eta\to\infty} \frac{\log \mathcal{N}(\eta)}{\log\eta}. \tag{B.11}$$

The counting function and its order are rather useful tools to deduce essential properties of entire functions.

B.2.2 Weierstrass Canonical Products and the Hadamard Theorem

In the course of the analysis of the relationship between the growth of an entire function and the location of its zeros, an analogue to the factorization of a polynomial into linear factors for transcendental entire functions is needed (see, e.g., [4, Section 2.6f], [12, Section 4.1]). With this, a particular infinite product representation of entire functions can be achieved, namely the Weierstrass canonical product. Therefore, the notions of convergence exponent and genus of a sequence (of zeros) are required [4, Definition 2.5.2f], [12, Section 3.2].

Definition B.3 (Convergence exponent). Given a sequence $(a_n)_{n\in\mathbb{N}}$ of complex numbers with $a_n \neq 0$, $\lim_{n\to\infty} a_n \to \infty$ the infimum of positive numbers γ for which the series

$$\sum_{n\in\mathbb{N}} \frac{1}{|a_n|^\gamma} \tag{B.12}$$

converges is called the convergence exponent.

The relationship between the convergence exponent of a sequence and its counting function is given in the following lemma [12, Section 3.2].

Lemma B.1. *The convergence exponent γ of the sequence $(a_n)_{n\in\mathbb{N}}$ is equal to the order ϱ_1 of its counting function.*

In addition, the convergence exponent of the zeros of an entire function and its order are related according to the theorem below [12, Section 3.2].

Theorem B.1. *The convergence exponent of the zeros of an entire function does not exceed its growth order.*

These two results already illustrate the importance of the convergence exponent for the analysis and characterization of entire functions.

Definition B.4 (Genus of a sequence). The smallest positive integer γ for which (B.12) converges is denoted by $g^s + 1$ and g^s is called the genus of the sequence $(a_n)_{n\in\mathbb{N}}$.

Note that g^s as defined above is not necessarily equal to the genus of the entire function $\hat{f}(s)$. Subsequently, assume that the sequence $(a_n)_{n\in\mathbb{N}}$ is of genus g^s. With this, consider now the infinite product

$$\Pi(s) = \prod_{n\in\mathbb{N}} \mathcal{G}\left(\frac{s}{a_n}, g^s\right), \tag{B.13}$$

where

$$\mathcal{G}(s, g^s) = \begin{cases} 1 - s, & g^s = 0 \\ (1 - s)\exp\mathcal{F}(s, g^s), & g^s > 0 \end{cases} \tag{B.14}$$

are the so–called Weierstrass primary factors with

$$\mathcal{F}(s, g^s) = \sum_{i=1}^{g^s} \frac{s^i}{i}. \tag{B.15}$$

It can be shown that the infinite product (B.13) converges absolutely and uniformly in every disk $\{s \in \mathbb{C} : |s| \leq R < \infty\}$ [12, Section 4.1]. Hence, $\Pi(s)$ is called the Weierstrass canonical product of genus g^s. Following Boas [4, Theorem 2.6.5], $\Pi(s)$ defines an entire function of a particular order.

Theorem B.2. *A canonical product $\Pi(s)$ of genus g^s is an entire function of order equal to the convergence exponent of its zeros.*

With these preliminary considerations one of the main theorems in the theory of entire functions can formulated, which provides a general representation formula for entire functions of finite order [12, Section 4.2].

Theorem B.3 (Hadamard theorem). *An entire function $\hat{f}(s)$ of finite order ϱ may be represented in the form*

$$\hat{f}(s) = s^m e^{P_q(s)} \prod_{n=1}^{\infty} \mathcal{G}\left(\frac{s}{a_n}, g^s\right), \tag{B.16}$$

where the sequence $(a_n)_{n\in\mathbb{N}}$ of genus g^s includes all nonzero roots of the function $\hat{f}(s)$, $g^s \leq \varrho$, $P_q(s)$ is a polynomial in s of degree $q \leq \varrho$, and m is the multiplicity of the root at the origin.

In addition, with the structural representation above the genus g^f of an entire function can be introduced, which can differ from the genus g^s of the sequence of its zeros [4, Definition 2.7.3].

Definition B.5 (Genus of an entire function). The genus g^f of an entire function $\hat{f}(s)$ is $\max(g^s, q)$ with q the polynomial degree in (B.16).

The product representations are particularly useful to determine connections between the growth of an entire function and the distribution of its zeros. Thereby, it is necessary to distinguish between entire functions of non–integer and integer order.

Theorem B.4. *The convergence exponent γ of the zero set of an entire function $\hat{f}(s)$ of non–integer order is equal to the order of growth ϱ of $\hat{f}(s)$.*

For a proof, see, e.g., Levin [12, Section 5.1]. If the entire function is of integer order, then no such simple result is available since the order might be larger than the distribution of its zeros might indicate. As an example consider $\exp(s)$, which has no (finite) zeros but is of order 1. Let a_ϱ denote the coefficient of s^ϱ in the polynomial $P_q(s)$ in the Hadamard representation (B.16). Then the following result holds, which traces back to Lindelöf [12, Section 5.2].

Theorem B.5. *If $\varrho = g^s + 1$, then $\hat{f}(s)$ is an entire function of minimal type for $a_\varrho = 0$ and of mean type for $a_\varrho \neq 0$. In the latter case the type of $\hat{f}(s)$ follows as $\tau = |a_\varrho|$.*

B.3 Functional Analysis

In the following, some basic functional analytic notions and results are summarized, which are used throughout this treatise. It is thereby assumed that the reader is familiar with the basic concepts of normed linear spaces. Herein, X denotes a Hilbert space with inner product $\langle \cdot, \cdot \rangle_X$ and induced norm $\| \cdot \|_X$, $\mathcal{L}(Z, X)$ is the space of bounded linear operators from the Hilbert space Z to the Hilbert space X with the induced norm. In addition, recall that two norms $\| \cdot \|_a$ and $\| \cdot \|_b$ on a space X are equivalent if there exist constants $c_1,\ c_2 > 0$ such that $c_1 \|\boldsymbol{x}\|_b \leq \|\boldsymbol{x}\|_a \leq c_2 \|\boldsymbol{x}\|_b$ for all $\boldsymbol{x} \in X$. This can similarly be defined for norms on subspaces. Given two Hilbert spaces V and X such that $V \subset X$ then the embedding $V \subset X$ is continuous (typically denoted by $V \hookrightarrow X$) if the identity operator on V is in $\mathcal{L}(V, X)$. Hence, there exists a constant $c \geq 0$ such that $\|\boldsymbol{x}\|_X \leq c \|\boldsymbol{x}\|_V$ for every $\boldsymbol{x} \in V$.

B.3.1 Fundamental Notions and Definitions

In order to make this section rather self–contained, some fundamental results are briefly recalled, which are used subsequently. For further details, the reader is referred to [7, 17, 9, 13, 19, 5, 1, 18].

Definition B.6 (Closed operator). Let X and Z be Hilbert spaces and $\mathcal{D}(\mathfrak{A}) \subset X$. The operator $\mathfrak{A} : \mathcal{D}(\mathfrak{A}) \to Z$ is called closed if its graph $\text{Graph}(\mathfrak{A}) = \{[\boldsymbol{x}, \mathfrak{A}\boldsymbol{x}]^T \mid \boldsymbol{x} \in \mathcal{D}(\mathfrak{A})\}$ is closed in $X \times Z$.

Moreover it can be shown that if $\mathfrak{A}$ is closed, then $\mathcal{D}(\mathfrak{A})$ is a Hilbert space with the graph norm $\| \cdot \|_{gr}$ defined as

$$\|\boldsymbol{x}\|_{gr}^2 = \left\| \begin{bmatrix} \boldsymbol{x} \\ \mathfrak{A}\boldsymbol{x} \end{bmatrix} \right\|_{X \times Z}^2 := \|\boldsymbol{x}\|_X^2 + \|\mathfrak{A}\boldsymbol{x}\|_Z. \tag{B.17}$$

By the closed graph theorem, a closed operator is bounded.

Theorem B.6 (Closed graph theorem). *If $\mathfrak{A} : X \to Z$ is closed, then $\mathfrak{A}$ is bounded if and only if $\mathcal{D}(\mathfrak{A})$ is closed.*

A closed operator can be also characterized by means of its resolvent set.

Definition B.7 (Resolvent, resolvent set, spectrum). If $\mathfrak{A} : \mathcal{D}(\mathfrak{A}) \subset X \to Z$, then the resolvent set $\rho(\mathfrak{A})$ of $\mathfrak{A}$ is the set of points $s \in \mathbb{C}$ for which the operator $s\mathfrak{I} - \mathfrak{A} : \mathcal{D}(\mathfrak{A}) \to Z$ is invertible and $(s\mathfrak{I} - \mathfrak{A})^{-1} \in \mathcal{L}(Z, X)$. The spectrum $\sigma(\mathfrak{A})$ is the complement of $\rho(\mathfrak{A})$ in $\mathbb{C}$. Moreover, $(s\mathfrak{I} - \mathfrak{A})^{-1}$ is called the resolvent.

Remark B.1. If $\rho(\mathfrak{A}) \neq \emptyset$, then $\mathfrak{A}$ is closed Tucsnak and Weiss [18, Remark 2.2.4].

B.3.2 Duality and Pivot Spaces

In order to deal with inhomogeneous boundary conditions or certain classes of unbounded input operators the concept of duality with respect to a pivot space has to be introduced.

For any Hilbert space X the dual space, i.e. the space of all bounded linear functionals on X, is denoted by X'. The dual space X' is a Hilbert space with the norm $\|\boldsymbol{x}'\|_{X'} = \sup_{\boldsymbol{y}\in X,\, \|\boldsymbol{y}\|_X \leq 1} |\langle \boldsymbol{x}', \boldsymbol{y}\rangle_{X',X}|$. Here, $\boldsymbol{x}'(\boldsymbol{y}) = \langle \boldsymbol{x}', \boldsymbol{y}\rangle_{X',X}$ denotes the duality pairing, i.e. the application of the linear functional $\boldsymbol{x}' \in X'$ to $\boldsymbol{y} \in X$. For such X and X' there exists a linear bijective map $\mathfrak{J}_R : X \to X'$ defined by $\langle \mathfrak{J}_R \boldsymbol{x}, \boldsymbol{y}\rangle_{X',X} = \langle \boldsymbol{x}, \boldsymbol{y}\rangle_X$ for all $\boldsymbol{x},\ \boldsymbol{y} \in X$.

Definition B.8 (Isomorphism, unitary operator). An operator $\mathfrak{J} \in \mathcal{L}(X, Z)$ is called an isomorphism from X to Z if $\mathfrak{J}^*\mathfrak{J} = \mathfrak{I}$ (identity in X) and $\mathfrak{J}\mathfrak{J}^* = \mathfrak{I}$ (identity in Z) with $\mathfrak{J}^*$ denoting the adjoint operator. Note that $\mathfrak{J}$ is an isomorphism if and only if $\|\mathfrak{J}\boldsymbol{x}\|_Z = \|\boldsymbol{x}\|_X$ and $\mathrm{ran}\mathfrak{J} = Z$. An isomorphism is also called an unitary operator.

With this, the Riesz representation theorem can introduced as follows.

Theorem B.7 (Riesz representation theorem). *Let X' be the dual space to X. Then X' can be canonically identified with X, i.e. for each $\boldsymbol{x}' \in X'$ there exists a unique element $\boldsymbol{x} \in X$ such that $\langle \boldsymbol{x}', \boldsymbol{y}\rangle_{X',X} = \langle \boldsymbol{x}, \boldsymbol{y}\rangle_X$ for all $\boldsymbol{y} \in X$. The mapping $\boldsymbol{x}' \mapsto \boldsymbol{x}$ is a linear isomorphism of X' onto X.*

From the Riesz representation theorem it follows that $\mathfrak{J}_R$ is an isomorphism. Hence, by not distinguishing between $\boldsymbol{x}$ and $\mathfrak{J}_R\boldsymbol{x}$ the space X can be identified with its dual space X'. In addition, the concept of duality can be used to properly introduce the adjoint operator $\mathfrak{A}^*$ to an operator $\mathfrak{A}$.

Definition B.9 (Adjoint operator). Let X and Y be Hilbert spaces and let $\mathfrak{A} \in \mathcal{L}(X, Y)$. The adjoint of $\mathfrak{A}$ is the operator $\mathfrak{A}^* \in \mathcal{L}(Y', X')$ defined according to $\langle \mathfrak{A}^*\boldsymbol{y}', \boldsymbol{x}\rangle_{X',X} = \langle \boldsymbol{y}', \mathfrak{A}\boldsymbol{x}\rangle_{Y',Y}, \forall \boldsymbol{x} \in X,\ \boldsymbol{y}' \in Y'$. By identifying X with X' and Y with Y' one has $\mathfrak{A}^* \in \mathcal{L}(Y, X)$ and the previous definition results in $\langle \mathfrak{A}\boldsymbol{x}, \boldsymbol{y}\rangle_Y = \langle \boldsymbol{x}, \mathfrak{A}^*\boldsymbol{y}\rangle_X, \forall \boldsymbol{x} \in X,\ \boldsymbol{y} \in Y$.

Consider now two Hilbert spaces V and X densely defined and with continuous embedding $V \subset X$. Then the function $\|\boldsymbol{y}\|_* = \sup_{\boldsymbol{x}\in V,\, \|\boldsymbol{x}\|_V \leq 1} |\langle \boldsymbol{y}, \boldsymbol{x}\rangle_X|$ for all $\boldsymbol{y} \in X$ is a norm on X. Let $\overline{V}$ denote the completion of X with respect to this norm. Then it can be shown that the operator $\mathfrak{J} : \overline{V} \to V'$ defined for any $\boldsymbol{y} \in \overline{V}$ according to $\langle \mathfrak{J}\boldsymbol{y}, \boldsymbol{x}\rangle_{V',V} = \lim_{n\to\infty} \langle \boldsymbol{y}_n, \boldsymbol{x}\rangle_X$ for all $\boldsymbol{x} \in V$, where $(\boldsymbol{y}_n)_n$ is a sequence in X such that $\boldsymbol{y}_n \to \boldsymbol{y}$ in $\overline{V}$ is an isomorphism from $\overline{V}$ to V' [18, Proposition 2.9.2]. By again identifying $\overline{V}$ with V', i.e. by no longer distinguishing between $\boldsymbol{y}$ and $\mathfrak{J}\boldsymbol{y}$ for all $\boldsymbol{y} \in \overline{V}$, it follows that $V \subset X \subset V'$, densely and with continuous embeddings. Then V' is called the dual of V with respect to the pivot space X or a Gelfand triple. The norm $\|\cdot\|_*$ defined on X is called the dual norm of $\|\cdot\|_V$ with respect to the pivot space X. Moreover, V is uniquely determined by V', i.e. V consists of those $\boldsymbol{x} \in X$

for which the inner product $\langle \boldsymbol{y}, \boldsymbol{x} \rangle_X$ regarded as a function of $\boldsymbol{y}$ has a continuous extension to V'.

The concepts introduced above in particular allow to characterize certain operator extensions, which are useful for the analysis of boundary control problems.

Lemma B.2. *Let V and X be Hilbert spaces such that $V \subset X$, densely and with continuous embedding, let $\mathfrak{A} \in \mathcal{L}(X)$, and denote by V' the dual of V with respect to the pivot space X. In this case,*

(i) if $\mathfrak{A}V \subset V$, then the restriction $\mathfrak{A}|_V \in \mathcal{L}(V)$;
(ii) if $\mathfrak{A}^* V \subset V$, then $\mathfrak{A}$ has a unique extension $\tilde{\mathfrak{A}} \in \mathcal{L}(V')$.

For a proof, see [18, Proposition 2.9.3].

B.3.3 The Spaces $\mathbf{X_1}$ and $\mathbf{X_{-1}}$

Based on the previous results, two Hilbert spaces, namely X_1 and X_{-1} can be introduced, which are important in the study of unbounded control and observation operators arising the study of PDE control problems. The assertions and proofs can be found, e.g., in [18, Section 2.10].

Lemma B.3. *Let $\mathfrak{A} : \mathcal{D}(\mathfrak{A}) \to X$ be a densely defined operator with $\rho(\mathfrak{A}) \neq \emptyset$. Then for every $\beta \in \rho(\mathfrak{A})$, the space $\mathcal{D}(\mathfrak{A})$ equipped with the norm $\|\boldsymbol{x}\|_1 = \|(\beta \mathfrak{I} - \mathfrak{A})\boldsymbol{x}\|_X$, $\forall \boldsymbol{x} \in \mathcal{D}(\mathfrak{A})$ is a Hilbert space, which is denoted by X_1. The norms generated for different β are equivalent in the graph norm and hence independent of the particular choice of β. Moreover, the embedding $X_1 \subset X$ is continuous. If $\mathfrak{L} \in \mathcal{L}(X)$ is such that $\mathfrak{L}\mathcal{D}(\mathfrak{A}) \subset \mathcal{D}(\mathfrak{A})$, then $\mathfrak{L} \in \mathcal{L}(X_1)$ (restriction of $\mathfrak{L}$ to X_1).*

The proof of this lemma is rather straightforward with the final claim on the restriction of the operator following from Lemma B.2.

By considering the adjoint $\mathfrak{A}^*$, the Hilbert space $X_1^d = \mathcal{D}(\mathfrak{A}^*)$ equipped with the norm $\|\boldsymbol{x}\|_{1,d} = \|(\bar{\beta}\mathfrak{I} - \mathfrak{A}^*)\boldsymbol{x}\|_X$, $\forall \boldsymbol{x} \in \mathcal{D}(\mathfrak{A}^*)$ and $\bar{\beta} \in \rho(\mathfrak{A}^*)$ or $\beta \in \rho(\mathfrak{A})$, respectively, can be introduced. It can be shown that X_1^d serves as pivot space.

Lemma B.4. *Let $\mathfrak{A} : \mathcal{D}(\mathfrak{A}) \to X$ be a densely defined operator with $\rho(\mathfrak{A}) \neq \emptyset$. By X_{-1} denote the completion of X with respect to the norm $\|\boldsymbol{x}\|_{-1} = \|(\beta\mathfrak{I} - \mathfrak{A})^{-1}\boldsymbol{x}\|_X$, $\forall \boldsymbol{x} \in X$. The norms generated for different β are equivalent in the graph norm and hence independent of the particular choice of β. Moreover, X_{-1} is the dual to X_1^d with respect to the pivot space X, i.e. $X_{-1} = \mathcal{D}(\mathfrak{A}^*)'$. In addition, if $\mathfrak{L} \in \mathcal{L}(X)$ is such that $\mathfrak{L}^*\mathcal{D}(\mathfrak{A}^*) \subset \mathcal{D}(\mathfrak{A}^*)$, then $\mathfrak{L}$ has a unique extension to an operator $\tilde{\mathfrak{L}} \in \mathcal{L}(X_{-1})$.*

Moreover, these results imply the following lemma, which is utilized for the introduction of boundary control systems.

Lemma B.5. *Let $\mathfrak{A} : \mathcal{D}(\mathfrak{A}) \to X$ be a densely defined operator with $\rho(\mathfrak{A}) \neq \emptyset$, let $\beta \in \rho(\mathfrak{A})$, and let X_1 and X_{-1} be as above. Then $\mathfrak{A} \in \mathcal{L}(X_1, X)$ and $\mathfrak{A}$ has*

a unique extension $\tilde{\mathfrak{A}} \in \mathcal{L}(X, X_{-1})$. *In addition,* $(\beta\mathfrak{I} - \mathfrak{A})^{-1} \in \mathcal{L}(X, X_1)$ *and* $(\beta\mathfrak{I} - \tilde{\mathfrak{A}})^{-1} \in \mathcal{L}(X_{-1}, X)$ *with* $\beta \in \rho(\tilde{A})$ *and these two operators are unitary.*

If $\mathfrak{A}$ is the generator of a C_0–semigroup $\mathfrak{T}(t)$ on X, then it follows from the previous results that for every $t \geq 0$, $\mathfrak{T}(t)$ has a unique restriction in $\mathcal{L}(X_1)$ and a unique extension $\tilde{\mathfrak{T}}(t)$ in $\mathcal{L}(X_{-1})$. These two families of operators are however similar to the original semigroup. In particular, the restriction of $\mathfrak{T}(t)$ to X_1 (considered as an operator in $\mathcal{L}(X_1)$) is the image of $\mathfrak{T}(t) \in \mathcal{L}(X)$ through the unitary operator $(\beta\mathfrak{I} - \mathfrak{A})^{-1} \in \mathcal{L}(X, X_1)$. Hence, these operators form a strongly continuous semigroup on X_1, whose generator is the restriction of $\mathfrak{A}$ to $\mathcal{D}(\mathfrak{A})$. The operator $\tilde{\mathfrak{T}}(t) \in \mathcal{L}(X_{-1})$ is the image of $\mathfrak{T}(t) \in \mathcal{L}(X)$ through the unitary operator $(\beta\mathfrak{I} - \tilde{A}) \in \mathcal{L}(X, X_{-1})$. Similarly, these extended operators form a C_0–semigroup $\tilde{\mathfrak{T}} = (\mathfrak{T}(t))_{t\geq 0}$ on X_{-1}, whose generator is $\tilde{\mathfrak{A}}$.

B.3.4 Sesquilinear Forms and the Lax–Milgram Theorem

Sesquilinear forms are, for instance, required to properly introduce weak formulations of PDE systems. For a comprehensive treatise of sesquilinear forms and their properties as well as weak form analysis, the reader is, e.g., referred to [17, 9, 19] and the references therein.

Definition B.10 (Sesquilinear form). The mapping $\sigma : V \times V \to \mathbb{C}$ is said to be a sesquilinear form or sesquilinear functional, respectively, if

(i) $\sigma(\phi_1 + \phi_2, \psi) = \sigma(\phi_1, \psi) + \phi(\phi_2, \psi)$
(ii) $\sigma(\alpha\phi, \psi) = \alpha\sigma(\phi, \psi)$
(iii) $\sigma(\phi, \psi_1 + \psi_2) = \sigma(\phi, \psi_1) + \sigma(\phi, \psi_2)$
(iv) $\sigma(\phi, \alpha\psi) = \overline{\alpha}\sigma(\phi, \psi)$

for all $\phi,\ \phi_1,\ \phi_2,\ \psi,\ \psi_1,\ \psi_2 \in V$ and $\alpha \in \mathbb{C}$.

The Lax–Milgram theorem provides an essential tool to analyse weak solutions to initial–boundary–value problems for different types of PDEs, see, e.g., [10, 17, 13, 6].

Theorem B.8 (Lax–Milgram). *Let* $\sigma(\phi, \psi)$ *be a sesquilinear form on a Hilbert space* X*, which is continuous and coerziv, i.e. there exist positive constants* c *and* k *such that*

$$|\sigma(\phi, \psi)| \leq c\|\phi\|_X\|\psi\|_X, \quad \Re\{\sigma(\phi, \phi)\} \geq k\|\phi\|_X^2$$

for all $\phi,\ \psi \in X$. *Let* f' *be any linear functional on* X. *Then there exist unique* $\phi_0,\ \psi_0 \in X$ *such that*

$$f'(x) = \sigma(x, \psi_0) = \overline{\sigma(\phi_0, x)} \quad \textit{for all } x \in X.$$

The reader is also referred to the Appendix by A.N. Milgram in [3].

B.4 Auxiliary Theorems and Lemmas

Lemma B.6.

$$(i) \qquad \sum_{j=0}^{l} \binom{l}{j} (l-j)!\,(j+k)! = \sum_{j=0}^{l} \binom{l}{j} (l-j+k)!\,(j)!$$
$$= \frac{(l+k+1)!}{k+1}, \qquad \forall k, l \in \mathbb{N} \tag{B.18}$$

$$(ii) \qquad \int_0^{\eta} \int_0^{r} \frac{s^{2k+l}}{(2k+l)!} \mathrm{d}s\mathrm{d}r = \frac{\eta^{2k+l+2}}{(2k+l+2)!}, \quad k, l \in \mathbb{N} \tag{B.19}$$

$$(iii) \qquad \int_0^{\sigma} \int_0^{r} (rs)^{n-1}(r+s)\mathrm{d}s\mathrm{d}r = \frac{\sigma^{2n+1}}{n(n+1)},$$
for $n \in \mathbb{N}_1$ *and* $\sigma \geq 0$ (B.20)

$$(iv) \qquad \int_{\sigma}^{\eta} \int_0^{\sigma} (rs)^{n-1}(r-s)\mathrm{d}s\mathrm{d}r = \frac{(\eta\sigma)^n(\eta-\sigma)}{n(n+1)},$$
for $n \in \mathbb{N}_1$ *and* $0 \leq \sigma \leq \eta$ (B.21)

$$(v) \qquad \int_{\sigma}^{\eta} \int_0^{\sigma} (rs)^{n-1}(r+s)\mathrm{d}s\mathrm{d}r = \frac{(\eta\sigma)^n(\eta+\sigma) - 2\sigma^{2n+1}}{n(n+1)},$$
for $n \in \mathbb{N}_1$ *and* $0 \leq \sigma \leq \eta$ (B.22)

The proof of Lemma B.6 is omitted but follows directly by induction. In addition, the successive application of Leibnitz's rule provides a rule to determine the derivatives of the product $c(z,t)x(z,t)$ up to an arbitrary order.

Lemma B.7. *Let* $c(z,t) \in C^{\infty}(\Xi)$ *and* $x(z,t) \in C^{\infty}(\Xi)$ *with* $\Xi = \Omega \times \mathbb{R}^{+}_{t_0}$, *then given* $l \in \mathbb{N}^r$ *and* $k \in \mathbb{N}$ *it holds that*

$$\partial_z^l \partial_t^k c(z,t)x(z,t) = \sum_{\gamma_0=0}^{k} \binom{k}{\gamma_0} \sum_{\boldsymbol{\gamma}=\mathbf{0}}^{l} \binom{l}{\boldsymbol{\gamma}} \partial_z^{l-\boldsymbol{\gamma}} \partial_t^{k-\gamma_0} c(z,t) \partial_z^{\boldsymbol{\gamma}} \partial_t^{\gamma_0} x(z,t). \tag{B.23}$$

References

1. Alt, H.: Lineare Funktionalanalysis, 4th edn. Springer, Heidelberg (2000)
2. Aoustin, Y., Fliess, M., Mounier, H., Rouchon, P., Rudolph, J.: Theory and practice in the motion planning and control of a flexible robot arm using Mikusiński operators. In: Proc. 5th IFAC Symposium on Robot Control, Nantes (F), pp. 287–293 (1997)
3. Bers, L., John, F., Schlechter, M.: Partial Differential Equations. John Wiley & Sons, Inc., New York (1964)
4. Boas, R.: Entire functions. Academic Press, New York (1954)
5. Brezis, H.: Analyse fonctionelle, Masson, Paris (1993)

6. Evans, L.: Partial Differential Equations. Graduate Studies in Mathematics, vol. 19. American Mathematical Society, Providence (2002)
7. Gohberg, I., Krein, M.: Introduction to the Theory of Linear Nonselfadjoint Operators. Translations of Mathematical Monographs, vol. 18. American Mathematical Society, Providence (1969)
8. Hua, C., Rodino, L.: General theory of PDE and Gevrey classes. In: Min-You, Q., Rodino, L. (eds.) General Theory of PDEs and Microlocal Analysis, pp. 6–81. Addison Wesley (1996)
9. Kato, T.: Perturbation Theory for Linear Operators. Springer, Berlin (1980)
10. Lax, P., Milgram, A.: Parabolic equations. In: Contributions to the Theory of Partial Differential Equations. Annals of Mathematics Studies, vol. 33, pp. 167–190. Princeton University Press, Princeton (1954)
11. Levin, B.: Distribution of zeros of entire functions. American Mathematical Society, Providence (1980)
12. Levin, B.: Lectures on Entire Functions. American Mathematical Society, Providence (1996)
13. Naylor, A., Sell, G.: Linear Operator Theory in Engineering and Science. Applied Mathematical Sciences, vol. 40. Springer, New York (1982)
14. Rodino, L.: Linear Partial Differential Operators in Gevrey Spaces. World Scientific Publishing Co. Pte. Ltd., Singapore (1993)
15. Rudolph, J.: Beiträge zur flachheitsbasierten Folgeregelung linearer und nichtlinearer Systeme endlicher und unendlicher Dimension. Berichte aus der Steuerungs– und Regelungstechnik. Shaker–Verlag, Aachen (2003a)
16. Rudolph, J.: Flatness Based Control of Distributed Parameter Systems. Berichte aus der Steuerungs– und Regelungstechnik. Shaker–Verlag, Aachen (2003b)
17. Tanabe, H.: Equations of evolution. Pitman Publ., London (1979)
18. Tucsnak, M., Weiss, G.: Observation and Control for Operator Semigroups. Birkhäuser, Basel (2009)
19. Wloka, J.: Partial Differential Equations. Cambridge University Press, Cambridge (1987)

Index